Donald W. Brown
David V. Duchane
Grant Heiken
Vivi Thomas Hriscu

Mining the Earth's Heat: Hot Dry Rock Geothermal Energy

Springer

The HDR Test Site at Fenton Hill, New Mexico, in late 1991

Donald W. Brown • David V. Duchane
Grant Heiken • Vivi Thomas Hriscu

Mining the Earth's Heat: Hot Dry Rock Geothermal Energy

Edited by Vivi Thomas Hriscu
Technical Illustration by Andrea Kron

Springer

Donald W. Brown
David V. Duchane (Ret.)
Grant Heiken (Ret.)
Vivi Thomas Hriscu (Ret.)
Los Alamos National Laboratory
Los Alamos, New Mexico
USA

ISBN 978-3-540-67316-3 e-ISBN 978-3-540-68910-2
DOI 10.1007/978-3-540-68910-2
Springer Heidelberg Dordrecht London New York

Library of Congress Control Number: 2012936976

Printed on acid-free paper

Springer is part of Springer Science+Business Media (www.springer.com)

Dedication

We dedicate this book to those who labored over many years to take the hot dry rock concept from simply a novel idea to a proven reality. Their imagination, creativity, long-term commitment, and hard work led to the outstanding technical achievements that are described in detail herein. Those achievements have laid a solid foundation for the development of HDR geothermal energy as a major energy resource for the 21st century and beyond.

Legal Statement

The Los Alamos National Laboratory strongly supports academic freedom and a researcher's right to publish; therefore, the Laboratory as an institution does not endorse the viewpoint of a publication or guarantee its technical correctness.

Acknowledgments

The 23 years of pioneering experiments that constituted the Los Alamos National Laboratory's Hot Dry Rock Project would not have been possible without the support of numerous entities, beginning with the U. S. Atomic Energy Commission (AEC). Its successor federal agencies, the Energy Research and Development Administration (ERDA) and the U. S. Department of Energy (DOE), continued the funding of the HDR effort. And from 1980 to 1986, the government of Japan and the Federal Republic of Germany also contributed, through an agreement developed under the auspices of the International Energy Agency (IEA).

The authors would like to particularly acknowledge the enthusiastic and unwavering support for the HDR concept shown by the late John E. (Ted) Mock, who directed the U. S. Department of Energy's geothermal program from 1982 to 1994, the period spanning the development and testing of the deeper Phase II reservoir at Fenton Hill, New Mexico, and by Allan Jelacic, now retired, who assumed leadership of the DOE's Division of Geothermal Energy following Dr. Mock's retirement in 1994. The financial support provided under their leadership made possible many of the technical achievements described herein and helped launch the production of this book, which no doubt will serve as one of the HDR Project's principal legacies.

It was through the persistent efforts of the late Mort Smith that the early funding was obtained for the nascent HDR Project. Without his efforts, there never would have been a Fenton Hill. Mort also inspired us to prepare this book and was a constant source of valuable information until his death.

Bob Potter, who originated the hot dry rock concept at Los Alamos, deserves special recognition. His unique expertise helped elucidate the initial drafts of several chapters of this book. Jim Thomson, a key member of the HDR field operations team responsible for the highly automated and reliable operation of the surface plant during the Long-Term Flow Test, provided much helpful technical input on the surface equipment and downhole operations. In addition, we thank Bert Dennis, the able leader of the Instrumentation Group during the HDR Project (starting with the Barley Canyon experiments in 1972), for his help in preparing the Appendix.

Thanks are also due the hundreds of hard-working scientists and engineers associated with the Fenton Hill HDR Project, who produced the reports from which portions of this book are drawn. The results cost them countless days and nights of effort, often under the pressure of deadlines and foul weather.

We would also like to recognize those who assisted in the practical aspects of preparing this volume for publication. Ruth Bigio, who left the Laboratory a few years ago, provided initial versions of several of the figures. Andi Kron, Los Alamos National Laboratory geologist-turned-cartographer/technical illustrator, was responsible for all of the final figures in the book. She not only

exercised laudable patience as we made endless changes to them, but her skill with graphics and her own scientific and technical background enabled her to improve many of them. The formatting and composition are the fine work of Carrie Dittmer (Dittmer Design, Golden, CO). Carrie has earned our particular gratitude for her dedication, good humor, and responsiveness in the face of multiple revisions of the manuscript. We thank Vicky Musgrave of the Los Alamos National Laboratory Research Library for expeditiously resolving problems with a number of the references; and Iosif Hriscu of the Halliburton Company (Duncan, OK) for help with some technical drilling details and terminology.

Finally, we would like to express our thanks and appreciation to our many colleagues around the world who took an interest in the Fenton Hill HDR Project. Many of them provided us with insights that both directly and indirectly contributed to the wide range of HDR issues summarized in this book.

Preface

The hot dry rock (HDR) geothermal energy concept was born of the recognition that the heat of the earth represents an almost inexhaustible source of clean, thermal energy for mankind. It was the pioneering efforts of Bob Potter and Mort Smith, two visionary scientists at Los Alamos National Laboratory in New Mexico, that led to the development of an effective and robust method of recovering useful energy from the vast regions of hot rock in the earth's upper crust. The heat from that rock—as Smith put it—"represents the largest and most broadly distributed supply of directly usable thermal energy that is accessible to man." In the ensuing years, other researchers at Los Alamos would help to make Potter and Smith's dream a reality.

This book tells the story of the pioneering experiments at Fenton Hill, near Los Alamos, which produced the world's first and—to date—only true HDR reservoirs. They were created in deep regions of jointed basement rock that had subsequently been tightly resealed by the deposition of secondary minerals (the almost universal situation where sufficient time has followed the period of deformation that produced the jointing).

As manager of the Hot Dry Rock Project during a period that yielded some of the most fruitful and significant technical results, I was particularly well positioned for the task of analyzing and synthesizing the findings from the numerous Fenton Hill tests and experiments. Over the past twelve years, the demands of writing this book have led me to carry out an exhaustive review of those findings and to revise and/or reinterpret them as called for—in light of present knowledge concerning the behavior of deep, jointed, crystalline basement rock in general and of confined, man-made HDR reservoirs in particular.

Some readers may find the length and level of detail of certain chapters excessive. But it should be noted that this book is intended not only to provide information useful to future exploiters of heat from the deep earth, but also to serve as the complete and definitive report on the 23 years of HDR operations at Fenton Hill—written from the perspective of one who was deeply involved from start to finish. To facilitate the reader's grasp of the most important events and findings, Chapter 2 has been structured as an "Executive Summary."

Donald W. Brown
Los Alamos, New Mexico

Contents

PART I

Hot Dry Rock Geothermal Energy: History and Potential of the Newest and Largest Renewable Energy Resource

Chapter 1

Serendipity—A Brief History of Events Leading to the Hot Dry Rock Geothermal Energy Program at Los Alamos

How far back in our past did humans begin to use hot water and steam coming from vents in the earth's surface to improve their lives? Did they make stops at such sites while moving from place to place, bathing in the warm pools or using the waters for cooking, and eventually construct villages near hot springs? We can only imagine in what ways man first availed himself of the earth's heat; but we can assume that human populations in various areas sooner or later encountered hot waters that were bubbling up to the surface after having been raised to high temperatures by circulation through deep, hot rock—and that they made use of the heated water.

In modern times, geothermal energy has been exploited through drilling into permeable zones within the earth's crust that are characterized by high heat flow. If the reservoir of hydrothermal fluid is sufficiently large, the depths are accessible to drilling, the temperatures are high enough, and the rock is sufficiently permeable, hot fluids can be brought to the surface for conversion to electrical power or for direct-heating use. But areas possessing these attributes (such as Larderello, Italy, where deep hydrothermal fluids have been commercially exploited for electricity generation since the early 1900s) are rare. In many regions, exploratory boreholes have been drilled to depths where temperatures were sufficiently high, but the permeability of the rock was negligible and only small amounts of fluid were present—in other words, the rock was hot, but essentially dry. The next logical step, then, was to consider *engineering* geothermal reservoirs in the far more numerous regions of the earth where rock at drilling-accessible depths was hot but contained no open, interconnected joints or faults.

The concept of extracting heat from man-made geothermal reservoirs originated in the early 1970s, at the Los Alamos Scientific Laboratory (now the Los Alamos National Laboratory) in New Mexico.[1] Established by the

[1]Much of this early history of hot dry rock (HDR) geothermal energy has been abstracted from the many papers written by HDR pioneer Morton C. Smith. His untimely death in 1997 brought an end to the detailed history of the HDR Program he had embarked upon. Fortunately, we already have the first volume, entitled *The Furnace in the Basement, Part I—The Early Days of the Hot Dry Rock Geothermal Energy Program, 1970–1973*. Published in 1995, it is superbly researched, extremely readable, and highly recommended as additional reading. The second volume, for which he had completed a great deal of the work, will be published by the authors of this book as soon as possible.

D.W. Brown et al., *Mining the Earth's Heat: Hot Dry Rock Geothermal Energy*,
DOI 10.1007/978-3-540-68910-2_1, © Springer-Verlag Berlin Heidelberg 2012

U. S. Army, then transferred to the Atomic Energy Commission (AEC) in the mid 1940s, the Laboratory[2] had as its primary mission the design and testing of nuclear weapons. So how did the scientists working there become involved in developing a unique form of renewable energy? The first serendipitous circumstance was the truly multidisciplinary character of the Laboratory and the uniquely "research-friendly" environment it offered. To design and test weapons required the efforts not only of weapons experts, but also of engineers, chemists, physicists, geologists, geophysicists, hydrologists, and health scientists. And to stay in the lead technologically required the "campus" atmosphere of freedom for creative thinking that was then the Laboratory's hallmark, as well as the kind of dedication for which Los Alamos scientists were known.

Developments at Los Alamos

Under the directorship (1945–1970) of Norris Bradbury, Los Alamos researchers were openly encouraged to "come up with ideas"—a challenge that was taken up by, among others, a group of chemists led by Eugene S. ("Robbie") Robinson. Robinson's group was interested in new techniques for drilling deep holes into the earth; it was not only the possible practical applications that sparked their interest (the "Mohole" deep earth sampling project was under consideration at the time), but also a kind of fascination about what could be done, what could be found, "down there."

Conventional drilling was based on the use of drill bits made of very hard materials that could break and grind solid rock. In 1960, members of Robinson's group conceived the notion that if the rock could be rendered liquid—melted—its penetration might be easier and faster (particularly as depth, and therefore rock temperature, increased), as well as cheaper. In early experiments, refractory metals such as tungsten and molybdenum, electrically heated to incandescence, were readily pushed through samples of igneous rock. These experiments confirmed that the energy needed to melt rock is similar to the energy required to break and pulverize it (on the order of 1 kcal/cm^3). The group then embarked on the developmental work that led to the creation of a rock-melting penetrator.

The new device proved capable of steady-state drilling through basalt boulders (the debris—glass particles—being pneumatically ejected as drilling progressed). In porous volcanic rocks, such as ash-fall tuffs, the penetrator was able to consolidate the rock as it advanced, creating a high-density glass lining for the hole—which eliminated the need to eject debris. The coupled heat-transfer and hydrodynamic behavior of the rock-melting process was analyzed through a new solution of the Navier–Stokes equations that was developed by B. B. McInteer, a member of Robinson's group (Armstrong et al., 1965).

[2]In this book we use "Los Alamos" and "the Laboratory" interchangeably to refer to the Los Alamos National Laboratory.

Although lack of funding terminated the rock-melting project in early 1963, the ensuing years saw considerable private speculation within the group about possible new advances in this area. In early 1970, at Norris Bradbury's direction, Robinson assembled an interdisciplinary ad hoc committee (Fig. 1-1) to study a rock-melting drill based on a new concept. Known as the "Nuclear Subterrene," this device would be powered by a compact nuclear reactor instead of by electricity; it would transmit thermal energy via heat pipes to a refractory metal shell surrounding the reactor (Robinson et al., 1971). Such a device would be capable of much more efficient boring of significantly larger holes (up to several meters in diameter) than the electrically powered rock-melting penetrator—opening up numerous applications for which smaller-scale drilling and excavating was costly and time-consuming (such as bores and tunnels for underground transport of gases, liquids, cargo, and people; large underground cavities for waste disposal or for storage and preservation of various materials; underground chambers for high-temperature and high-pressure processing operations; shafts for mining and exploration; underground laboratories for scientific studies; and—not least—the creation of man-made geothermal energy systems).

Fig. 1-1. The Ad Hoc Committee on Rock-Melting Drills (clockwise from left): Don Brown, Bob Potter, Bob Mills, B. B. McInteer, John Rowley, Mort Smith (behind Rowley), and Dale Armstrong.
Source: *The Atom*, 1971

In addition to most of the original members of the rock-melting project, the committee included experts in needed disciplines, and outside consultants were called upon for assistance with specialized matters. The committee conducted its study through most of 1970 and summarized its conclusions—how the Subterrene would be constructed, how it would work, and its principal applications—in a report for submission to Harold Agnew, the new Laboratory Director. The report would essentially be a proposal for the establishment of a major program to develop the Subterrene.

It was as part of this process that another link in the serendipitous chain was forged: Bob Potter, an influential and creative member of Robinson's team, had long been interested in the application of deep-drilling technology to the recovery of geothermal energy, which would involve accessing the hot crystalline rock typically found deep in the earth's crust. Potter's imagination was sparked by an article in the *Journal of Geophysical Research* describing hydraulic fracturing experiments carried out at the Oak Ridge National Laboratory (Sun, 1969). Using the hydraulic fracturing technology developed by the petroleum industry to access "tight" hydrocarbon reservoirs, Oak Ridge was investigating whether fracture systems could be created in the sedimentary layers of the earth's crust for the disposal of radioactive waste. Potter reasoned that if hydraulic fracturing could be used to develop fracture systems in sedimentary rock, the technology could also be used to fracture[3] crystalline rock.

The Oak Ridge experiments provided other insights that were pivotal as Potter's aspirations for the Subterrene became more and more drawn in the direction of geothermal applications. The experiments involved two relatively shallow wells: an injection well, down which water was pumped at a pressure that would induce fracturing of the surrounding rock (through slots cut in the casing); and an observation well, located about 30 ft (9 m) to the west. By the time about 9000 gal. (34 000 L) of water had been pumped into the injection well, a sudden rise in pressure was noted in the observation well, indicating that the hydraulically induced fracture (or fractures) had intersected that well. It became clear that such fractures could extend tens to hundreds of meters into the surrounding rock. This finding, in combination with the knowledge that rocks become progressively hotter with depth, made it only a short step to the next realization: the idea began to jell that, at depths where rock temperatures were hot enough for commercial applications, hydraulic fractures could serve as underground flow paths for a heat-mining system. Heat from the fracture surfaces would be transferred to fluid pumped into them via the injection well, and the hot fluid would then be

[3]Today, we often use the more accurate term "pressure-stimulate"—it now being clear that crystalline rock is characterized by pre-existing networks of joints or fractures that have become sealed by mineral deposition and are reopened through hydraulic pressurization.

brought back to the surface via the second (production) well—an efficient means of recovering geothermal heat. The hot dry rock geothermal energy concept was born.

Building on Potter's concept, Mort Smith postulated that (owing to the combined effect of increasing temperature, increasing overburden stress, mineral alterations, and deposition of secondary minerals) both the porosity and permeability of crustal rock would diminish progressively with depth. He believed this geologic situation—the presence of low-porosity hot rock at depth—to be extremely common throughout the world, in contrast to the rarity of natural hydrothermal systems. If HDR was exploitable, then, nearly every area of the world could, given adequately deep boreholes, be considered to possess an abundant geothermal resource at depth.

Mort Smith and Don Brown, who were knowledgeable in conventional rotary drilling techniques, then supplied the final link in the chain of serendipitous events: they reasoned that the development and testing of an HDR system need not wait for success in the Subterrene Program, but could proceed in parallel, using then-available oilfield drilling equipment. Most of the committee—and especially Potter, McInteer, Smith, and Brown—concurred that HDR was at least as important as the Subterrene. When the proposal was submitted to Director Agnew in November 1970, therefore, it contained (as Appendix F) a detailed presentation of Bob Potter's HDR concept and the suggestion that once the Subterrene Program was under way, a second major program be instituted to develop HDR geothermal energy systems. (The document was reproduced by Mort Smith in a more polished form the following April, for use as a "sales tool" [Robinson et al., 1971].)

Note: The Nuclear Subterrene would never be developed. In 1973, under the leadership of John Rowley, the Program would be redirected from an emphasis on large-diameter tunneling and boring applications to support of geothermal drilling and exploration. With the approach of a worldwide oil crisis (the Arab oil embargo of 1973), which was driving renewed interest in alternative energy technologies, it was difficult to argue against the logic of developing HDR geothermal systems as soon as possible. Moreover, anticipated major cutbacks in the Laboratory's multimillion-dollar Rover Program—to develop a hydrogen-cooled nuclear rocket engine for space exploration—was creating a need for new programs at the Laboratory. (By 1976, lack of interest in Washington would lead to a withdrawal of funding and cancellation of the Subterrene Program. Fortunately, the HDR Project would be the beneficiary, at least in terms of manpower.)

Hot Dry Rock in Its Infancy

In March 1971, the Laboratory's newly appointed Associate Director for Research, Richard Taschek, launched the Hot Dry Rock Geothermal Energy Development Project—as yet unfunded—under the leadership of Mort Smith and with Eugene Robinson as coordinator. The HDR concept would be patented three years later (Potter et al., 1974).[4]

In those early years, the HDR Project at Los Alamos was very informal. The "geothermal group" began by gathering and studying available information on the geology and geophysics of geothermal areas, as well as on hydrology, drilling, rock mechanics, reservoir management, and hydraulic fracturing. Physicists working with the group modeled the efficiency of heat extraction from an HDR reservoir (Harlow and Pracht, 1972). Early on, a closed-loop earth circulation system was envisioned that would incorporate heat exchangers at the surface to transfer the heat from the hot geofluid (pressurized water) to another working fluid—a so-called binary cycle. Such a system would have the advantages of being simple, safe, and environmentally benign, and could be designed on the basis of existing technology.

The Los Alamos team believed that man-made geothermal systems could be created in the deep crystalline "basement" almost anywhere that geothermal gradients were high enough for heat mining to be commercially attractive—the principal economic issue being the cost of drilling. Without the means to explore far and wide, they went looking "just over the hill" west of Los Alamos, in the Jemez Mountains. The major feature of this area is the Valles Caldera, formed only about 1 million years ago.

Along the trace of the bounding ring-fracture, post-caldera eruptions of rhyolitic lavas occurred as recently as about 50 000 years ago. Primarily inside the physiographic rim, hot springs and a few fumaroles were surface indicators of a large thermal resource (magma body) underlying a portion of the caldera; and extensive faulting suggested subsurface joint permeability, making the caldera a prime target for hydrothermal geothermal exploration and development. In the 1970s and 1980s, in an independent effort (funded mainly by the U. S. Department of Energy [DOE] and the Public Service Company of New Mexico), the Union Oil Company of California carried

[4]The HDR patent was written by Don Brown, with the able assistance of Paul Gaetjens, a Laboratory patent attorney. Almost the entire HDR concept was Bob Potter's; Mort Smith added a section on the augmentation of heat production through thermal stress cracking, and Don Brown contributed a section on a single-well heat production concept using insulated, coaxial casing. (Later, to honor Eugene Robinson—the Project's financial "godfather" in the early days, who was suffering from terminal cancer—Don Brown replaced his name as third author with that of Robinson.)

out extensive drilling and testing along a major northeast-trending fault structure within the caldera. They did find a high-temperature hydrothermal system, but its power-generation potential was only about 25 MW_e, half that required (at that time) to make a commercial venture feasible.

The Los Alamos team reasoned that recent volcanic activity along the ring-fracture would have produced a region of elevated temperature that would extend radially outward from the caldera at least several miles. In late 1971, the measurement of geothermal gradients in a number of shallow, augered holes surrounding the caldera verified this hypothesis and showed that the western flank was particularly attractive for HDR development. In early 1972, four deeper holes were drilled in that area for measuring temperature gradients and heat flows. Three of these holes were located roughly along an arc parallel to and 2–3 miles (3–5 km) west of the ring-fracture; the fourth was located 4.5 miles due west of the ring-fracture.

As shown in Table 1-1, the heat-flow values for the three holes closest to the caldera (A, B, and C) were found to be uniformly high—in the range of 5–6 cal/cm^2 • sec (worldwide average heat flow is about 1.5 cal/cm^2 • sec). In contrast, the heat flow for hole D was only about one-third as high.

Table 1-1. Heat-flow values in intermediate-depth test holes

	Hole A	Hole B	Hole C	Hole D
Date completed	10 Apr 1972	13 Apr 1972	16 Apr 1972	18 Apr 1972
Distance from ring fault (mi)	2.0	2.4	3.0	4.5
Depth (ft)	590	650	750	500
Heat flow (cal/cm^2 • sec)	5.13×10^{-6}	5.50×10^{-6}	5.88×10^{-6}	2.20×10^{-6}

The Precambrian-age crystalline basement rocks of the area were thought to lie about 2600 ft below the surface. Similar rocks, when tested at university laboratories, had proved to be nearly impermeable, indicating that a basement-rock environment such as that found in the Jemez Mountains could be ideal for testing and development of the HDR concept. On the basis of these findings, the team selected the Fenton Hill area, just west of the Valles Caldera (Fig. 1-2). An essentially nonvolcanic terrain, Fenton Hill exhibited elevated thermal gradients; the crystalline basement rock lay at reasonable depths; and the entire region was public land, part of the Santa Fe National Forest.

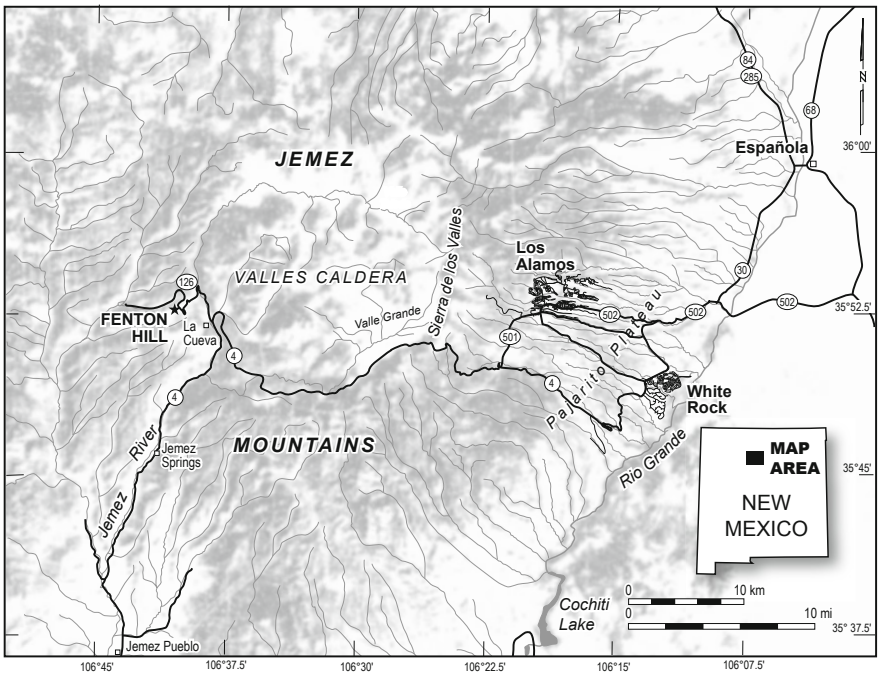

Fig. 1-2. The region west of Los Alamos. The Fenton Hill area is shown west of the Valles Caldera.

A site in Barley Canyon, located on the arc formed by heat-flow test holes A, B, and C, was picked. It was decided to drill in the canyon bottom, which would reduce the amount of drilling by some 300 ft, thereby saving considerable time and money (but this would later prove to be a mistake, when thawing of the very heavy snowfall of the winter of 1972–73 turned the work area into a muddy bog).

In the spring of 1972, the drilling of the first deep exploratory borehole, Granite[5] Test No. 1 (GT-1), was begun. Precambrian crystalline basement rocks were encountered at 2105 ft (642 m), and by June 1 the hole had reached a depth of 2430 ft (741 m), some 325 ft into the basement. After being cased to a depth of 2400 ft with 5-in.-diameter, 13 lb/ft K-55 casing, the hole was deepened 145 ft by continuous coring. The final depth was 2575 feet (785 m), 470 ft into the crystalline basement. An examination of the drill cuttings obtained during the first 325 ft of basement drilling (before the casing was set) showed that the rock was primarily augen gneiss. The

[5]Although the term "Geothermal Test Hole" appears in numerous HDR publications and reports, the original term—and the one that was used in the permits and original paperwork—was "Granite Test Hole."

rocks penetrated during the continuous-coring phase were 50 ft of true granite, 40 ft of gneiss, and finally 55 ft of amphibolite. This first exploratory borehole exhibited a bottom-hole temperature of 100.4°C and a mean gradient of over 100°C/km—outstanding for any geothermal area.[6]

Figure 1-3, an enlarged view of the Valles Caldera and the region to the west, shows the location of GT-1 in relation to the caldera and the four heat-flow holes. (Most of the area known at that time as Baca Location No. 1 is currently the Valles Caldera National Preserve.)

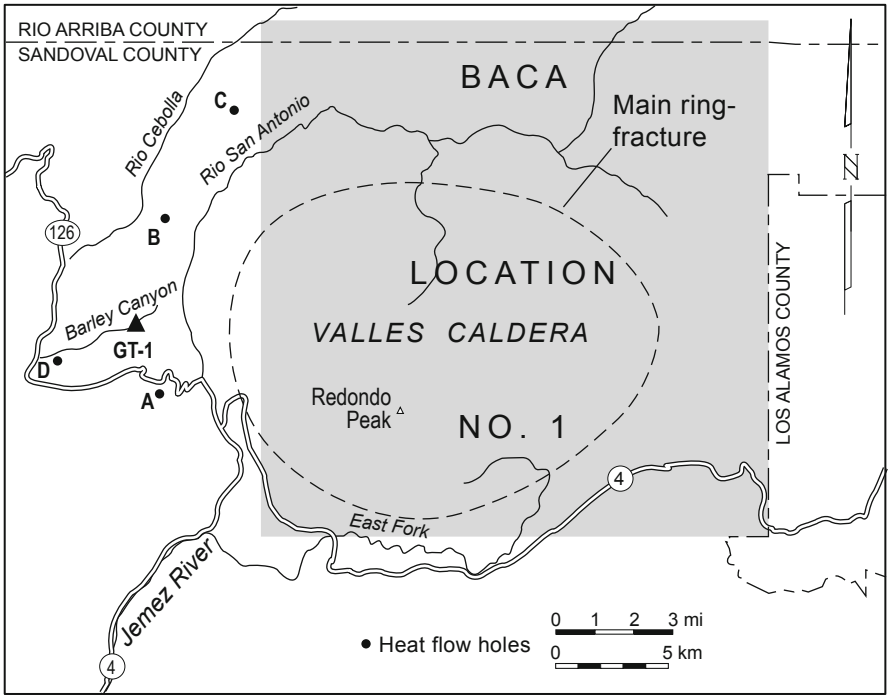

Fig. 1-3. Enlarged view of the Valles Caldera area, showing GT-1 and the four heat-flow test holes (A, B, C, and D). The dashed line delineates the trace of the main ring-fracture.
Adapted from Smith, 1995

[6]As would be discovered later, all the heat-flow and temperature-gradient measurements made in the Fenton Hill area were strongly affected by the hot aquifer originating from the caldera and flowing to the west on top of the Precambrian surface.

The First Experiments in Hydraulic Fracturing

In early 1973, a series of hydraulic fracturing experiments were conducted—with considerable difficulty—in the 145-ft continuously cored Precambrian interval of GT-1.[7] These first-ever "fracturing" experiments in deep, hot crystalline rock were intended to verify the suitability of such rocks for field testing of an HDR reservoir.

In conventional hydraulic fracturing of sedimentary formations containing petroleum or natural gas, a "packed-off" interval[8] of the borehole is pressurized until the overpressure fractures the borehole wall. According to the then-accepted theory of hydraulic fracturing in unjointed sedimentary formations ("homogeneous" isotropic rock) in regions where the earth stresses are typical (i.e., the maximum earth stress is vertical), the induced fracture should be vertical, planar, and normal to the axis of the least principal earth stress, which acts horizontally. With continued pressurization, the fracture should extend radially outward from the borehole for hundreds of feet, forming what is referred to as a "penny-shaped vertical fracture." This theory, which had its origin in the classic 1946 paper by I. N. Sneddon, formed the basis for the original HDR system design (Fig. 1-4).

But when the Los Alamos team applied this simple theory to the hydraulic fracturing of the Precambrian crystalline rocks penetrated by GT-1—as though this melange of ancient metamorphic and igneous rocks were "unflawed and homogeneous"—they made a serious error in judgment. Worse, that error would be perpetuated in HDR geothermal programs carried out later in other countries and in HDR research conducted by several universities (much of which, at least initially, was supported by Los Alamos). The investigators all assumed that a single fracture would be created and that it would be penny-shaped and vertical, providing a large area for the transfer of heat from the fractured hot rock to the circulating fluid.

It is important to note that this concept was not abandoned until the early 1980s (even later in Japan). Eventually, both the British HDR team working at Rosemanowes[9] and the Los Alamos team realized that, except for possibly a short distance immediately adjacent to the borehole wall, hydraulic fracturing was not actually breaking open intact crystalline rock against its inherent tensile strength. Rather, perhaps with one exception (see

[7]These experiments are more thoroughly covered in Mort Smith's excellent report on the early days of HDR, *The Furnace in the Basement, Part I* (Smith, 1995).

[8]The interval to be fractured is isolated between a pair of removable seals called "packers." This "straddle" packer assembly is connected by a pressure line ("frac" string) to high-pressure pumps on the surface.

[9]From 1977 to 1988, personnel from the Camborne School of Mines carried out the first large-scale geothermal research project in Europe, in the Carnmenellis granite (Cornubian Batholith) of a former granite quarry at Rosemanowes, in the southwestern Cornwall peninsula.

Table 1-2 and related discussion), pre-existing—but sealed—joints were being opened. The conventional theory of hydraulic fracturing had ignored the presence of these flaws in the basement rock. (For additional information, see *Properties of the Deep Crystalline Basement as They Relate to HDR Reservoirs* in Chapter 2.)

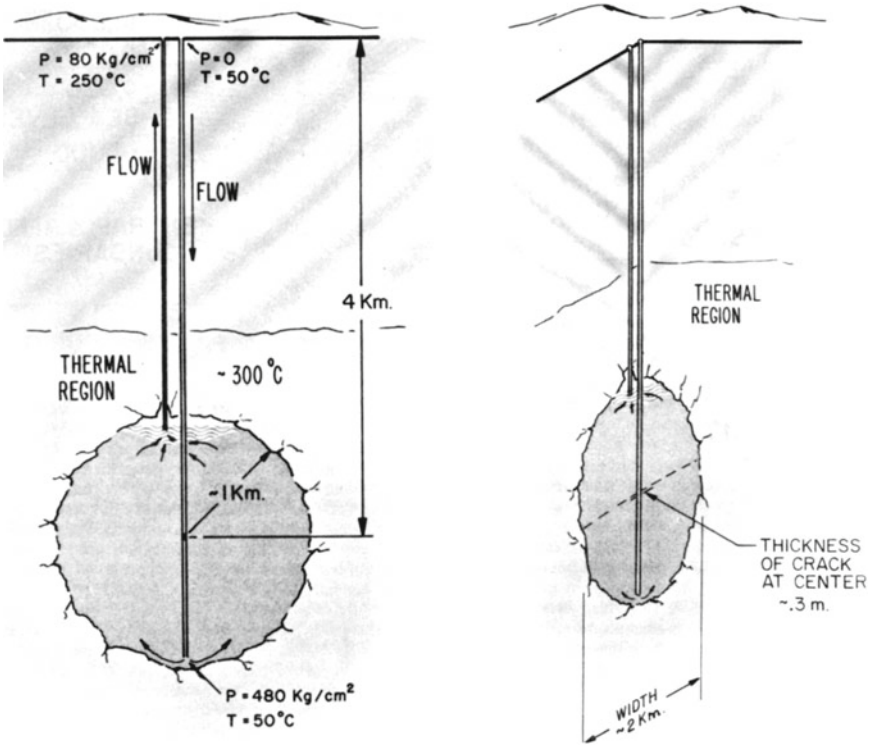

Fig. 1-4. Originally proposed model for an HDR geothermal energy system. Source: Robinson et al., 1971

Planned and directed by Don Brown, these first attempts to fracture the basement rock were funded by the Division of Physical Research of the AEC. They were uniquely successful and would not soon be replicated—for three reasons:

- Because this lower section of the GT-1 borehole had been drilled with diamond core bits, the borehole wall was very smooth, enabling many short intervals to be isolated with straddle packers.
- The diameter of the lower borehole was only 4 1/4 in., allowing the use of smaller and more efficient packer elements (the success of sealing with packers appears to decrease inversely with hole diameter).
- The working depths were fairly shallow, making the numerous packer repairs relatively easy.

The plan was (1) to isolate, and then hydraulically fracture, seven short intervals (7–9 ft) within the cored open-hole section of the borehole; (2) by setting a bridge plug just below the deepest mini-fracture and an inflatable packer just above the shallowest, to pressurize the interval encompassing all the mini-fractures—in the hope that they would coalesce; and (3) with further pumping, to extend the single composite fracture radially outward.

Note: At that time, how the jointed crystalline basement would behave under pressurization was not well understood (previous hydraulic fracturing experience, in the oil industry, had been limited to sedimentary rocks). It had been surmised that the composite fracture, when extended, would be vertical and perpendicular to the least principal earth stress, which was assumed to be horizontal. And from analyses based on the diagnostic tools available at this very early stage of the HDR Project, what would *appear* to have taken place is exactly that (even though it was a resealed joint rather than a true hydraulic fracture): the only discernible feature would be a single vertical crack extending the entire length of the 117-ft straddled interval (from 2427 ft to 2544 ft) and striking approximately N45W.

Both inflatable and compression-set straddle-packer assemblies were used to isolate seven separate intervals of jointed rock, which represented several rock types in the Precambrian basement. These intervals were sequentially pressurized at very low pumping rates (about 1 gpm), by small, air-driven positive-displacement pumps. Despite innumerable problems with the packers and many aborted runs (due primarily to packer leakage), and despite harsh winter conditions at the 8400-ft elevation, eventually all seven of the intervals were successfully stimulated at moderately low pressures (Table 1-2). Examination of cores and of impression packers showed that all but one of these intervals contained obvious resealed natural joints. The one interval that did not show such joints (the granite interval tested on March 27—see Table 1-2) did contain structural flaws, which probably explains why the rock in this interval fractured at a modest pressure—much lower than would have been expected for true, unflawed crystalline rock.

None of the seven "hydraulic-fracturing" (joint-opening) events was energetic enough to be detected by the surface array of seismic detectors. In a final fracturing experiment (of April 4, 1973: see Table 1-2), much higher injection rates—4.5 to 5 BPM (180–200 gpm or 12–13 L/s)—were achieved with commercial pumping equipment (Halliburton Services). As supported by a recent re-examination of the GT-1 data, this experiment opened one large joint over the entire 117-ft straddled interval. Borehole televiewer surveying, conducted by Birdwell, indicated that this joint was essentially vertical (aligned with the almost vertical borehole), oriented northwest–southeast, and connected all seven of the smaller aligned joint openings. It was because these incomplete (lacking any seismic verification) observations appeared to confirm the "vertical, penny-shaped fracture" theory that the team would stay with its original model for an HDR system (Fig. 1-4) for the next several years.

Table 1-2. Hydraulic fracturing experiments in GT-1

Date	Mean depth of joint, ft (m)	Pumping pressure, psi (MPa) Breakdown	Extension	Fluid-acceptance pressure, psi (MPa)*	Rock type
7 Mar 1973	2497 (761)	1320 (9.1)	___	___	Gneiss
14 Mar 1973	2534 (772)	___	1050 (7.2)	___	Amphibolite
19 Mar 1973	2464 (751)	1380 (9.5)	1175 (8.10)	900 (6.0)	Granite
23 Mar 1973	2545 (776)	1323 (9.12)	___	___	Amphibolite
24 Mar 1973	2428 (740)	1170 (8.1)	1015 (7.0)	925 (6.38)	Gneiss
27 Mar 1973	2454 (748)	1702 (11.73)	1300 (9.0)	965 (6.65)	Granite
28 Mar 1973	2444 (745)	1515 (10.44)	1250 (8.6)	920 (6.3)	Granite
4 Apr 1973	2484 (757) (117-ft [36-m] straddled interval)	___	1090 (7.5)	___	Composite

Source: Smith, 1995
*upon repressurization

Following these stimulation tests, Bob Potter analyzed the actual recorded pressure traces (those available) and noted that in each case, repressurization brought about a linear rise in the pressure curve followed by a "turning over" (deviation) at the point where the previously opened joint had begun to accept fluid. Potter at first identified this fluid-acceptance pressure (see Table 1-2) as the joint-opening pressure, and therefore as a measure of the *least principal earth stress* (σ_3)—on the assumption that the joint is orthogonal to the direction of this stress. We now understand that as the opening (or "jacking") pressure of a closed joint is approached, the joint starts to pressure-dilate even though many of the surface asperities are still in contact. Therefore, the initial fluid-acceptance pressure is *not* the joint-opening pressure—the latter being 100 to 200 psi higher.[10]

At a very low injection rate, the joint-extension pressure (column 4 of Table 1-2) actually more closely approximates the joint-opening pressure than does the fluid-acceptance pressure (column 5). In other words,

[10]This topic is discussed more fully in Chapter 3 (see in particular Fig. 3-6).

in this region the true least principal earth stress at a mean depth of 2428 ft is 1015 psi—the lowest of the six extension pressures recorded (on March 24). At the low injection rate of about 1 gpm, any frictional effect on the pressure could be ignored; in contrast, for the April 4 stimulation of the composite joint, at an injection rate approaching 200 gpm, the flow-induced frictional pressure loss probably explains the somewhat higher extension pressure of 1090 psi.

The drilling and testing of GT-1 laid to rest the concerns of several "experts" that

1. it would be difficult if not impossible to drill into hot crystalline rock with conventional rotary drilling equipment;
2. crystalline rock could not be hydraulically fractured;
3. because of the assumed presence of open faults and joints, the permeability of crystalline rock would be too high to contain water under pressure.[11]

The results of the experiments in Barley Canyon added needed credibility to the Laboratory's concept for an HDR energy system: that hydraulic stimulation of hot basement rock could create open joints through which pressurized fluid could be circulated. Some earth scientists continued to doubt that such a system could work or that scaling problems due to mineral dissolution could be overcome; but the GT-1 results were sufficiently encouraging to gain financial support from the AEC for the development of a deeper heat-extraction loop to investigate and demonstrate the technical feasibility of such a system. Indeed, this next step had been envisioned from the beginning of the HDR Project.

On the basis of experience gained from the work in Barley Canyon, Don Brown selected a nearby site for long-term HDR testing, which would last until 1996. Known as the Fenton Hill HDR Test Site, it was located 1.5 miles (2.5 km) south of GT-1 and 1.8 miles (2.9 km) west of the caldera ring-fracture, on a broad mesa that had been burned clear of trees during a forest fire in 1971. Not only was it high and dry—in contrast to the muddy conditions of Barley Canyon—but it was adjacent to an all-weather road (necessary in winter, given the 8700-ft [2650-m] elevation) and to electricity and telephone lines. The U. S. Forest Service granted the Laboratory a permit to use 20 acres for HDR experiments. In late 1973, the DOE finally approved funding to drill a 4500-ft-deep exploratory hole, thus launching the more than 20 years of research and development covered in this book.

---

[11] Contrary to these experts' expectation that the Precambrian permeability values would be in the millidarcy range, measurements made in GT-1 through the summer of 1973 showed a constant value of 7.7×10^{-8} darcy (0.077 microdarcy) for the 175-ft open-hole interval.

Chapter 2

The Enormous Potential for Hot Dry Rock Geothermal Energy

The concept of hot dry rock (HDR) geothermal energy originated at the Los Alamos National Laboratory. In 1970 it was proposed as a method for exploiting the heat contained in those vast regions of the earth's crust that contain no fluids in place—by far more widespread than natural geothermal resources (HDR represents over 99% of the total U. S. geothermal resource). Although often confused with the small, already mostly commercialized hydrothermal resource, HDR geothermal energy is completely different from hydrothermal energy. Whereas hydrothermal systems exploit hot fluids in place in the earth's crust, an HDR system[1] recovers the earth's heat via closed-loop circulation of fluid from the surface through a man-made, confined reservoir several kilometers deep. The technology bears little similarity to that of the hydrothermal industry, and unlike hydrothermal, it is applicable almost anywhere—hence the claim that HDR is ubiquitous.

The present-day concept of an HDR geothermal system has evolved considerably from the concept proposed by Bob Potter in 1970 and described in the original U. S. patent (see Chapter 1). As shown in Fig. 2-1, a first borehole is drilled and used for hydraulic pressurization of the naturally jointed basement rock—opening flow paths in the sealed rock mass. The reservoir of circulation-accessible hot rock thus created is then accessed by two production boreholes, drilled into the ends of the elongated reservoir region.

This current HDR concept also recognizes features of the earth's deep, hot crust that were not well understood during the early years of the HDR Project. It is now known that

- The deep crystalline basement is not homogeneous and isotropic, but is highly flawed—on a scale covering many orders of magnitude: from microcracks of a millimeter or so to an interconnected network of joints measuring a few centimeters to several meters, to faults extending tens of meters to several kilometers.
- Whereas open joints and faults are typical in the shallow, cooler layers of the earth's crust (to a depth of about 1 km), the joints and faults in the deep basement will typically have been resealed by the precipitation of secondary minerals dissolved in the hot, circulating fluids. Invariably then, the only open flaws in the basement are the microcracks[2]—except in regions that have undergone recent faulting or folding.

[1]The term "HDR geothermal system" typically refers to the *pressurized, closed-loop circulating system*, consisting of the HDR reservoir, the injection borehole, the production borehole(s), the surface piping, and the injection pumps.

[2]Evidence for these open microcracks in the earth's crust is given in Kowallis and Wang, 1983; Simmons and Richter, 1976; Swanson, 1985; and Wang and Simmons, 1978. The pervasive array of fluid-saturated microcracks gives rise to the finite, but very small (nanodarcy range), permeability of the crystalline basement.

D.W. Brown et al., *Mining the Earth's Heat: Hot Dry Rock Geothermal Energy*,
DOI 10.1007/978-3-540-68910-2_2, © Springer-Verlag Berlin Heidelberg 2012

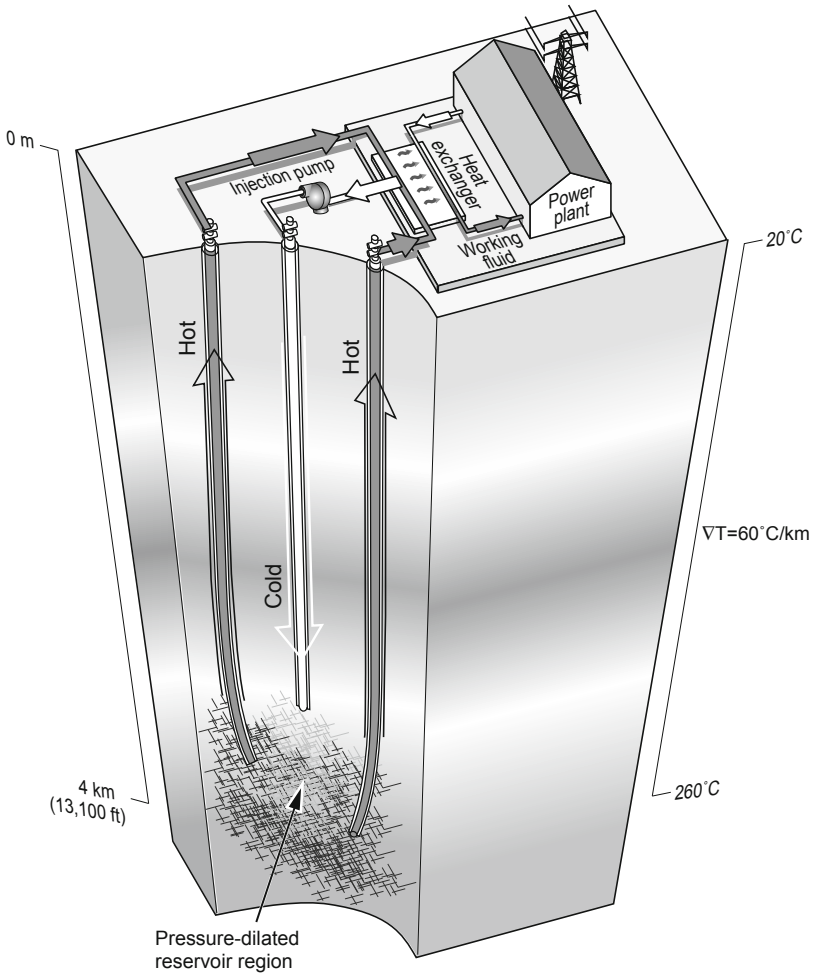

Fig. 2-1. Present-day conceptualization of a closed-loop HDR system. Source: HDR Project files

- It is the network of pre-existing joints in the crystalline basement that ultimately controls the deformation of the rock mass during hydraulic stimulation. These joints, resealed by mineral deposits, are still more permeable than the adjacent rock and open at much lower stimulation pressures than those required to fracture the adjacent rock. As the network of pressure-dilated joints is extended and these joints intersect other joints, they appear to be terminated (truncated) by the intersected joints rather than to cross them. At the intersections, the high-pressure fluid in the extending joints will be diverted into the truncating joints, forming a dendritic pattern of interconnected joints.

Because the greatest portion by far of the earth's deep, hot crust is essentially sealed, it is available *only* for HDR development. Invariably, therefore, an HDR reservoir would be developed within a previously sealed rock mass and would remain totally surrounded by sealed rock.

Between 1974 and 1995, two separate HDR reservoirs were created in deep, hot crystalline rock, extensively studied, and then flow-tested for almost a year each. These experiments took place at the Fenton Hill HDR Test Site in the Jemez Mountains of north-central New Mexico, about 20 miles west of Los Alamos. The "Phase I" and "Phase II" reservoirs were created at depths of 2700 m and 3600 m, and temperatures of 180°C and 240°C, respectively. During the flow testing, thermal power production ranged from 4 MW for extended routine production intervals to as high as 10 MW for one 15-day period—proving beyond a doubt that it is technically feasible to recover useful amounts of thermal energy from HDR. To the authors' knowledge, these are still the only true HDR reservoirs created anywhere in the world. (As discussed below, the open reservoirs created in Japan, England, Europe, and Australia do not meet the criteria for HDR.)

Of the many insights gained during the creation and flow testing of the two HDR reservoirs at Fenton Hill, the most profound are these two:

1. **An HDR reservoir is confined**. This means that except for a small—and slowly decreasing—pressure-dependent diffusion of fluid from its boundaries, the reservoir of pressurized fluid is totally contained.
2. **An HDR geothermal system is fully engineered.** By "fully engineered," we mean that every aspect of the system—including the injection and production wells, the HDR reservoir, and the pressurized flow system—is engineered (as opposed to those partially engineered systems that are based on the pressure-stimulation of an existing, but unproductive or only marginally productive hydrothermal region). The central component of the HDR system is the man-made reservoir, which is created in an essentially impermeable region of hot crystalline rock through the use of hydraulic stimulation methods to open, pressure-dilate, and extend a network of pre-existing sealed joints.

These two key insights are discussed in more detail below.

The Magnitude of the HDR Resource

It has been pointed out in several recent publications (e.g., Tester et al., 1989a; MIT, 2006) that the HDR geothermal resource represented by the vast regions of hot rock at accessible depths in the earth's crust far exceeds that of the combined total of the world's fossil energy resources. Figure 2-2, in which various major energy resources are plotted on a logarithmic scale, shows that the potential energy supply from HDR is exceeded only by that from fusion energy (and it is still not known whether the latter will

ever be developed for commercial power generation). In the case of HDR geothermal energy, the technology has already been proved via the two successful field demonstrations at Fenton Hill.

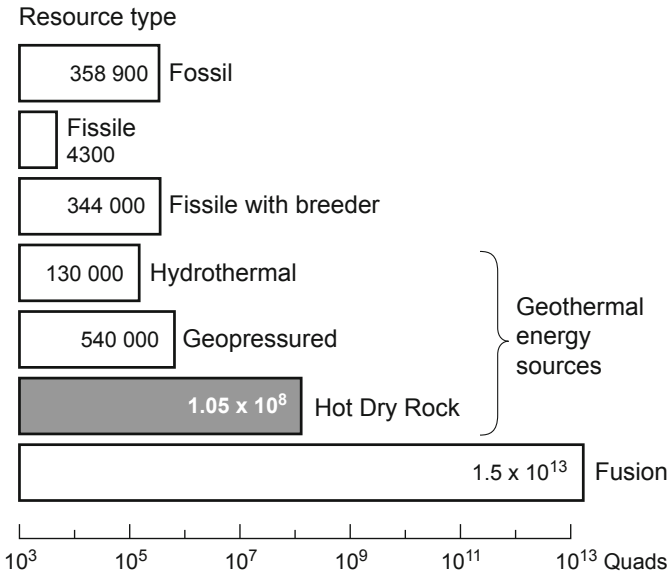

Fig. 2-2. Estimates of the worldwide resource base for geothermal and other energy sources.
Adapted from Armstead and Tester, 1987

Figure 2-3 presents a simplified geothermal gradient map for the U. S. Obviously, rock at temperatures suitable for a commercial-scale HDR power plant (generally recognized as above 150°C) is typically found at shallower depths in the western part of the country; but with the maturing of the HDR industry, most parts of the U. S. will become available for HDR development. In contrast to the very limited hydrothermal resource, therefore, the HDR resource can be considered essentially *ubiquitous*.

The size and distribution of the U. S. HDR resource are adequately discussed in two recent publications: *Assessment of Moderate- and High-Temperature Geothermal Resources of the United States* (USGS, 2008) and *The Future of Geothermal Energy* (MIT, 2006). Suffice it to say that the HDR resource is so large as to almost trivialize a discussion of its quantitative size. HDR researchers over the next 20 years will look back at the pioneering work done at Los Alamos National Laboratory and ask only why it took so long for the country to finally discover HDR.

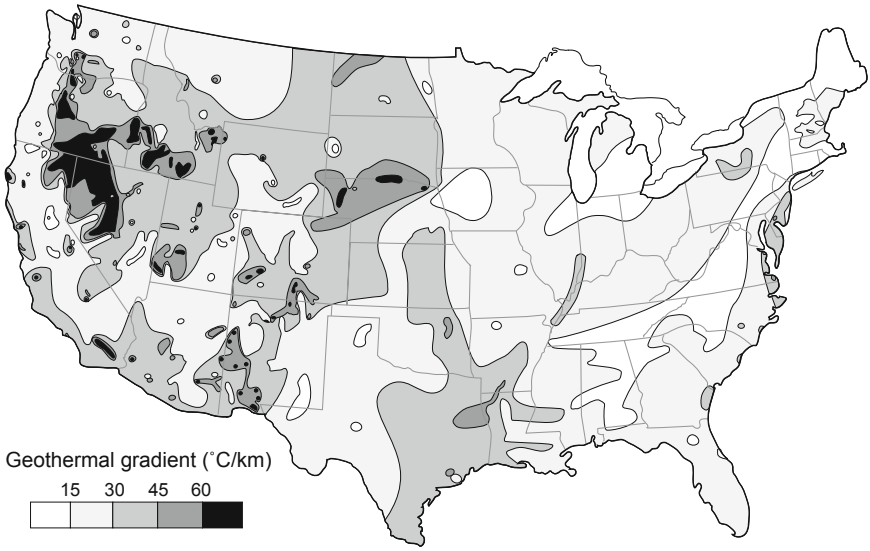

Fig. 2-3. Geothermal gradient map of the U. S.
Source: Kron et al., 1991

Properties of the Deep Crystalline Basement as They Relate to HDR Reservoirs

The Permeability of the Rock Mass

The essential feature of an HDR reservoir is that its permeability is man-made. How the reservoir will perform is only marginally related to the original permeability of the rock mass, and then only through the diffusion of pressurized fluid from the boundaries of the pressure-stimulated reservoir region (the so-called "water loss" from the reservoir). The deep, crystalline rock mass that forms the "basement" in almost all tectonically quiescent regions of the earth's crust will have a very low permeability, because the number of open faults and joints decreases rapidly with depth; it is thought that open joints, in particular, are virtually nonexistent at crustal depths below about 2 km. (Obviously, in developing an HDR reservoir, one would avoid regions of recent tectonism containing open faults or joint systems.)

Suitable crystalline rock masses would typically have permeabilities in the nanodarcy range at depths of 3–4 km (Brown and Fehler, 1989; SKB, 1989). On the basis of core studies, this very small, but finite, permeability is attributed to a sparse but interconnected network of microcracks within the matrix rock. (The resealed joints themselves probably have permeabilities one to two orders of magnitude greater than that of the matrix rock, but still very low.)

Most crystalline rocks in the depth range of 1–10 km have undergone natural modification, through two competing processes: (1) fracturing (due to deformation), which tends to open fluid conduits such as joints, faults, and breccia zones; and (2) sealing/healing of such permeable features. As hot fluids move through joints or faults in deep crystalline rocks, changes in the chemistry and temperature of the fluid can cause minerals to be precipitated. The accumulation of these minerals over time in joints or faults can reduce, and finally essentially stop, fluid flow. These sealing processes vary with depth (and therefore temperature and stress conditions), mineralogy, and fluid composition (Khilar and Folger, 1984; Carter, 1990). Heat-induced stresses can have similar effects, causing joints to close and thereby impede fluid flow. Other causes of reduced joint permeability include the formation of gouge material during shear displacement (Olsson, 1992) and lithostatic stresses—which, at elevated temperatures, cause dissolution at points of higher stress and re-precipitation at points of lower stress (Lehner and Bataille, 1984). Both the rate and degree of sealing appear to increase with depth and temperature. The very few areas of high permeability in the earth's crust, then, will be those rare hydrothermal regions in which jointing or faulting processes are currently active (for example, along portions of recently active faults within the Basin and Range Province of the western U. S.).

Sealed Joints in the Deep Basement: Potential HDR Reservoir Flow Paths

The principal geologic mechanisms that contribute to the jointing of crystalline rocks are tectonic activity (faulting, folding, and regional uplift) and lowering of the lithostatic stress by erosion. Folding is seen mainly in older rocks that were involved in ancient and deep-seated episodes of metamorphism, thrusting, or mountain-building. Regional uplift is always followed by erosion of the overburden, which gradually decreases the lithostatic stress on the underlying rocks, again resulting in jointing.

When a region of deep, hot basement rock is targeted for the development of an HDR reservoir, it is the network of interconnected joints in the rock mass—however formed and then resealed in the past—that controls how the reservoir develops. Knowledge of the orientations of the one or more joint sets in the rock mass would be desirable, but the nature of this network is not something that can be ascertained from the surface, or even by observation via a nearby drilled hole or an adjacent HDR reservoir. The orientations of the fluid-conductive joints within the HDR reservoir region will be determined after the reservoir is created, through analysis of microseismic data in concert with flow-testing results and post-stimulation borehole surveys.

The orientations of the several sealed joint sets relative to the contemporary stress field will determine which joints open first and at what pressures, how the pressure-dilating region will develop, and what the ultimate geometry of the HDR reservoir will be. The confined (pressure-tight) nature of a true HDR reservoir means that it can be operated, or circulated, at an elevated pressure relative to the least principal earth stress at the depth of the reservoir. Most important, the pressure of the circulating fluid would hold open—*against the joint-closure stresses*—one or more of the interconnected sets of the previously pressure-stimulated joints, thus giving rise to the man-made reservoir's porosity and permeability.

The Geological and Hydrological Setting of Fenton Hill: Influence of the Valles Caldera

As shown in Fig. 2-4, the Fenton Hill HDR Test Site is located 1.9 miles west of the 1.26-million-year-old, main ring-fracture of the Valles Caldera, and 4.3 miles southwest of San Antonio Mountain, a post-caldera rhyolitic dome that erupted along the ring-fracture as recently as 560 000 years ago. Although clearly outside the caldera, the test site is located on the ash-fall-tuff apron that extends several miles to the west of the caldera proper. Because of this proximity to recent volcanic activity, the deep basement rock at Fenton Hill has been affected by heat and pore fluid diffusing radially outward from the caldera over the last million years or more.

A major reason for the selection of this site was the expectation that proximity to the caldera would gain an additional increment over the regional heat flow. (In other respects, Fenton Hill is not very different from many other potential HDR sites in the western U. S.) However, the measured geothermal gradient (over 100°C/km) in the Paleozoic sedimentary rocks was misleading, being augmented by heat from the 100°C groundwater flowing west from the caldera on top of the Precambrian surface.

In addition, this site was centrally located within a large fault block whose principal faults—one mapped to the east, and one inferred (from hydrothermal activity) to the west—are roughly parallel. These two north-trending faults have essentially the same orientation as the deeper HDR reservoir later developed, which exhibited little tendency to grow in the direction of either of these deep faults. The basement rock is at a depth of about 2400 ft (730 m), and is a melange of Precambrian igneous and metamorphic rocks. Of more importance for HDR development, the rock mass is criss-crossed with an array of joints that, below a depth of about 3000 ft, have been resealed with secondary minerals. Except for the slightly permeable joints, the rock mass is extremely tight—in the range of nanodarcies. Because the joints are somewhat more permeable than the matrix rock, pressurized fluid can slowly diffuse into and then open them against the joint-closure stress.

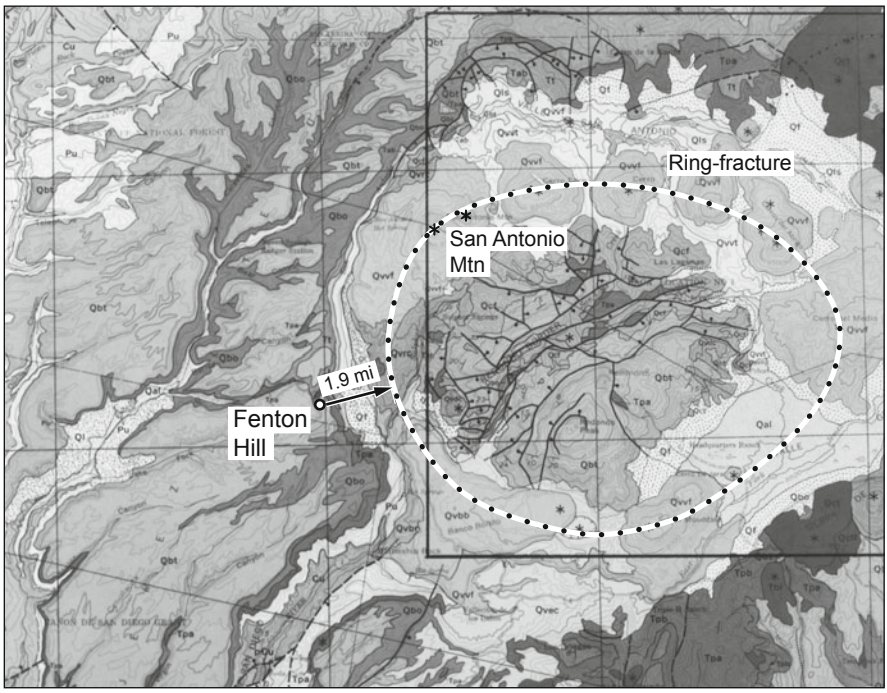

Fig. 2-4. The geological and structural setting of the Fenton Hill HDR Test Site, located to the west of the Valles Caldera in the Jemez Mountains of north-central New Mexico. (The large dots show the inferred position of the main ring-fracture of the Valles Caldera; the rectangular outline on the right delineates the Baca Location No. 1.)
Adapted from Smith et al., 1970

The Paleozoic sediments on top of the Precambrian surface were significantly altered by the hydrothermal outflow coursing westward from the caldera. Over time, this underground "river," at a temperature of just above 100°C, dissolved areas of the deepest limestone, producing an interconnected network of very large solution cavities. This cavernous zone was responsible for repeated losses of circulation, which severely hindered efforts to drill through the limestones and into the granitic rocks below. (Aggravating this situation was the fact that in this mountainous terrain, the water table was almost 1800 ft subhydrostatic!)

As it turned out, the enhanced temperature gradient (which enabled the desired reservoir temperature of about 200°C to be reached at shallower depths, reducing drilling costs) was offset by the damage caused by the high concentration of dissolved hydrogen sulfide (H_2S) in the pore fluid. Diffusing outward through the joint-filling materials, the H_2S caused

hydrogen embrittlement of the high-strength steels used in the hydraulic fracturing and pressure-stimulation work. Pipe failures occurred repeatedly, most at pressures less than half those for which the steel was rated.

If we were to select an HDR site in the area today, on the basis of our current knowledge, it would be at least twice as far west of the ring-fracture as the existing site. The much lower amounts of CO_2 and H_2S in the pore fluid would more than compensate for the need to drill to greater depths to reach rock of temperatures equivalent to those at Fenton Hill.

A True Hot Dry Rock Reservoir is *Confined*

That a true HDR reservoir is confined is probably the most profound insight garnered from the 21 years of HDR research at Fenton Hill (Brown, 1999; Brown, 2009). What confines a true HDR reservoir region is the inherent tightness of the surrounding sealed rock mass, combined with the "stress cage" formed at its periphery by the earth's elastic response to the pressure-dilation of the reservoir (see Chapter 6 for a discussion of the "stress cage" concept). A confined HDR reservoir exhibits two characteristics not found in open, hydrothermal systems:

1. Water loss is extremely low, as has been verified experimentally. For example, Fig. 2-5 shows the water-loss profile from Expt. 2077, conducted in 1992 (see Chapter 7). For this experiment, the Phase II reservoir was maintained at a pressure level of 15 MPa (2200 psi) for a period of 17 months, by intermittent pressurization with a small, positive-displacement pump. As shown in the figure, the rate of water loss from this reservoir (a seismically determined volume of 0.13 km^3) decreased continuously over this time, to a final rate of about 2 gpm—less than the flow from a garden hose. If the Phase II reservoir had been *open*, the water loss, instead of decreasing, would have stayed relatively constant. (Note that the method of reporting HDR water loss as a percentage of production flow is nonsensical. Water loss is a function of the pressure at the periphery of the reservoir, which is not particularly related to the flow rate.)
2. At a constant injection rate and pressure (higher than the joint-opening pressure), the growth of the reservoir region is linear with time. This relationship is illustrated in Fig. 2-6: the growth in volume of the Phase II stimulated region corresponds linearly to the increase in the volume of injected water. If the stimulated region had been open instead of confined, the increase in seismic volume would have flattened out with increasing injection volumes (as often occurs with hydro-frac operations in the oil industry).

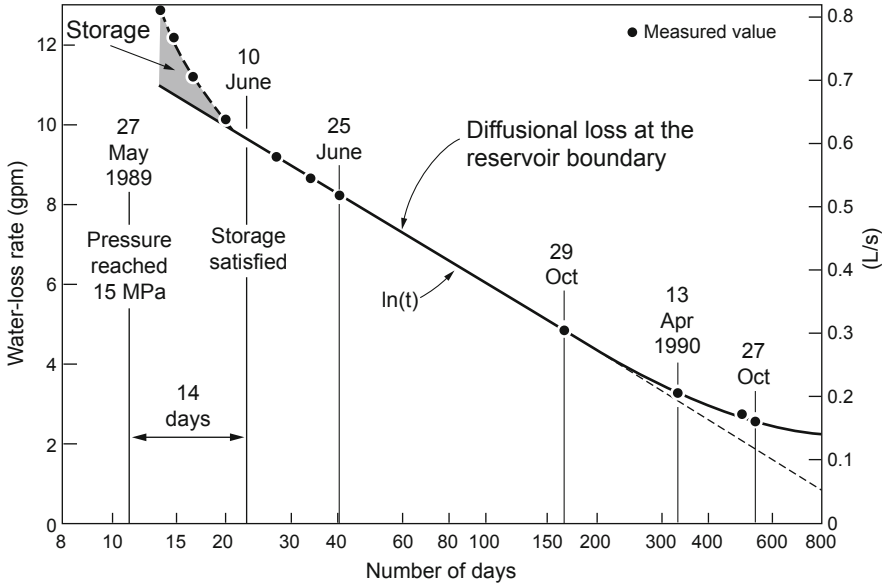

Fig. 2-5. Water-loss rate vs log (time) during the 15-MPa pressure plateaus of Expt. 2077 (diffusion of pressurized water to the far field).
Source: Brown, 1995b

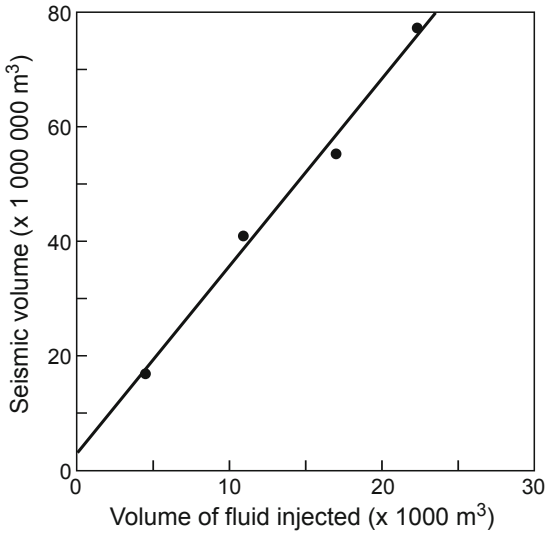

Fig. 2-6. Linear relationship between seismic volume and volume of injected fluid.
Source: Brown, 1995b

A True Hot Dry Rock Geothermal System is *Fully Engineered*

The creation of an HDR reservoir in a region of previously tight basement rock enables the system to be engineered in all its aspects. Those geothermal projects elsewhere in the world claiming to be HDR and/or "engineered" are only partially so. The reservoirs at Hijiori and Ogachi in Japan are both within volcanic calderas and associated with open, fluid-conductive fault and/or joint systems, making them *hot wet rock*, or HWR, geothermal systems.[3] In the late 1980s, hydraulic stimulation was successfully carried out at both these sites. But a few years later, recognizing the undeniably open (hydrothermal) nature of these regions, the Japanese researchers created a new project for HWR geothermal reservoir design (described in Takahashi and Hashida, 1993). Figure 2-7, taken from that publication, illustrates their view of the HWR concept vs that of HDR.

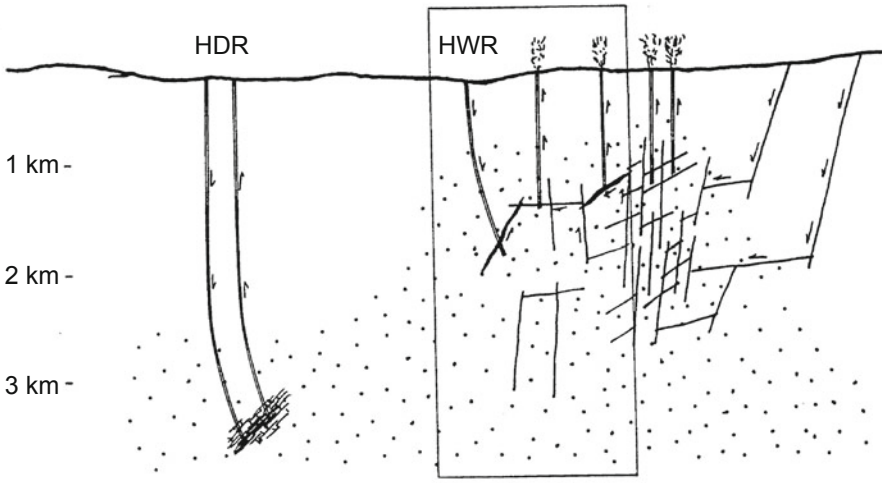

Fig. 2-7. The concept of a hot wet rock (HWR) geothermal reservoir. Source: Takahashi and Hashida, 1993

[3]so named by the Japanese in the early 1990s.

It appears that the "HDR" projects in the Cooper Basin of Australia are also open and unconfined. And the European "HDR" project at Soultz-sous-Forêts (Alsace) was renamed an enhanced geothermal system (EGS) project in 2001. In two extended flow tests, this system achieved only about a 30% recovery of injected fluid—highlighting the very open nature of the reservoir (Gérard et al., 2006).

All of these HWR systems are partially "engineered" (e.g., the natural joint/fault permeability has been enhanced by pressure stimulation, and in some cases also through zone isolation using casing strategies and/or downhole pumping of the production well or wells); but because the reservoirs in question are not confined, none of these systems is *fully* engineered.

Only an HDR system with a reservoir enclosed and sealed at its boundaries can be fully engineered—that is, all key parameters can be controlled:

- Production temperature, by selecting the drilling depth
- Size of the HDR reservoir, by specifying the amount of fluid injected
- Reservoir injection pressure and flow rate
- Production well backpressure
- Placement of production wells for optimum productivity

Development of an HDR System

The system is developed through a series of distinct operations, as described in the following subsections.

Selection of a Site

Don Brown's direct involvement with the process of selecting Fenton Hill as the site of the world's only true HDR reservoirs affords him a unique understanding of the criteria to be used in choosing a site for the *next* HDR development—an electric power generating system. Such a site would be selected primarily to satisfy the requirements of the community it would serve, and only secondarily for the geological conditions (of which the most important is the absence of active faults at the proposed reservoir depth). The major criteria would be as follows:

- Proximity to a municipal load center, offering water and power availability as well as road access
- Tectonic quiescence of the targeted reservoir region
- An appropriate type of rock at the depth of the reservoir (almost any crystalline basement rock would be appropriate; it is the joint structure that primarily determines the characteristics of an HDR reservoir)
- Suitable geothermal gradient—at least 40ºC/km, as determined from an intermediate-depth exploratory borehole (drilled at least 500 ft into the basement rock to preclude any compromising of the gradient data from groundwater flows in the sediments above the basement)

Almost without exception, the terrain at depth would consist of igneous or metamorphic rock in which once-open joints have been hydrothermally resealed. The rock mass would exhibit very low initial porosity and permeability (i.e., it would be a region of hot, but essentially dry, rock). In such areas boreholes could be routinely drilled to depths of 11 000 to 16 000 ft (3400 to 4900 m). Only at such depths is it possible to (1) attain sufficiently hot temperatures for good commercial viability[4] and (2) ensure that the rock beyond the periphery of the HDR reservoir would remain tightly sealed, and therefore that the reservoir would be confined.

Drilling of an Injection Borehole

An injection borehole would be drilled to a depth at which the rock temperature is suitable for the generation of electricity. This first borehole would be drilled essentially vertical (no directional drilling would be involved because, before reservoir stimulation, very little would be known about the stimulation characteristics of the target reservoir region—e.g., the shape and orientation of the pressure-stimulated region, and the pressure required to open, and then extend, the contained array of joints). The injection borehole would be completed by cementing-in a short (about 1000-ft) scab liner 1000–2000 ft off bottom, to pressure-isolate the lower portion of the hole, and then installing a "frac string" (high-pressure pipe used in hydraulic fracturing operations) from the top of the scab liner to the surface.[5]

Initial Pressurization Testing

With the injection borehole complete, the deep rock mass is "interrogated" through pressurization. This testing gathers data essential for planning the creation of the HDR reservoir. A contract mini-frac truck (having a maximum flow rate of 5 BPM) and superlative instrumentation would be employed to determine

- the permeability of the exposed rock mass at a very low injection rate and a controlled pressure
- the initial "formation" breakdown pressure (the pressure level at which the most favorably oriented joints start accepting fluid)
- the asymptotic joint-extension pressure
- the presence of any open faults
- the orientation of the fluid-accepting joints (through pre- and post-test Schlumberger FMI logs)

---

[4]At a mean depth of 14 000 ft and with a temperature gradient of 40°C/km, the reservoir temperature would be about 180°C.

[5]High-temperature/pressure inflatable packers, used to isolate the open-hole portion of the borehole during the Phase II experiments at Fenton Hill, proved to be unreliable (see in particular Chapters 4 and 6 for detailed accounts of packer problems). Even after a long period of collaborative development and testing by the Laboratory and an industrial partner, a 50% success rate was the best obtained.

Creation of the Reservoir

An HDR reservoir is created within a previously impermeable body of hot, crystalline basement rock, by means of high-pressure, hydraulic-stimulation ("hydro-frac") techniques commonly employed in the oil and gas industry. However, when used to create an HDR reservoir, these pressure-stimulation operations are generally much larger in scale and use higher pressures. The rock surrounding an isolated, open-hole interval at the bottom of the injection borehole is pressurized, in one or several stages of hydraulic stimulation, to create a very large (~1 km^3) region of pressure-dilated rock.

Via the injection well, fluid pressure is used to open a multiply interconnected array of pre-existing but resealed joints within the rock mass, such that a series of flow paths is formed that traverse the reservoir. These flow paths will later be accessed by the production wells. The flow impedance of each of these individual paths may be relatively high, but their aggregate impedance, as they carry fluid across the HDR reservoir, will be much lower.

During the initial development and subsequent growth of the HDR reservoir region, seismic activity will be monitored. As a result of the pioneering work done at Los Alamos, analysis of pressure-induced microseismicity has become the principal tool for determining the shape and orientation of this reservoir region (the observed "cloud" of microseismic event locations delineates the boundaries of the reservoir) as well as significant features of its internal structure (Albright and Hanold, 1976; Albright and Pearson, 1982; House et al., 1985; Fehler et al., 1987; House, 1987; Fehler, 1989; Roff et al., 1996; and Phillips et al., 1997). This information will be critical for determining the optimum locations for the production wells and the drilling trajectories that will best access the reservoir.

From the knowledge gained from the development of two separate HDR reservoirs at Fenton Hill, one can surmise that the typical HDR reservoir would be ellipsoidal in shape. This is because the stress field at depth in the earth's crust is invariably anisotropic. Within the Basin and Range Province of the western U. S. (which harbors most of the highest-grade HDR resources), the maximum earth stress is typically vertical, and the least principal earth stress is horizontal. Such a stress state would result in an elongate reservoir region whose smallest dimension is horizontal and whose larger dimensions are near vertical and approximately orthogonal to the direction of the least principal earth stress. The Phase II reservoir at Fenton Hill—which has been described as a steeply inclined, elliptical-shaped "pillow" sitting on edge, with its largest dimension in a north–south direction—appears to have followed this pattern of development.

The Initial Closed-Loop Flow Test (ICFT), performed in mid 1986 (see Chapter 7), in particular revealed that under high injection pressure (4570 psi [31.5 MPa]), the growth of the reservoir was predominantly

toward the south—in the direction away from the production well (which was north of the injection well). The result was a "stagnant" high-pressure, southern reservoir region without any path to the production well. With this portion of the reservoir essentially isolated, the ICFT achieved a power production level of only 10 MW_{th}. But had a second production well been drilled into that southern portion of the reservoir, it is estimated that at least twice that—20 MW_{th}—would have been available from this HDR reservoir.

This elongated reservoir shape suggests that the best configuration for HDR reservoir production would be a centrally located injection well and *two* production wells, one near each end of the ellipsoidal reservoir region (Brown and DuTeaux, 1997). Because it is in these elongated boundary regions that the reservoir is preferentially extending during pressure stimulation, the two production wells would act as "pressure-relief valves": inhibiting reservoir growth in these critical regions and thereby enabling reservoir operation at even higher injection pressures than would be possible with a single production well.

The productivity of the reservoir is directly dependent on the flow impedance, or degree of resistance to flow through the reservoir (a concept unique to HDR geothermal energy). Flow impedance is usually expressed in units of psi/gpm or MPa per L/s. The overall flow impedance of the reservoir has three components: the *body impedance* (across the greatest extent of the dilated reservoir), the *near-wellbore outlet impedance* (near the production wellbores), and the *near-wellbore inlet impedance* (near the injection wellbore). These are discussed further in Chapter 4. With higher injection pressures, the principal flow paths across the reservoir would be further dilated, reducing the body impedance and increasing reservoir productivity.

Drilling of the Production Wells

The HDR circulation system would be completed by drilling *two* production wells to intersect the reservoir near the ends of the elongated reservoir region (the boundaries determined by seismic data).

Flow Testing

The completed HDR geothermal system would be flow-tested to determine the optimum production flow rate. Test parameters would include the available range of injection and production pressures. In the event that the cumulative flow rate from the production wells is too low, pressure/temperature cycling operations would be instituted to reduce the near-wellbore outlet impedances of these wells. In addition, laterals could be drilled from near the bottom of each production well to increase productivity.

Seismic Risks Associated with HDR Geothermal Energy

Because of the environmental consciousness of the HDR staff, seismic monitoring was a "given" for all the pressure-stimulation activities, starting with the experiments in Barley Canyon.

In the summer of 1972, Prof. Bert Slemmons, an expert on earthquakes from the University of Nevada, spent five weeks investigating the fault structure and earthquake history of the Fenton Hill area and assessing potential earthquake hazards associated with the planned hydraulic fracturing operations. (A very large body of data already existed on Fenton Hill. The Valles Caldera—one of the classic calderas in the U. S.—and its environs had been extensively studied by a number of geoscientists over the preceding years [e.g., Smith et al., 1970]).

Dr. Slemmons reported his findings in a Los Alamos National Laboratory publication (Slemmons, 1975). On the basis of low-sun-angle photography augmented by field studies, he confirmed the presence of the known faults in the area and discovered a previously unmapped minor fault in Virgin Canyon, 2.5 miles southeast of Fenton Hill. This fault had a very low average rate of movement, and trended away from Fenton Hill. There also appeared to be no earthquake hazard from other faults within a 15-mile radius of Fenton Hill. (Except for the Virgin Canyon fault, none was found that had displaced the geologically young surface volcanic rocks.)

Dr. Slemmons also collected and analyzed all available earthquake data for New Mexico. He concluded that the level of seismic activity in the region surrounding Fenton Hill was very low; that hydraulic-fracturing experiments in this area involved very little seismic risk from natural fault activity or local earthquakes; and that such experiments were not likely to activate any of the known faults in the area—including the closest and most recent one in Virgin Canyon.

During the ensuing 22 years, the magnitude of the largest induced seismic event was only about 1.0 on the Richter Scale (Leigh House, Los Alamos National Laboratory, personal communication, May 2009). It is notable that for the 844 microearthquakes reliably located during the MHF Test in 1983 (on the basis of arrival times recorded by five downhole geophone stations), the range of magnitudes was –3 to 0 (House et al., 1985). It is the confined nature of the reservoir in an HDR system that explains the greatly reduced seismic risk vis à vis "enhanced" hydrothermal reservoirs. Only *within the pressurized envelope* of the stimulated HDR region is seismic activity generated—and then typically at magnitudes below zero on the expanded Richter scale. Any nearby faults would be shielded from activation (pressure stimulation) by the pressure-sealed boundary of the HDR reservoir.

In contrast, the pressure-stimulation of regions within or adjacent to known hydrothermal systems (e.g., the HWR systems at Hijiori and Ogachi in Japan, and the "HDR" systems now being developed deep below the Cooper Basin in Australia) carries a significantly higher risk because of the *open* (unconfined) nature of these systems. As an example, such a pressure-stimulation was recently attempted at Basel, Switzerland, within the southeastern margin of the Upper Rhine Graben—an area of "elevated seismic activity."[6] To enhance hydrothermal flow in the deep granitic basement, 11 600 m^3 of water was injected over six days into a deep injection well ("Basel 1," drilled *within* the city). The bottom-hole temperature of this well, at a depth of 5000 m, was about 195°C. With injection pressures finally reaching as high as 29.6 MPa (4300 psi), on December 8, 2006, a magnitude 2.7 earthquake occurred. As pre-planned, injection was terminated. Four hours later (at a shut-in "reservoir" pressure of about 19 MPa), a magnitude 3.4 earthquake shook the city and brought the entire effort to a halt (Dyer et al., 2008). Even so, because of the large volume of water injected at high pressure into the fault system, tremors continued for a year or more. Although such a high level of induced seismicity has rarely if ever been seen in other HWR stimulations around the world, it stands as a warning of what *could* occur if an open hydrothermal system is subjected to high-pressure stimulation.

Note: The injection pressures used at Basel (29.6 MPa) were only slightly higher than those routinely used during flow testing of the Phase II reservoir at Fenton Hill, which averaged about 27.3 MPa.

The Economics of HDR Geothermal Energy

The researchers most involved with the development of HDR geothermal energy believe that the preferred route for HDR commercialization is the generation of electricity. This belief has been shared by the U. S. Department of Energy (DOE) throughout its long association with the HDR Geothermal Energy Program at Los Alamos, simply on the basis of economics. At the same time, it is possible that some concentrated, direct-heat applications (such as those described in Tester et al., 1989a) could be brought on board competitively. For instance, HDR geothermal heat could be used directly to supply feed-water heating for a co-located, fossil-fuel electric power plant; in this case—in light of the current tax credit for renewable energy and anticipated cost incentives for reductions in carbon dioxide emissions (e.g., a carbon tax)—the economics of HDR direct heat could be favorable. Although it may not be intuitively obvious, if an HDR system cannot

[6]In 1356, an earthquake with an estimated magnitude of 6.2 destroyed parts of the medieval city of Basel.

economically generate electric power under the given conditions, it probably cannot economically be used for direct heating either. With a direct heating system, the cost of transporting the pressurized hot water to its final destination would be significantly higher than for natural gas. This assertion is based on present-day natural gas prices. As a corollary assertion, HDR-derived geothermal heat of only moderate temperature is not economical compared with natural-gas heating.

At the time of this writing (spring 2012), it is difficult to accurately forecast the economics of constructing an HDR power plant, particularly when no such plant has ever been built. The primary capital costs are those of drilling the deep injection well, developing the pressure-stimulated HDR reservoir, and then drilling the two production wells. These costs are estimated to represent about two-thirds of the total capital investment for a complete HDR power generating system (depending principally on the depth of the wells).

In the summer of 2010, oil prices were considerably lower than they are at present. In past months a number of factors—not least the widespread upheavals in the Middle East—have intervened to return prices to their 2008 levels. Given the impossibility of predicting such fluctuations, an estimate provided in 2008, of about $24 million for drilling and completing three boreholes to 13 500 ft (Louis Capuano Jr., ThermaSource, Inc., personal communication, September 2008), remains the best currently available. But a further consideration is that a new drill-bit technology on the horizon (David Hall, Novatek International, Inc., personal communication, June 2011) could cut that cost in half!

In estimating the power output of an HDR plant, the principal unknown is the productivity of the reservoir. On the basis of the flow testing of the deeper (Phase II) reservoir at Fenton Hill, the output of a three-well system is projected to be at least 20 MW_{th}. Further, if an HDR plant were to be established at the decommissioned Fenton Hill site, this productivity could be increased through various strategies—the most viable being the drilling of a lateral from the bottom of each of the production wells, which could conceivably increase power output to near 40 MW_{th}. Other strategies include pressure- and/or temperature-cycling (to reduce the near-wellbore outlet impedance), both of which appear to be attractive approaches but must be verified through field demonstrations.

In reality, then, until the first true HDR power-generating system is up and running, the actual costs for such a revolutionary new power source can only be guessed at. (Note: such a system was very close to being constructed when the DOE withdrew funding in 1995—see Duchane, 1995d).

Armstead and Tester (1987), in discussing the generation of electric power from HDR geothermal resources, considered both open (flashed-steam) and closed (binary-cycle) systems. It has been the Los Alamos HDR Project's contention since the early 1980s that a closed-cycle earth loop is the preferred approach, from both environmental and water-use standpoints. With this type of system, the heat contained in the produced geofluid (the fluid being maintained at a pressure sufficient to ensure that it remains liquid) is transferred via a heat exchanger to vaporize a secondary working fluid, which is then expanded through a turbine, producing mechanical power. The secondary working fluid is next condensed in a cooling tower or an air-cooled heat exchanger, repressurized, and returned to the primary heat exchanger to be reused.

Milora and Tester (1976) considered seven possible working fluids for a binary-cycle system. The variation in thermodynamic availability of each of these as a function of temperature, over the range of probable geofluid production temperatures from 100°C to 300°C, is shown in their Figure 3-3. A commercial HDR development at typical production temperatures would be on the high side of this range; therefore, according to this analysis, ammonia appears to be the best working fluid.

The true picture of the economics of HDR power generation must await commissioning and then operation of a prototype power plant—not yet even in the planning stage. Further, the principal economic issue of reservoir productivity must await pre-operational flow testing of the reservoir, which would be carried out before a binary-cycle power plant is constructed. During this flow testing, several proposed methods of production enhancement would be evaluated.

Using an HDR Reservoir for Load-Following

A very significant experiment was conducted in July of 1995, near the end of the long-term flow testing of the Phase II reservoir (see Chapter 9). This experiment demonstrated a concept referred to as "load-following," whereby an HDR reservoir can be operated for several hours each day with greatly increased thermal power production (Brown, 1996a, 1997b).[7]

For six days, while the injection pressure was held steady at 3960 psi (27.3 MPa), a 20-hour period of high-backpressure (2200 psi [15.2 MPa]) operation was alternated with a 4-hour period of greatly increased production flow (maintained through a controlled decrease in the backpressure—to a final value of 500 psi). The last two of the six 24-hour cycles are shown in Fig. 2-8.

[7]Only a few weeks after this experiment all flow testing was halted, and at the end of the fiscal year the DOE terminated the HDR Project.

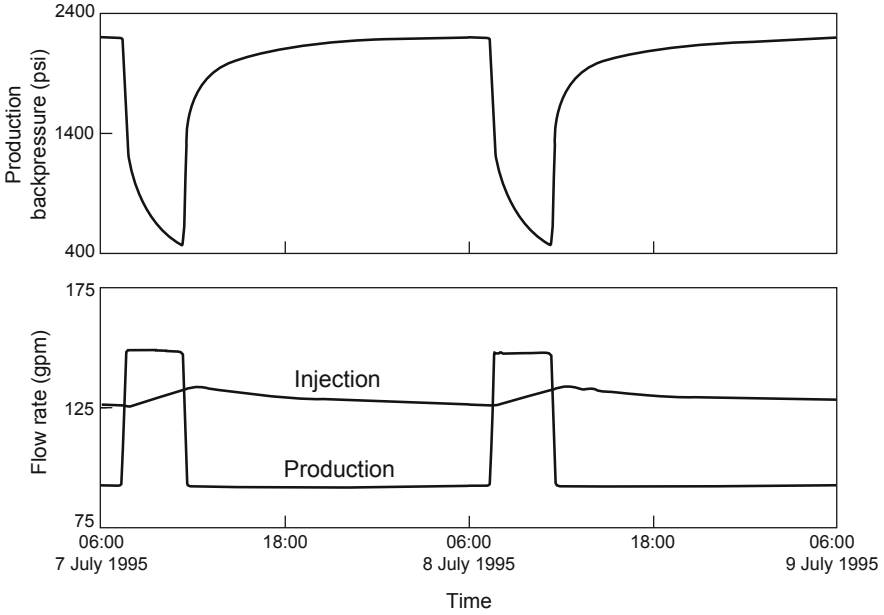

Fig. 2-8. Injection and production flow profiles vs the controlled variation in the production well backpressure during the last two daily cycles of the Load-Following Experiment (1995).
Source: Brown, 1996a

During the 4-hour portion of the daily cycle, the production flow rate was increased by a constant 60%. With the associated 10°C increase in the production fluid temperature, the overall power level achieved was 65% higher than that of the preceding 20-hour period of steady-state operation.

As shown in the figure, for each cycle the production well backpressure began at 2200 psi and ended at 500 psi. However, to maximize reservoir power production during the 4-hour portion of the cycle, the backpressure for the 20-hour portion could have been increased somewhat (e.g., to 2400 psi) and the final pressure could have been dropped to near 182 psi (the saturation pressure for water at 190°C). These operational changes would have increased the power multiplier for the 4-hour period of enhanced production from 1.65 to closer to 2.0—a considerable improvement.

When an HDR reservoir is used in this advanced operational mode, one can also take advantage of the principle of "pumped storage"—the storage of additional pressurized fluid within the reservoir. In essence, during the Load-Following Experiment at Fenton Hill, a portion of the high-pressure reservoir fluid stored near the production well was being vented down

(temporarily produced) during the 4 hours; then, during the next 20-hour period of steady-state operation at a backpressure of 2200 psi, the reservoir was reinflated by injection at a somewhat higher rate (the rate gradually returning to its previous steady-state level during the subsequent 20-hour period).

Note: During flow testing of the Phase II reservoir, it took only about two minutes to nearly double the reservoir's power production, by simply opening the motor-driven throttling valve on the production well. Making use of this HDR load-following capability would reduce the local electric utility's need to draw on its natural-gas-fired "spinning reserve" during times of peak demand (a very costly—but also very common—method of load-following, particularly during the summer air-conditioning season).

The demonstrated ability of HDR geothermal systems, operating in a base-load mode, to provide peaking power upon demand confers on HDR power plants an additional cost advantage that has not been considered in *any* of the HDR economic studies done so far. The premium for peaking power is typically more than twice the base-load price. For example, for a base-load busbar price of 9 cents/kWh and a peaking price of 21 cents/kWh for 4 hours, the overall effective price would be 11 cents/kWh—a premium of 2 cents/kWh, which could markedly change the profitability of an HDR power plant.

The pumped storage aspect of this experiment was not particularly emphasized at the time. The experiments at Fenton Hill suggest that upon reinflation, the region surrounding the production well behaves like an elastic spring, storing pressurized fluid for delivery the following day. The recent growth of wind power (often generated at night) presents an appealing opportunity for exploiting this aspect: excess wind power could be used to power an additional injection pump during all or a portion of the 20-hour reinflation phase—the supplemental store of pressurized fluid thus created turning the HDR reservoir into a kind of "earth battery." Most of this excess pressurized fluid could be recovered the next day in the form of increased power generation for peak demand periods. In other words, the reservoir could be hyper-inflated to a mean pressure level *above* that used for steady-state operation, enabling a greater quantity of pressurized fluid to be stored during the off-peak hours. The quantity would be limited only by the requirement to keep the pressure below a level that would cause renewed—or excessive—reservoir growth.

The Challenges of HDR Technology

In the early days of the HDR Project, a number of concerns—or challenges to implementation of the technology—were expressed by the earth sciences community. Ongoing research of the HDR geothermal energy concept at Los Alamos National Laboratory and the field experiments at Fenton Hill led to successful resolution of most of these. In addition to the two most important ones (water loss and induced seismicity, discussed above), these challenges included the following:

- *Controlling growth of the reservoir region.* During Phase II, when the reservoir was tested for over two years at a very high pressure (3960 psi), there were no indications of reservoir growth.
- *Preventing chemical scaling*. After years of flow with hot, mineral-laden water through the mild-steel, air-cooled heat exchanger, only a very thin—and actually protective—coating of iron carbonate was found (possibly owing to the injection of fine-grained calcium carbonate during the Massive Hydraulic Fracturing [MHF] Test in December of 1983—see Chapter 6). Further, no detrimental build-up of mineral deposits was found in any of the surface plumbing or downhole piping. Therefore, chemical scaling proved to be a non-issue.
- *Creating sufficient reservoir volume for a commercial-scale operation*. The Phase II reservoir at Fenton Hill had a circulation-accessible volume of at least 20 million m^3—sufficient for the continuous production of at least 20 MW of thermal energy for at least 10 years with very little thermal drawdown. In addition, if sufficient heat-transfer volume is a concern, before power production begins the circulation-accessible reservoir volume can easily be increased through additional pressure stimulation, at a very modest cost.
- *Achieving higher productivity.* Increasing the rate at which energy can be extracted from the man-made reservoir is the primary remaining challenge to the commercialization of HDR geothermal energy. This rate is dependent on the flow impedance ("I" in the following equation), which determines the amount of water that can be circulated through the pressure-dilated reservoir region for a given set of reservoir inlet and outlet pressures (as measured at the surface):

$$I = \frac{\text{(injection pressure – production pressure)}}{\text{production flow rate}}$$

Reservoir productivity is particularly closely linked to the near-wellbore outlet impedance (see also the discussion of flow impedance in Chapter 4). This impedance can be significantly reduced by operating the production wells at an elevated backpressure, which keeps the reservoir flow outlets partially dilated. These outlets would otherwise be held almost closed by the combination of the wellbore stress concentration and the decreasing differential pressure[8] as the flow converges to the production wellbores.

- *"Short-circuiting" of flow within the reservoir.* This concern was allayed by very favorable data from the Long-Term Flow Test of the deeper reservoir (1992–1995). Tracer testing showed that the flow patterns became *more* diffuse with time, suggesting that more of the reservoir was being accessed as flow continued—with no tendency toward short-circuiting.

A Major Observation and a Practical Lesson

A major observation from our Fenton Hill HDR reservoir testing and development is that the characteristics of the jointed rock mass are variable, and unpredictable. For example, the joint-extension pressure in the Phase I reservoir was only about 2000 psi, whereas the corresponding joint-extension pressure for the Phase II reservoir—only 2300 ft (700 m) deeper—was 5500 psi, a remarkable difference. This pressure is controlled not by the earth stresses per se, but by the orientations of the principal flowing joints relative to the earth stresses—something that cannot (as yet) be discerned from borehole observations nor, assuredly, from the surface! Although microseismic observations are essential to understanding HDR reservoir development, there is much more to do in this field—particularly in understanding/discerning that portion of the induced seismicity that is specifically related to the opening of the joints that constitute the principal flow paths.

[8]This *differential pressure*—the difference between the pressure of the circulating fluid acting to open the joints and the normal stress acting to close them—rapidly declines from its positive value in the body of the reservoir to a neutral and finally a negative value as the flow converges to the reservoir's outlets into the production boreholes. This phenomenon, unique to HDR reservoirs, explains why an increase in the production-well backpressure decreases the near-wellbore outlet impedance. It follows that the larger (i.e., the more negative) this differential pressure, the more tightly closed are the joints in the vicinity of the production well.

The most practical lesson from the Laboratory's HDR work is that the engineering of an HDR geothermal system begins with the creation of the reservoir from the initial borehole. The reservoir is then accessed by two production wellbores drilled to near the boundaries of its (seismically determined) ellipsoidal volume. To first drill two boreholes, and then try to connect them by hydraulic pressurization, is almost impossible. (The reason for drilling *two* production wellbores is twofold: First, to markedly increase productivity by much more fully accessing the reservoir; and second, to permit even higher reservoir operating pressures to further dilate the flowing joints and further reduce the body impedance, while constraining additional reservoir growth.)

PART II

First Demonstration of the Hot Dry Rock Geothermal Energy Concept: Development of the Phase I Reservoir at Fenton Hill

Chapter 3

Phase I Drilling and Initial Attempts to Establish Hydraulic Communication

The world's first demonstration of the hot dry rock (HDR) geothermal energy concept took place at Fenton Hill, New Mexico, in the mid to late 1970s. The objective was to create a large, man-made HDR reservoir in rock at an appropriate temperature (~200°C) and accessed by two deep boreholes, completing the pressurized earth circulation loop.

As described in Chapter 1, the original concept of an HDR geothermal energy system was developed in 1970 by Bob Potter (Robinson et al., 1971). Figure 3-1 illustrates the concept as it was published two years later (Brown et al., 1972). The then-anticipated location for such a system was somewhere in the Basin and Range Province of the western U. S.—hence the 8000 ft of sedimentary and volcanic rocks estimated to overlie the basement rock and the assumed temperature of 300°C at 15 000 ft (technical specifications, such as hole diameters and pipe sizes, were included to enable thermal power production to be calculated).

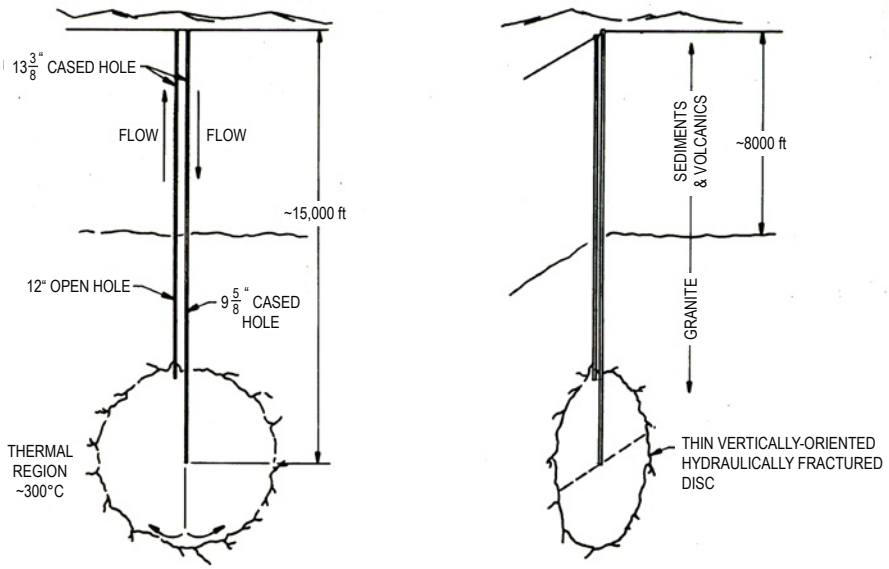

Fig. 3-1. The originally proposed system for developing a dry geothermal reservoir in the western United States as a commercial energy source (1972).
Source: Brown et al., 1972

D.W. Brown et al., *Mining the Earth's Heat: Hot Dry Rock Geothermal Energy*,
DOI 10.1007/978-3-540-68910-2_3, © Springer-Verlag Berlin Heidelberg 2012

In those early days, Don Brown briefed Atomic Energy Commission (AEC) Headquarters staff and other interested parties on the simplicity of creating an HDR reservoir in hot crystalline rock—generally outlined as

- drilling a vertical borehole to a depth at which the rock temperature is suitable for power generation;
- using proven oilfield techniques of hydraulic fracturing to create a large vertical fracture from the bottom of this hole; and
- using conventional directional drilling techniques to drill a second borehole to intersect the vertical fracture.

(Note: at the time, the directional drilling component was considered no more difficult than "hitting the broad side of a barn." Little did we know!)

The HDR concept published in 1972 was kept general for a very specific reason: The potential for HDR geothermal energy in the Basin and Range Province is huge, and not nearly enough was yet known for a particular site to be specified. As described in Chapter 1, that same year the nascent HDR group at the Laboratory undertook some initial studies in the Fenton Hill region of the Jemez Mountains, just west of the Valles Caldera. On the basis of regional geology and heat flow measurements in this region, they drilled the first exploratory borehole (GT-1), in Barley Canyon, to a depth of 2575 ft. The encouraging results obtained from GT-1 then led to selection of a nearby site for long-term HDR experiments.[1]

The principal objective of the Phase I operations at the new Fenton Hill site was to assess the suitability of the deep Precambrian basement in this area for containing a pressurized HDR circulating system. Here, pressurized-fluid injection testing would be done in a second borehole (Granite Test Hole 2, or GT-2), at several depths. From the beginning, GT-2 was envisioned as an exploratory borehole—like GT-1, but considerably deeper (4500 to 6000 ft). It would be used, first, to confirm the suitability of Fenton Hill as the location for the world's first man-made heat-mining system; and second, as a deep seismic observation station during the hydraulic fracturing operations and experiments involved in reservoir development (and, later on, as a reservoir-interrogation and diagnostic borehole, separate from loop operations).

[1]This site soon came to be known as the Fenton Hill HDR Test Site, referred to by the Laboratory as Technical Area 57 (TA-57), or simply as "Fenton Hill."

Summary of Phase I Drilling and Attempts to Create a Reservoir

The GT-2 borehole was the first to penetrate deep into the hot Precambrian basement rock at the Fenton Hill HDR test site. But as HDR Project priorities shifted, there were some significant departures from the original plan. One was that during the later stages of drilling, the role of GT-2 as an exploratory and then reservoir-interrogation borehole, separate from the reservoir-creation and production boreholes, was changed. After the establishment of the Energy Research and Development Administration (ERDA) out of the former AEC in January 1975, and the ensuing increase in micro-management by the ERDA Division of Geothermal Energy (DGE), the decision was made that GT-2 would become the injection well for the first-ever HDR reservoir test. The Laboratory acquiesced to the change, which meant that only one of the planned two additional boreholes (referred to as EE-1 and EE-2, for "Energy Extraction") was drilled for Phase I experiments; and that GT-2 was twice deepened beyond its planned depth, for a total of three stages of drilling.

When GT-2 was completed on December 9, 1974, its final depth was 9619 ft (2932 m) and its bottom-hole temperature was 197°C. Soon thereafter, a favorably oriented joint was opened by hydraulic pressurization near the bottom of GT-2, to form the initial reservoir heat-exchange system (per the then-prevalent hydraulic fracturing theory of a penny-shaped, vertical fracture created in homogeneous, isotropic crystalline rock—see Fig. 3-1). The second well, EE-1, was drilled next; but after much heated discussion and analysis, the plan for the directional drilling of this well was changed from that shown in Fig. 3-1. Rather than being aimed at the upper portion of the GT-2 joint, EE-1 was drilled directly under the bottom of GT-2, to intersect the lower portion of the joint (which, according to the theory, would grow symmetrically and near vertically, upward and downward, from the injection point). The original roles of the two wells were thus reversed: EE-1 became the injection well and GT-2 the production well.

There were two primary reasons for this change in strategy: first, the concern that if EE-1 was drilled across the plane of the created fracture above the bottom of GT-2, it might intersect that borehole; and second, since it was presumed that the fracture was near-vertical, if EE-1 was drilled directly under the bottom of GT-2, it could not help but intersect the lower extension of the fracture (almost regardless of the fracture's orientation in plan view). Another consideration was that the creation of a deeper inlet for circulating fluid appeared to offer a better flow/heat-transfer situation. According to the concept of

Fig. 3-1, the inlet fluid, being cold, should "fall" by gravity to the bottom of the large, pressurized, penny-shaped fracture, then be heated as it rose buoyantly to the production well.

However, instead of hitting "the broad side of the barn"—the large target thought to be presented by the joint at the bottom of GT-2—the trajectory of EE-1 was inadvertently turned *away* from GT-2 less than 30 ft short of the target! Owing to a 180° error in the seismic analysis of the acoustic ranging data, the HDR Project geophysicists thought that at depth, EE-1 was west of GT-2 rather than still east. They convinced the Project management that EE-1 had been drilled past the bottom of GT-2 when in fact it had not. The 180° error came to light only some 18 months later—December 1976—when magnetic ranging and better-coupled acoustic ranging experiments were performed. Further confirmation came in the spring of 1977, when high-temperature gyroscopic survey tools specially developed for the Laboratory were run in GT-2.

Much of the intervening year and a half was spent attempting to create an HDR reservoir between the two boreholes. After all these efforts, the flow impedance achieved—24 psi/gpm (2.6 MPa per L/s)—was adequate, but still higher than a "desirable" level (about 10 psi/gpm, or 1 MPa per L/s). Further, the 24-psi/gpm impedance was not maintained, but subsequently increased (to 100 psi/gpm) when the multi-joint flow connection between the boreholes became plugged with detritus from the quartz-leaching experiment. Instead of attempting to reopen the plugged joints and further pressure-stimulate the connecting joints, the staff decided to redrill GT-2 to intersect the near-vertical joint that—according to seismic data—had been opened at a depth of about 9050 ft, behind the casing in EE-1.

Planning, Drilling, and Testing of the GT-2 Borehole

The Drilling Plan

The original plan for the GT-2 borehole was that it would have a final depth of between 4500 and 6000 ft (depending on available funding)—penetrating 2000+ ft into the Precambrian basement rock underlying the Jemez Plateau. A borehole of this depth would make it possible to

- obtain additional information on the geology of the deeper Precambrian basement, and
- assess the permeability of the rock mass, ideally to a depth of 6000 ft.

Personnel from the HDR Group at the Laboratory (Group Q-22) prepared a detailed drilling and casing plan for GT-2, including materials and equipment. After the plan had been reviewed by outside drilling engineers (from Fenix and Scisson, Inc.) and minor changes made, a bidding package

was completed on October 13, 1973. The Q-Division office reviewed the final plan (Fig. 3-2) and delivered it to the Laboratory Supply and Property Department on November 21. The successful bidder was Calvert Western Exploration Co. of Tulsa, Oklahoma.

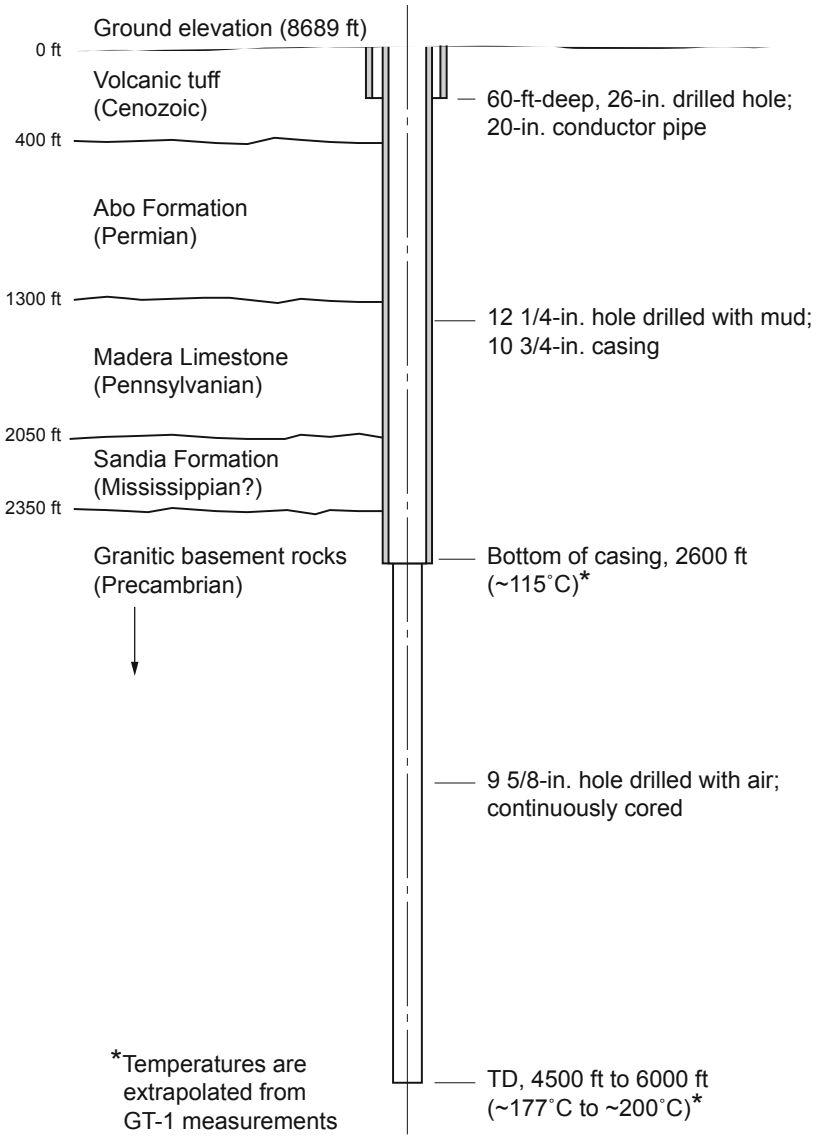

Fig. 3-2. Final plan for drilling and casing of the GT-2 borehole, showing the anticipated stratigraphic section and expected bottom-hole temperatures. Based on Pettitt, 1975a (Appendix C)

This "final" plan, however, would turn out to be only the first of three stages of development of GT-2 (Table 3-1). In the end, budget and time considerations would dictate a number of modifications.

Table 3-1. Drilling operations—GT-2 borehole

Drilling stage	Start date	Final depth
1	17 February 1974	6356 ft (1937 m)
2	30 August 1974	6702 ft (2043 m)
3	12 October 1974	9619 ft (2932 m)

In addition to the details of the drilling and casing program (see Pettitt, 1975a), the plan contained in the bidding package called for the driller to (1) continuously core from the top of the Precambrian granitic rocks to a depth of at least 4500 ft, using air as the circulating medium; and (2) as directed by the Laboratory, conduct hydraulic fracturing tests and run logs and surveys. Core analysis would allow the determination, as a function of depth, of several properties of the rock matrix:

- petrology (including age);
- mechanical and acoustic properties;
- thermal conductivity;
- the nature of the joint fill materials;
- porosity and permeability (inferred from laboratory testing that replicates the *in situ* state of stress); and
- the nature and geochemistry of potential rock–water interactions.

InfoNote

In retrospect, the priority given to coring in the drilling plan was unjustifiably high considering the cost and time involved. As would be learned in the course of reservoir testing (see Chapter 9), the matrix data yielded by core materials are not truly relevant to reservoir development and flow performance (for example, whether the rock matrix is granite, diorite, or amphibolite affects the behavior of the reservoir only minimally). The physical properties that do influence reservoir development and flow are those of the rock mass, which are controlled primarily by the nature and orientations of the principal joint sets. The most important of these properties are overall permeability and compressibility, which determine how flow through the network of joints will change with the level of pressurization. Although a few matrix properties are representative of the rock mass as well (such as thermal conductivity, because the joint porosity is so small), the majority are useful primarily for reservoir modeling.

Most of the information on the first stage of drilling and the extensive testing operations performed in GT-2 is taken from Pettitt (1975a and b) and Blair et al. (1976).

Stage 1 Drilling

Drilling in the Surface Volcanic Rocks

On February 17, 1974, the drilling of the GT-2 borehole began in the Bandelier Tuff, which is exposed at the surface at Fenton Hill. At a depth of 77 ft (24 m),[2] a 65-ft (20-m) string of conductor casing having an outer diameter of 20 in. (510 mm) was set and cemented to the surface just above ground level. Drilling then continued, with a 12 1/4-in. (311-mm) Smith Tool Company (STC) steel-tooth, tricone rock bit, through the 450 ft (137 m) of surface volcanic rocks and into the underlying Permian sedimentary formation.

Drilling Through the Paleozoic Sedimentary Formations and into the Granitic Rocks

After some 780 ft (240 m) of red clays, siltstones, and sandstones of the Permian Abo Formation had been penetrated, drilling proceeded below 1230 ft (375 m) in Pennsylvanian rocks of the Madera and Sandia formations. (The transition between Permian and Pennsylvanian rocks in this region of northern New Mexico is typically determined by the increasing amounts of limestone in the red beds; when limestone is more abundant than red sediments, the rocks are no longer considered of Permian age.) In addition to STC bits, Security and Hughes Tool Company bits were used in the sedimentary formations, but the two STC bits drilled over twice the distance—nearly 600 ft each.

Drilling in the Madera limestone was proceeding at rates averaging 6–8 ft/h when a massive loss of circulation occurred on February 28, at a depth of 1916 ft (584 m)—an occurrence that was to be repeated during the drilling of all subsequent boreholes at Fenton Hill (it had already been experienced during the drilling of GT-1 in Barley Canyon, but in that first exploratory hole the situation was somewhat easier to manage because of the much smaller—6 3/4-in.—diameter of the upper portion of the borehole). At the GT-2 site at this depth, the borehole was apparently passing through a "vuggy" limestone interval, in which solution cavities had been created by hot water (~100°C) flowing westward above the Precambrian granitic rocks. The source of this hot fluid was probably the ring-fracture bounding the Valles Caldera immediately to the east of Fenton Hill.

---

[2]Unless otherwise specified, all depths given for Fenton Hill drilling operations were measured from the top of the Kelly bushing and along the incline of the borehole (the so-called "slant depth"—typically obtained from incremental drill pipe measurements). In the case of GT-2, the Kelly bushing was 13 ft above ground level (equal to an elevation of 8701.5 ft above mean sea level at Fenton Hill). Because GT-2 was drilled essentially vertical, the "true vertical depth" (TVD)—the depth of the completed borehole derived from surveyed depth measurements along its incline—was only a few feet less than the wireline-measured total depth (TD).

After a week of various attempts to seal off the problem zone, including the addition of lost-circulation materials to the drilling fluid and two cementing operations, it was evident that further efforts would probably not be successful.[3] With the condition of the hole continuing to deteriorate, the only solution was to run casing as soon as possible. On March 9, the hole was reamed to a diameter of 17 1/2 in., and a 13 3/8-in. (340-mm) surface casing string was set at a depth of 1604 ft (489 m) and cemented in place, with a Baker cement shoe installed at the bottom and a Baker float collar at 1573 ft (480 m). Although casing to about 1900 ft—just above the loss zone—would have been even better, the condition of the hole at that time made it impossible; and the 1600 ft of casing did mean that all of the Abo Formation and a significant portion of the interbedded red clays in the Madera Formation were cased off.

Drilling resumed on March 17, with a 12 1/4-in. bit and with water as the circulating medium; but when circulation was lost again at 1889 ft (576 m), water was abandoned in favor of air drilling and the much-lower-density drilling fluid used with it. Because the original plan had called for air to be used in drilling the Precambrian basement once the 10 3/4-in. intermediate casing string had been run and cemented, most of the equipment needed for air drilling was already on site.[4] The drilling fluid, an emulsion of soap, bentonite, and Gel-Foam having the consistency of a milk shake and a density of about 1 lb/gal., was used to stabilize and lubricate the hole, reducing somewhat the continuing problems with caving and stuck drill pipe. Even so, on March 25 drilling had to be halted at a depth of 2230 ft because of serious caving in the Madera Formation, some 300 ft higher, where the very low pressure of the column of foam in the borehole was now allowing significant inflows of water. (What had previously been a loss zone turned into a production zone when the pressure environment of the borehole decreased from full hydrostatic to very subhydrostatic.) Eight successive cementing operations were carried out over the next three days, to try to seal off this zone and stabilize the hole. Air drilling then resumed, and on March 30 the top of the Precambrian basement was reached at 2404 ft; but caving of the

[3]In fact, right to the end of the Fenton Hill experiments, none of the various lost circulation materials tried would be even marginally successful. To the dismay of the vendors of these materials, any substance that could be pumped through the rig's mud pumps (the positive-displacement pumps used to circulate the drilling fluid) without plugging them up would in no way seal off severe loss zones of the type encountered at Fenton Hill.

[4]The air-drilling equipment included three heavy-duty Ingersoll-Rand air compressors (each rated at 300 psi [2.1 MPa] and 2400 SCFM for an elevation of 8700 ft), a booster pump designed to boost the compressor output to 1500 psi (10 MPa), a mist pump (16 gpm at 1500 psi), and related piping. In addition, the compressed air services contract included the services of an engineer and two operators for approximately seven weeks.

overlying sedimentary rocks continued to present serious problems. In addition, just above the Precambrian surface a much more significant hot "aquifer" was encountered. Like the one some 400 ft higher, it appeared to be flowing toward the west, supplied by hot geothermal fluids from the Valles Caldera ring-fracture just to the east. Over time, this flow had washed out large cavities in the limestone that probably measured several feet across.

Drilling proceeded into the crystalline basement rock, but inflow of water from the formation was increasing; at 2463 ft, it became necessary to again cement the lower section of the hole (from 2463 ft up to 2105 ft). Following the cementing, which was done in four stages, drilling resumed and succeeded in deepening the borehole another 72 ft, to a depth of 2535 ft (773 m), 131 ft into the Precambrian basement.

Unfortunately, despite the cement jobs, caving of the sedimentary formations above had became so serious that even with air drilling the hole could not safely be deepened further in the absence of casing. On April 5, the planned deep string of 10 3/4-in., K-55 casing (45.5-lb/ft) was run from the surface into the top of the Precambrian basement, to the full drilled depth of 2535 ft. A Baker cement shoe was installed on bottom and a Baker float collar at a depth of 2404 ft. The float collar was installed this high in the string to prevent overdisplacement of the cement from the annulus between the casing and the granitic rocks, and to ensure that the cement would extend upward at least to the deeper loss zone, in the lower part of the Sandia Formation (at about 2380 ft).

On April 6 the lower section of casing, from 2535 ft up to the deeper loss zone, was tag-cemented by Dowell.[5] About 10 000 gal. of water was pumped into the empty casing (the static water level being about 1700 ft below ground level), followed by 2400 gal. of cement slurry. After a rubber plug had been inserted on top, the cement was displaced down the hole with 14 700 gal. of water. The amount of displacement water was calculated to leave about 30 ft of cement above the float collar, such that the cement would rise in the annulus to the region of the loss zone in the Sandia Formation. Once the cement had set, a 9 5/8-in. STC button bit was used (with air) to drill out, first, the cement and the plug on top of the float collar; then the float collar; then the cement remaining in the casing between the float collar and the cement shoe; next the cement shoe; and finally any cement and debris remaining at the bottom of the hole. To ensure that the hole was in good shape for the upcoming coring operations, it was then deepened to 2547 ft.

[5]The Farmington, NM, station of Dowell Cementing Services, then a division of Dow Chemical Company.

Note: The loss zones encountered during the drilling of GT-2 would also affect the drilling operations of the next three boreholes: EE-1, EE-2, and EE-3. The contract engineers for EE-2 and EE-3 in particular approached the problems posed by these loss zones according to their previous oilfield experience. The higher zone, in the Madera Formation (~1900 ft), was the easier of the two; it was usually handled by setting an intermediate casing string just above it, then loading the drilling fluid with lost-circulation material as this zone was being traversed. The massive loss zone immediately on top of the Precambrian surface (2380–2400 ft) was much more difficult. A number of different approaches were tried, but none was very successful.

Drilling in the Precambrian Crystalline Complex

The original GT-2 drilling plan for the Precambrian basement rock called for continuous, wireline-retrievable coring to a depth of at least 4500 ft, and if possible 6000 ft. The specified core bit was a type developed for the JOIDES (Joint Oceanographic Institutions for Deep Earth Sampling) program[6] and used to drill deep-ocean-floor basalts, somewhat softer and more easily drilled than the granitic rocks at Fenton Hill. The Smith Tool Company manufactured fifteen JOIDES-type 9 5/8-in. core bits for the HDR Project. This bit, shown in Fig. 3-3, incorporated four tungsten-carbide-insert (TCI) roller cutters that produced a 2 7/16-in.-diameter core.

Fig. 3-3. The JOIDES-type core bit manufactured by Smith Tool Company for the Fenton Hill HDR Project. Source: Pettitt, 1975a

[6]Darrell Sims, while working at the Scripps Institution of Oceanography in La Jolla, CA, was instrumental in designing the JOIDES coring system for the *Glomar Challenger* (the JOIDES drilling ship). He later joined the Laboratory's Group Q-22 (the initial HDR group led by Mort Smith) and was deeply involved in planning the drilling of the GT-2 borehole.

To provide the additional clearance needed for wireline retrieval of the core barrel—without having to break out the Kelly after each coring run—a special large-bore, rotating drilling head had been procured for the continuous wireline coring operation. However, before the entire wireline coring system was mobilized, several trial runs were carried out to check the system's viability for coring in the Precambrian basement at Fenton Hill (which turned out to be a wise move). The first two trial runs had actually been conducted during drilling in the Madera Limestone (despite the lost-circulation problems being encountered at the time): one at a depth of 2078 ft and the other at 2248 ft. Neither recovered intact core, only chips. Two more trial runs took place in the Precambrian basement, the first from 2547 to 2580 ft and the second from 2580 to 2600 ft. After each run, the Kelly was broken out and a wireline was run through the drill pipe to latch onto and recover the core barrel.

These trial runs were an abject failure. Owing to both the poor design of the core barrel and the apparent unsuitability of the JOIDES bits for drilling in granitic rock (see *Stage 1 Coring*, below), it appeared that continuous coring would not work in the Fenton Hill Precambrian basement—despite an "on-the-fly" redesign of the core-barrel/bit interface by Laboratory engineers, to place the "core catcher" right on top of the bit. With only 7 of the initial order of 15 JOIDES bits having been received from the manufacturer, one additional tactic was tried: STC was asked to modify the remaining 8 bits by replacing the innermost carbide inserts (which cut the outer diameter of the core) with the hardest tungsten carbide buttons available. But even after these two modifications, the JOIDES coring system was just not up to the job at Fenton Hill. Therefore, the decision was made to drill ahead with the STC 9JS bits, and core only as directed by the Project team.

As noted above, the GT-2 drilling plan also called for air drilling of the basement rock (Ingersoll-Rand personnel, on the basis of their experience in the mining industry, had convinced the HDR Project drilling engineers that air drilling would achieve a higher rate of penetration at a lower over-all cost than either water or mud). Another perceived advantage was that air would be more practical at Fenton Hill because water had to be hauled to the site.

The 10 3/4-in.-diameter intermediate casing string dictated a maximum bit size of 9 5/8 in. (244 mm) for drilling of the crystalline basement rock below 2535 ft. The selected hard-rock bits (which had been ordered when continuous coring was still the plan, for the eventuality that conventional drilling might be needed as a back-up) were STC 9JS full-face, TCI bits. These standard mining bits had been developed to drill the hardest, most abrasive ore-bearing rocks encountered in the mining industry—including taconite, chert, granite, quartzite, and other hard igneous and metamorphic rocks. Specifically designed for air drilling, these bits were fitted with hardened, open bearings that were both cooled and flushed clean of cuttings by air (unlike the sealed-bearing bits then being manufactured for the oil

industry by the Hughes Tool Company). In addition, having built-in jets, the STC 9JS bits could be adapted for water drilling by welding shut the air courses (copper tubes) through which clean air was directed to the open bearings; the bearings would then instead be "lubricated" with clean water flowing through the jets.

Drilling with air progressed rapidly in the crystalline basement, interrupted by four more coring runs and several cementing operations to repair zones of excessive water inflow. On April 23, when the drilled depth had reached 3542 ft, water was being produced from the hole at such a rate (estimated at over 400 gpm) that the settling pond was close to overflowing. A series of commercial logging tests that day indicated that the casing was undamaged, dispelling concerns that a hole in the casing could have been the source of the inflow and suggesting instead that the water was coming from the brackish aquifer above the granitic surface and was flowing around the bottom of the casing through a breach in the cement. (This conclusion would soon be refuted by operations deeper in the borehole.)

In an attempt to seal off the supposed breach in the casing cement with additional cement—a so-called casing-shoe "squeeze" job—a wireline-activated, open-hole bridge plug was set at 2580 ft, 45 ft below the casing shoe. Next, a removable packer was run in on drill pipe and set inside the casing at a depth of 2400 ft, and a slurry of 300 sacks of cement was injected into the interval between the packer and the bridge plug. Although this was enough to fill the packed-off interval two times over, it would later be determined that the cement had flowed around the bridge plug and on down the hole.

The drill pipe was removed and the residual cement, which filled the hole from 2400 ft down to the bridge plug, was drilled out; but before the bridge plug was broached, water began flowing into the hole at such a rate that air drilling could not continue. Following another attempt to cement off the water inflow (still assumed to be coming around the bottom of the casing), the hole was cleared of cement and the bridge plug was drilled through. The hole promptly filled with water again, to a level of about 1700 ft—indicating continued flow communication with the aquifer above the granitic surface. It now appeared probable that the open-hole bridge plug had not held against the differential fluid pressure—in excess of 1500 psi—exerted during the squeeze cement job and the subsequent air drilling.

Efforts now focused on looking deeper to locate the source of the water inflow. An inflatable Lynes open-hole packer was run in on drill pipe and set in the borehole below the casing shoe. Injection testing below the packer was carried out with a full hydrostatic head of water augmented by some pump pressure. The results indicated that the borehole was accepting water across a wide interval *below* 3150 ft. (Later, a caliper log showed that a portion of the borehole at about 3220 ft was enlarged, apparently representing the intersection of a fracture zone with the borehole.) On May 4, a

slurry of 300 sacks of cement was pumped into the hole through open-ended drill pipe, filling the bottom portion (from 3542 ft up to 3119 ft). Once set, the cement was successfully drilled out with air. The hole was then deepened to 3556 ft, but once again it filled with water. The fact that the deep cement plug had effectively sealed off the water until it was drilled out demonstrated conclusively that the route of the inflow was not around the bottom of the casing but through open fractures in the basement rock.

At this point, it was decided to switch to water drilling, even though this might mean drilling without returns through any additional open fractures in the basement rock. A pump was installed in the reserve pit to supply the additional water needed (and simultaneously draw down the large quantity of water produced during air drilling). Drilling progressed in the granitic rocks to a depth of 3666 ft without excessive water losses, suggesting that the very fine drilling cuttings were slowly sealing the open fractures. A comprehensive suite of temperature logs run by the Laboratory yielded a temperature profile without significant perturbations, signifying that the borehole was tight below about 3600 ft.

Because the plan was to return to air drilling, two attempts were made to "squeeze off," with cement, the open fractures between 3150 and 3600 ft—both with disastrous results. In the first attempt, on May 9, cement formulated to set in 1 3/4 hours at 26°C was pumped in through open-ended drill pipe and ended up "flash-setting" in the drill pipe in only 19 minutes! Twenty-nine stands (about 2600 ft) of pipe full of cement had to be pulled out and sent to Farmington, NM, to be drilled out (meanwhile, additional pipe was rented so that operations could continue). Drilling with water resumed, taking the hole to 3728 ft. Further temperature measurements indicated that water was still flowing out of the hole at about 3600 ft (a caliper log run several weeks later showed that the section of borehole between about 3550 and 3600 ft was also enlarged, presumably representing another fracture zone in the basement rock).

The second "squeeze cementing" attempt took place on May 15: open-ended drill pipe was run into the hole to 3680 ft, then cement was injected (150 sacks in about 20 minutes). This time the cement formulation had been lab-tested to allow a pumping time of 1h 37 min at 110°C, providing an ample margin in case of unforeseen delays. Unfortunately, because the bottom of the drill pipe was positioned below the major inflow zone between 3550 and 3600 ft, and there was a large pressure differential between the cement in the borehole and the underpressured inflow zone, the drill pipe was "sucked" against the borehole wall—a phenomenon known in the drilling industry as *differential sticking*. The pipe could not be moved as the cement proceeded to set up. When the cement within the drill pipe was tagged, its top was found to be at a depth of 3232 ft; the cement was then drilled out with small-diameter drill pipe and a 3 1/2-in. bit. Next, service company acoustic equipment was used to determine the depth at which

the outside of the pipe was cemented in the hole, and a fishing job ensued ("fishing" is drilling parlance for the removal from the hole of any damaged pipe, stuck tools, drill bits, debris, etc.): with a deep, back-off explosive shot, all but 330 ft of the drill pipe was pulled out of the hole.

On May 19, after successive joints of drill pipe had been "washed-over" and then unscrewed, hard cement was finally encountered in the annulus at a depth of 3556 ft. By May 28, this cement had been laboriously reamed out of the annulus (with washover pipe fitted with a variety of cutter faces, including diamonds), slowly freeing the remaining drill pipe, section by section. Finally, the hole having been cleared, air drilling began again and reached a new depth of 3814 ft. But water was still flowing in at a rate of between 60 and 70 gpm—primarily because neither of the squeeze cementing jobs had been successful in sealing off the open fault intersections with the borehole.[7]

Note: It was only much later, during flow testing of the Phase I reservoir, that the true nature of the "flowing fractures" traversed by the GT-2 borehole in the upper crystalline basement became apparent. With production approaching 400 gpm under modest air-drilling differential pressures, the inflow must have been through open fault zones—not through unsealed, but tight, "fractures" in the basement rock. To produce this amount of water, the *en echelon* set of fractures making up these fault zones must have undergone considerable recent displacement, and consequent shear dilation (often referred to in the HDR literature as "self-propping"). The two fault zones intersected by the GT-2 borehole—one at 3220 ft and one between 3550 and 3600 ft—were probably relatively recent (but minor) steeply dipping fault zones that had not been detected when the Fenton Hill site was originally investigated.

At this point, considering that the rate of penetration with air drilling was not particularly impressive (5–6 ft/h), that the air compressors, booster pumps, and additional personnel required were costly, and that it was becoming progressively harder to blow the produced water from the hole, the decision was made to evaluate air drilling vs water drilling under

[7]In oil-well drilling, water channels and other voids in casing cement are sometimes sealed by the slow pumping of additional cement into (and through) the poor-quality cement. As setting of the new cement begins, it causes the pumping pressure to gradually increase, which forces the still-plastic cement slurry into the remaining voids and channels in the original cement (hence the name "squeeze" cement job). However, it is improbable that an open joint (or fault zone) in crystalline basement rock can be similarly "squeezed off" with cement. Without the pressure needed to dilate the joint intersection with the borehole, the closed joint will act as a sieve, filtering out the cement particles from the slurry; as the water passes through, it leaves a thick buildup of dehydrated cement at the joint entrance.

actual field conditions. Two successive drilling runs were carried out with STC 9JS bits, one with air and the other with water, during which drilled footage, drilling time, bit wear, and other key parameters were recorded. When the results showed that water drilling had a small but distinct advantage over air drilling (Table 3-2), the decision was made to use water for all subsequent drilling operations. On June 2 the air compressors were shut down, and two days later the contract with Ingersoll-Rand for compressed air was terminated.

Table 3-2. Drilling performance: air vs water

Parameters measured	Air as circulating medium	Water as circulating medium
Drilled interval	199 ft (61 m)	237 ft (78 m)
Drilling time (h)	39	42
Bit wear	0.25 in. (0.6 cm)	0.125 in. (0.3 cm)
Reamer wear	0.125 in. (0.3 cm)	0.0625 in. (0.2 cm)
Drilling rate	5.1 ft/h (1.6 m/h)	6.1 ft/h (1.9 m/h)
Drill-string weight (weight on the bit)	44 000 lb	45 000 lb
Drilling speed (rpm)	40	44

As drilling proceeded, fluid continued to be lost into the fault zones, most of it probably in the 3550- to 3600-ft zone. In an effort to seal off these fault zones, as well as aid in removal of drill cuttings, beginning on June 10 small amounts of bentonite and lost-circulation material were added to the drilling fluid. Eventually, the water loss decreased from several tens of gpm to only about 2.5 gpm.

With drilling progressing at a steady rate, numerous temperature-logging and coring runs were interspersed with drilling runs in a standardized sequence, to obtain maximum information on the characteristics of the basement rock in the lower section of the hole. At a depth of 4915 ft, the first reconfigured JOIDES coring bit and the modified coring assembly were used to cut 6 ft of core in less than 2 hours, with 100% core recovery (in contrast, the average recovery on the previous six JOIDES coring runs had been only 26%). The last three major bit runs—of 313, 239, and 310 ft—were all uneventful and deepened the borehole to 5979 ft.

With time, it became possible to predict the life of an STC 9JS bit. At 40–50 rpm and a bit load of 38 000–42 000 lb, a bit could be expected to last about 60 hours and to drill nearly 300 ft (91 m)—an average of about 5 ft/hr. By that time the bit was usually about 1/4 in. under gauge and missing 15–25 buttons, and the bottom reamers were between 1/16 and 1/8 in. under gauge. For this reason, after about 50 hours of bit rotation, the drilling rate was closely monitored. If a significant fall-off from the average

rate of 5 ft/h was measured, or if the bit began to run rough or torque up, drilling was stopped and the bit was changed. In this way, it was possible to obtain maximum use from the bits while minimizing the risk of disintegration (typically the loss of one of the three roller cones, as evidenced by a sudden onset of very rough drilling).

Following the two final coring runs, Stage 1 drilling was completed on July 14, 1974. The total drilled depth was 6356 ft (1937 m). The major drilling runs in the basement rock are summarized in Table 3-3, and the rock types are shown in the geologic cross section, Fig. 3-4.

Table 3-3. Major Stage 1 drilling runs in the GT-2 borehole

Drilled depth, ft (m)	Drilled interval, ft (m)	Drilling time (h)	Rock type	Drilling medium	Average penetration rate, ft/h (m/h)
2857–3147 (871–959)	290 (88.4)	27	Monzogranitic gneiss, biotite-granodioritic gneiss	Air	10.7 (3.2)
3182–3463 (970–1056)	281 (85.6)	32.5	Monzogranitic gneiss, biotite-granodioritic gneiss	Air	8.6 (2.6)
3814–4013 (1163–1223)	199 (60.7)	39	Monzogranitic gneiss	Air	5.1 (1.6)
4013–4270 (1223–1302)	257 (78.3)	42	Monzogranitic gneiss, monzogranite	Water	6.1 (1.9)
4279–4556 (1304–1389)	277 (84.5)	49.5	Monzogranite, monzogranitic gneiss	Water	5.6 (1.7)
4556–4835 (1389–1474)	279 (85)	60.5	Monzogranitic gneiss, granodioritic gneiss	Water	4.6 (1.4)
4921–5234 (1450–1595)	313 (95.4)	65	Monzogranitic gneiss, biotite-granodioritic gneiss, biotite-tonalite gneiss	Water	4.8 (1.5)
5240–5479 (1579–1670)	239 (72.8)	51	Monzogranitic gneiss, biotite-granodioritic gneiss	Water	4.7 (1.42)
5669–5979 (1728–1822)	310 (94.5)	55.5	Monzogranitic gneiss, hornblende-biotite schist, amphibolite	Water	5.6 (1.7)

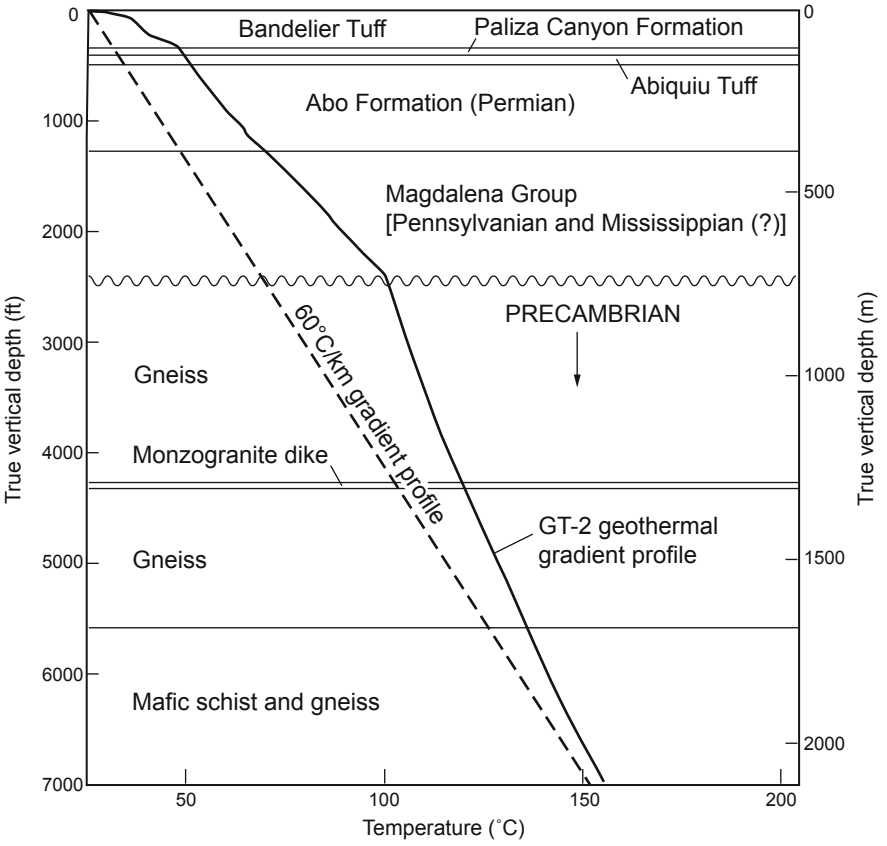

Fig. 3-4. Geologic cross section of the Precambrian basement and overlying formations, showing the geothermal gradient. (Note: the information in this figure is more generalized than the petrographic information given in Tables 3-3 and 3-4.)

The very pronounced "knee" in the gradient profile at the top of the Precambrian (2404 ft) illustrates the magnitude of the hydrothermal outflow from the caldera. At this depth, the convection of heat into the overlying sedimentary rocks from this flow effectively doubled the gradient to the ground surface—from just over 60°C to about 120°C. The dashed line in the figure represents the 60°C gradient.

During the air drilling of GT-2, the production of hot fluid from this loss zone was in excess of 1000 gpm (the air compressors were acting as lift pumps). Such a high rate of production from this very subhydrostatic aquifer, flowing westward on top of the Precambrian surface, shows what a prolific—albeit low temperature—geothermal resource had been tapped into (little wonder that it presented such an obstacle to the drilling efforts)!

Stage 1 Coring

The Stage 1 coring runs are summarized in Table 3-4.

Table 3-4. Stage 1 coring runs in the GT-2 borehole

Coring run	Cored interval, ft (m)	Recovery (%)	Core bit (J=JOIDES type; C=Christensen)	Rock type
1	2078–2098 (633–640)	25[a]	J	Clay, limestone chips
2	2248–2258 (685–688)	50[a]	J	Shale, limestone chips
3	2547–2580 (776–786)	35[a]	J	Leucocratic quartz monzonite[b]
4	2580–2600 (786–793)	33[a]	J	Leucocratic quartz monzonite[b]
5	283 1–2844 (863–867)	30	J	Granitic[b]
6	2844–2857 (867–871)	20	J	Quartz monzonite[c]
7	3151–3182 (960–970)	20	J	Biotite granodiorite[b]
8	3464–3476 (1056–1060)	17	J	Leucocratic quartz monzonite[b]
9	3694–3705 (1126–1129)	100	C	Leucocratic quartz monzonite[b]
10	4278–4285 (1304–1306)	85	C	Leucocratic granodiorite and quartz monzonite[b]
11	4892–4897 (1491–1493)	100	C	Biotite trondhjemite, leucocratic granodiorite, and quartz monzonite[b]
12	4915–4921 (1498–1500)	100	J	Leucocratic quartz monzonite[b]
13	5234–5240 (1595–1597)	38	J	Quartz monzonite, granodiorite[b]
14	5487–5492 (1672–1674)	90	C	Quartz monzonite[c]
15	5654–5660 (1723–1725)	92	J	Hornblende biotite schist[c]
16	5980–5986 (1823–1825)	100	J	Hornblende biotite schist[c]
17	6150–6156 (1875–1876)	66	J	Quartz monzonite[c]
18	6156–6162 (1876–1878)	100	J	Quartz monzonite[c]

Table 3-4. (Continued)

Coring run	Cored interval, ft (m)	Recovery (%)	Core bit (J=JOIDES type; C=Christensen)	Rock type
19	6344–6350 (1934–1936)	16	J	Granodiorite[b]
20	6350–6356 (1936–1937)	5	J	Granitic chips[c]

[a] Core barrel retrieved via wireline
[b] Determined from petrographic examination of thin sections
[c] Determined by hand examination

Source: Pettitt, 1975a
Note: These core samples were later re-evaluated and the gneissic textures described. The information in Table 3-3 and Fig. 3-4 reflects the later data.

As discussed above, many mechanical difficulties were encountered with the modified version of the wireline core-retrieval system developed for the JOIDES program. The primary modification was to enable the coring assembly—which for the JOIDES program was normally dropped from the surface into a water-filled borehole—to function in the air-drilled GT-2 borehole. Concurrently, a mechanism was added that would enable the orientation of a core in the undisturbed rock to be determined. After the failure of the two trial wireline-recovery coring runs in basement rock (Runs 3 and 4 in Table 3-4), two additional coring runs were made without wireline recovery. But core recovery was still poor because cores were jamming in the core barrel. Given the time constraints of the project, the continuous-wireline-recovery coring system was not developed further; the JOIDES core bits were used in the conventional manner (the core barrel being tripped out of the hole with the drill string following each coring run).

Unfortunately, the use of harder carbide inserts on the bits and the lowering of the core barrel to just above the bit did not improve recovery on the conventional coring runs (compare Runs 5 through 8 with Runs 3 and 4 in Table 3-4). The performance of these bits at Fenton Hill was roughly on a par with that attained in the Deep Sea Drilling phase of the JOIDES program (about 25% recovery in basalt). Diagnosis of the core recovery problem took a fair amount of time, and meanwhile another two coring runs were made with the JOIDES bits (Runs 7 and 8)—with even poorer results. Upon reflection, Darrell Sims recalled that the deep ocean basalt cores obtained from the *Glomar Challenger* (the JOIDES program drilling ship) were typically "eye-shaped," with smooth, rounded corners. This phenomenon had been explained as exfoliation of the basalt into thin slices as a result of stress relief after cutting, followed by "tumbling" in the core barrel. Now, at Fenton Hill—in a much different type of rock—similar rounded, "eye-shaped" slices of core were being seen. The obvious conclusion was that the core bit itself

was causing the problem; examination revealed that it was oscillating laterally, breaking off thin slices as it cut out the core. To restrain this sideways motion, a full-diameter blade stabilizer was custom-designed to fit directly above the bit.

The redesigned JOIDES coring assembly with added blade stabilizer was employed for all but one of the remaining runs. With the blade stabilizer, core recovery more than tripled, averaging about 84% for coring runs 12 through 18. This recovery rate was comparable to that achieved with conventional diamond bits (about 95%), but the rate of penetration and bit life were up to four times greater. (The problems experienced during the last two JOIDES runs were related to excessive wear on the blade stabilizer.)

Stage 1 Hydrology Experiments

HDR Project personnel never intended to develop an HDR geothermal heat-mining system at the shallow depths and modest rock temperatures (ca. 146°C) attained during the first stage of drilling of the GT-2 borehole (down to 6356 ft). At the same time, they recognized that the success of any pressurized HDR system would ultimately depend on the ability to access a large volume of low-permeability basement rock, capable of containing the heat-exchange system without excessive water losses at the boundaries. It was for this reason that one of the principal objectives of the GT-2 drilling program was to investigate the permeability of the Precambrian rock mass at Fenton Hill at depths greater than the 2575 ft reached by GT-1. Such investigations seemed particularly warranted in light of the fault zones encountered during air drilling at 3220 ft and between 3550 and 3600 ft, through which large amounts of water flowed into the borehole.

An oilfield method of measuring borehole permeability known as drill-stem testing was adapted for use under the very tight borehole conditions of GT-2 (permeabilities anticipated to be in the low-microdarcy to several-hundred-nanodarcy range—lower by a factor of at least 1000 than those of typical petroleum-bearing formations). This method involves isolating potential production intervals from the borehole fluids and then actually producing the formation under several subhydrostatic pressures to measure the permeability.

The intervals of the GT-2 borehole to undergo drill-stem testing were selected on the basis of two criteria: smoothness of the borehole wall and absence of pre-existing joints intersecting the borehole (the presence of intersecting joints often led to enlargement of the hole). Caliper data were used to identify the portions of the borehole that were nearest to true gauge, the expectation being that these sections would offer better chances for seating packers without leakage (and might also be "tighter" than other portions of the borehole). Unfortunately, from start to finish the tests would

be plagued with leakage problems: the packers either did not seat properly, ruptured against the rough borehole wall, or failed to function for other reasons. This "thorn in the side" of the HDR Project would persist for an entire year—through the testing periods of the next two stages of drilling.

Between July 17 and August 4, 1974, following Stage 1 drilling and coring, about 16 drill-stem tests were conducted in the 2600- to 2900-ft (792- to 884-m) and 4700- to 6200-ft (1433- to 1890-m) depth intervals. All of the packers used in these tests were from the Johnston Division of Schlumberger, Ltd. Typically, soft rubber packers were used in a straddle configuration (one packer above and one below the test zone), with the spacing between packers ranging from 90 to 408 ft (27 to 124 m). This testing assembly also incorporated a pressure-balancing feature—a tube extending through the packer assembly equalized the pressure between the open hole below the lower packer and the annulus above the upper packer, by providing a path for flow as the packers were compressed and set. In addition, this feature gave an immediate indication if the lower packer failed during a pressurization test: fluid broaching the lower packer from the pressurized interval would flow upward via the tube into the annulus above the upper packer, thereby forcing fluid in the annulus to flow out at the surface.

For the first few tests, packers having a diameter of 8 1/2 in. (216 mm) were used, but these turned out to be too small to seat properly under the applied drill-string compressive load. A slightly larger, 9 1/4-in. (232-mm)-diameter size proved to be more satisfactory. Even so, the rubber packers were often torn and ruptured from being dragged across the rough, irregular walls of the drillhole. Typically, at the end of each test, at least one of the packers would need to be replaced. Other problems encountered during the early tests—malfunctioning equipment, leaking drill pipe, and plugging of fittings by drill cuttings—were corrected in later stages.

The last two tests were done in the lowest section of the hole, with only a single upper compression packer (the bottom of the hole acting as the lower packer). A string of drill collars was made up, near the top of which were installed the upper packer and the multi-flow evaluator (MFE). The thus-modified drill-stem test assembly was lowered into the hole until it rested on the bottom; additional string load was then applied to compress the upper packer, causing it to expand and seat against the borehole wall. The drill pipe, which had been run in empty, was now partially filled with water to prevent steam blowoffs, and the main control valve in the MFE was opened to allow water from the formation to flow into the interval between the packer and the bottom of the hole. Following the tests, a 0.66-gal. sample of fluid was trapped in the MFE sampler chamber and brought to the surface for analysis. The results showed that this fluid was not reservoir "pore fluid," but rather some of the borehole fluid pumped from the surface when the drill pipe was partially filled with water.

Unfortunately, none of the 16 drill-stem hydrology tests yielded any definitive results—only evidence that all the tested intervals appeared to be very tight. Indeed, because the basement rock was so tight, no measurable reservoir pore fluid was produced during any of the tests, even after a number of attempts to modify the straddle-packer configuration. However, despite being only qualitative in nature, the tests did indicate that the granitic rock had a very low permeability and would be able to contain pressurized water with acceptably low leakage rates.

Stage 1 Fracturing (Pressure-Stimulation) Tests

Following the hydrology experiments, several tests were carried out in the GT-2 borehole to investigate whether the deeper basement rock could be fractured at reasonable surface pressures and to measure the amount of fluid injected into the created fracture as it extended away from the borehole. It had been assumed, on the basis of the successful hydraulic fracturing in the GT-1 granitic rocks at pressures up to 2000 psi, that there would be little trouble doing the same in GT-2. However, the open-hole section of the GT-2 borehole differed in two significant ways from that of GT-1: first, the diameter of the granitic section was much larger—9 5/8 in. as compared with only 4 1/4 in.—making packer sealing considerably more difficult; and second, in contrast to the very smooth granitic walls of GT-1 (which had been continuously cored with diamond core heads), the rotary-drilled walls of GT-2 were quite rough and thus less conducive to tight packer sealing. These problems would be a constant source of frustration during the hydraulic fracturing attempts in GT-2.

The results of the hydrology experiments, the condition of the borehole wall, and geophysical logging data (which indicate the least-fractured, lowest-permeability locations) were all used to select six zones of the open hole for the hydraulic fracturing tests. Each zone was selected, and the tests carried out, before the next zone for testing was decided upon.

Zone 1	2775–2865 ft (843–873 m)
Zone 2	2600–2680 ft (793–817 m)
Zone 3	4730–4880 ft (1442–1487 m)
Zone 4	4880–5020 ft (1487–1530 m)
Zone 5	5314–5394 ft (1620–1644 m)
Zone 6	4617–5153 ft (1407–1571 m)

Johnston packers were again used for most of the hydraulic fracturing tests, at various spacings and, this time (in an effort to control leakage), in a "double straddle" configuration—two packers above and two below the test zone. The lower pair of packers was held in position by a hook-wall anchor at the lower end of the pipe string, and the upper pair was inserted into the pipe string at the selected spacing interval.

In these early days, the Project had not yet acquired a positive-displacement pump for fracture initiation and extension tests. Instead, water was pumped into the hole by three 10-gal., 5000-psi pressure accumulators manifolded together. The flow was regulated by an electromechanical control valve and could be accurately maintained at rates ranging from 1 to 20 gpm (0.06 to 1.3 L/s).

InfoNote

Throughout this book, we attempt to consistently use the units in which the original measurement was made. For instance, if psi was the unit of a pressure transducer or pressure gauge used in a particular operation, the relevant text will use psi (sometimes with its MPa equivalent, for the convenience of non-U. S. readers). Another example: when pumping equipment belonging to the HDR Project was used for fluid injection, the original unit of measurement for the flow rate was gpm (gallons per minute), whereas when rental pumping equipment was used, the unit of measurement was BPM (barrels per minute—1 BPM = 42 gpm).

Figure 3-5 shows the depth at which each fracturing test was carried out as well as the type of packer used (plotted by date of test).

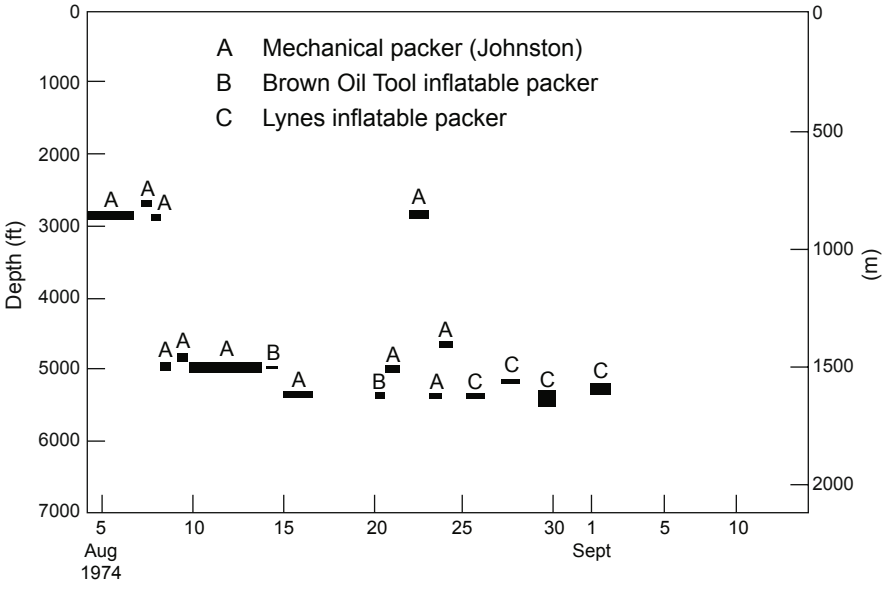

Fig. 3-5. Stage 1 fracturing tests in GT-2 with mechanical and inflatable packers, plotted by date of test.
Source: Blair et al., 1976

The first test took place August 6, 1974 (in Zone 1). Not only did the Johnston packers initially hold up to a pressure of almost 1400 psi without leaking, but a successful "hydraulic fracture" was initiated. (As discussed in Chapters 1 and 2, only several years later would it become clear that all Fenton Hill "fractures" were actually pre-existing but resealed joints that were being reopened.)

The opening of this joint was evidenced by a small—but distinct—pressure overshoot, reflecting the fracture "breakdown" point. This often-observed phenomenon is represented schematically in Fig. 3-6, along with a typical pressure profile observed during reinflation. The latter deviates from the straight-line compressibility curve for the water in the frac string at the point where the reclosed joint just starts to accept fluid—i.e., at this pressure, the stress-closed joint first becomes slightly permeable. However, only with additional pressurization does the joint actually jack open against its closure stress. This phenomenon was first observed during the hydraulic fracturing experiments in GT-1 (see Chapter 1).

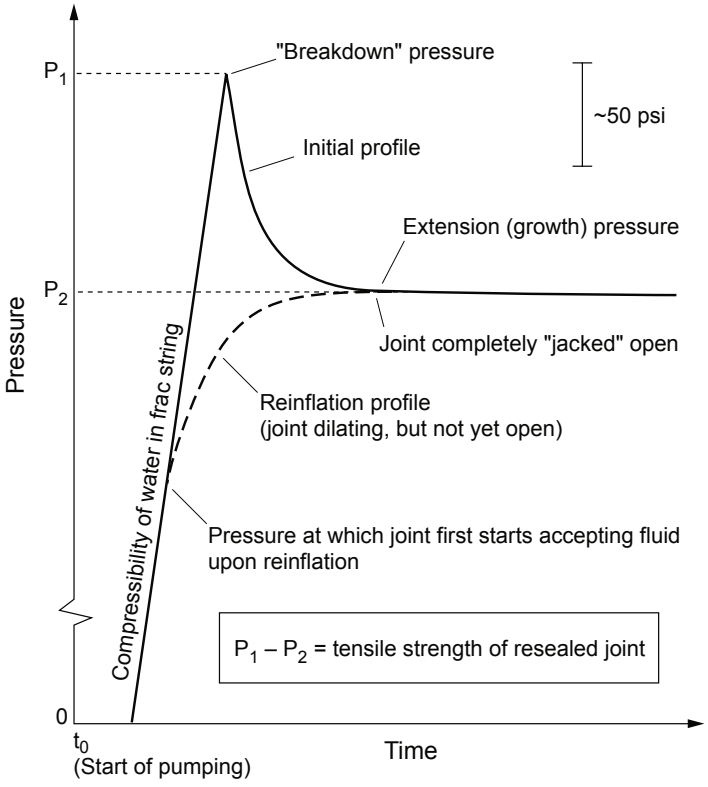

Fig. 3-6. Conceptualization of the pressure overshoot at the initiation of a "fracturing" event (opening of a resealed joint) and the pressure profile during subsequent reinflation of the joint, both at a constant rate of injection.

During the August 6 test, the joint initially opened at a pressure of 1397 psi. Then, as the joint was further opened and extended at a constant injection rate of 19 gpm, the pressure dropped rapidly and leveled off at 1286 psi. The difference between these two pressures—111 psi—was interpreted as representing the tensile strength of the joint-filling material. This overshoot was too small to reflect the creation of a fresh hydraulic fracture in unflawed granitic rock, considering that the rock at the borehole wall would have had a breakdown pressure of at least several thousand psi (according to laboratory tensile-strength testing). This first "fracturing" test was terminated by flow around the packer, as would be all the others in this series.

Following this first successful "fracturing" test, the Johnston straddle packers were tried higher up in the borehole (Zone 2) and then in the deeper Zones 3 and 4. But none of these fracturing attempts were successful: with the pumping pressure on the straddled interval reaching only 500–1000 psi (below the fracture initiation pressure), the packers leaked so badly that the tests could not be continued. For all but the last few tests, the packers were fitted with flexible, hard-rubber elements (90 durometer). Softer packer elements (70 durometer) were tried for the last few tests; with these elements, the packers withstood pressures as high as 1600 psi (11 MPa) before leaking. Drill-stem weights, ranging from 80 000 to 150 000 lb, were then added to further compress the packers, but did not stop the leakage. This series of tests with Johnston mechanical packers was terminated on August 14.

On August 20 and 21, a two-day pressurization test was attempted in Zone 5 with Brown Oil Tool inflatable packers in a straddle configuration. But the packers either burst or leaked when inflated, prompting a return to the Johnston packers for the next four days of testing.

Finally, a series of pressurization tests was carried out in Zones 5 and 6 (August 26–30 and September 2, 1974) with Lynes inflatable packers, again in a straddle configuration. On August 30, with the packers centered at a depth of about 5150 ft, a pressure of 1300 psi (9 MPa) was attained before the packers leaked. In a photograph of the upper packer used for this test (Fig. 3-7), the predominant impressions are of two calcite-filled joints having an inclination of about 70° that had been eroded during drilling operations. Also visible is a more steeply dipping joint (the fainter and narrower crack inclined in the opposite direction) that was opened during this test, probably at a pressure of about 1300 psi (the pumping records give no clear indication of joint inflation). Because of the repeated failure of the packers to satisfactorily hold pressure, this joint and the one opened on August 6, during the first brief fracturing test, were the only two clearly defined joints opened during these open-hole tests.

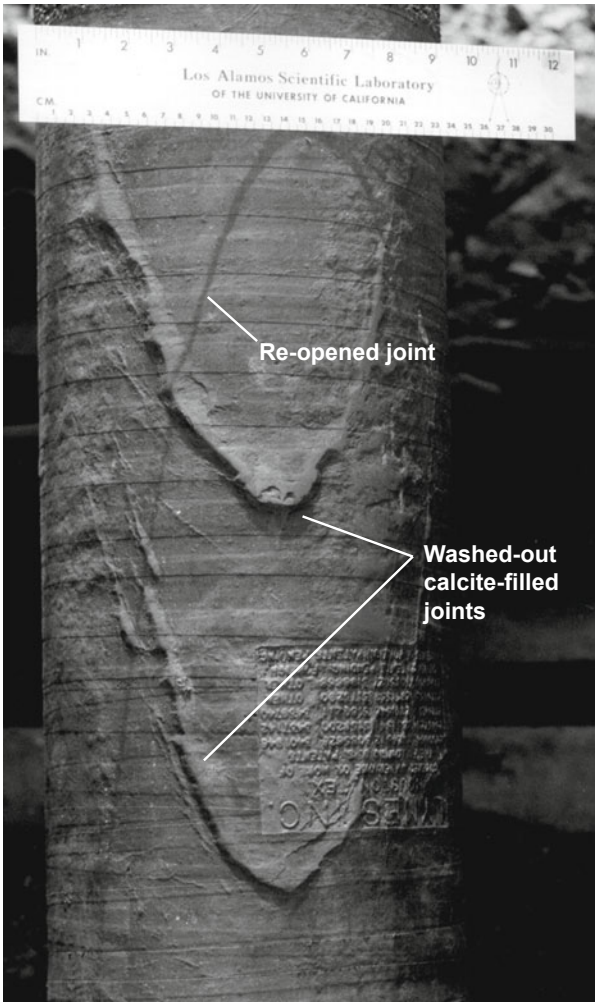

Fig. 3-7. Photograph of the upper Lynes packer (set at about 5100 ft in GT-2), showing impressions of two 70° eroded joints and a steeply inclined joint opened during the pressurization test of August 30, 1974.
Source: Pettitt, 1975b

On August 30, 1974, while awaiting the arrival of new Lynes packer elements for additional hydraulic fracturing attempts, the field engineers decided to drill ahead instead of placing the rig on standby. Besides productive use of the wait time, this additional drilling would provide a fresh section of hole for further fracturing and hydrologic testing. The information on the second stage of operations in GT-2 is based mainly on Pettitt (1975b and c) and Blair et al. (1976).

Stage 2 Drilling

After the 6200- to 6356-ft section of the hole had been reamed, drilling with an STC 9 7/8-in. TCI mining bit began on August 31 and ended on September 5 at a depth of 6696 ft. The hole was then cleaned by circulation of water through open-ended drill pipe, and a Laboratory temperature probe was run in through the pipe. Following the pumping of a thick "pill" of bentonite and Cellex (about 800 gal.) to the bottom of the hole to reduce thermal convection, the drill pipe and temperature probe were set on bottom. The bottom-hole temperature, extrapolated from measurements taken over the next 20 hours, was 146.2°C. Then a JOIDES core-bit assembly was employed to deepen the hole to 6702 ft (this was technically a coring run—No. 21—but no core was recovered).

On September 8, 1974, in preparation for hydraulic fracturing, a hydrology experiment was conducted below the 6499-ft (1981-m) depth to evaluate the permeability of the lower portion of the hole. This experiment, carried out at modest pressures for 1 hour, used a compression-set packer assembly that rested on the bottom of the hole. It was made up of three Johnston packers at the top of a 203-ft section of drill collars, with the bottom of the lowest packer at 6499 ft. The lack of any perceptible pressure drop in the shut-in, pressurizing system after one hour indicated "zero" inflow over the 6499- to 6702-ft depth interval.

Stage 2 Pressure-Stimulation Tests

Pressure testing of the fresh new open-hole interval at the bottom of GT-2 afforded an excellent opportunity to clarify whether true hydraulic fractures were being created in intact rock, or pre-existing joints intersecting the borehole were being opened. (In this as in all subsequent injection tests involving pressurization of a significant interval of borehole, it would be found that the applied hydraulic pressure was opening existing joints rather than fracturing unflawed rock.)

After the borehole had been vented, more weight was stacked on the compression-set packers and the bottom interval was pressurized to about 2000 psi—much higher than during the hydrology experiment—in an attempt to create a hydraulic fracture. But at this high pressure, packer leakage once again forced a shut-in, terminating the test. From surface indications, there had been no evidence of hydraulic fracturing during this pressurization (no sudden drop in pressure followed by a pressure plateau). At the same time, it was a significant accomplishment for the then-available open-hole packers; previously, pressures in the range of 1300–1600 psi could not be attained without severe packer leakage.

When the Johnston packer assembly was retrieved, the bottom of the lowest packer—set at a depth of 6499 ft—bore impressions of several opened joints about 6 in. apart and dipping 70° (a "real" hydraulic fracture—a "hair-line"—would not have been visible on the soft rubber). The opening pressure for these inclined joints, therefore, had indeed been reached—albeit at a very low injection flow rate, in view of the ongoing problems with packer leakage. In fact, given the trouble-plagued history of packer usage for hydraulic fracturing to this point in GT-2, it was decided that the Lynes packers that had been ordered would not be used for the remaining Stage 2 tests. Instead, a scab liner with a polished bore receptacle (PBR) on top would be run and cemented in at the top of this new interval.

Arrangements were made with the Halliburton Oil Well Cementing Company, and the work got under way immediately. The bottom section of the borehole was backfilled with coarse sand to a depth of 6525 ft, a cement plug was placed on top of the sand to a depth of 6501 ft, and the cement was faced off to 6510 ft to provide a firm bottom for landing the scab liner. On September 10, a 210-ft section of 20 lb/ft, 7-in. steel casing (inner diameter 6.46 in.) was run in on drill pipe, set onto the plug, and then picked up 12 ft. The PBR at the top of the liner was a 3 1/2-ft flared section, with a machined inner surface into which the PBR mandrel would seat. The liner was cemented in place from its lower end (6498 ft) up to 6288 ft.

After a 24-hour wait for the cement to set, a 6 1/8-in. bit was run down through the liner, the residual cement and cement plug were drilled out, and the sand was washed out of the bottom of the hole. On September 13, the PBR mandrel assembly was run in on 5 1/2-in. drill pipe and seated with a 140 000-lb drill-string weight. The 204-ft open-hole interval below the scab liner (6498–6702 ft) that was now isolated for pressure testing was referred to as Zone 7. In essence, the failed packers had been replaced with a pressure-tight, steel-and-cement "packer," a technique that would be employed several more times during the HDR Project when attempts to use conventional packers were unsuccessful. The borehole configuration for further pressurization testing at the bottom of GT-2 is shown in Fig. 3-8.

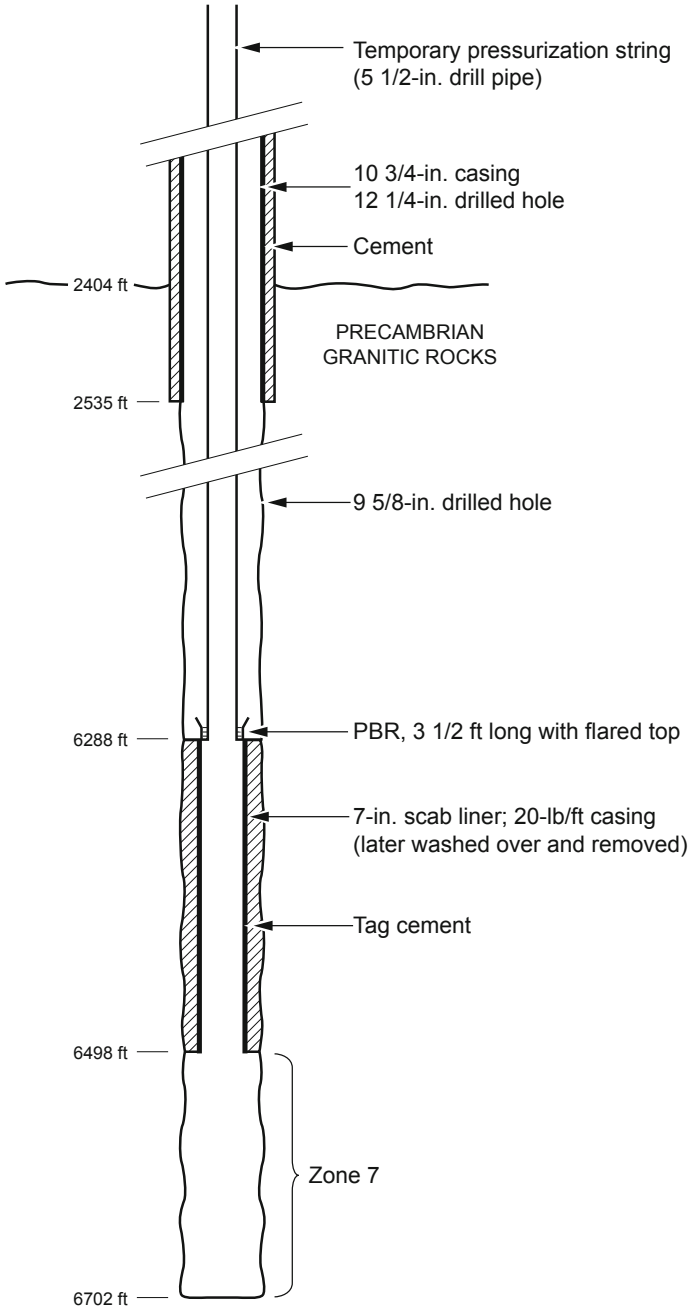

Fig. 3-8. Configuration of the GT-2 borehole through Stage 2 drilling and liner installation.

Pressurization testing in Zone 7 recommenced on September 14, with a commercial, truck-mounted "frac" (injection) pump. Only the first test of this series yielded meaningful data. After that test, unfortunately, the surface packoff assembly—through which the cable for the downhole temperature instrument was run—began leaking and continued to leak until it finally failed completely. Figure 3-9 shows the surface pressure profile for the first test, during which fluid was injected at a rate of 3 BPM (8 L/s) for just under 1 minute. The profile did not exhibit the anticipated "breakdown-pressure" excursion, but simply a sharp rise in pressure and then an abrupt leveling off at about 2500 psi before shut-in. This pressure behavior strongly indicated that one or more joints had been opened at or below a pressure of 2500 psi. (The quality of the recording was quite poor, obscuring the details of this very brief period of joint opening and fluid injection.)

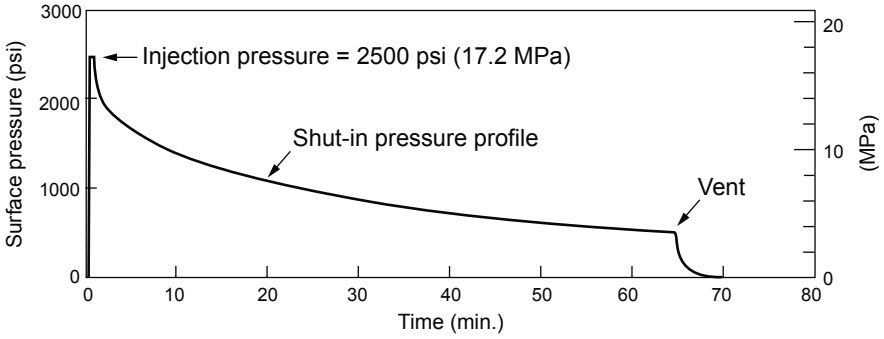

Fig. 3-9. Surface pressure during the first hydraulic fracturing test below the cemented-in liner (Zone 7) in GT-2. At a pumping rate of 3 BPM (8 L/s), some 105 gal. of fluid was injected in about 1 minute.
Adapted from Blair et al., 1976

Since many HDR staff had expected a real hydraulic fracture of unjointed granitic rock, at the time this result was not accepted as meaningful. However, it is now recognized that this was the most significant pressure-stimulation test that had been run so far in GT-2. The shape of the pressure profile is strongly indicative of a joint opening, with a very sharp rise followed by an abrupt "flattening out." The shut-in pressure profile following the joint opening is also typical of one for a previously sealed joint.

That the opening pressure for the stimulated joint(s) was as high as 2500 psi suggests a significant contribution to the joint normal stress from the overburden stress (σ_1)—indicating inclined joints that could well be at an angle of about 70°. If the joints opened had been near-vertical, their opening pressures would have been much lower (closer to the least principal earth stress of 1015 psi measured in GT-1—see the discussion following Table 1-2 in Chapter 1).

Further evidence that a joint (or joints) had been opened near the top of Zone 7 comes from the temperature fluctuations seen on temperature logs taken below the liner during these injection tests.

InfoNote

In the ideal case—rarely seen in the field—of a borehole drilled in a homogeneous and isotropic rock mass (with no flaws, such as pre-existing but resealed joints), hydraulic fracturing of the borehole wall takes place when the injection pressure is increased enough to just balance the minimum circumferential (hoop) stress concentration at the borehole wall (created when rock is removed by drilling) plus the tensile strength of the rock. During initial fracturing, a pressure "overshoot" occurs that is equal to the tensile strength of the rock; then, upon repressurization, the fracture reopens at a pressure equal to the minimum stress concentration at the borehole wall.

The "real" case—nearly always seen in the field—is that the rock mass contains a network of resealed joints. Under pressurization, a favorably oriented joint intersecting the borehole wall will open first—with a pressure overshoot roughly equal to the tensile strength of the joint-sealing material, which is much lower than that of the rock (in the range of 50 to 250 psi). In the oil industry, hydraulic fracturing is done in sedimentary rock, which typically has a tensile strength on the order of a few hundred to 1000 psi. In contrast, in laboratory testing, the Precambrian granitic rocks at Fenton Hill show tensile strengths of about 5000 psi, even when some microcracking (from stress relief following coring) is present. In the authors' experience over many years at Fenton Hill, no true "hydraulic fracturing" was ever observed.

To repair the leaking surface packoff assembly, the drill string had to be raised somewhat, which meant that the PBR mandrel had to be withdrawn from the PBR. Following the repair work, the mandrel was reset and pumping resumed. But when annulus outflow was observed shortly thereafter, pumping was again halted and the PBR mandrel was pulled out of the hole. Inspection revealed that the nylon chevron seals had been badly damaged during the reseating operation. The damage was so severe that the PBR sealing approach was abandoned; the rest of the pressurization tests in Zone 7 would instead be carried out with a casing packer set inside the liner. On September 21, a Baker Oil Field casing packer was run in on drill pipe and set inside the liner at a depth of 6325 ft.

The next two days were occupied with further injection testing. Flow into the opened joints was measured by means of a Schlumberger spinner logging tool, as water was pumped into the joints in increasing volumes (the largest single injection being 4600 gal. [17 000 L] at pressures of about 2500 psi [17.2 MPa] and flow rates of 3–4.5 BPM [8–12 L/s]). On the basis of results from 20 spinner runs, two zones of fluid acceptance—inclined joints—were identified: one at 6529–6540 ft (1990–1993 m) and one at

6559–6568 ft (1999–2002 m). From September 25 to 27, these two joints were further inflated/extended through three further injections, of 11 000, 20 000, and 36 000 gal. (42 000, 76 000, and 136 000 L), again at a maximum injection pressure of 2500 psi and a maximum flow rate of 4 BPM (11 L/s). (It should be noted that the two joints extensively "exercised" during this injection testing were different from—somewhat deeper than—those that had left impressions on the lowest Johnston packer during the first hydraulic fracturing test, before installation of the liner.)

One observation from the injection testing in Zone 7 that provoked a great deal of discussion was that despite repeated pumping and venting, much less than half of the injected fluid was recovered for each test. Several theories were proffered: (1) The pressurized joints were connected to a permeable, but much lower pressure, zone beyond the borehole that absorbed most of the flow; (2) permeation of the fracture walls by the fluid accounted for most of the loss; and (3) the intersections of the joints with the borehole, like pressure-activated diodes, were snapping shut with the release of borehole pressure and trapping the injected fluid within the pressure-dilated joints.

On a Sunday morning (September 28), when no one else was around, Roland Pettitt and Don Brown arranged with the Western Co. to perform a sand-fracturing operation. (In those days, such operations were possible without much procurement hassle—just the approval of Harry Allen, then director of the Supply and Property Division!) Pumping proceeded at a rate of 9 BPM (24 L/s), injecting 4500 gal. of treated water into the joints of Zone 7 (the water had been jelled with a cross-linked polymer mixed with 9500 lb of sand, for a sand loading of just over 2 lb/gal.; the polymer effectively suspended the sand in the fluid, preventing its loss during pumping). Because the mixture was highly viscous, the pumping pressure rose to about 2950 psi during this "treatment," opening the joints even wider. Following injection, the pump was shut in and the borehole immediately vented, leaving the joints "sand-propped." Over 90% of the injected fluid was returned in less than an hour, and continued venting recovered another 8%, for a total recovery of 98%!

Note: With the Western pump truck still on site, this would have been an ideal time for an injection test to determine the low-rate (3/4–1 BPM) injection pressure for the sand-propped joints. Unfortunately, this unique opportunity was missed.

This ad hoc experiment demonstrated the validity of the third theory—that the joints were snapping shut and trapping fluid within them. Beyond being an interesting experiment in its own right, it would have a profound influence on the HDR Project in the years to come: from it was born the recognition that the near-wellbore outlet impedance was controlled by joint closure. This meant that HDR reservoir production could be significantly increased only by finding ways to reduce the impedance created when joints

"snap shut" as a result of the injection pressure falling below the jacking pressure—i.e., below the closure stress normal to the plane of the joint.

By this time, it seemed obvious to some of the HDR staff that hydraulic pressure was opening pre-existing joints, not creating new vertical fractures. But for others—including Mort Smith, the HDR Project Manager, and several other high-level Project staff—the "penny-shaped fracture" theory still held sway. According to this theory, the way to develop a large HDR reservoir was to create a series of *en echelon* vertical fractures from an inclined borehole.[8] One of the ideas proposed to control the spacing of such an array of "penny-shaped" fractures was to fracture through discrete sets of perforations in casing, a method that appeared to offer a more straightforward way of controlling the inlet and outlet flow conditions of the reservoir than an open-hole completion. This idea was purely experimental; at the time, there was no established "theory" for fracturing crystalline rock through perforations (nor is there today!). A few of the HDR staff had hypothesized that because the jet-cut holes in the casing would extend at least several inches into the rock—beyond the high-stress region immediately next to the borehole—one might reach a point at which true hydraulic fractures would be initiated. They also surmised that in the absence of any overriding rock tensile strength, the pressures required to initiate fracturing might be somewhat lower. Thus, with the scab liner already cemented in place, the joints below it having been thoroughly exercised, and the cost of the experiment very low, it seemed an opportune time for the first-ever attempt at fracturing granitic rock through perforations in casing.

On September 30, eighty jet perforations were made in the cemented-in liner over a small (10-ft) zone: from 6370 to 6380 ft. A Johnston straddle packer assembly was then lowered into the hole and set over the 6345- to 6390-ft interval, bracketing the perforated zone. When this zone was pressurized with the Western Co. pump, the pressure rose to 1850 psi (12.8 MPa), but continuous flow up the annulus indicated leakage in the packer assembly, and there was no evidence of hydraulic fracturing of the rock exposed behind the perforations. The assembly was removed, and a Baker packer was set in the casing above the perforated zone, at 6330 ft.

[8]Nine years later, in the late fall of 1983, Dr. John Whetton (then division leader of the Earth and Space Sciences [ESS] division and manager of the HDR Program), Dr. Hugh Murphy, group leader of ESS-4 (Geoengineering), and Don Brown, project manager for HDR operations at Fenton Hill, visited the Halliburton Research Laboratory in Duncan, OK, to consult with world-recognized experts in the field of hydraulic fracturing about the upcoming Massive Hydraulic Fracturing Test at Fenton Hill. To a man, the Halliburton experts were convinced that a fresh and continuous vertical fracture could be created in the deep crystalline basement at Fenton Hill—despite the evidence to the contrary presented by Don Brown (showing that the multiple attempts to create hydraulic fractures had succeeded only in opening pre-existing joints).

But, the sand-propped joints below the liner were left exposed to the pressurizing fluid—first, because it was easier to carry out the test without having to install a bridge plug below the perforated zone (the plug would have had to be shipped to the site from Farmington); and second, because it was assumed that joints in the rock behind the perforations would open at a pressure lower than the 2500 psi at which the sand-propped joints had initially been opened (on September 14). The Western Co. pump was used to pump water into the hole for one hour at a low rate of 3/4 BPM (2 L/s) and a maximum pressure of 1950 psi (13.4 MPa). The system was shut in for 15 minutes, then vented. About 92% of the 2012 gal. of injected water was recovered.

Witnessing the unusually high fluid recovery upon venting, in combination with the low injection pressure, the HDR field engineers realized that most if not all of the injected water had gone not through the perforations—as some of the HDR staff had predicted—but into the sand-propped joints below the liner. To satisfy those few who still insisted that even a single fracture might possibly have been created through the perforations, this possibility was investigated by testing for flow communication between the joints below the liner and the supposed fracture. On October 2, the Baker packer was run in on drill pipe and set in the liner at a depth of 6432 ft, below the perforations (thereby exposing the perforated zone to the annulus outside the drill pipe), and Zone 7 was pressurized once again. The pumping continued for 2 hours at a rate of 3/4 BPM (2 L/s) and injection pressures as high as 2185 psi. Despite the prolonged pumping and high pressure, absolutely no flow communication with the annulus was observed. The zone below the liner was then vented, and within 5 hours 85% of the injected fluid had been recovered. Once again, the evidence indicated that the sand-propped joints below the liner were accepting all the flow.

In a final effort to fracture through the perforations, a more capable system was devised to straddle the 6370- to 6380-ft perforated zone. The drill pipe was made up with a bridge plug on bottom and a Baker packer above, then run into the hole and set with the top of the bridge plug at 6432 ft and the bottom of the packer at 6328 ft (a straddled interval of 104 ft). The Western Co. pump was then used to pressurize the rock behind the perforated zone. After several "false starts" due to pump problems, pressurization became steady at a rate of 4 BPM (11 L/s). During this fracturing test, a joint indeed was opened through the perforations, at about 6375 ft—but only with pressures far above any used previously. As shown in Fig. 3-10, the pressure reached a maximum of 3860 psi (26.6 MPa). But even at this high level, the surface pressure and the flow rate show typical joint-opening profiles, not those that would be seen if true hydraulic fracturing of unflawed rock had taken place. Starting about 20 minutes into the test, the pressure rises very steeply and linearly as the fluid in the drill pipe is compressed, then "rounds off" as fluid begins to permeate into the sealed joint (which is

still significantly more permeable than the surrounding rock). As the joint is progressively jacked open, the pumping pressure profile flattens out at its maximum and then gradually decreases as the pressure-dilated portion of the joint grows. This behavior made it obvious that one of the perforations in the rock had intersected a joint, facilitating its opening through hydraulic pressurization. A total of 2470 gal. of water was injected into this joint over the course of the test.

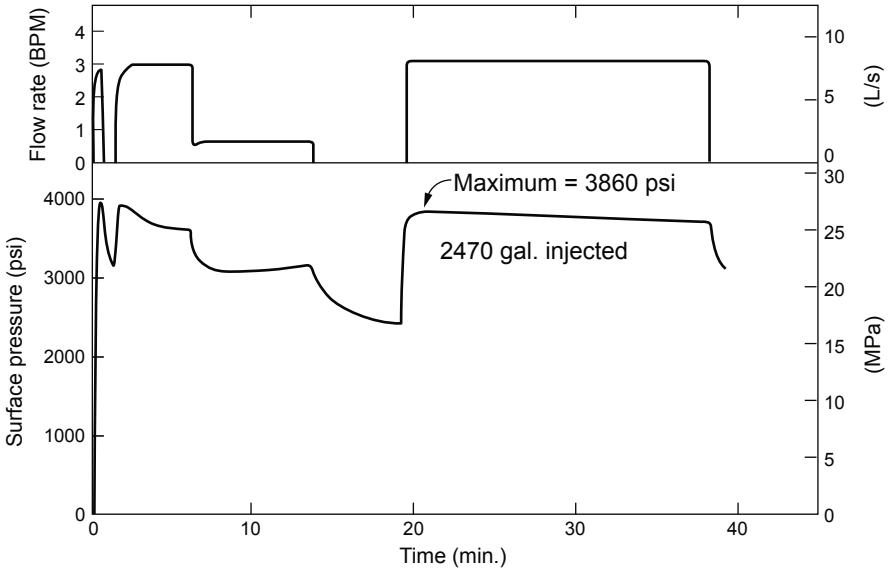

Fig. 3-10. Pressure stimulation through perforations in casing: pressure and flow profiles during stimulation of a high-opening-pressure joint in the 6370- to 6380-ft depth interval of the GT-2 borehole.
Source: Blair et al., 1976

By now, the HDR staff were becoming aware that to locate joints having low opening pressures, a far greater number of joints would need to be accessed—which would require pressurizing an interval much longer than 10 ft. The joint opened through the perforations, at a depth of 6375 ft, had an opening pressure significantly higher than those of the joints opened in Zone 7, below. Evidently the component of the vertical stress acting perpendicular to it was greater, indicating that it was more inclined toward the horizontal than the Zone 7 joints. Conventional analytical techniques were used to determine the probable inclination of this pressure-stimulated joint: Given a roughly north–south direction (orthogonal to the least principal earth stress of 1240 psi), and with the maximum earth stress being vertical and equal to the overburden stress, one can easily calculate the inclination of the joint—about 40° from the vertical.

The next day, the bridge plug and packer assembly were loosened and lowered, and the packer was reset at 6422 ft (below the perforations). This bottom section of the hole was then pressurized to 2200 psi (15.2 MPa) at a flow rate of 1.5 BPM (4 L/s), to ascertain whether there was now flow communication between the joint that had been opened through the perforations and those in the zone below the scab liner. When a brief but rapid rise occurred in the annulus water level, followed by a smaller, steady discharge of 3 gpm from the flow line, it looked possible (although the evidence was very tenuous) that a small amount of water was being "squeezed" out of the joint behind the perforations as the sand-propped joints below the liner were pressurized.

The Stage 1 and 2 hydrology tests and pressure-stimulation experiments showed that true rock fracturing had not taken place in GT-2, but rather preexisting joints had been opened and extended (dilated). Another observation was that although the rock at depth appeared to be extensively jointed, the rates of fluid leakage were quite small. On the basis of these findings, the Fenton Hill site was judged to be suitable for the development of a deeper HDR system.

Another Revision to the Plan

Considering what it had already cost to drill GT-2 to this depth, and the relatively low incremental cost to further deepen this exploratory borehole, the Project staff decided to continue drilling to about 9600 ft—at which depth the rock temperature was estimated to be about 200°C. This additional work would provide information on the geology, hydrology, and character of the rock mass at this greater depth, which would be important for confirming the suitability of the Fenton Hill site for the world's first demonstration of HDR heat extraction. Accordingly, a schedule was drawn up for a third stage of drilling, including coring, testing, and post-drilling diagnostic logging operations. Previous experience suggested that each bit would be able to drill about 500 ft of hole in three days. The plan was to drill to depths of approximately 7920 ft, 8420 ft, 8930 ft, and 9440 ft; at each of these depths, the hole would be circulated clean, a 24-hour bottom-hole temperature measurement would be taken, and a 10-ft core would be cut.

Once the drilling of GT-2 was complete, a longer (600-ft) scab liner/PBR assembly would be cemented in just off bottom. This assembly would provide a very good platform for pressure stimulation of the basement rock below the liner, eliminating the problems and uncertainties encountered so frequently with the unreliable open-hole packers. It would also offer a standard environment for anchoring and setting the much more reliable high-temperature, high-pressure casing packers (if needed). Finally, it would make available a test interval long enough to thoroughly investigate

fracturing through perforations. The suggestion was also made that, should fracturing through perforations succeed in creating a large joint system that was connected to the joint(s) below the liner, it might be possible to set up a one-hole circulation experiment. By pumping through drill pipe and a deep-set packer into a zone below the liner, water would be circulated up through the interconnected joints, through the perforations above the packer, and finally into and up the annulus outside the drill pipe. To allow for these various options, an extensive series of hydrology, geophysical, and pressurization tests was planned to follow the third stage of drilling.

The information on Stage 3 operations is abstracted largely from Pettitt (1975b and c), Blair et al. (1976), and Smith (in preparation).

Stage 3 Drilling

After the bridge plug and packer assembly had been removed from the GT-2 borehole, preparations began to remove the scab liner. A washover drilling assembly was put together and run into the hole on drill pipe, but the operation met with some difficulties: first and foremost, the basement rock was extremely hard (typically, washover operations are employed in the much softer sedimentary rock found in oilfield situations); second, the outer diameter of the PBR section at the top of the liner was almost equal to the inner diameter of the washover bit; and third, the centralizer fins that had been welded to the outside of the liner extended almost to the borehole wall. On two different occasions, the washover bit became stuck and then the jarring tools broke and had to be fished out of the hole. It was only on October 11 that the last piece of the liner assembly was finally removed from the hole. A full-face, 9 7/8-in., STC Q9 (TCI) mining bit with a junk basket was then run in to ream out the residue of the cement that had held the liner in place. By early on October 12, the bit had reached the hole bottom at 6702 ft.

Drilling now proceeded, with a new STC Q9 bit and water as the circulating fluid. The bit managed to drill only 15 ft of new hole before its action became very erratic, an indication that considerable junk remained at the bottom of the hole from the washover operation. The bit was pulled and a magnet was run into the hole, which retrieved a large number of metal chips. Drilling then resumed, with another STC Q9 mining bit. By October 16, this bit had reached a depth of 7102 ft, having drilled 385 ft in 48 actual drilling hours—or 8.0 ft/h. (Five additional magnet runs and three viscous mud sweeps had been interspersed with the drilling, to further clean the hole of metal particles.)

With the hole apparently finally clean, the first coring assembly was made up with a 9 5/8-in. × 4 1/2-in. Christensen diamond core bit. Coring of a 2-ft interval, from 7102 to 7104 ft (Coring Run 22) obtained approximately 75% core recovery (a 6-in. stub of core was left at the bottom of the hole when the assembly was pulled). On October 18, drilling recommenced with

the last available 9 7/8-in. STC Q9 mining bit. During this run, while the bit was drilling at a depth of 7107 ft, the drill pipe broke at a tool joint at about 6000 ft. By October 20 the pipe had been fished out of the hole, and drilling then resumed with the same bit, taking the hole to a depth of 7485 ft. This STC bit averaged 5.6 ft/h in 67 hours of drilling.

The Arab oil embargo of 1973 had given rise to a huge upsurge in domestic oil drilling, and a consequent shortage of drilling equipment—including the 9 7/8-in. STC bits that had been used for Stage 3 drilling to this point. For this reason, the remainder of the Stage 3 drilling program was carried out with Dresser-Security 9 5/8-in. H10J bits. On a rock-hardness scale of 1 to 10, these bits were designated 10: capable of drilling the hardest, most competent rock types (such as chert, quartzite, taconite, and granite). The first run with a Security bit took the hole to 7918 ft in 58.5 hours—an average penetration rate of 7.4 ft/h, which was significantly better than the rates achieved with the STC bits. Following this bit run, the bottom-hole temperature was measured over a 24-hour period; the recovering temperature was 161°C, which extrapolated to 164°C at infinite time.

After a short coring run—only 1 ft—with a Christensen diamond bit (Run 23), drilling began again on October 29 with a new H10J bit. Eighty-one hours and 658 ft later, the hole depth had reached 8577 ft—again at a very respectable rate for penetration of granitic rock, 8.1 ft/h. When the bit was finally pulled on November 2, it was found to be 1/8 in. under gauge, but all three cones were still reasonably tight, indicating minimum wear of the bearings. At this depth, the deviation of the hole from vertical was 2 1/8°, in a westward direction. Following a 24-hour bottom-hole temperature measurement, a JOIDES bit was used for a 10-ft coring run (No. 24), to 8587 ft; core recovery was 70%.

A break in drilling, between November 4 and 7, was used to return to a joint previously opened higher in GT-2—in the 6535- to 6564-ft interval, within Zone 7. In an attempt to determine the orientation of that joint, several runs were carried out with Lynes impression packers. The most successful of these yielded an impression about 4 ft long, of a vertical joint centered at 6535 ft; this no doubt was the upper "inclined" joint identified earlier (September 22–23) by spinner logging over the depth interval 6529–6540 ft. It had been identified as inclined because of its apparent short (11-ft) intersection with the borehole. However, the impression packer now showed it to be vertical, but truncated at the top and bifurcated at the bottom (Fig. 3-11). The orientation of this joint was found to be approximately northeast–southwest—a somewhat surprising result given the direction of the least principal earth stress at this depth (inferred to be east–west, roughly orthogonal to the normal faulting exhibited by the caldera ring-fracture zone immediately to the east).

Fig. 3-11. Lynes packer showing impression (enhanced by chalk rubbing) of a vertical joint centered at 6535 ft.
Source: Pettitt, 1975c

Note: During a later attempt to determine the orientation of the "target" joint opened at about 9600 ft in GT-2,[9] the NE–SW orientation of the joint at 6535 ft would be invoked. But the underlying assumption, that the orientation of the higher joint could be extrapolated downward more than 3000 ft to the bottom of GT-2, was a misguided one and would confuse subsequent efforts to determine the best trajectory during directional drilling of EE-1 to intersect the target GT-2 joint.

[9]See *Stage 3 Pressure-Stimulation Tests* below.

Drilling began again on November 7, but two days later, at a depth of 8842 ft, problems developed with the rotary swivel. The swivel was replaced, a new H10J bit was run in, and over the next 75 hours the borehole was deepened by 672 ft, to 9514 ft. When the bit was pulled after this very long bit run in very hard granitic rock with only water as the circulating fluid, it was found to be only 1/8 in. under gauge and the cones were only slightly loose—a remarkable performance even by today's standards.

The next two days were spent measuring temperatures within the borehole, for use in formulating the cement for the planned installation of a 608-ft scab liner. Before being run into the hole, the drill pipe was fitted with a specially fabricated, low-conductivity phenolic end section, for better thermal insulation of the temperature sonde from the drill pipe (this end section, having a diameter nearly that of the borehole, would also inhibit fluid convection in the narrow annulus separating it from the borehole wall). Following the temperature measurements, two JOIDES coring runs (Nos. 25 and 26) deepened the hole to 9537 ft.

On November 19, a 10-ft-long, 7 7/8-in.-diameter pilot hole was drilled from the bottom of the 9 5/8-in.-diameter borehole to provide a ledge for landing the liner. The bit was then pulled and replaced with a coring assembly fitted with a 7 7/8-in.-diameter Christensen diamond core bit. Because of fluid circulation problems, coring progressed very slowly: it took some 8 hours to cut 2.7 ft of core. When the coring assembly was withdrawn from the hole, only the inner core barrel (no core) was still attached; the outer core barrel, the core bit, and the stabilizer had been left at the bottom of the hole.

On the morning of November 25, fishing tools were being lowered into the hole when the hydraulic brake on the drilling rig failed and the traveling block (with 9200 ft of drill pipe attached) fell onto the rotary table. Although the drill pipe remained in the elevators and was caught at the rotary table, the severe jolt caused a tool joint to separate, sending the bottom 4000 ft of pipe to the bottom of the hole. This pipe now had to be fished from the hole as well (once it was out, 85 of the joints required straightening). Finally, on November 29, the outer core barrel was fished from the hole, but the bit and stabilizer were not recovered. Milling and washover operations, which continued until December 7, ground up both—along with any core that had been cut. The bottom of the hole was then cleaned up by drilling ahead to a depth of 9581 ft (2920 m) with a 9 5/8-in. TCI bit.

On December 8, a new pilot hole was drilled to create the ledge for landing the scab liner. This time the hole was centralized; it was drilled 5 ft deep with a 7 7/8-in. bit made up on the bottom of a 9 5/8-in. stabilizer. On the last day of drilling in GT-2, December 9, 1974, the 7 7/8-in. pilot hole was deepened another 33 ft to provide a 38-ft open-hole section ("rat hole") below the ledge. At a final depth of 9619 ft, GT-2 was now the deepest borehole ever drilled in granitic rock. It was probably also the hottest: the

equilibrium bottom-hole temperature measured at 9607 ft was 197°C, and the geothermal gradient was 60°C/km (compared with 50°C/km at about 6000 ft). On the basis of information derived from deviation and directional surveys, the bottom of GT-2 was calculated to be offset from the surface location by about 360 ft, to the northwest.

With Stage 3 drilling complete, the 608-ft, 7 5/8-in. scab liner, with a PBR assembly at the top, was successfully landed on the ledge at 9581 ft and cemented into the hole. (Although the casing was slightly smaller in diameter than the centralized 7 7/8-in. hole below it, the pull of gravity held the casing to the low side of the modestly inclined borehole.) Once set, the cement in the liner and in the open-hole interval below the liner was drilled out with a 6 3/4-in. bit. A system was then designed to enable pressure stimulation of the open-hole region below the liner after release of the drilling rig: a string of 4 1/2-in.-diameter, high-pressure casing with a PBR mandrel on bottom was run into the hole and stabbed into the top of the PBR. Testing showed that the casing assembly and the liner were pressure-tight. On December 20, the drilling rig was released.

Table 3-5 shows the major Stage 3 drilling runs, and Table 3-6 shows the Stage 3 coring runs. Figure 3-12 is a schematic representation of the completed GT-2 borehole.

Table 3-5. Major Stage 3 drilling runs in GT-2

Drilled depth, ft (m)	Drilled interval, ft (m)	Drilling time (h)	Rock type	Average penetration rate, ft/h (m/h)
6717–7102 (2047–2165)	385 (117)	48	Biotite-granodioritic gneiss, biotite-tonalite gneiss	8.0 (2.4)
7107–7485 (2166–2281)	378 (115)	67	Biotite-tonalite gneiss, biotite-granodioritic gneiss, monzogranitic gneiss	5.6 (1.7)
7485–7918 (2281–2413)	433 (132)	58.5	Granodioritic gneiss, monzogranitic gneiss	7.4 (2.3)
7919–8577 (2414–2614)	658 (200)	81	Monzogranitic gneiss, biotite granodiorite	8.1 (2.5)
8587–8842 (2617–2695)	255 (78)	30.75	Biotite granodiorite	8.3 (2.5)
8842–9514 (2695–2900)	672 (205)	75	Biotite granodiorite	9.0 (2.7)

Table 3-6. Major Stage 3 coring runs in GT-2

Coring run	Cored interval, ft (m)	Recovery (%)	Core bit (J=JOIDES-type; C=Christensen)	Rock type*
22	7102–7104 (2164.7–2165.3)	75	C	Biotite tonalite monzogranite
23	7918–7919 (2413.4–2413.7)	100	C	Leucocratic monzogranite
24	8577–8587 (2614–2617)	70	J	Biotite monzogranite pegmatite
25	9519–9527 (2901–2904)	50	J	Biotite granodiorite
26	9527–9537 (2904–2907)	50	J	Biotite monzogranite

* All rock types were determined by petrographic examination of thin sections.

Note: As mentioned earlier, after the creation of ERDA in January 1975, the plan for GT-2 as an exploratory borehole and, later, for reservoir interrogation—separate from the HDR circulation loop—was abrogated by Division of Geothermal Energy (DGE) management at ERDA headquarters in Washington, DC. Instead, GT-2 was to become the first "leg" of the circulation loop, i.e., the reservoir creation and injection well. However, several role reversals and two redrillings later, GT-2 would finally end up as the production well for the Phase I reservoir.

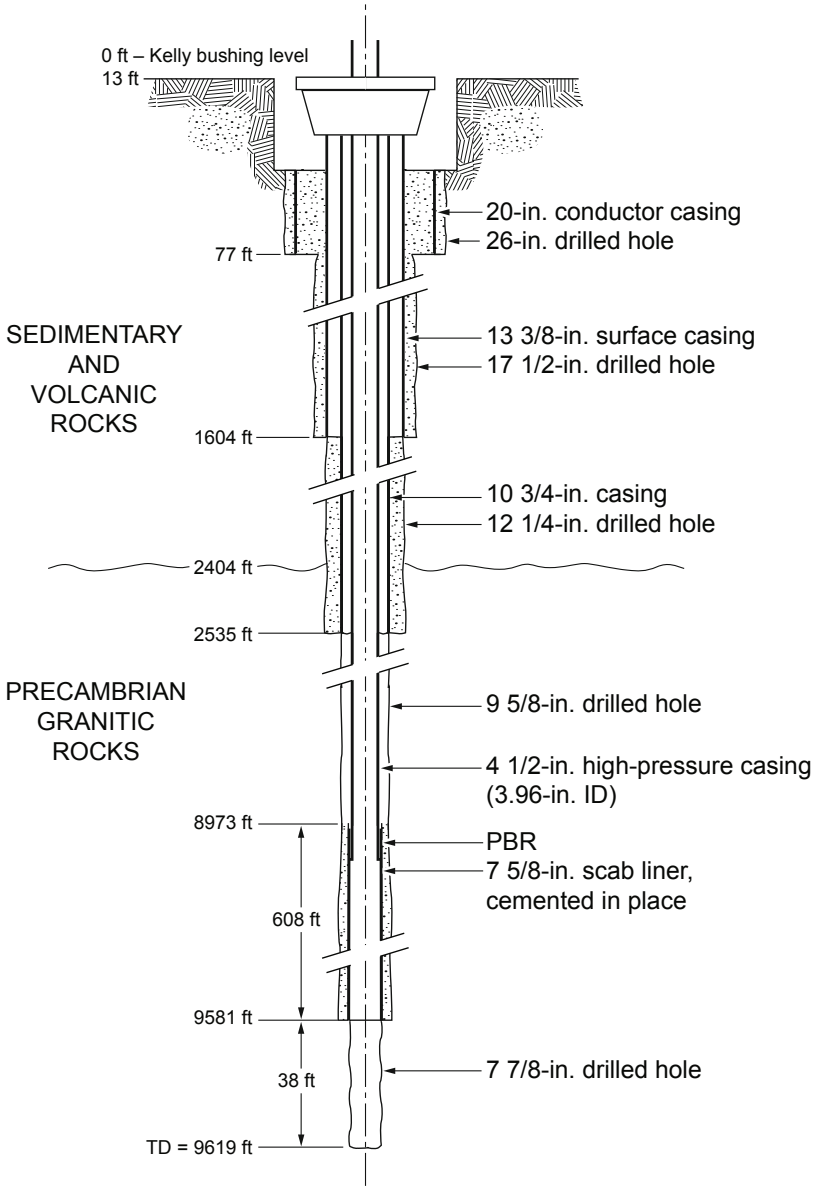

Fig. 3-12. The GT-2 borehole, as completed in December 1974.
Source: Blair et al., 1976

Physical Properties of the Rock Matrix (as Derived from GT-2 Cores)

With the GT-2 borehole completed to a depth of 9619 ft, the core samples that had been taken intermittently during drilling were analyzed for information regarding the properties of the rock matrix. As noted earlier, core materials do not generally yield data relevant to reservoir development and flow performance, but they do yield data useful for reservoir modeling.

In Situ Permeability (Inferred from Laboratory Measurements)

The *in situ* permeability of the crystalline rock matrix is stress-dependent and determines how much water will be lost by diffusion to the region beyond the boundary of the pressure-dilated reservoir. Despite its importance in computing this loss, *in situ* permeability is generally not included in descriptions of the physical properties of crystalline rock because, being stress-dependent, it is very difficult to measure in the laboratory. This is particularly true at the very high stress levels of interest—those representing deep *in situ* conditions, under which the matrix permeability is completely controlled by the network of interconnected, pre-existing microcracks. But when the rock is removed from its deep environment by coring, these stresses are relieved, strain relaxation (expansion) takes place, and a fresh fabric of microcracks overprints and completely dominates the *in situ* fabric. The only way to replicate the *in situ* conditions is to reclose the new microcracks—a difficult task at best. The sample, essentially in the shape of a cube cut from the original core, must be repressurized in a special triaxial stress fixture. The very small residual permeability of the sample can then be measured. Unfortunately, one can never be entirely certain that the fresh microcracks have been closed precisely enough to eliminate some minor influence on the measured permeability.

Only a very few researchers, such as Gene Simmons at MIT and those rock mechanics specialists working with the HDR Project at Los Alamos, have attempted to obtain relevant permeability values by such a technique. The permeabilities for two GT-2 core samples measured in this way at Los Alamos are given in Fig. 3-13, as a function of confining pressure at 24°C up to 5000 psi (34.5 MPa). As shown, the difference in permeability between the two samples is close to an order of magnitude, suggesting that—at least in the case of the deeper sample—the stress fixture could not totally reclose all the fresh microcracks. The figure also shows that during the first 1000 psi or so of compression, the measured permeabilities of both samples changed very rapidly: they dropped by an order of magnitude as the fresh set of microcracks was being reclosed.

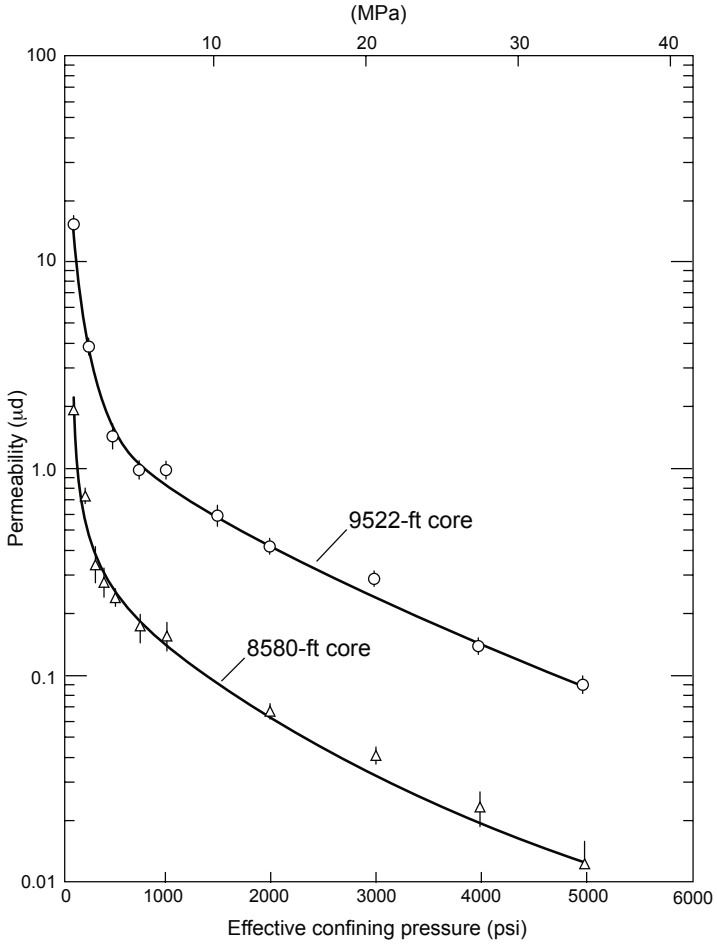

Fig. 3-13. Permeability as a function of effective confining pressure at 24°C (based on two granitic core samples from GT-2).
Adapted from HDR, 1978

Microcrack Porosity

As with the matrix permeability, the microcrack porosity of the crystalline matrix must be measured under conditions of *in situ* stress. The data shown in Fig. 3-14, based on the work of Gene Simmons at MIT, shows how porosity values vary according to depth of core retrieval. The apparent large spread in these data undoubtedly reflects not only the difficulty of making the measurements, but the vagaries in recovery and handling of the core samples. The surprising result from these measurements is that the average deep porosity at Fenton Hill is on the order of 0.0001 (0.01%)—100 times smaller than porosity values typical of "tombstone" granites.

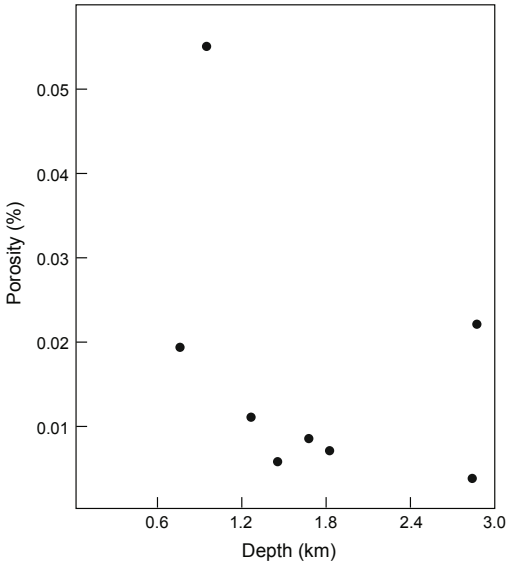

Fig. 3-14. *In situ* microcrack porosity as determined by differential strain analysis (after Simmons and Cooper, 1977).

Thermal Conductivity

The predominant heat transfer mechanism within an HDR reservoir is convection, by the fluid flowing through the dilated joints. The thermal conductivity (λ) of the rock matrix, which is primarily dependent on the matrix mineralogy, is used in thermal modeling of the reservoir (to calculate the transfer of heat from the interiors of the rock blocks to the joint surfaces). Table 3-7 summarizes the thermal conductivity results obtained from GT-2 cores.

Table 3-7. Thermal conductivity of rocks from GT-2, W/(m-K)

Depth (ft)	0°C	50°C	100°C	150°C	200°C	250°C
λ Parallel to core axis*						
2580	3.785	3.475	3.206	2.998	2.820	2.680
4918	3.800	3.475	3.209	2.981	2.797	2.646
5964	2.900	2.714	2.565	2.440	2.341	2.260
6153a	3.475	3.222	2.992	2.836	2.713	2.608
6153b	3.413	3.143	2.921	2.735	2.584	2.466
6156	2.908	2.777	2.625	2.503	2.393	2.292
λ Perpendicular to core axis*						
8579	3.125	2.990	2.852	2.750	2.660	2.595
9608	3.115	2.906	2.728	2.587	2.473	2.376

*A cut bar comparator was used for the parallel measurements and a needle probe for the perpendicular measurements.

These conductivity values compare quite favorably with those in standard handbooks listing rock physical properties (e.g., S. P. Clark, *Handbook of Physical Constants*, 1966). The variation with temperature—an average decrease of 22% between 0°C and 200°C for the first six core samples measured—is in particularly good agreement with the values given in this handbook for Barre and Rockport granites (–17% and –23%) and for quartz monzonite (–22%).

Other Physical Properties

A number of other physical properties (including density, P-wave and S-wave sonic velocities, and elastic parameters) were measured on samples from 17 cores taken in the 2570- to 5240-ft (780- to 1600-m) depth interval of the Precambrian basement rock in GT-2.

Densities were determined in the laboratory by the U. S. Bureau of Mines and were found to be in good agreement (±2%) with field density logs collected by a service company (Table 3-8).

Table 3-8. Density: laboratory vs field measurements (averaged values)

	Density (g/cm^3)	
Sample depth, ft (m)	U. S. Bureau of Mines Laboratory	Field logs
2580 (786)	2.64	2.70
2600 (792)	2.66	2.71
2844 (867)	2.62	2.64
2857 (871)	2.61	2.64
3151 (960)	2.66	2.68
3464 (1056)	2.61	2.62
3697 (1127)	2.63	2.63
4279 (1304)	2.63	2.60
4894 (1492)	2.64	2.59
4915 (1498)	2.64	2.64
5234 (1595)	2.69	2.55

The ambient-temperature P-wave and S-wave velocities were also measured in both the field and the laboratory. In this case, the comparison (Table 3-9) did not show such close agreement. The laboratory-measured velocities were consistently lower than the field-measured ones—attributable primarily to the superimposed array of fresh, stress-relief-derived microcracks in the cores.

Table 3-9. P-wave and S-wave velocities: laboratory vs field measurements (averaged values)

Sample depth, ft (m)	P-wave velocity (km/s)		S-wave velocity (km/s)	
	Lab	Field	Lab	Field
2600 (792)	5.89	6.03	3.43	3.43
2850 (869)	5.88	6.33	3.47	3.52
3151 (960)	4.98	5.78	2.91	2.97
3464 (1056)	5.66	6.02	3.19	3.43
3697 (1127)	5.87	5.86	3.49	3.51
4279 (1304)	5.86	5.99	3.43	3.49
4894 (1492)	5.85	5.93	3.47	3.52
4915 (1498)	5.53	5.98	3.39	3.54
5234 (1595)	5.90	6.03	3.42	3.56

The P-wave and S-wave velocity data were then used to calculate average elastic parameters (Table 3-10).

Table 3-10. Average elastic parameters, as derived from P-wave and S-wave velocity data

Elastic parameter	Lab	Well log
Young's modulus (GPa)	71.6	78.7
Shear modulus (GPa)	30.2	31.4
Bulk modulus (GPa)	47.0	54.1
Poisson's ratio	0.257	0.255

Stage 3 Hydrology Experiments

Static hydrology testing in the rat hole, to estimate the permeability of the exposed rock mass, began on January 8, 1975. At that time, the water level in the 4 1/2-in.-diameter high-pressure casing string was at 120 ft below the ground surface, whereas the level in the annulus around it (above the scab liner) was at 325 ft below the surface. The fact that the two levels had not equilibrated over the nearly five weeks of inactivity since the completion of GT-2 indicated that the casing string and PBR were pressure-tight. Observations throughout the next week revealed that the level in the casing (the inner diameter of which was 3.96 in.) was dropping about 5 ft per day, while that in the annulus was dropping about 7 ft/day.

The significance of these water-level measurements in the annulus—approximately 6600 ft of exposed borehole—is of course open to much interpretation because there are so many unknowns: the wall of the borehole was intersected by a number of open joints of unknown surface area that

were pressure-stimulated during earlier experiments; it had been exposed to a varying head of water in the annulus; and the diffusion of fluid—some into microcracks in the rock matrix along the entire borehole wall and some into joints—took place over a protracted period and at varying water levels. These many unknowns rendered rock permeability analyses almost impossible for the extensive section of exposed borehole above the liner.

However, for the rat hole, which was drilled nine months after the beginning of drilling and testing in the basement rock, the permeability of the rock adjacent to the borehole surface is much easier to estimate. Assuming (on the basis of fluid diffusion modeling) that after a one-month "soak" at almost full hydrostatic pressure, the pressurized fluid would have penetrated the borehole wall to a depth of about 3 cm, one can derive a rock permeability on the order of 0.01 microdarcy—very low indeed. Core permeability measurements (see Fig. 3-13) proved to be in good agreement with this estimate.

Three pressurization hydrology experiments took place on January 28, at surface pressures of 400, 800, and 1200 psi (below the joint-opening pressure of about 1400 psi), but no data or analyses were reported for these experiments.

Stage 3 Pressure-Stimulation Tests

The numerous joint stimulation and inflation tests carried out between January and May 1975 in the 38-ft rat hole (at the bottom of GT-2, below the cemented-in scab liner) are summarized in Figs. 3-15 and 3-16.[10] Their purpose was to obtain data that could be used to

- determine the joint-breakdown pressure, the joint-inflation pressure, and the flow-rate-dependent joint-extension pressure; and
- develop techniques to determine the orientation of a "hydraulic fracture" and measure its surface area during each stage of extension.

It appears that over the course of these tests, one favorably oriented, resealed joint at about 9600 ft was pressure-opened, repeatedly inflated and vented, and finally extended. (It should be remembered that at this time, the concept of the penny-shaped vertical fracture still dominated the thinking of the Project staff.)

Figure 3-15 summarizes the results of the first series of eleven tests. These included pressurization, constant-pressure, and pressure-decay tests, at surface pressures ranging from 400 to 1600 psi (and one brief—unplanned—excursion to 1750 psi on March 8).

[10]The lack of detail in these figures is unfortunate, but in the case of these particular experiments, no additional information is available from the reports of the time, except for some brief notes in Mort Smith's *The Furnace in the Basement Part II.*

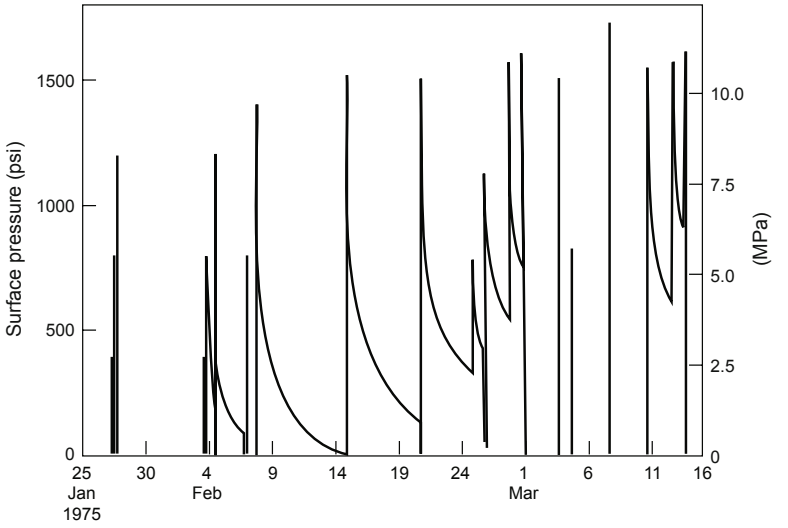

Fig. 3-15. Pressurization testing in the bottom 38 ft (rat hole) of the GT-2 borehole, January 25–March 16, 1975.
Source: Blair et al., 1976

The rat hole was pressurized to 1400 psi for the first time on February 8. With the pressure held at that level, 200 gal. of water was injected, indicating that a joint intersecting the rat hole (at a depth of about 9600 ft) had been opened by pressure-stimulation. The joint was then vented all the way down to zero pressure. Over the next several weeks, each time the rat hole was repressurized (to slightly higher levels—on the order of 1500 psi) and then vented, this joint accepted the same amount of fluid: about 200 gal. This finding, which indicated no growth of the joint, led—finally—to a "best guess" that the extra volume represented fluid storage in a near-vertical, unsealed or reopened ancient joint (not a true hydraulic fracture). In addition, water loss from the pressurized volume was very small, indicating that this joint was tightly confined within the rock mass and that the permeability of its exposed surfaces was very low.

An inadvertent pressurization of the rat hole to 1750 psi on March 8 further opened and extended this joint, to a volume of about 800 gal. It appears that this near-vertical joint was oriented approximately perpendicular to the least principal earth stress at that depth (1240 psi above hydrostatic pressure).[11] If this was indeed a single joint, its radius, calculated on the basis of elastic fracture mechanics, would have been about 100 ft. The permeability of the

[11]This value for the least principal earth stress at 9600 ft in GT-2 is not much larger than the mean 1015 psi measured at 2428 ft in the GT-1 borehole, demonstrating that at Fenton Hill, the least principal earth stress does not vary greatly with depth. This observation is consistent with the expected tectonic stress environment for the extensional Rio Grande Rift immediately to the east.

dilated joint's surfaces and, most important, of its sealed periphery, was very low—about 0.3 microdarcy (but still higher than the 0.01 microdarcy calculated for the wall of the 38-ft rat hole before stimulation).

The next series of tests took place from mid April through early May 1975 (Fig. 3-16). On April 21, some 1600 gal. of water was pumped into the rat hole at 8.5 gpm. The pumping pressure reached 1700 psi and was held there for 3 hours, during which time a number of seismic signals were observed at the surface (an indication that the joint was pressure-dilating and probably undergoing some shear displacement). The hole was then shut in overnight and the pressure decay recorded. The next day the system was vented and the procedure repeated, with similar results—except that the amplitude of the seismic signals and the rate of pressure decay were both smaller. It appears that the first set of seismic signals represented the extension of the joint—to a calculated radius of about 200 ft—whereas the second set (after venting), which was less energetic, represented only the reinflation of the previously extended joint. In a further reinflation test, both the joint-opening and reinflation pressures rose slightly, by about 20 psi. This phenomenon would be observed again in 1993–95, during the long-term flow testing of the Phase II reservoir, and is probably attributable to a localized increase in pore-fluid pressure just ahead of the undilated tip of the sealed—but somewhat permeable—joint. As Mort Smith observed, this effect might prove useful for broadening the pressure range over which a circulation loop could be operated without causing uncontrolled extension of joints (a very perceptive observation for this early stage in pressure testing of opened joints!).

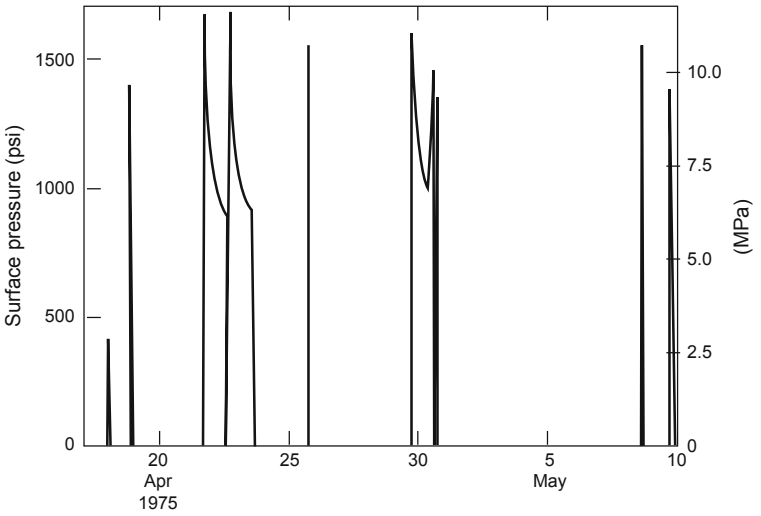

Fig. 3-16. Pressurization testing in the bottom 38 ft (rat hole) of the GT-2 borehole, April 15–May 10, 1975.
Source: Blair et al., 1976

Another important observation of Mort Smith's at this time was that the geology of the Precambrian basement was much more complex than previously thought. The bottom 1120 ft of the GT-2 borehole traversed a very uniform, intrusive granodiorite, which—like the basement rock above it—was criss-crossed by many ancient joints. But because these joints were all tightly sealed with secondary minerals, the rock mass had very low permeability, making it well suited for the containment of a pressurized circulation loop.

Water-loss measurements were used to assess how pressurization was affecting fluid flow into the surfaces of the 9600-ft-deep opened joint: at a surface pressure of 600 psi, the rate of water loss from the rat hole was 1 gpm; at 900 psi it was 4 gpm; and at 1200 psi it was 5.6 gpm. A total of 600 gal. of water was injected in this series of tests, of which about half was recovered in the first two hours of venting and 95% in four days. The obvious conclusion is that at this depth, water losses from a pressurized circulation loop should be very low.

A final series of pressurization tests were carried out during July and August, 1975 (Fig. 3-17), to further study fracturing through perforations (it would be the last such effort; with its termination, this reservoir completion concept was finally, and unequivocally, "laid to rest"). This series of tests even included an attempt to grow two "fractures" simultaneously—by pressurizing them at the same time—with the hope of fracture coalescence (if the "fractures" were truly vertical, they would be almost coplanar in a borehole inclined only 2° from the vertical).

To prepare for the testing, the 4 1/2-in. casing string was removed from the hole and five 10-ft-long zones of the scab liner (centered at depths of 9150, 9250, 9350, 9450, and 9550 ft) were perforated. For each pressurization, a Baker straddle packer assembly was set across a selected perforated zone (each zone was pressurized several times). The lowest opening pressures recorded—on the order of 1800 psi—were for Zone B (centered at 9250 ft), indicating that this zone contained, or was closely connected to, the most favorably oriented joint(s) pressurized during these tests. Toward the end of the tests, the joints at 9450 ft and 9550 ft were pumped simultaneously (see D+E in Fig. 3-17). Then the lower joint (E) was pressurized by itself, but there was no evidence of communication with the upper joint. However, because the lowest perforations apparently had become plugged with drill cuttings, the pressure rose to nearly 5000 psi, making this test inconclusive.

With each pressurization, the result was somewhat different, but the tests did demonstrate that higher pressures—higher than those required to open and extend the favorably oriented joint exposed in the rat hole below—were always required to stimulate joints through perforations. It was this finding that brought an end to such tests. In addition, in about a third of these tests, the packers leaked or ruptured (most of these were not even recorded and thus do not appear in the figure).

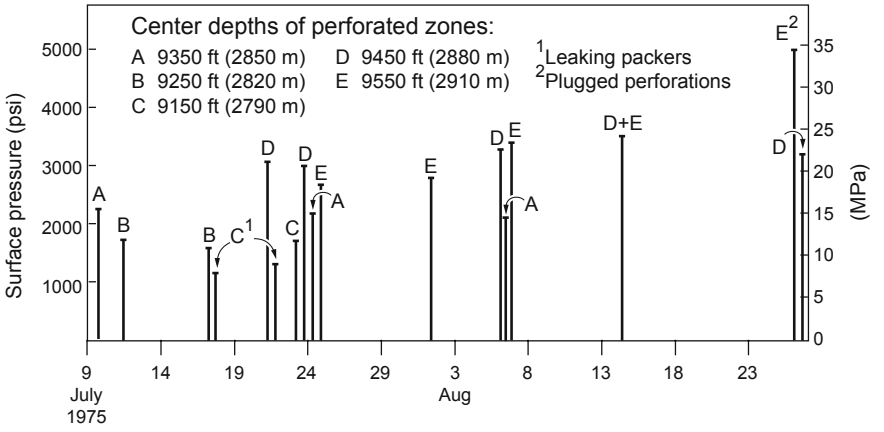

Fig. 3-17. Results of "fracturing" through perforations in the scab liner in GT-2, July and August 1975.
Source: Blair et al., 1976

Planning, Drilling, and Testing of the EE-1 Borehole

The Drilling Plan

The original drilling plan for EE-1, the designated production well for the two-hole circulating system, called for the upper part of the hole to be offset from GT-2 by about 250 ft to the north, and drilled nearly vertically to a depth of about 7000 ft. (This part of the plan assumed that EE-1 would drift off to the northwest as GT-2 had done, following a more or less parallel path.) Then, conventional directional-drilling techniques would be used to gradually rotate the lower portion of the borehole to the south until it intersected the upper part of the large joint opened at a depth of about 9600 ft near the bottom of GT-2 (the concept shown in Fig. 3-1). This joint was believed—from the interpretation of pressure-stimulation data—to be near-vertical with a radius of about 200 ft and to have a northwest–southeast orientation. To intersect it from a direction roughly perpendicular to its plane, EE-1 would need to be directionally drilled.

But during the late summer of 1975, while the vertical portion of EE-1 was still being drilled, a serious disagreement would arise among the HDR Project staff regarding the orientation of the GT-2 joint—whether its strike was northwest–southeast, northeast–southwest, or somewhere in between. However, given the general agreement that the joint was probably near-vertical, and thus should extend directly below the bottom of GT-2 whatever its orientation, after much discussion the decision would be made to directionally drill the lower portion of EE-1 to pass about 50 ft directly beneath the bottom of GT-2, rather than to one side or the other of the upper

extension of the joint. This drilling path would also prevent inadvertent drilling into the GT-2 borehole, a risk with any attempt to intersect the upper part of the pressure-opened joint. This change in plans meant that the roles of GT-2 and EE-1 would be reversed: GT-2, now the shallower borehole, becoming the production well and EE-1 the injection well. Fortunately, a final casing string had not yet been run and cemented in place in GT-2, precluding a serious problem: had the casing been run, it would have been set in compression before cementing for an injection role, rather than tensioned for a production role.

The drilling site for EE-1 (Fig. 3-18) was located 252 ft roughly north of GT-2 (on a bearing of N14E) and only about 8 ft higher in elevation. As detailed in Table 3-11, EE-1 would be drilled in two stages, to a final inclined depth (TD) of 10 053 ft (3064 m). Much of the information on the drilling and testing operations in EE-1 is taken from Pettitt (1977b) and Blair et al. (1976).

Fig. 3-18. Aerial view of the Fenton Hill site, showing GT-2 on the left (with a workover rig over it), and EE-1 in the center.
Source: HDR Project photo archive

Table 3-11. EE-1 drilling operations

Drilling stage	Start date	Final depth, ft (m)
1	May 26, 1975	6886 (2099)
2	Aug. 31, 1975	10 053 (3064)

Stage 1 Drilling

Stage 1 drilling began on May 8, 1975. A hole 10 ft deep and 4 ft in diameter was drilled, into which a 10-ft length of 30-in.-diameter corrugated metal pipe was cemented as the conductor casing. The next day a letter of intent was sent to Signal Drilling Company of Denver, Colorado, and a week later Signal began moving equipment for its No. 5 drilling rig to the EE-1 location. Mobilization was complete by May 25 (Fig. 3-19). The top of the Kelly bushing was set at 8711.3 ft (2655 m), 15 ft above the ground level of 8696.3 ft.

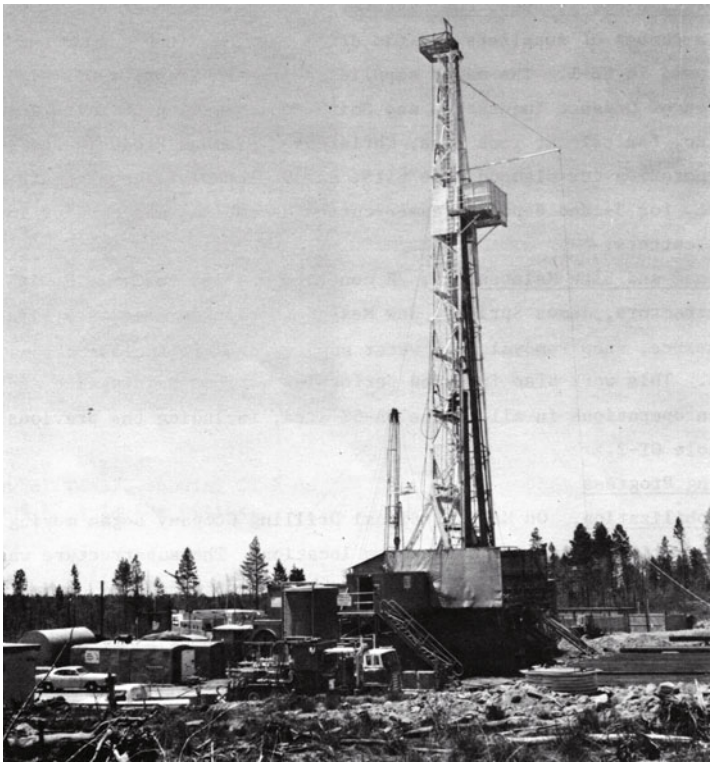

Fig. 3-19. Signal Drilling Company rig No. 5 on location over EE-1. Source: Pettitt, 1977b

Drilling in the Surface Volcanic Rocks and Sedimentary Formations

The portion of the EE-1 borehole that passed through the Bandelier Tuff and the upper part of the Abo Formation—to a depth of 599 ft—was drilled with 17 1/2-in. steel-tooth bits. Then, because there had been repeated losses of mud at the surface around the very short (10-ft) conductor casing, the hole was reamed out to a diameter of 26 in., and a deep string of 20-in. surface casing

was run in to 580 ft. After the casing had been cemented to the surface, drilling continued in the Abo Formation and on into the Madera Formation, with 17 1/2-in. TCI and steel-tooth bits. In anticipation of the lost-circulation zone that had been encountered during the drilling of GT-2 (at a depth of about 1900 ft, in the Madera Formation), the drilling fluid was loaded up with lost-circulation material—at a high concentration, but one that could still be pumped—as this depth was approached. Even so, on June 12, at a depth of 1905 ft, all circulation was lost and the drill pipe became stuck. After several hours' effort, the pipe was freed and pulled from the hole. The jets were removed from the bit, the concentration of lost-circulation material in the drilling mud was increased to 30%, and the drill string was started back into the hole.

Drilling in the Madera limestone then proceeded satisfactorily, but only with the continual addition of lost-circulation material (cottonseed hulls, Fibertex, and Gelflake) to the drilling mud to control fluid flow into the 1905-ft loss zone. However, when the cavernous limestone interval in the lower part of the Sandia Formation was encountered at a depth of 2359 ft, circulation was again completely lost and the pipe became stuck once more.

Efforts to restore circulation and free the stuck pipe continued for two days, during which five "pills" of 40% lost-circulation material (2800 gal. each) were pumped down the hole. But these efforts proved fruitless, and finally GO-International Logging was called out. They determined that the "free point" for the drill string was 80 ft off bottom, whereupon an explosive "string shot" was detonated at a tool joint 110 ft off bottom and the joint was unscrewed. The remaining pipe was withdrawn from the hole early on June 21. The washover assembly used to recover the 110 feet of drill string at the bottom of the hole encountered numerous bridges in the shale sections of the Abo and upper Madera formations, and lost-circulation problems continued. By June 24 the remaining bottom-hole assembly had been recovered; but since circulation had not been re-established, the team decided to try to cement off the cavernous limestone interval in the lower Sandia Formation. For the first attempt, a cement mixture with added lost-circulation material (bentonite chips and Gelflake) was pumped down the hole, but it did not fill in the zone. Next, a "gunk" squeeze was attempted, with a mixture of cement and bentonite in a slurry of diesel oil to slow down the cement hydration—again without success. A final attempt, with a 100-sack batch of cement containing Cello-flake lost-circulation material, along with 3% calcium chloride as a cement accelerator, did appear to seal off the loss zone.

Unfortunately, after the cement plug had been drilled through, renewed drilling in fresh limestone proceeded only 1 ft before circulation was completely lost again. This time the losses were not only at the bottom of the hole but also in the 1900-ft region above, in the upper Madera and Abo formations. With no fluid in the borehole above about 1700 ft to stabilize them, these red clays were swelling and sloughing, seriously hampering

drilling. In an effort to stabilize the borehole, two cement plugs were set, at 1900 ft and 2100 ft. The Project staff then decided to drill ahead into the granitic basement without returns—a very risky operation given the likelihood that the drill string would become stuck yet again. Additional water-hauling trucks were engaged, and drilling commenced. The Precambrian surface was encountered at a depth of 2401 ft, and drilling without returns continued to 2431 ft, but with considerable difficulty.

At this juncture, the team decided that running casing was their only hope for stabilizing the hole. A three-stage cement job was designed: first, the lowest 71 ft of casing—from the bottom of the hole up to the cavernous limestone interval at about 2360 ft—would be tag-cemented; second, with a stage collar placed in the casing string at a depth of 1783 ft (bypassing the 2360- to 1905-ft interval, which could not be cemented because of the severe lost-circulation conditions), the casing would be cemented up to 800 ft; and third, the top portion—from about 800 ft to the surface—would be secured by cementing through a second stage collar.

Before the casing was run, the borehole was reamed repeatedly, from about 1500 ft down to 2200 ft, in an attempt to maintain its full 17 1/2-in. diameter. But the attempt was only partially successful: the clay beds continued to swell and squeeze into the borehole, restricting the diameter—sometimes to the point that the reaming assembly had to be "drilled" back out of the hole before the next run could begin.

Before the reaming assembly was pulled out of the hole, several pills of bentonite mud mixed with Baroid Torq-Trim were pumped in to help lubricate the borehole walls for the running of the casing. Finally, on the afternoon of July 3, a string of 13 3/8-in. intermediate casing (54.5 lb/ft, Type K-55) was started into the hole, with a Baker cement shoe on bottom and two backup float collars. The deeper collar was positioned one joint above the bottom of the casing and the shallower one three joints above; thus, once the casing was on bottom, their depths would be 2390 ft and 2307 ft, respectively. During run-in, two stage collars (each with a cement-retaining basket below to block the annulus outside the casing) were installed in the casing string for the second and third cementing stages; these were positioned such that, once the casing was on bottom, one would be at 1783 ft and the other at 790 ft below the rig floor. However, the installation of these stage collars assumed that each of the planned sequential cementing operations would be successful; no thought had been given to contingencies—even though, considering all the troubles encountered in drilling into the granitic rocks, contingency planning should have been paramount.

The next morning, as the casing was being slowly lowered through the still-swelling clay zones in the Abo and Madera formations, to everyone's dismay it stopped completely—its lower end about 200 ft off bottom. But after an hour or so, ever so slowly it finally slid on down and into the granitic basement! The casing was landed at a depth of 2431 ft.

Note: The cementing of the intermediate casing string in EE-1 would turn out to be almost a complete failure—rescued only at the last moment with a well-thought-out repeat tag cementing of the bottom 71 ft of casing. The net results of the various stages would be as follows:

- Stage 1 (tag cementing of the bottom of the casing): failed
- Stage 2 (cementing through the stage collar at 1783 ft): failed
- Stage 3 (cementing through the stage collar at 790 ft): partially succeeded (two-thirds of the cement went through the stage collar and into the annulus)
- Repeat tag cementing of the bottom of the casing: succeeded

Many factors would later be identified as having contributed to this near-failure: (1) the supervisors and cementers who were attempting cementing operations in a mountainous setting, beset with severe lost-circulation problems, were experienced primarily in "flat-land" oilfield methods; (2) technical supervision was poor—the drilling supervisors failed to understand the significance of the very subhydrostatic water-level measurements following the tag-cement job, which indicated that the casing was in direct fluid communication with the loss zone at 2360 ft; and (3) presence/oversight by Group Q-22 personnel was inadequate—personnel in the field tended to accept the recommendations of the hired drilling/cementing "experts" without critical review.

Cementing of the Intermediate Casing String

In preparation for the first stage (tag cementing of the bottom 71 ft of casing), some 16 000 gal. of bentonite mud was pumped in to stabilize the borehole. Then 8800 gal. of cement slurry containing Pozzolan, silica flour, and Cello-flake was pumped into the casing. Following a brief pause in pumping for flow to be switched from the cement blender to the water supply, a rubber plug was released from the cementing head at the surface and water was pumped in to displace it down the casing. This turned out to be a mistake: In the particular mountainous environment of Fenton Hill, the severe lost-circulation conditions created by a water table some 1700 ft below ground surface meant that the top 1700+ ft of the casing was filled with air instead of water.[12] Thus, during the pause in pumping, the cement flowed down the casing and out into the loss zone by gravity, sucking air behind it; when the plug was released, followed by displacement water, it could only "rattle" its way down the casing, almost in free fall. It is difficult to estimate the velocity of the plug as it fell, but as evidenced by the

[12]In the typical oilfield setting, the water table being near-surface, such severe lost-circulation problems are rare (the casing would be filled with water instead of having a column of air at the top). Thus, in a conventional tag-cement job, first the cement and then the plug would be pumped slowly down the casing, followed by a carefully measured amount of displacement water (to just pump the plug to bottom while forcing the cement through the cement shoe and up the annulus).

lack of a pressure pulse, it did not reach the upper float collar (at 2307 ft) intact—thereby failing to create the necessary seal. The consequence was that the water flowed around the plug and overdisplaced all of the cement—through the cement shoe at the bottom of the casing, up the annulus outside the casing, and out into the loss zone at about 2360 ft. Several water-level measurements, made following the tag-cement job, showed the casing to be empty of any fluid down to a depth of 2157 ft—a sure sign that the lowest section was not cemented (even a short interval of cement behind the casing would have caused it to be full to the surface).

The report on this episode (Pettitt, 1977b) makes it clear that the rig supervisors knew at the time that the plug had not seated properly. But unfortunately, they did not realize that the tag-cement job had failed, nor did they understand the significance of the water-level measurements: the fact that the aquifer flowing through the cavernous Madera limestone at 2360 ft was in hydraulic communication with the water inside the casing should have made it obvious that the displacement water had washed all the cement out into this very subhydrostatic loss zone. The rig supervisors could have found out what had happened simply by attempting to fill the casing with water. But they did not.

Note: The lesson imparted by the failure of the tag-cementing attempt was that under such severe lost-circulation conditions, no plug or displacement water should follow the cement. The cement should be allowed to fall by gravity and "U-tube" around the cement shoe.

Thinking, then, that the tag-cement job had (somehow) succeeded, the rig supervisors proceeded to begin the second stage. Late on July 4, after the sliding sleeve on the deeper stage collar (at 1783 ft) had been shifted upward to open the cementing ports, placement of the second-stage cement began. A 9500-gal. slurry of cement, similar to that used for the tag cementing, was injected into the casing and was followed by tandem rubber plugs and displacement water. But the results were almost identical to those of the tag-cementing stage: when the plugs—pushed by the displacement water—hit the deeper stage collar at high velocity, either the collar or the plugs were not strong enough to withstand the impact. The plugs then "sailed on by," but not before managing to knock the sliding sleeve on the collar back down, reclosing the ports (both plugs would later be found on top of the upper float collar near the bottom of the hole). The water continued to flow on down the casing, pushing the cement ahead of it. Once again the lost-circulation zone at about 2360 ft took the cement as fast as it flowed in, leaving the casing essentially empty. In other words, the rapidly falling cement flowed not through the open ports in the stage collar as intended, but on down the casing—past the rubber plug on top of the upper float collar near the bottom of the casing, out the cement shoe, and back up into the loss zone at 2360 ft. Water-depth measurements following the second

stage of cementing showed that the casing was empty all the way down to the deeper stage collar at 1783 ft. After all this effort, the 13 3/8-in. intermediate casing string remained completely uncemented.

Evidently now realizing that something must have gone wrong with the second stage of cementing, the rig supervisors suspended cementing operations.[13] The reports of the time state that the third stage was delayed until fluid circulation could be established through the cementing ports at 790 ft and back to the surface via the annulus. Since circulation is absolutely essential for any cementing through stage collars—and should have been established before the second stage—this is tantamount to an admission that the third stage, if undertaken without circulation, would fail just as the second stage had; and that even with the cementing ports on the lower stage collar open, the flow path of least resistance for the cement would be the same as during the second stage.

Nevertheless, the rig supervisors proceeded to open the cementing ports on the upper stage collar at 790 ft and pumped fluid into the casing to circulate through these ports. To their surprise, all flow was lost. Assuming that it was going through the ports but then somehow bypassing the cement basket in the annulus below the collar and traveling down the outside of the casing, they concluded that the cement basket would need to be plugged. (In reality, the flow was going all the way down the inside of the casing, past the damaged rubber plug on top of the upper float collar at 2307 ft, out the cement shoe at the bottom of the casing, and back up the annulus to the loss zone at 2360 ft.)

The operation to plug the cement basket—which in fact had not been breached—consisted of pumping in three successive 25 000-gal. pills of bentonite mixed with 30%–50% lost-circulation material. The first two pills flowed down and out the bottom of the casing into the deep loss zone, with no returns. With the third pill, the space around the damaged plug on top of the upper float collar was almost completely closed off, which forced most of the flow to finally go through the cement ports in the stage collar at 790 ft and back up the annulus (a fraction of the flow was still going all the way down the casing and into the loss zone at 2360 ft). This "fix," although not the intended one, did at least temporarily establish a significant degree of circulation.

On July 6 the third stage—cementing of the 800-ft length of annulus above the upper stage collar—began. This stage should have been relatively simple; but when the cement was injected, instead of the full volume going through the cement ports, about one-third went on down the casing. (The calculated volume for this annular region, most of which was within the

[13]It appears that they were still unaware that the tag-cementing job had not succeeded either.

580 ft of 20-in. surface casing, was 890 ft^3. The amount of cement actually injected, with the standard allowance for a 20% excess, was some 1070 ft^3—which left about 140 ft of annulus still empty.)

The following day, after the cement had set up, its top was tagged with a 1-in.-diameter pipe run down the annulus. The remaining void was then filled, to within a few feet of the surface, with an additional 170 ft^3 of cement pumped in through this pipe.

The last "surprise" of this cementing project evidently brought with it—finally—some revelations. When the rig supervisors made a bit run to clear the casing, they found it essentially clear (except for a small amount of cement and the plug inside the upper stage collar) until the bit encountered the plugs on top of the upper float collar at 2307 ft. The upper two plugs, from the failed second-stage cementing job, were drilled through uneventfully. However, as the tattered plug directly on top of this float collar (the plug pumped down during the first tag cementing) was being drilled up, circulation was totally lost. At last the supervisors understood that it was this faulty plug, damaged in transit down the casing, that had caused the tag-cement job to fail; and that circulation was achieved before the third stage only because the bottom of the casing had been temporarily sealed by the lost-circulation material packed in around the plug—now broken up and washed away. After assessing the situation, they decided to clear the rest of the casing and then very carefully repeat the tag cementing, this time through open-ended drill pipe.

The successful tag cementing of the bottom 71 ft of the casing was done on July 7: a cement slurry (225 sacks of Class B cement containing 3% calcium chloride, mixed with 25 sacks of Cello-flake) was pumped in, allowed to fall by gravity (with no displacement water following), and to "U-tube" around the casing shoe at 2431 ft.

Drilling in the Precambrian Basement

For drilling of the crystalline basement rock, the only available TCI hard-rock bits of the desired 12 1/4-in. (311-mm) diameter were the STC Q9J and Security H-100 bits. Both makes were employed, so that their performances could be compared. The tungsten-carbide inserts of the Smith bit were somewhat softer than those of the more advanced, oilfield-type Security bit, which also had prelubricated and sealed roller bearings and was designed only for use with mud or water as a circulation medium. The weights on the bits ranged from 60 000 to 70 000 lb and the rotational speeds from 40 to 50 rpm. The H-100 Security bits would be found to outperform the STC Q9J bits—their rate of penetration averaging nearly 7 ft/h and their useful life exceeding 100 hours, almost twice as long as that of the Q9J (attributed to the sealed roller bearings and harder carbide inserts of the H-100).

Drilling in the crystalline basement below the intermediate casing began on July 9, with a 12 1/4-in. STC Q9J bit and water as the circulating fluid. A survey of the hole at 2509 ft showed the trajectory to be N52W, 3/4°.[14]

The first bit change was at 2785 ft, when drilling became erratic. The bit was pulled, and examination revealed that two of the three cones were almost completely locked up and four buttons were missing. Even so, the bit was still in gauge. The next bit, a Security H-100, drilled 650 ft in 107.5 hours—a remarkable performance for a 12 1/4-in. bit drilling in granitic rock (the average rotational speed for this bit run, at a load of 65 000 lb, was 44 rpm). When pulled and examined, the bit was missing about one-third of the buttons and was 3/8 in. under gauge. Drilling then continued, the STC Q9J and Security H-100 bits being used on alternate runs.

In contrast to the experience with the GT-2 borehole, there was no increase in drilling-fluid losses (at that time, about 200 gal./h) as EE-1 was being drilled through the 3600- to 3700-ft depth interval. By this depth, the inclination of the hole had increased to 2° in the direction N75W. During drilling below 3700 ft, the inclination of the hole would continue to increase gradually—as had the inclination of GT-2—reaching about 6° (in a northwesterly direction) by 6500 ft.

Drilling progressed smoothly until August 5, when, at a depth of 5985 ft, the penetration rate suddenly increased from 6 ft/h to 19 ft/h—indicating that a brecciated fracture zone had been encountered. The plan had been to drill to 6300 ft, case the hole with 10 3/4-in. casing, and then continue drilling with 9 5/8-in. bits. However, this drilling "break" so near that depth created concern that the rock at 6300 ft might not be suitable for setting casing, owing to the potential for seepage of water through the brecciated rock below the casing shoe. The plan was therefore altered: the hole would be deepened to at least 6420 ft, with 12 1/4-in. bits, before setting of the deep casing string. As drilling continued, the zone of brecciated rock was found to extend downward about 255 ft, to 6240 ft. At this depth, the penetration rate decreased again, to about 10 ft/h.

On August 8, when the 6420-ft depth had been reached, the hole was circulated to cool it and clean the fluid preparatory to logging operations. From August 8 to 12, open-hole diagnostic logs were run by Dresser-Atlas Petroleum Services between about 2430 ft and the bottom of the hole. These logs included 4-arm caliper, Acoustilog, Densilog, Laterolog, and Spectralog; a gamma-ray detector was used in conjunction with many of the logs to enable accurate depth correlations. In addition, a suite of supporting diagnostic logs was run on August 11, over various intervals of the open hole, by the Birdwell Division of Scientific Services Corp.

---

[14]The notation we use for borehole trajectories is azimuth or direction first, inclination or angle second. For example, N52W, 3/4° would mean the borehole has a surveyed direction of N52W and an inclination of 3/4 degree from the vertical.

On August 13, a deep string of 10 3/4-in. casing (51 lb/ft, K-55) was run and landed at a depth of 6420 ft. To prevent malfunctioning of the displacement plug and/or float collars, as had occurred during first- and second-stage cementing of the intermediate casing string, tandem float collars were installed at the bottom of the casing string and an aluminum plug-landing baffle 40 ft above the upper float collar. The displacement plug to be used was a Halliburton cast aluminum plug, designed to withstand high landing pressures.

A single-stage cementing operation—to cement only the bottom 1000 ft of the casing—was performed the same day by Halliburton Oil Well Cementing Co. of Farmington, NM. First, a 400-gal. "pad" of water was injected; then 2250 gal. of cement slurry was pumped down the casing, followed by the aluminum plug and 25 750 gal. of displacement water. Following an 18-hour wait for the cement to set, a 9 5/8-in. Security H10J TCI bit was run into the hole to drill out the aluminum plug and float collars. Drilling with this bit then proceeded to a depth of 6874 ft in 50 hours (9.1 ft/h), producing a well-isolated open-hole interval for a series of fracturing experiments (although the nearby brecciated zone should have given the Project staff pause when planning such experiments).

Before testing began, a 12-ft coring run was made (to 6886 ft) with an STC-modified 9 5/8-in. JOIDES core bit. Only 3 ft of core was obtained (25% recovery). From petrographic examinations of thin sections from this core, the rock was classified as a leucocratic monzogranitic gneiss.

Stage 1 Pressure-Stimulation Tests

On August 23, 1975, the Laboratory's newly designed high-temperature geophone package (Fig. 3-20) was deployed for the first time, in the GT-2 borehole. (The 4 1/2-in. high-pressure casing string, which had been removed from the hole for the experiments with fracturing through perforations, had not been reinstalled, allowing for passage of the 5-in.-diameter geophone package.) The package contained 12 geophones, arranged in three sets—one vertical and two horizontal—to record tool motion on the three orthogonal axes. The four geophones in each set were connected in series to average their outputs, which were then sent to an amplifier to increase gain. Housed with its batteries in an ice-filled Dewar flask, the amplifier and batteries were protected from the downhole temperature for about 12 hours. At the bottom of the geophone package was a locking arm to force the geophones against the borehole wall. The ideal position for this arm was on the high side, pressing the package—aided by gravity—against the low side of the hole. Unfortunately, because the package would rotate randomly as it was lowered into the hole, the locking arm was often positioned such that the package was lifted somewhat off the low side of the hole before being forced against the wall; as a consequence, the coupling was less effective.

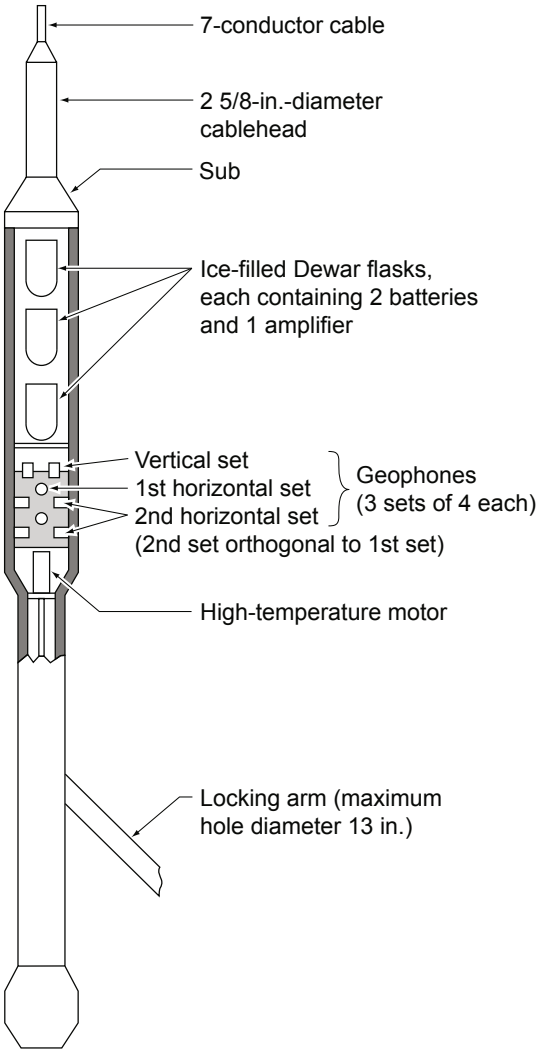

Fig. 3-20. Schematic view of the Laboratory's first high-temperature geophone package (ca. 1975).
Source: Pettitt, 1977b

With the geophone package positioned at a depth of 6585 ft in GT-2, the open-hole interval of EE-1 was pressurized with a commercial pump, provided by The Western Co. of Farmington, NM. From a beginning rate of about 1 BPM (2.7 L/s), injection pumping was gradually increased to 5.5 BPM (14.6 L/s) at a maximum injection pressure of only 1200 psi. At first there was no evidence of fracture initiation (i.e., the opening of a sealed joint or joints), but considerable backflow occurred when the

borehole was vented—suggesting that a pre-existing joint system had been opened and extended. Because no seismic signals were recorded on the geophone in GT-2, this joint opening was thought to be essentially aseismic—without tensile rock fracturing or joint shear displacement. In hindsight, it is possible that joint-opening signals were present but were not observed during this first attempt at "fracture" mapping. The data recording system had two shortcomings: the frequency of the downhole amplifiers was not sufficiently high, and the surface system did not yet employ the high-speed Ampex tape recording system (it would be added a few months later). Signals of frequencies greater than about 125 Hz, therefore, would not have been recorded.

Two days later, on the assumption that the joint newly opened in EE-1 was located deeper than about 6500 ft, an inflatable Lynes packer was set at a depth of 6480 ft (60 ft below the bottom of the casing). It was hoped that with pressurization of this 60-ft annular interval of open hole isolated between the top of the packer and the casing shoe, another joint might be opened. Fluid would be pumped down the annulus between the drill pipe and the casing with the Project's recently acquired positive-displacement, 9-gpm Kobe pump. Before pressurization began, a small Laboratory pump was used to inflate the packer to 1500 psi (beyond that point, the packer would be maintained at an internal pressure about 200 psi above the injection pressure).

Injection pumping then began, at a constant rate of 9 gpm. The pressure rose rapidly to about 1900 psi and then dropped back to about 1400 psi. Some 800 gal. of fluid was injected at the latter level—this pressure behavior indicating that another sealed joint had been opened; but no seismic signals were recorded at the geophone in GT-2, signifying that this was again a true tensile-opening joint (without a significant shear component and therefore almost aseismic). A self-potential electric log run later indicated that a joint had been opened between 6437 and 6454 ft, about in the middle of the isolated open-hole interval, and that its intersection with the borehole was about 17 ft long. Although the strike of this hydraulically opened joint was not determined, from the length of its intersection with the borehole and the borehole inclination of about 6°, one can infer that the joint was within 2° of vertical.

Following this experiment, the Lynes packer was deflated and the entire open-hole interval below the casing was repressurized with the Kobe pump. The results were, to say the least, anomalous! At a constant injection rate of 9 gpm, the highest pressure achievable was now only 300 psi—strongly suggesting the presence of an open joint system somewhere below the packer-setting depth of 6480 ft (and possibly connected to the GT-2 borehole through one of the previously opened joint systems at about that depth in GT-2). The Lynes packer was then moved 240 ft farther down the borehole and reset at a depth of 6720 ft. When the Kobe pump was used to pressurize this longer (300-ft) open-hole annular region between the

casing shoe and the packer, 500 gal. of water was injected at a pressure of 1375 psi—indicating that the low-pressure open joint system was located below the packer.

At this juncture, the team decided to cement up the open joint system at the bottom of EE-1. If left open, it would constitute a lost-circulation zone with a very low fluid-acceptance pressure, posing problems for subsequent drilling operations. Halliburton Oil Well Cementing Co. was called out from Farmington, NM, and on August 26 the bottom of the borehole was cemented back with 1750 gal. of cement slurry pumped through open-ended drill pipe. The top of the hardened cement was subsequently tagged at 6480 ft, the depth at which the Lynes packer had first been set.

With the lower part of the borehole now filled with cement, the open-hole interval from 6480 ft up to the casing shoe was repressurized a number of times; the pressure behavior was similar to that seen earlier, when the joint in this interval (6437–6454 ft) was initially opened. On August 27, a Lynes packer was run in and the interval was pressurized to 1850 psi in an attempt to obtain an oriented impression of this joint. Unfortunately, when the packer was pulled, it was found that the soft rubber sleeve had been left behind in the hole. A second attempt on August 30, with a tandem Lynes impression packer positioned over the 6437- to 6454-ft interval (two 5-ft elements, one centered at 6438 ft and one at 6449 ft), succeeded: the 9-gpm Kobe pump was used to reinflate the joint at a pressure of 2000 psi, then for four hours the packer was pressurized at 2300 psi with a smaller Laboratory pump. When the packer assembly was pulled from the hole, it showed definite impressions of the joint, oriented in a northwest–southeast direction.

Stage 2 Drilling to 9168 ft

As had happened with GT-2, the EE-1 borehole drifted off toward the northwest during the first stage of drilling. However, its inclination increased more rapidly than that of GT-2, to 5 3/4° at 6490 ft and to 6° at 6874 ft. As shown in Fig. 3-21, the direction of EE-1 at 6886 ft was almost due west. Therefore, if the large joint emanating from the bottom of GT-2 was oriented northeast–southwest, as inferred by some of the team—though on a very tenuous basis (extrapolation, to a depth 3000 ft deeper, of the orientation found the previous November for the joint at 6535 ft)—then the EE-1 borehole at the end of Stage 1 drilling was well beyond the joint and not favorably positioned for intercepting it as originally planned.

In contrast, however, the packer impression taken in EE-1 on August 30 indicated that the joint intersecting the borehole at a depth of about 6450 ft had a northwest–southeast orientation. Given this seemingly conflicting information, the HDR Project staff decided to rotate EE-1 rapidly from a westerly to a southerly direction and then continue drilling to the south so that it would pass directly below GT-2. As noted earlier, this strategy would maximize the probability of intersecting the joint opened from the bottom of GT-2 regardless of its orientation.

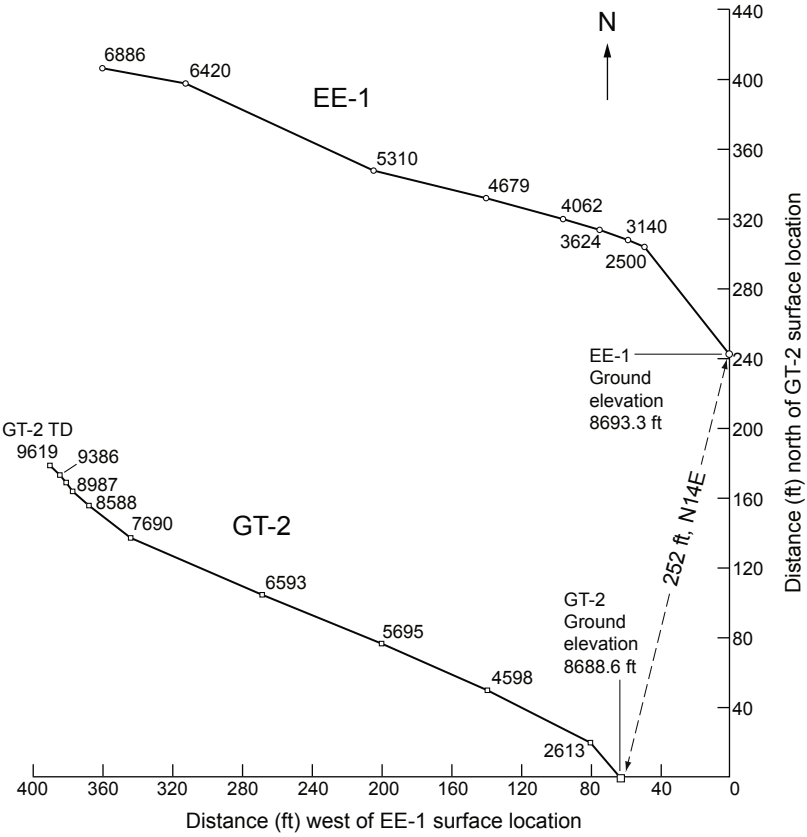

Fig. 3-21. Plan view of the drilling trajectory of the completed GT-2 borehole in relation to that of the EE-1 borehole at the end of Stage 1 drilling, based on magnetic single-shot surveys conducted during drilling. (Note that three gyroscopic surveys of GT-2 done later, in February and March of 1977, all showed the northward curve below 7690 ft as less pronounced; it is probable that the magnetic survey was distorted somewhat by the higher levels of magnetic minerals in the deeper granitic rocks.)
Adapted from Blair et al., 1976

The directional drilling equipment then available in the oil industry was rated for a maximum temperature of about 180°C (350°F). The Project staff believed that with occasional cooling of the assembly during run-in, such equipment would be just adequate for drilling EE-1 on the planned inclined southerly path to about 9600 ft (at which depth the rock temperature was about 200°C).

More uncertain were the temperature capabilities of the available hole-surveying equipment: inquiries to both Sperry-Sun and Eastman Whipstock revealed that their gyroscopes were rated for maximum temperatures of only

about 150°C. In contrast, the more commonly used Eastman Whipstock magnetic survey tools were rated at 200°C for 2 hours when heat-shielded, which appeared to be just adequate. For this reason, magnetic surveying was selected as the primary method of determining the relative locations of the two boreholes as drilling proceeded.

A Dyna-Drill assembly was selected for the directional drilling of EE-1. Unlike conventional rotary drilling equipment, the Dyna-Drill incorporates its own downhole, positive-displacement motor (PDM), eliminating the need to rotate the drill pipe. This specially designed motor consists of a multi-stage Moyno pump incorporating a metal rotor and an elastomeric stator (a rubber-like element molded with a spiral passageway having an oblate cross section).

The first Dyna-Drill run, which started at a depth of 6886 ft on August 31, 1975, turned the hole 21°—from N78W to S81W—in 65 ft of directional drilling. At this new depth (6951 ft), the trajectory of the borehole was S81W, 5 1/2°. An Electronic Yaw Equipment (EYE) steering tool, manufactured by Scientific Drilling Controls of Newport Beach, CA, was used to direct and check the course of the directional drilling. For the next 82 ft, the hole was rotary-drilled with a limber assembly, rotating it southward another 11° to a trajectory of S70W, 6° at a depth of 7033 ft. These two drilling runs, which added 147 ft of depth and rotated the hole 32°, marked the first time that directional drilling had been accomplished in hot granitic rock!

Two additional Dyna-Drill runs of 139 ft and 140 ft, with a 75-ft conventional rotary drilling run between them, deepened the borehole to 7387 ft. By this depth, EE-1 had been rotated an additional 90°, to S23E—past its target direction of due south—and its inclination had been increased to about 8°. Conventional rotary drilling along with one more Dyna-Drill run (from 8200 ft to 8313 ft) then took the borehole to 9168 ft. The hole trajectory had now been rotated back 43°, through south again, to S20W, 4 1/2°.

Stage 2 Final Drilling: Attempt to Connect EE-1 with the Joint at the Bottom of GT-2

Magnetic single-shot surveys were taken at various depths during directional drilling between 6886 and 9110 ft. The trajectory of the EE-1 borehole based on these surveys is illustrated in Fig. 3-22. It was confirmed by magnetic multishot surveying done on September 16 by Eastman Whipstock, over the depth interval 6700–8990 ft (2040–2740 m).

Figure 3-22 shows that at a depth of 9110 ft in EE-1 (and 9068 ft in GT-2, the vertically equivalent depth taking into account the steeper inclination of this borehole), the horizontal distance between the two holes was 40 ft, with EE-1 almost due north of GT-2. Furthermore, on its current trajectory of S20W, 4 1/2°, EE-1 was aimed directly at the bottom of GT-2 rather than the planned 200 ft below it. With the bottom of GT-2 still some 500 ft deeper

than EE-1 at this point, as shown in the figure, the inclination of EE-1 would have had to be even steeper—about 2 1/2° from the vertical—for the borehole to pass 200 ft beneath GT-2 (the remaining 500+ ft of drilling would allow for only 30 ft of advancement horizontally).

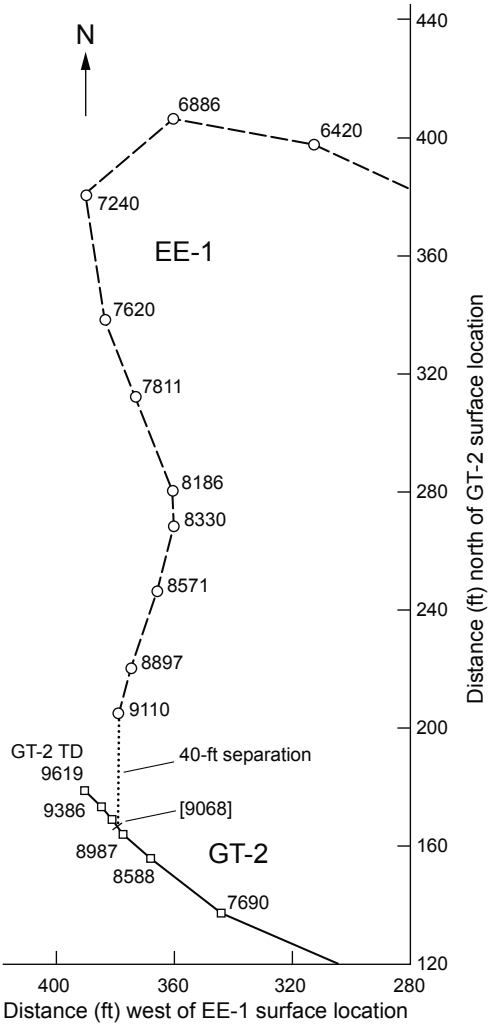

Fig. 3-22. Plan view of the drilling trajectory of the EE-1 borehole between 6886 ft and 9110 ft, in relation to that of GT-2. Trajectories are based on magnetic single-shot surveys conducted during drilling (as were the Stage 1 drilling trajectories shown in Fig. 3-21). The dotted line represents the horizontal distance between EE-1 at 9110 ft and GT-2 at 9068 ft.
Adapted from Blair et al., 1976

First Series of Seismic Ranging Experiments

On September 20, a series of seismic ranging experiments was performed at a depth of 9100 ft in EE-1, with two principal objectives: (1) to measure the horizontal distance from EE-1 to GT-2, and (2) to determine the compass direction from EE-1 to GT-2 at this depth. In preparation for these experiments, the 4 1/2-in. high-pressure casing string, needed to guide wireline tools into the GT-2 scab liner, had been reinstalled (it would be needed later, as well, for repressurization of the joint(s) opened below the scab liner the previous spring). The new geophone package—now fitted with a brass-tipped locking arm to improve coupling to the borehole wall—was positioned in EE-1 at a depth of 9100 ft. Then detonator caps were run into the GT-2 scab liner and sequentially fired at depths of 9018, 9068, and 9118 ft. The horizontal distance between the two holes at 9100 ft in EE-1 and 9068 ft in GT-2—as derived from the difference between the first-arrival times of the compressive and shear signals received by the geophone—was 52 ft. (The rock properties used for this calculation were 5.85 km/s for the P-wave velocity and 3.38 km/s for the S-wave velocity, with a travel-time accuracy of ±1 ms.) This distance compares quite favorably with the 40-ft distance obtained via magnetic single-shot data for the same depth (Fig. 3-22); but the ranging data were considered the more accurate, suggesting that the true GT-2 trajectory at this depth was somewhat south of that shown in Fig. 3-22.

The seismic ranging experiments did not, however, yield any data regarding the relative horizontal positions of the two boreholes at the 9100-ft depth. Without any seismic direction data to confirm the positions shown in Fig. 3-22, the team decided to continue drilling EE-1 toward a target directly beneath GT-2.

Second Series of Seismic Ranging Experiments

Over the next four days, three additional rotary drilling runs deepened EE-1 to 9575 ft; the azimuth of the borehole at this depth was almost due south, at an inclination of 3 3/4°. The horizontal path of EE-1 between 8897 and 9575 ft, calculated on the basis of magnetic single-shot survey data, is depicted in Fig. 3-23. If it was correct (at the time, there was no reason to think otherwise), EE-1 had progressed 30 ft farther south between 9100 and 9575 ft, and in that case would have intersected the GT-2 borehole at a depth of about 9560 ft! (It would turn out that this was not the case—later gyroscopic surveys in GT-2 would reveal that the single-shot data were somewhat in error, having placed the bottom of GT-2 some 35 ft north and 30 ft east of its true location.)

A second series of ranging experiments—interspersed with a couple of pumping experiments—began September 26 at the new EE-1 depth of 9575 ft.

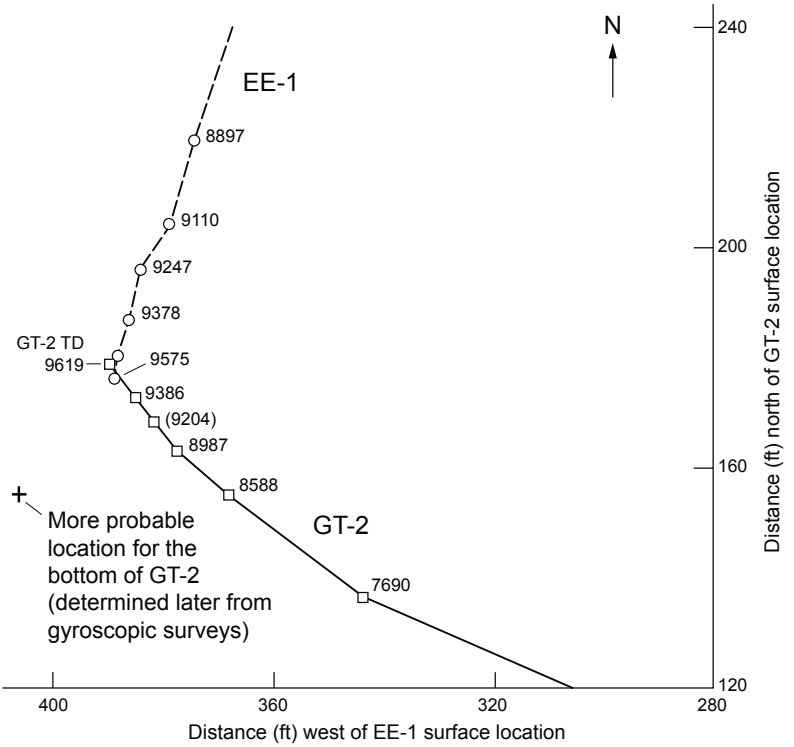

Fig. 3-23. Close-up view of the trajectory of the EE-1 borehole between 8897 and 9575 ft, in relation to that of the GT-2 borehole (as calculated from magnetic single-shot survey data).

For the first pumping experiment, the geophone package was placed on the bottom of EE-1 with the geophones at 9565 ft. The 9-gpm Kobe pump was then used to reinflate the major joint at the bottom of GT-2. But the injection of 3600 gal. of water over a period of 7 hours, at a maximum pressure of 1600 psi, produced no discernible seismic signals at the EE-1 geophone.

When GT-2 had been vented, a ranging experiment was done to verify the relative borehole positions shown by the single-shot survey data in Fig. 3-23. Three GO-International detonators were made up on the Dresser-Atlas cable with a Laboratory-designed firing mechanism; a geophone trigger assembly ensured precise timing of the shots, to an accuracy of ±0.05 ms. The detonators were run into GT-2 and fired at depths of 9531 and 8581 ft. This time, the signals received indicated that at the 9531-ft depth in GT-2 and the vertically equivalent depth of 9565 ft in EE-1, the horizontal distance between the two boreholes—to an accuracy of ±1 ft—was 26 ft (rather than essentially zero, as the single-shot data had shown). Unfortunately, owing to a malfunction of the Eastman camera, the orientation

of the seismic package in EE-1 was not measured, and thus once again no seismic information was obtained concerning the relative positions of the boreholes. The critical question remained, then: was EE-1 at 9575 ft west or east of the bottom of GT-2?

On September 29, following a two-day hiatus for instrument and equipment repairs and modifications, a second pumping experiment took place. The joint at the bottom of GT-2 was inflated again, this time with the Western pump. Some 3500 gal. of water was injected, at a rate of 3.7 BPM (10 L/s) and a maximum pressure of 2200 psi. The Western pump was then shut off, and pumping continued with the Kobe pump for another 1 1/2 hours while induced-potential logs were run in EE-1. The logs indicated additional growth of the joint—beyond the 400-ft diameter calculated for the previous extension of the joint, on April 21.

Third Series of Seismic Ranging Experiments

A third series of ranging experiments, aimed at resolving the growing concern about the relative positions of the two boreholes, took place on September 30. This time, the compass orientation of the geophone sonde in EE-1 would be determined as well: a high-temperature Eastman Whipstock compass was specially installed in the geophone sonde, the readings from which would be verified by setting off a surface dynamite explosion a mile and a half away and recording the acoustic signals (whose direction was known). With reliable orientation data for the geophone sonde, its direction with respect to the detonators—i.e., to the GT-2 borehole—could be obtained via the hodogram seismic-analysis technique, and its distance from GT-2 could be obtained from the first arrivals of the P-wave and S-wave signals.

After GT-2 had been vented down, the geophone package was set on the bottom of EE-1 (the actual depth of the geophones was 9558 ft). Unfortunately, owing to faulty electrical connections through the cablehead, the locking arm on the geophone package could not be extended. Coupling of the package to the borehole wall was therefore very poor—which by itself can render direction information ambiguous. (Ideally, the geophone package should move as a unit with the borehole wall—a nearly impossible feat given its weight, even with the locking arm perfectly oriented to press the package against the low side of the borehole, assisted by rather than fighting gravity.) Further, when the detonators were fired in GT-2, at depths of 9535 and 9512 ft, the detonator package was lying against the low side of the hole; this skewed position made a reliable reading even less likely (for direction measurements to be unambiguous, the explosions have to be symmetrical in the borehole, transmitting a compressive sound wave equally in all directions). By this time, long exposure of the geophone package to the high-temperature environment had taken its toll: only one horizontal set of geophones was operating. But this set received good signals from

the detonators, and it also received good signals when the surface dynamite charge was exploded in a shallow hole on Cebollita Mesa, about 1 1/2 miles to the southeast of Fenton Hill.

A ranging calculation based on the P- and S-wave arrivals from the GT-2 detonator shots showed a horizontal separation of 26 ft between the boreholes, consistent with that found four days earlier. Hodogram analysis of the acoustic signals, based on the compass-measured (and dynamite-blast-verified) orientation of the geophone package in EE-1, showed the position of EE-1 as almost due west of GT-2.

Note: At this stage, with the EE-1 borehole at 9575 ft, a heat-shielded magnetic multishot survey could have been done immediately by Eastman Whipstock, with existing equipment, to validate the results of the ranging experiments. Had this been done, the trajectory shown in Fig. 3-23 for the EE-1 borehole would have been seen to be wrong and could have been corrected. Unfortunately, at the time the HDR Project was under the direction not of engineers but of geophysicists, who had more confidence in the seismic direction data—which would later prove to be fallacious—than in the magnetic survey data.

In a final injection test late on September 30, the Western pump was used to further extend the joint at the bottom of GT-2, providing a better target for EE-1 when drilling resumed the next day. Some 12 000 gal. of water was injected into this joint over a period of 90 minutes (the largest volume previously injected had been 3500 gal., the day before). The pumping followed a stepped profile: the injection rate was increased in 1-BPM steps until it reached about 4 BPM at an injection pressure of 2250 psi. During this test, the calculated diameter of the GT-2 joint was effectively doubled, from 400 to 800 ft.

The most significant result of this injection test was that, for the first time, seismic signals from a pressure-dilating and extending joint were recorded on a nearby geophone. Although the sources of the microseismic signals were not well located, it was possible to derive the distances from the geophone to the foci of these few events. It should be noted that these signals exhibited a much higher shear than compressive component, implying that they were related to shear slippage between the faces of the pressure-dilating joint.

EE-1 Inadvertently Turned Away from the GT-2 Target

Directional drilling was resumed on October 1, from the 9575-ft depth, with a Dyna-Drill assembly. In about 115 ft of drilling, EE-1 was turned rapidly to the east by almost 90°, and at the new depth of 9690 ft the bottom of the hole had progressed horizontally eastward by about 7 ft. Although the actual drilling time was only a little over 4 hours, the need to change the bit between runs prolonged the operation to October 3. As drilling proceeded,

the target joint at the bottom of GT-2 was kept inflated by intermittent pumping with the 9-gpm Kobe pump. It was anticipated that if and when the joint was intersected, the outflow into EE-1 would be large enough to cause the GT-2 wellhead pressure to drop dramatically. However, the rate of this pressure decrease—being strongly dependent on the rate of outflow into EE-1—could be "masked" if it occurred during one of the repeated pumping shut-ins (Fig. 3-24).

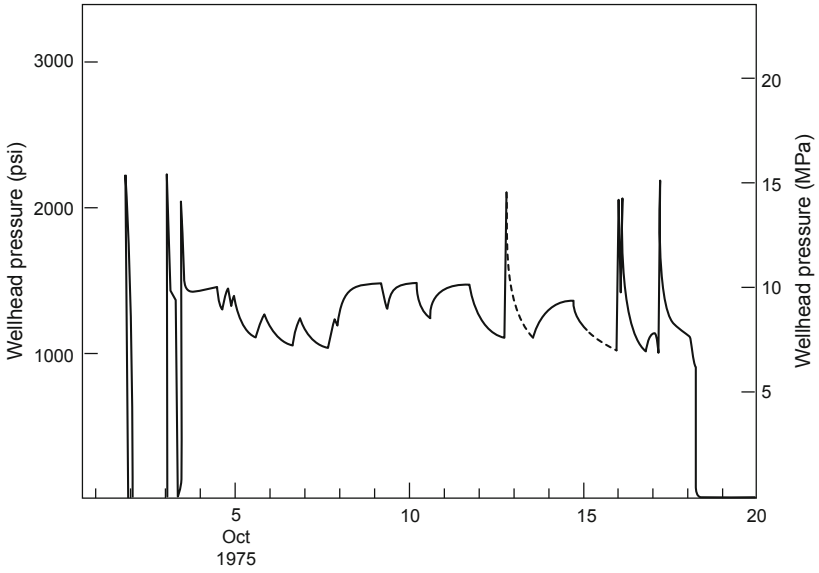

Fig. 3-24. Pressurization history in GT-2 during the directional drilling of EE-1 (pressure declines indicate pump shut-ins).
Source: Blair et al., 1976

A shallow break in the casing at 270 ft interrupted drilling for a couple of days (October 4 and 5). This would have been an excellent time to vent down GT-2 and conduct another seismic ranging experiment to determine whether EE-1 was in fact approaching GT-2 or was instead moving away. The depth in EE-1 that was vertically equivalent to the bottom-hole depth in GT-2 (9619 ft) was 9653 ft. At this depth, EE-1 was horizontally displaced eastward by about 3 ft with respect to its position at 9575 ft. Using the then most recent distance calculation of 26 ft—derived from the second and third ranging experiments—the measured distance would have been either 23 ft (26 – 3 ft, i.e., closer) or 29 ft (26 + 3 ft, i.e., farther away). Had that exercise been carried out at the time, the error in the hole positions would have been discovered—and simply by cementing a whipstock into the bottom of EE-1, the borehole could have been turned back to the west and drilled just a couple of hundred feet more to intersect the target joint below the bottom of GT-2!

Instead, the casing break was repaired by cementing, and directional drilling continued—one 76-ft Dyna-Drill run and a rotary drilling run taking the hole to a depth of 9791 ft. But when the Dyna-Drill was run back in on October 7, it failed after just one foot of drilling: the stator blades sheared off, apparently before they could be adequately cooled by the circulating fluid. The trajectory reading at this depth was N77E, 7°. While a new Dyna-Drill was en route from the manufacturer, the hole was rotary-drilled to a depth of 9877 ft, where the inclination was 7 1/4°.

Seismic Interrogation of the GT-2 Target Joint

On October 10, 1975, the lowermost part of GT-2 was pressure-stimulated again with the Western pump. The total injection volume was only slightly greater than that of the September 30th injection test (12 400 gal. vs 12 000 gal.); but this experiment was specifically designed to seismically interrogate the joint(s) intersecting the GT-2 borehole behind or just below the scab liner, by positioning the geophone package sequentially at four different depths near the bottom of EE-1 (9211 ft, 9409 ft, 9656 ft, and 9856 ft). An Eastman Whipstock magnetic survey tool attached to the bottom of the geophone package allowed the compass orientation of the package to be determined at each depth.

After the geophone package had been run into EE-1, water was pumped into GT-2 through the high-pressure casing string connected to the top of the scab liner. For about 1 1/4 hours, the bottom of the borehole was pressurized to 2150 psi with a pumping rate of about 4 BPM. During this time, the geophone package in EE-1 was placed successively at each station for a 15-minute interval, then returned to the first station (9211 ft) for the last 15 minutes. It should be noted that although the horizontal distance between these stations and the midpoint of the scab liner in GT-2 (about 9280 ft) was only 40–70 ft, the vertical distance between the two deeper stations and the midpoint of the liner was much greater (576 ft for the deepest station, at 9856 ft). Because of these greater distances and the steep angles of arrival, the seismic signals originating near the scab liner in GT-2 were highly attenuated—which meant that their location depended primarily on the much less sensitive vertical geophones. (Seven years later, during Phase II reservoir development, this difference in sensitivity would be quantified and definitively attributed to the impaired vertical coupling of the geophone package to the borehole wall.)

Joint-related microseismic events—characterized by seismic signals having distinct P-wave and S-wave arrivals—were recorded at three of the four stations in EE-1 (unfortunately, the surface readout from the geophone package was temporarily lost during the 15-minute recording interval at 9409 ft).

Assuming that the foci of such events originate from the plane of the dilating joint—as seems reasonable—these signals form seismic maps of the joints, in both space and time. Figure 3-25 is a representation of these maps: the plane(s) of the GT-2 joint(s) are shown as least-squares-fit horizontal projections based on the events recorded at the three depths in EE-1. The indicated planes assume that the stimulated joint(s) were vertical and varied only in their strike.

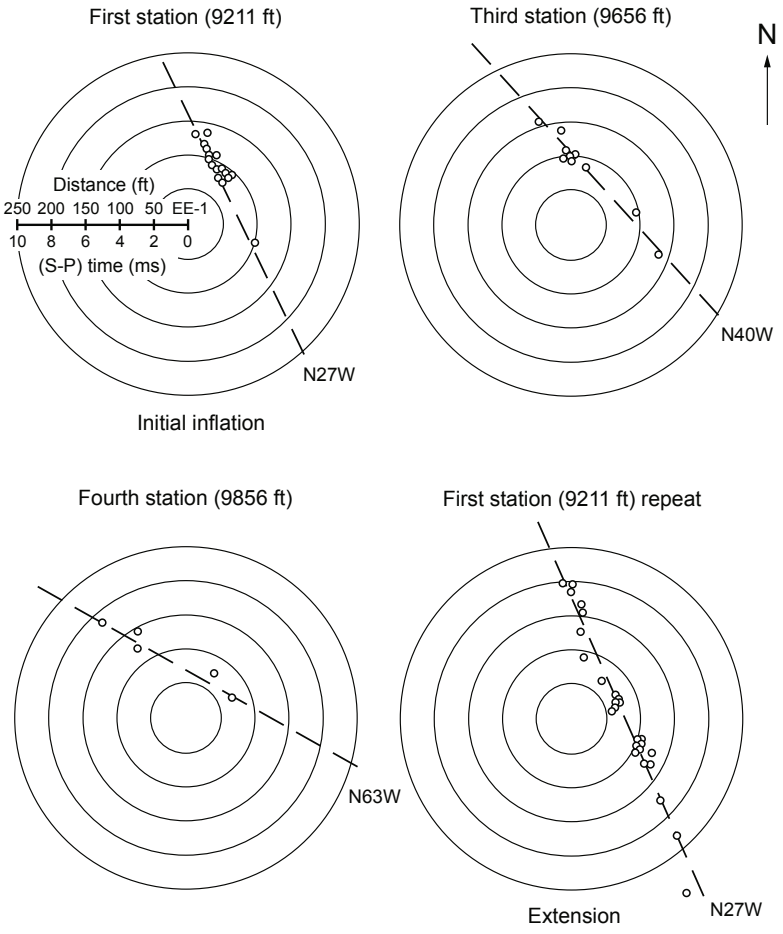

Fig. 3-25. Plane(s) of the GT-2 joint(s), as determined by the seismic experiment of October 10, 1975.
Source: Blair et al., 1976

InfoNote

The use of seismic signals for determining the direction to a microseismic event is limited by the "non-unique" nature of the focal-point data—these data being based in part on the azimuthal approach of the seismic signals to the geophone station. Although there were cases in which the foci for an individual event would define a planar zone of seismicity, and thus allow a planar solution for determining the direction of approach, a 180º ambiguity remained (i.e., without a known focal mechanism for an individual event, two locations—in opposite directions from the geophone station—were equally possible). Ultimately, the solution to this problem was to use a combination of stations: one or more in each borehole.

With an injected fluid volume only slightly greater than that of the September 30 experiment, the October 10 experiment would not be expected to cause extension of the previously deflated GT-2 joint(s) until very late in the pressurization. This is precisely what occurred, as Fig. 3-25 shows. During the first 15-minute recording interval, seismicity was concentrated near the first geophone station (within 140 ft), suggesting initial inflation. Then, when the geophone was returned to this station near the end of the experiment, much of the seismicity was farther away (some as far as 300 ft), indicating joint extension.

Figure 3-25 suggests the possibility that three separate joints were pressure-stimulated near the bottom of GT-2, the most definitive of which was approximately symmetrical about the geophone depth of 9211 ft and striking N27W. At the same time, the observation that each of these three joints "just happens" to be symmetrical about one of the three pre-selected geophone stations in EE-1 casts doubt on the notion of three separate joints. The two deeper "joints" are suspect for two reasons: First, the number of located seismic events is relatively small; and second, if the seismicity originated from the stimulated joint striking N27W (which is probable), the very steep approach angle and greater distance to the deeper geophone stations would have considerably clouded the hodogram analysis. For these deeper stations, accurate analysis was particularly difficult because of the inordinate reliance on the vertical geophone signal. It is possible that the seismicity recorded at the 9656- and 9856-ft depths originated from the deeper reaches of the joint centered at 9211 ft. Given these shortcomings and uncertainties, the most probable scenario is that a single joint was interrogated in GT-2 and that its strike was N27W.

Many of the microseismic signals generated by the inflation and subsequent extension of the GT-2 joint exhibited discernible P- and S-wave arrivals—though in some cases, the P-wave did not emerge from the background noise clearly enough for events to be accurately located. Location of the focus of an event requires (a) distance to the event and (b) arrival

direction of the P-wave. The distance is calculated from the time interval between the P- and S-wave arrivals and from the propagation velocities of the two signals. Because P-waves are linearly polarized in the direction of signal propagation, the arrival direction of the P-wave is specified by its azimuth and inclination (which are determined by analyzing the hodograms of the two components of the P-wave velocity amplitude as derived from the geophone recordings).

Even though in most cases the onset of the P-wave can be determined to within a cycle, the sense of the first arrival is usually uncertain, creating an ambiguity of 180° in azimuth measurements. However, in the particular case of the experiments of October 10, the orientation (i.e., strike and dip) of the joint was unaffected by this ambiguity: with the recording geophone in EE-1 so close to the point of joint initiation in GT-2, the maps of the event foci were essentially centro-symmetric to it.

This experiment marked the first time that the foci of microseismic events resulting from the hydraulic stimulation of a deep, hot region of jointed basement rock had been (a) clearly located in space and (b) definitively associated with the reinflation or extension of pre-existing joints.

Final Attempts to Stimulate the Deeper Part of EE-1

Following the seismic experiment, the Western pump was replaced by the Kobe pump. Pressurization of GT-2 was continued at 9 gpm while the geophone package was removed from EE-1 and a Laboratory self-potential (SP) tool was run in. At about 9500 ft, an electric anomaly was noted that appeared to be the same as one detected by a Dresser-Atlas SP log run in late September—implying a zone of fluid entry in EE-1. Then, at a depth of 9856 ft, a second SP anomaly was seen; the latter was detected again during two subsequent SP logging runs. During these tests, a small amount of water was observed flowing out of EE-1—the first evidence (although trivially small: about 1 gpm) of a flow connection between the two boreholes—probably via a tortuous, multiple-joint flow path having very high impedance.

A final core was taken in EE-1 during this period—from 9877 to 9881 ft—with an American Coldset Corporation diamond bit having a 9 5/8-in. (244-mm) outer diameter and a 6-in. (152-mm) inner diameter. Core recovery was only about 17%.

The final drilling run (with a 9 5/8-in. rotary drilling assembly) took place October 12, 1975, completing EE-1 at a depth of 10 053 ft. A temperature log was run on October 13; it identified the EE-1 fluid entry point at 9500 ft by registering a sharp, 4°C–5°C temperature drop immediately below that depth (the water flowing into and then up the EE-1 borehole from the fluid entry point was being heated as it traversed the jointed rock adjacent to the borehole). A repeat temperature log run the same day verified the fluid entry point at 9500 ft, but repeat SP logging did not show the anomaly seen three

days earlier at 9856 ft. The equilibrium temperature at hole bottom was 205.5°C and the geothermal gradient was about 60°C/km.

With EE-1 complete except for installation of casing, several more temperature logs, electric logs, and pumping and hydraulic pressurization experiments were done, ending on October 22. The results confirmed the existence of a "weepy" flow connection between GT-2 and EE-1—a cause for some celebration, but perhaps even more consternation: considering the quantities of water being injected into GT-2, the rate of flow into EE-1 at 9500 ft was very low (only about 1 gpm), indicating that the flow impedance was extremely high; and therefore, most definitely no HDR reservoir had been created.

On October 14, 1975, in the hope that the hydraulic connection could be improved, a Lynes inflatable packer was set at 9600 ft in EE-1 to isolate the bottom of the borehole from the rest of the open-hole interval. Next, GT-2 was pressurized with the Western pump; when the pressure reached 2100 psi, the pump was moved to the EE-1 wellhead and the 9-gpm Kobe pump was used to continue injecting into GT-2. At 9 gpm, the GT-2 injection pressure dropped rapidly to 1800 psi, then continued falling more slowly. With the Western pump now connected to the drill pipe at EE-1, the region below the packer was pressurized at increasing injection rates—up to about 2.1 BPM (5.6 L/s) at 2400 psi. But after the injection of 3700 gal. into EE-1, the Lynes packer failed. During the pressurization of EE-1, while injection into GT-2 was maintained at 9 gpm, the pumping pressure continued to drop at a steadily decreasing rate until it finally stabilized at 1500 psi.

Pumping into GT-2 continued with the Kobe pump while EE-1 was vented and the failed packer was pulled from the hole. During this time, the injection pressure at GT-2 dropped further, then stabilized once more, at 1190 psi. The vent flow from EE-1 finally stabilized at about 4 gpm (0.25 L/s)—this somewhat improved flow connection from GT-2 suggesting that a new flow path had been opened into EE-1 below 9600 ft, at a pressure of about 2400 psi.

The next day, while pumping into GT-2 continued at a pressure of 1190 psi, the flow from EE-1 was measured at 5 gpm. Temperature and SP logs run in EE-1 both showed very sharp anomalies at 9650 ft, indicating the new point of fluid entry. With this sign that a deeper—and potentially better—flow connection to GT-2 might exist, further pressurizations were planned to try to open up this EE-1 joint (or joints). Lynes inflatable packers were run several more times over the next few days. The first packer hung up at about 9600 ft while being run in, necessitating reaming of the 9570- to 9918-ft section of the hole. On October 17 the next packer was run in, to a depth of 9822 ft, but failed to set. When the drill pipe was pulled from the hole, it was discovered that the packer assembly had sheared off and been left in the hole. A third packer was tried the next day, but could not be lowered below 9278 ft; when it was pulled out, the lower third of the

packer assembly was missing. At this point, a bit run was made to 10 022 ft, pushing the several packer remnants to the bottom of the hole.

Finally, on October 20, a fourth packer was successfully set at a depth of 9791 ft. The Western pump was then used to pressurize the bottom 260 ft of the borehole. The pressure reached 3300 psi before there was evidence of water bypassing the packer—but no borehole breakdown occurred. At the time this behavior was surprising, considering that the pressure to which the borehole had been subjected was far above the least principal earth stress (about 1240 psi above hydrostatic at this depth).

The following day, one more attempt was made to hydraulically fracture the lower part of the borehole, but the Lynes packer seated prematurely at about 800 ft and had to be withdrawn. Thus ended the effort to hydraulically fracture EE-1 below 9800 ft.

Note: Subsequent work several years later would show that the portion of EE-1 below about 9650 ft was actually within the deeper (Phase II) reservoir region, in which joint-opening pressures were considerably higher.

Completion of the EE-1 Borehole

On October 23, 1975, a final (composite) casing string, with a Halliburton cement shoe installed on the bottom, was run into EE-1 to a depth of 9599 ft. Sometime in the few weeks before the running of this casing, a high-temperature, magnetic multishot survey was done in EE-1 by Eastman Whipstock. The exact date is uncertain, because the survey was neither described nor referred to in any of the reports of the time. But in a report published about three years later, after the redrilling of GT-2, the position shown for the EE-1 borehole is based on data from that October 1975 Eastman Whipstock survey (Fig. 20 in Pettitt, 1978b). Obviously, by 1978 the drilling personnel had recognized that these earlier magnetic multishot data represented the best knowledge of the EE-1 borehole trajectory—better than the data from any of the later (1977) gyroscopic surveys in EE-1.

The upper section of the final casing string was 8 5/8-in., 32-lb/ft, Grade J-55 pipe; the 999-ft-long lower section consisted of 7 5/8-in., 26.4-lb/ft, Grade N-80 pipe (the lower section was smaller in diameter to provide additional annular clearance for the cement in the 9 5/8-in. drilled hole). As the lower section was being run in, a Halliburton float collar and baffle plate were installed two joints (about 80 ft) above the float shoe. In preparation for cementing, the casing was flushed with about 400 gal. of water.

A day later, the lower section of casing was tag-cemented by Halliburton Oil Well Cementing Co. Some 1800 gal. of highly retarded cement slurry, consisting of almost 25% silica flour (5760 lb), was pumped into the casing; it was followed by an 8 5/8-in.-diameter wiper plug of soft rubber, flexible enough to fit into the lower 7 5/8-in. section of casing. Then, with 24 000 gal. of water (an amount calculated to just fill the casing down to the float collar), the cement was displaced down the casing, around the bottom

of the float shoe at 9599 ft, and up into the annulus. When the wiper plug on top of the cement "bumped" the valve on the float collar, pumping was stopped and the annulus was shut in. After shut-in, the surface pressure on the annulus was 800 psi—higher than would have been expected for a 1200-ft column of tag cement—suggesting that flow from GT-2 into EE-1 below the casing shoe was contributing to this pressure.

The GT-2 borehole was kept pressurized during the cementing operation, to prevent any cement from entering the fracture connection. Unfortunately, there was also an unintended consequence: the pressurized water from GT-2, flowing at a rate of about 1 gpm into the lowermost part of the EE-1 borehole outside the casing, slowly displaced the cement upward. As anyone familiar with cementing would realize, this water flow tended to channel upward, creating flow paths through the slowly hardening cement.

InfoNote

We emphasize in the strongest terms that the error in cementing the EE-1 casing should not have occurred. There was no evidence at that time, nor has any come to light since, that—at the modest pressures used for cementing—cement will flow into joints in the crystalline basement that had been pressure-opened and then depressurized. In fact, during the early drilling of GT-2, deliberate attempts to close off fluid inlets with cement not only failed but had disastrous results, as described earlier in this chapter. The belief on the part of the EE-1 drilling supervisors (and some HDR staff) that a flowing joint might inadvertently be closed off with cement stemmed from lack of understanding of what had happened during the drilling of GT-2.

After a 24-hour wait for the cement to set, a bit run was made to clean out the casing, drill out the float collar and float shoe, and clean the hole to bottom. But the bit encountered no cement between the float collar and float shoe, raising suspicions that there could be a problem with the cement around the lower part of the casing. However, after the float shoe had been drilled through, the tag-cement job was pressure-tested with the rig pumps to about 1000 psi, which revealed no problem.

Before the drill rig was released on October 27, a cement-bond log was run by Dresser-Atlas. It revealed that—owing to the unintended upward displacement of the cement (accompanied by "water-cutting" and channeling of the lower portion, in the annulus outside the 7 5/8-in. casing)—bonding from the cement shoe at 9599 ft to 9020 ft was only 30% to 50%. Over the 9020–7900 ft interval (in the smaller annulus outside the 8 5/8-in. casing, which was less affected by the water-cutting and displacement), bonding was good—95% to 98%. The completed EE-1 borehole, including the details of the casing cement job, is shown in Fig. 3-26.

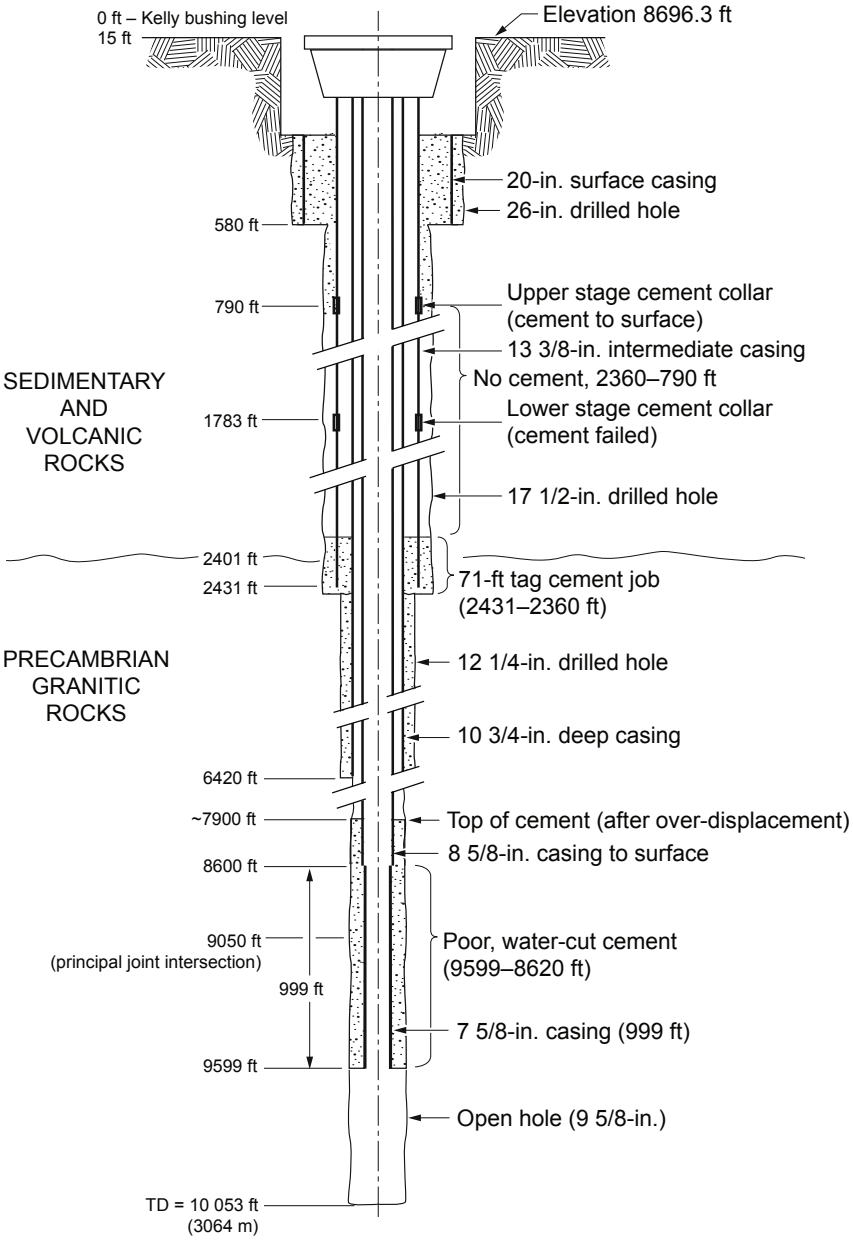

Fig. 3-26. The EE-1 borehole, as completed in October 1975.

Fast Forward: Where the Boreholes Really Were

Because the final 500 ft of drilling took the EE-1 borehole away from, rather than toward, the N27W-striking joint emanating from the bottom of GT-2, the hoped-for reservoir connection was not achieved. By the time magnetic multishot surveying was done later in October, the hole had already been turned in the wrong direction and been completed to its final depth of 10 053 ft. (The Project staff, not yet aware of the true relative positions of the boreholes, believed that the flow connection between them could be significantly improved.)

It would be nearly a year and a half before additional survey data shed more light on this issue. In 1975, the Laboratory had signed contracts with both Eastman Whipstock and Sperry-Sun for the development of high-temperature gyroscopic surveying tools.[15] When tested in both boreholes in early 1977, these tools would perform well in GT-2 (a borehole with only modest horizontal displacement) but only marginally in EE-1, with its much greater horizontal displacement. In fact, it would be found that for EE-1, none of the five gyroscopic surveys was as accurate as the Eastman Whipstock magnetic multishot survey of October 1975. For GT-2, the Eastman Whipstock gyroscopic survey was not only better than either of the Sperry-Sun surveys, it was also superior to the magnetic single-shot surveys performed during drilling (which may have been adversely affected by the magnetic mineral content of the deeper granitic rocks).

Figure 3-27, which combines the best trajectories for the two boreholes (1975 magnetic multishot survey in EE-1 and 1977 gyroscopic survey in GT-2), shows that the trajectories depicted in Fig. 3-23 had been somewhat in error—by about 1/2%. The bottom of GT-2 was

[15] When the Fenton Hill experiments began in 1974, most of the techniques, equipment, and instruments needed for characterizing a 10 000-ft-deep HDR reservoir in basement rock, at temperatures above 200°C, did not exist. Conspicuously lacking were reliable methods of borehole surveying at temperatures far higher than those encountered in petroleum drilling up to that time. For example, the magnetic surveying techniques used in the effort to determine the relative positions of GT-2 and EE-1 had produced conflicting results, because of both magnetic anomalies (due to the varying magnetite content of the basement rock) and the elevated temperatures. This need for better survey data would lead the Laboratory to negotiate contracts with Eastman Whipstock and Sperry-Sun, both of Houston, TX, for the development of high-temperature (at least to 200°C) gyroscopic borehole-surveying tools. The tools built by the two groups would use the same basic design: a vacuum heat shield and a Cerrobend (low-melting-temperature) heat sink to protect the gyroscope and batteries. The Eastman package would feature a surface readout, whereas the Sperry-Sun tool would be entirely self-contained with internal recording.

actually some 35 ft farther south and 30 ft farther west than had been indicated by magnetic single-shot surveys (Figs. 3-21 through 3-23); and at 9575 ft, EE-1 was actually 37 ft farther south and 15 ft farther west than shown in Fig. 3-23.

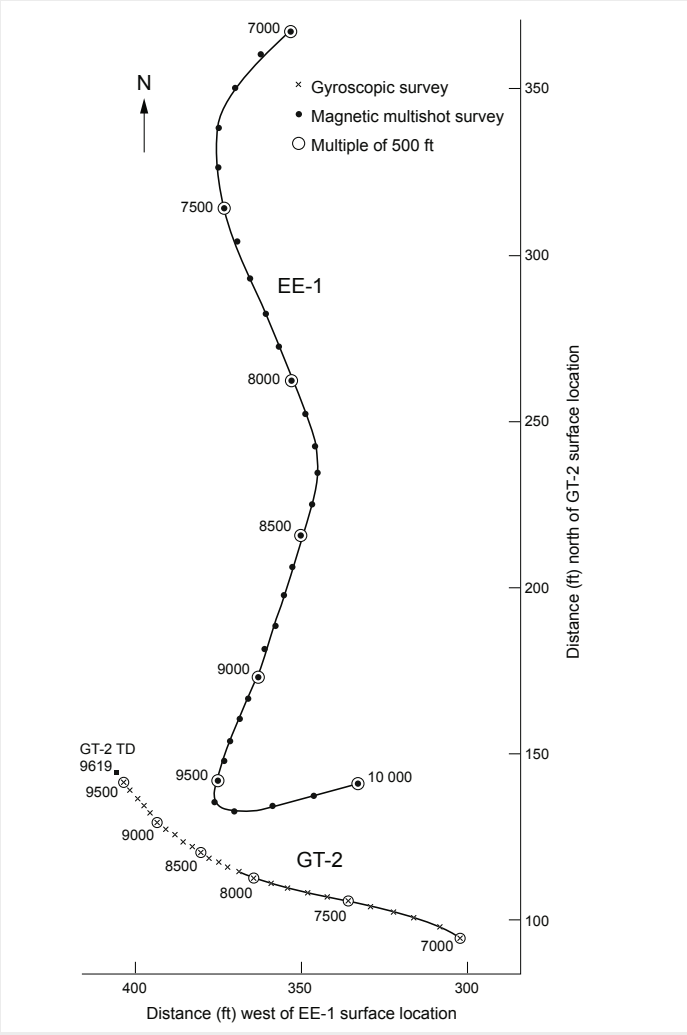

Fig. 3-27. Plan view of the trajectories of the completed GT-2 and EE-1 boreholes below 7000 ft, based on the Eastman Whipstock high-temperature magnetic multishot survey of EE-1 (October 1975) and the Eastman Whipstock high-temperature gyroscopic survey of GT-2 (January 1977).
Adapted from Pettitt, 1978b

But much more serious, the seismic data analysis that showed EE-1 at 9575 ft as almost due west of GT-2 was in error by 180º! The hodogram method used for the analysis is inherently subject to an ambiguity of 180º with regard to the direction of the received seismic signals: if the geophone and/or detonator coupling is poor—as it was in this case—the sign of the initial rise in the P-wave arrival is not definitive.) The October 1975 magnetic multishot survey of EE-1, in combination with the 1977 gyroscopic survey of GT-2 (Fig. 3-27), would show the true position of EE-1 at that depth to be nearly due *east* of GT-2. The region of near-intersection of the two boreholes seen in Fig. 3-27 is magnified in Fig. 3-28, which also gives the measured horizontal distances between the two at 9100 ft and 9575 ft in EE-1. These distances—52 ft at 9100 ft and 28 ft at 9575 ft—corroborate those found by seismic ranging at the same depths, i.e., 52 ft and 26 ft.

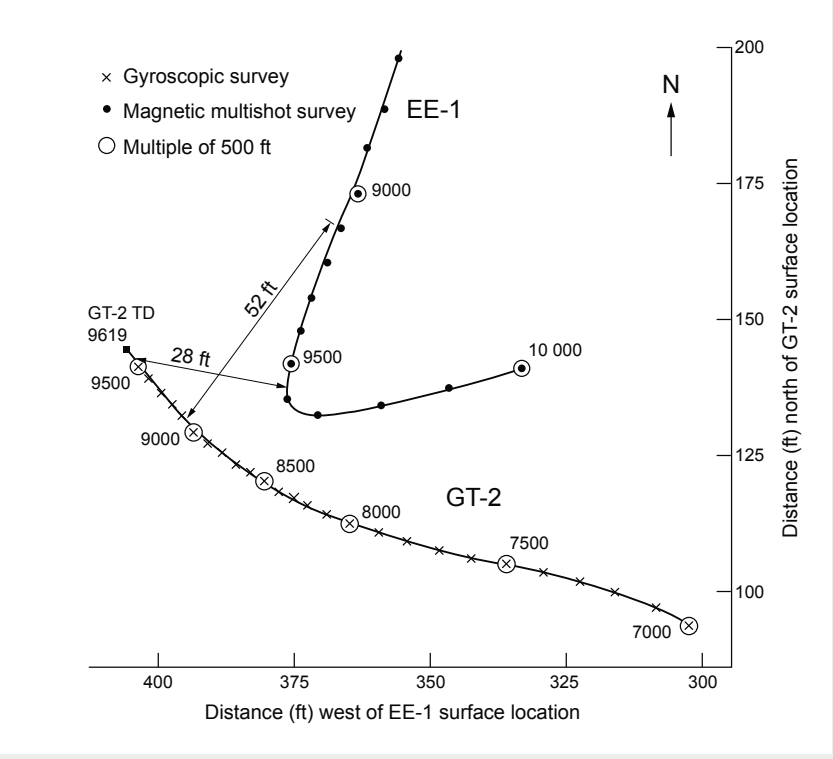

Fig. 3-28. Magnified view of the region of closest approach of the borehole trajectories shown in Fig. 3-27.

As noted above, if magnetic multishot surveying of EE-1 had been done when the bottom of the hole was at 9575 ft, the results would have stopped the project "dead in its tracks" until a concerted diagnostic effort could resolve the question of where the boreholes really were relative to one another! Instead, when directional drilling recommenced in October 1975, the turning of the EE-1 trajectory in a very tight arc to the east (ultimately, to N77E at a depth of 9690 ft) took the borehole in the wrong direction—away from GT-2 and from the target joint. The decision was entirely based—even in the face of conflicting data—on the erroneous determinations, obtained via seismic analysis, of the position of EE-1 vis-à-vis GT-2. Continued drilling on this path, to the final depth of 10 053 ft, then carried EE-1 ever farther from its intended target!

The remainder of this chapter describes how the true positions of the boreholes were eventually clarified and how the direction of the HDR Project was modified as a result.

Studies of the Deep Joints Stimulated from EE-1 and GT-2 and Attempts to Improve the Hydraulic Connection (November 1975–November 1976)

The HDR Project staff recognized that the hoped-for low-impedance hydraulic communication between GT-2 and EE-1 had not been achieved because the deeper portion of EE-1 had failed to intersect the large joint emanating from the bottom of GT-2. The ready answer for this failure was that the downhole geometry at Fenton Hill—both of the boreholes themselves and of the surrounding jointed rock—was not well understood. This indeed was a factor, particularly given that the relative positions of the two boreholes were still not known; but of course the major factor was that because of the misinterpretation of seismic data using the hodogram method, the two boreholes had been getting farther apart, rather than closer, as EE-1 was deepened below 9575 ft. As emphasized earlier, this confusion could and should have been resolved before drilling proceeded—techniques for doing so were available—but it was not.

Believing, then, that the Project's major need at this stage was better knowledge of the downhole environment, the team decided that the coming year's work would focus on studies designed to

- characterize, through a variety of interrogation techniques, the geometry (size, strike, and dip) of the principal pressure-stimulated joint near the bottom of GT-2 and of the one or more joints pressure-stimulated below 9000 ft in EE-1, and
- improve the hydraulic communication between the two boreholes.

These studies, carried out between November 1975 and November 1976, involved numerous experiments and tests. For many of these, a new, larger Kobe pump—having a nominal pumping rate of 34 gpm—was used. (This pump, procured by the HDR Project in late 1975, was thereafter referred to as the "big Kobe pump" and the original 9-gpm pump as the "small Kobe pump.") To facilitate later reference, the experiments in this series were numbered, beginning with Experiment 101. However, not all of the experiments originally proposed were actually conducted; some experiments ended up with null results because of failed instrumentation or equipment, severe weather, or other problems; and in a few cases the chronological order of experiments differed from that indicated by their numbers. Table 3-12 lists the most important of the experiments, and these are referred to as appropriate in the discussion that follows.

The information in this section is taken mainly from Blair et al. (1976), HDR Geothermal Energy Development Project (1978), and Pettitt (1978b).

Table 3-12. Major experiments and tests to investigate the deep system of joints and improve hydraulic connectivity (November 1975–November 1976)

Expt. No.	Date	Description	Remarks
101	6 Nov. 1975	Background temperature log in GT-2.	Temperature anomalies at about 9200 ft (a hole had been milled in the liner) and 9450 ft (liner was perforated); bottom-hole temperature constant at 197°C.
102	12 Nov. 1975	Pumping into GT-2 at 9 gpm and 1000 psi.	Measured EE-1 outflow of 2.2 gpm.
104	2 Dec. 1975	Background temperature log in EE-1.	No anomalies noted. Bottom-hole temperature = 205.5°C.
105	3–4 Dec. 1975	Temperature log in GT-2 during pumping into EE-1 at 34 gpm (injection pressure = 1150 psi).	EE-1 injection = 13 600 gal.; GT-2 outflow = 10 680 gal.—75% from 9200 ft, 25% from 9450 ft.
106	23–24 Dec. 1975	Pumping into EE-1 at 34 gpm, followed by temperature logging (injection pressure = 1360 psi).	EE-1 injection = 11 600 gal.; GT-2 outflow = 7000 gal. at 9 gpm. No temperature change. Impedance = 155 psi/gpm (17 MPa per L/s).
109	11 Feb. 1976	Induced-potential and self-potential logs in EE-1.	Logs show conductive zone from 9770 to 9780 ft (below casing at 9599 ft).
111	16–19 Mar. 1976	Pumping into EE-1 at several pressures, up to 1320 psi, with GT-2 shut in.	EE-1 injection = 27 000 gal.; GT-2 pressure = 950 psi. After shut in of both wells for 53 hours, EE-1 = 705 psi, GT-2 = 730 psi.

Table 3-12. (Continued)

Expt. No.	Date	Description	Remarks
114	4–7 Feb. 1976	Measurement of flow rate potential of hydraulic connection with joint system inflated.	Both holes pressurized in steps to about 1300 psi, then GT-2 slowly vented (25 psi/h) at 14–20 gpm. Measured σ_3 in GT-2 =1240 psi. Final flow impedance = 50 psi/gpm (5.5 MPa per L/s).
115	23–24 Mar. 1976	Residence-time analysis of joint system by means of tracer techniques. EE-1 injection pressure held at 1300 psi.	EE-1 injection = 60 080 gal. with 100 gal. sodium fluorescein dye. Substantial tracer dispersion seen in interconnected joint system.
116	20–21 Mar. 1976	Iodine tracer injections into GT-2 and EE-1. Gamma-ray logging in both boreholes and cement-bond log in GT-2 (all by Dresser-Atlas).	EE-1 joint intersection from 9610 to 9690 ft, oriented N54W. GT-2 injection at 9200 ft through liner where Otis packer previously milled out and liner breached.
117	3–5 Mar. 1976	Mapping of EE-1 joint. Injection into EE-1 first at 4 BPM and 1600 psi, then at 5 BPM and 1700 psi, with geophone package in GT-2.	Orientation of geophone package achieved. Many discrete seismic signals received from different azimuths and depths.
119	27–29 April 1976	Residence-time analysis of deflated joint system (pumping into EE-1 with sodium fluorescein dye at a controlled pressure of 700 psi, GT-2 vented).	EE-1 injection = 31 540 gal. with 1.8 gal. of concentrated dye. First dye appearance in GT-2: 2500 gal. after maximum calculated short-circuit time. 91% of injected volume recovered. Final impedance = 75 psi/gpm (8.2 MPa per L/s).
120	11–14 May 1976	Constant-pressure injection into EE-1 (34 gpm, 1350 psi) for 90 hours. Flow from GT-2 maintained at 10 gpm.	Steady-state circulation established. Low-pressure flow impedance = 26 psi/gpm (2.8 MPa per L/s); EE-1 injection = 182 730 gal.; GT-2 production = 145 750 gal. (80%).
122	6 May 1976	Seismic mapping of EE-1 joint at 9650 ft.	Many problems with faulty geophones, lightning strikes, and power outages. No seismic data.

Table 3-12. (Continued)

Expt. No.	Date	Description	Remarks
122A	10 May 1976	Continuation of Expt. 122—injection into EE-1 of 41 400 gal. at 5 BPM and 1200 psi (injection pressure very close to σ_3 measured during Expt. 114). With GT-2 vented, flow reached about 50 gpm.	When GT-2 shut in, pressure leveled off at 1102 psi in 1 hour; when vented, flow impedance dropped to 24 psi/gpm (2.6 MPa per L/s) at end of injection—an early indication of the opening up, behind the casing, of a higher joint (later located at 9050 ft) that would develop into the major flow connection for EE-1.
127	16–17 June 1976	Ranging experiment to confirm borehole separation at 9100 ft.	46-ft separation measured, consistent with the 52-ft separation measured earlier at this depth.
129	22–29 June 1976	Seismic mapping of EE-1 joint at 9050 ft.	50 320 gal. injected into EE-1. "Sufficient" seismic signals obtained.
133	19–21 July 1976	Measurement of flow impedance during pumping into EE-1 at flow rates of 34 and 43 gpm and pressures up to 1550 psi; measurement of temperature profile inside GT-2 high-pressure string and liner to detect outflow from GT-2 joint into region behind scab liner and into annulus just above liner.	Temperature measurements in GT-2 showed flow from EE-1 into GT-2 joint now exiting that joint between 9015 and 9100 ft—through channeled cement behind scab liner and then into annulus above liner (rather than into borehole through high-impedance milled hole in liner, as before). This change in exit flow path caused overall flow impedance to drop from 100 psi/gpm to 30 psi/gpm (3.3 MPa per L/s).
137	1–11 Nov. 1976	Flow test to ascertain baseline parameters for sodium carbonate leaching experiment (250 000 gal. injected at low rate).	Flow rate and pressure information analyzed. Flow impedance at end of test stabilized at 75 psi/gpm.
138	11–18 Nov. 1976	Sodium carbonate used to leach quartz from contact surface of 9050-ft in EE-1; borehole shut in on 17 Nov. at 1200 psi.	Test results evaluated. Flow impedance *increased*, to 90–100 psi/gpm.
144A	7 Oct. 1976	Temperature log in GT-2 with new thermistor.	Temperature logging over full depth of borehole.
144B	21 Oct. 1976	Temperature log in EE-1 with new thermistor.	Temperature logging over full depth of borehole.
145	14 Oct. 1976	Repeat of ranging experiment in GT-2 (at 9020, 9090, and 9390 ft)	Results of Expt. 127 confirmed.

Temperature Logging to Detect Fluid Entry/Exit Points

The temperature log in GT-2 (Expt. 101) indicated that injected water was exiting the borehole—not only at the bottom of GT-2, but also through the scab liner at about 9200 ft (where a packer had been milled out) and through perforations at about 9450 ft. This information suggested that the GT-2 joint was of significant extent and possibly made up of several closely spaced *en echelon* joints.

On November 12, during pumping into GT-2 with the small Kobe pump at 9 gpm and a pressure of about 1000 psi (Expt. 102), the outflow from EE-1 was measured at 2.2 gpm—suggesting at best a marginal flow connection. Three weeks later, Expt. 104 (background temperature logging in EE-1) showed no points of residual fluid inflow.

During Expt. 105 (December 3–4), EE-1 was pressurized at 34 gpm for a total of 400 minutes while temperature logging was done in GT-2. Comparison of the size of the temperature anomalies at 9200 and 9450 ft led to the conclusion that the outflow rate at 9200 ft was about three times that at 9450 ft. However, because of the very short distance—38 ft—from the bottom of the scab liner at 9581 ft to hole bottom (and the considerably larger diameter of the open hole vis-à-vis the liner), it was not possible to detect a temperature anomaly associated with inflow from the joint opened below the liner in early 1975.

Joint Mapping Experiments

The lengthy series of experiments that occupied the first half of 1976—tests and retests of the tortuous flow connection between the two boreholes—left the staff rather incredulous that the supposedly direct connection between EE-1 and the joint extending downward from the bottom of GT-2 did not result in a very low flow impedance. The best impedance achieved, after repeated pressure-exercising of the connecting network of joints, was 26 psi/gpm. Experiments 115 and 116 (tracer tests) showed a high degree of dispersion, confirming the complexity of the interconnecting joint network.

Experiment 117, performed in early March of 1976, was an attempt to map the EE-1 joint opened the previous October at a depth of 9650 ft and then repressurized twice in December of 1975.[16] This experiment was essentially a repeat of the October 10, 1975 seismic experiment, but with the roles of the boreholes reversed—injection into EE-1 and seismic recording in GT-2.

---

[16]This joint was initially opened on October 14, 1975 (at a pumping rate of 2.1 BPM [5.6 L/s] and pressures up to 2400 psi), and the fluid entry point was identified the next day. The joint was later repressurized twice at a rate of 34 gpm—first on December 3–4, 1975 (Expt. 105, when 13 600 gal. of water was injected at a pressure of 1150 psi) and again on December 23–24 (Expt. 106, when 11 600 gal. was injected at a pressure of 1360 psi).

On March 3, the geophone package was positioned in GT-2 (at hole bottom—9619 ft—because the magnetic orientation tool attached to the sonde needed to be in an uncased portion of the borehole). For two hours the EE-1 joint was reinflated with the injection of 9040 gal. of water at a rate of 4 BPM (11 L/s) and a pressure of 1600 psi; during that time the geophones recorded 15 microseismic events.

Following an overnight shut-in, the geophone package was again positioned at 9619 ft in GT-2. This time the EE-1 joint was reinflated and then extended over a 2 1/2-hour period, by the injection of an additional 22 000 gal. of water at a rate of 5 BPM (13 L/s) and a pressure of 1700 psi). On this second day, 65 microseismic events were recorded—at a rate of less than one per minute during joint reinflation, but then at double that rate during the joint-extension stage.

Because of the low signal-to-noise ratio, which rendered the P-wave arrival times uncertain, none of the events of the second day could be used to map the orientation of the EE-1 joint. And of the 15 events of the first day, which were randomly distributed in time, only six provided information usable for mapping. On the assumption that the EE-1 joint was vertical,[17] its plane—as derived from those six event locations—would be as shown in Fig. 3-29, with a strike of N54W. This plane would place the joint about 75 ft southwest of the geophone location in GT-2. Even if the position of EE-1 relative to the bottom of GT-2 had been as shown in Fig. 3-23, as believed at the time, such a location for the EE-1 joint would be improbable to say the least: the trace of the joint would have been outside the lower boundary of the figure by quite a bit. And with respect to the true relative positions of the two boreholes—which would be discovered only the following spring—such a location would have been virtually impossible.

[17]Open-hole portions of both boreholes, beginning with GT-2 in 1975, were periodically surveyed by the USGS with their high-temperature borehole televiewer, a sonic scanning tool that can detect and map natural joints and induced fractures intersecting the borehole wall. These surveys, and analyses of the vertical extent of temperature anomalies in the boreholes, indicated that the principal joints connected to EE-1 and GT-2 were essentially vertical.

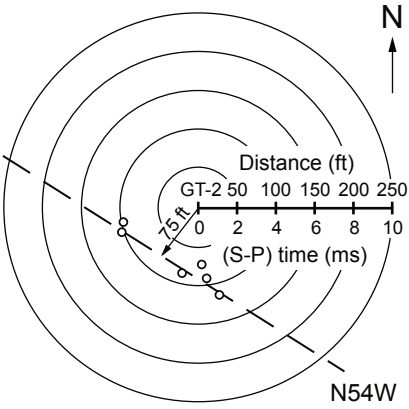

Fig. 3-29. Plane of the EE-1 joint at 9650 ft, as determined during Expt. 117 in early March, 1976.
Adapted from Blair et al., 1976

A radioactive iodine survey (part of Expt. 116) and temperature logging followed Expt. 117, aimed at measuring the orientation of the EE-1 joint at its intersection with the borehole. Both methods yielded a height of 80 ft for the joint intersection, with a midpoint at 9650 ft. On the basis of the known inclination and direction of the EE-1 borehole at 9650 ft, and assuming that the joint was vertical, the strike was calculated to be N54W, the same as that determined by Expt. 117 (Fig. 3-29). It is obvious that, given the borehole positions shown in Fig. 3-27, a N54W-striking joint intersecting the EE-1 borehole at 9650 ft could not at the same time occupy the position in space shown in Fig. 3-29 (75 ft southwest of GT-2). Experiment 117, then, again demonstrated the 180° ambiguity inherent in the hodogram method when determining direction to individual microseismic events. In reality, the EE-1 joint was 75 ft northeast of the bottom of GT-2 (but the orientation shown in Fig. 3-29—N54W—was still correct).

From April 27 to 29, to further investigate the joint system connecting the two boreholes, GT-2 was vented and a dye tracer was injected into EE-1 (Expt. 119). Some 31 540 gal. of water containing sodium fluorescein was pumped into the borehole at a controlled injection pressure of 700 psi. The subsequent recovery of 91% of the injected fluid indicated that the joint system was very tight, i.e., diffusion of fluid into the surfaces of the pressurized joints was very small.

A third experiment to map the orientation of the EE-1 joint at 9650 ft took place a couple of weeks later, in two parts (122 and 122A); but the experiment failed because of a faulty vertical geophone, which severely hampered the hodogram analysis. The injection pressure at which some 41 400 gal. of water was injected into EE-1, at a rate of 5 BPM, was about 1200 psi—

somewhat lower than those of previous high-injection-rate experiments (for example, the pressure during Expt. 117 had been 1600 psi). This was the first of a number of signs that the fluid was no longer entering only the joint at 9650 ft. Another was the leveling off of the flow impedance (which had been declining) at 24 psi/gpm—the lowest value measured to date. In fact, given the high rate of injection, this lower impedance suggested that a significant portion of the flow was now going up behind the casing and out a new joint opening (which would later be located at about 9050 ft).

Note: At this juncture, in mid 1976, the results of the tests and experiments performed so far had led to the following conclusions regarding the tenuous flow connection between the two boreholes:

- Nearly parallel joint systems had been developed from the bottoms of GT-2 and EE-1.
- The impedance to flow between the boreholes was too high for a meaningful heat extraction experiment to be carried out.
- The rock between the GT-2 and EE-1 joints presented a considerable obstacle to reducing flow impedance.

Although some additional experiments were planned, to attempt to reduce the flow impedance, redrilling one of the boreholes was increasingly viewed as the most practical option for achieving a viable HDR heat-extraction system at Fenton Hill. Preliminary studies for a redrilling program began in June 1976, and specifications for the program were written in July 1976. In January 1977, along with continuation of flow testing and other experiments, a small group was formally organized for in-depth study of the problems anticipated in redrilling and to make recommendations for directionally drilling out of one borehole to intersect the joint system opened near the bottom of the other.

The final EE-1 mapping experiment (Expt. 129), which was performed in late June of 1976, would yield a surprising result. During this experiment, 50 320 gal. of water was injected into EE-1 at a rate of about 1.7 BPM (4.5 L/s), in four stages (each lasting one day), while the geophone package was positioned at four different stations within the scab liner in GT-2. Unfortunately—because of the low signal-to-noise ratio of the seismic recording system and differences in the frequency response between the high-temperature geophones—the only usable seismic data came from the fourth day, when 11 locatable events were finally recorded by the geophone package at 9360 ft. A map of these events is shown in Fig. 3-30 (traces of a typical microseismic event, recorded by the vertical and two horizontal geophones, appear below the map). The locus of activity in the figure is roughly linear and strikes northwest. The seismic traces shown highlight the difficulty of picking the P-wave arrival as it emerges from the background noise, as opposed to the relative ease of picking the subsequent S-wave arrival.

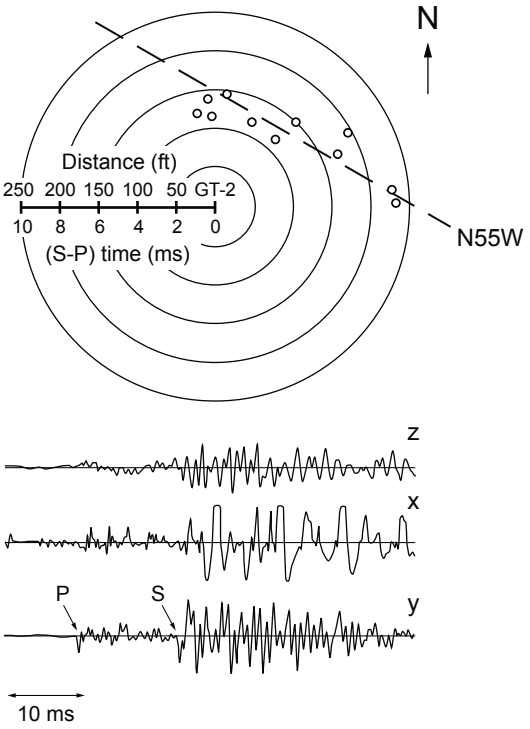

Fig. 3-30. Plane of the higher EE-1 joint (subsequently located at 9050 ft), as determined during Expt. 129 in late June, 1976. Also shown is a typical microseismic event recorded during this experiment.
Source: HDR, 1978

The surprise came when the results of Expt. 129 were compared with those of Expt. 117 (Fig. 3-29). The joint located during Expt. 117 had been mapped as southwest of GT-2, whereas the one mapped during Expt. 129 was clearly to the northeast. (The problem, as would be seen later, was that the position of the GT-2 borehole—shown in Fig. 3-23—was in error; the joint located during Expt. 117 actually lay almost on top of GT-2, rather than southwest.)

The different injection pressures recorded for Expt. 117 (1600 psi) and for Expt. 122A (1200 psi) suggests that two separate, but essentially parallel, joints had been pressure-stimulated in EE-1: during Expt. 117, the N54W-striking joint that intersected the borehole at 9650 ft (originally opened in October 1975) was reinflated; then, during Expt. 122A, a new joint having a strike of N55W was opened higher up, behind the EE-1 casing. This higher joint is the one that was very tenuously mapped—on the basis of only 11 events—during Expt. 129. Later temperature logging, radioactive tracer testing, and other diagnostics (Expt. 156, in February of 1977) would locate

this joint at 9050 ft. Its opening was apparently the result of repeated pressure and temperature cycling in EE-1 during Expts. 114, 117, 119, 120, and 122A, which allowed water to finally work its way up through the cement behind the casing (already substantially channeled by water during the original cementing job, when GT-2 had been kept pressurized) and open a weakness in the borehole wall.

This higher joint was slightly permeable and must have had a very favorable orientation relative to the earth stresses. Pressure data for this joint, obtained from the shut-in GT-2 borehole during Expt. 122A, showed the lowest equilibrium reinflation/extension pressure ever measured in this depth range—only 1100 psi—making it the closest yet to being orthogonal to the least principal earth stress.

The new joint connection thus created in EE-1 would have serious ramifications for all subsequent flow experiments in this series. The deeper joint, at 9650 ft, had more promising attributes—e.g., a deeper entry point for heat transfer and a closer physical proximity to the GT-2 joint; but although still receiving some flow during Expt. 122A, when the flow impedance hit its lowest value of 24 psi/gpm, by now this deeper flow connection to GT-2 was essentially inactivated (it required an injection pressure of 1500–1600 psi for significant inflow, whereas the injection pressure for the higher joint was only 1200 psi).

In mid July, the flow impedance between EE-1 and GT-2 was further investigated by injection into EE-1 at the fairly low rates of 34 and 43 gpm (Expt. 133). A few months earlier, in March 1976, a radioactive tracer test in the scab liner of GT-2 (part of Expt. 116) had shown that approximately 85% of the flow from GT-2 into its principal joint was entering through the milled-out hole in the scab liner, at a depth of 9200 ft. At that time, this flow connection was the vertically highest indication of that joint, and therefore had the lowest entry/exit pressure. Now, during Expt. 133, fluid from EE-1 began flowing into this joint and thence into the open annular region of GT-2—above the scab liner and outside the high-pressure casing—accompanied by a marked decrease in the flow impedance (from 100 psi/gpm to 30 psi/gpm). Temperature logging inside the scab liner showed that the region of outflow extended from 9100 ft up to 9015 ft, behind the upper part of the liner (evidently through the region of poorly bonded cement). In other words, the outflow from the GT-2 joint was now passing through an open area, one less restrictive to flow than the milled-out hole in the scab liner.

The fact that the GT-2 target fracture was initially accessed from below the scab liner (at about 9600 ft), then at several interim points along the liner (via perforations), and finally from behind the upper part of the liner (whose top was at 8973 ft), shows the unusual continuity of this joint. Indeed, if one examines the trace of the GT-2 borehole below 9000 ft—the portion containing the scab liner (see Fig. 3-27)—it is easy to see how that portion of the hole and a vertical joint striking N27W could lie in essentially the same plane.

Note: At this stage in the experimental sequence, the overall flow impedance between EE-1 and GT-2 had been reduced to 24–30 psi/gpm (Expts. 122A and 133). Therefore, had GT-2 been completed to just above the top of the scab liner, to directly access the very good flow connection observed during Expt. 133, from the GT-2 borehole to the GT-2 joint, a satisfactory HDR flow loop could have been developed without redrilling (and considerable expense and time could have been saved). With EE-1 as the injection well and GT-2 as the production well, additional stimulation of the GT-2 joint would probably have created a flow loop with an overall impedance of only a few psi/gpm when operated under high-backpressure conditions. (See the discussion of reservoir flow impedance and its relationship to reservoir productivity in Chapter 2.)

Quartz-Leaching Experiments to Reduce Flow Impedance

Experiments 137 and 138, referred to as the quartz-leaching experiments, were designed as a final attempt to reduce the flow impedance between the two boreholes. Silica (quartz) would be removed from the surfaces of the joint network connecting the higher joint in EE-1—now recognized as the major flow connection, although its exact depth had not yet been pinpointed—with the large joint near the bottom of GT-2.

Experiment 137 was designed to ascertain baseline parameters, particularly steady-state flow rate and overall flow impedance, as a basis for evaluating the effects of sodium-carbonate dissolution of silica from the joint surfaces during Expt. 138. Some 250 000 gal. of water was injected into EE-1 over about 7 days, at a controlled pressure of 1200 psi and a flow rate ranging from 43 gpm initially to 20 gpm at the end of pumping. Near the end of this phase of injection, GT-2 production leveled off at 15 gpm and a steady-state flow impedance of 75 psi/gpm was recorded.

On the afternoon of November 11, 1976—immediately following Expt. 137 and without any interruption of pumping or change in rate or injection pressure—Expt. 138 began. This silica-leaching experiment consisted of injecting a large volume (nearly 48 000 gal.) of a 1-normal solution of sodium carbonate at a controlled injection pressure of 1200 psi. By the next day, the injection flow rate had increased from the final Expt. 137 value of 20 gpm to 88 gpm; it then gradually declined, reaching 9 gpm, and finally showed another small increase. With the injection of the first 25 000 gal. of the carbonate solution, the GT-2 outflow decreased from the 15 gpm measured at the end of Expt. 137 to 12 gpm. It would remain at that lower value for the remainder of the experiment.

At about noon on November 12, a significant increase in bicarbonate concentration was observed in the GT-2 effluent, but the fluoride concentration (20 ppm) was still relatively low and the silica concentration was unchanged at 200 ppm. After 47 870 gal. of carbonate solution had been

injected, the injection fluid was switched back to water. By mid afternoon the silica concentration of the effluent had begun to increase, reaching 1400 ppm by 22:00 that night; over the same period, the fluoride concentration rose to 140 ppm. The two eventually peaked at 2500 ppm and 190 ppm, respectively. On November 17, after the cumulative injection of 426 000 gal. of fluid during Expts. 137 and 138, EE-1 was finally shut in.

The results of these two experiments were at best confusing. Even though geochemical analyses of the GT-2 effluent showed that between 1 and 2 tons of silica had been leached from the fracture system during Expt. 138, the overall flow impedance, rather than decreasing, increased from the 30 psi/gpm level of Expt. 133—to 75 psi/gpm during Expt. 137 and then to 90–100 psi/gpm during Expt. 138. A review of the downhole flow situation existing at that time may shed some light on why.

Seven months earlier, during Expt. 122A, the long-term flow impedance of the joint system connecting EE-1 to GT-2 was measured as 24 psi/gpm. It was at this stage, evidently, that most of the water injected into EE-1 began flowing out of the borehole via the higher (9050-ft), N55W-striking joint. The flow through this joint would have been essentially lateral until it reached the very sharp intersection with the N27W-striking GT-2 joint, which probably lay about 100 ft northwest of the injection point in EE-1.[18]

At an injection pressure of 1200 psi, the EE-1 joint would have been "jacked open"—and therefore one can assume that its body impedance was at least as low following the carbonate treatment as before. The most likely explanation for the much higher overall impedance, then, is that the impedance across the intersection with the GT-2 joint was significantly higher following the treatment. Mineral residues liberated during the leaching of silica, from both the casing cement and the surfaces of the 9050-ft joint in EE-1, probably ended up partially plugging the interconnection between the two joints (and possibly portions of the GT-2 joint as well).

[18] An argument can be made for a flow connection via one or more inclined joints, but at no time during the pressure-testing of EE-1—after the opening up of the 9050-ft joint—was the borehole subjected to the elevated pressures (3500 psi and above) needed to open such connecting joints. A set of inclined joints would be opened later in Phase I reservoir testing, after the bottom of the EE-1 casing had been re-cemented and the deeper joint (at 9650 ft) reactivated.

The Awakening: Early 1977

The realization that the silica-leaching experiment had degraded rather than improved the flow impedance of the system, supplemented by the results of some further experiments in the winter of 1976–77, finally made the reality of the situation obvious to almost everyone: Because the drilling trajectory for EE-1 had been turned away from the target joint at the bottom of GT-2 several tens of feet short of intersection, the planned direct connection between the two boreholes had not been achieved. Moreover, it did not appear (at least to the Project management) that the 100-psi/gpm flow impedance between the two boreholes could reasonably be reduced to anything near the hoped-for value of 10 psi/gpm or less.

Thus, there was no longer any alternative: if an adequate flow connection was ever to be achieved, one or the other of the two deep boreholes would need to be redrilled. With EE-1 cased to about 9600 ft, the obvious choice was to redrill GT-2 to intersect the joint opened behind the casing in EE-1.

Naturally, redrilling meant that the positions of GT-2 and EE-1 relative to one another—which at that time were still uncertain (was EE-1 east or west of GT-2?)—would need to be unequivocally determined. In addition, the actual height and orientation of the EE-1 joint at 9050 ft would need to be verified. A series of experiments designed to resolve these issues took place between December 1976 and March 1977 (Table 3-13).

Table 3-13. Experiments to determine the relative positions of GT-2 and EE-1 and to characterize the major EE-1 joint (December 1976–March 1977)

Expt. No.	Date	Description	Remarks
149	2 Dec. 1976	Magnetic ranging experiment between 9655 and 9735 ft in EE-1, to determine the relative positions of GT-2 and EE-1.	With Sperry-Sun survey compass at GT-2 bottom (9619 ft), bar magnet lowered in EE-1; compass response shows bottom of EE-1 east of GT-2 (not west, as previously found seismically by the hodogram method).
150	12–13 Jan. 1977	Seismic experiment to confirm borehole positions (large geophone package, modified for better acoustic coupling, run into EE-1; detonators fired in GT-2).	Considerably improved seismic first-arrival data confirm EE-1 position as east, not west, of GT-2 in the deeper region of interest.
156	7–11 Feb. 1977	Cement-bond log and radioactive iodine tracer study of fluid injection path(s) in EE-1, by Dresser-Atlas.	Little or no cement behind casing from 9599 ft up to 8980 ft, allowing water to flow up annulus and into the higher joint; tracer results show this joint to be major flow connection in EE-1 and locate it at 9050 ft.

Table 3-13. (Continued)

Expt. No.	Date	Description	Remarks
157	28–31 Jan. 1977	Surveys of EE-1 and GT-2 with newly developed, high-temperature Eastman Whipstock gyroscopic tool.	The Eastman Whipstock survey of GT-2 turned out to provide the best data for the location of this borehole. (Both Eastman Whipstock and Sperry-Sun tools run on Laboratory logging cable.)
	14–16 Feb. 1977	Surveys of EE-1 and GT-2 with Sperry-Sun heat-hardened gyroscopic tool.	
159A	8 Mar. 1977	Shear-shadowing experiment to determine upper extent of major EE-1 joint at 9050 ft. Geophone package positioned in GT-2 at 9045 ft; three detonators fired in EE-1 at 9038 ft. Joint tested first depressurized (to obtain background response) and then inflated (by injection into EE-1 at a pressure of 1550 psi).	Detonator position very inappropriate for a joint intersecting the borehole at about 9050 ft. Faulty experiment design (based on belief that the joint being tested was the deeper one—at 9650 ft) led to placement of detonators much too close to joint intersection. Result: Moderate shear-wave attenuation with joint pressurized.
159B	9 Mar. 1977	Repeat of Expt. 159A at shallower depth (8487 ft in EE-1, 8544 ft in GT-2), thought to be well above upper extent of joint. *(This depth range later chosen as target zone for redrilling.)*	Significant shear-wave attenuation at this depth with joint pressurized. Result unexpected (this experiment, like 159A, erroneously designed to test joint originating at 9650 ft).
159C	21 Mar. 1977	Repeat of Expt. 159A at 8762 ft in EE-1, 8794 ft in GT-2.	Maximum shear-wave attenuation at this depth, demonstrating origin of EE-1 joint at 9050 ft, not 9650 ft.
159D	22 Mar. 1977	Repeat of Expt. 159A at 8000 ft in EE-1, 8123 ft in GT-2.	Insignificant attenuation of shear waves—implying upper extent of EE-1 joint just below 8080 ft.
160	16 Mar. 1977	Induced-potential (IP) measurement of EE-1 joint at 9050 ft to determine upper extent of dilated region.	With current electrode at 9700 ft in EE-1, GT-2 surveyed with voltage probe while EE-1 joint first deflated, then inflated. Marked decrease in GT-2 voltage potential seen in 8500- to 9000-ft interval during inflation. Results consistent with those of Expt. 159D—show joint extending upward to about 8300 ft.

Additional Ranging Experiments

For Experiment 149 (a magnetic ranging experiment), a 25-ft-long permanent magnet was lowered into EE-1 below the casing, after which a heat-shielded Sperry-Sun survey compass was positioned at 9619 ft in GT-2 (at the bottom of the open-hole interval). With the magnet positioned at several different depths, the calculated and observed compass deflections consistent with an EE-1 location east of GT-2 showed excellent matches (all the observed deflections would have been reversed if EE-1 were west of GT-2).

These unequivocal magnetic ranging results totally contradicted all the hodogram-based directional inferences from the acoustic ranging experiments that had been done in the summer and fall of 1975, which had shown EE-1 as west of GT-2. It was this discrepancy—now undeniable—that finally "turned on the light" with regard to the 180° directional ambiguity of the hodogram method: the HDR Project seismologists at last realized that their previous interpretations of the P-wave first-arrival sign had been erroneous. At the same time, they realized that in the absence of other choices, the hodogram method would continue to be used in reservoir development operations—and therefore it was imperative that the problem of ambiguous directional indications be resolved.

In preparation for further experiments and borehole surveys, DA&S Oil Well Servicing Co. of Hobbs, NM, was called out to Fenton Hill to remove the pressure string and polished-bore-receptacle (PBR) mandrel from GT-2. By December 20 these operations were complete, and in mid January 1977 Expt. 150 took place. This seismic ranging experiment was designed to test the efficacy of some improved equipment: a detonator holder that would position the detonators in the center of the borehole (to ensure symmetrical explosions) and a new, 6-in.-diameter geophone instrument package that would seat more firmly against the borehole wall.

With the geophone package at 9560 ft in EE-1, twelve detonators were fired at the vertically equivalent depth in GT-2 (within the scab liner). Between firings, the geophone package was raised and reseated so that various package orientations could be tested. The standard deviation of the data for a single measurement was 8.6°. Experiment 150 was successful and confirmed the results of Expt. 149 (for which the standard deviation of the data was 2.6°): the mean bearing of EE-1 in relation to GT-2 was 101°—in other words, east! Happily, the new equipment worked well, and the direction information obtained via hodogram analysis was at last correct!

Gyroscopic Borehole Surveys

The fallacious geophysical data interpretations of the previous year having been recognized, the HDR Project team now focused on obtaining, via a new set of surveys, a "most-probable" picture of the GT-2 and EE-1 trajectories—particularly the relative positions of the two boreholes at depth, which would be essential for planning the redrilling program. (As noted

above, even after these surveys it would be the EE-1 trajectory indicated by the magnetic multishot survey obtained more than a year earlier that would become the final "anointed" one.)

In early 1977, Expt. 157 began. Both EE-1 and GT-2 were surveyed with Eastman Whipstock's newly developed high-temperature gyroscopic tool. After seal failures caused the first two attempts to be aborted, in late January both boreholes were successfully surveyed. But disturbingly, the results showed a separation between the boreholes (at around 9500 ft) of 46 ft—not in very good agreement with the numerous acoustic ranging measurements showing a separation of about 26 ft. In mid February, the new high-temperature gyroscopic tool developed by Sperry-Sun was tried. Multiple surveys were run in both boreholes, but the results only added to the uncertainty (and rather deflated the high hopes of the HDR Project staff, after they had commissioned and funded the development of this new tool). The various gyroscopic surveys of the two boreholes below about 8000 ft are compiled in Fig. 3-31.

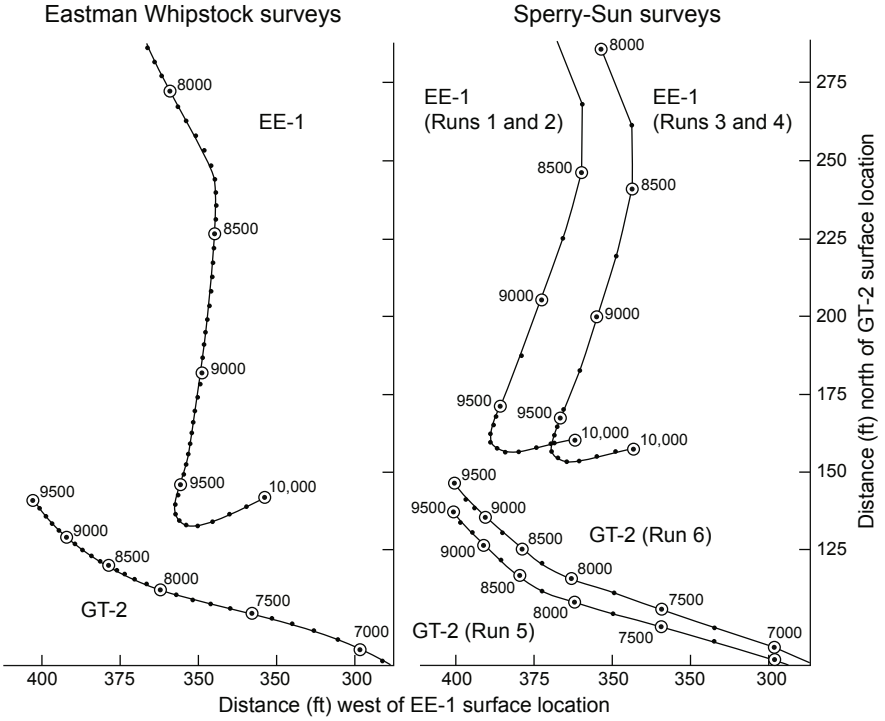

Fig. 3-31. Trajectories of the EE-1 and GT-2 boreholes as shown by high-temperature gyroscopic surveys (January–February 1977).
Source: HDR, 1978

Immediately evident in Fig. 3-31 is the lateral spread among the EE-1 surveys, which is greatest between the Eastman Whipstock survey and those by Sperry-Sun, but also significant between Sperry-Sun runs 1 and 2 and Sperry-Sun runs 3 and 4. The three gyroscopic surveys of GT-2 were much more internally consistent: they show the bottom of GT-2 about 40 ft south of the location indicated in Fig. 3-21 (which was based on magnetic single-shot surveys taken during drilling). It is likely that the differences among the EE-1 surveys were due mainly to the more tortuous and longer path of the borehole through the directionally drilled interval, and to the cumulative error in the sequential readings taken from the surface. The only real conclusion that can be drawn from this figure is that EE-1, at 9500 ft, was east of GT-2.

The analyses, discussions, and debates that followed Expt. 157 eventually led the team to conclude that

- for the EE-1 borehole, the October 1975 Eastman Whipstock magnetic multishot survey (Figs. 3-27 and 3-28) was much more accurate than any of the five gyroscopic surveys;
- the Eastman Whipstock gyroscopic survey of GT-2 (which fell between the two Sperry-Sun surveys) gave the best trajectory for GT-2.

These conclusions meant that (1) the borehole separation at 9575 ft was 28 ft, consistent with that measured earlier by acoustic ranging (26 ft); and (2) at GT-2 hole bottom (9619 ft), the bearing from GT-2 to EE-1 was approximately 100° (about east), consistent with the magnetic ranging findings of Expt. 149.

Additional Tracer and Cement-Bond Surveys

In early February 1977, a radioactive-iodine tracer survey (Expt. 156) and a cement-bond log were employed to more precisely define the flow path identified in EE-1 by several temperature logs (the temperature-log results had revealed a significant "counter-current" flow behind the casing—traveling up through the region of poor cement and then exiting the annulus via the joint at 9050 ft).

The tracer survey results were very revealing and would markedly influence the flow testing and redrilling activities to come. The principal finding was that more than 90% of the water injected down the casing was turning around at the casing shoe (at 9599 ft), thence flowing upward in the annulus outside the casing, and finally entering the surrounding rock mass through the joint at 9050 ft. The zone of fluid outflow from the annulus was about 33 ft long (from 9082 ft up to 9049 ft). In other words, these tracer results unequivocally showed that the joint constituting the major flow connection in EE-1 was the one at 9050 ft, not the deeper joint at 9650 ft.

The cement-bond log showed that up to about 8980 ft, there was now essentially no cement behind the EE-1 casing—not surprising, because the cement, being rich in silica, would have lost much of that component during the silica-leaching experiment (No. 138).

Shear-Shadowing Experiments

These experiments—Nos. 159A, B, C, and D—along with an induced-potential (IP) experiment (No. 160, see below) would provide the final data needed to select the best path for redrilling GT-2 to intersect the upper part of the EE-1 joint. The shear-shadowing experiments were devised to measure the height of the opened portion of this joint. With the point of fluid entrance assumed to be roughly in the center of the inflated joint, a drilling target near its upper extent would provide the optimum separation distance for heat transfer from the joint to the circulating fluid.

Simply stated, the shear-shadowing principle is based on the fact that shear waves are not transmitted through fluid. Therefore, when an acoustic signal is transmitted across a fluid-inflated joint, the shear phase will be attenuated compared with that of a signal transmitted across the same joint depressurized. The degree of attenuation depends on the width and lateral extent of the joint at the signal-crossing depth, both of which would be expected to be greatest near the center of the joint.

These experiments lasted two weeks. High-temperature explosive detonators were run into EE-1 on a wireline and positioned sequentially at several depths. For each experiment, a geophone package was positioned at a corresponding depth in GT-2 and the detonators were fired, transmitting acoustic signals across the upper EE-1 joint—first with the joint depressurized and then with it inflated. It was anticipated that the maximum shear-wave attenuation would be seen at about the joint's mid-height, where the inflated cross section is greatest (in the case of the now-principal EE-1 joint, near its intersection with the borehole at 9050 ft).

It appears that for some obscure reason, the geophysicist in charge of this experiment was still working on the premise that the major flow connection in EE-1 was via the joint originating at 9650 ft—even though by now it was recognized that the higher joint, at 9050 ft, was accepting the bulk of the flow. Because of this lack of understanding, probably coupled with some ongoing confusion about the relative positions of GT-2 and EE-1, the shear-shadowing experiments were designed to measure a joint 600 feet deeper than the true principal joint. However, with the deeper joint now barely accepting any fluid, the joint actually interrogated was the one at 9050 ft. The positions of the two boreholes relative to that joint and the locations of the detonators and geophones (defining the acoustic-signal path) for each of the four experiments are shown in Fig. 3-32.

For Experiment 159A, the geophone package was positioned in GT-2 at 9045 ft and detonators were fired in EE-1 at 9038 ft (within a few feet of the intersection of the joint with the borehole)—first with the joint depressurized and then with it inflated. While the joint was inflated, attenuation of the shear waves was only moderate, as could be expected because the exact depth of the detonators relative to the joint intersection with EE-1 was uncertain within several tens of feet (at this depth, cable measurements

typically have an uncertainty of ± 30 ft). At the time, those conducting the experiment—who still believed the joint being inflated was the one at 9650 ft—viewed this result as anomalous.

For Expt. 159B, the geophone package was positioned at 8544 ft in GT-2 and detonators were fired at 8487 ft in EE-1. With the EE-1 joint inflated, shear-wave attenuation was significant—again viewed as an anomalous result by those who still thought the principal joint was the one at 9650 ft. But as is obvious from Fig. 3-32, the acoustic-signal path B–B would have passed (side to side) through the center of the inflated joint (at 9050 ft), and about 550 ft above its intersection with the EE-1 borehole.

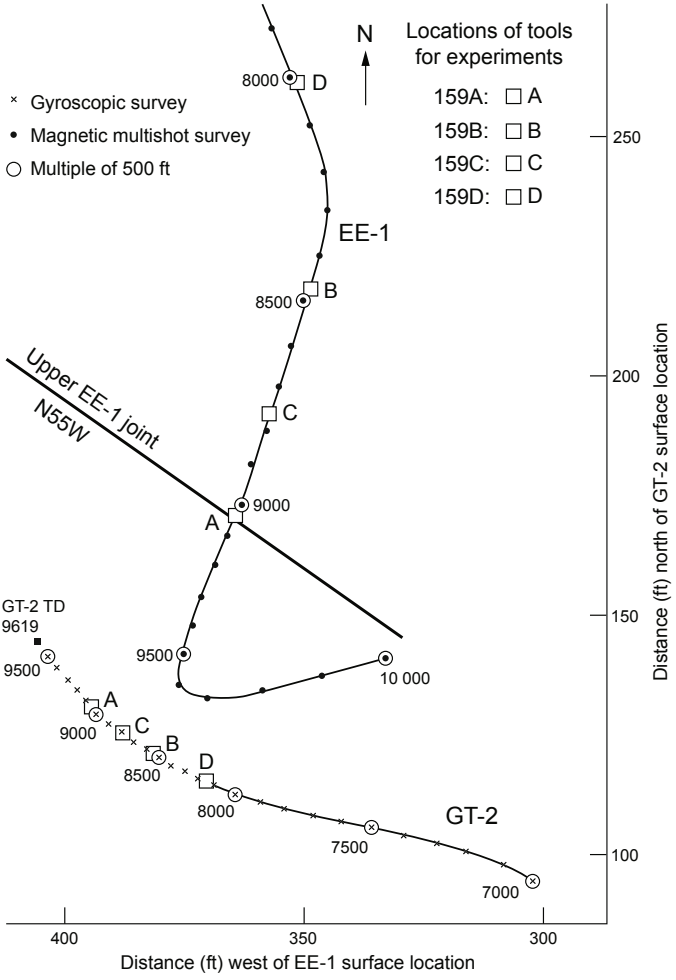

Fig. 3-32. Positions of the EE-1 and GT-2 boreholes and locations of detonators and geophones during the four shear-shadowing experiments. The acoustic-signal paths are A–A, B–B, C–C, and D–D.

For Expt. 159C, the geophone package was positioned at 8794 ft in GT-2 and the detonators were fired at 8762 ft in EE-1. With the EE-1 joint inflated, shear-wave attenuation was maximum, a result consistent with the path of the acoustic signals (C–C) in Fig. 3-32, which again passed through the midpoint of the joint—but this time only about 280 ft above its intersection with the borehole.

Finally, for Expt. 159D, the geophone package was positioned at 8123 ft in GT-2 and the detonators were fired at about 8000 ft in EE-1. The mean depth of path D–D in Fig. 3-32, therefore, was about 8080 ft—some 1000 ft above the nominal center of the EE-1 joint at 9050 ft. A plot of the acoustic signal power vs time for Path D–D (Fig. 3-33) shows that its mean depth would be very near the upper limit of the joint: the S-wave for the inflated joint is not much smaller (75%) than that for the collapsed joint—i.e., the attenuation of the signals is relatively small, as would be expected if they were passing through the very top of the inflated portion of the EE-1 joint.

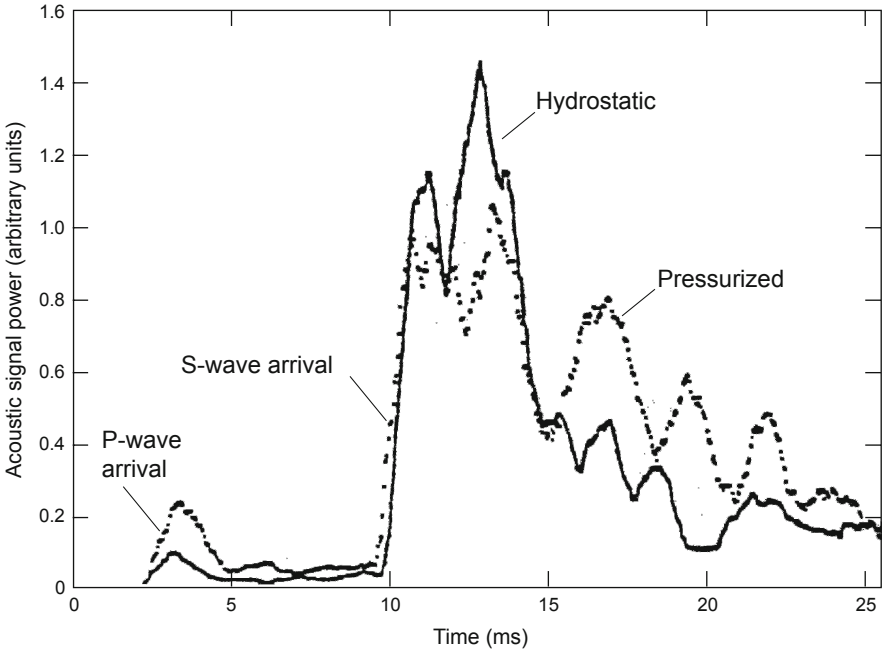

Fig. 3-33. Signal power vs time for acoustic-signal path D–D (mean depth = 8080 ft). The arrival of the P-wave is shown at about 2.5 ms, and the arrival of the S-wave about 7 ms later.
Source: HDR, 1978

Experiment 159D provided a clear indication that the optimum target for a redrilled GT-2 lay a few hundred feet below the 8080-ft mean depth of the acoustic-signal path D–D.

Note that the overall height of the inflated portion of the EE-1 joint at 9050 ft, as derived from the shear-shadowing experiments (and assuming a symmetrical inflation about the injection point) is about 2000 ft—a most significant dimension, because it implies an astounding degree of flow continuity for a heterogeneous rock mass!

Induced-Potential Survey of the EE-1 Joint

As the final experiment in this series (Expt. 160), the EE-1 joint originating at 9050 ft was surveyed electrically. With the current electrode placed at 9700 ft in EE-1, a wireline voltage probe was used to survey the induced voltage generated over the lower part of GT-2 (7400–9100 ft), first with the EE-1 joint deflated and then with it inflated by injection into EE-1. The results of this IP survey indicated that the inflated joint extended upwards to a depth of about 8300 ft, 750 ft above its point of intersection with the EE-1 borehole (its assumed center). The most pronounced decrease in the voltage potential in GT-2 was between 8500 and 9000 ft, which would correspond to the interval of greatest inflation of the EE-1 joint. (Note: with the steel scab liner in GT-2, its top at 8973 ft, the portion of the inflated EE-1 joint below this depth could not be surveyed electrically.)

Summary: The Situation Leading up to Redrilling of GT-2

Figure 3-34 shows, in plan view, what was known by the end of March 1977 about the geometry of the principal near-vertical joints opened up near the bottoms of GT-2 and EE-1.

The GT-2 Principal Joint

The principal joint developed near the bottom of GT-2 was initially opened in mid February 1975, at a depth of about 9600 ft, by pumping into the 38-ft rat hole below the scab liner at an injection pressure of 1400 psi. Over the next two months this joint was repeatedly inflated and vented; then on April 21, with the injection of 3600 gal. at an injection pressure of 1600 psi and a pumping rate of 9 gpm, it was finally extended to a (calculated) diameter of about 400 ft. About four months later, during the deep drilling of EE-1, the Western pump was used to further extend this GT-2 "target fracture" to a calculated diameter of 800 ft, by the injection of 12 000 gal. of water at a pressure of 2250 psi and a rate of about 4 BPM (11 L/s).

October 10 of that year saw the first-ever seismic interrogation of a dilating joint in deep, hot granitic rocks. With the geophone package positioned at several depths in EE-1, the Western pump was used to reinflate the

GT-2 joint and eventually extend it somewhat (injecting at a rate of 4 BPM and a pressure of 2150 psi). The measured orientation of this joint, during both its initial inflation and subsequent extension, was N27W. However, the major seismic activity in GT-2 now appeared to be at a depth of about 9300 ft, suggesting an upward growth of the dilated region. During this testing, the measured width of the dilated portion of this joint was roughly 500 ft.

On July 21 of the following summer (1976), during injection into the recently drilled EE-1, the outflow from the GT-2 joint was observed to be exiting behind the scab liner at a depth as high as 9015 ft—which would indicate a vertical extent for this joint of at least 600 ft (not considering any downward growth from its initial point of inflation at about 9600 ft).

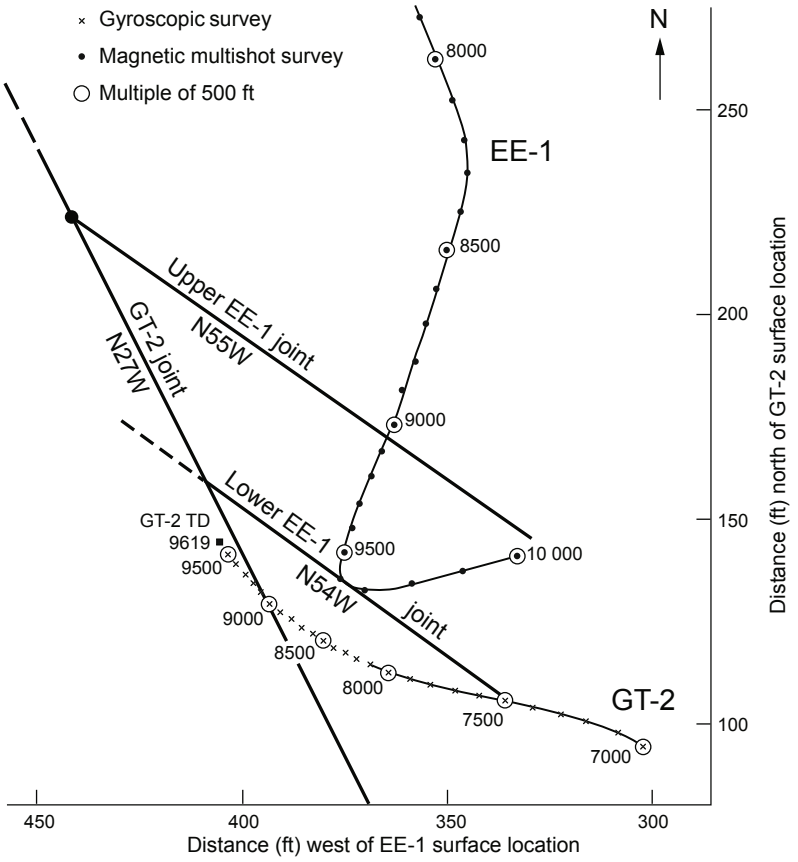

Fig. 3-34. Region of closest approach of GT-2 and EE-1, in plan view, showing the seismically determined orientations of the three principal joints pressure-stimulated near the borehole bottoms.

The EE-1 Principal Joints

Near the bottom of EE-1, two principal joints were sequentially pressure-stimulated: the first at about 9650 ft and the second at about 9050 ft. The deeper joint was first opened on October 14, 1975, by injection with the Western pump at a rate of 2.1 BPM (5.6 L/s) and pressures up to 2400 psi. Its measured strike was N54W.

The higher joint, up behind the casing, was first opened in May of 1976. This joint had a strike of N55W and exhibited a somewhat lower opening pressure (1200 psi—vs 1600 psi for the deeper joint under similar injection conditions).

EE-1 to GT-2 Flow Impedance

Once the upper joint in EE-1 became active, the inter-borehole flow impedance dropped to more reasonable values than those initially observed—albeit still too high for a productive circulation loop. The following values were obtained during the 1976 flow testing:

26 psi/gpm (Expt. 120)
24 psi/gpm (Expt. 122A)
30 psi/gpm (reached after an initial value of 100 psi/gpm—Expt. 133)

But then, inexplicably, the flow impedance increased during Expt. 137, to 75 psi/gpm, and then again following the quartz-leaching experiment (No. 138), to 90–100 psi/gpm. These data suggest that the interconnection between the two joints was tenuous and subject to being repeatedly plugged and then cleared by flow-through.

Reflections on the Geometry of the Joint System

From an examination of Fig. 3-34, it is tempting to draw some inferences concerning the flow geometry between EE-1 and GT-2. First, if the fluid injected into EE-1 flowed 100 ft laterally to the northwest, turned the sharp corner into the GT-2 joint at the point of vertical intersection, and then flowed back towards GT-2, such a path would explain many of the experimental observations. The major flow impedance would be expected to occur at the very confined intersection of the two joints—a contact zone of unknown, but significant, height.

Second, it is clear that by the end of 1976, the Laboratory had managed to develop a true HDR reservoir between the GT-2 and EE-1 boreholes. The flow geometry was lateral rather than vertical, but would have been sufficient for an initial heat-mining experiment. A year or more of work, not to mention the considerable costs associated with twice redrilling GT-2, could have been saved if such an experiment had gone forward. Further, the development of the deeper, hotter Phase II reservoir—the primary Project objective—would have been achieved that much sooner.

Chapter 4

Phase I Reservoir Development—Redrilling and Flow Testing

In early 1977, the condition of the two deep boreholes at Fenton Hill was as follows: The GT-2 borehole had been drilled to a depth of 9619 ft (2832 m) and a 7 5/8-in. scab liner had been placed and cemented from 8973 ft to 9581 ft, leaving a 38-ft "rat hole" below the liner (see Fig. 3-12). The EE-1 borehole had been drilled to a depth of 10 053 ft (3064 m) and cased from 9599 ft to the surface with a composite casing string (999 ft of 7 5/8-in. casing from 9599 ft to 8600 ft, and 8 5/8-in. casing above 8600 ft—see Fig. 3-26).

The plan was to first remove from GT-2 the temporary, 4 1/2-in. high-pressure casing string that had been used to pressure-stimulate the rat hole and to guide wireline tools into the scab liner. The next step was to mobilize a drill rig over GT-2, set a cement plug just below the desired sidetracking depth, and sidetrack the borehole at about 8200 ft (2500 m). Finally, the sidetracked hole would be drilled directionally into the large joint that had been pressure-stimulated from EE-1 at a depth of 9050 ft (behind the casing). With the true positions of the boreholes now finally known, redrilling GT-2 from a kickoff depth of about 8200 ft and on a trajectory of N30E (see Fig. 3-32) would take the new borehole toward the EE-1 joint at almost a right angle.

Summary of Phase I Reservoir Development and Testing

As detailed in Chapter 3, the HDR Project team had spent more than a year attempting to develop a low-impedance flow connection between EE-1 and GT-2. An unintended consequence of these efforts was erosion of the poor cement surrounding the bottom of the final casing string in EE-1 and, eventually (February–May 1976), the opening of a joint behind this casing, at 9050 ft, through which flow continued to increase. Ultimately, a connection to GT-2 was achieved via this joint at a moderate flow impedance—about 24 psi/gpm—but this was judged to be too high.

Unfortunately, it was not recognized at the time that a multiply jointed HDR reservoir had in fact been created between the two boreholes, and that it could have been further developed with more "aggressive" pressurization (such as that carried out following the re-cementing of the final EE-1 casing, described in this chapter). Thus, this nascent, multiply jointed reservoir was abandoned and instead the

D.W. Brown et al., *Mining the Earth's Heat: Hot Dry Rock Geothermal Energy*,
DOI 10.1007/978-3-540-68910-2_4, © Springer-Verlag Berlin Heidelberg 2012

lower portion of GT-2 was twice redrilled directionally (creating the "legs" GT-2A and GT-2B). The second redrilling finally achieved a satisfactory hydraulic connection with the joint opened from EE-1 at a depth of 9050 ft, giving rise to the "original Phase I reservoir."

When three tests of this flow connection between the boreholes (Run Segments 1, 2, and 3) were conducted between late 1977 and mid 1978, it became evident that the original Phase I reservoir was principally a single-joint connection between EE-1 and GT-2B, with a very limited surface area and not much opportunity for expansion. Therefore, following these tests, the bottom 600 ft of casing in EE-1 was re-cemented to seal off the flow path behind the casing into the 9050-ft joint. Then, the higher-opening-pressure, deeper joint (at 9650 ft), originally opened in October of 1975, was pressure-stimulated much more aggressively. The development and extension of this deeper joint essentially created an enlarged Phase I reservoir, but with the same multiple outlets into the GT-2B borehole as the original reservoir. Two more flow tests (Run Segments 4 and 5) followed the pressure stimulations of the deeper EE-1 joint; the second of these tests, which ended in late December 1980, lasted more than nine months.

However, the 9050-ft joint in EE-1 continued to play a significant role in the enlarged Phase I reservoir; as pressurized flow testing continued, fluid from the reservoir entered the EE-1 annulus via this joint and progressively worked its way up through the incompletely re-cemented region just above the 9050-ft depth. Eventually a major bypass flow developed, which by early 1981 rendered EE-1 unsuitable for further testing of the reservoir.

In the end, the Phase I HDR reservoir at Fenton Hill was developed in a way very different from that originally planned, and through a stepwise process that would bring a much clearer understanding of what "hydraulic fractures" in basement rocks really are. Only in the early 1980s was it finally recognized (except by a few diehard members of the HDR staff) that the "penny-shaped fracture" theory—although valid for an isotropic and homogeneous medium—could not be applied to the Fenton Hill granitic basement, which was neither isotropic nor homogeneous. In reality, the rock was not being fractured at all; instead, the hydraulic pressure was opening a number of pre-existing (but resealed) joints in the rock mass. The flow geometry was therefore much more complicated than first thought: it consisted of a complex network of pressure-dilated joints—probably having different orientations, and therefore different opening (or jacking) pressures.

Redrilling of the GT-2 Borehole

The information in this section is extracted mainly from Pettitt (1978b).

Sidetracking and Directional Drilling of GT-2A

In mid December 1976, the temporary 4 1/2-in. casing string was removed by DA&S Oil Well Servicing Co. of Hobbs, NM. Arrangements were then made to procure a drilling rig from the Noble Drilling Corp. of Midland, TX, for the redrilling of GT-2. On March 29, 1977, mobilization of rig No. N115 got under way at Fenton Hill. Once the drilling structure had been erected, the elevation of the Kelly bushing was measured as 8714.9 ft.

On April 7 a cement plug was set in the hole by Halliburton Oil Well Cementing Company of Farmington, NM, and was faced off to 8263 ft. The first attempt to sidetrack off this plug took place two days later. The drilling assembly, which consisted of a tungsten-carbide-insert (TCI) hard rock bit, a Dyna-Drill motor, a 2° bent sub, and an Eastman Whipstock single-shot orientation tool, was oriented to drill out the side of the hole in a N30E direction, to intersect the 9050-ft joint in EE-1 at about a right angle. The motor, however, failed to turn and had to be withdrawn. When inspection revealed that it was plugged with cement cuttings, it was replaced with a new Dyna-Drill motor. On April 10, the assembly was run in again and drilling began in the N30E direction. But after seven hours of drilling, to a depth of 8342 ft, the drilling assembly was still in the original borehole and had not managed to sidetrack into the granitic sidewall.

The next day a second cement plug, made up of a harder mix with less retarder and water, was set by Halliburton and faced off to 8163 ft (100 ft higher in the hole than the first plug). On April 12, a drilling assembly consisting of a 1 1/2° bent sub, yet another Dyna-Drill motor (this one having a 1 1/2° bent housing), and a 9 7/8-in. Security H7SGJ steel-toothed bit, was run in. But because the hole had not been adequately cleaned out, some 75–100 ft of cement fill had accumulated on top of the plug. As drilling proceeded through this fill, the two collars above the motor became clogged with cuttings and the motor stopped turning. The same steel-toothed bit was then run back in the hole on a straight rotary drilling assembly, and the hole was flushed with a mixture of Baroid Quickgel and soda ash (often referred to as a "mud sweep") to lift the cement cuttings out of the hole.[1] Next, the drilling assembly with the bent housing and motor was equipped with a new Security steel-toothed bit to enable timed drilling. But after 20 ft of drilling—all of it through cement, to a depth of 8183 ft—it was clear that the attempt was not succeeding: the bit showed extreme wear on the outer edges of the external row of teeth. (Note: steel-toothed bits do not drill granitic rock!)

[1]Mud sweeps became standard practice for cleaning and circulating the hole at the end of each drilling run.

With experience in GT-1 having shown that diamond bits would drill granitic rock—albeit at only about 1 ft/h—a Christensen 9 7/8-in. side-cutting diamond bit was now tried, with the same drilling assembly. This bit drilled 15 ft—from 8183 ft to 8198 ft (apparently "somewhat" into the granitic sidewall), but trouble with the Dyna-Drill on the morning of April 15 prevented continuation of drilling. When a follow-up rotary drilling run with a TCI bit ended up drilling only cement, a specially designed 9 5/8-in. side-cutting Christensen bit was tried—with some success.

Over the next week, five more attempts were made to sidetrack the hole using a variety of diamond and TCI bits. Two of these, consecutive diamond-bit runs, actually sidetracked the hole a short distance; but the follow-up bit run (with a stiff rotary drilling assembly and a TCI bit) ended with the bit drifting back into the original hole and drilling ahead in cement to 8280 ft. At this point, plans were made to underream the hole to create a ledge for sidetracking.

On April 23 a three-cone, TCI underreamer assembly was used to enlarge the diameter of the GT-2 borehole from 9 5/8 in. to 16 in. over the 8110- to 8120-ft depth interval. The following day, Halliburton placed a 150-sack cement plug through open-ended drill pipe, up to a depth of 8040 ft. After the plug had been faced off to 8110 ft with a 9 5/8-in. bit, a Dyna-Drill assembly was made up with a 7 7/8-in. Christensen side-cutting diamond bit and a 2° bent sub above the motor. On April 25 and 26, the cement was drilled through asymmetrically: a hole about 8 in. in diameter was drilled along the low side of the 16-in.-diameter interval, to just above the ledge at 8120 ft. (The inclination of GT-2 at this depth was 3.4°.)

Next came a directional drilling run, with a 2° bent sub, a Dyna-Drill, and a new 7 7/8-in. diamond bit. Beginning on the low side of the borehole from the ledge formed at 8120 ft, this run proceeded in a northeasterly direction (out the right side of the hole) to 8128 ft. The load on the bit began to increase at this depth, and as drilling progressed to 8140 ft (at a controlled rate of 1–2 ft/h), the bit load needed to drill ahead at this rate increased from 5000 to 8000 lb.

This increasing load on the bit and the presence of some granitic chips in the cuttings indicated that the hole had been successfully sidetracked. The diamond drilling assembly was then pulled, and the hole was reamed—full diameter—from 8110 ft to 8139 ft with a Dyna-Drill assembly having a 2° bent sub and a 9 5/8-in. Smith 9JA button bit. Two very short (1 ft each) Dyna-Drill runs followed, the first with a 9 5/8-in. diamond bit and the second, a clean-out run, with a Smith 9JA bit. On April 29, the final diamond-bit run took place (with a 2° bent sub, Dyna-Drill motor, and 9 5/8-in. bit), deepening the hole to 8144 ft before the bit stopped cutting. The cuttings were showing increasing amounts of granitic chips.

After the diamond bit assembly had been pulled from the hole, a Dyna-Drill assembly with a 2° bent sub and a Smith 9JA button bit was run in.

Five feet of drilling later, at 8149 ft, 60% of the cuttings were granitic chips. Continued drilling, with the load gradually increased to 12 000 lb and at a penetration rate of 10–12 ft/h, deepened the hole to 8154 ft—at which depth 95% of the cuttings were granitic chips. The records show that GT-2 was considered sidetracked at a depth of 8144 ft, with the directionally drilled new hole (called GT-2A) departing the old borehole out the right side in a NE direction, roughly perpendicular to the NW direction of the old borehole.

Note: The sidetracking of GT-2 was the first effort of its kind in deep basement rock. It took 22 days and about $300 000 to learn how to sidetrack a borehole in granitic rock, but it was hoped that this learning experience would benefit all future sidetracking programs at Fenton Hill (and elsewhere).

With the drilling of the GT-2A borehole under way, pressurization of EE-1 began with the big (34-gpm) Kobe pump to inflate the 9050-ft target joint. Drilling of GT-2A continued with the same Dyna-Drill assembly, on the planned NE course and at a rate of 12 ft/h, to a depth of 8215 ft. The bit began to run rough at this depth, and when the drilling assembly was pulled, examination of the bit showed it had three cracked or chipped buttons and was 1/8-in. under gauge. For the next run, a rotary drilling assembly was made up with a Monel collar, a reamer, and a 9 5/8-in. Smith 9JA bit on bottom. The hole was first reamed to 8215 ft and then drilled ahead to 8357 ft. A hole survey at this new depth showed a trajectory of N39E, 6°.

On May 4, with a new Smith 9JA bit, drilling continued to 8496 ft, at which depth the direction of the hole was N25E and the inclination 9 1/4°. To limit any further increase in inclination, the drilling assembly was pulled from the hole and replaced with a stiffer one. The new assembly, consisting of a button bit, a 3-point reamer, a short drill collar, and a second 3-point reamer, did maintain the inclination at about 9°. The next drilling run took GT-2A to a depth of 8736 ft, through the upward extension of the EE-1 joint. As GT-2A intersected this joint—at 8645 ft, on May 5—the pressure at EE-1 began to drop at about 0.5 psi/min even though the injection was constant at 34 gpm. This joint intersection was about 400 ft above the fluid inlet point in EE-1 (9050 ft), providing a heat-transfer surface believed to be adequate.

Note: Several of the joint-interrogation experiments performed during the months preceding the redrilling of GT-2 had identified the upper extent of the EE-1 joint (see Chapter 3). Experiments 159B and 159D (shear-shadowing) indicated that it was just below 8080 ft, and Expt. 160 (induced-potential) showed it at 8300 ft. Thus, the actual intersection with this joint at 8645 ft, which the outflow from GT-2A confirmed, should have been anticipated.

Inexplicably, instead of stopping when the drilling run ended at 8736 ft and setting up to stimulate the joint intersection at 8645 ft, the drilling managers replaced the bit with a new Smith bit and drilled on for an additional two days—to a depth of 9184 ft (reached on May 8). During this time, the measured outflow from GT-2A remained constant at about 7 to 9 gpm. Not unexpectedly, given the joint orientations shown in Fig. 3-34, no further indications of joint intersection were exhibited in GT-2A during this long drilling excursion to the northeast.

The geometry of the EE-1 joint is shown in relation to the drilling trajectories of GT-2, GT-2A, and EE-1 in Fig. 4-1 (magnified plan view).

Using (1) the measured N55W strike and the 9050-ft intersection of this joint with the EE-1 borehole, (2) the depth of the joint's intersection with GT-2A (8645 ft), and (3) the distance from the 405-ft vertical projection of the joint to the intersection at 8645 ft (13 ft, as shown in the figure), one can calculate an actual inclination for this joint of 1.9° to the SW—very close to vertical!

Pressurization of the Joint Intersection

A significant connection to the EE-1 joint having been established, plans were now finally developed to pressure-stimulate this joint intersection. High-temperature Lynes inflatable packers[2] would be used to pressure-isolate the upper portion of the GT-2A borehole while the interval below the packer was pressurized. For the first pressurization (Expt. 161), on May 11, a packer was set at 8275 ft—about 370 ft above the joint intersection. Pumping was initiated at a rate of 4 BPM (11 L/s) and a pressure of 1550 psi. Shortly thereafter, flow was observed coming out of the annulus—indicating that at least a portion of it was bypassing the packer—and pumping was terminated. When the packer was removed from the borehole, it was found that the exterior rubber element had been completely stripped off.

The next day, in preparation for Expt. 162, another Lynes packer was set—this time at a depth of 8245 ft. After only 20 minutes of pressurization of the borehole below the packer, at 1600 psi and a pumping rate of 1 BPM, some bypass flow was again observed out the annulus. But when a check of the load on the packer indicated that it was still holding (at least mechanically), pumping was increased to 5.5 BPM (14.6 L/s) to pressure-stimulate the GT-2A joint intersection. Over the next three hours, the injection pressure rose to 1830 psi and the annulus outflow increased to 75 gpm (about 1/3 of the pumping rate). After 1000 bbl (42 000 gal.) had been pumped, the experiment was terminated. When the packer was pulled, again the rubber element was missing. On May 12 the drilling rig was placed on standby to conserve funds.

[2]The previous August (1976), a sole-source purchase request had been issued to Lynes United Services for the fabrication of six 8 5/8-in., high-temperature open-hole packers and two mandrel assemblies. Following successful testing of the packers (15 hours at a temperature of 400°F and a pressure of 2300 psi) at the Lynes facility in Houston, TX, they had been sent to Hobbs, NM, for storage until scheduled for use at Fenton Hill.

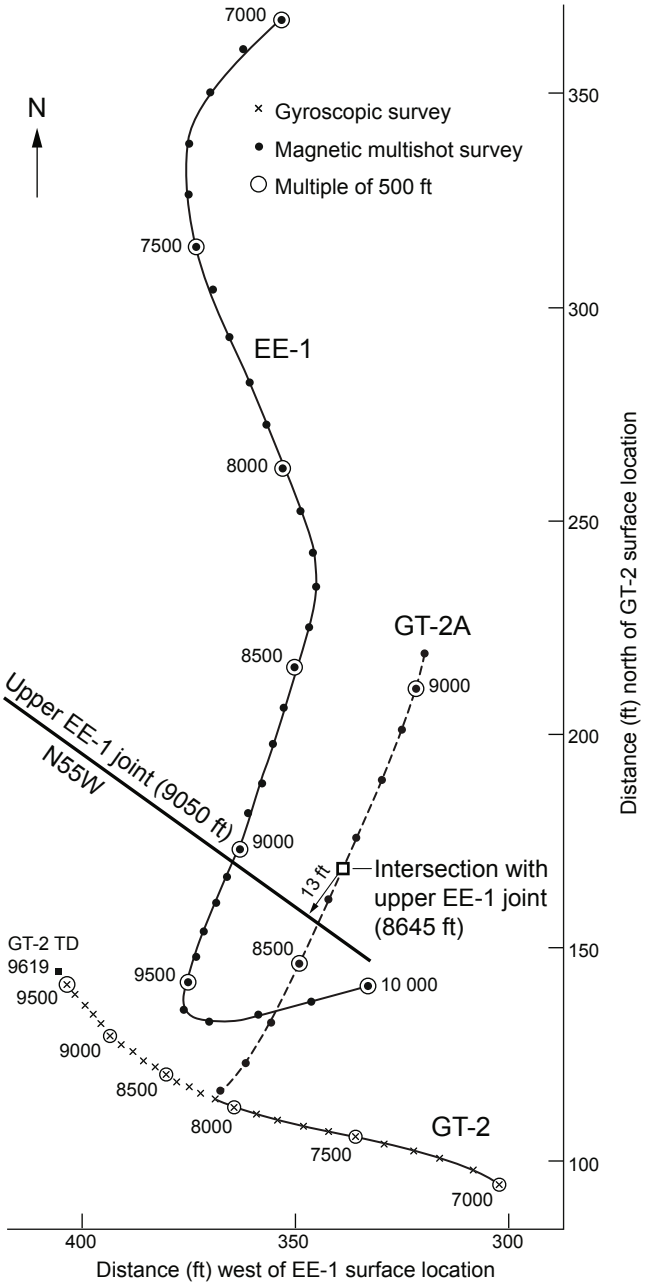

Fig. 4-1. Plan view of the 9050-ft EE-1 joint in relation to the trajectories of GT-2, GT-2A, and EE-1.

To evaluate the flow impedance of the now-direct joint connection between EE-1 and GT-2A, EE-1 was pressurized at 34 gpm with the big Kobe pump (Expt. 163, which began on May 17). The measured flow impedance varied from 10 to 35 psi/gpm (1.1 to 3.8 MPa per L/s). Unfortunately, the reports of the time pertaining to this experiment are very vague—no actual measurements are given for parameters such as the temporal variation of the EE-1 injection pressure, the GT-2A production pressure, and the GT-2A production flow rate. The fact that the flow impedance for the 9050-ft EE-1 joint was already considerably lower—by about one-third—than that measured at the end of the quartz-leaching experiment (Expt. 138) should have given the Project managers some pause. After an entire year (November 1975–November 1976) had been devoted to trying to improve the EE-1 to GT-2 flow impedance, it now showed significant improvement in a single week—and that with only the Project's 34-gpm Kobe pump.

But the flow impedance was considered still too high to proceed with flow testing. As explained in the Chapter 3 summary, before the redrilling of GT-2 the intrinsic impedance of the multiple-joint flow connection between EE-1 and GT-2 had been in the 24-to 30-psi/gpm range until the quartz-leaching experiment, when the flow path apparently became clogged with detritus. When the GT-2A leg was drilled, this flow path was reduced to a single-joint flow connection—now direct but still partially plugged, with an opening pressure of 1100–1200 psi. Had this joint been hyper-dilated, by injection into EE-1 at the high pressures possible with a commercial pump (around 2400 psi at 5 BPM [13 L/s]), it is probable that the flow path could have been cleared—which would have dropped the flow impedance to an acceptable level (about 10 psi/gpm). Indeed, as discussed later in this chapter (see *Run Segment 4*: *October–November 1979*, below), an even greater drop in impedance could have been achieved by the simultaneous imposition of a modest backpressure at GT-2A. Unfortunately, there was no attempt to try such strategies. Instead, the decision was made to cement off the GT-2A leg and to sidetrack anew, along a lower trajectory.

Sidetracking, Directional Drilling, and Flow Testing of GT-2B

The plan for the second redrilling was to sidetrack from GT-2A, at a depth of 8300 ft—out the left side in a northerly direction—to intersect the EE-1 joint at a depth of 8800 ft (just 250 ft above its intersection with EE-1).

On May 18 the drilling rig was reactivated, open-ended drill pipe was run in to 8437 ft, and cement was pumped in to plug about 300 ft of the GT-2A leg above that depth. Drilling was begun with a very simple assembly, incorporating a stabilizer, a drill collar, and a 9 5/8-in. Smith 9JA TCI bit, in the hope of achieving a kickoff. The top of the cement was encountered at 8135 ft. As drilling proceeded, it appeared that the bit was not "digging in," but just scraping along the low side of the hole. This assembly was pulled and replaced with one consisting of a 2° bent sub, a Dyna-Drill motor, and a smaller (7 7/8-in.) Smith 9JA button bit. With the bit oriented in

a northerly direction, the drilling assembly was worked up and down the hole in an attempt to find an irregularity in the borehole wall as a kickoff point for sidetracking. When no satisfactory "ledge" was found, drilling ahead on the cement plug proceeded at a slow rate of 1 ft/h. The only indication that "some" granitic rock had been drilled was that, by the end of the drilling run, the load on the bit had increased to 5000 lb.

The drilling assembly was then pulled from the hole. Inspection of the bit revealed that it was 1/4 in. under gauge, and the outer row of buttons showed severe wear. The same Dyna-Drill assembly was employed for two more drilling runs with 9 5/8-in. Smith 9JA bits. The first reached a depth of 8269 ft without any appreciable bit load. Following five orientation surveys (carried out once the drilling assembly was on bottom), the second run advanced several feet at a slow rate of 1 ft/h and with a load of only 2000 lb. With continued drilling, the penetration rate was gradually increased to 3 ft/h as the load increased to 3000 lb. By the morning of May 22, at a depth of 8300 ft, the load had increased dramatically—to 9000 lb. Drilling was continued another 14 ft, then the drilling assembly was pulled. This time the bit was well worn across its entire face, confirming that granitic rock was being drilled and that the sidetracking had succeeded. (The 8270-ft depth would later be considered the depth at which the hole had been sidetracked, on the basis of borehole survey data.) The new leg was referred to as GT-2B.

InfoNote

Although neither the sidetracking of GT-2A nor that of GT-2B required the use of a whipstock, both required considerable "finesse" on the part of the directional driller. GT-2A was sidetracked off a ledge formed by underreaming a section of the borehole from 9 5/8 in. to 16 in. and starting the drilling with a 7 7/8-in. special side-cutting diamond bit. GT-2B was sidetracked off a naturally occurring ledge in the borehole wall, with a 7 7/8-in. button bit. In both cases, the portion of the borehole below the ledge was plugged back with cement to aid in sidetracking. Given the success of these operations, the following steps should guide future development of HDR systems having production wells with multiple (forked) completions for enhanced productivity:

1. Obtain the services of a directional driller who has sidetracked boreholes in hard crystalline rock without using a whipstock.
2. Let the directional driller order the necessary downhole motors, bent subs, and surveying equipment for the job.
3. To enable the borehole to be used as part of a multiple-well completion, do not place a cement plug in the initial borehole.
4. At the desired depth off the bottom of the initial borehole, underream a considerable length of the hole with a limber assembly to form a good ledge, particularly on the low side of the hole.
5. Slowly drill off the ledge to the side with a mud motor and bent sub, initially using a special side-cutting diamond bit having a somewhat smaller diameter (e.g., a 7 7/8-in. bit in a 9 5/8-in. hole).

Next, a reamer assembly (no Dyna-Drill) was run in with a new 9 5/8-in. Smith 9JA bit, and the hole was drilled ahead, at an increasing load, to 8380 ft. At this depth a magnetic survey showed a trajectory of N6E, 3°. Drilling continued at 9 ft/h and a load of 40 000 lbs; by the 8415-ft depth, the cuttings were almost all granitic chips. After another 150 ft of drilling (to a depth of 8565 ft), the bottom-hole assembly was pulled.

Concurrent with the running of the next assembly—a Dyna-Drill with a new Smith 9JA bit—the EE-1 joint was pressurized with the big (34-gpm) Kobe pump. When drilling reached 8686 ft, the assembly was pulled; the Smith bit was then re-run with a 6-point reamer to ream the hole full-depth. A bottom-hole survey showed a trajectory of N77E, 5 1/4°, which was more easterly than desired.

On May 26, the EYE steering tool was used to more closely control the drilling direction. After a full day of efforts to get the EYE tool to perform properly in the difficult downhole environment, it was found that the extreme curvature of the borehole was preventing correct orientation of the Dyna-Drill assembly. The assembly was replaced with a conventional rotary assembly, and 30 ft of straight drilling with a Smith 9JA bit took the hole to 8716 ft. At this depth, directional drilling began anew, with the EYE steering tool guiding a Dyna-Drill and a Smith 9JA bit below a 2° bent sub. At midnight on May 28, a sharp decrease in the injection pressure at EE-1 indicated that the target joint had been intersected, at a depth of 8769 ft (somewhat higher than the anticipated 8800 ft). This time, a plan was in place to immediately halt drilling and core through the joint to obtain a sample of it.

The borehole was surveyed, the drilling assembly was pulled from the hole, and on May 29 an 8 1/2-in. Christensen core bit was run in. The 4-ft core that was cut (to 8773 ft, with a 50% recovery) consisted of a biotite granodiorite and exhibited three joint planes—two still sealed with calcite, and one apparently reopened. This core turned out to be an incredible stroke of luck in terms of confirming the nature of the pressure-opened joints forming the Phase I reservoir: the reopened joint in the core was an *actual sample* of one of the ancillary joints connecting the principal (9050-ft) EE-1 joint to GT-2B.

The following day, a Dyna-Drill assembly with the EYE steering tool was run in, but troubles with both prevented any drilling. This was the last attempt at directional drilling in GT-2B. Over the next couple of weeks, several experiments were performed in GT-2B to assess the nature of the new flow connection from EE-1 (Table 4-1).

Table 4-1. Initial experiments and tests to investigate the EE-1 to GT-2B flow connection (31 May–17 June 1977)

Expt. No.	Date	Description	Remarks
165	31 May 1977	Initial system flow impedance measurement.	Measured impedance = 15 to 18 psi/gpm (1.6–2.0 MPa per L/s).
166	1–3 June 1977	Pressurization of the 8769-ft joint connection in GT-2B to reduce flow impedance, with a Lynes packer set at 8706 ft. Western pump used to inject into GT-2B at rates varying from 1 to 5 BPM; then to inject into EE-1 at 2.5 BPM.	During injection into EE-1, water discharge temperature at GT-2B reached 130°C. Final EE-1 to GT-2B flow impedance (with very low backpressure of 70 psi at GT-2B) = 9.5 psi/gpm (1.0 MPa per L/s).
167	8–9 June 1977	Monitoring of pressure during injection into EE-1 (big Kobe pump) while drilling ahead in GT-2B.	Second, larger pressure response at EE-1, leading to another coring operation in GT-2B, at a depth of 8894 ft.
168	9 June 1977	Temperature logging in GT-2B during injection into EE-1, to determine flow split between two possible fluid entrances in GT-2B. Temperature logging in EE-1 during injection with the big Kobe pump (GT-2B shut in).	None of four separate temperature logs confirmed existence of second fluid entrance near bottom of GT-2B.
169	16 June 1977	System flow impedance tested during injection into EE-1 at 5 BPM (final test before casing of GT-2B.)	EE-1 to GT-2B flow impedance about 10 psi/gpm.
170	17 June 1977	Repeat of GT-2B temperature log during injection into EE-1 at 1 BPM for 9 h—to again test whether flow was split between two fluid entrances.	Again, temperature logging did not confirm second fluid entrance near bottom of GT-2B.

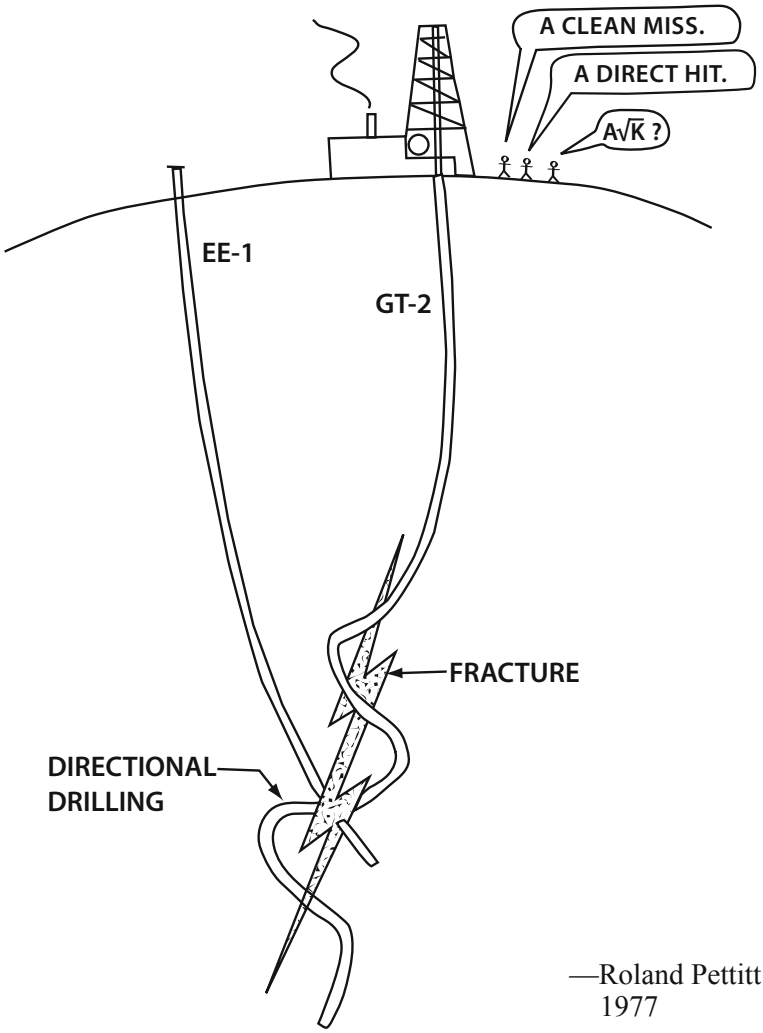

—Roland Pettitt
1977

For Expt. 165, the big Kobe pump was used for an 8-hour pumping test to measure the flow impedance of the joint connection from EE-1 to GT-2B. The impedance measured was 15 to 18 psi/gpm. A conventional drilling assembly was then used to ream GT-2B to bottom and to drill an additional 5 ft of hole, to a depth of 8778 ft. Subsequent temperature logs in GT-2B showed the principal fluid inlet at 8769 ft, with a possible minor fluid entrance above this point, at about 8670 ft. (Note: It is interesting that this minor fluid entrance was almost directly above that of the deeper EE-1 joint [at 9650 ft]. If both fluid entries in fact represented the same vertical joint, or a closely spaced joint set, its connection to GT-2B would be a lengthy [±1000 ft] and probably a tortuous one, which may explain the anomalous geochemical results that would be obtained during later flow testing—Run Segment 2 in particular.)

On June 1, Expt. 166 began with the running of a high-temperature Lynes packer into GT-2B; it was set at a depth of 8706 ft to permit the pressurization and stimulation of the 8769-ft joint intersection. Pumping with the rental Western pump began at 1 BPM and was slowly increased to 5 BPM (13 L/s), at a final injection pressure of 1830 psi. This pressure-stimulation in GT-2B was followed by a similar operation in EE-1. With the drill rig placed on standby, the Western pump truck was moved to EE-1 and the joint connection to GT-2B was pressure-stimulated for 20 hours at an injection rate of 2.5 BPM (6.6 L/s). The injection pressure at EE-1 was only 1000 psi, and the backpressure at GT-2B was maintained at 70 psi to prevent boiling in the surface piping. By the end of Expt. 166, the outlet temperature at GT-2B had increased to 130°C. This series of pressure stimulations succeeded in reducing the overall system flow impedance to 9.5 psi/gpm. (Because of ongoing problems with leakage, Lynes inflatable packers were not used again during Phase I testing. They would be used repeatedly during the establishment of the Phase II reservoir, but only after much further development between the Laboratory and Lynes United Services.)

Drilling recommenced on June 8, at 8778 ft, and continued to 8879 ft, at which depth the drilling assembly was pulled and the borehole was surveyed with a magnetic multishot tool. The bottom 60-ft section was then reamed with a 9 5/8-in. Smith 9JA bit, and the following day drilling proceeded another 14 ft (to 8893 ft). At this depth, there was a second, larger pressure signal at EE-1—suggesting another joint intersection. Drilling was shut down, and the 8893- to 8898-ft interval was cored with a Christensen diamond core bit; but no core was recovered. Subsequent temperature logging (repeatedly proven to be a good indicator of flowing joint intersections with the borehole) did not confirm a joint intersection at the then-deepest point, 8898 ft. (Note: later, during Run Segment 2, temperature logging and spinner surveys would reveal two GT-2B flow connections near the borehole's final drilled depth of 8907 ft—one at 8880 ft and a second just below 8900 ft.)

On June 12, Dresser-Atlas surveyed GT-2B from 2540 ft to 8900 ft with their 4-arm caliper logging tool ("Laterolog") and a spectral gamma logging tool ("Spectralog"). Two days later, Dresser-Atlas also ran two acoustic logs in GT-2B. The Spectralog showed a uranium spike at about 8769 ft (suggesting the presence of mineral-filled joints), and the Laterolog indicated a joint intersection at roughly the same depth.

In retrospect, these logs were mainly a waste of time and money. The Laterolog could not detect the very small amount of fluid contained in the closed (unpressurized) joint at 8769 ft and was thus completely useless (moreover, the spikes seen in the counterpart Laterolog previously run in EE-1 were later found to be fallacious). The acoustic logs were uniform and featureless over the surveyed interval and served only to confirm a value found earlier—via active acoustic ranging—for the sonic velocity of the

rock (5.85 km/s). The only possibly meaningful information yielded by these logs was that from the 4-arm caliper survey, which confirmed the presence of the two calcite-filled joints observed in the core taken on May 29.

Experiment 169, a final assessment of the EE-1 to GT-2B flow impedance, was conducted on June 16. The Western pump injected into EE-1 at 5 BPM (13 L/s), again pressure-stimulating the principal joint at 9050 ft. When the impedance was found to be about 10 psi/gpm—judged adequate for a meaningful heat extraction experiment—plans were made to complete GT-2B so that flow testing could begin.

Experiment 169 also included a period (several hours) of pressurization of the region behind the casing. The injection pressure reached as high as 1400 psi, higher than that required to initially open the joint at 9050 ft. The result was the opening of several other joints intersecting the EE-1 borehole in this region—most of them above the 9050-ft depth. Figure 4-2, a temperature survey done in EE-1 following Expt. 169, reveals these additional joints as well as the principal fluid entrance at 9050 ft.

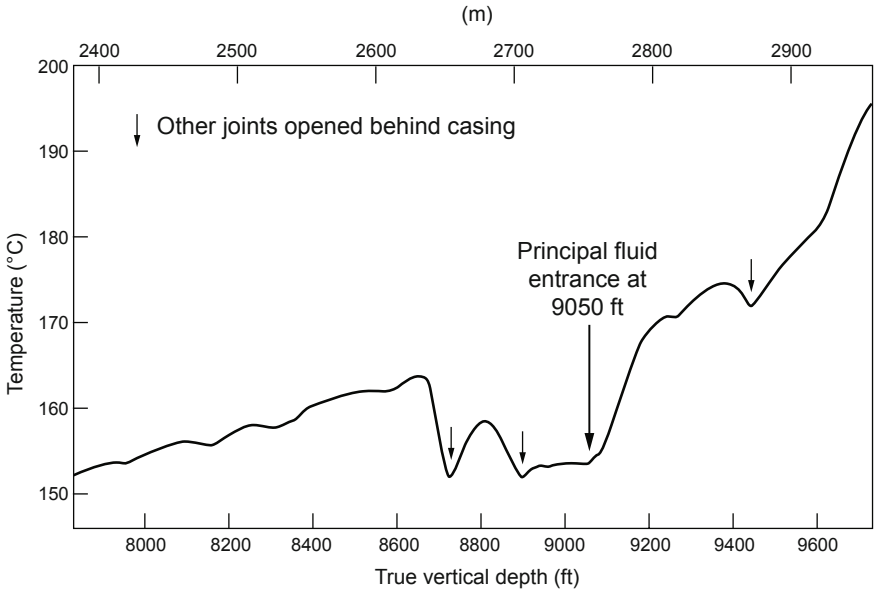

Fig. 4-2. Temperature survey of the lower part of EE-1 following Expt. 169. The depths shown are "true vertical depths"—about 50 ft less than the depths measured along the borehole.
Adapted from HDR, 1978

There was no evidence that any of these other joints were connected to GT-2B, but their presence would complicate subsequent analyses during flow testing of the Phase I reservoir. It is probable that these joint intersections

received some pressurized water via a micro-annulus that formed between the cement and the rock (even though the casing in this interval was adequately cemented, it is likely that the injection of cold fluid down the borehole caused thermal contraction of both the casing and the cement). Even a small flow of water through such a micro-annulus could permeate into these joints, facilitated by the lower earth stresses farther up the borehole.

The next day the flow situation in GT-2B was assessed once more (Expt. 170): temperature logging during injection into EE-1, at 1 BPM for 9 hours, again showed only one production zone—the one at 8769 ft.

On June 18 and 19, two more coring runs deepened GT-2B to its final drilled depth of 8907 ft. The first run, with a diamond core bit, recovered no core; but the second, with a newly developed Stratapax four-cone, TCI core bit (Smith Tool Co.), cut 5 ft of hole with an 89% recovery. The Stratapax bit was designed with four outer roller cones (to cut out the entire portion of hole surrounding the 3-in. central core area) and four inner Stratapax cutters. These cutters—polycrystalline diamond compacts mounted on pedestals—maintained core diameter by compensating for the wearing of the innermost carbide buttons on the roller cones (any increase in diameter could cause the core to jam in the core barrel). The rock, a biotite granodiorite, exhibited several distinct joint surfaces that apparently had been mechanically opened during the coring process. As shown in Fig. 4-3, by the end of the coring run, the Smith bit—which drills in a much rougher fashion than a diamond core bit—had lost three of the four studs holding the synthetic diamond cutters.

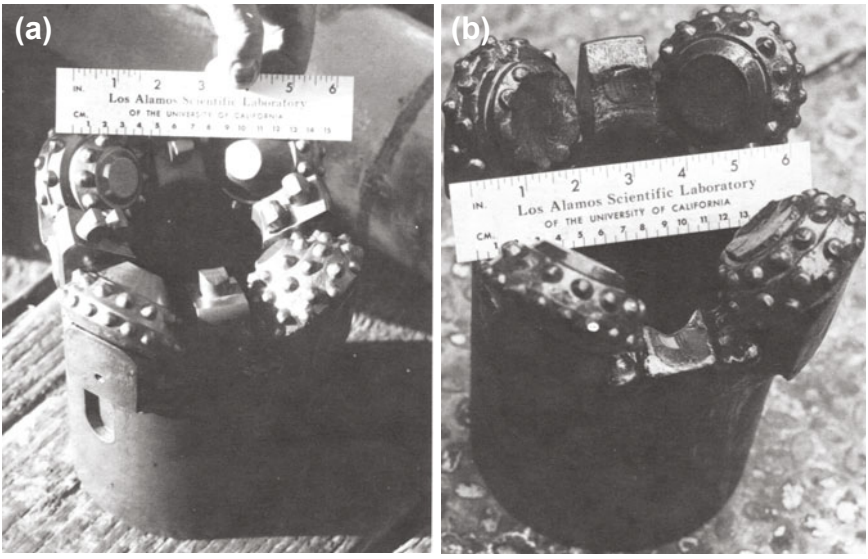

Fig. 4-3. The Smith Tool Co. Stratapax core bit (a) before drilling and (b) after a 5-ft coring run in granitic rock.
Source: Pettitt, 1978b

Completion of GT-2B

The first step in completing GT-2B was to set a cement plug in the borehole above the depth of the primary flow connection at 8769 ft. (Because the inclination of the hole at this depth was near-vertical, no bridge plug was needed to prevent the cement from flowing on down the hole.) On June 20, the cement (50 sacks) was placed through open-ended drill pipe at a depth of 8650 ft. However, when a drill bit was run into the hole to face off the plug, no solid cement was encountered. It appeared that the cement had been dispersed by continuing flow from EE-1 (which, although shut in, was still somewhat pressurized from previous pumping operations). The next day EE-1 was vented, after which the cementing operation was repeated—this time successfully. The top of the hard cement was tagged at 8515 ft and faced off to 8572 ft.

To case the hole, a string of 7 5/8-in. (194-mm) production casing was run from 2 ft above the cement plug to the surface, made up as follows:

- 2620 ft of 33.7 lb/ft, grade S-95 casing at the bottom
- 2800 ft of 33.7 lb/ft, grade N-80 casing in the middle
- 3158 ft of 33.7 lb/ft, grade S-95 casing at the top

The grade S-95 casing was used for both the bottom and top sections because once the casing job was complete, compressive stresses would be greatest at the bottom and tensile stresses would be greatest at the top. A Halliburton float shoe was installed on the bottom of the string and a Halliburton float collar was set in the string one joint (40 ft) above the shoe.

As the casing string was run in, 22 centralizers were spaced along the bottom 20 joints (about 800 ft). After the pipe had tagged the cement plug, it was lifted up 2 ft (putting the bottom of the casing at 8570 ft). The casing was then hung from the surface, and the bottom 1500 ft was tag-cemented by Halliburton Oil Well Cementing Company.

Before cementing, the weight of the casing string—as recorded on the rig weight indicator—was 252 000 lb (corresponding to a weight in air of 289 000 lb). The casing slips on the rig floor supported most of this weight while the cement hardened. Next, the cement shoe and the cement plug were drilled out, the borehole was washed to bottom, and the casing was tensioned by hydraulic casing jacks placed over the hole. Finally, the casing was landed in the wellhead with a load of 410 000 lb (as measured by load cells). According to calculations, it would remain in tension at the surface during reservoir production at temperatures up to 180°C.

Figure 4-4 shows the trajectories of the original GT-2 borehole and the GT-2A and GT-2B sidetracked legs, in relation to EE-1.

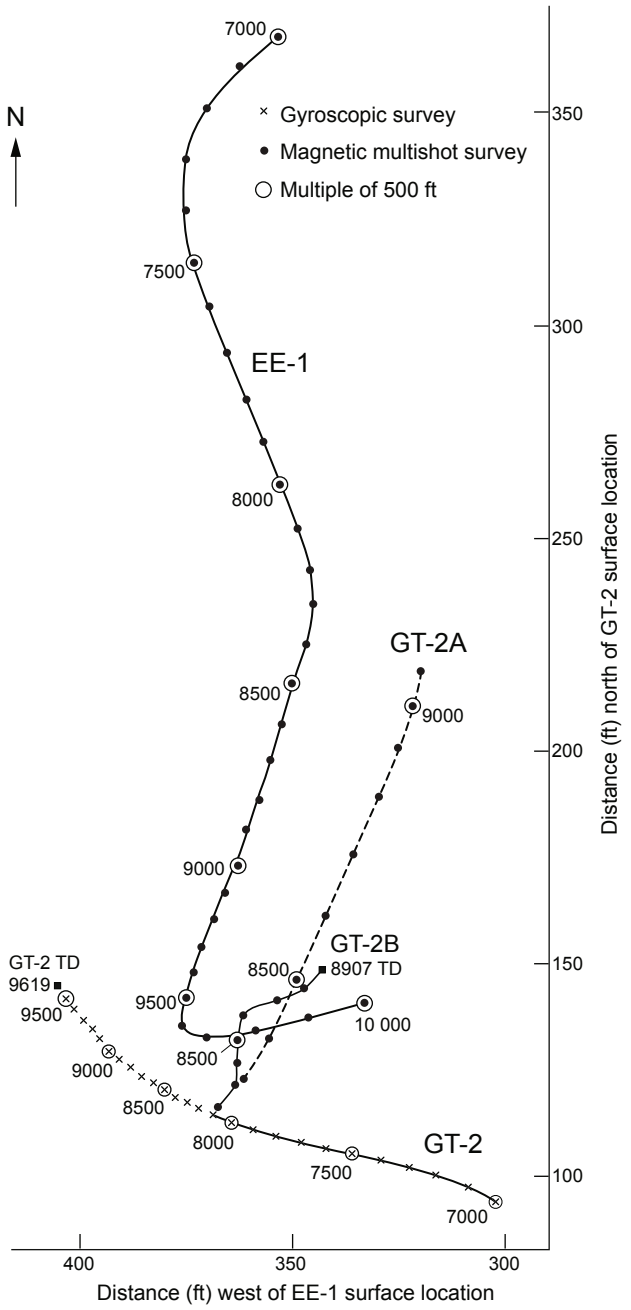

Fig. 4-4. The paths of GT-2, GT-2A, and GT-2B in relation to EE-1 (in plan view).
Source: Pettitt, 1978b

A Conceptual Model of the Phase I Reservoir

In mid 1977, after the GT-2B borehole had been completed, a conceptual model of the Phase I reservoir was developed on the basis of data from the various flow tests, geophysical logs, and temperature surveys. This model, shown in Fig. 4-5, included

1. an essentially vertical pressure-stimulated joint—at that time called a "fracture"—originating from EE-1 at a depth of 9050 ft and striking N55W, as determined by seismic monitoring (see Fig. 3-30);
2. the location of this joint and of all three very steeply inclined boreholes within the very narrow—ca. 50 ft—width of the reservoir region, shown in cross section in Fig. 4-5 (shaded area);
3. an intersection of the GT-2A borehole with the upper extension of this joint, at a depth of 8645 ft (evidenced by a marked pressure perturbation at EE-1, which was pressurized at a constant rate of 34 gpm during the drilling of GT-2A);
4. significant fluid entry points into GT-2B (detected during the drilling of that leg of the borehole) *but no actual intersection of the EE-1 joint*;
5. one or more flow connections, of unknown orientation, from the 9050-ft EE-1 joint to the GT-2B borehole, as evidenced by flow testing (see Expts. 165–170, above);
6. a zone between the EE-1 joint and the GT-2B borehole that appeared, on the basis of *known* joint structures, to be devoid of any connecting flow paths.

Although a number of HDR staff contributed to this concept, in no sense did it reflect a consensus view. To resolve the apparent contradiction between (5), which implies that flow connections did exist in the intervening zone, and (6), which implies the opposite, an additional feature had to be postulated:

> Several joints, dipping about 30° to the northwest across the region between EE-1 and GT-2B, could be inferred on the basis of clusters of borehole anomalies—temperature, geophysical (spectral gamma spikes, signifying uranium), and flow (indicated by spinner surveys). Such joints are represented by the dotted lines in Fig. 4-5.

However, several facts argue against this part of the conceptual model. First, the notion of the 30°-inclined joints was arrived at by an almost arbitrary joining of data points: drawing of straight lines between clusters of anomalies along the GT-2B and EE-1 boreholes (such as the flow connection—then minor—shown in the figure at 8894 ft). One might just as easily have joined these anomalies otherwise, e.g., in a way that would result in SW-dipping 45° joints. Second, there was no seismic evidence for a set of 30°-dipping joints. And third, the injection pressure required to open such a set of sealed joints would have been on the order of 2800 psi. There had been no pressurization of either borehole that high; the highest injection pressure used up to this time was 1830 psi (during Expts. 162 and 166 in May and June of 1976).

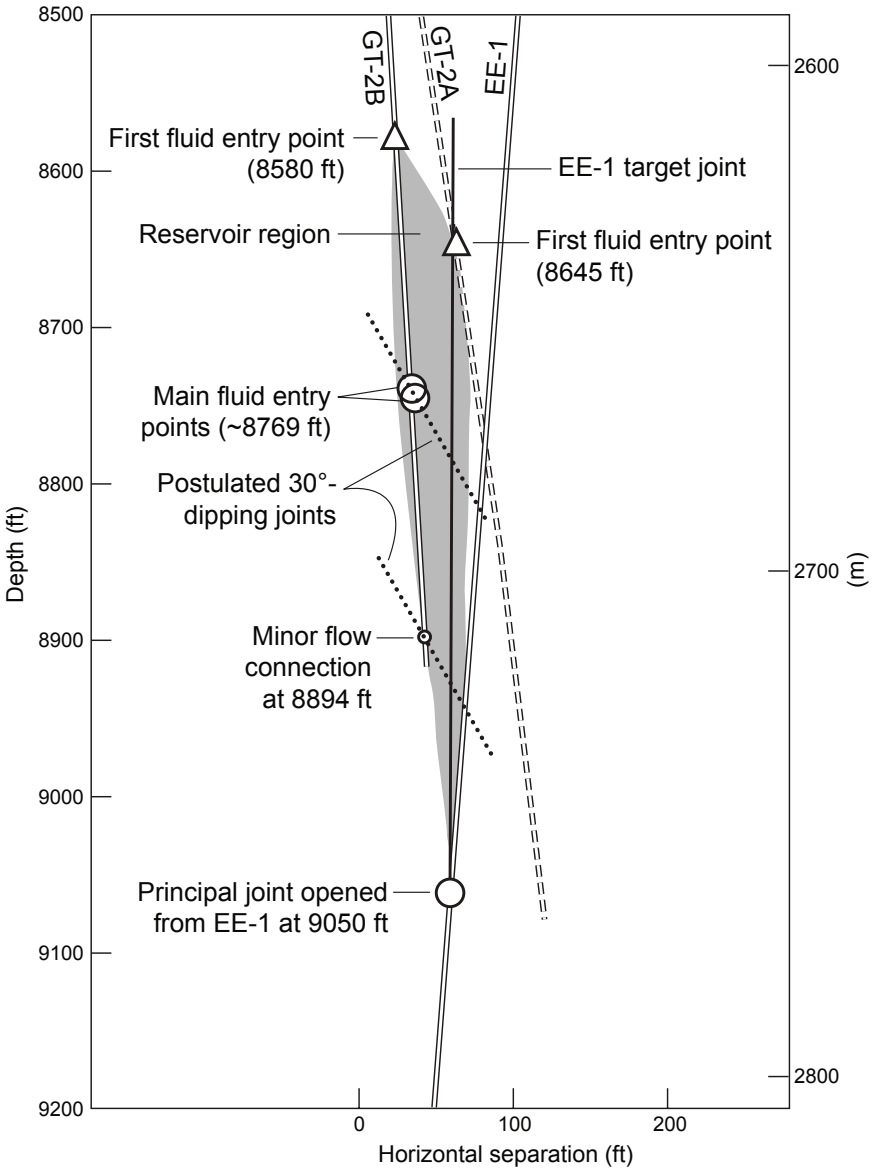

Fig. 4-5. The Phase I reservoir region as conceptualized following the drilling and testing of GT-2B (viewed in the N55W direction, along the plane of the 9050-ft joint in EE-1). Major fluid entry points detected during drilling are shown.
Adapted from HDR, 1978

What, then, was the true nature of the flow connections between the EE-1 joint and the GT-2B borehole? As discussed below (see sections on Run Segments 2 and 3), it is more likely that these connections were formed by a set of near-vertical joints having strikes somewhat oblique to the EE-1 joint, i.e., approximating the N27W strike of the GT-2 joint (see Fig. 3-34). For instance, a vertical joint striking N35W—a 20° rotation from the N55W strike of the 9050-ft EE-1 joint—would have had a closure stress of about 1500 psi, well within the range of the stimulation pressures used.

The Phase I Surface Facility

Many pieces of equipment and special installations had to be put in place before flow testing of the Phase I reservoir could begin. Figure 4-6 shows the major components of the surface facility in the fall of 1977.

Water Storage

A large (500-bbl [80 000-L]) rectangular storage tank was situated just outside the wooden fence surrounding the GT-2 location, and a smaller (6000-gal.) circular storage tank was situated just outside the fence surrounding the EE-1 location. The earthen reserve pit used for the drilling of EE-1 had been enlarged into a 400 000-gal. water storage pond for the venting of EE-1, venting of the surface loop, or auxiliary water storage. In addition, the larger of the two reserve pits used during the redrilling of GT-2 was used as necessary for the venting of that borehole.

Injection Pumps

Two multistage, centrifugal pumps were procured and installed vertically (in concrete-walled cellars). Each was rated at 250 gpm with a differential pressure of 1350 psi. During loop operations at a backpressure of 175 psi, the suction pressure of these pumps would be about 150 psi—which equates to a maximum EE-1 injection pressure of 1500 psi at 500 gpm.

Surface Flow Loop

The hot production fluid from GT-2 flowed through a long, insulated pipe to an air-cooled heat exchanger that was purchased and installed in 1977 (see Fig. 4-6).[3] Once cooled, the fluid traveled to the injection pumps near EE-1, where sufficient makeup water was added to reach the specified injection flow rate (a makeup pump supplied this additional water, from the cylindrical storage tank adjacent to EE-1). The pressurized fluid from the injection pumps was injected into EE-1, completing the surface loop.

[3]This heat exchanger was one of the few "constants" at the Fenton Hill Test Site (another being the positions of the boreholes). Even the roads were moved as the Project developed. The heat exchanger was used for all closed-loop flow testing, including the Long-Term Flow Test, which ended in 1995.

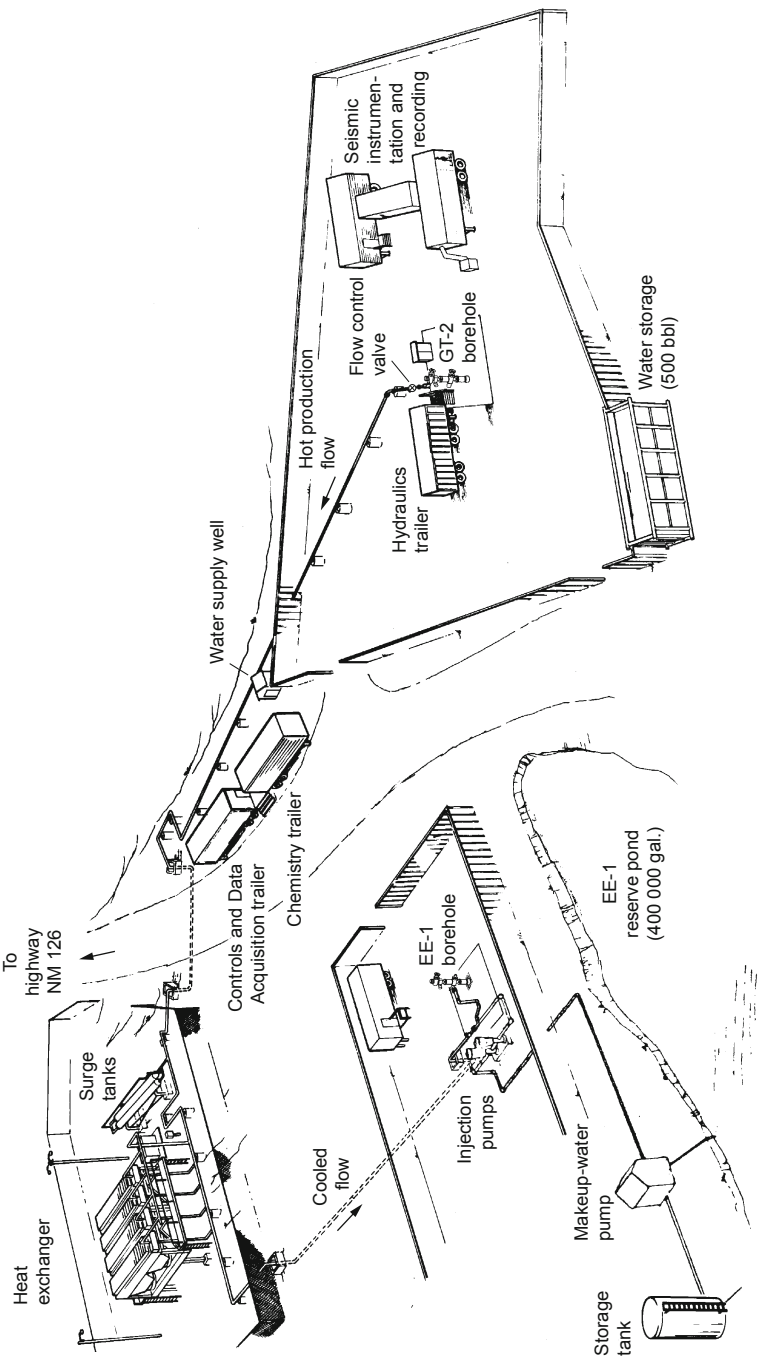

Fig. 4-6. Major components and structures of the Fenton Hill surface facility (fall 1977, before the start of Phase I flow testing).
Source: Tester and Albright, 1979

On-site Water Well

In the summer of 1976, a well had been drilled on site as a source of potable water for all domestic uses as well as for drilling, fracturing, and circulation operations (before that, water had been trucked in from the nearby community of La Cueva). The well was 450 ft (137 m) deep and 6.25 in. (15.9 cm) in diameter; the bottom 60 ft was lined with a 5 5/8-in. (14.3-cm) slotted screen. This well brought a reliable supply of naturally potable water from a perched aquifer on top of the Permian formation, at a rate of about 40 gpm (2.5 L/s).

Controls and Data Acquisition Trailer

The Controls and Data Acquisition (CDA) Trailer was the "hub" for all the activities involved with the flow testing of the Phase I reservoir. All the data for the surface system—flow rates, pressures, temperatures, changes to certain valves (those not controlled directly in the field), etc.—were fed to this trailer; alarms signaling critical conditions in any of several major parameters were displayed here; and the operation of the injection pumps and of the four-component heat exchanger was controlled from here. This trailer was also the site of many spirited discussions as the flow testing proceeded.

Chemistry Trailer

The "Chem" Trailer was positioned next to the CDA Trailer and adjacent to the water well and to the flow line connecting GT-2 to the heat exchanger. It contained a host of sophisticated chemical analysis equipment, which would be used almost continuously for over 15 years—through the end of the Long-Term Flow Test (LTFT).

Seismic Instrumentation and Recording

This complex of trailers was the heart of seismic monitoring during Phase I testing. Signals from all the surface seismic stations were recorded here, as were those from the downhole geophones when deployed. The surface array consisted of nine stations located on a radius of about 2 miles (3.2 km) from the EE-1 wellhead; in addition, during pumping into either GT-2B or EE-1, a geophone would usually be installed in the other borehole.

Flow Testing of the Phase I Reservoir, 1977–1978

The information in this section is abstracted mainly from Tester and Albright (1979) and HDR Geothermal Energy Development Program (1979).

With GT-2B complete and some initial reservoir flow testing and interrogation having been done, the surface equipment for the closed energy-extraction loop was installed and checked. Everything was ready by September except for the primary circulation pumps and the final configuration of the CDA Trailer. The Project managers, who were anxious to have a significant reservoir flow test to report by the end of the fiscal year (September 30, 1977), decided to activate the loop and run an initial segment of the HDR demonstration (planned to last 10 000 hours in all) with rented pumping equipment and a "jury-rigged" CDA Trailer.

Run Segment 1: September 1977

Run Segment 1, also known as Expt. 176, was a 4-day (96-hour) flow test designed as a preliminary checkout of the closed-loop heat-extraction system (numerous "bugs" were anticipated) and as an initial assessment of the reservoir's flow characteristics. Over the four days of this test—carried out at injection pressures varying between 1000 and 1350 psi—the water loss decreased from 86 to 30 gpm, total dissolved solids in the produced fluid remained low (<400 ppm), and there was no induced seismicity.

Analysis of the surface pressure behavior during several Run Segment 1 flow shut-ins led to the conclusion that the flow impedance of the reservoir system had two major components and one minor component. The major components are (1) the impedance across the principal joint—the simplest form of an HDR reservoir—called the *body impedance*; and (2) the impedance in the highly stressed and flow-restricted zone where one or more joints connected the principal EE-1 joint to the production wellbore, referred to as the *near-wellbore outlet impedance*. The body impedance during Run Segment 1 was 3.7 psi/gpm (0.4 MPa per L/s), and the near-wellbore outlet impedance ranged from 7.3 to 11 psi/gpm (0.8 to 1.2 MPa per L/s). (Note: A near-wellbore outlet impedance higher than the body impedance would also be found during testing of the multiply jointed Phase II reservoir more than a decade later, and would prove to be characteristic of HDR reservoirs.)

The minor component of the overall reservoir flow impedance, called the *near-wellbore inlet impedance*, is the impedance to flow from the injection borehole into the body of the reservoir, through the first few meters of the connecting joints. This impedance was initially small (about 1 psi/gpm or less), but diminished even more, to an almost unmeasurable value, as the cold injection flow continued to induce thermal contraction of the already pressure-dilated inlet joints.

By the end of this test, the produced thermal power had risen to 3.2 MW at a production flow rate of 100 gpm and an outlet temperature of 130°C. Run Segment 1 demonstrated for the first time that heat could be extracted from a man-made HDR reservoir at a usefully high rate. Further, it raised expectations that no significant problems would be encountered during sustained closed-loop operation of the system.

On October 11 and 12, following Run Segment 1, Dresser-Atlas surveyed the condition of the casing cement at the bottom of EE-1, using both acoustic cement-bond logs and radioactive iodine tracers. They found that the bonding signal was almost totally absent below about 9000 ft, and that nearly all of the injection flow (>90%) was exiting the EE-1 borehole through the 9050-ft joint—via the annular flow path up behind the casing—supporting many previous measurements of a split flow in EE-1 (see, for example, Expts. 122A, 129, and 156 in Chapter 3).

Run Segment 2: January–April 1978

Run Segment 2, a 75-day period of closed-loop, low-backpressure operation, was the first true evaluation of the thermal and flow characteristics of a pressure-dilated joint network dominated by a single near-vertical joint—the configuration of the Phase I HDR reservoir at this time. Water was pumped into the reservoir through EE-1, at injection pressures varying from about 1200 psi (day 5) to 870 psi (day 72), and recovered via GT-2, the production well. The recovered hot water was then passed through the water-to-air heat exchanger to be cooled to 25°C. To it was added a quantity of makeup water to replace water lost from the reservoir by permeation into the surrounding rock mass. Finally, the water was reinjected into EE-1.

The variation in the reservoir production temperature, as measured at a depth of 8530 ft in GT-2B, is depicted in Fig. 4-7. The drawdown (rate of decline) in this temperature over the 75 days of Run Segment 2 was considerable: from an initial value of 175°C to 85°C.

At this time, several numerical models were being developed to estimate the heat-transfer surface of the reservoir. One of these suggested that the drawdown profile of Fig. 4-7 would correspond to a heat-transfer surface of about 86 000 ft^2 (8000 m^2). If one assumes (1) a single flowing joint making an almost direct connection between EE-1 and GT-2B and (2) a roughly rectangular joint with an inlet at 9050 ft in EE-1 and an outlet at 8769 ft in GT-2B (i.e., a height of 281 ft), a heat-transfer surface of this size (one side) would imply an accessible joint width of about 300 ft.

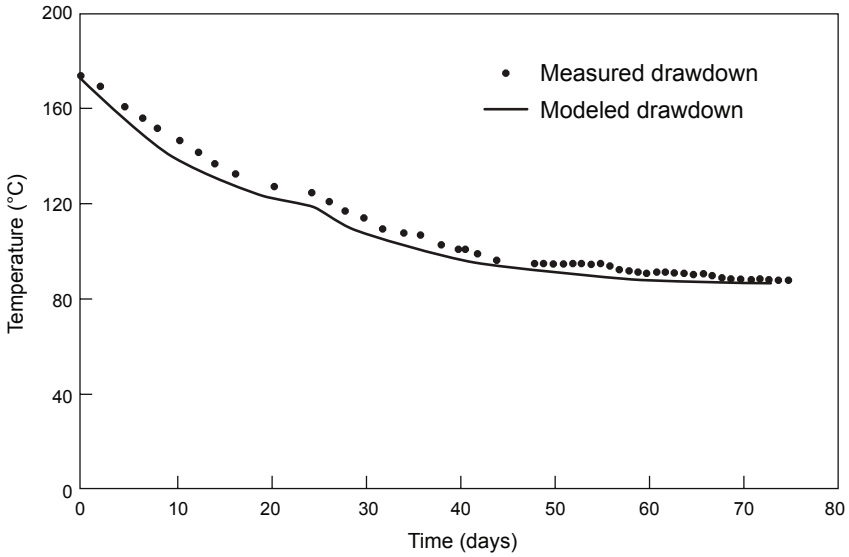

Fig. 4-7. Variation in the reservoir production temperature during Run Segment 2, as measured at 8530 ft in GT-2B. Also shown is the modeled thermal drawdown of the reservoir, based on a constant joint area of 86 000 ft^2. Source: Tester and Albright, 1979

The modeled thermal drawdown profile of Fig. 4-7 closely follows the measured profile for the entire 75 days, which suggests that the effective heat-transfer surface remained unchanged during this test and was not significantly added to by thermal stress cracking along the cooled joint surfaces.

The net thermal power produced during Run Segment 2 is shown in Fig. 4-8. It represents the amount of heat transferred from the reservoir rock to the fluid flowing in the joint(s), less the amount lost to the rock surrounding the borehole during the flow to the surface. For the last 28 days of the test, net thermal power averaged about 4.3 MW.

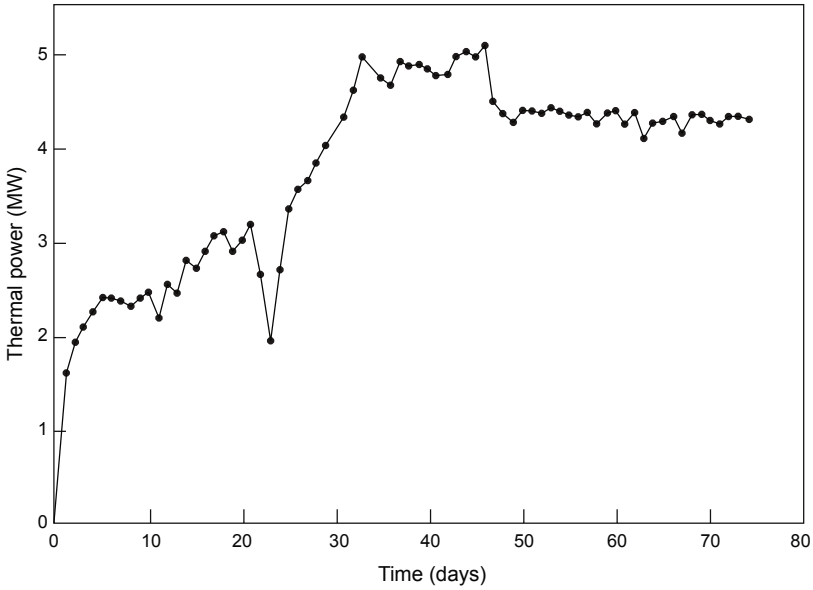

Fig. 4-8. Thermal power production during Run Segment 2.
Source: Tester and Albright, 1979

One of the confounding aspects of the Phase I reservoir was the apparent complexity of the flow connections to the GT-2B borehole. During Run Segment 2, 58 temperature surveys were done between 8530 and 8900 ft in the GT-2B production interval. (When the temperature tool was not being used for surveys, it was "parked" at 8530 ft, just above the shallowest production zone, continuously recording the mixed-mean reservoir production temperature.) Three of these surveys, taken 7 days, 12 days, and 16 days after the beginning of power production, are depicted in Fig. 4-9. They illustrate how flow inlets tended to change or develop as the flow test proceeded. For instance, the major flow connection at 8769 ft appears to increase with time, becoming even more pronounced on the February 13 survey; a higher flow entrance (at 8620 ft) increases only modestly during the span of the three surveys; the anomalous (high-temperature, low-flow)

fluid entrance at 8670 ft[4] is essentially unchanged over the 9 days covered by the surveys; and on the February 13 temperature profile, one or more flow entrances are again indicated near the bottom of the borehole[5] (in addition to a completely new, cooler fluid entrance that appears to have developed at about 8820 ft). In other words, after only 16 days of production one sees a considerable change in the flow connectivity to the GT-2B production interval, with at least four joint connections. Most of these changes probably resulted from the continuing pressurized flow from EE-1.

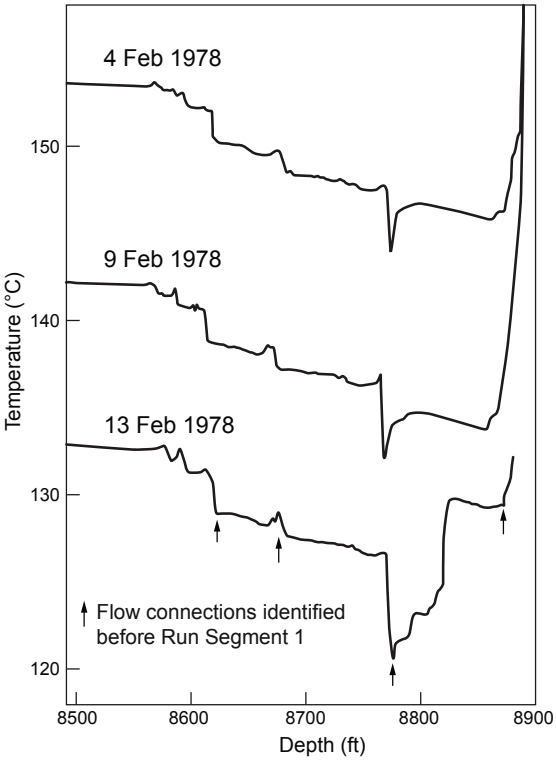

Fig. 4-9. Three temperature surveys taken in the open-hole interval of GT-2B during the early part of Run Segment 2.
Adapted from Tester and Albright, 1979

[4]The fact that its presence made almost no change in the mixed-mean temperature of the flow up the borehole indicates that this inlet had a very low rate of flow.

[5]Evidently none of the three temperature surveys reached the GT-2B TD of 8907 ft, probably to avoid risking damage to the tool with a hard landing on bottom. For this reason, the depths of flow entrances in this vicinity are not easily identifiable, except possibly for the one at about 8880 ft (seen most clearly in the February 13 survey).

Given the proximity of the boreholes to the 9050-ft joint (see Fig. 4-5), it is likely that the cooling effects of Run Segment 2 extended into significant portions of the reservoir region by the end of this 75-day flow test, resulting in thermal contraction and, possibly, some additional cooling-induced joint openings.

As noted by Hugh Murphy in the report on this run segment (Tester and Albright, 1979), even a cursory look at these temperature surveys leads one to conclude that the connectivity between the reservoir and the production well was highly complex. As alluded to earlier, this complexity would suggest an array of near-vertical, low-opening-pressure joints connecting the 9050-ft EE-1 joint to the GT-2B production interval, rather than the set of high-opening-pressure, 30°-dipping joints that had been postulated by some HDR staff (Fig. 4-5).

The circulating fluid was sampled at a number of locations around the surface loop[6] during Run Segment 2, and its geochemistry was carefully monitored for the entire 75 days. The results were anomalous. As shown in Fig. 4-10, the silica content of the produced fluid generally *increased* over the course of the test, while the reservoir production temperature (Fig. 4-7) *decreased*. Such a fluid geochemistry behavior suggests the inflow into GT-2B of a small amount of hot, saturated fluid not associated with the flow from the principal joint—an inference supported by the concentration curves of the other dissolved species (calcium, magnesium, lithium, sodium, potassium, chloride, bicarbonate, fluoride, and sulfate), all of which increased with time. The path through which this fluid was circulating apparently remained at or close to the initial reservoir temperature and had a large contact area. It was postulated that the EE-1 joint at 9650 ft was contributing this fraction of hot fluid to the GT-2B production flow, via a long, tortuous—i.e., multiple-joint—path that entered GT-2B at about 8670 ft, as shown in Fig. 4-9. (Note: Nearly a year later, with the re-cementing of the EE-1 casing and the closing off of the annular space that was the main pathway for the flow into the 9050-ft joint, it would be determined that this secondary flow path was the only remaining connection between EE-1 and GT-2B.)

A model was developed for predicting the silica concentration as a function of time under the postulated scenario that 5% of the GT-2B production flow was being continuously recirculated through this secondary flow path (the 5% value is supported by analysis of an EE-1 temperature log taken 19 days after Run Segment 2—see below). The result is the "predicted" curve for silica shown in Fig. 4-10.

A recent re-analysis of the relevant experimental data shows that the probable secondary flow path connected to GT-2B first became apparent

[6]Sampling locations were the GT-2 wellhead, the input to the heat exchanger, the makeup-water line just upstream of the injection pumps, and the input to EE-1.

following Expt. 165, when temperature logs not only confirmed the principal joint intersection at 8769 ft but also revealed a minor—but hot—fluid entrance at about 8670 ft. This flow path showed up again in the three successive GT-2B temperature logs (Fig. 4-9) as a small but recurring step temperature rise, and subsequent fall, of about 3°C. This temperature pulse probably denoted the intersection with the borehole of the joint to which this small secondary flow path was connected, and suggested an inflow at a nearly constant rate and temperature. The three temperature logs of Fig. 4-9 also showed decreasing mixed-mean reservoir production temperatures with time (154°C, 142°C, and 133°C, respectively) as measured at a depth of 8530 ft, just above the production interval.

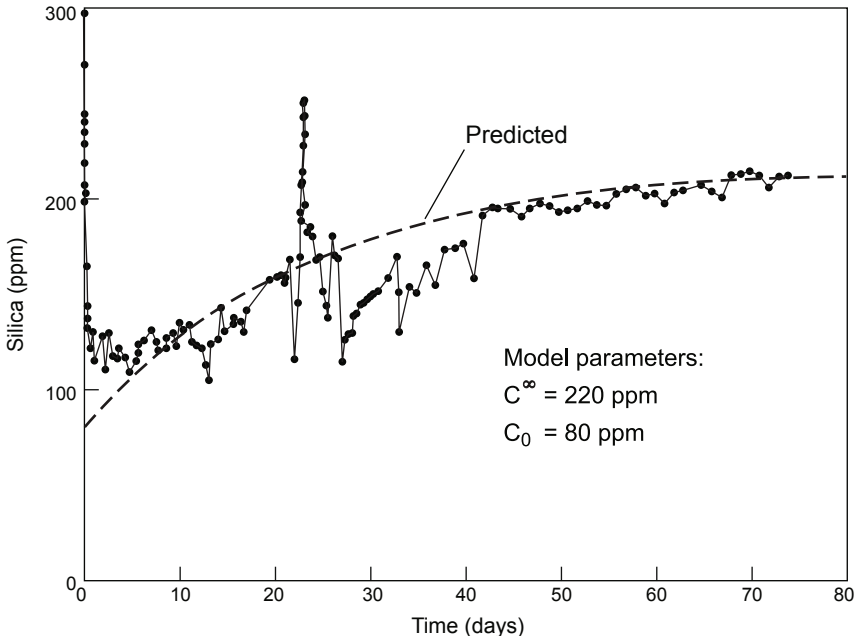

Fig. 4-10. Measured and model-predicted silica concentrations in produced fluid during Run Segment 2.
Source: Tester and Albright, 1979

Nineteen days after the end of Run Segment 2, a temperature log in EE-1 located the principal fluid inlets, but also several irrelevant—and confusing—broad zones of fluid entry (Fig. 4-11). Unfortunately, as has often been observed, a temperature depression does not always mean a significant inflow of cold water. In some cases, a small temperature depression may be caused by long-term permeation of cold fluid into a joint (or jointed interval)—as can occur when the individual joints are filled with secondary mineralization that is somewhat more permeable than the surrounding rock matrix.

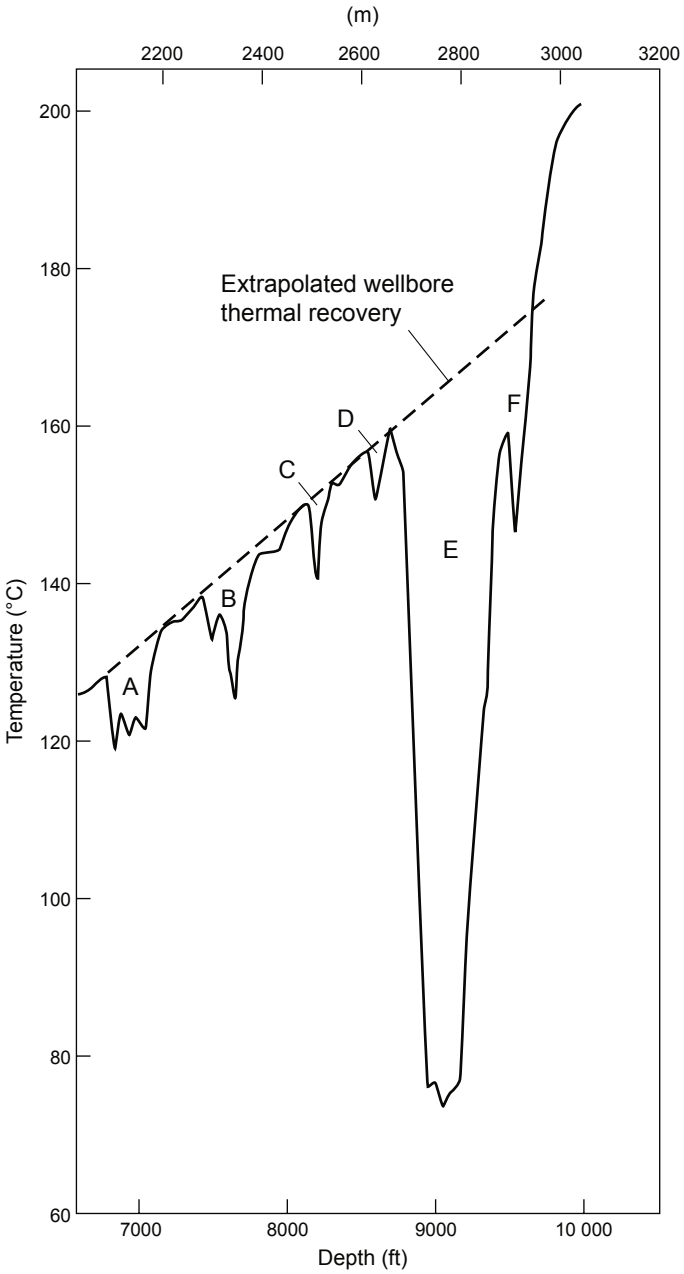

Fig. 4-11. Temperature profile taken in the injection well (EE-1) on June 2, 1978—19 days after the end of Run Segment 2 injection. Depression "E" is the principal fluid inlet into the joint at 9050 ft.
Source: Tester and Albright, 1979

The temperatures plotted in Fig. 4-11 illustrate this phenomenon. Anomalies A and B are in the open annulus behind the casing and above the top of the cement at 7900 ft. With no significant annular pressure or flow (the annulus was open to the atmosphere at the surface), it is hard to explain these anomalies except as artifacts of the previous testing of the borehole, accentuated by the very significant cooling—for 75 days—of the injection borehole, wherein temperature recovery may not always be uniform. Anomalies C and D occur behind the well-cemented portion of the casing, where flow, if any, would have been minimal, pressure was nil, and outflow at the surface was very minor.

In contrast, the anomalies at 9050 ft and 9650 ft (E and F, respectively) represent true, flow-induced depressions associated with the principal identified joints intersecting EE-1. The estimated flow fraction represented by temperature depression F is 5%. (Note the sharpness of this depression, which indicates a single joint intersection with the borehole, whereas each of the two upper temperature anomalies [A and B] occurs over about 400 ft of the hole—much too wide for single joint intersections.)

As shown in Fig. 4-12, the flow impedance of the reservoir increased gradually, from 13 psi/gpm (1.4 MPa per L/s) at the beginning of Run Segment 2 to a maximum of 15.5 psi/gpm (1.69 MPa per L/s) on day 8; for the rest of the test it showed an overall decrease, to a final value of 3 psi/gpm (0.3 MPa per L/s). These impedance values were obtained from the difference between the EE-1 injection pressure and the GT-2B production pressure (both measured at the surface), divided by the production flow rate. The results were then corrected for buoyancy—the difference between the integral mean fluid density in the injection well and that in the production well times the average reservoir height—and converted to psi. (This correction, which amounted to +260 psi early in Run Segment 2, dropped rapidly to about +120 psi by day 35 and then remained constant to the end of the test on day 75.)

A comparison of the flow impedance profile in Fig. 4-12 with the production temperature profile in Fig. 4-7 suggests a strong correlation between reservoir impedance and temperature. The most likely explanation for this correlation is that the principal flowing joint dilated as it cooled, particularly where the joints connecting it to GT-2B intersected that wellbore (the near-wellbore outlet impedance)

The flow impedance exhibited a number of step-changes during Run Segment 2. The most significant of these, which occurred on day 22, is shown on the flow impedance profile (Fig. 4-12) and also on the temperature and power profiles (Figs. 4-7 and 4-8)—a sudden drop in impedance of 4 psi/gpm that nearly doubled the production flow rate at GT-2B, requiring a shut-down of the entire surface system for over 3 hours. Following this impedance drop (which was attributed to a slight shear displacement of the joint faces, probably due to a lowering of the effective joint-closure stress with cooling), it took many hours to get the flow loop running smoothly again. Flow rates, makeup-water pressures, louver settings on the heat exchanger, and throttle-valve settings all had to be readjusted.

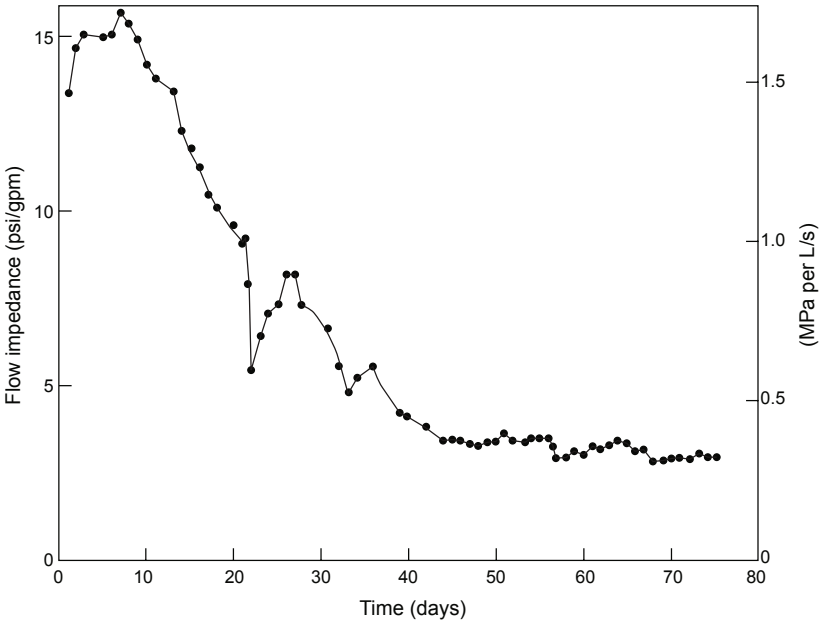

Fig. 4-12. Net flow impedance during Run Segment 2 (corrected for buoyancy).
Source: Tester and Albright, 1979

The plan was to maintain the EE-1 injection pressure at 1200 psi (somewhat below the joint-closure stress) throughout Run Segment 2. However, after 30 days the flow impedance had declined to the point (see Fig. 4-12) that the pumps could no longer maintain this level of injection pressure. From then on, the test was run at a constant rate of injection—230 gpm—with a constant backpressure of 250 psi at GT-2B. The resulting pressure profile is shown in Fig. 4-13.

The first component of the overall flow impedance, the body impedance, was computed by assuming a constant aperture for the pressure-dilated joint of 0.2 mm—an assumption that depends on the decline in pressure across the body of the joint being only modest (that is, from the inlet to near the outlet at GT-2B, where the streamlines of flow through the interconnecting joints rapidly converge into the pinched-off intersections of these joints with the wellbore). The result was about 3 psi/gpm (0.3 MPa per L/s), which compares quite favorably with the 3.7-psi/gpm (0.4-MPa per L/s) value deduced for this component during Run Segment 1. It is likely, therefore, that early in Run Segment 2, before the effects of cooling had reached the region of the near-wellbore outlet impedance, the overall flow impedance of about 15 psi/gpm (1.6 MPa per L/s)—observed on day 9—consisted of a 3.0-psi/gpm body impedance and a 12-psi/gpm near-wellbore outlet impedance.

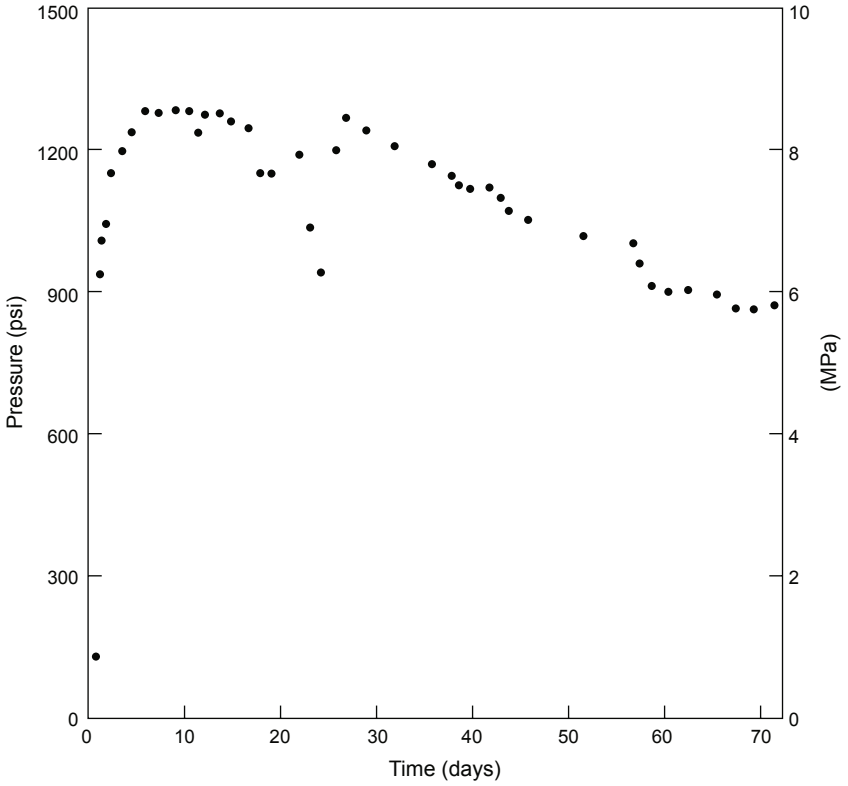

Fig. 4-13. Profile of EE-1 injection pressure during Run Segment 2. Adapted from Tester and Albright, 1979

Figure 4-14 shows that the water loss from this early version of the Phase I reservoir (essentially one joint) decreased continually during Run Segment 2, as diffusion from the periphery of the pressure-stimulated portion of the joint slowly declined.[7] Reservoir water loss is inherently a very "noisy" measurement, because it is calculated by subtracting the production flow rate from the injection flow rate—both much larger quantities, measurement of which is complicated by repeated flow shut-ins for repair of pumps or other surface system components. At the beginning of Run Segment 2, as the principal joint was reinflated, the apparent water loss was equal to the injection flow rate of 230 gpm (100% loss). But by the end of the test, the loss rate had dropped to 2 gpm, less than 1% of the injection rate.

[7]Note, however, that had the injection pressure at EE-1 been maintained at a level somewhat *above* the joint-closure stress, the principal joint would have continued to slowly pressure-dilate (extend) in the regions farthest from its 9050-ft intersection with EE-1, resulting in somewhat higher water losses—some of the "lost" fluid being stored in an ever-dilating joint (i.e., an expanding reservoir region).

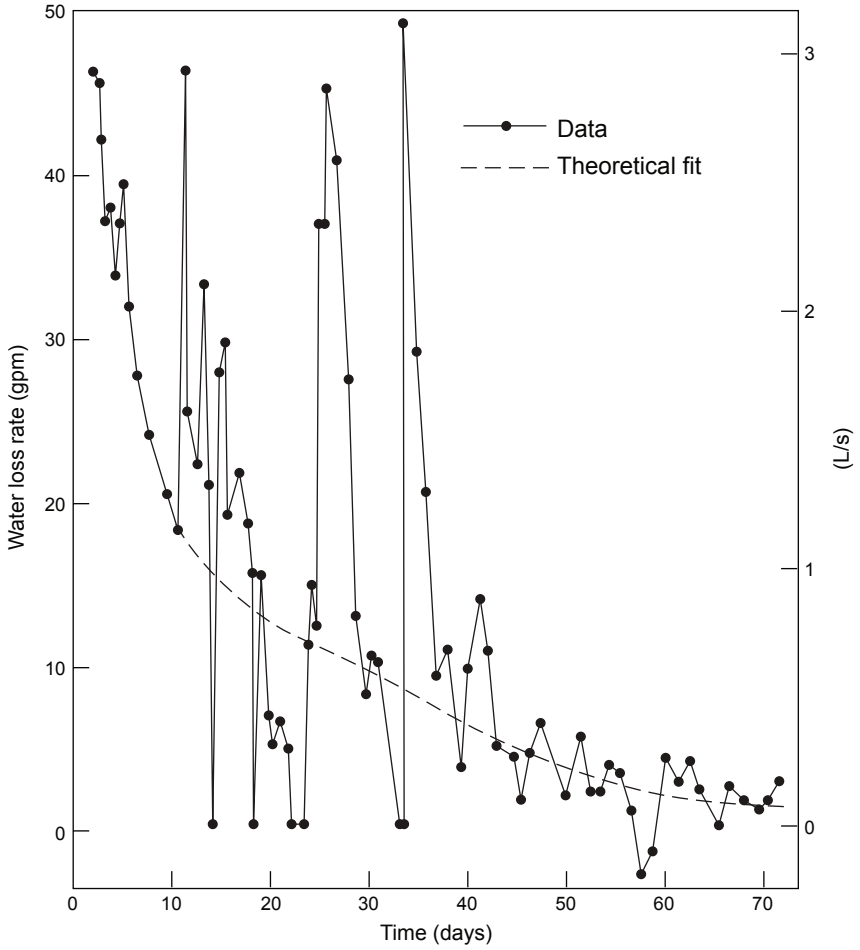

Fig. 4-14. Rate of water loss during Run Segment 2.
Source: Tester and Albright, 1979

The chemical composition of the fluid produced during Run Segment 2 was benign. At the end of the test, the level of total dissolved solids was 2000 ppm and there was no evidence of scaling in the surface flow equipment. No measurable seismicity was induced at the site at any time during this run segment. However, as pointed out earlier (see Fig. 4-7), the relatively rapid thermal drawdown of the produced water, from 175°C to 85°C, indicated that the effective heat-transfer surface within the reservoir was small—about 86 000 ft^2 (8000 m^2)—and essentially confined to the single joint connecting EE-1 and GT-2B.

Toward the end of Run Segment 2, a small annular bypass flow developed outside the casing at EE-1. Although estimated to be less than 1 gpm—not

considered very significant at the time—this flow was an indication that the casing cement was beginning to deteriorate and portended a major change in plans.

Note: In their report on Run Segment 2, the authors, realizing that the relationships between the geometric, thermal, and chemical properties of the fracture system were very complex, commented that "a unique model consistent with all the data does not exist, at least with the information we now have on the properties of the reservoir." (Tester and Albright, 1979)

Run Segment 2: A Milestone

The 75-day Run Segment 2 in 1977 represented the first-ever successful operation of an engineered HDR system. The thermal power production of over 4 MW, although modest for this closed-loop circulation test, conclusively demonstrated the viability of the HDR geothermal energy concept.

Following this successful field demonstration, the DOE directed the expansion of the Project into a national effort. Known as the Hot Dry Rock Geothermal Energy Development Program, it would be managed from Los Alamos (HDR, 1979).

In addition to the Fenton Hill Project, the new national HDR Program would comprise all other HDR development and support activities (such as instrumentation, HDR exploration techniques, and economic studies) as well as all HDR-related projects elsewhere in the U.S.

A key activity under the expanded Program was to be the selection of a second experimental HDR site, geologically and geographically disparate from Fenton Hill. The Division of Geothermal Energy (DGE) of the U.S. DOE felt that the development of such a second site was necessary to establish that

1. the basic HDR reservoir development techniques employed at Fenton Hill (pressure stimulation of a tight, but jointed, rock mass) can be used in other types of hot basement rock, and
2. the proximity of a young silicic volcano to an HDR system is *not* a prerequisite for the success of the HDR concept.

Run Segment 3: September–October 1978

Known as Experiment 186, or the High-Backpressure Flow Experiment, Run Segment 3 was designed to confirm, or refute, Don Brown's assertion that by imposing a very high backpressure at the production well—thereby increasing the fluid pressure within the joint(s) connected to the GT-2B

borehole to a level *higher* than the joint-closure stress(es)—the reservoir flow impedance could be dramatically reduced. (Implicit in this assertion was an acknowledgment that the reservoir consisted primarily of a single, near-vertical joint.) A second objective for Expt. 186 was added by the Project managers: to determine whether operation under high-backpressure conditions would increase the effective heat-transfer surface.

Run Segment 3 lasted only 28 days—cut short when the flow bypass that had been developing in EE-1, through and around the poor-quality casing cement, began discharging significant amounts of fluid out the annulus at the surface. But during those brief four weeks, under a constant backpressure of 1400 psi and a constant injection pressure of about 1330 psi at EE-1, not only did the overall flow impedance of the joint drop precipitously, but the biggest factor in this impedance drop was the almost total elimination of the stress-induced near-wellbore outlet impedance.

The temporal variation in the overall flow impedance for Run Segment 3, shown in Fig. 4-15, was determined from a combination of measured and calculated buoyancy data. After peaking on day 2 at 2 psi/gpm, the impedance dropped steadily over the remainder of the flow test, to a final value of 0.5 psi/gpm on day 28. (The corresponding value on day 28 of Run Segment 2 was 7 psi/gpm, 14 times greater!) These impedance results were a real "eye opener"! They clearly demonstrated that operation under high-backpressure conditions could dramatically reduce the near-wellbore outlet impedance.

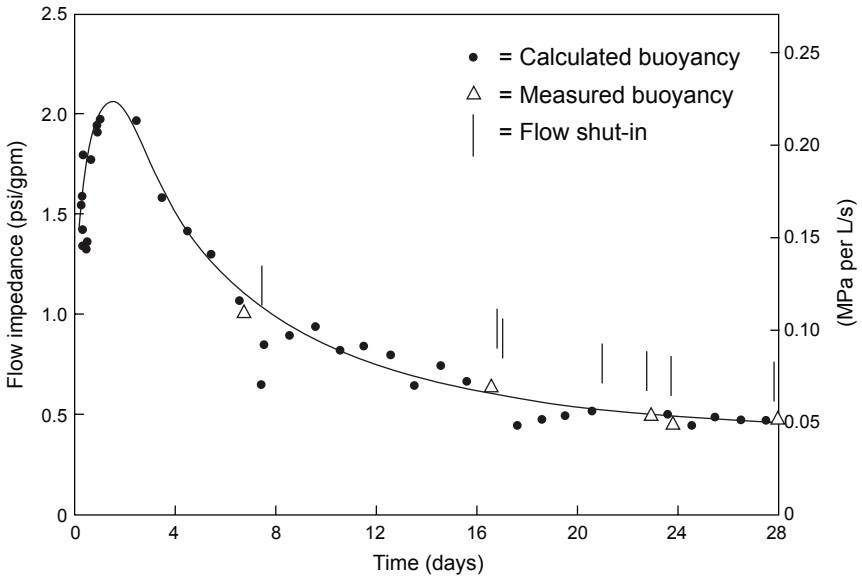

Fig. 4-15. Flow impedance during Run Segment 3 (corrected for buoyancy). Source: Dash et al., 1981

This component had accounted for approximately 80% of the overall flow impedance during the early stages of Run Segment 2 (that is, 12 of the 15 psi/gpm on day 2). It was almost completely eliminated when the production-well backpressure was increased to a level above the joint-closure stress, negating the stress-induced pinch-off of the joints at their intersection with the GT-2B borehole.

These results, then, further confirmed that there was no need to postulate a connecting set of tightly closed, 30°-inclined joints, as depicted in Fig. 4-5. (Note: Some HDR Project staff who still held to this concept were attempting to use it to explain the high outlet impedance of Run Segment 2. However, had the connectivity between the EE-1 joint and the GT-2B borehole been solely via a set of 30°-dipping joints, per the concept shown in Fig. 4-5, the outlet impedance would have been far higher than it was.)

Figure 4-16 shows a revised conceptual model of the Phase I reservoir based on the data from Run Segments 2 and 3. The features of the model shown in Fig. 4-5 remain valid except that the postulated 30°-dipping joints are replaced by a set of near-vertical joints striking about N27W. Running oblique to the trend of the 9050-ft EE-1 joint, they connect that joint with the GT-2B borehole at the three most significant depths indicated in Fig. 4-9—about 8620 ft, 8769 ft, and 8900 ft (the deepest of these three representing various measurements from 8880 ft to just below 8900 ft)—and possibly at other depths as well. The existence of such an *en echelon* set of N27W-striking joints is supported by at least the following observations:

- There were multiple connections between the 9050-ft EE-1 joint and the open-hole interval of GT-2B.
- A N27W-striking joint had previously been identified close to the Phase I reservoir and at about the same depth, near the bottom of GT-2 (see Figs. 3-25 and 3-34).

Note that the lateral distance from the 9050-ft joint to the GT-2B borehole via the deepest N27W connecting joint(s) is only about 10 ft, providing a very short, low-impedance flow connection.

Note: As our understanding of an HDR reservoir evolved, several HDR staff were becoming aware that not all the rock in the pressure-stimulated region would be readily accessible to the circulating fluid at the lower reservoir operating pressures. These less-accessible areas include the far boundaries of the dilated joints; the rock adjacent to joints having opening pressures higher than the reservoir operating pressure; and areas remote from the production well and therefore not adequately "swept" by the circulating fluid. This realization led to the concept of a *circulation-accessible* portion of the reservoir: that portion of the stimulated region that was in good thermal communication with the lower-pressure circulating fluid.

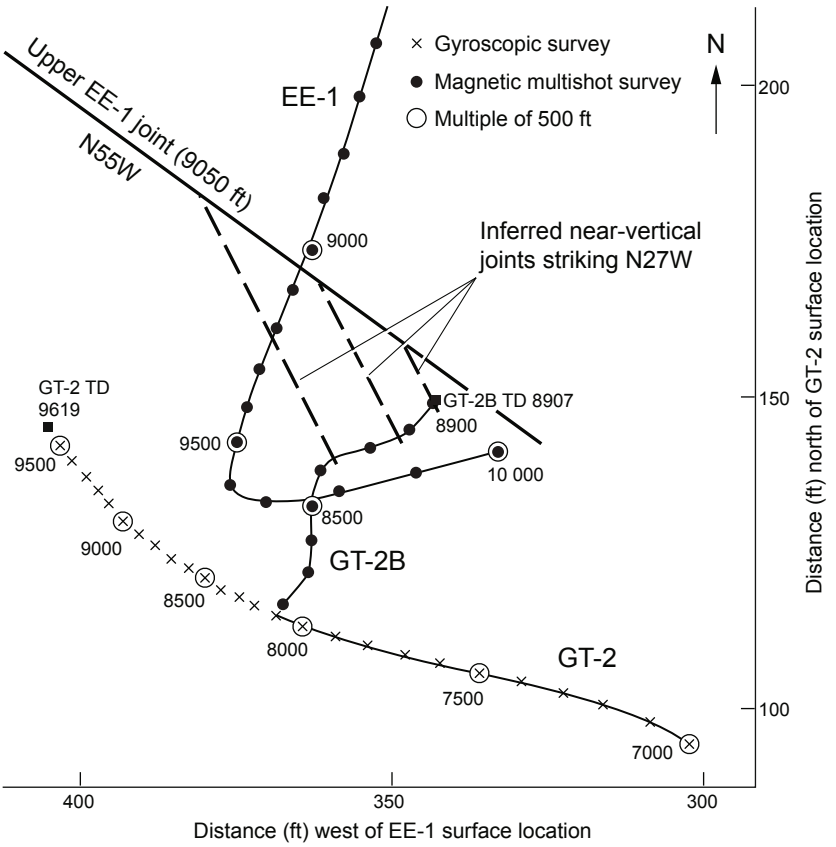

Fig. 4-16. Plan view of the single-joint Phase I reservoir as conceptualized after Run Segment 3.

During Run Segment 3, the measured production temperature at a depth of 8500 ft in GT-2B declined from 135°C to 98.5°C, a drawdown again consistent with an effective heat-transfer surface of 86 000 ft^2 (8000 m^2) for one side of the joint. In other words, high-backpressure operation did not produce an increase in the size of the circulation-accessible portion of the reservoir, as had been anticipated by some. The average thermal power production was 2.1 MW, compared with 3.1 MW during Run Segment 2.

One of the major conclusions drawn from Run Segment 3 was that the various pressure stimulations of EE-1 between mid 1976 and March 1977, before the redrilling of GT-2 (see Chapter 3), had merely opened, and then extended, a single natural joint that now effectively connected EE-1 to GT-2B. This joint was nearly orthogonal to the least principal earth stress, which was oriented approximately NE–SW. Then, during Run Segment 3,

the pressures used—an injection pressure of 1330 psi and a backpressure of 1400 psi—were sufficient to jack open the entire joint (and were probably close to those required to jack open the set of connecting oblique joints shown in Fig. 4-16 as well).

InfoNote

When the fluid pressure within a previously opened joint approaches the closure stress, the joint becomes increasingly permeable as more and more of the asperities previously in contact separate. The process is thus a continuous one, of ever-increasing permeability, as the joint passes from a tightly closed state to a fully opened one. In fact, it has been shown experimentally in the field (not the laboratory) that at fluid pressures above the closure stress, the joint continues to dilate, further compressing the surrounding rock.

The density difference between the cold injection wellbore (higher fluid density) and the hot production wellbore (lower fluid density) produced a *negative* pressure difference across the reservoir—a buoyant drive that boosted the effective pumping pressure. If the joint-opening pressure could have been maintained by some means other than pumping (for instance, injection of a high-density brine), the reservoir would have circulated naturally by buoyant drive alone.

Figure 4-17 compares a spinner survey taken in GT-2B during Run Segment 3 with one taken near the end of Run Segment 2. The Run Segment 2 survey displays five flow entrances, rather uniformly distributed along the production interval; the two deepest of these—at about 8880 ft (also identified on the February 13 temperature survey shown in Fig. 4-9) and at the borehole TD (8907 ft)—represent almost 40% of the flow. In contrast, the survey done under the high-backpressure flow conditions of Run Segment 3 (October 12, 1978) shows some 70% of the flow entering through these two deepest joint intersections. (Note: Obviously, since the bottom-hole depth is 8907 ft, there is some depth error in this survey.[8]) The remaining 30% entered above 8850 ft, through other connecting joints. It appears that the high-backpressure operation altered the flow connections to GT-2B, virtually shutting off the flow entrance at 8769 ft that had been significant during Run Segment 2 and markedly opening up the ones near the bottom of GT-2B.

[8]These and other discrepancies (e.g., Fig. 4-9) between the depths of the joint intersections with GT-2B measured by various logs are due to (1) the difference in cable stretch on different logging runs, (2) the weights of the logging tools used, and (3) the degree of cable drag in the borehole. Variations of up to 30 ft have been observed for different measurements identifying the same borehole feature.

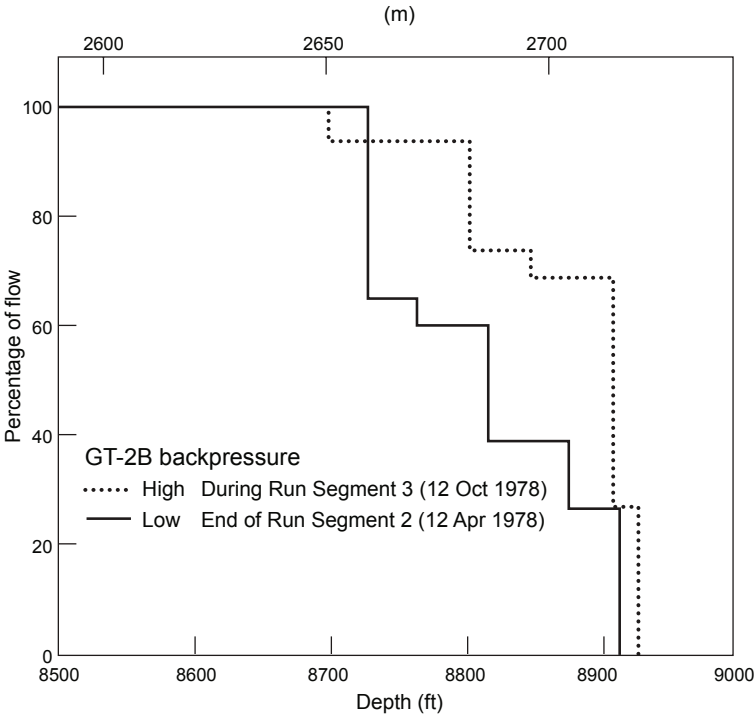

Fig. 4-17. Fractional production flow distribution in GT-2B under high-backpressure conditions (Run Segment 3) compared with that under low-backpressure conditions (Run Segment 2).
Adapted from HDR, 1979

Given the vanishing flow impedance of Run Segment 3, the joint connections shown in Fig. 4-16 must have behaved in much the same way as a direct joint connection, i.e., their closure stresses would be similar to one another, but somewhat greater than that of the EE-1 joint. This behavior would in turn imply that they were near-vertical and at most a few tens of degrees oblique to the strike of the EE-1 joint. The spinner survey done near the end of Run Segment 2, showing a rather uniformly distributed flow among at least five connecting joints, reflects the true complexity of the reservoir at that time.

The annular bypass flow at EE-1 that brought a premature end to Run Segment 3 had been steadily increasing as the casing cement continued to deteriorate; by day 28, when the test was terminated, it had reached a level of 55 gpm.

Run Segments 1–3: General Observations

The poor casing cement job done three years earlier (October 1975) not only led to the annular bypass flow at EE-1 but, by opening up a major flow path to the joint at 9050 ft, ultimately shifted the focus of the stimulation efforts to that joint. If the cement job had been adequate, the EE-1 joint at 9650 ft would have been the primary one stimulated during all the attempts to establish flow communication with GT-2. And had that been the case, the Phase I reservoir would undoubtedly have been developed more quickly—and in a much different fashion, probably without the redrilling of GT-2. If one mentally deletes the 9050-ft joint from the plan-view geometry shown in Fig. 3-34 (Chapter 3), some of the possible strategies can be visualized. Instead of the costly and time-consuming redrilling of GT-2, the strategy of choice would probably have been repeated injections into both EE-1 and GT-2, at higher rates and pressures and for much longer periods. Such a strategy would probably have ultimately produced a reservoir of multiple interconnected joints, not unlike the deeper Phase II reservoir that would be created several years later (see Chapter 6).

The very low flow impedance achieved during Run Segment 3 was important for understanding how interactions between earth stresses and fluid pressures control joint flow in the hot crystalline basement, which in turn determines the productivity of the reservoir. However, from the standpoint of long-term HDR power production, it was not an altogether favorable achievement. With such a low impedance, the reservoir envisioned for the next phase of operations (Phase II)—a set of parallel vertical joints—would undoubtedly have been plagued by short-circuiting of flow if operated under high-backpressure conditions. For such a reservoir, a high near-wellbore outlet impedance would have been a "blessing in disguise": essentially decoupling the individual joint flows from the effects of cooling-induced thermal dilation. In other words, if initial flow in one of the parallel vertical joints should be somewhat greater than in the others (as is likely), with continuing reservoir operation the increasing flow in that joint would produce a greater and greater degree of cooling, and of cooling-induced thermal dilation, than in the other joints. Eventually, this process would lead to short-circuiting, i.e., most of the flow being channeled through this "favored" joint while very little flowed through the other joints. But a high near-wellbore outlet impedance, being largely unaffected by temperature, would tend to stabilize this flow behavior and lessen the chances of short-circuiting. Further, the measure of flow control thus provided would be much less complicated than the wireline-actuated sliding sleeves and other hardware that some Project staff were working on to control the flow from the injection well into the envisioned multiple-inlet reservoir.

Tracer studies conducted during Run Segments 2 and 3 suggest that cooling-induced thermal dilation affects the reservoir *through-flow fluid volume*.[9] This volume (calculated as the integral mean fluid volume) varied from 34 400 L to 56 200 L during Run Segment 2 and from 33 100 L to 49 600 L during Run Segment 3. It is interesting to note the return to this smaller fluid volume at the start of Run Segment 3, when it was nearly the same as at the beginning of Run Segment 2—reflecting the thermal recovery of the reservoir during the intervening 5 months.

EE-1: Re-cementing of the Casing and Reactivation of the Deep Joint (9650 ft)

The problems that developed near the end of Run Segment 3, resulting from the poor-quality casing cement job of three years earlier, led to the decision to re-cement the bottom section of the EE-1 casing. Repair of this section would (1) eliminate the annular bypass flow problem that had prematurely terminated Run Segment 3, and (2) shut off flow to the 9050-ft joint (this joint, the principal entrance into the Phase I reservoir, had been stimulated to the extent possible; it was clear that further stimulation would not produce any significant enlargement of the reservoir). Once the 9050-ft joint had been closed off, the plan was to expand the Phase I reservoir via the deeper EE-1 joint. The much greater separation between inlet and outlet would improve the potential for a much larger heat-transfer surface.

Note: It would turn out that although the multiple-joint reservoir thus produced indeed provided a much larger heat-transfer surface, the loss of the direct joint connection between the two wells ultimately resulted in a flow impedance in the 10–15 psi/gpm range (far from the 1-psi/gpm impedance obtained under high-backpressure flow conditions during Run Segment 3). What had been demonstrated during Run Segment 2, it would be seen later, was that the EE-1 joint at 9650 ft was not connected to GT-2B directly but via a set of joints having strikes oblique to that of the 9650-ft joint—thus the much higher flow impedance.

Re-cementing of the EE-1 Casing—January 1979

In mid January 1979, the bottom 600 ft of the EE-1 casing was re-cemented to plug the flow channels in the cement between the casing shoe at 9599 ft and the joint entrance at 9050 ft. This cement—originally water-cut during

[9]The volume of fluid flowing through the reservoir at a selected time is determined from tracer studies, by one of a number of methodologies. The one used throughout this book—except for Run Segment 5—is the *integral mean fluid volume*. Other methodologies used, and cited in the HDR literature, include the Median volume and the modal volume. The latter, which was used for Run Segment 5 because the integral mean fluid volumes were erratic, is that volume of tracer circulated through the reservoir from the time of tracer entry until the time the tracer concentration at the outlet reaches a maximum.

its placement three years earlier, by inflow from the pressurized GT-2 borehole—had initially provided a tenuous seal. But early in 1976 it was penetrated and eroded by high-pressure water during pressure and temperature cycling, then further eroded and chemically attacked during Expt. 138, the quartz-leaching experiment. (The designers of that experiment, knowing that the cement in the annulus contained 40% silica, should have realized that the hot sodium carbonate leachate they were using to remove silica from the joint faces would first attack the cement behind the casing!)

For the re-cementing operation, Halliburton designed and tested a Class H portland cement stabilized with 80% silica flour for longer-term temperature stability. To prepare the borehole, the open-hole interval was backfilled with sand to within a few feet of the casing shoe. Then the cement was pumped down the casing, around the casing shoe, and up the annulus. Pumping continued until the pressure increased significantly, at which point pumping was suspended and the pressure on the casing maintained until the cement had set. Then the residual cement in the casing was drilled through and the sand was washed out of the open-hole interval. As shown in Fig. 4-18—cement-bond logs run by Halliburton in EE-1 before the cementing operation (January 8) and after it (January 16)—the cement in the annulus between 9599 and 9050 ft went from 0% bonding to 70%–98% bonding. Repeated pressurization and temperature cycling during the subsequent two months confirmed that the 9050-ft injection region in EE-1 was completely isolated. The only flow connection to GT-2 was now the one at 9650 ft, in the open-hole region just below the casing.

On February 14, 1979, a radioactive-bromine tracer study (Expt. 194) was done to test the integrity of the remedial casing cement job and to locate the remaining EE-1 joint connection(s). This study detected no signs of flow behind the re-cemented casing, and clearly showed the principal joint connection at 9650 ft.

While Expt. 194 was in process, the circulating flow impedance between EE-1 and GT-2B was measured and found to be a surprisingly high 137 psi/gpm (14.9 MPa per L/s)! This value was only about 10% lower than that measured during Expt. 106, three years earlier (before activation of the lower-impedance joint connection at 9050 ft). Considering all the reservoir development work done since that time, a better result had been hoped for!

During injection into EE-1, GT-2B was shut in several times so that the pressure rise could be measured. Analysis of the GT-2B pressure rise suggests that cross-flow from EE-1 was entering GT-2B through the same joint system that was active during Run Segment 2, before the re-cementing of the EE-1 casing. In other words, the joint at 9650 ft must also be connected to this joint system, albeit via a much longer and more tortuous flow path. This conclusion was confirmed by gamma logging done under pressure in GT-2B: the tracer appeared at the same joint entrances identified by temperature and spinner surveys during Run Segments 2 and 3.

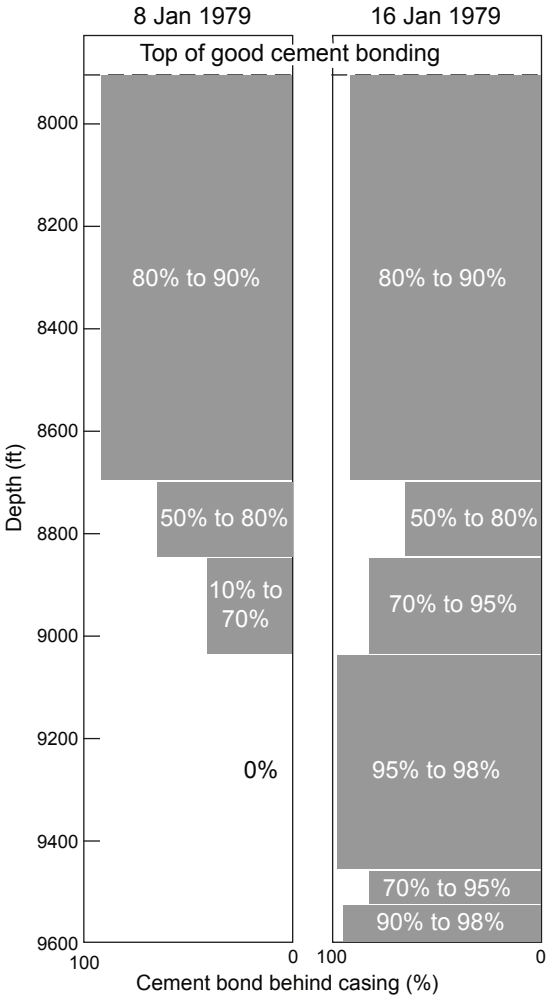

Fig. 4-18. Cement bond logs run in EE-1, January 1979. Adapted from HDR, 1980

Experiments 203 and 195, Seismicity, and Inferred Reservoir Volume

Given the high flow impedance measured during Expt. 194, the HDR staff realized that extraordinary measures—that is, stimulation at much higher flow rates and pressures—would be needed to achieve a suitable flow impedance through the reconfigured Phase I reservoir. (Interestingly, some prominent staff members viewed this strategy still in terms of "massive hydraulic fracturing," to drive upwards the small "hydraulic fracture" previously created at the 9650-ft depth in EE-1.) Whatever the divergent reasons for the

approach, in March 1979 the 9650-ft joint in EE-1 was stimulated twice at flow rates and pressures that, for the time, were very high.[10] Seismic activity was recorded on a triaxial geophone placed at 8810 ft in GT-2B—a location just 840 ft higher than the EE-1 injection point.

The first of these stimulations (Expt. 203) was conducted on March 14, with two principal objectives:

1. To test the integrity of the re-cementing job
2. To reduce the impedance of the flow connection to GT-2B through aggressive pressure-stimulation of the joint intersecting EE-1 at 9650 ft

Experiment 203 consisted of injection of some 160 000 gal. of water into the joint, over about 6 hours—during which time the injection rate was maintained at 10 BPM (except for some initial transients caused by trouble with the rental pumping equipment). The injection pressure rose to 2800 psi in the first 30 minutes and continued to rise, reaching 2880 psi after an additional hour of injection. It then slowly declined to 2730 psi. At the end of 5 hours of pumping, the system was shut in for 15 minutes for repair of a blown-out pressure transducer connection. Pumping at 10 BPM was then resumed for an additional 1 1/4 hours. The final injection pressure was 2130 psi—a significant drop, possibly suggesting that the inadvertent pressure-cycling caused by the 15-minute shut-in had brought about a re-arrangement of the joint geometry. The lack of any evidence during this test of a "fracture breakdown" pressure made it clear that no new joints had been opened below the casing shoe in EE-1 (i.e., that the joint at 9650 ft was simply being pressure-dilated and possibly extended or better interconnected with other nearby joints).

Because high-backpressure operation during Run Segment 3 had succeeded in significantly reducing the reservoir flow impedance, an attempt was made to replicate these results during Expt. 203. However, the cable pack-off at the surface (required for the deep geophone package in GT-2B) unfortunately leaked erratically—sometimes at rates exceeding 100 gpm—making it impossible to measure the flow impedance under steady-state, high-backpressure conditions.

A high-temperature Sperry-Sun magnetic multishot compass was attached to the geophone package, to enable its orientation to be determined; but at the anticipated downhole temperature the life of the geophone was limited, and after 5 hours the package had to be pulled up and parked near the surface.

---

[10]This EE-1 joint was initially opened in 1975. As discussed in Chapter 3, before the completion of EE-1 a Lynes packer was set at a depth of 9600 ft and the entire open-hole region, down to 10 053 ft, was pressurized with a Western Co. pump. A joint centered at 9650 ft and striking N54W was opened and extended with an injection flow of 2.1 BPM (5.6 L/s) and pressures up to 2400 psi. During the spring of 1976, following the completion of EE-1, this joint was further pressure-stimulated numerous times (see discussions of Expts. 111, 116, 117, and 120 in Chapter 3).

The second stimulation (Expt. 195),[11] which took place on March 21, was designed to further improve the inter-well flow connectivity. Because a pressure limitation of 3000 psi had been specified for the EE-1 casing, the injection rate was not predetermined (sufficient rental pumping capacity from the Western Co. was on hand to inject at rates up to 20 BPM [53 L/s]). For this test, a pressure lock had been fabricated and installed at the GT-2 wellhead, into which the geophone package could be pulled while the well-bore was under high pressure.

The major part of Expt. 195 was conducted with GT-2B shut in. After an initial repressurization of the joint system at an injection rate of 3 BPM, and then an increase to 16 BPM, the rate had to be cut back to 12 BPM to avoid exceeding the casing pressure limit. This injection rate was maintained for 90 minutes while the injection pressure slowly decreased, then was increased again to 16 BPM to re-establish a 3000-psi injection pressure. In all, some 200 000 gal. of fluid was injected into EE-1 in 6 1/2 hours.

After the higher-pressure, seismic portion of the experiment had been completed, the geophone package was returned to the surface and secured in the pressure lock. The injection rate was then reduced to about 10 BPM, and controlled venting of GT-2B began at surface pressures of 1400–1500 psi. With GT-2B producing at up to 100 gpm, the high-backpressure flow impedance slowly decreased from 14 to 12 psi/gpm.

Don Brown, the Project's advocate for high-backpressure reservoir circulation, was perplexed by this result. He had reasoned that if the joint intersecting EE-1 at 9650 ft was directly connected to GT-2B, the high-backpressure flow impedance should have been no more than 1 psi/gpm. That it was so much higher indicated the presence of an intervening set of joints connecting the 9650-ft joint with the set of joints intersecting GT-2B. This observation added to the Project staff's evolving view of the HDR reservoir—that it consisted of a network of interconnected joints.

During this production testing of the enlarged Phase I reservoir, the water loss was about 75%, most of which was going into further extending and inflating the interconnected joint system.

Considerable microseismic activity was recorded during Expt. 203 and during the latter part of Expt. 195. As shown in Fig. 4-19, the activity began almost at the outset of Expt. 203 and continued at a high, steady rate for the next 4 1/2 hours (after which the geophone package had to be pulled up to avoid temperature-related problems). During Expt. 195, the onset of seismicity was delayed by about 2 hours as the region that had been pressure-dilated

[11] As noted in Chapter 3, experiments were not always conducted in the order in which they had been proposed (and numbered).

and shear-stress-relieved during Expt. 203 was aseismically reinflated by the injection of the first 65 000 gal. of fluid. It was apparently only near the end of this second stimulation test that vigorous, seismically active growth (like that seen during Expt. 203) resumed. During the two experiments, the cumulative number of events and the rates at which they occurred far exceeded those recorded during previous injection tests; in addition, the event locations were at much greater distances from the injection point.

Analysis of the seismic signals revealed that from the fluid entry point at 9650 ft, the pressure-stimulated region extended upward to at least 8530 ft (2600 m). This distance—1120 ft (340 m)—was more than three times that of the previous reservoir region tested during Run Segments 1–3, suggesting that the effective heat-transfer surface would be significantly greater.

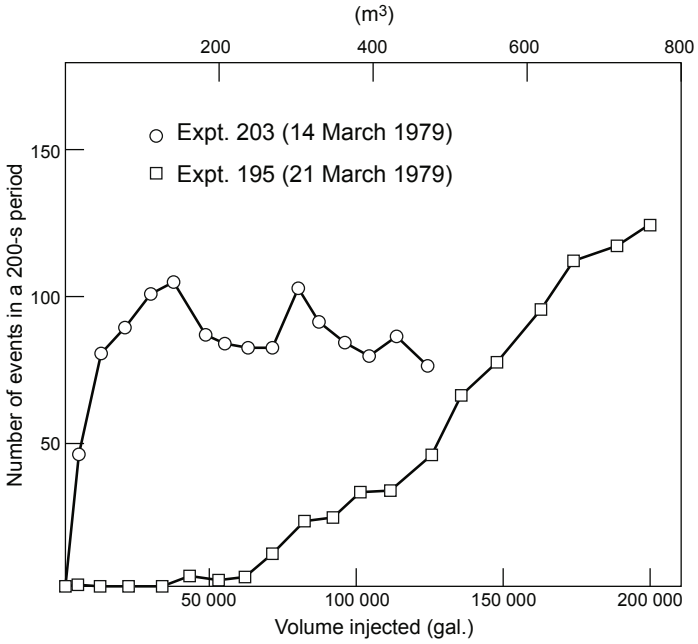

Fig. 4-19. Microseismic activity recorded during high-rate injection into EE-1 in March 1979 (Expts. 203 and 195).
Source: HDR, 1980

Figure 4-20 is a horizontal projection of the locations of the microseismic events that occurred during Expt. 203. From a statistical analysis of the stereographic projections (not shown), the microseismic activity of both Expts. 203 and 195 is confined to a near-vertical zone dipping from 85° to 89°. The salient feature is the strike of this zone: N15W. A reservoir region consisting of multiple interconnected joints striking in this direction—rotated 40° toward the intermediate principal stress (away from

N55W)—would explain both the higher injection pressures required during both stimulation tests and the significant shear release within this zone. A near-vertical geometry is supported by the spatial progression of the seismicity, with the earliest events occurring close to the injection point in EE-1 and then progressing upward and outward within this N15W-striking zone. These joints lie at greater oblique angles to the N55W strike of the 9650-ft EE-1 joint (about 40°) than those in the older portion of the reservoir did to the then-active joint at 9050 ft (10°–20°). The tortuous flow across this zone of intersecting joints gives rise to an "interior" flow impedance that modifies the overall flow impedance from EE-1 to GT-2B—making it significantly higher than that of the single-joint reservoir region tested during Run Segment 3.

The length of the seismically active region, as shown projected onto a horizontal plane in Fig. 4-20, is about 500 m (1600 ft), and its mean width is about 90 m (300 ft). It is interesting to note that the region surrounding the injection point in EE-1 (almost directly below the location of the geophone in GT-2B, at the center of the figure) is relatively quiet.

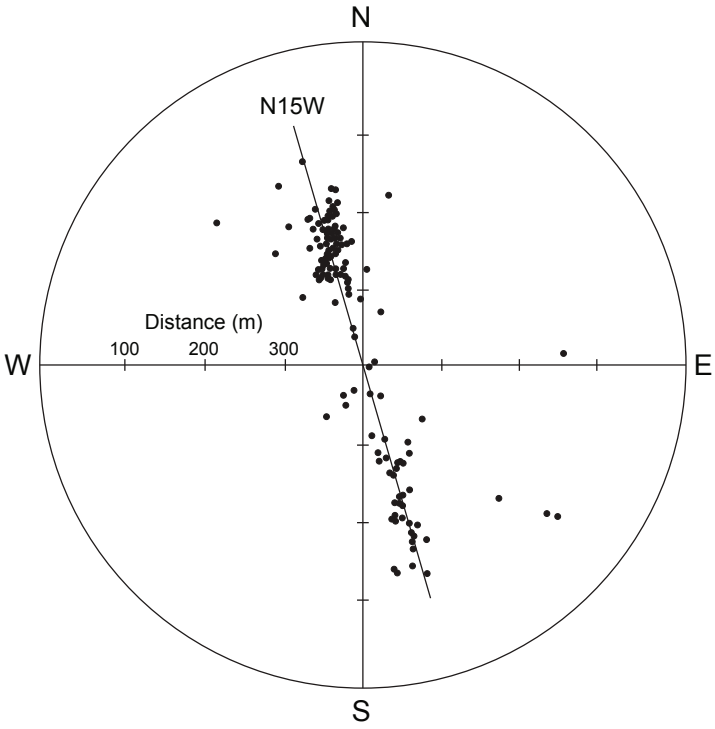

Fig. 4-20. Horizontal projection of the microseismic activity recorded during Expt. 203 (March 14, 1979).
Source: HDR, 1980

Figures 4-21a and 4-21b represent the seismic activity in vertical section: the first view perpendicular to the strike of the activity (in the direction N75E), and the second view along the "plane" of the activity, in the direction N15W. These two views show the seismically active region to be confined to a semi-circular zone having a radius of 270 m and a mean width of about 90 m. The rock volume corresponding to this seismically delineated region, or *seismic volume*, would be 10 million m^3.[12] Assuming that all the water injected into this region during Expts. 203 and 195 went into joint dilation (160 000 gal. + 200 000 gal., or a total of 1360 m^3), the seismic volume would have a porosity of 1.4×10^{-4}.

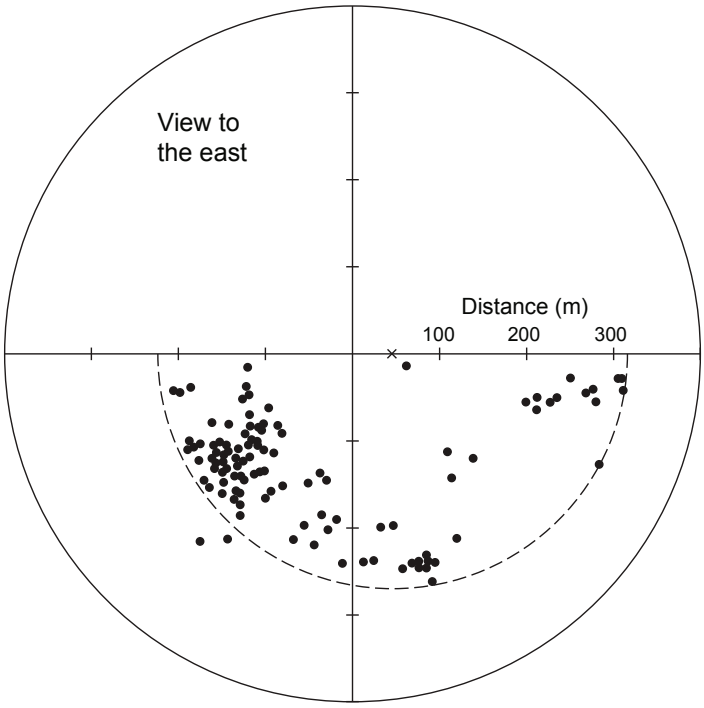

Fig. 4-21a. Vertical projection of the microseismic activity recorded during Expt. 203, as viewed in the direction N75E.
Source: HDR, 1980

[12]Throughout this book, reservoir rock volumes are given only in cubic meters; heat-transfer areas are given either in square meters or in square feet with the equivalent in square meters.

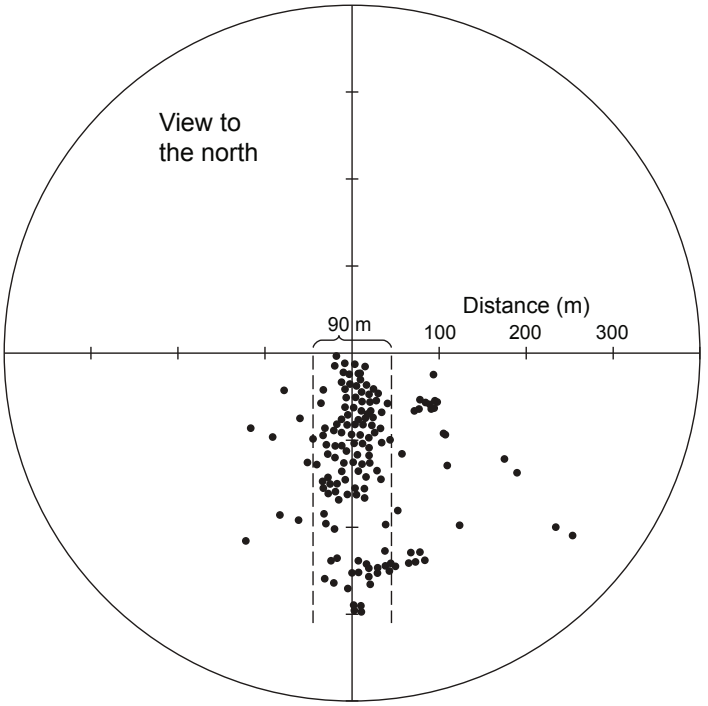

Fig. 4-21b. Vertical projection of the microseismic activity recorded during both Expt. 203 and Expt. 195, as viewed in the direction N15W.
Source: HDR, 1980

The True Measure of an HDR Reservoir: Rock Volume

The preceding discussion introduced the concept of a reservoir *volume*. For the older, essentially single-joint Phase I reservoir region, the metric for evaluation was the *heat-transfer surface*—the amount of joint surface accessible to the circulating fluid. It is in a multiply jointed HDR reservoir that *volume* becomes the more significant metric. It is the volume of rock accessible to the circulating fluid that is the most important parameter for reservoir heat production. (Recall once again that at this time, many of the HDR Project staff did not yet recognize the multiply jointed character of the enlarged Phase I reservoir created during Expts. 203 and 195; they believed that the reservoir of Run Segments 2 and 3 consisted of a single, "penny-shaped fracture" and that what these high-flow and high-pressure experiments had created was a second, larger, such fracture.)

With our understanding of the more complex nature of an HDR reservoir comes the realization that the reservoir comprises two distinct rock *volumes*:

1. The *seismic* rock volume—the stimulated region of rock enclosing the foci of most of the microseismic events produced by the initial pressurization. (We assert that no joint slippage—the mechanism by which these events are generated—can occur without the action of pressurized fluid to first dilate the joint.) This seismic rock volume has associated with it a *fluid* volume, which is the volume of fluid initially used to pressure-stimulate (usually at relatively high pressures) that seismic volume.
2. The *circulation-accessible* rock volume—the smaller volume of rock accessed by the circulating fluid during closed-loop reservoir production (at pressures lower than those used to create the seismic volume). At typical production pressures, which are selected to prevent reservoir growth and to minimize pumping costs, many of the pressure-dilated joints—particularly those having higher opening pressures and those located at the periphery of the seismic region—are not readily accessible to the circulating fluid. This circulation-accessible rock volume, which can be viewed as the *active* reservoir volume for heat transfer, cannot be measured directly; it must be obtained from modeling studies based on a known (or reasonably estimated) mean joint spacing and conducted after a significant degree of reservoir thermal drawdown. However, the fluid volume associated with this rock volume, the *through-flow fluid volume*, can be determined through tracer techniques.

It is important to note that these two rock volumes represent the end points of a continuum of volumes that are dependent upon the mean reservoir operating pressure. Thus, intermediate volumes can be "engineered" to meet particular objectives, such as enhancing reservoir productivity by increasing the circulation-accessible rock volume.

(Because the notion of the penny-shaped fracture would continue to dominate the thinking of some of the HDR Project staff, the term *heat-transfer surface* continues to appear below in discussions of tests and experiments based on that thinking.)

State of Stress within the Phase I Reservoir

From earlier testing, combined with the results of Run Segment 3, one can conclude that the least principal earth stress at the depth of the Phase I reservoir (9000–9600 ft) has a value of about 1240 psi, or 8.6 MPa (see Expts. 114 and 122A in Table 3-12, Chapter 3). Dey and Brown (1986), using a different methodology, found values of 9.6 MPa (1390 psi) for the least principal earth stress and 21.6 MPa (3130 psi) for the intermediate principal stress for a depth of 9500 ft in the Phase I reservoir region. For the direction of the least principal earth stress within the reservoir, a very elegant determination was made by Burns (1988). Using borehole televiewer images of a large number of borehole breakouts, he determined a direction of N110.7E (±10.3°).

Using standard rock mechanics relationships and the minimum joint-closure stress measured during Expt. 203 for the near-vertical joints oriented N15W (2130 psi), one can obtain the intermediate principal earth stress (σ_2) directly, as follows:

$$\sigma_{normal} = \sigma_3 \cos^2\phi + \sigma_2 \sin^2\phi,$$

where

σ_3 (least principal stress) = 1240 psi,

σ_{normal} (closure stress on N15W joints, oriented N75E) = 2130 psi,

and

ϕ (angle between the normal to N15W joints and least principal stress direction [N111E]) = 36°,

σ_2 = 3800 psi (reasonably close to the value determined by Dey and Brown)

Note that this value for σ_2 is about one-third the overburden stress (σ_1) of 10 900 psi at a depth of 9500 ft. (Because the tectonic regime at Fenton Hill is *extensional*, the maximum earth stress is vertical.)

Flow Testing of the Enlarged Phase I Reservoir, 1979–1980

The information in this section is abstracted mainly from Dash et al. (1981), HDR Geothermal Energy Development Program (1979), Murphy et al. (1980a), HDR Geothermal Energy Development Program (1980), Murphy et al. (1981a, 1981c), and Zyvoloski et al. (1981a).

Run Segment 4: October–November 1979

Run Segment 4 (Expt. 215) was designed as four stages of operation with the following planned parameters (some of which were changed during the actual operation):

1. An early period of additional pressure stimulation of the EE-1 joint at 9650 ft, at an injection rate of 10 BPM
2. A 36-hour low-backpressure flow test (at an injection pressure of 1800 psi and a production borehole backpressure of 160 psi)
3. A two-stage high-backpressure flow test (at an injection pressure of 1800 psi and production borehole backpressures of 900 psi for the first stage and 1700 psi for the second)
4. A 14-day heat-extraction flow test at low backpressure (an injection pressure of 1400 psi and a production pressure of 160 psi)

Note: The centrifugal pumps recently purchased by the Laboratory were not capable of injection pressures above about 1500 psi. For this reason, only the fourth stage was carried out with these pumps. Rental pumping equipment from the Western Co. was used for the first three stages.

The first stage of Run Segment 4 was essentially a repeat of Expt. 195 (the second high-flow, high-pressure stimulation test following the re-cementing of the EE-1 casing). The injection of 200 000 gal. of fluid, at a pressure of 2900 psi and a rate of 10 BPM (26.5 L/s), lasted about 8 hours, with GT-2B being vented at a low-backpressure level of 160 psi during the entire test. The production rate at GT-2B increased from 15 to 100 gpm over the 8-hour period, for a final flow impedance of 27 psi/gpm (essentially the same as that measured during Expt. 122A in May 1976).

The second stage consisted of circulation of the reservoir for an additional day, at the same backpressure of 160 psi but with an injection pressure of 2450 psi. The production flow rate increased slowly during this stage to 116 gpm—reflecting a somewhat improved flow impedance of 19.7 psi/gpm.

The third stage of Run Segment 4 followed immediately, but the injection pressure, at a near-constant 2420 psi, was higher than that planned; and only one high-backpressure level (1480 psi) was used instead of two. During 60 hours of circulation, the production flow increased to 131 gpm,

for a measured flow impedance of 7.3 psi/gpm—much improved. Seismic monitoring indicated that low-level seismic activity occurred only during this third stage, and only at magnitudes of –1.5 or less on the extrapolated Richter scale. Activity was detected at distances up to 2300 ft from the injection point, suggesting that the injection pressure of 2420 psi was producing a slowly growing stimulated region.

The fourth and final stage of Run Segment 4, which began on October 30 and lasted 16 days, was designed as a heat-extraction experiment preparatory to the much longer Run Segment 5. This stage was a closed-loop operation: the produced geofluid was cooled and then recirculated, with sufficient makeup water added to replace the fluid lost from the boundaries of the pressure-dilated reservoir region. (The makeup water was supplied initially from the reserve pond and later, as less was needed, from the on-site water well.) The injection pressure was maintained at about 1400 psi and the production pressure at a low 160 psi.

At the beginning of the fourth stage, the system was shut in so that the surface plumbing could be re-configured for the closed-loop flow system that would incorporate the Laboratory's newly acquired centrifugal pumps. Then, about a week later, both wells were again shut in briefly so that the shut-in behavior of the reservoir—both the injection and production sides—could be observed and the several components of the overall flow impedance determined (see *Reservoir Flow Impedance* below).

Under the low backpressure of the fourth stage and at a flow rate of about 95 gpm, the overall reservoir flow impedance slowly declined, reaching 13.1 psi/gpm near the end of this stage. The water loss varied over the 16 days, finally stabilizing at a rate of 20 gpm (17% of the injection rate). After an initial transient period of two days, the average thermal power production became almost constant at 3 MW (at a constant reservoir outlet temperature of 153°C, as measured at a depth of 8500 ft).

Run Segment 4: Observations

Through-Flow Fluid Volume of the Reservoir

Residence-time studies, using sodium fluorescein dye tracers, showed an initial through-flow fluid volume that varied from 207 000 L to 283 000 L. This integral mean fluid volume is four to five times that of the original Phase I reservoir, as measured at the beginning of both Run Segments 2 and 3. Such an increase in volume would suggest that the enlarged reservoir accessed from EE-1 had been not only pressure-dilated but also cooled and thermally dilated by the high-pressure stimulations of Expts. 203 and 195. To those still giving credence to the vertical-hydraulic-fracture concept, a fluid volume increase of this magnitude might imply a heat-transfer surface that had also grown by a factor of as much as five—to about 430 000 ft^2 (40 000 m^2). However, the essentially constant reservoir outlet temperature

during Run Segment 4 (i.e., no drawdown) means that the heat-transfer surface for the enlarged Phase I reservoir tested during this run segment cannot be determined. Notwithstanding, some brave HDR staff did publish their guesses—based on these changes in fluid volume—that the heat-transfer surface was about 480 000 ft^2 (45 000 m^2).

InfoNote

For a reservoir consisting of only a few flowing joints, under conditions of constant temperature and pressure and with no change in the joint aperture, an increase in the tracer-derived through-flow fluid volume should be indicative of the amount of new heat-transfer surface created. However, for reservoir operations that involve pressurized circulation, the attendant cooling will produce some degree of thermal contraction; and changes in inlet and/or outlet pressures will bring about changes in the pressure-dilation of the joints. This fluid volume, then, is not a reliable basis for calculating an increase in heat-transfer surface unless these temperature and pressure effects can be corrected for—in most cases a very difficult task.

Reservoir Temperatures

Figure 4-22 shows the temporal variation in reservoir-associated temperatures, obtained from both geochemistry and fluid-temperature measurements, during Run Segment 4. The most striking feature is the agreement between the two geochemistry-derived curves (measured by Na-K-Ca and quartz geothermometers)—in particular for days 16–24—and the almost 40°C difference between those curves and that of the reservoir outlet temperature (measured by the wireline temperature tool located at about 8500 ft). The explanation for this discrepancy is fairly simple: the geothermometers are primarily influenced by temperature-dependent chemical dissolution as the injected fluid flows across the hottest part of the reservoir, i.e., the region near the 9650-ft joint entrance. In contrast, the reservoir outlet temperature would (unfortunately) be most influenced by flow across those regions of the reservoir near GT-2B that had been cooled earlier, during the 3 1/2 months of power production during Run Segments 2 and 3 (the associated thermal drawdowns for these run segments were 85°C and 98.5°C, respectively).

In other words, the marked difference between the average of the geothermometer readings (190°C) and the reservoir outlet temperature (ca. 153°C), particularly over the last 8 days of steady-state reservoir operation, clearly reflects (1) the heating to 190°C of the fluid flowing through the newly opened joints connected to the 9650-ft inlet from EE-1, and (2) the cooling of the fluid back down to 153°C as it flowed through the joints connected to the GT-2B borehole (the temperatures of these joints were still recovering from the cooling of Run Segments 2 and 3).

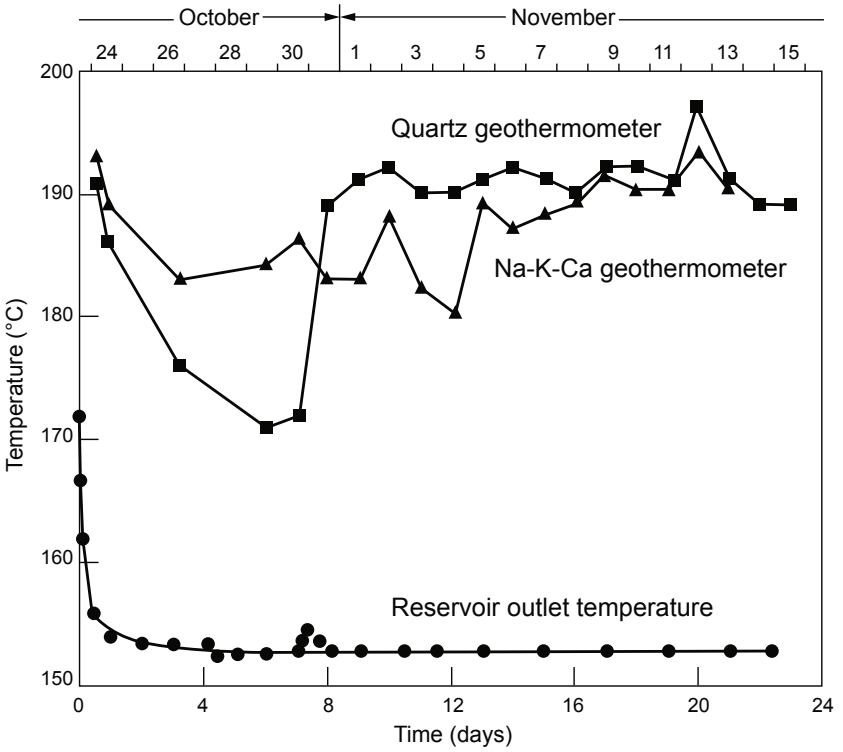

Fig. 4-22. Reservoir outlet temperatures measured during Run Segment 4. Source: Murphy et al., 1980a

Note: The principal objective of Run Segment 5, the 9-month flow test, would be to determine the effective heat-transfer surface of the enlarged Phase I reservoir. As mentioned above, the analytical models being used were not incorporating the notion of reservoir *volume* because it was not yet recognized that the enlarged reservoir was a multiply jointed one. The objective of this run segment was somewhat compromised, therefore, by the complex flow situation: an unknown flow geometry in the newer, multiply jointed portion of the reservoir, combined with an interior set of joints of unknown nature between this newer portion and the older, severely cooled one. The problem was, how to estimate a heat-transfer surface when the parameters of any numerical computation would depend on the particular geometric reservoir model adopted, and when the only available parameter was the temporal variation of the reservoir outlet temperature. Even that parameter—owing to these simultaneous heating and cooling processes—would behave in an unexpected fashion (actually *increasing* slightly for the first 100 days of Run Segment 5—see *Run Segment 5* below).

Reservoir Flow Behavior

During the multiple flow excursions of Run Segment 4, a decoupling became apparent between the surface injection and production conditions. Operation at either high backpressure or low backpressure had almost no effect on the injection flow rate; that is, the rate required to maintain a constant pressure of 2450 psi tended to gradually increase irrespective of the backpressure at GT-2B—as if one side of the reservoir "didn't know what the other side was doing." One would expect, then, that had the flow test been operated at a constant injection rate, the injection pressure would likewise have been unaffected by high or low backpressure at GT-2B and would have slowly declined.

The insensitivity of the enlarged reservoir to inlet or outlet pressure variations contrasts with the much more "connected" inlet-to-outlet behavior observed for the predominantly single-fracture reservoir tested during Run Segments 2 and 3. Primarily responsible is the difference in flow impedance—both magnitude and distribution—between the two portions of the reservoir. For example, after a few days of flow testing during Run Segment 3, cooling-induced thermal dilation caused the inlet flow impedance to vanish; the elevated backpressure, by effectively jacking open the joint connecting the boreholes, brought the combined body and outlet impedances to a very low 1.0 psi/gpm. Under similar conditions, the residual flow impedance (which consisted almost entirely of body impedance) for the third stage of Run Segment 4 was 7.3 psi/gpm—more than seven times higher.

An analysis of the GT-2B borehole flow and temperature data from Run Segment 4 (Murphy et al., 1980a) showed that the flow through the enlarged Phase I reservoir was being conveyed to the production well via the same set of joints that had connected the older, smaller reservoir to GT-2B during Run Segments 2 and 3. This observation represented a real "breakthrough" in understanding for some of the HDR staff, who were finally recognizing that the flow geometry of the enlarged Phase I reservoir was that of a complex, multi-jointed region rather than a simple vertical "fracture." On the basis of linear heat diffusion theory (Wunder and Murphy, 1978), it was estimated that at the beginning of Run Segment 4, after thermal recovery from the cooldown of Run Segments 2 and 3, the set of joints connected to GT-2B had surface temperatures of 150°C–155°C (very close to the measured reservoir outlet temperature of 153°C shown in Fig. 4-22).

Figures 4-23 and 4-24 show, respectively, the pressure responses at GT-2B and EE-1 on November 6, 1979, during the brief shut-in period of the fourth stage. Both indicate the presence, not far from the reservoir inlet and outlet, of a large region of high-pressure fluid. With the cessation of flow across this region—the highly impeded interior portion of the reservoir—the pressure at GT-2B rose rapidly; in less than 5 minutes it reached nearly 1200 psi. During the same time interval, the pressure at EE-1 dropped from 1400 psi to 1200 psi. In other words, this 1200-psi pressure at both boreholes represented the approximate fluid pressure within the multiply jointed interior region, or "body," of the reservoir.

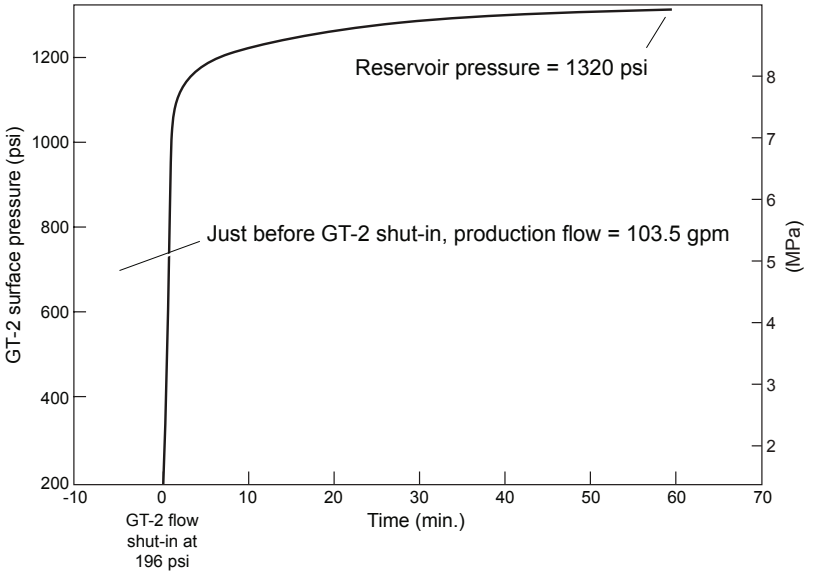

Fig. 4-23. Pressure history at GT-2B during a brief shut-in of both wells (about one-third of the way through the fourth stage of Run Segment 4). Source: Murphy et al., 1980a

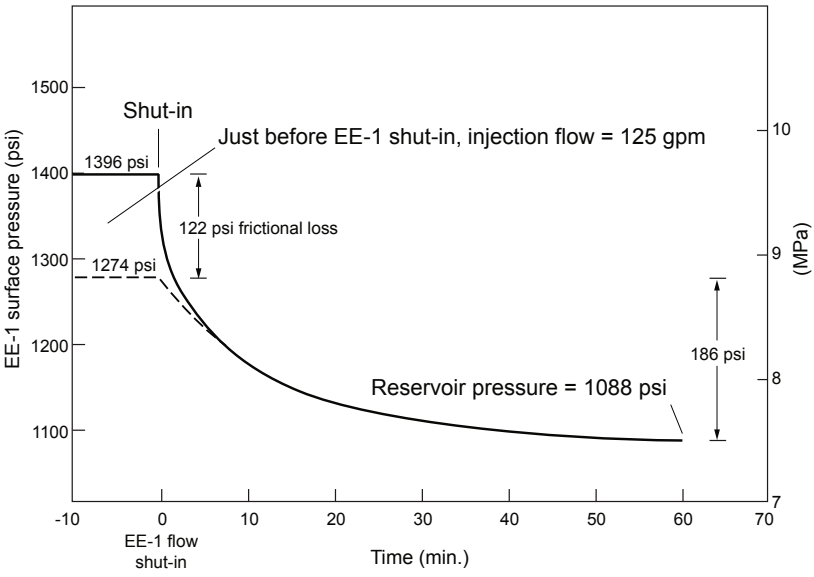

Fig. 4-24. Pressure history at EE-1 during a brief shut-in of both wells (about one-third of the way through the fourth stage of Run Segment 4). Source: Murphy et al., 1980a

Reservoir Flow Impedance

The flow and pressure data obtained during Run Segment 4 constitute a crucial data set on the performance of the enlarged Phase I reservoir. From it emerges a new picture of the composite flow impedance of this reservoir.

InfoNote

From Run Segment 4 forward, we give flow impedance values as directly measured:

Impedance = inlet pressure minus outlet pressure divided by the production flow rate, uncorrected for the mean fluid density difference between the injection and production wells.

There are two reasons for this convention, particularly as regards the overall flow impedance: (1) Subtracting the outlet from the inlet pressure gives the actual pressure difference that had to be supplied by the circulating pumps; and (2) Under most of the flow-testing conditions from October 1979 on, the mean temperatures in the injection and production wells would remain almost constant (in particular, the more density-sensitive production temperature would change very little—e.g., only 7°C during Run Segment 5 and no change during the LTFT in the 1990s).

It should be made clear, as part of the discussion of flow impedances in the enlarged Phase I reservoir, that the joint connections to the GT-2B borehole did not change as a consequence of the reservoir enlargement. Therefore, the high-backpressure impedance values obtained during Run Segment 3 are applicable to the older portion (connected to GT-2B) of the enlarged Phase I reservoir as well. After 7 days of circulation, the overall flow impedance for Run Segment 3 was 1.0 psi/gpm. Since by this time cooling-induced thermal dilation had reduced the inlet flow impedance to less than 0.1 psi/gpm, the 1.0 psi/gpm impedance represents the sum of the body and near-wellbore outlet impedances (but predominantly the latter, because the principal joint was being pressurized at a level above its closure stress and was therefore dilated).

Table 4-2 lists the average operating conditions for the second, third (last 8 hours), and fourth stages of Run Segment 4. These data reveal a surprising phenomenon: the marked effect, on the overall reservoir flow impedance at low backpressure, of imposing a 2 1/2-day period of operation at high backpressure. As can be seen, the overall impedance dropped during the fourth stage to about two-thirds of its second-stage value—from 19.7 psi/gpm to 13.1 psi/gpm. The only logical explanation for this behavior is a shifting or relative movement among the multiple joints opened within the newer, interior portion of the reservoir (which accounts for the body impedance), brought about by a brief imposition of high backpressure at GT-2B concurrent with an elevated (2450 psi) injection pressure at EE-1. A comparable decrease in impedance would be seen again at the end of Run Segment 5, when high pressures (ca. 2200 psi) were imposed on both wellbores during the Stress-Unlocking Experiment—see below.

Table 4-2. Average operating conditions during the last three stages of Run Segment 4

	Second stage 27 October 1979 (08:00–16:00 h)*	Third stage 30 October 1979 (00:00–08:00 h)*	Fourth stage 3–15 November 1979*
Backpressure	LOW	HIGH	LOW
GT-2B			
Production flow (gpm)	116	129	95
Temperature (°C)	154	153	153
Backpressure (psi)	160	1480	160
EE-1			
Injection flow (gpm)	246	380	120
Pressure (psi)	2450	2420	1400
Overall flow impedance (psi/gpm)	19.7	7.3	13.1
Apparent water loss (gpm)	130	251	25
Thermal power (MW)	3.8	4.2	3.1

* interval over which data are averaged

The most remarkable aspect of the impedance reduction illustrated in Table 4-2—and the most significant for subsequent HDR reservoir development efforts—was the ease of accomplishing such a reduction. It required only 2 1/2 days and a modest-size commercial pump truck (at a rental cost of about $10 000 per day in today's dollars). Further, reducing the flow impedance from 19.7 psi/gpm to 13.1 psi/gpm increased the potential reservoir production by about 50%. Even though Run Segment 4 did not provide ideal test conditions for isolating the different components of the reservoir flow impedance (two of which were undergoing changes), some significant conclusions can still be drawn:

1. During high-backpressure operation (third stage), nearly all of the 7.3 psi/gpm flow impedance derives from the joint connections between the body of the reservoir and the set of joints connected to GT-2B.[13] The near-wellbore inlet impedance, after several weeks of cold injection, would be very small (0.1 psi/gpm or less), owing to cooling-induced thermal dilation of the inlet joint connected to EE-1. The impedance across the interconnected joints making up the body of the reservoir should also have been very small: with opening pressures in the 1400- to 1600-psi range, all these joints should have been held widely open ("pressure-propped") by an injection pressure in excess of 2400 psi.

[13]In this new, enlarged Phase I reservoir, in addition to the near-wellbore inlet impedance, the body impedance, and the near-wellbore outlet impedance, a fourth impedance component was being added: the "interior" impedance to flow caused by the acute-angled intersections of the joints in the body of the reservoir with those flowing into GT-2B.

In other words, under conditions of both high backpressure and elevated injection pressure, the overall impedance appears to consist of the near-wellbore outlet impedance, i.e., of the joints connected to GT-2B (about 1 psi/gpm, as measured during the high-backpressure Run Segment 3) plus the "interior" impedance across the acute-angled intersections of these joints with those in the body of the reservoir (about 6 psi/gpm). The latter, inferred impedance should have been largely insensitive to the level of reservoir pressurization because of the turbulent and restricted nature of flow at joint intersections.

2. When the difference between the flow impedance of Run Segment 2 and that of Run Segment 3 is compared with the difference between the impedances of the third and fourth stages of Run Segment 4, there is a significant discrepancy—one that unfortunately cannot be resolved. During the early parts of both Run Segment 2 and Run Segment 3, the injection pressures were very similar; only the backpressure changed, from 250 psi during Run Segment 2 to 1400 psi during Run Segment 3. The sharp drop in overall impedance seen when the high backpressure of Run Segment 3 almost completely eliminated the near-wellbore outlet impedance allows one to conclude that nearly all (~80%) of the overall flow impedance of Run Segment 2 (13 psi/gpm on day 14) was attributable to the near-wellbore outlet impedance. In contrast, during the fourth stage of Run Segment 4, not only was the backpressure significantly reduced from the level of the third stage, but the injection pressure was too. The resulting overall flow impedance of about 13 psi/gpm is higher than that of the third stage—but how much of the increase is attributable to the drop in backpressure, and how much to the drop in injection pressure? The only way to answer this question would have been to insert a test stage between the third and fourth stages—one that repeated the conditions of the second stage (low backpressure and elevated injection pressure), which would have revealed the influence of the low backpressure by itself.

3. Although it is tempting to attribute the entire increase in the overall reservoir flow impedance (from 7.3 psi/gpm during the third stage to 13.1 psi/gpm during the fourth) to an increase in the near-wellbore outlet impedance, this does not correlate well with the larger decrease in impedance of Run Segment 3 (to 1 psi/gpm from the 13 psi/gpm of Run Segment 2) given an equivalent change in backpressure.

Note: The issue of the impedance of the reservoir has been given particular emphasis because the reservoir conditions observed at the end of Run Segment 4 would be those obtaining throughout the upcoming extended flow test (Run Segment 5).

Seismicity: What Does it Say About the Reservoir?

The seismicity recorded during the third stage of Run Segment 4 presents an anomalous picture when compared with that recorded during Expts. 203 and 195, the preceding high-flow stimulation tests (Fig. 4-25). Why did the injection of 160 000 gal. (during Expt. 203) and of 200 000 gal. (during Expt. 195) each produce a much higher level of microseismic activity than the injection of *2 million* gal. during the first three stages of Run Segment 4? (As illustrated in Fig. 4-25, only a small amount of seismicity occurred near the end of the third stage.) The injection pressures varied from 2900 psi during the first stage to 2420–2450 psi during the second and third stages—not much lower than the 2900-psi injection pressures used during Expts. 203 and 195.

As shown in Murphy et al. (1980a), the integrated water loss at the end of the high-backpressure third stage (after 4 1/2 days of high-rate injection) was about 1.4 million gal. This fluid, amounting to *four times* the total quantity injected during Expts. 203 and 195, had to have gone somewhere. It is estimated that most of this 1.4-million-gal. water loss was actually going into additional reservoir growth at the boundaries of the previously stimulated region.

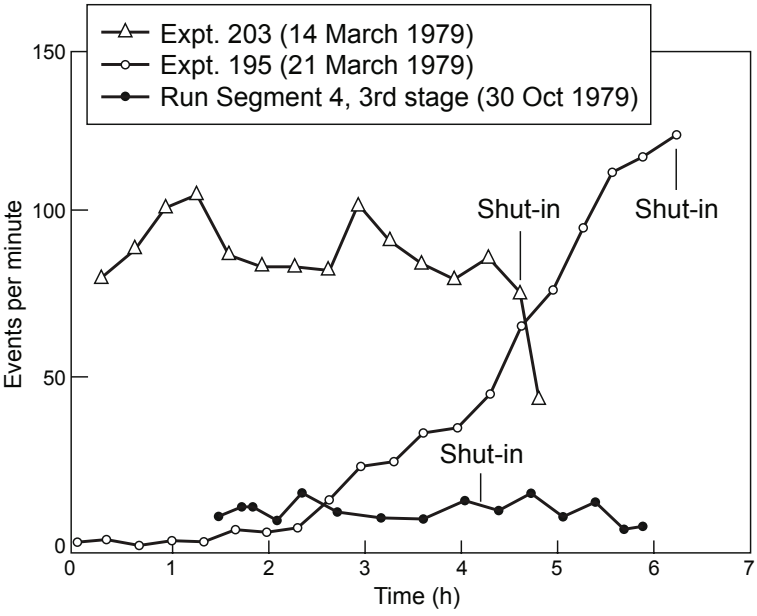

Fig. 4-25. Microseismic activity recorded during the third stage of Run Segment 4, compared with activity during high-rate injection into EE-1 in March 1979 (Expts. 203 and 195).
Source: Murphy et al., 1980a

The puzzle, then, is that growth as extensive as this should have been accompanied by marked seismicity. But as the figure shows, the seismicity of the last 4 hours of the third stage—when the reservoir would have been extending most actively—was low and constant, and remained so even after shut-in of the flow system during the first 2 hours of the fourth stage. Considering that almost 30 years have passed since these tests were done, it is very hard to determine what actually happened. It may well be that during the third stage, the geophone package was not adequately coupled to the GT-2B borehole for good seismic monitoring. But one can only guess.

Figure 4-26 illustrates the distribution of seismicity, collapsed onto a horizontal plane, recorded[14] during a 4 1/2-hour period near the end of the third stage of Run Segment 4. As one can see, the seismic activity tends to be concentrated in the NE quadrant, out to distances of about 600 m.

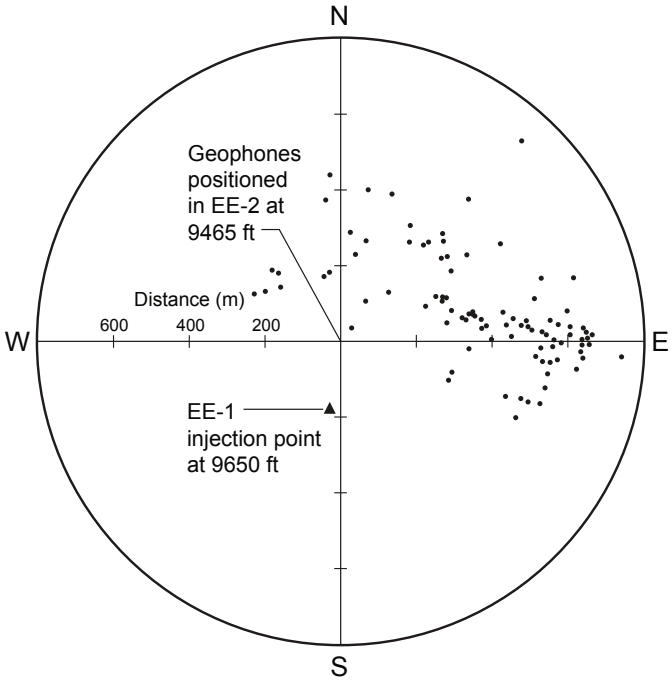

Fig. 4-26. Plan view of the microseismic activity recorded near the end of the third stage of Run Segment 4 (October 30, 1979).
Adapted from Murphy et al., 1981a

[14]on a triaxial geophone package placed at a depth of 9465 ft in the new EE-2 borehole. With drilling of this borehole (for the Phase II operations) well advanced by this time, EE-2 was occasionally used as an observation borehole during the last part of Phase I testing.

The staff guiding the HDR Project at this time, still enamored with the penny-shaped-fracture theory, concluded that most of the 2 million gal. of water injected into EE-1 during the first three stages of Run Segment 4 (except for the modest amount produced at GT-2B) had simply permeated into the rock mass surrounding the vertical "fracture" created during Expts. 203 and 195. This fracture, according to the theory, would have extended mainly upwards from the 9650-ft flow entrance in EE-1. However, the seismic activity depicted in Fig. 4-26 maps a very large stimulated region that is *laterally* distributed. As noted above, it is likely that the bulk of the injected water was simply being stored in the very large pressure-dilated joint system created during Expts. 203 and 195 and then greatly extended by the 2-million-gal. injection—at surface pressures of over 2400 psi—during the first three stages of Run Segment 4 (which were essentially a continuation of Expts. 203 and 195).

The relatively low level of seismicity accompanying the creation of this very large stimulated region, a diffuse pattern extending outward over 600 m, remains unexplained—and perplexing. (Note: This pattern of seismicity, although shown in Murphy et al., 1981a, is not discussed therein nor in other reports of the time. It differs considerably from that reported a year earlier [Murphy et al., 1980a] and must have resulted from a global re-analysis of the microseismic event locations recorded during this massive injection.) Given the average injection pressure of 2440 psi, one would have expected considerable seismicity. However, if the joints being dilated during Run Segment 4 were oriented nearly perpendicular to the least principal earth stress (about 1240 psi), their opening—even of a large array—would have been mostly aseismic (particularly as regards shear waves, because such joints would not exhibit significant shear displacement). While this might largely explain the low level of seismicity, the fact that the pattern is so broad and diffuse indicates that there must have been at least some seismicity arising from interconnecting joints having other orientations.

What would prove most relevant to subsequent analyses is the excessive cooling of the central portion of the enlarged Phase I reservoir, as the cold injected fluid continued to flow outward to the boundaries of this expanding pressure-stimulated region.

At the conclusion of Run Segment 4, only two principal issues remained unresolved:

1. What was the internal structure of the enlarged Phase I reservoir?
2. What was the effective heat-transfer surface?

Answering the second question was the main objective of the Run Segment 5 flow test, which would end up lasting more than 9 months. But even a partial answer to the first question would have to await a review of all the Phase I reservoir testing—at a much later date.

Run Segment 5: March–December 1980

Like other tests of the Phase I reservoir, Run Segment 5 (also known as Expt. 217) was preceded by a number of start-up operations, which began on February 27: background temperature logs in both EE-1 and GT-2B, testing of the surface piping and related equipment, and concurrent testing of the data acquisition system. Some preliminary flow tests[15] were carried out from March 3 to 10, during which the reservoir was circulated in both directions, at injection rates varying from 9 to 110 gpm and for periods varying from 3.4 to 91.7 hours.

Finally, March 10 saw the start of a 281-day period of mostly sustained heat extraction—the only interruptions being a 7-day shut-in starting on day 68, a 2-day fresh-water flush beginning on day 105, and the 2-day Stress-Unlocking Experiment (SUE) in early December. (The objective of the SUE was to relieve to some extent the thermal stresses induced by the extraction of 15 million kWh of heat during Run Segment 5. This experiment is discussed below.) While GT-2B was maintained at a backpressure of about 200 psi, the initial EE-1 injection pressure of 1400 psi slowly declined to about 1200 psi (because of a lack of pumping capacity); the reservoir water-loss rate decreased to 7 gpm; and thermal power production averaged 3 MW.

About halfway through Run Segment 5, the makeup-water flow rate began to increase and water began flowing from the annulus at the surface, indicating that a renewed annular bypass flow was developing. This flow was slowly eroding the cement in the annulus above the 9050-ft joint intersection—both the original poor cement and the newer cement that had been "squeezed" into this zone during the re-cementing of the bottom 600 ft of the EE-1 casing. (As Fig. 4-18 shows, the re-cementing had sealed off the principal flow path existing throughout Run Segments 2 and 3—from below the casing, thence upward through the essentially empty annulus behind the casing, and into the 9050-ft joint. But it had not completely sealed the poor cement in the annulus *above* 9050 ft). The new bypass flow, instead of coming from below the casing, originated from the reservoir itself—following a downward path to the EE-1 borehole through the 9050-ft joint (i.e., in the direction opposite that in which the earlier reservoir had been circulated), then upward through the re-cemented annulus and out at the surface.

Finally, the overall reservoir flow impedance remained at about 13 psi/gpm during flow testing, the same as that measured under low-backpressure flow conditions during the fourth stage of Run Segment 4. Although originally planned as a 3- to 6-month experiment, Run Segment 5 was gradually extended almost to Christmas 1980 (a total of 293 days, including the 12-day start-up period) and nearly ran the HDR crew to exhaustion. It was finally terminated by Rod Spence, the HDR Project

[15]The last of these tests of the reservoir's start-up behavior, which began the morning of March 10 with injection into EE-1 at a rate of 110 gpm, was actually the beginning of the extended circulation phase of Run Segment 5.

Manager, on December 16. After having carefully plotted the production zone outlet temperature—daily—for the preceding several months, he concluded that nothing more could be learned by continuing to circulate the Phase I reservoir, now compromised by the annulus leak. In fact, 5 months earlier, when the renewed bypass flow developed at EE-1, some HDR staff had already pronounced Run Segment 5 "dead in the water." But others wanted to continue the flow testing, hoping to glean additional information (and besides, a "9-month flow test" sounded impressive).

Comparison of Reservoir Through-Flow Fluid Volumes: Run Segments 2–5

The through-flow fluid volumes for the Phase I reservoir—as determined by tracer studies done during Run Segments 2 through 5—are shown in Table 4-3, in terms of both integral mean and modal volumes. It was noted earlier (see footnote 9) that the authors consider the former measure to be the more reliable overall. The major reason for this—although never mentioned in the HDR literature—is that the through-flow fluid volume could never be *greater* than that allowed by the circulation-accessible rock volume at a given operating pressure.

Table 4-3. Through-flow fluid volumes

	Elapsed time (days)	Integral mean fluid volume (m^3)*	Modal fluid volume (m^3)*
Original reservoir			
Run Segment 2 (75 days, low backpressure)			
9 Feb 1978	8	34.4	11.4
1 March 1978	28	37.5	17.0
23 March 1978	50	54.7	22.7
7 April 1978	65	56.2	26.5
Run Segment 3 (28 days, high backpressure)			
28 Sept 1978	10	33.1	3.8
13 Oct 1978	25	56.5	11.4
16 Oct 1978	28	49.6	20.8
Enlarged reservoir			
Run Segment 4 (21 days)			
26 Oct 1979	—**	207	136
29 Oct 1979	0	230	144
2 Nov 1979	2	262	121
12 Nov 1979	12	283	129
Run Segment 5 (281 days)			
16 April 1980	38	404	155
9 May 1980	61	1100	161
3 Sept 1980	178	1311	178
2 Dec 1980	268	581	187

* All volumes are given in m^3 to facilitate comparisons among the data sets.

** This tracer study was done two days before the beginning of Run Segment 4.

For the very lengthy Run Segment 5, however, the integral mean volume calculations were too erratic to be considered reliable, and the reservoir modal fluid volume was therefore used instead to ascertain changes in volume. This volume was somewhat larger for Run Segment 5 than for Run Segment 4, and increased slowly over the 8 months (mid April–early December 1980). The average of the Run Segment 4 and 5 values (151 m^3) is about five times the modal volume at the end of Run Segment 2. Similarly, the average integral mean volume during Run Segment 4 (245 m^3) was about four and a half times the integral mean volume at the end of Run Segment 2.

Temperature Conditions in the Reservoir at the Beginning of Run Segment 5

Before Run Segment 5 began, the temperature situation in the central portion[16] of the extensive seismic volume constituting the Phase I reservoir was one of significant cooling. But being unanticipated, this fact was mostly unrecognized. Figure 4-27 shows a temperature survey done in EE-1 on February 27—eleven days before the start of circulation—in relation to the temperature gradient measured in the fall of 1975, soon after completion of this borehole. The two major depressions in the temperature curve represent, first, the cooling produced in the original reservoir during Run Segments 2 and 3 (by injections into the 9050-ft joint) and then the marked cooling of the rock on either side of the 9650-ft inlet joint to this central portion of the reservoir (from the initial temperature of 197°C seen on the 1975 gradient to an average of about 155°C). This second cooling episode, brought about by the massive injection of cold fluid during Run Segment 4, is the most important inference from the temperature data—an understanding of which is key to understanding Run Segment 5 and the overall thermal performance of the Phase I reservoir.

Note that Fig. 4-27 also gives strong evidence of a pair of entrances from EE-1 into the enlarged Phase I reservoir during Run Segment 4. The temperature dip at a depth of about 9500 ft indicates the second joint entrance, flow into which was coming from behind the casing (through the cement in the lower part of the re-cemented annulus, which had shrunk slightly, forming a microannulus that would slowly be eroded by the continuing flow). The intersection of this 9500-ft joint with EE-1 had been identified in October 1975, before the casing of the borehole, by several geophysical and temperature logs (see Chapter 3).

[16]This rock volume, which was much smaller than the seismic volume, is the region that would eventually be accessed by the lower-pressure circulating flow during Run Segment 5.

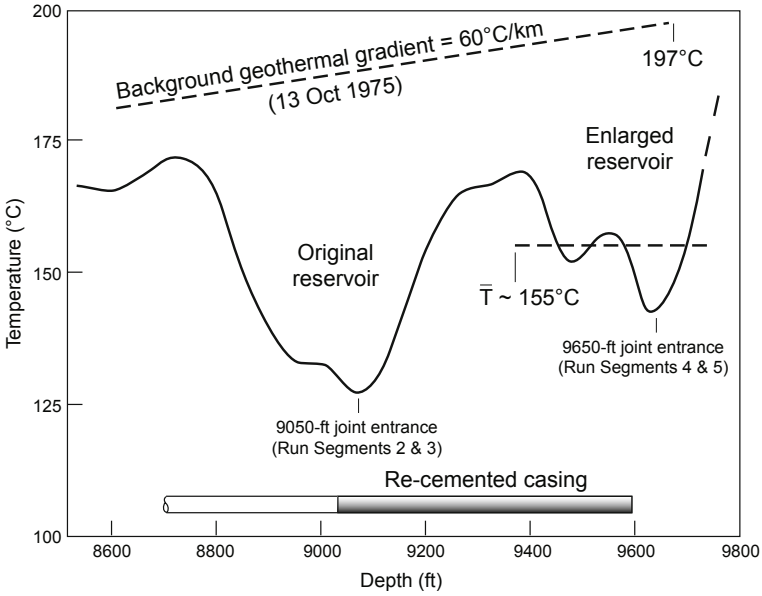

Fig. 4-27. Static temperature log taken in EE-1 on February 27, 1980 (12 days before Run Segment 5 circulation began).
Adapted from Zyvoloski et al., 1981a

The perpendicular spacing between these two flowing joints (6 ft—as shown in Fig. 4-28) is especially significant. It helped dispel one of the early HDR myths: that two nearby joints could not be open simultaneously (the theory being that the first joint opened would squeeze nearby parallel joints, keeping them tightly closed). From the data shown in Fig. 4-27, this theory is obviously false.

What is remarkable is that this non-flowing temperature log shows how far the cooling wave produced by the repeated injections, first into the 9050-ft joint and then into the 9650-ft joint, had moved laterally from these joint entrances into the surrounding rock. Figure 4-28 depicts the cooled region in relation to the trajectory of the EE-1 borehole, the only place where reservoir temperature measurements could be made. Also shown in this figure, to elucidate the spatial relationship between the reservoir inlets and outlets, is the trace of the short production interval in GT-2B.

The cooling produced by the injections into the 9050-ft joint (Run Segments 2 and 3) evidently persisted at least 16 months after the end of Run Segment 3, when these temperature measurements were taken. One can derive the width of this cooled zone first from Fig. 4-27, in which the temperature depression is seen to begin at about 8750 ft and to end at about 9300 ft; and second from Fig. 4-28, in which the horizontal distance between those two depths in EE-1 is seen to be about 40 ft (the cooled zone being roughly orthogonal to the trace of the 9050-ft joint). However, the width of

the cooled zone around the 9650-ft joint is harder to obtain, because—as seen in Fig. 4-28—the EE-1 borehole did not traverse that joint but was instead turned sharply eastward at that depth. Even so, by extrapolating the half-width of the cooled zone that was measurable (from 9300 ft to 9650 ft in Fig. 4-27) to an equal distance below the joint in Fig. 4-28, one obtains an approximate overall width of 75 ft. (Note that the cooling waves for the two joints, as depicted in Fig. 4-27, overlap at a depth of about 9300 ft—thus the flattened "plateau" in temperature above and below this depth.)

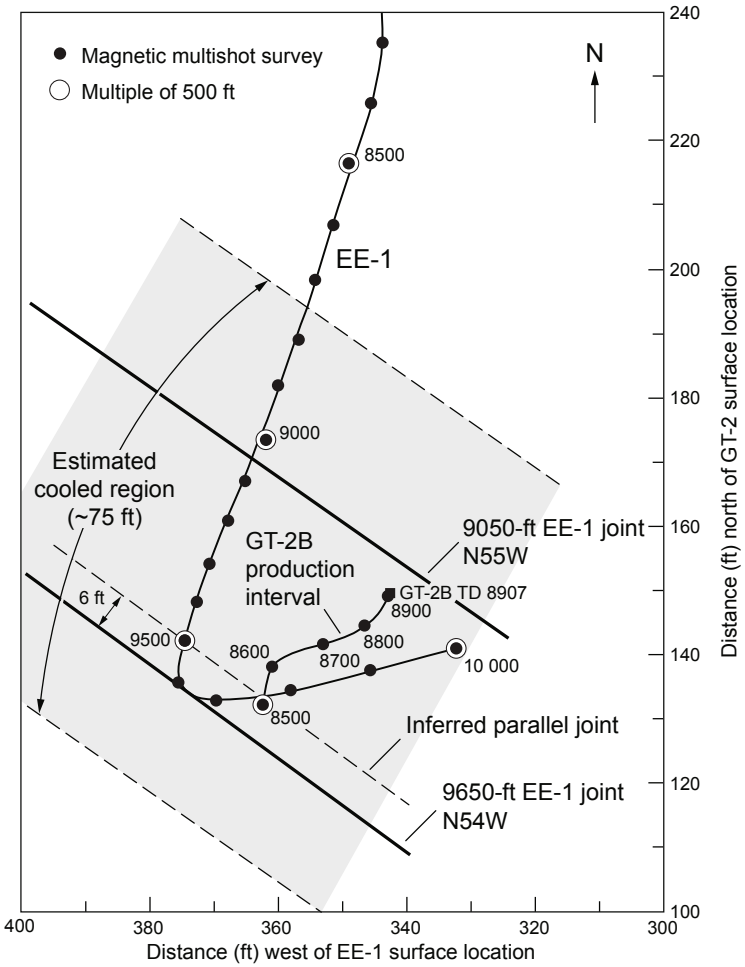

Fig. 4-28. Large cooled region produced during Run Segments 2, 3, and 4 in relation to the trajectory of the deeper part of EE-1 and the two principal pressure-stimulated joints, whose orientations were determined from seismic measurements. (This figure is essentially a magnified view of the EE-1 portion of Fig. 3-34.)

Figure 4-28 suggests that during Run Segment 5, the flow through the reservoir was primarily vertical—upward and somewhat outward through the array of joints associated with the entrance at 9650 ft in EE-1, then through unknown (but obviously existing) connections to the 9050-ft joint, and finally exiting via the set of joints connecting the 9050-ft joint to the production interval in GT-2B (about 8600–8900 ft, as shown in Fig. 4-28). How much of the rock volume pressure-stimulated during Expts. 203 and 195 might have been in direct communication with this flow is only conjecture; but given the extensive joint system indicated by this large seismic region, it is likely that the circulating flow also had some lateral component in the N15W–S15E direction, via the extensions of the 9650-ft joint (see Figs. 4-20 and 4-21).

The great extent of this seismic volume also makes it easy to envision the comparatively small jointed region connecting EE-1 to GT-2B as an inlet "manifold"—first for the large amounts of fluid injected to the far reaches of the seismic region during Expts. 203 and 195, and then for the 1.4 million gal. injected during Run Segment 4. All the cold fluid injected before Run Segment 5 would have contributed to the severe cooling of this vertical "manifold" of jointed rock—but the only cooling that is actually evident is that shown in Figs. 4-27 and 4-28.

Hydraulic and Related Data

Run Segment 5 pressures and flow rates are shown in Figs. 4-29 and 4-30. Clearly visible are the effects of the 7-day shut-in that began on day 68.

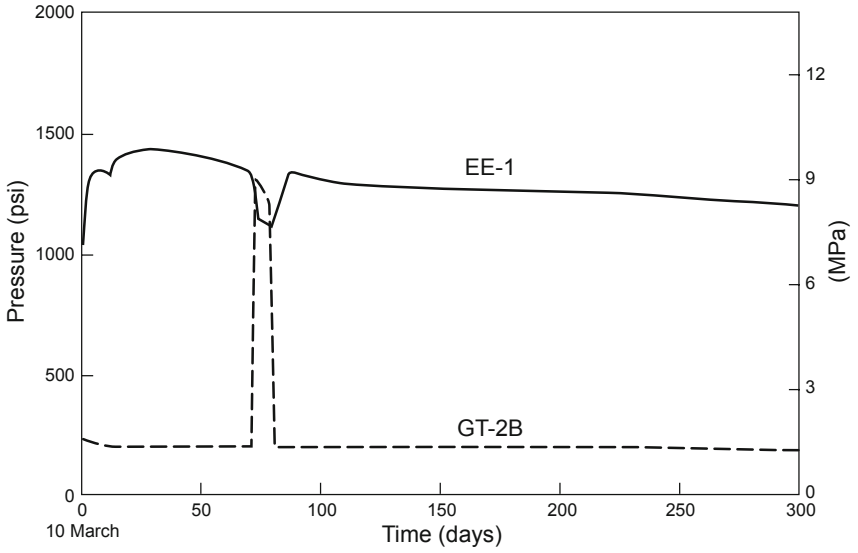

Fig. 4-29. Wellhead pressures during Run Segment 5.
Source: Zyvoloski et al., 1981a

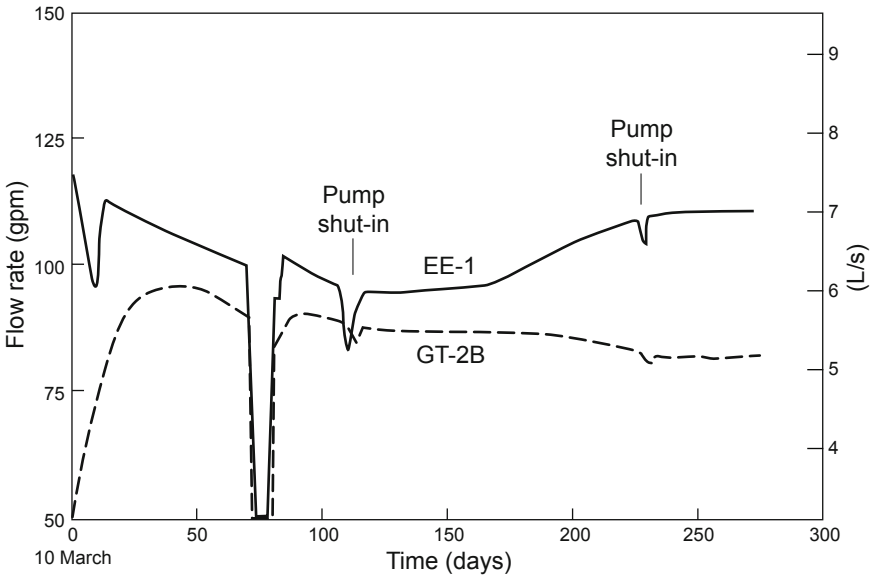

Fig. 4-30. Wellbore flow rates during Run Segment 5.
Source: Zyvoloski et al., 1981a

Figure 4-31 illustrates the variation, during Run Segment 5, in the makeup-water flow rate required to maintain a constant injection rate at EE-1—which under steady-state conditions could be assumed to be equal to the reservoir water-loss rate. According to several analysts, the only data in this figure that were considered appropriate for comparison with reservoir water-loss data from previous run segments were those up to about day 70. The 7-day shut-in that began on day 68 and the open-loop segment of the fresh-water flush (days 105 and 106) both caused major perturbations in the makeup-water data used for water-loss calculations.

The renewed annular bypass flow that began to develop in EE-1 on about day 160 is reflected in Fig. 4-31 by the apparent increase in the makeup-water flow rate beginning at about that time. This secondary flow, from the reservoir to the surface, was penetrating the remedial cement in the annulus above the 9050-ft joint intersection at an ever-increasing rate. (This bypass flow can also be detected in Fig. 4-30: the injection and production flow rates begin to diverge at about day 160.) The flow of hot water to the surface via this alternate path was clearly detrimental to accurate thermal modeling of the reservoir! For example, it added several degrees to the normal heating of the injection flow: the reservoir inlet fluid temperature, as measured at 9600 ft in EE-1, increased from 70°C on day 160 to 78°C by day 200.

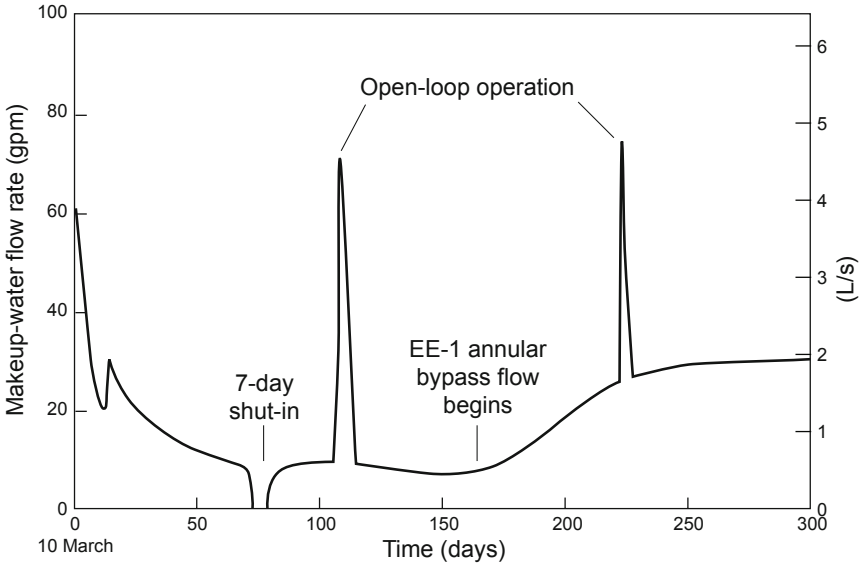

Fig. 4-31. Water-loss rates during Run Segment 5.
Source: Zyvoloski et al., 1981a

Finally, Fig. 4-32 shows the overall reservoir flow impedance during Run Segment 5 (uncorrected for buoyancy effects). After the very long—about 30 days—start-up transient, this impedance leveled out at about 13 psi/gpm, very close to that measured during Run Segment 4.

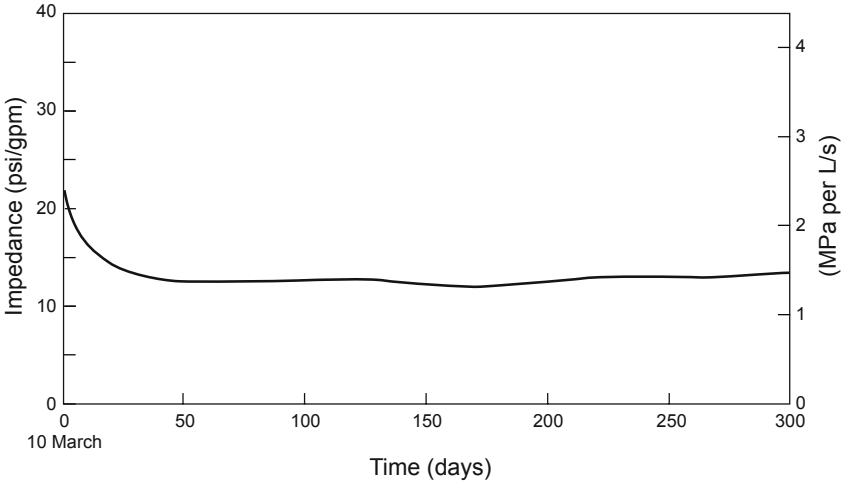

Fig. 4-32. Overall reservoir flow impedance during Run Segment 5.
Source: Zyvoloski et al., 1981a

Modeling of the Heat-Transfer Surface

Considering the geometrical unknowns and the poorly defined temperatures of the rock near the reservoir inlet, the modeling done to determine the effective heat-transfer surface—the main objective of Run Segment 5—was reasonably successful. The principal parameter used in these modeling efforts was the temporal variation in the outlet temperature. The analytical cooldown profile shown in Fig. 4-33 was based on an aggregate heat-transfer surface of 50 000 m^2, as predicted by the "Independent Fractures Model." (This heat-transfer model was initially developed to analyze the Run Segment 2 reservoir, then expanded to accommodate two series-connected joints for the analyses of Run Segment 5. It was so named because it was used to model, independently, the heat-transfer surface of each of the "fractures" [joints] constituting the enlarged reservoir—the 9050-ft joint of the original Phase I reservoir and the 9650-ft joint through which the enlarged reservoir was created.)

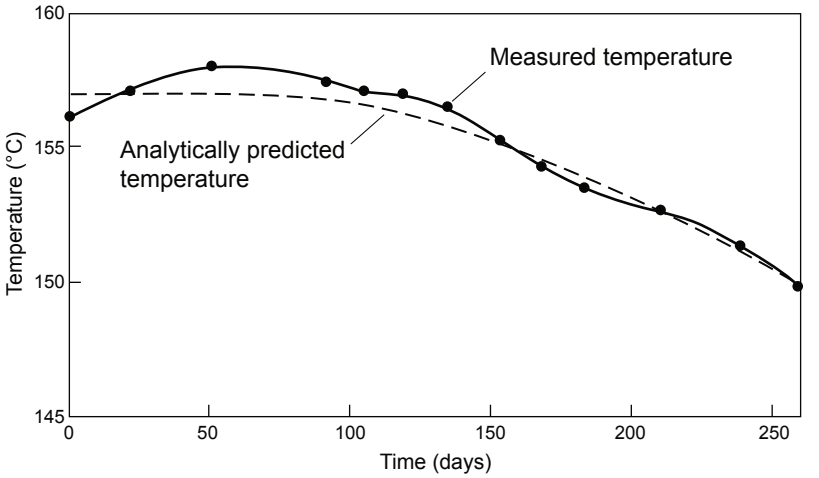

Fig. 4-33. The cooldown temperature profile for Run Segment 5 predicted by the Independent Fractures Model (based on a heat-transfer surface of 50 000 m^2), compared with the outlet temperature profile for the reservoir as measured in the casing at 8500 ft—just above the several production zones in the open-hole interval of GT-2B.
Adapted from Zyvoloski et al., 1981a

As shown in the figure, the measured outlet temperature rose during the first 50 days of Run Segment 5, from 156°C to 158°C—a very strange behavior for an HDR geothermal reservoir, and one that would suggest a modest heating (by a somewhat warmer flow from the interior of the reservoir) of the previously cooled joints connected to GT-2B. For the next 50 days, the outlet temperature was nearly constant, dropping only 0.7°C

(to 157.2°C), suggesting an almost isothermal reservoir at a temperature of about 157°C during this period. The modeled profile shows the temperature constant at 157°C for the first 75 days (halfway between the initial and maximum measured temperatures); then after day 140 and for the rest of Run Segment 5, the outlet temperature declines more sharply, in close agreement with the measured cooldown profile—a strong indication that by this time the cooling "wave" produced by the cold inlet fluid had reached the reservoir outlet.

The heat-transfer surface for Run Segment 5 was estimated by incorporating the temperature data from Fig. 4-33 and the Run Segment 5 production flow rates from Fig. 4-30 into the Independent Fractures Model (Table 4-4). This numerical simulation results in a thermal drawdown of 7°C in 185 days (from day 75 to day 260).

Table 4-4. Heat-transfer surface of the Run Segment 5 reservoir based on the Independent Fractures Model

Original reservoir (Run Segments 2 and 3)	One joint, modeled surface = 15 000 m^2
Enlarged reservoir (Run Segments 4 and 5)	One additional joint, modeled surface = 35 000 m^2
Total surface (both joints)	50 000 m^2

However, one salient feature of the measured reservoir cooldown shown in Fig. 4-33 escaped the analysts: The near-constant production temperature for the first 100 days or so implies that the *effective* mean temperature of the circulation-accessible rock volume was about 157°C—before significant cooldown began at the production well. Further, when the cooling wave from EE-1 finally reached GT-2B (on about day 75), the reservoir cooldown proceeded as if the entire 50 000-m^2 heat-transfer surface was at this mean temperature. In other words, the rock in the region of the inlet was no longer at a temperature of 197°C, as had been measured in 1975. Obviously, in an interconnected, multiply jointed reservoir, individual flow paths could, and did, have different surface temperatures. This phenomenon is illustrated in Fig. 4-34, which shows temporal variations in outlet temperatures measured at three zones within the GT-2B production interval (identified as separate joint outlets by both temperature and spinner logging during Run Segment 5). Note that the upper zone had the highest temperature, an intuitively anomalous behavior. However, the reservoir model shown in Fig. 4-16 suggests that this zone, having the longest flow path, would have enhanced heat transfer (through more contact with the hotter rock in this region) but at the same time the lowest flow rate (because of the greater resistance to flow). This is indeed what the Run Segment 5 data show (Zyvoloski et al., 1981a).

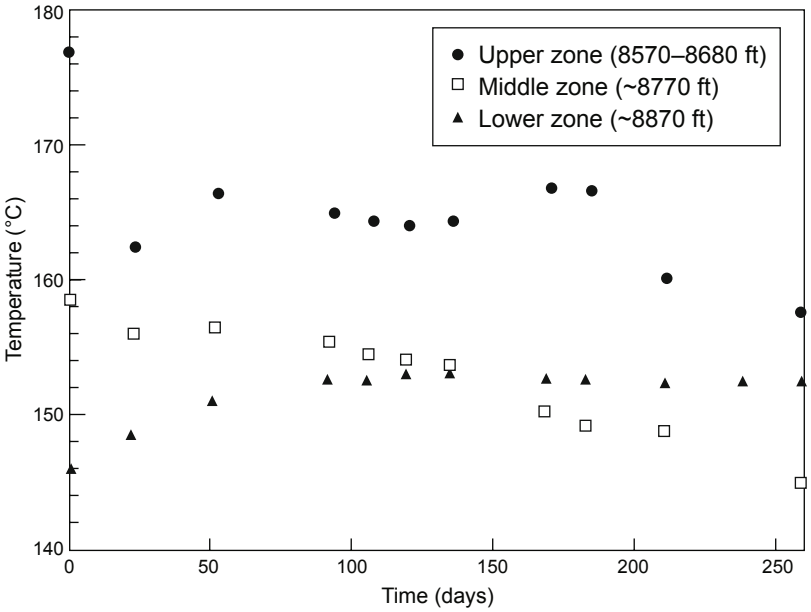

Fig. 4-34. Outlet temperature histories as measured at three individual zones of the production interval in GT-2B (plotted on an expanded scale). Source: Zyvoloski et al., 1981a

At the same time that some Project staff were modeling the reservoir's heat-transfer surface using the assumptions of the Independent Fractures Model, others were starting to explore the notion of an HDR heat-transfer *volume* that would be implicit in a conceptual model based on a complex, multiple-joint geometry.

Heat-Transfer Volume of the Reservoir

At the time the Phase I reservoir was being tested, there were only two ways of estimating the circulation-accessible rock volume (or effective heat-transfer volume). The first method is based on (1) the joint porosity, as determined for the seismic volume (1.4×10^{-4}—see discussion of Fig. 4-21a and b above) and (2) the known through-flow fluid volume. The main constraint with this method is that it is often difficult to determine an appropriate value for the latter parameter. For the enlarged Phase I reservoir, the through-flow fluid volume was determined early in Run Segment 5 (after the major reservoir growth produced by Run Segment 4, but before additional cooling had occurred). The most appropriate measure of this volume would be the integral mean volume, i.e., the 404 m^3 shown in Table 4-3 for

the beginning of Run Segment 5. Although erratic during this run segment, this volume is still more appropriate for this purpose than the modal volume, which showed almost no increase between the beginning of Run Segment 4 and the early part of Run Segment 5 (even after the injection of over 2 million gal. of additional water, the modal volume increased only from 136 to 155 m^3). Using a through-flow fluid volume of 404 m^3 and a porosity of 1.4×10^{-4}, one obtains an estimated circulation-accessible rock volume of 2.9 million m^3.

The second method is based on geometric and seismic information. In the case of the enlarged Phase I reservoir, only the height dimension of the circulation-accessible rock volume is reasonably well constrained—the 950-ft (290-m) height from the EE-1 entrance at 9650 ft to the mean production interval in GT-2B at 8700 ft (Fig. 4-28). The low (1300-psi) reservoir pressure during Run Segment 5 produced few locatable signals—only 11—which were clustered along a 650-ft-long region oriented a little east of north. Using a height of 950 ft, a length of 650 ft, and the 75-ft width of the cooled region shown in Fig. 4-28, one obtains an estimated circulation-accessible rock volume of 1.3 million m^3 (46 million ft^3)—less than half that derived by the first (porosity-based) method.

Geothermometer Measurements

The Run Segment 5 geothermometer measurements were adversely affected by the presence of one or more flow paths carrying hot fluid between EE-1 and GT-2B at very low rates. Evidence for these flow paths was observed during Run Segments 2 and 3. Further evidence was obtained during Run Segment 4 and is shown in Fig. 4-35, which includes the rationale for and method used to calculate the temperatures of their entry points into GT-2B (from temperature-probe and spinner flow data obtained near the end of Run Segment 4). Note in particular the November 9 calculated point at 225°C. The flow path suggested by such a temperature would have passed well below the bottom of EE-1 before finally exiting into GT-2B at 8660 ft—and would obviously have complicated the geochemical results, especially the geothermometer measurements. However, because the flows associated with these paths were very low (3 gpm or less), the anomalous temperatures shown in Fig. 4-35 are somewhat uncertain.

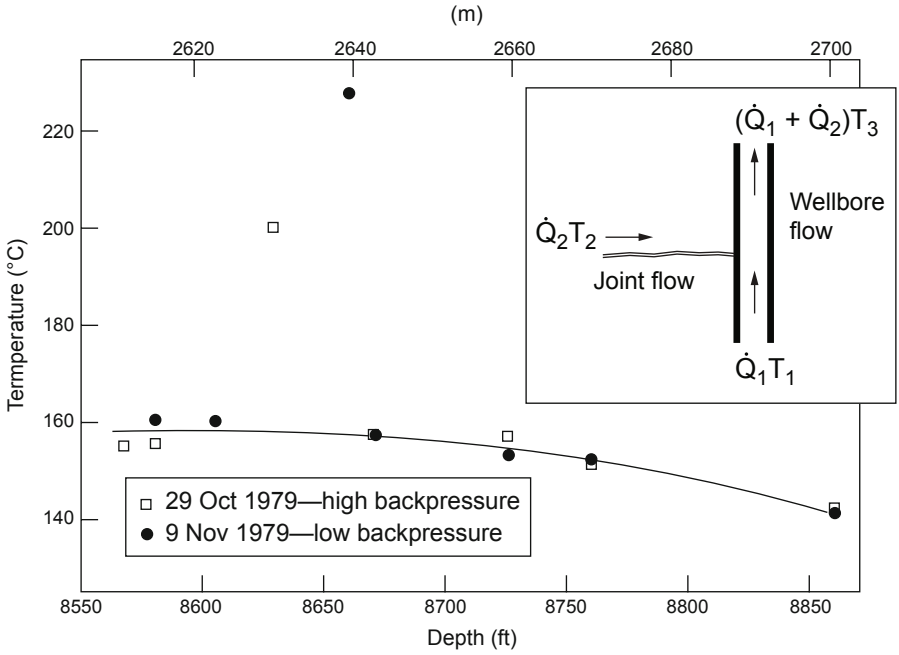

Fig. 4-35. Calculated temperatures of fluid entering GT-2B at various points along the production interval during Run Segment 4. The method of calculation is shown in the inset. T_1 and T_3 are the measured temperatures, $\dot{Q}_1$ and $(\dot{Q}_1 + \dot{Q}_2)$ are the spinner-measured flow rates, and T_2 is the derived inflow temperature at the intersection.
Source: Murphy et al., 1980a

Figure 4-36 depicts the computed silica and Na-K-Ca geothermometry temperatures for Run Segment 5, compared with the measured outlet temperature of the reservoir. The discrepancy of about 30°C between these two kinds of measurements can probably be attributed to the one or more low-flow-rate, high-temperature flow paths connecting EE-1 to GT-2B.

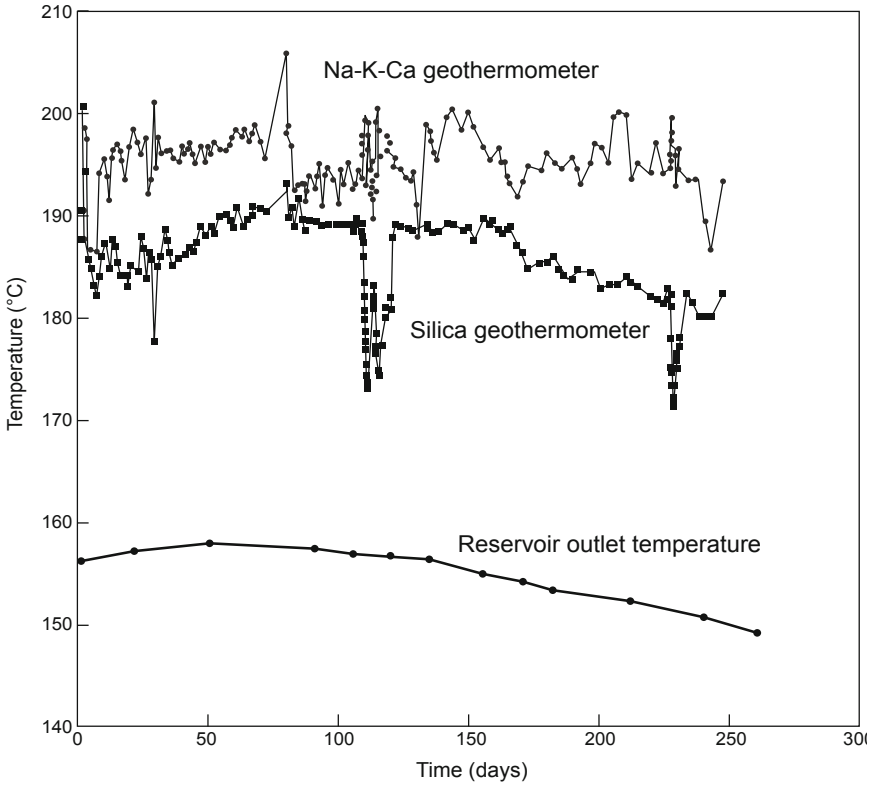

Fig. 4-36. Comparison of the calculated geothermometer temperatures with the mixed-mean reservoir outlet temperature.
Source: Zyvoloski et al., 1981a

Influence of the Nearby Valles Caldera on Dissolved Minerals, Gases, and the Geothermal Gradient

As discussed in detail in Chapter 2, the environment deep beneath Fenton Hill was influenced by diffusional processes associated with the eruption of the nearby Valles Caldera about 1 million years ago. No one disputes that the enhanced geothermal gradient at Fenton Hill results directly from the radial diffusion of heat from the caldera, a process that has been active over the past million or so years. (In fact, this elevated geothermal gradient is one of the main reasons for which Don Brown selected Fenton Hill as the HDR site.) It should then follow that the outward radial diffusion of volcanically derived fluids from the caldera would likewise have been occurring over the past 1 million years.

The evidence is overwhelming that the connate fluid in the deep system of sealed joints in the Precambrian basement at Fenton Hill is derived from the then-active volcano immediately to the east. (The added heat has been a blessing, but the associated fluids have been a real headache! For example, because of the presence of dissolved hydrogen sulfide [H_2S]—a very poisonous, volcanically derived gas—in the produced fluid from the Phase II reservoir, the entire site had to be posted as hazardous and then monitored continuously during Phase II reservoir development and testing.)

Geochemistry Results

Figure 4-37 depicts the variations with time in the concentrations of five dissolved species (silica, sodium, chloride, potassium, and boron) in the produced fluid during Run Segment 5. What is remarkable is the rapidity with which equilibrium was reached—for most of them, within 20 days after the start of circulation. Thereafter, for the rest of Run Segment 5, the concentrations changed very little, in spite of the gradually decreasing fluid temperatures (Figs. 4-33 and 4-34). This would suggest that the elevated—but near-steady-state—species concentrations were strongly affected by the small portion of the production flow that was traversing the very large system of semi-permeable joints in the seismic volume via one or more high-temperature, low-flow paths; and that these joints contained sufficient entrained fluid to stabilize the geochemistry of the produced fluid.

In all of these curves, one can discern the influence of the fresh-water flush, an experiment carried out from June 26 through July 7. Fresh water was injected into EE-1 to totally replace the recirculating flow, the production flow being vented to the GT-2 pond. After about two days of open-loop operation, during which some 250 000 gal. of fresh water was injected, closed-loop flow was re-established.

The effect of the fresh-water flush is most evident in the silica concentration curve, which after 10 days "snapped back" to 228 ppm, its value before the fresh-water flush. This behavior suggests that the fresh-water flush had little effect on the hot, auxiliary flow paths, the fluid in them having reached equilibrium with rock at 195°C–198°C. The concentrations of boron, potassium, sodium, and chloride were a little slower in returning to their previous values, suggesting that these were at least partially controlled by the concentrations of those species in the joint-filling fluid just beyond the active-circulation region. In addition to their inability to "rebound" as quickly following the fresh-water flush, the very high concentrations of chloride and boron would be more indicative of hot fluid derived from the nearby caldera than of fluid in quiescent equilibrium with a hot granodioritic rock mass.

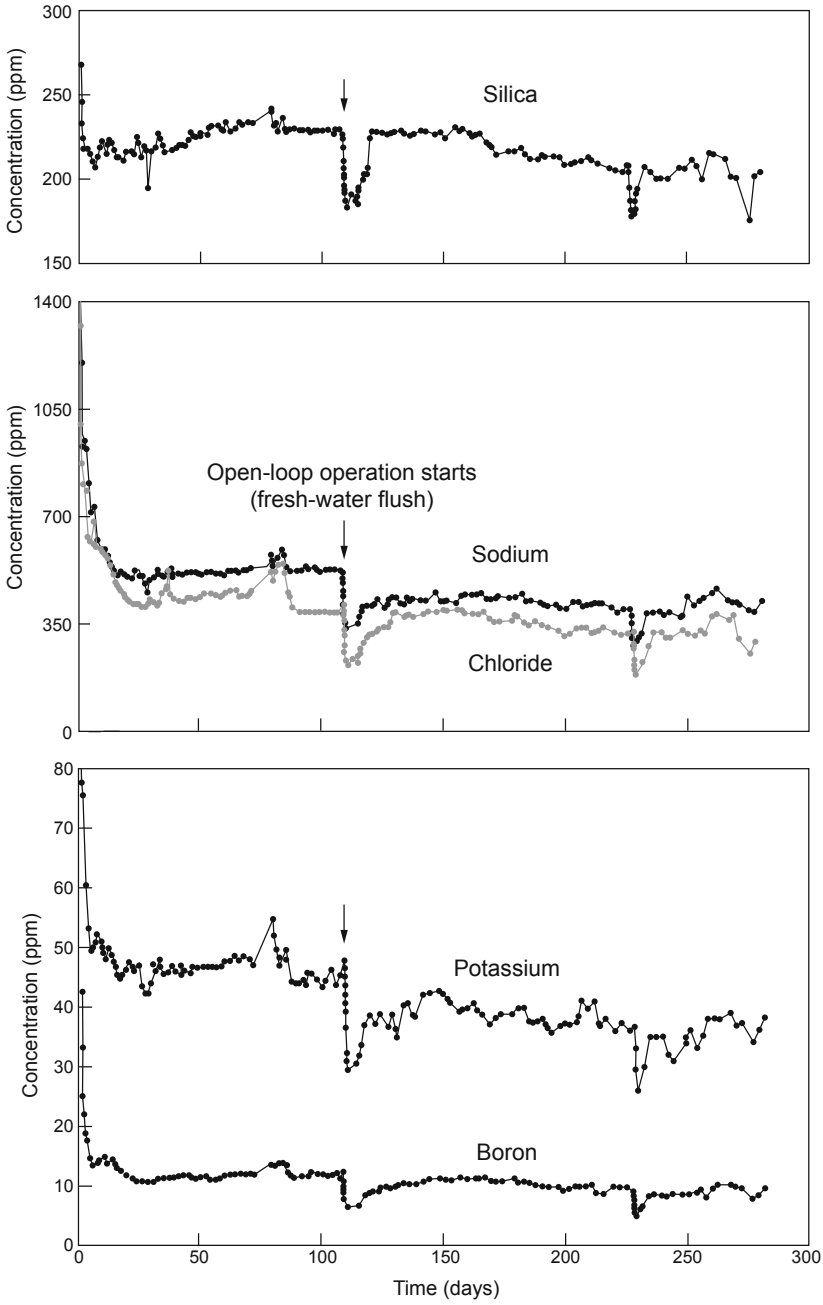

Fig. 4-37. Variation in concentrations of five dissolved species in the produced fluid during Run Segment 5.
Source: Zyvoloski et al., 1981a

For example, there were no boron-containing minerals within the Phase I core samples, but boron in the produced fluid averaged about 10 ppm, not atypical for a volcanically derived joint-filling fluid.

At the time of Run Segments 4 and 5, a different theory was advanced by several HDR staff to explain the generally elevated species concentrations measured in the circulating fluid. This theory—now believed to be fallacious—was that the circulating fluid was flushing out pore fluid contained in the regions of the rock blocks adjacent to the joint surfaces within, and just beyond, the circulation-accessible rock volume. (This "pore" fluid was assumed to be the connate fluid filling the sparse array of tightly closed—but still interconnected—microcracks[17] in these rock blocks.) However, with the rock blocks of the "active" reservoir being *compressed* as they were, it is almost inconceivable that the very small amount of pore fluid within them could be readily accessed by the higher-pressure fluid circulating through the joint network.

The more reasonable explanation is that at least a portion of the fluid filling the joints within the seismic reservoir volume had originated from the caldera and was being circulated, at a very low flow rate, to the production well during Run Segment 5. Such an explanation is supported by the chemical composition of the dissolved gases in the produced fluid—in particular the continuing high levels of dissolved CO_2 (70%–80% of the gas fraction) and the presence of hydrogen sulfide (ranging from 300 to 1000 ppm).

Stress-Unlocking Experiment

This experiment, known as the SUE, was designed primarily to determine whether the reservoir flow impedance of Run Segment 5 (a near-constant 13 psi/gpm) could be significantly reduced by repressurization of the reservoir at significantly higher levels (auxiliary pumping equipment was enlisted for this purpose). The principal result of the SUE was a reduction in the overall reservoir flow impedance of about 37%—from 13.5 psi/gpm to 7.8 psi/gpm.

Note: A decrease in flow impedance had been achieved by this means during Run Segment 4: while fluid was injected into EE-1, beginning at 2450 psi and ending at about 2420 psi, the backpressure at GT-2B was held at 160 psi, then increased to 1480 psi (second and third stages). Next, the injection pressure was reduced to 1400 psi and the backpressure at GT-2B returned to 160 psi (fourth stage). The result of this multiday pressure excursion was a drop in the overall flow impedance of 34% (from 19.7 psi/gpm to 13.1 psi/gpm, as shown in Table 4-2). But this achievement was largely unrecognized at that time.

[17]The average porosity of the microcracks representative of the rock blocks within the circulation-accessible reservoir volume was measured as 10^{-4} (Simmons and Cooper, 1977).

The underlying rationale for the SUE was as follows: as the reservoir cooled during Run Segment 5, the individual rock blocks within the cooled reservoir region would have undergone thermal contraction but would have been prevented from moving by the confining earth stresses. An increase in the reservoir pressure to a level above the least principal earth stress would have partially relieved these "locking forces," allowing for at least some movement (any movement would be along the joint surfaces bounding these blocks).

To best comprehend the SUE, one must understand the sequence of pumping operations (which well was being pressurized at a given time, and at what level). The experiment began on December 9, with injection into EE-1 for one hour at 5 BPM and a pressure of about 1200 psi. The injection flow rate was then increased in two steps—to 10 BPM and to 18 BPM—and two hours later throttled back somewhat (to 15 BPM) and maintained at that level for the rest of the EE-1 injection phase. During these variations in flow rate, the injection pressure increased from 1600 psi to 2200 psi. After 7 hours and the injection of 270 000 gal. of fluid, EE-1 was shut in and GT-2B was pressurized instead, at 10 BPM for just 25 minutes; during this brief time, the injection pressure at GT-2B increased from an initial shut-in value of 1700 psi to 1900 psi. This phase of the SUE had to be terminated prematurely because of excessive pump vibration.

As shown in Fig. 4-38, seismicity during the SUE was modest until late on December 9, when the rising shut-in pressure at GT-2B finally exceeded 1500 psi—the pressure for a warm column of fluid in GT-2B that would correspond to a pressure of about 1300 psi for a cold column of fluid in the injection well—the condition under which previous reservoir stress measurements had been made. Because the least principal earth stress within the Phase I reservoir region was close to 1300 psi (see *State of Stress within the Phase I Reservoir* above), the level of seismicity along the most favorably oriented joints within the cooled portion of the reservoir began increasing rapidly above this threshold.

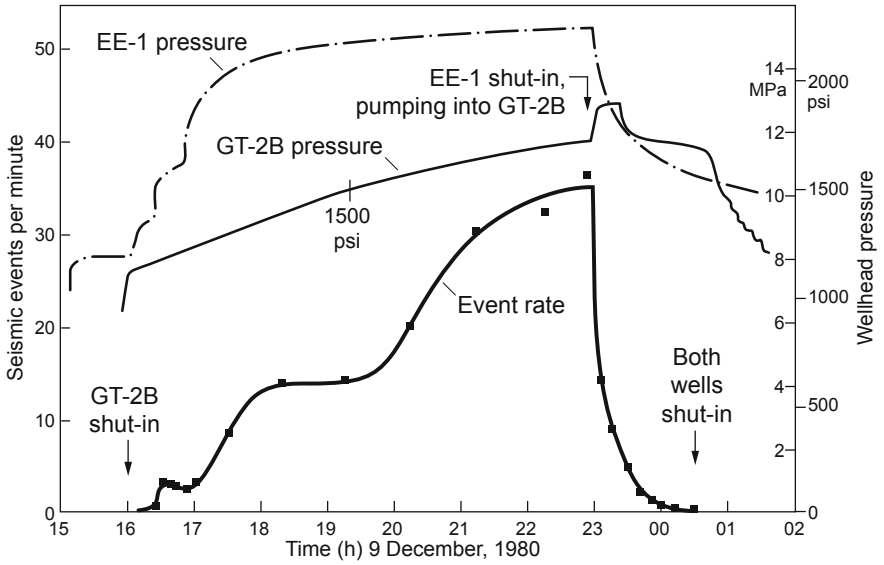

Fig. 4-38. Correlation between seismic event rates and system pressures during the SUE.
Source: Murphy et al., 1981a

Figure 4-39 shows, in plan view, the seismicity produced during the brief SUE. Occurring mostly in the SE quadrant, these events were restricted to the cooled central portion of the reservoir and extended out no more than 200 m—a pattern different from those seen during previous episodes of reservoir growth. For example, the seismicity produced during the very large injection of Run Segment 4 extended outward almost 800 m from the injection point (see Fig. 4-26). The seismicity during the SUE indeed appears to have resulted from a realignment of some of the rock blocks within the cooled portion of the active reservoir, when the reservoir pressure was increased enough to allow movement along the bounding joints.

When reservoir pressure during the SUE was further increased (ultimately to 1900 psi, as measured at GT-2B), the rate of seismicity—still emanating from the thermally depleted central portion of the reservoir—accelerated markedly. Although at least equal to the 20-events-per-minute average recorded near the end of the third stage of Run Segment 4 (at pressures above 2400 psi), it was still much lower than the seismicity produced during Expts. 203 and 195 (Fig. 4-25).

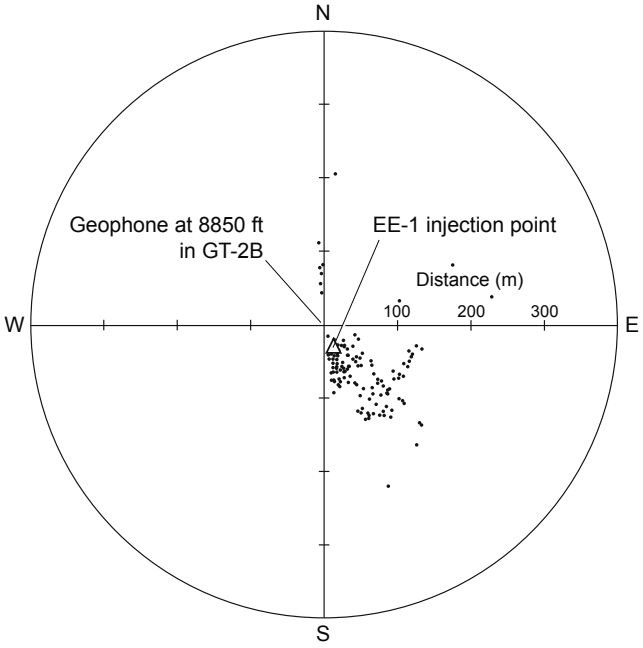

Fig. 4-39. Plan view of the seismicity produced during the SUE (as recorded at the GT-2B station).
Source: Murphy et al., 1981a

Radioactive tracer experiments were conducted both before the SUE and after it. The results are given in Table 4-5, for the integral mean and modal volume determinations.

Table 4-5. Reservoir through-flow fluid volumes before and after the SUE (m^3)

Tracer experiment	Integral mean volume	Modal volume
Pre-SUE (2 Dec 1980)	581	187
Post-SUE (12 Dec 1980)	1118	266
Increase (%)	92	42

The changes in these volumes associated with the SUE are attributed to a rearrangement of the rock blocks in the cooled region of the reservoir, suggesting an overall increase in the joint apertures. As discussed earlier, the authors believe that the integral mean volumes represent the more realistic values; whether they in fact do cannot be proved, but no doubt the trends are valid.

Nor is it certain what actually caused the reduction in the overall reservoir flow impedance, the primary objective of the SUE. Analysis of the shut-in pressure behavior at both wells indicates that the main factor was

a 43% reduction in the near-wellbore outlet impedance. This impedance, however, is the one that should have been least affected by the cooling of the reservoir and the concomitant shifting of the rock blocks.

Following the SUE, steady-state operating conditions were re-established for another week. Final shut-down took place December 16, 1980.

The Phase I reservoir was tested for over nine months at an average power level of 3 MW_{th}. However, with only a modest change in operating conditions—i.e., the use of pumping equipment capable of higher pressures, to operate the reservoir at an injection pressure of 2400 psi and a backpressure of 1400 psi—the power level of the HDR system could easily have been increased 50%, to 4 1/2 MW_{th}, for at least 6 months. A high-backpressure operating scenario of this kind would prove to be very successful in the 1990s, during the testing of the Phase II reservoir.

The seismic data used to define reservoir geometry during the various run segments were also used to evaluate the potential for seismic risks associated with HDR geothermal energy extraction. These data showed no evidence that Phase I reservoir development or testing presented any seismic hazard. The largest event detected by the downhole package during Run Segment 4 had a magnitude of –1.5 on the extrapolated Richter scale, or an energy release roughly equivalent to that of a 10-kg mass dropped 3 m (10 ft).

Led by Hugh Murphy, a number of HDR staff lobbied the Laboratory for a continuation of Phase I reservoir testing during the time that the Phase II reservoir was being developed. However, Rod Spence, then the HDR Project Manager, decided to abandon the Phase I reservoir and to concentrate the staff's efforts on the deeper Phase II reservoir. Today, 31 years later, it is illuminating to read Hugh's comments on the subject (Dash et al., 1981):

> The summary of heat extraction tests in Run Segments 2 through 5. . . indicates that the. . .[reservoir is] of modest size. However, other indications, such as geochemical, microseismic, water losses, and venting volume measurements, suggest that the reservoir is potentially much larger. In particular, the microseismic data suggest that we have forced water, that is, gained access to distances very far from the injection well . . . .Furthermore, the microseismic data suggest that this larger potential reservoir is not planar, but highly jointed and multiply fractured, so that this potential reservoir, if sufficiently exploited, would represent a volumetric rather than an areal source of heat.

Although numerous problems and delays beset the development and testing of the Phase I reservoir, it must be remembered that this was the first-ever test of an HDR reservoir in deep, hot, crystalline rock. Most important is that the overall success of the endeavor represented the first true milestone in the establishment of a totally novel (and vast) renewable energy resource for the 21st century—not only for the United States, but for the entire world.

PART III

Engineering the HDR System: Development and Testing of the Phase II Reservoir at Fenton Hill

Chapter 5

Planning and Drilling of the Phase II Boreholes

The Phase I reservoir at Fenton Hill, which extended over the approximate depth interval 8000–10 000 ft, had indeed demonstrated the technical feasibility of the HDR concept, but at a temperature (157°C) and thermal power (3 MW) lower than desirable for commercial power production. The Phase II reservoir was planned for development at a depth of 12 000–14 000 ft, to test the HDR concept at a temperature and rate of geoheat production more appropriate for a commercial power plant, and with a reservoir large enough to sustain a high level of thermal power for an extended period (at least 10 years).

To understand how and why the Phase II HDR system at Fenton Hill developed as it eventually did, one needs to realize that the planning for this system was a "work in progress" from about mid 1979 through mid 1982. Its evolution was driven by the continually changing demands of the ongoing work at Fenton Hill; by the varying levels of funding from the U. S. Department of Energy (DOE); and by the political and technical cross-currents among DOE personnel, Laboratory staff, and those managing the HDR Program at Los Alamos.

As late as the spring of 1979, while Run Segment 5—the first-ever long-term flow test of an HDR system—was under way to test the enlarged Phase I reservoir, the (still evolving) plan for the Phase II system called for the drilling of only one new borehole, EE-2. This new borehole would be used as the Phase II injection well, while one of the existing Phase I wells—probably GT-2—would be deepened to serve as the production well for the deeper and hotter system.

> "This new well, EE-2, will be drilled to a total depth corresponding to a bottom-hole temperature of at least 275°C. We intend to create the new [HDR] system . . . with a heat-production capability of about 20 MWt. Further, we will use this system to demonstrate extended reservoir lifetime. . .for a [thermal] drawdown that will not exceed 20% in 10 years of operation." (HDR, 1979)

The principal objective of the drilling program for EE-2 was to gain access to a large volume of hot rock at depths of 12 000–14 000 ft for subsequent reservoir development. On the basis of temperature-gradient data from the deeper portions of GT-2 and EE-1, where bottom-hole temperatures were about 180°C, attaining the desired reservoir temperature of 275°C would require a TVD (true vertical depth) of about 14 000 ft (4300 m) for the new borehole. (As will be seen, this rock temperature would actually be reached at a TVD of only 12 700 ft [3870 m], because of the directional drilling of the EE-2 borehole toward the caldera; with the temperature gradient increasing with depth below about 6500 ft [2000 m], the bottom-hole temperature at 14 405 ft, at the completion of drilling, would be about 317°C—considerably hotter than the original target temperature!)

D.W. Brown et al., *Mining the Earth's Heat: Hot Dry Rock Geothermal Energy*,
DOI 10.1007/978-3-540-68910-2_5, © Springer-Verlag Berlin Heidelberg 2012

Only after the drilling of EE-2 was in process, later in 1979, did it become known that the following year would bring higher levels of funding to the HDR Program. With this news, the plan to deepen GT-2 (or possibly EE-1) was dropped in favor of drilling a second new borehole, EE-3—to be started immediately after the completion of EE-2: the drill rig would simply be skidded about 150 ft to the northwest. This decision was quite reasonable considering not only the small diameter of the casing in GT-2 (7 5/8 in.) but also the condition of EE-1 following the 9-month flow test (Run Segment 5) that ended in December 1979. By late 1979, a significant bypass flow had developed: fluid was now flowing from the pressure-stimulated Phase I reservoir region, via the annulus above the cemented-in portion of the casing in EE-1, to the surface—in parallel with the production flow in GT-2B.

The Phase II Development Plan

The development plan for the Phase II HDR reservoir is shown in Figs. 5-1 and 5-2. The plan stipulated that the lower portions of the injection and production wells would be directionally drilled—which would be both expensive and difficult.

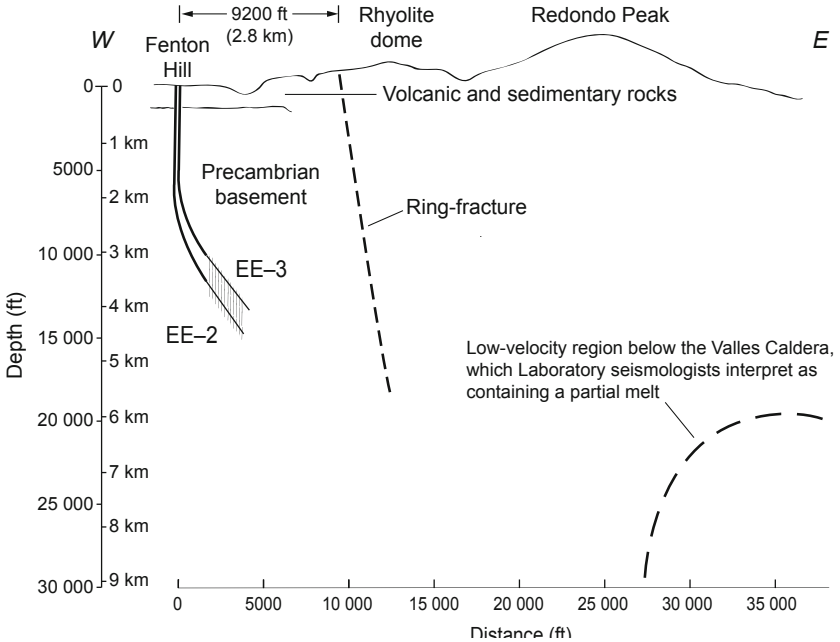

Fig. 5-1. The geological setting of the Phase II HDR system in relation to the adjacent Valles Caldera. The size and depth of the low-velocity region are adapted from Roberts et al. (1991) and Steck et al. (1998).

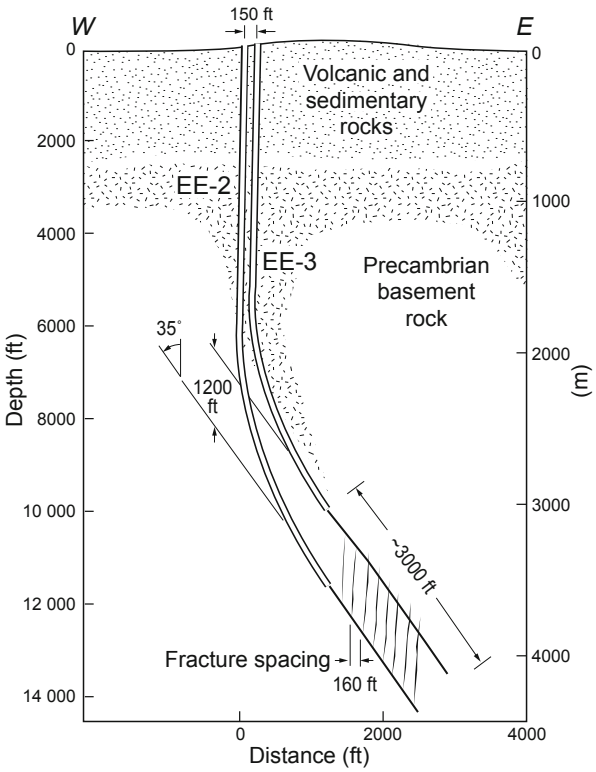

Fig. 5-2. Cross section of the Phase II HDR system (as planned). Adapted from HDR, 1980

The rationale for this plan was based on a critical, but nonetheless erroneous, assumption (later referred to as the *Phase II assumption*): that the continuous, near-vertical, northwest-striking principal joints observed in the Phase I reservoir region between about 8000 and 10 000 ft (2440 and 3050 m)—see Chapter 4, Fig. 4-28—would also be present some 4000 ft deeper into the structurally complex Precambrian basement *and* would control the development of the Phase II reservoir. The plan called for drilling EE-2 and EE-3 vertically to a depth of about 6500 ft (2000 m) and then directionally toward the east (that is, roughly across the strike of the two principal vertical joints that had been pressure-opened in the Phase I reservoir). The lower portions of the two boreholes would be drilled to position EE-3 directly above EE-2, with a vertical separation of about 1200 ft (370 m). The planned final inclination of the boreholes was 35° from the vertical, so that starting from the bottom of EE-2 and working

upward along the borehole, up to 12 intervals could be sequentially isolated with inflatable packers, separated by about 160 ft; each interval would be pressurized to create a vertical "fracture" that would then be driven upward to intersect the EE-3 borehole.

However, it would turn out that the near-vertical, northwest-striking joints that had been opened as the principal joints in the Phase I reservoir region, although present in the Phase II reservoir region, were no longer continuous but were truncated by an array of significantly inclined joints. These inclined joints were continuous and had much higher opening pressures (near 6400 psi [44 MPa], vs about 2200 psi [15 MPa] for the vertical joints). Thus, the pressures used to open the inclined joints within the Phase II reservoir would hyper-dilate the vertical joints, making them very significant in terms of fluid storage and reservoir connectivity; but the vertical joints *were not the major flow paths*. (These conclusions were based on extensive analyses of flow, pressure, tracer, and microseismic data obtained during the development and testing of the Phase II reservoir.) It was the inclined joints that were the major flow paths and would ultimately determine the geometry of the Phase II reservoir.[1]

Unfortunately, the Phase II reservoir would develop in roughly the same direction as the inclined portions of the two boreholes (i.e., with an eastward inclination of about 60°). The resulting geometry would be that of a thin ellipsoid tilted to the east, its greater dimensions in the north–south and inclined directions and its smallest dimension in the direction from EE-2 toward EE-3. Such a geometry was the worst possible one for trying to connect EE-2 to EE-3 by hydraulic fracturing.

In addition, owing to the credence given the erroneous underlying "Phase II assumption," during the two years of Phase II drilling considerable time would be devoted to developing methods for controlling the flow in individual vertical "fractures"—so that no single one would over-cool, thermally dilate, and garner most of the flow (the dreaded notion of thermal short-circuiting in a parallel-channel HDR system).

Construction of the larger, deeper, and hotter Phase II HDR system was initiated in 1979. The EE-2 and EE-3 boreholes would be drilled from locations about 150 ft (50 m) apart at the surface to approximate TVDs, respectively, of 14 000 ft (4300 m) and 13 000 ft (4000 m).

[1]Even though the two reservoirs were separated by only about 600 ft (the bottom of the Phase I reservoir being at about 10 400 ft and the upper extent of the Phase II reservoir at about 11 000 ft), their joint structures differed significantly.

Planning and Drilling of the EE-2 Borehole

In October 1978, a detailed plan for the drilling of EE-2, the intended injection well for the Phase II HDR system at Fenton Hill, was submitted to Los Alamos National Laboratory by Grace, Shursen, Moore & Associates of Amarillo, Texas. The drilling plan included wellhead sketches and detailed specifications for all equipment and materials needed for the project, including bits, hydraulics, tubular goods, drilling fluids, drilling assemblies, and pressure-control equipment.

For any directional drilling required at depths shallower than 9800 ft (3000 m), where temperatures are below 200°C, a downhole positive-displacement motor (PDM) would be used. The bit rpm for this type of motor is moderate and is controlled directly by the flow rate of the drilling fluid; in addition, the bit reaction torques are reproducible and familiar to directional drilling engineers, which means that the direction of drilling can in most cases be controlled by single-shot surveying between motor runs—obviating the need for the much more expensive, continuous-readout surveying provided by downhole steering tools.

Because PDMs have temperature-sensitive elastomer stators and radial bearings that do not withstand temperatures higher than about 200°C, they were not specified for directional drilling below 9800 ft (3000 m). For the deeper drilling, two specially designed high-temperature turbodrills were purchased. Developed jointly by Los Alamos National Laboratory and Maurer Engineering, Inc. of Houston, Texas, these 7 3/4-in. (197-mm) turbodrills were designed with specific operating characteristics to match (to the extent possible with a turbodrill) the rpm, torque, bit weight, and power capacity required to drill granitic rock with the conventional rock bits selected for use at Fenton Hill. However, because the turbodrills rotate at very high speeds (250–400 rpm), it was expected that using them with tungsten-carbide-insert (TCI) rock bits—which are typically rotated at 40–60 rpm—would wear the bits down much faster and shorten their life.

During drilling below 11 000 ft (3350 m), a core would be taken approximately every 600 ft as a means of gaining additional information about the reservoir region.

In early 1979, expecting that the substantial increase in drilling activity in the Rocky Mountains area would make it difficult to obtain a drill rig, the Laboratory solicited bids from more than 30 contractors. Bids were received from three of these. The selected contractor was the Brinkerhoff-Signal Drilling Company (a division of Petrolane Corporation). Before the drill rig was mobilized at EE-2, a 28 1/2-in. conductor pipe was installed in a 76-in.-diameter, 83-ft-deep bored hole[2] and concreted in place—except for the top 2 ft, which would serve as a cellar.

[2]Note that in Fig. 5-4, this depth is shown as 110 ft—as measured from the Kelly bushing after completion of the borehole.

Because of the complexities involved in drilling deep, hot, and—worse—deviated holes, Grace, Shursen, Moore & Associates was awarded a purchase order contract to provide continuous on-site supervision. Whereas drilling engineers from the Laboratory had supervised the Phase I drilling, now contract drilling engineers (with some assistance from Laboratory engineers) were to direct the operation of the drill rig and the work of the crews. As will be seen, this decision would turn out to be an unfortunate one. In addition, the contract supervisors would be responsible for coordinating specific Laboratory operations, such as wireline temperature logging. The management duties were generally carried out on a rotating basis by two drilling engineers, with a third available for occasional relief duty.

The information on the drilling of the EE-2 borehole is drawn largely from Helmick et al., 1982.

Drilling in the Volcanic Rocks

The drilling of EE-2 began on April 3, 1979 (Fig. 5-3 shows the Brinkerhoff-Signal rig No. 56 in operation). Penetration of the 460 ft (140 m) of Bandelier Tuff, for which a 26-in. (660-mm) bit was employed, presented no problems and was completed in two days.

Fig. 5-3. The EE-2 drilling location, viewed to the east, in the spring of 1979. The heat exchanger, the tower over GT-2, and the numerous trailers, tanks, and pipelines associated with the first two flow tests of the Phase I reservoir are visible behind and to the right of EE-2.
Source: HDR Project photo archives

Drilling in the Paleozoic Rocks

On April 6, at a depth of 460 ft,[3] the Abo Formation (Permian red beds) was encountered. The borehole—despite "fanning" at a low bit load and a high rotational speed of 150 rpm—began to deviate from vertical and by 938 ft (286 m) had reached an inclination of 5°. A "hole-straightening" assembly was then used to drill the next 400+ ft. The Pennsylvanian-age shales and limestones of the Magdalena Group (Madera and Sandia formations) were penetrated on April 14, at a depth of 1250 ft (381 m); and by a depth of 1342 ft (409 m) the hole had been brought back to 1.5° from vertical. Drilling then continued, with a 26-in. bit, through the Madera Formation to a depth of 1784 ft (544 m). Interbedded limestones and red, sandy-clay/shale units, ranging in thickness from 5 to 25 ft, were encountered throughout. (In this area, the contact between the Permean-age Abo Formation and the Madera Formation is defined as the depth at which limestone becomes more abundant than red clays and shales.)

On April 20, a string of 20-in.-diameter surface casing was run in to a depth of 1783 ft (543 m)—unusually deep for surface casing, but the intent was to case off as much of the unstable Madera Formation as possible. (Because of the experience with the Phase I wells, it was expected that the first major lost-circulation zone would be encountered at about 1900 ft.) The casing was then cemented to the surface.

Beginning on April 22, the cement was drilled out with a 17 1/2-in. (445-mm) bit, and drilling then continued below the casing at a rate of 10–12 ft/h. Between the depths of 1883 and 1889 ft, approximately 630 gal. (2400 L) of drilling fluid was lost into the same lost-circulation zone that had previously been encountered in the drilling of the GT-2 and EE-1 boreholes (the severe lost circulation at that time had resulted in significant problems of borehole swelling and caving above the loss zone). Lost-circulation material was added to the circulating fluid, and as drilling progressed the zone sealed off. Drilling continued steadily at 8–10 ft/h until circulation was lost again on April 26, at 2354 ft (717 m), in a cavernous section of limestone overlying the granitic basement.

Note: It should be remembered that the static water level in the deep sedimentary rocks at Fenton Hill was about 1700 ft below the ground surface, which contributed to the severity of the lost-circulation problems.

Owing to the experience with the earlier boreholes, what was thought to be an appropriate course of action had been included in the drilling plan and was now implemented: supplemental water was immediately trucked onto the site so that drilling could continue despite the lost circulation. Referred to as "drilling without returns," this operation was an expensive one at

[3]Depths in the EE-2 borehole were measured from the top of the Kelly bushing, which was 8720 ft (2660 m) above mean sea level.

Fenton Hill. Although an on-site water well had been drilled in 1976, this well—at a pumping rate of about 40 gpm—was able to provide only a fraction of the water required. Some water was available from La Cueva, 5 miles away, but most had to be hauled from Los Alamos, a distance of 27 miles (45 km) over mountainous roads. In addition to the expense, the need to haul water slowed down the drilling process, the water being used at a much faster rate than it could be brought in. Equally important, drilling without returns was very risky in that the cuttings could accumulate and become compacted around the upper part of the drilling assembly, which could then become stuck. Even though the stabilizers did become clogged with clay, the cavernous limestone section was penetrated quite rapidly, and without major problems, to the surface of the granitic basement at a depth of 2402 ft (732 m).

Drilling in the Precambrian Crystalline (Plutonic and Metamorphic) Complex

Vertical Drilling

A 17 1/2-in., very hard formation bit was used to drill the uppermost part of the Precambrian basement rock; it achieved a rate of 7 to 12 ft/h, about the same as that in the Paleozoic limestones above. On April 28, at a total depth (TD) of 2593 ft (790 m), drilling was halted because of excessive pipe drag—which indicated tight spots (due to the squeezing of shale zones, mainly in the Madera Formation above 2050 ft). The EE-2 borehole would remain at this depth for the next eleven days.

The drilling plan called for running an intermediate string of 13 3/8-in. casing into the granitic basement, to stabilize and seal off the Paleozoic sedimentary rocks above the Precambrian surface. Before run-in of the casing, an attempt was made to seal off the bottom part of the Sandia Formation—the cavernous limestone interval on top of the Precambrian surface. First, a high-viscosity mud was pumped in to fill the portion of the hole in the granitic basement (2593 ft up to 2402 ft); then 200 sacks of a cement mixture was pumped through open-ended drill pipe on top of the mud, in the hope of creating a plug that would fill and seal off about 100 ft of the worst part of the cavernous limestone. On April 29, while drill pipe was being run in the hole in preparation for drilling out the cement plug (which, it turned out, had been overdisplaced), the first of a series of obstructions was encountered at about 2063 ft, in the upper part of the Sandia Formation—in a zone of untreated clays in which hydration could not be prevented. With the pressure of the very subhydrostatic fluid (mostly water) in the borehole much too low to prevent it, the hydrating and swelling clays were being squeezed into the borehole, aggravating its instability. (Drilling-mud stabilization could not be used, because drilling mud could not be retained in the hole.) Despite reaming, drilling, and washing to a depth of 2127 ft (648 m), the obstructions could not be adequately cleared.

Finally, high-viscosity mud was used to stabilize the section of the hole below the static fluid level of about 1700 ft, allowing reaming to continue to the full drilled depth of 2593 ft (790 m). When no cement was found on top of the granitic rocks—as had happened during several similar cementing attempts in GT-2 at about the same depth—it should have been clear that the cement had been overdisplaced into the lost-circulation zone overlying the granitic surface. Nevertheless, preparations began to place a new cement plug so that the 13 3/8-in. intermediate casing could be run. This time a wad of burlap bags was set *below* the loss zone, at about 2450 ft (750 m), to keep the cement from displacing the less-dense drilling mud filling the granitic section of the borehole below this depth. A 300-sack slurry of cement was pumped on top of the bags through open-ended drill pipe.

When EE-2 was re-entered on April 30, additional obstructions were encountered below 2230 ft (680 m), but as before, little or no cement was found. It was now obvious that pumping of cement—at a density almost twice that of water—from the surface into a very subhydrostatic loss zone essentially guarantees overdisplacement of the cement into the loss zone. Thus, cementing efforts were abandoned. But because of deteriorating hole conditions, trouble was anticipated in running the casing. A "Texas shoe"[4] was installed in place of the guide shoe at the bottom of the casing string. After the hole had been conditioned with high-viscosity mud, run-in of the 13 3/8-in. casing began, aided by a casing power swivel. However, when the casing encountered severe obstructions and could not be rotated through them beyond approximately 2260 ft (690 m), there was no alternative but to withdraw the casing joint by joint and lay it back down on the racks—a difficult and time-consuming operation. Next, a bit and reamer were run in on drill pipe, and the hole was rapidly reamed again to a full 17 1/2-in. diameter. Time was now of the essence, because the clay intervals were continuing to hydrate, swell, and squeeze off the borehole.

On May 3, the run-in of the 13 3/8-in. casing finally took place. During run-in, each joint was measured and its length added to the running total (the nominal joint length of 40 ft could vary by up to two feet, plus or minus). But most unfortunately, as the driller was adding up the lengths—on paper, as was common oilfield practice, rather than with a calculator—he made an error in addition of an even 100 ft (which should have been caught; an operation as critical as this one should have been double-checked by the contract drilling supervisor, who was not on site at the time!). This error would have severe repercussions for almost all the EE-2 drilling in the crystalline basement over the next eleven months. The immediate consequence was that the casing, while being run in at a rather good rate, came to a very

[4]A "Texas shoe" is a cutting/drilling shoe. When rotated, it would allow the casing to cut and ream its way to bottom through the swelling Madera clay zones exposed below the 20-in. surface casing (which was set at 1783 ft).

abrupt stop at what the contract drillers thought to be a depth of only 2493 ft. In reality, the casing shoe was sitting on solid rock at the bottom of the hole, at a depth of 2593 ft! Believing that they had hit an obstruction, they made several attempts to get past this "obstruction" by running the casing harder and harder into the bottom of the hole—which "corkscrewed" and partially collapsed it. Finally, they had no choice but to cement the casing in place where it had landed. (The reports of the time erroneously state that the casing was cemented in at 2493 ft, 100 ft off bottom.)

The plan for cementing the 13 3/8-in. casing string was devised on the basis of past experience with GT-2 and EE-1. Only the section of casing set into the granitic rock—that is, the section below the "vuggy limestone" loss zone at 2380 ft—was to be tag-cemented, because it was known that the cement would rise no higher in the annulus than this zone (owing to the difference in density between the cement and the water in the annulus, any excess cement would flow into the loss zone). Then, to stabilize this casing inside the 20-in. surface casing string, the annulus between the two would be cemented through an external packer/stage collar from about 1785 ft to the surface. This stage collar had been inserted during run-in of the 13 3/8-in. casing string, such that it would end up at a depth of 1785 ft (544 m) when the bottom of the casing was at 2593 ft. The stage collar would then be very close to the bottom of the 20-in. casing, which had been set at 1783 ft—and that in fact was the case.

Unfortunately, the tag-cementing job failed: when the wiper plug placed on top of the column of cement (to separate the cement from the displacement water) reached the float collar at the bottom of the casing string, it failed to seal—allowing the cement to be overdisplaced into the brackish aquifer flowing in the cavernous limestone on top of the Precambrian basement. (It is probable that the rubber seals on the plug were damaged by their passage across the rough, collapsed areas of casing above the float collar.) On May 5, a retrievable cement retainer was run in on the bottom of the drill pipe. Once it had been set inside the casing at a depth of 2411 ft (735 m), cement was pumped down the drill pipe and through the cement retainer, filling both the casing below the retainer and the annulus outside the casing up to the loss zone, successfully completing the tag-cementing job.

The second stage of cementing was carried out next: the cement was pumped down the 13 3/8-in. casing, through the open stage collar at 1785 ft, and back to the surface through the annular space outside the casing.

On May 7, a 12 1/4-in. (311-mm) drilling assembly equipped with a TCI button bit was run into the hole; it encountered cement at a depth of 1740 ft (530 m), about 45 ft above the stage collar—precisely where the cement *should* have been encountered with the bottom of the casing at 2593 ft and the stage collar at 1785 ft, but 100 ft deeper than the contract drillers expected! The cement and cementing hardware left behind after the second

stage of cementing were drilled through, then the drilling assembly was lowered until it encountered the plugs and other hardware left inside the casing during the tag cementing. These too were drilled through. Finally, on May 8, drilling in the granitic rocks recommenced with a new bit, deepening the hole by 26 ft, to a measured depth of 2619 ft.

Over the eleven months from May 1979 to March 1980, a litany of drilling and casing problems would ensue—almost all of them directly related to the collapse and corkscrewing of the 13 3/8-in. casing when it was repeatedly rammed into the granitic rock at the bottom of the hole.

On May 8, while drilling was proceeding at 2619 ft, the bit torqued up and had to be pulled. When inspection revealed that the inner sections of all three cones were missing, a specially ordered, 11 1/4-in.-diameter fishing magnet was run in to retrieve them. But the magnet could not be passed through an apparent obstruction in the casing at a depth of about 2390 ft (728 m), where it was known that a major cavernous region existed in the Sandia Formation. It can be inferred that over this depth interval, the borehole had a much larger "diameter" than the drilled diameter of 17 1/2 in.

After the magnet had been withdrawn, a previously used 12 1/4-in. bit was run in to attempt to clear the "obstruction"—which, in reality, was simply one of the areas of bent and buckled casing. Still unaware of the true situation, the contract engineers then spent several hours attempting to ream through the "obstruction" with the used bit. Finally, circulation was lost. The reaming had succeeded in cutting through the casing, and as shown by a subsequent temperature survey, fluid was escaping into the loss zone through a hole in the casing at about 2400 ft.

Next a second magnet, smaller in diameter (10 in.), was run in; but the 9-in.-diameter, relatively stiff assembly of drill collars above the magnet could not pass through the badly contorted casing. A 12 1/8-in.-diameter swedge with jars, run in to try to open the restriction in the casing, encountered tight spots at 2380 ft (725 m) and 2420 ft (737 m). A near-full-diameter casing roller (but without the stiff drill collars) was then run in to 2465 ft (751 m), with very little resistance. The fact that a nearly full-diameter casing roller assembly—which is limber—was able to pass through when a 9-in. drill collar assembly—which is longer and stiffer—could not, should have been a dead giveaway that the problem was collapsed casing (regardless of where the bottom of the casing was believed to have landed).

A series of logs done by Schlumberger on May 11 and 12 indicated breaks in the casing in the 2370- to 2390-ft and 2434- to 2468-ft depth intervals. Additional surveys were conducted over the next three days: temperature and spinner logging (Laboratory equipment), a McCullough casing inspection log, and Birdwell cement-bond and collar-locator logs. These surveys indicated damaged casing between 2380 and 2400 ft, buckled casing at 2480 ft, and a gap or split at 2400 ft. Water was exiting through a hole in the casing at 2380 ft (725 m) and flowing upward, outside the casing, into

the cavernous limestone region between 2354 and 2360 ft. (Note: one can only assume that by this time—although the official documentation makes no mention of it—the contract drilling supervisors were aware of the error made when the pipe lengths were added up, which had led to the severe damage of the casing. In particular, the collar-locator log, which would routinely have been run clear to bottom, would have shown the casing shoe at about 2590 ft, exactly where it should have been.)

On May 16, an attempt was made to seal off the lost-circulation zone outside the casing by cementing through the hole in the casing at 2380 ft. Three joints of open-ended drill pipe were run in through the blow-out preventor; then 400 sacks of Regulated Fill-up Cement (RFC) was pumped into the casing, followed by 1000 sacks of cement containing 40% sand; these materials were then displaced by 1850 gal. (7100 L) of water to effect a hydrostatic-pressure squeeze on the slurry (as if one could squeeze off a lost-circulation zone!).

When the drilling assembly was run back into EE-2, the cement was encountered at 1788 ft (545 m), and drilling through with a steel-toothed bit achieved full circulation (obviously, the cement had sealed the inside of the casing *above* the hole and splits). Then the bit ran into the same region of damaged casing at 2380 ft that had just been cemented. In an attempt to clear it, more reaming was carried out—which only damaged the casing further: metal flakes were appearing in the return fluid. After several passes with a magnet and junk basket, some 30 lb (14 kg) of metal fragments was recovered from the borehole.

Drilling into the remaining debris and fill at the bottom of the borehole began at a depth of 2405 ft (733 m), with a 12 1/4-in. bit. Almost immediately about 30% of the drilling fluid was lost through the hole and the splits in the casing. (Clearly, the massive cementing operation of May 16 had failed to close off the cavernous lost-circulation zone in the limestone above the granitic basement—as had the previous multiple cementing operations attempted during the drilling of GT-2 and EE-1 in the Paleozoic sedimentary rocks.) The injection of some 15 000 gal. (57 000 L) of lost-circulation material (a thick, bentonite-loaded fluid containing wood chips and cottonseed hulls) reduced fluid losses to 10% and finally restored full circulation by the following day. When the bit was pulled, it exhibited "flats" on all three cones, and an additional 12 lb (5.4 kg) of metal cuttings was found in the junk basket. The tight section of casing between 2380 and 2410 ft (725 and 735 m) was then milled, but when the next bit was run in to wash and clean the borehole below 2420 ft, circulation was lost twice—probably because the lost-circulation materials again proved insufficient for sealing off the severely underpressured loss zone in the Sandia limestone above. Circulation was restored once again by the addition of more lost-circulation material.

Shortly thereafter, circulation was lost again in the same region (ca. 2380 ft). Additional cement (300 sacks) was pumped through the hole

and/or splits in the casing into the cavernous limestone on top of the granitic surface, followed by 590 gal. (2300 L) of displacement water. The next day, the cement was drilled out to a depth of 2417 ft (737 m) with full returns. Drilling-out of fill and debris continued to 2602 ft (793 m)—at which point circulation was again completely lost. With the fluid level in the borehole at about 1700 ft (500 m) below ground, a 4200-gal. (16 000-L) "pill" of high-viscosity lost-circulation material was pumped through open-ended drill pipe (run in to a depth of 1525 ft) and was followed by 600 sacks of cement. On May 28, drilling resumed and succeeded in deepening EE-2 by about 22 ft, to 2641 ft (805 m); but then circulation was completely lost once more.

Yet another massive cementing operation was now decided upon. First, RFC (200 sacks) was pumped into the hole; it was followed by 1000 sacks of cement and then by another 1000 sacks of cement mixed with 400 sacks of silica flour. (Cementing jobs were now requiring more and more massive amounts, because the milling and cutting of the casing in several places had created new openings into the lost-circulation zone.) A steel-toothed bit was used to drill out the cement in the 1358- to 2391-ft (414- to 729-m) depth interval, *finally* restoring full circulation. Over the next 16 days, new drilling in the basement rock deepened the hole by nearly 1700 ft (518 m), to 4340 ft (1323 m)—an average of just over 100 ft/day.

On June 19, after eight hours of very rough drilling at about 4340 ft with essentially no penetration, the bit was withdrawn for examination. Two 12-in. blades were missing from one of the blade stabilizers of the bottom-hole assembly (BHA). After two retrieval attempts with a magnet, one of the blades was recovered, and a third attempt brought up several pounds of metal cuttings. When two further retrieval attempts produced nothing, a hard-formation bit was run in to crush the remains of the blade left in the hole. In the junk basket were found the badly worn ends of the blade, and one more pass with the magnet brought out the central piece.

Note: When the original two boreholes, GT-2 and EE-1, were drilled under the direction of Laboratory personnel, more expensive roller stabilizers were used instead of blade stabilizers. These were very effective and created no problems requiring fishing operations.

On June 22, during drilling at a depth of 4362 ft (1330 m), circulation was completely lost once again. According to a Laboratory temperature survey, the problem zone was in the 1800- to 2400-ft (550- to 730-m) depth interval. A retrievable casing squeeze packer was run in on drill pipe to a depth of 1508 ft (460 m), and the annulus above the packer was then filled to the surface with water to maintain a backpressure on the packer. A quantity of RFC (200 sacks) was then pumped in below the packer and through the splits and holes in the 13 3/8-in. casing, followed by 500 sacks of cement. After the cement had set, the packer was retrieved and the residual cement was drilled out.

Three days of steady drilling began June 25, with full returns. With the hole depth now at 4855 ft (1480 m), a Maurer turbodrill was employed for the first time, in a test run, at a modest hole temperature of about 115°C. Driving a Security H-100 bit (a TCI button bit designed for drilling extremely hard rock), the turbodrill deepened the hole 57 ft, to 4912 ft, in 3h 45 min.—an average of 15.2 ft/h. In contrast, the previous conventional (rotary) drilling run with a comparable 12 1/4-in. button bit, had drilled 493 ft of hole in just over 53 h—an average of 9.2 ft/h.

As drilling progressed in the crystalline basement, the deviation of the hole had been gradually increasing to the west, reaching an inclination from vertical of 6° by 4870 ft (1484 m). (Note: EE-2 was surveyed periodically, to monitor its trajectory, to a depth of 15 273 ft, close to the final TD. All these surveys were done with an Eastman Whipstock magnetic, single-shot survey tool run on a wireline.) Drilling over the next seven days—through July 7—was steady, with only minor problems, and deepened the hole to 6492 ft (1979 m).

A Last-Minute Change in the Planned Drilling Direction

As outlined above, the Phase II reservoir development plan called for drilling the EE-2 and EE-3 boreholes directionally across (orthogonal to) the strike of the two principal joints opened by pressurization of EE-1 during the development of the Phase I reservoir. These joints exhibited a roughly N55W strike (Fig. 4-28), meaning that the azimuth of the directionally drilled portion of EE-2 *should have been* N35E. However, in a last-minute revision to the drilling plan, the azimuth for the last 3000 ft of directional drilling was inexplicably changed to N70E.

This new azimuth would be roughly orthogonal to the array of joints stimulated during Expts. 203 and 195 (mid March 1979), and it is possible that the change in plan was based on the seismic results of those experiments (see Chapter 4, Fig. 4-20). The drilling plan for EE-2 produced by Grace, Shursen, Moore & Associates in 1978 (reproduced as Appendix E of the 1979 Annual Report) had specified a drilling direction of N45E. This direction was reiterated in the 1980 Annual Report (as ". . .in a northeasterly direction, approximately perpendicular to the northwesterly strike expected of the hydraulic fractures"). There is no information in the reports of the time explaining how or why the change to a N70E direction came about.

Because of the tendency of the borehole to drift northward, the major consequence of the change in azimuth to N70E was that the Maurer turbodrill had to be used repeatedly to turn the borehole back toward the east. The high rotational speeds of the turbodrills meant

faster drilling rates, but also very severe gauge wear on the bits; the drilling runs were therefore very short, averaging about 60 ft. In addition, each turbodrilled interval had to be reamed with a conventional drilling assembly, which added considerably to the cost and complexity of the directional drilling. Nevertheless, the N70E azimuth would be maintained or even exceeded during most of the directional drilling of EE-2 (reaching almost N80E below 14 000 ft). Later, this N70E azimuth would be maintained for the directional drilling of EE-3.

It would turn out that the maintenance of this very difficult azimuth for over 6000 ft of directional drilling in EE-2 had absolutely no relevance to the ultimate development of the Phase II reservoir.

Directional Drilling

At the new TD of 6492 ft, the trajectory of the EE-2 borehole was S77W, 5 1/2°. Because the azimuth was about 180° from the newly mandated one (N70E), on July 8, 1979, directional drilling began to rotate the hole—first toward the north and then around toward the east.

The directional-drilling strategy for EE-2 was to alternate runs of a downhole motor guided by a steering tool (which primarily changes the azimuth of the borehole) with runs of a rotary drilling assembly (which primarily deepens the hole while maintaining or perhaps increasing the inclination and, secondarily, eases tight zones and/or reams out sections left undergauge by the turbodrill). Once the borehole inclination had reached about 35°, rotary drilling with a "stiff" angle-maintaining assembly would be used to deepen the borehole without changing the azimuth.

During the first of the downhole motor runs, an Eastman Whipstock wireline-guided Directional Orientation Tool (DOT) was used to control the direction. But the DOT was plagued by intermittent signal losses, and the hole direction had to be checked every 60 to 90 ft with a single-shot tool.

The PDMs—Dyna-Drill and Baker—used for directional drilling proved to be quite successful at this depth and temperature (130°C). Between motor runs with the directional-drilling equipment, the hole was reamed and deepened with stiff rotary drilling assemblies to maintain inclination and azimuth. By July 15, the hole had been deepened to 6818 ft (2078 m); its trajectory was now N37W, 4 3/4°, representing a change in direction of 66°.

By July 18, another motor run had increased the hole depth to 7184 ft (2190 m) and rotated the borehole an additional 76°, to N39E at an inclination of 3 1/4°. Over the next five days, angle-building, rotary drilling assemblies were used to deepen the hole another 1020 ft, to 8204 ft (2501 m). The inclination was increased at a rate of just over 1° per 100 ft, but the azimuth of the hole was now drifting back to the north (from N40E to N13E). In an

attempt to correct this drift, a Dyna-Drill motor was employed again, but after drilling had progressed just 22 ft, the motor failed. The temperature at this depth was about 140°C.

Directional drilling with the turbodrills and the Eastman Whipstock DOT continued through August, with numerous interruptions for reaming and for repairing small washouts at drill-pipe tool joints. By August 14, with the hole depth at 9082 ft (2768 m), the inclination had been increased to 15° and the direction corrected to N34E. At this point, the poorly performing Eastman Whipstock DOT was replaced with a Sperry-Sun "Hades" wireline directional tool; but this tool did not operate well in the very high downhole temperatures either, and three of them failed in succession. The remaining directional drilling would be completed with a Scientific Drilling Controls EYE tool; by monitoring the orientation setting and progress of the downhole motor, this tool enabled better control of the trajectory. (Note: most of the directional drilling still lay ahead, and at ever-increasing downhole temperatures.)

For the next stretch of directional drilling (684 ft), which ended on September 2, five different Maurer turbodrill runs were interspersed with rotary reaming and drilling runs, in an attempt to control the borehole trajectory. But even with the EYE tool, the net result was that the inclination of the hole *decreased* by 3° (to 12°), while the azimuth "bounced around" but ended up somewhat increased (by 8°), to N42E, at a depth of 9766 ft.

By September 9, the depth of the hole had reached 9917 ft (3023 m), and two runs with a Baker PDM (also guided by the EYE tool) had increased the inclination of the hole from 12° to 16 1/4° and turned the azimuth farther to the east, to N59E. Although by now the bottom-hole temperature had increased to about 180°C, a poor Maurer turbodrill run (which managed to drill only 20 ft) led the drilling supervisors to return to the Baker PDM. In spite of the temperatures, the Baker motor was able to drill 63 ft—at least partially dispelling the notion that these PDMs were inferior to the Maurer turbodrill in all high-temperature conditions.

By September 12, three more Maurer turbodrill runs had increased the hole depth to 10 035 ft (and dropped the inclination back slightly, to 15 1/2°). While the region near the bottom of the hole was being rotary-reamed (always a necessity following Maurer turbodrill runs), circulation was lost. The drill pipe was immediately withdrawn, and the lost-circulation zone was identified by a temperature survey as lying within an interval of damaged casing between 1800 and 2000 ft. A caliper log revealed that there was a new break in the 13 3/8-in. casing at a depth of approximately 1800 ft. A mixture of 200 sacks of cement with additions of Gilsonite (12.5%) and Celloflake (0.25%) was pumped down the empty casing through five stands of open-ended drill pipe. The mixture was followed, half an hour later, by an additional 400 sacks of cement—but this time, the cement was not followed by displacement water. The top of the cement plug was encountered at a

depth of 1380 ft (421 m); when the plug had been drilled through, its lower end was measured at 1865 ft (568 m), indicating that the amount of cement retained within the casing was about 250 sacks (the remaining 350 sacks would have gone into the lost-circulation zone below).

Further rotary drilling on September 15 succeeded in deepening the hole, but by only 32 ft—to 10 067 ft (3068 m)—and the bit was now showing signs of being plugged. Drilling was halted, and during an attempt to clear the plug, the drill pipe parted at a depth of 4549 ft (1387 m). Dia-Log, Inc., of Odessa, TX, was called out for free-point determinations and break-out services. After several back-off attempts, the upper part of the drill string was unscrewed at a depth of 6510 ft (1980 m) and removed from the hole. One more back-off then succeeded in unscrewing and removing an additional 3100 ft of the drill string, clearing the borehole down to 9612 ft (2930 m).

The next 18 days were occupied with fishing operations to clear the rest of the hole of drill pipe and the stuck BHA. During this period, 8000 ft of wireline was also lost in the hole. An attempt to retrieve the wireline with "spaghetti pipe" ended when the spaghetti pipe itself broke downhole. These fishing tools then had to be themselves fished out, and on top of everything the drill pipe broke in the hole several more times. At last, on October 6, Dailey jars set for 90 000 lb_f were used to remove the stuck BHA.

Rotary drilling finally resumed on October 7. A 403-ft (123-m)-long angle-building rotary drilling assembly was employed to drill 366 ft (112 m) of new hole, to a depth of 10 433 ft. In the course of drilling, the inclination of the hole was increased from 15 1/2° to 17° in a N77E direction. The Maurer turbodrill, with the EYE tool, was then used to deepen the hole another 119 ft (to 10 552 ft) and to increase the inclination to 21° while decreasing the azimuth by 7° (to N70E).

After the hole had been reamed, rotary drilling recommenced on October 14 with a more "limber" BHA that incorporated smaller-diameter drill collars (6 5/8 in. in place of 8 in.). This assembly proved to be much more successful in building hole angle. Over the next 24 days, the hole was deepened by 1024 ft, to 11 576 ft (3528 m), while its inclination was increased from 21° to 34 1/2°, very close to the target inclination of 35°. By now, the azimuth of the hole had drifted back toward the north by 23°, to N54E.

Borehole-Reduction Drilling, Coring Runs, and Attempt to Repair the 13 3/8-in. Casing

On November 7, 1979, drilling began to reduce the 12 1/4-in. borehole to a final size of 8 3/4 in. (22 cm), in two 20-ft stages: first to 11 596 ft (3577 m) with an 11-in. (280-mm) bit, and then to 11 616 ft with a 9 5/8-in. (244-mm) bit. Finally, the hole was drilled ahead 118 ft (to a depth of 11 734 ft) with an 8 3/4-in. bit. A 7 7/8-in. STC Stratapax core bit (pictured in Chapter 4, Fig. 4-3) was then employed for the first of seven coring operations.

A length of core measuring approximately 4 ft (1.2 m) and having a diameter of 3 in. (7.6 cm) was obtained from the 11 734- to 11 743-ft (3577- to 3579-m) depth interval. Drilling with 8 3/4-in. bits then continued for the next nine days (interrupted by frequent on-bottom milling and by magnet runs to retrieve lost bit cones and pieces of the 13 3/8-in. casing that had fallen down the hole). Surveying at a depth of 12 266 ft (3739 m) showed a hole trajectory of N59E, 35°.

The second coring run took place on November 20, between 12 266 and 12 276 ft (3739 and 3742 m). This run saw the first attempt to orient a core; the selected device was an Eastman Whipstock core-orienting tool protected with a heat shield. To help preserve the film within the tool, the bit was pulled after only 10 ft of coring; even so, the "temperature-hardened" orienting tool suffered severe heat damage, to the point that the film was blackened and thus yielded no orientation information. In addition, no core was recovered (the cuttings indicated that the zone in which coring had been attempted was highly jointed). On November 26, after four rotary drilling runs had deepened the hole by 572 ft, the third coring operation recovered 8 ft of core between 12 848 and 12 856 ft.

Drilling with 8 3/4-in. bits continued for another 11 days, but considerable reaming and working of the drill string was needed to keep its pulling force below an acceptable limit (400 000 lb). On December 2, all the standard drill collars (except the nonmagnetic Monel collar)—weighing a total of some 30 000 lb—were removed from the BHA to reduce downhole torque and drag. The BHA then consisted of a bit, a junk basket, a 6-point roller reamer, a 3-point roller reamer, a short drill collar, a second 3-point roller reamer, the Monel collar, and a third 3-point roller reamer; above the BHA were nine joints of heavy-weight drill pipe (HWDP), a jar, and two more joints of HWDP. To reduce hole drag, the Baroid friction-reducing agent Torq-Trim II, a triglyceride-alcohol mixture, was added to the circulating fluid (at a rate of approximately 125 gal. [475 L] /day) for the remainder of the drilling.

The fourth core was cut on December 8, between 13 454 and 13 464 ft (4101 and 4104 m). In the course of further drilling, numerous magnetic single-shot survey attempts either yielded no picture or ended with the tool stuck in the pipe. On December 12, drilling was suspended at a depth of 13 657 ft (4162 m) so that extensive reaming operations could be carried out to try to reduce hole drag. A reamer assembly, consisting of a bit and a string reamer, was run in to ream out doglegs present at depths of 3050 ft (930 m), 6600 ft (2010 m), and 6900 ft (2100 m). During this time, the drill string was inspected (by Tuboscope Inspection Service) and the tool joints on the drill pipe were hard-banded. Rotary drilling of the 8 3/4-in. hole recommenced on December 20 and reached a depth of 13 955 ft (4253 m)—298 ft in 22 hours, for an average penetration rate of 13 1/2 ft/h! (To this day, this is an outstanding performance for a TCI bit drilling in granitic rock.) The trajectory of the hole at this depth was N74E, 35°.

Note: Eight months later, temperature measurements would show that at a hole depth of just 12 700 ft, the actual formation temperature already exceeded the target temperature of 275°C. Unfortunately, no diagnostic temperature measurements were done in late 1979, even with the hole TD now close to 14 000 ft. Had they been done, it would have been clear that all the objectives of the EE-2 portion of the Phase II reservoir development plan had essentially been met. The 9 5/8-in. casing string could have been run at this time (December 20, 1979), to isolate the projected reservoir interval below 11 500 ft (3500 m) from all the region above, and the job would have been done! More than four months of time and well over $2 million in direct project costs (for rig time, contract drilling supervision, special tools, commercial logging, fishing operations, etc.) would have been saved—as would the cost of an additional 4 1/2 months of support provided by the Laboratory's Borehole Instrumentation Group (for temperature and TV surveys as well as numerous other site support activities).

The fifth coring operation was begun soon after the 22 hours of drilling to the new TD. While the coring assembly was being washed to bottom, a 90% loss of returns occurred, which then gradually dropped below 30%. It was decided to continue the coring run and to later do a temperature survey to locate the depth of the fluid loss (probably again somewhere in the damaged region of the 13 3/8-in casing). A 7 1/2-ft length of core was obtained between 13 955 and 13 963 ft (4253 and 4256 m).

Temperature surveying on December 21 revealed that fluid losses were occurring at a depth of about 2375 ft (724 m). The next day, while the drill pipe was being run in (in preparation for cementing operations), an obstruction was encountered at 1762 ft (537 m) in the 13 3/8-in. casing string. An impression block, run in on drill pipe, confirmed that the collapsed casing below that depth had suffered further damage.

The next three months turned into an absolute driller's nightmare. The collapsed 13 3/8-in. casing string, with its multiple tears and holes, was rapidly deteriorating, in addition to which large quantities of fluid were repeatedly disappearing through breaks in the casing into the seemingly boundless lost-circulation zone just above the Precambrian basement. Attempt after attempt to repair the casing, undertaken concurrently with efforts to control the fluid losses into the lost-circulation zone, brought more frustration than success. The major "weapon" being used to combat fluid losses was a succession of ever larger cementing operations, to try to close off the lost-circulation zone. These involved a wide variety of cement formulations and approaches—all of which turned out to be futile (in terms of stopping the losses for more than just a few days). The eventual total of 22 remedial cementing jobs took 6600 sacks of cement, equivalent in volume to more than 10 000 ft^3.

Multiple operations were carried out in an attempt to open up the collapsed casing: numerous runs with casing rollers or string reamers, others with mills (concave-faced, flat-faced, and tapered) or swedges, interspersed with magnet runs to collect the accumulated metal pieces and grindings. A wireline video camera was used to survey the damaged casing at critical points, and when larger tools would not pass through restricted areas of casing, lead impression blocks were run in on drill pipe to assess the nature of the blockage.

That the casing was continuing to deteriorate was clearly illustrated by two video camera surveys. The first, run on December 29, revealed that an "obstruction" at 1792 ft was in reality a large split, where the casing was folded inward like the lid of a tin can. Above this zone of split casing, in the 1762- to 1783-ft depth interval, the video camera also observed numerous smaller splits (ranging from about 1/4 in. to 3 in. wide), through which rubble could be seen behind the casing. Then, on January 6, 1980, just a week after the camera had been lowered to 1793 ft, another camera run could not progress beyond 1771 ft, at which depth new damage—jagged pieces of metal—could be seen.

On February 1, a 12 1/4-in. combination mill-and-swedge assembly was successfully worked through the damaged casing. It was then used to clean the open-hole portion of the borehole all the way down to 9100 ft (2790 m), clearing it of the debris that had fallen down the hole during the many casing repair operations (the mill-and-swedge assembly probably just pushed much of the accumulated debris ahead of it). On February 7, while the section of the borehole below 11 000 ft was being cleaned of debris, circulation was again lost through the damaged 13 3/8-in. casing at a depth of about 2350 ft. Another month and a half of cementing attempts, interspersed with milling, reaming, and swedging operations, ensued. Finally, on March 22, after three months of agony, frustration, and expense, the contract drilling supervisors decided to abandon further efforts to seal off the cuts and splits in the 13 3/8-in. casing and to run the 9 5/8-in. casing string as soon as possible to save the hole!

Running and Cementing of the 9 5/8-in. Casing

The borehole would need to undergo an extensive cooldown before the casing could be run, which would require large amounts of water (owing to the continuing loss of fluid into the cavernous limestone overlying the granitic basement). The water was hauled to the site by truck, at that time the only way to obtain such large amounts. A 12 1/4-in. bit was run in on the 5-in. drill pipe, then cooldown pumping began and continued at a rate of approximately 800 gpm (50 L/s) for three days, after which the drill pipe was withdrawn. On March 28, the 9 5/8-in. production casing was run in to

the setting depth of 11 578 ft (11 351 ft TVD).[5] Cooling water was again pumped down and around the casing, at rates of 500–800 gpm (31–50 L/s), for another four days.

The original drilling plan called for cementing the 9 5/8-in. casing to the surface in four stages, to limit the external pressure that would be exerted against it (a full 11 578-ft column of cement outside the casing, at a density of about 2 g/cc, would exert a pressure of about 5000 psi (34.5 MPa)—possibly sufficient to cause collapse of the casing and/or breakdown (hydraulic fracturing) of the rock mass near the bottom of the borehole. For this reason, three stage collars were to be placed in the casing string, at about 8000 ft (2440 m), 5000 ft (1520 m), and 2000 ft (610 m). At the last moment, however, the plan was considerably revised: not only was the drilling of EE-2 now far over-budget, but it was becoming clear that a multiple-stage cementing job would be more complex and difficult than originally thought. In particular, the cementing job planned for the section of hole above the stage collar at 2000 ft would not work at all because of the numerous holes in the surrounding 13 3/8-in. casing, which opened directly into the massive loss zone beyond. Given these considerations, the decision was made to tag-cement only about the bottom 1000 ft (300 m) of the casing, leaving the remainder of the annular space (between the top of the cement and the static water level at about 1700 ft) filled with water.

The tag-cementing job began with the pumping of 13 700 gal. of a heavy, barite-loaded mud (having a density of about 2 g/cc) down the casing to stabilize the open hole below the casing shoe and to prevent the cement from flowing on down the inclined borehole. The mud was followed by 200 gal. of water. Then the bottom wiper plug was dropped, and a slurry of 3100 gal. of cement and silica flour was pumped on top of it (an amount that ended up filling about 960 ft of the annulus). Next, the top wiper plug was released and displaced with water to the bottom of the casing. It landed in the float-collar plug catcher and held pressure. As soon as possible after the tag cementing, the drill string was run in open-ended to just above the float collar at 11 496 ft, for the post-cementing cooldown. For four days, water was circulated down the drill pipe and up the annulus between the drill pipe and the casing, at 200 gpm (13 L/s).

On April 3, a Dia-Log caliper log was run to a depth of 11 493 ft (3504 m) to obtain baseline measurements of the diameter of the production casing. After rubber protectors had been installed on the drill-pipe tool joints to protect the casing during subsequent downhole work, the float collar and plugs were drilled out and work began to drill up/mill up the considerable debris left in the hole below the casing setting depth of 11 578 ft.

[5]This depth was selected to coincide with that of the ledge formed when the 12 1/4-in.-diameter hole was reduced to 11 in. in diameter (November 7, 1979—see above).

Final Drilling

Milling and cleaning of the hole to TD continued until April 24, 1980, when new footage was drilled for the first time in 126 days (since December 21, 1979). By May 1, with only minor difficulties, EE-2 had been deepened from the previous TD of 13 963 ft (4256 m) to 14 501 ft (4420 m). The next day the sixth coring run took place: a 7 7/8-in. core bit was used to retrieve approximately 3 ft of core from the depth interval 14 501–14 504 ft. An Eastman Whipstock magnetic multishot tool having a wireline insertion and recovery mechanism was also used during this run, in a second attempt to obtain oriented core. But the overshot grapple on the wireline came unscrewed during insertion, making early recovery impossible. When the tool was withdrawn with the bit, it was found that excessive heat had damaged both the film and the tool. Preparatory to the seventh (and final) coring run, the borehole was deepened to 14 962 ft—458 ft in 42 hours, for an average penetration rate of 10.9 ft/h.

On May 6 the crew recovered 2 ft (0.6 m) of core from the depth interval 14 962–14 966 ft. Then, with only one additional drilling run needed to complete EE-2 to its target depth, the newly developed STC 8 3/4-in., 7GA rock bit was used for a final rotary drilling run from 14 966 ft to 15 273 ft, which took just 22 1/2 hours—an outstanding penetration rate of 13.6 ft/h.

Note: It turned out that none of the seven EE-2 coring runs (one of which recovered no core) contributed significantly to the knowledge base required to further develop the HDR concept. The money and effort could have been better spent in other ways.

Two very brief turbodrill runs on May 12 (test runs of the smaller, 5 3/8-in. [137-mm] Maurer turbodrill) then deepened the hole by another 16 ft. Its final TD was 15 289 ft (4660 m), corresponding to a measured TVD of 14 405 ft (4391 m). An Eastman Whipstock magnetic single-shot survey, at a depth of 14 962 ft, showed its final trajectory as N79E, 35°—even farther to the east than the intended N70E azimuth. In August 1980, a gyroscopic survey was run by Sperry-Sun to check the cumulative trajectory data obtained during drilling (Eastman Whipstock magnetic single-shot surveys). The results did corroborate the earlier ones: the two types of data coincided almost exactly.

The borehole as completed is shown schematically in Fig. 5-4. The measured bottom-hole temperature was 317°C.

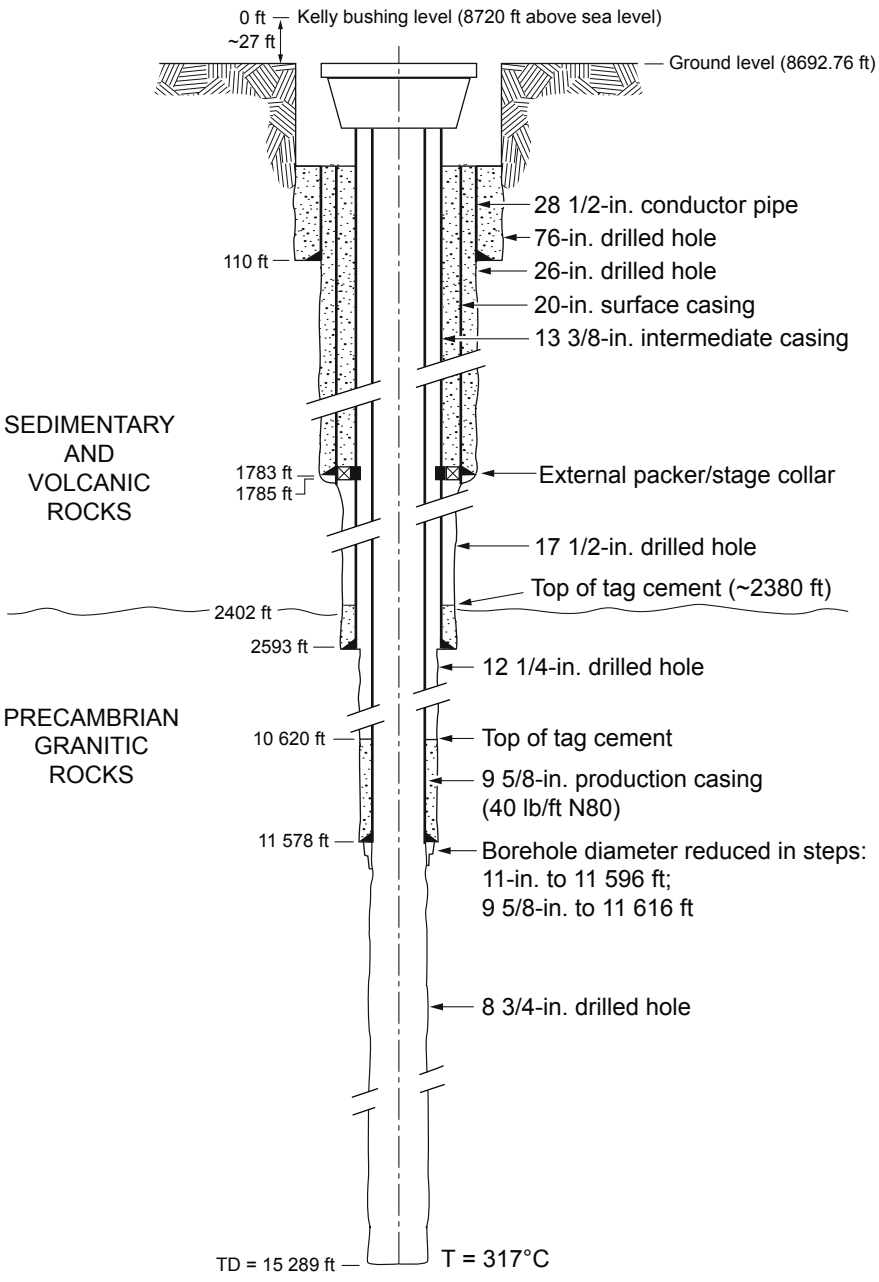

Fig. 5-4. Schematic diagram of the EE-2 borehole as completed.

Reflections on the EE-2 Drilling Operation

Table 5-1 lists the time spent on each of the principal activities that took place during the drilling of EE-2 (as a percentage of the total time, 410 days). As can be seen, activities to remedy problems occupied 34.5% of the time, or 141 days. Of course, not all of these problems were associated with directional drilling; but as explained earlier, that part of the drilling operation was based on the "Phase II assumption" (that the vertical joints stimulated during Phase I would also constitute the major flow paths in the Phase II reservoir region)—an assumption that would later prove wrong. In other words, in the time (and for the money) spent only on drilling problems, the entire EE-2 borehole could have been drilled vertically to 14 500 ft—which would have been all that was required. (In the final analysis, the directional drilling of the lower part of EE-2 would not contribute in any way to the development of the Phase II reservoir, and would actually turn out to be an impediment.)

Table 5-1. Time spent on principal activities during the drilling of EE-2 (410 elapsed days)

Activity	Incremental time (%)	Cumulative time (%)
Drilling-related		
Drilling	15	
Tripping drill pipe	24	
Reaming	5	45.5
Coring	0.5	
Directional drilling	1	
Remedial operations related to		
Collapsed casing	23	
Fishing	8	
Lost circulation	2.5	34.5
Failures of directional-drilling tools	1	
Casing-related		
Running casing	3	
Circulating to cool	3	7
Cementing	1	
Logging		3
Other activities		10

As shown in Figs. 5-5 and 5-6 (plan and sectional views), EE-2 was drilled essentially as planned—albeit with a final azimuth below 14 000 ft of about N80E (Fig. 5-5); but the final depth was greater (14 405 ft TVD instead of the target 14 000 ft), and the bottom-hole temperature was higher (317°C, instead of the target 275°C). As mentioned earlier, it is puzzling why drilling was not stopped months sooner (in late December), at a borehole depth just shy of 14 000 ft and a rock temperature well in excess of the 275°C objective!

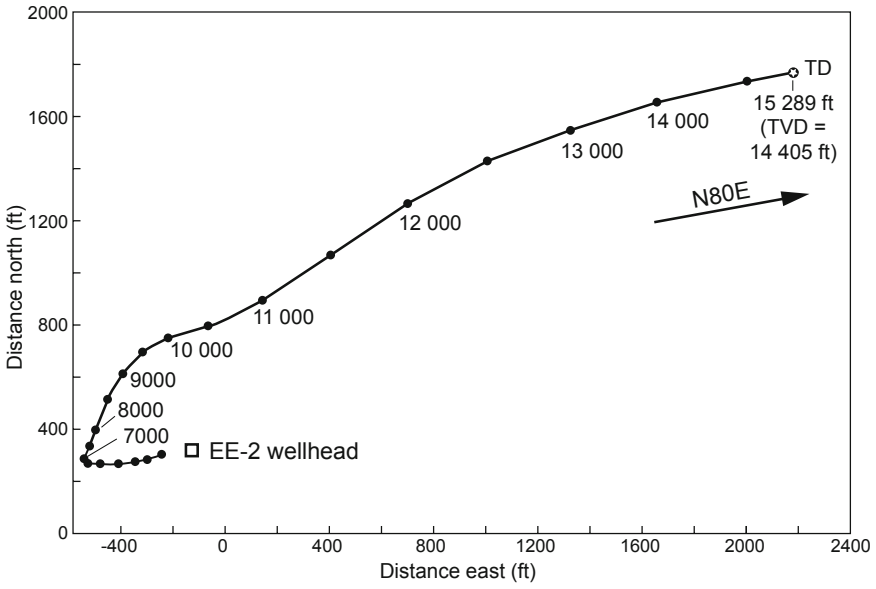

Fig. 5-5. Plan view of the EE-2 borehole trajectory, based on data from a magnetic multishot survey following completion of the borehole. Adapted from Helmick et al., 1982

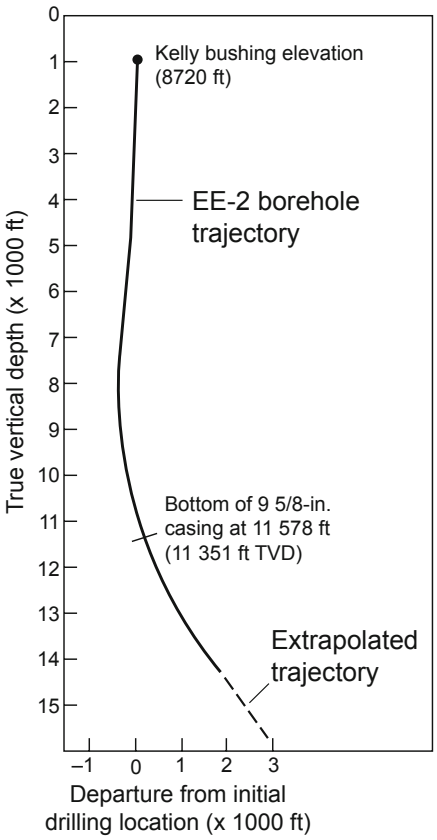

Fig. 5-6. Sectional view of the EE-2 borehole trajectory, projected onto a N71E–S71W vertical plane (from magnetic single-shot survey data). Adapted from Helmick et al., 1982

Equipment and Materials: Performance in the EE-2 Borehole

Drilling Fluids

The drilling fluids used in EE-2 were essentially the same as those used in the two boreholes drilled earlier at Fenton Hill: bentonite mud with lost-circulation additives for drilling in the volcanic and Paleozoic rocks, and water with moderate amounts of various corrosion- and friction-reducing additives for drilling the very hard rock of the crystalline basement.

Volcanic and Paleozoic Sedimentary Rocks

While the 26-in.- and 17 1/2-in.-diameter sections of the borehole were being drilled, a polymeric flocculant was used to keep the hole clean and control the buildup of natural "mud" in the drilling fluid, generated from the red shales of the Abo and Madera formations. In the two previous boreholes (GT-2 and EE-1), filtration-reducing agents had been used during drilling through these shales, to protect the walls of the borehole from water adsorption (and consequent hydration and swelling); but none were used in EE-2. No appreciable increases in natural mud solids or problems with wall instability were noted as a result of this omission (that is, until the later encounter with the massive lost-circulation zone, when the hole was emptied of drilling fluid down to about 1700 ft, resulting in sudden loss of control of the now-exposed clay sections of the Abo and Madera formations—see below). When the known lost-circulation zone at about 1900 ft was being drilled through, pre-treatment of the drilling fluid with 20% lost-circulation materials limited fluid losses to only about 1500 gal. (5700 L), a great improvement over the previous lost-circulation episodes at about this depth in GT-2 and EE-1.

When the major lost-circulation zone—the cavernous limestone region in the lowermost part of the Sandia Formation just above the granitic basement—was reached in late April 1979, the drilling supervisors resorted to drilling ahead without returns to a depth of 2593 ft (790 m). Over the next 11 months (until the running and cementing of the 9 5/8-in. production casing in late March 1980), very large amounts of drilling fluids and water were lost into the cavernous limestone, through the numerous cuts and splits that had developed in the collapsed 13 3/8-in. casing. Large amounts of supplemental water were of course needed during this period, and were trucked to the site. But for the most part, the massive losses of fluid were not accurately recorded at the time—no doubt because of the severe drilling difficulties that constantly occupied the attention of the crew.

Precambrian Crystalline (Plutonic and Metamorphic) Rocks

Drilling of the Precambrian crystalline-complex rocks required a completely different drilling fluids program from that used for drilling the volcanic and sedimentary rocks above. Problems associated with this major portion of the hole included extreme abrasiveness, extreme temperatures (as high as 317°C), and occasional instability in some fractured zones. Below a depth of about 6500 ft (1980 m), directional drilling rotated the azimuth of the hole from west to almost due east and gradually increased the inclination from near vertical to 35° from vertical, which (in combination with the abrasiveness of the formation) caused significant torque and drag problems.

Drilling fluid costs reached their highest levels by far on those occasions when circulation was completely lost into the cavernous limestone overlying the granitic basement. Each time, the entire drilling fluid inventory had to be replaced.

When lost circulation was not a problem, and drilling was proceeding with full returns, other factors controlled the amounts of drilling fluid needed, and hence the cost. For example, the use of Torq-Trim II increased the cost of drilling fluids by about one-third. This organic lubricant, which cut drilling torque almost in half (a number of twist-offs—parting or breaking of the drill pipe at tool joints—were attributable to a combination of fatigue, torque, flexure, and tension applied to the tool joints), was effective only at temperatures below 190°C; and large volumes—on the order of 400 000 gal. (1 500 000 L)—of circulating drilling fluid were required for adequate cooling during its use. High temperatures caused the Torq-Trim to degrade into what became known as "black gunk," a very thick mixture of the "cooked" lubricant combined with drill cuttings (mostly sand) and other drilling residue, that was found coating the surfaces of the casing, of the open hole, and of logging tools and other instruments run into the hole. In addition, given the high torque and drag, minimizing corrosion-related failure of the drill pipe was a concern. The use of an ammonium bisulfite oxygen scavenger and an organic descaler in combination with caustic soda, which maintained pH in the range of 9–10, kept corrosion well below the standard 2 lb/ft^2/yr. Again because of the high temperatures, large volumes of circulating fluids were needed when these products were in use, which also raised the cost of drilling fluids by about one-third.

Bits Used in the Crystalline Basement Rocks

The 12 1/4-in.-diameter section of the EE-2 borehole in the basement rock (2593–11 576 ft) was drilled with TCI button bits, typically having sealed bearings. A 6-point TCI roller reamer was almost always positioned directly above the bit to maintain the gauge of the hole as the bit gauge wore down. (In addition, when an angle-maintaining rotary drilling assembly was being used, 6-point roller reamers were positioned within the drill collars.) Even so, the very abrasive drilling environment meant that bit life was typically shorter than under normal conditions. The performance of the TCI bits used with the Maurer turbodrills was predictably poor; at the turbodrills' much higher rotational speeds (350–500 rpm), gauge wear was severe and greatly reduced the useful life of the bits.

The 8 3/4-in.-diameter section of the borehole (11 616–15 289 ft) was also drilled with TCI button bits, along with 6-point TCI roller reamers to help maintain the gauge of the hole. This deeper section of EE-2 was drilled at an ever-increasing angle to the east, under the erroneous "Phase II assumption" that the hydraulic fractures created from this borehole would be essentially vertical, continuous, and striking approximately northwest. Thirty-one 8 3/4-in. bits were used to drill this portion of EE-2, twenty of which were geothermal bits specially designed and manufactured by STC for drilling in hot, deep, granitic basement rocks. These TCI bits, Model 7GA, were

open-bearing (i.e., nonsealed, so that they could be cooled and lubricated by the drilling fluid). Additional features that made them more durable and effective than other then-available TCI bits were

- harder carbide buttons on the gauge row of the cones,
- hard facing for extra wear resistance on the structural members that anchor the cutting wheels,
- built-up wear pads and carbide inserts on the shanks,
- additional clearance in the open bearings to permit greater circulation of drilling fluid.

These features increased the life of the STC 7GA bits, one consequence of which was to reduce the number of times the BHA had to be withdrawn from the hole to replace a worn bit. This advantage alone more than offset the 10% higher cost of these bits. They became the preferred bit for all the deeper, hotter drilling at Fenton Hill.

The bit selected for coring in EE-2 was the STC hybrid roller-cone Stratapax with polycrystalline-diamond cutters. (The modified JOIDES bits that had been used for coring in GT-2 and EE-1 gave fair results in both core recovery and bit life, but only at moderate depths and lower temperatures; and the diamond-core bits that had been tried, while yielding good core, were too costly for extensive use because of their extremely short bit life—typically only about 5 hours, translating to less than 5 ft of core at a cost of over $10 000 for the bit alone.) The Stratapax bit had a 7 7/8-in. (200-mm) outer diameter and a 3-in. inner diameter (i.e., cores cut with this bit would have a 3-in. diameter); it incorporated four cones with TCI buttons and four (instead of the prototype six) polycrystalline-diamond cutter pads mounted on tungsten-carbide pedestals. The bit was used with a 15-ft (4.6-m)-long Hycalog core barrel having an outer diameter of 6 1/4 in.

Rotational speeds during coring ranged from 35 to 50 rpm and bit weights from 10 000 to 20 000 lb. A bit was replaced when its penetration rate slowed to about half the initial rate. The condition of five of the Stratapax core bits was evaluated by STC after use in EE-2. The overall appearance of the cutting elements was very good, according to STC, with no excessive wear noted. The bits used for coring runs 1 and 3 could have been reused by replacing the polycrystalline-diamond cutter pads and the pedestals; the bit from Run 2 was in good enough condition to be reused in Run 7; and the bit from Run 5, also in good condition, was reused for Run 6 (during which the pedestals broke off). Despite breakage of the Stratapax pedestals and wearing of the seals when exposed to higher-than-expected temperatures, the overall good performance of these bits makes them the first choice for future coring operations in abrasive crystalline rock.

Directional Drilling Equipment

Motor-Driven Equipment

Table 5-2 gives particulars on the three types of downhole motors used for directional drilling in EE-2.

Table 5-2. Downhole motors used in EE-2

Type	Diameter, in. (mm)	Temperature rating (°C)	Length, ft (m)	Supplier
PDM*	6 3/4 (170)	~175	20 (6.1)	Baker Service, Houston, TX
PDM	7 3/4 (200)	~155	20 (6.1)	Dyna-Drill, Smith International, Irvine, CA
Turbodrill	7 3/4 (200)	~320	20.7 (6.3)	Maurer Engineering, Houston, TX

*Postive-displacement motor
Source: Helmick et al., 1982

The high-temperature turbodrill, which was developed jointly by Los Alamos and Maurer Engineering, Inc., of Houston, Texas, required the use of a steering tool. Of the three different types of steering tools tried in EE-2, only one—the Scientific Drilling Controls EYE tool—displayed the capability to perform reliably at temperatures above 200°C. Many of the failures of the other steering tools can be attributed to thermal degradation of the cablehead and wireline.

A turbine tachometer (rpm indicator) enabled the speed of the downhole motor to be determined from the surface: as the shaft of the turbine revolved, perturbations in the blades generated pressure pulses that were then transmitted through the fluid column in the drill string to the surface, driving the tachometer. To improve the resolution of the pressure-pulse signal, nitrogen-operated dampers were placed in series in the fluid column, at the outlet of the triplex rig pumps. The transmission of vibrations and shock waves from the bit to the motor was attenuated by two high-temperature-rated shock absorbers.

Other devices used to increase the effectiveness of the motor-driven equipment were a bent sub (1/2° to 2 1/2°) containing a latch-in orienting sleeve, which was included in the assembly just above the motor (to provide a directed side thrust to the bit); and a nonmagnetic drill collar (Monel) installed directly above the bent sub (to eliminate magnetic disturbance to the magnetometer of the steering tool from the steel in the parts of the assembly above and below the tool).

Thirty-three motor-driven runs were made in EE-2 (Table 5-3). Of the three types of downhole motors used, the Maurer turbodrill demonstrated the greatest capability to operate in high-temperature downhole environments (Table 5-4). All of the PDMs suffered thermal degradation of the elastomer stators at temperatures approaching 200ºC.

Table 5-3. Motor-driven directional drilling equipment: Summary of performance in EE-2

Motor type	Number of runs	Average hours per run	Average footage per run, ft (m)	Average rate of penetration per run, ft/h (m/h)
Maurer turbodrill	21*	2.8	59.8 (18.2)	21.6 (6.6)
Dyna-Drill PDM	6	4.5	54.7 (16.7)	12.3 (3.7)
Baker PDM	4	7.8	48.8 (14.8)	6.2 (1.9)

* Does not include two short test runs of the smaller (5 3/8-in. [137-mm]) Maurer turbodrill at the bottom of the hole.

Source: Helmick et al., 1982

Table 5-4. Typical performance of Maurer high-temperature turbodrill (7 3/4-in.-diameter) in EE-2

Date	October 12–13, 1979
Depth interval	10 433–10 552 ft (3180–3216 m)
Drilling footage	119 ft (36 m)
Formation temperature	230°C
Shock absorber	None
Bit	12 1/4-in. STC Q9JL
Weight on bit	≤ 20 000 lb
Bent sub	1 1/2°
Flow rate	348 gpm (22 L/s)
Estimated rotary speed	300–400 rpm
Change in angle of inclination	About 4° (from 17° to 21°)
Total rotating time	4.5 h
Penetration rate	26 ft/h (8 m/h)
Condition of bearing	No broken faces, but less than 1/2 h drilling life remaining

Source: Helmick et al., 1982

The turbodrill played a key role not only in controlling the azimuth, or direction, of the EE-2 borehole, but sometimes in increasing the inclination. Below approximately 9000 ft, an average increase in the angle of inclination of about 2° per 100 ft was required to attain a 35° inclination by 11 000 ft. For example, on October 11 a single-shot survey at 10 433 ft (3180 m) revealed an inclination of only 17°; the turbodrill succeeded in increasing the inclination to 21° within a drilling interval of only 119 ft (see Table 5-4).

Rotary Angle-Building and Angle-Maintaining Assemblies

The Maurer turbodrill was the tool of choice for azimuth corrections; but because a turbodrill run was comparatively short and had to be followed by reaming, a rotary drilling assembly would typically be used once the desired azimuth had been attained, to maintain or increase the inclination of the hole while keeping the azimuth near-constant. The rotary drilling assemblies used in EE-2 generally performed well, as did the roller reamers that were always used with them as wall-contact tools.

Directional Surveying Equipment

During rotary drilling operations, single-shot directional measurements were taken at regular intervals. At shallow depths and moderate temperatures, a magnetic single-shot tool was run either on a 3/32-in. (2.4-mm) slick line (a wireline with no electrical conductors) or dropped in go-devil fashion down the drill string, before the bit was tripped out of the hole. At temperatures above 121°C, however, a more heat-resistant, smaller-diameter single-shot tool, encased in a Dewar-type heat shield, had to be used. In addition, as the inclination approached 35°, a 5/8-in. (16-mm) braided wireline had to be substituted for the slick line to effectively handle the increased drag during retrieval of the tool. Finally, at temperatures above 200°C, various operational techniques designed to cope with the elevated temperatures had to be used (such as taking precautions to exclude water vapor from inside and outside the Dewar flask).

Drill String

The performance of the drill pipe was remarkably good considering the hostile environment to which it was exposed and the lack of routine tool-joint inspections (the most significant consequence of which was tool-joint failures). Severe and rapid abrasive wear of the pipe was observed, and although no downhole failures were attributed to this abnormal wear, it did result in early replacement of some 4000 ft of drill pipe. The rate of wear was retarded somewhat by periodic applications of tungsten-carbide hard banding on the tool joints.

Fatigue failures were surprisingly rare considering the length of the directionally drilled borehole and the magnitude of axial and torsional loads applied to the drill string. Inspection of the drill pipe by Tuboscope's Amalog IV service showed that the two that did occur could both be attributed to the growth of cracks that developed from sharp, deeply penetrating corrosion pits. These cracks were within 20 in. (50 cm) of a tool joint or connection and involved Grade E, 19.5-lb/ft drill pipe having a nominal outer diameter of 5 in. (127 mm). The low incidence of fatigue failure is due in part to efforts to avoid doglegs and in part to the use of lower-yield-strength (75 000-psi) drill pipe for all but the upper 3500 ft of the string.

After numerous washouts and twist-offs in the drill collars, the boxes and pins of the BHA were inspected by Magnaflux testing on the rotary floor.

Logging Instrumentation

Logging surveys in EE-2, for which both commercial and Los Alamos-developed instruments were used, were aimed largely at locating lost-circulation zones, identifying holes and breaks in the collapsed 13 3/8-in. casing, and determining the integrity of the casing and the cement (no further attempts were made to obtain geophysical information). Commercial companies handled as much of the logging as they were capable of, but the commercial logging tools performed marginally at best. This was particularly true of the temperature, caliper, and sonic tools, which often failed at the elevated temperatures to which they were exposed at depth. In addition, the commercial cableheads (connections between the tools and the electrical cable) were poorly designed and remained water-tight for only a few hours at most.

Because of these shortcomings, Los Alamos began to design and produce some of the needed instrumentation (then unavailable from industry) and would continue to develop an entire suite of high-temperature logging tools and geophones to support the HDR Project[6] (see the Appendix). A particularly critical need was for tools that would allow temperature logging of the borehole at will, since the variation in fluid temperature along the borehole is the most sensitive indicator of points of fluid entry or exit (temperature is a much more definitive indicator than fluid velocity). Temperature-logging tools designed by the Laboratory incorporated an ingenious "armor" structure that allowed the thermistor probes, which were very lightweight and delicate—and thereby capable of rapid equilibration with changes in temperature—to be fully exposed to the borehole fluid as the tool was moving but protected from contact with rock ledges or other borehole obstructions. The logging cables on which these tools were run, manufactured by the Rochester Corp. of Culpeper, VA, were 7/16-in.-diameter, double-armored, 7-conductor cables insulated with Tefzel (sintered TFE Teflon) for a high-temperature rating of 315°C.

The geothermal gradient measured in EE-2 by means of such logging tools (augmented by measurements obtained in GT-2 and EE-1) is shown in Fig. 5-7, along with the geologic section for EE-2. The deeper portion of the geologic section (below about 10 000 ft) was based on analyses of cores and drill cuttings from EE-2. (See Chapter 2 for a detailed discussion of the unique geologic/geothermal-gradient conditions found at Fenton Hill as a result of its proximity to the recently active Valles Caldera.)

[6]somewhat to the chagrin of the DOE, who disliked the appearance of competition with industry.

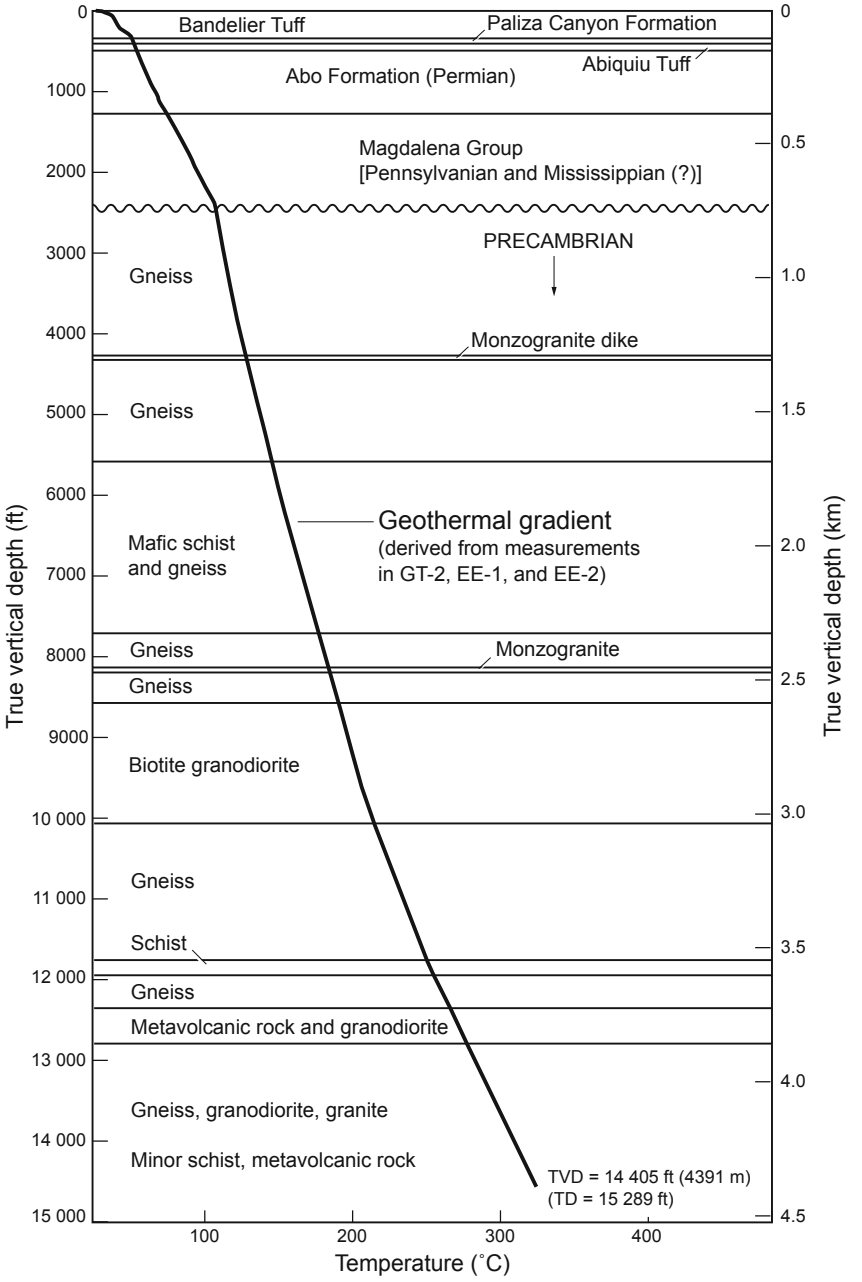

Fig. 5-7. EE-2 geothermal gradient profile (derived from measurements in GT-2, EE-1, and EE-2) and geologic cross section.
Adapted from Rowley and Carden, 1982

In addition to the temperature-logging tools, Laboratory-designed instruments used in EE-2 included a combination temperature/spinner tool used to simultaneously measure the temperature of the water and its rate of flow down the casing as a function of depth—information critical for locating lost-circulation zones or breaks in the collapsed 13 3/8-in. casing. An abrupt increase in temperature at a given location indicated that water was flowing out through the casing and into the loss zone at that point; and information on the amount of water exiting the casing at that depth, provided by the spinner tool, served to corroborate the temperature data. (The combined temperature and spinner surveys were run while water was being pumped down the hole, so that the water above the lost-circulation zone or casing-break would be cold and in motion, while that below the zone or break would be hot and static.) In addition, a three-arm (individually recording) caliper tool developed by Los Alamos was used to inspect the casing for breaks or changes in thickness; and a Los Alamos downhole video camera was employed to identify the nature of the collapsed zones, tears, and breaks in the 13 3/8-in. casing and to visually inspect the 9 5/8-in. production casing for suspected wear at 670 ft (204 m).

All of the Laboratory-designed logging tools were deployed from two commercial-type logging vans, purchased by the Laboratory in the late 1970s.

Three Observations from the Drilling of the EE-2 Borehole

Attempts to Seal the Sandia Formation Loss Zone

During the drilling of the two earlier boreholes (GT-2 and EE-1), the Laboratory drilling supervisors had concluded that no amount of cement or lost-circulation material was capable of sealing off the cavernous loss zone in the Sandia Formation overlying the granitic basement. It was on the basis of this experience that they developed the plan for drilling the portion of EE-2 that would traverse the lowermost part of the Sandia Formation (which presented the most severe lost-circulation conditions) and penetrate the underlying basement rock. That plan was to rapidly drill ahead without returns to the casing setting depth (about 200 ft into the granitic basement), then promptly run and cement the intermediate casing string.

Unfortunately, the contract personnel supervising the drilling of EE-2, who were inexperienced with severe lost circulation, did not follow this plan; instead, using their limited prior experience in similar environments, they tried to seal off the loss zone. Further, the technique they used—the addition of silica flour to the cement—was not effective. Only after five days of effort—which cost close to $100 000 and produced nothing but further deterioration of the red beds of the Madera Formation—was the

sealing effort finally abandoned, the borehole drilled into the granitic rocks without returns, and the casing run.

Attempts to Repair the Intermediate Casing

The collapse of the lower part of the casing string and the subsequent attempts to work through and repair the tight, collapsed interval (which created tears and holes in the casing, bringing the borehole into direct fluid communication with the very large loss zone on top of the granitic surface) resulted in repeated losses of circulation. In retrospect, this major drilling problem could have been solved by a common and proven technique: that of setting a smaller casing string inside the intermediate casing (for example, during mid June 1979, when full circulation had temporarily been restored and drilling was proceeding at a depth of about 4000 ft, a "repair" string of 10 3/4-in. casing could easily have been run and cemented inside the 13 3/8-in. casing). Such a measure would have required a reduction in the size of the drilled hole, from 12 1/4 in. to 9 5/8 in., but this would have been only a minor setback in the Phase II reservoir plans. Instead, repair attempts took the form of ever more massive cementing jobs, which provided at best very temporary relief.

Testing of a New Core Bit

The performance of the new STC four-cone core bit was outstanding, especially considering the very short amount of hard-rock coring time that had been devoted to its development. Five of these bits were tested in EE-2 (before the most severe hole problems began in late December 1979); their average penetration rate was 9 ft in 2 1/2 h, or 3 1/2 ft/h—about three times the highest rate previously seen with diamond core bits. With additional development time and field testing, it is possible that this core bit might eventually replace the much more costly diamond bits typically used for coring in granitic and metamorphic rocks.

Planning and Drilling of the EE-3 Borehole

One of the major challenges posed by the Fenton Hill HDR Project was that of drilling the lower portion of the Phase II production well, EE-3, on an inclined trajectory that would track directly above EE-2, with a vertical separation of about 1200 ft (370 m). The drilling of such a deep borehole, and one with such a precise trajectory, in hot, hard, crystalline rock had never before been attempted. This pioneering directional drilling effort was reviewed in Rowley and Carden (1982), from which much of the following information is adapted.

Drilling Plan

The drilling plan for EE-3, like that for EE-2, was dictated by the "Phase II assumption" (later seen as fallacious) and called for a controlled-trajectory borehole aligned with the EE-2 borehole. The part of the plan calling for directional drilling of the deeper portion of the borehole was based on the survey data obtained for the 8 3/4-in. (22-cm)-diameter portion of EE-2 below about 11 600 ft (Fig. 5-5). The plan is summarized as follows:

1. Drilling of the 2400-ft (730-m) section of volcanic and sedimentary rocks—and then sufficiently far into the crystalline basement to set casing—would follow the same guidelines as in the EE-2 plan, including without-returns drilling of the deeper lost-circulation zone and about 150 ft (50 m) into the underlying crystalline basement. The 13 3/8-in. (340-mm) casing would be set into the basement rock and tensioned after cementing to guard against compressive failure caused by the thermal expansion associated with hot water production.
2. At a kickoff point of about 6500 ft (2000 m), the 12 1/4-in. (31-cm)-diameter borehole would be angled toward the northeast and the inclination would be gradually increased, to match the northeast direction (about N80E) and 35º inclination of the lower 3000 ft of the EE-2 borehole. That is, the bottom portion of the EE-3 borehole would follow the course of EE-2 but lie 1200 ft directly above it.
3. The directional drilling of EE-3 would have two target parameters:
    - a TVD such that the borehole terminates 1200 ±50 ft above the 14 405-ft (4391-m) TVD of EE-2; and
    - a lateral deviation of ±100 ft (±30 m) from the horizontal projection of the EE-2 trajectory.

(Note that, in retrospect, both of these target parameters were excessively restrictive—and costly—considering that the true orientations of the joint systems in the Phase II reservoir region were not known, nor was the direction in which the reservoir would actually develop.)

4. A 9 7/8-in. (25-cm)-diameter transitional section of borehole would be drilled, about 20 ft (6 m) long, between the 12 1/4-in. borehole and the lower 8 3/4-in. borehole.
5. The final section of the EE-3 borehole would be drilled with an 8 3/4-in. (222-mm)-diameter bit and with stiff (angle-maintaining) drilling assemblies.
6. Magnetic single-shot surveys would be taken every 60 ft (20 m); the azimuth would then be corrected by means of high-temperature turbodrill runs, to maintain the path of the EE-3 borehole parallel to that of the EE-2 borehole (within the ±100-ft horizontal tolerance specified).
7. Once drilling had reached the anticipated TD of about 14 400 ft, a 9 5/8-in. (244-mm) production casing would be run from the surface to the bottom of the 12 1/4-in. section of the hole. This casing string would be cemented and tensioned to prevent excessive thermal stresses at the wellhead during hot water production.

Various equipment items had already been tested during the controlled-trajectory drilling of EE-2. With respect to downhole motors, it had been established that at temperatures below 200°C—which at Fenton Hill corresponds to depths less than about 10 000 ft (3000 m)—a PDM could be used for both angle building and azimuth control; at temperatures above 200°C (depths exceeding 10 000 ft), a high-temperature-rated turbodrill would be needed to adjust the azimuth of the borehole.

The directional-drilling strategy for EE-3, like that for EE-2, was to alternate runs of a downhole motor guided by a steering tool with runs of a rotary angle-building drilling assembly; then, once the inclination of the borehole had reached about 35º, to rotary-drill with a stiff, angle-maintaining assembly to deepen the hole without changing its azimuth. In the case of EE-3, however, because of the need to position the borehole with respect to the already-drilled EE-2, even greater attention had to be given to controlling the azimuth and inclination.

Figure 5-8 shows the EE-3 drilling location at Fenton Hill in the fall of 1980, with the Brinkerhoff-Signal rig No. 56 in operation.

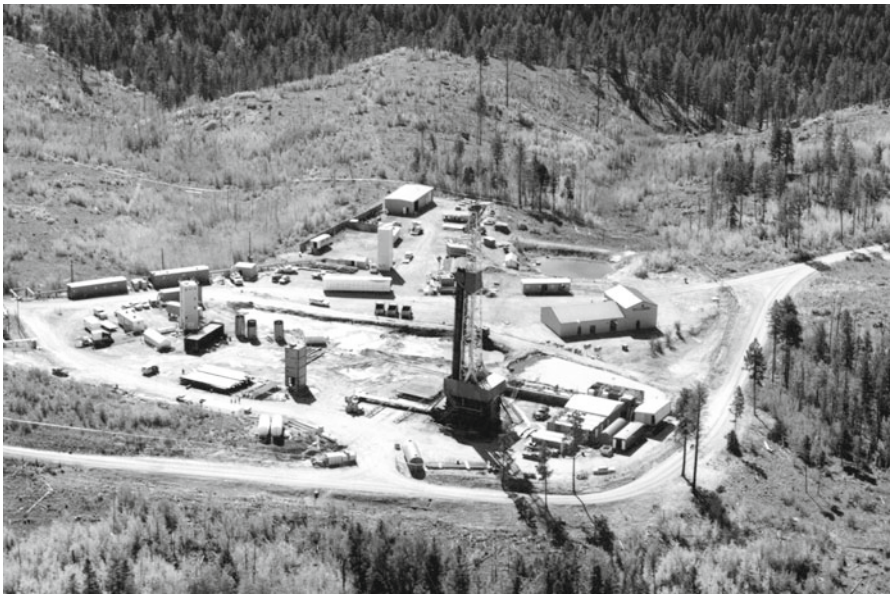

Fig. 5-8. The EE-3 drilling location, viewed to the southeast. The logging tower over the recently completed EE-2 borehole is directly to the left of the EE-3 location. The towers over EE-1 and GT-2, and the various facilities associated with the long-term flow testing of the Phase I reservoir (which was proceeding concurrently with Phase II drilling), are visible in the background.
Source: HDR Project photo archives

Drilling Through the Volcanic and Sedimentary Rocks and into the Granitic Basement

On May 20, 1980, with the derrick still raised, the drill rig was skidded from EE-2 to the new EE-3 location 165 ft to the west. At this location, an 80-ft-deep,[7] 76-in.-diameter hole had been bored and a 30-in.-diameter steel conductor pipe concreted in place (except for the top 2 ft, which would serve as a cellar).

Drilling of a 26-in.-diameter hole through the volcanic and sedimentary rocks began on May 22. As with all the previous boreholes at Fenton Hill, the EE-3 borehole met with no serious loss of circulation until, at a depth of 1923 ft, the bottom of the hole "fell out" (the top of the washed-out loss zone was subsequently determined to be at 1894 ft). While the hole was being re-entered to drill ahead, the bit struck a bridge at 480 ft, but washing to bottom succeeded in re-establishing circulation. Then, during a second attempt to drill ahead, a more serious obstruction was encountered at 505 ft. This obstruction was successfully drilled through, after which the hole was reamed to near bottom—where circulation was again completely lost at 1894 ft.

Two attempts were made to seal off the lost-circulation zone by pumping thixotropic cement into the hole. The first plug (500 sacks of cement) was set at TD (1923 ft) but unfortunately was overdisplaced from the hole; the hole was then washed and reamed to TD without returns. A second attempt to place a cement plug (with another 500 sacks) succeeded, and so did the drilling through of the unstable clay zones above the plug, which were swelling and sloughing. The plug was penetrated to a depth of 1775 ft (541 m), but because of the continuing sloughing of the borehole walls and bridging of the hole in the red clays of the Abo and Madera formations above the lost-circulation zone, it became obvious that drilling could not proceed further until the borehole could be better stabilized. On June 9, therefore, a 20-in. (508-mm)-diameter string of surface casing was run in. But the continued swelling and sloughing of the unsupported clay zones above 1900 ft formed a bridge in the borehole that could not be penetrated. The casing could not be run in to full depth and had to be set at 1580 ft (480 m).

Note: All three of the previous boreholes drilled at Fenton Hill had encountered this same severe lost-circulation zone at about 1900 ft. For this reason, it is difficult to understand why the 20-in. surface casing was not set earlier—on May 31, at the more appropriate depth of 1872 ft—which would have saved nine days of rig time and cased off an additional 290 ft of the trouble-prone Madera Formation. (Major problems during the drilling of EE-2 were probably averted by the addition of large amounts of lost-circulation material to the drilling fluid *before* this zone was encountered; but in that instance luck may also have played a role!)

[7] In Fig. 5-12, this depth is shown as 107 ft—as measured from the Kelly bushing after completion of the borehole.

A slurry containing 2400 sacks of cement was pumped down the casing and up into the annulus behind the casing, but when it did not reach the surface, an additional 650 sacks of cement was pumped down the annulus from the surface to finish the job. Once the cement had hardened, it was drilled out; drilling then recommenced, now with a 17 1/2-in. bit, until circulation was lost again at 1860 ft. Another attempt to seal the lost-circulation zone with a massive infusion of cement (2500 sacks) was unsuccessful. The decision was made to drill on into the granitic basement—even though this meant drilling without returns, which was not only dangerous but expensive (even more so now, the water supply from La Cueva having been exhausted).

The granitic basement was encountered at a depth of 2404 ft (733 m), after which drilling continued another 162 ft to a depth of 2566 ft (782 m). A 13 3/8-in. string of casing was run into the hole, the casing shoe was landed at 2552 ft (778 m), and the casing was then cemented in two stages. First, a slurry of 200 sacks of cement was injected to tag-cement the lower 148 ft (45 m) of the casing into the granitic rock; when this cement had set, the casing was tensioned with casing jacks to a load of 725 000 lb (to prevent excessive compression loads on the casing caused by the high-temperature fluids expected to be produced from the reservoir through EE-3). The tensioning of the casing produced an axial stretch recorded as 19 in. (48 cm) at the wellhead. The second stage consisted of cementing the casing from a depth of 1403 ft (428 m) to the surface, through a cementing stage collar; just below this collar was set an expandable, external casing packer (to prevent the cement from flowing down the annulus and into the lost-circulation zones below).

Drilling in the Precambrian Crystalline (Plutonic and Metamorphic) Complex

Vertical Drilling

A 12 1/4-in. (311-mm) steel-tooth bit was used to drill out the cementing hardware (cementing sleeve, float collar, plugs, and shoe), as well as the cement below the shoe. Then, on June 30, the steel-tooth bit was replaced with a TCI bit and the drilling assembly was run back in the hole. It was rotated slowly (40 rpm) and at a low bit load to avoid damaging the casing and the cement. This precaution was continued until the top reamer of the BHA[8] was at a depth of 2640 ft, 88 ft below the 13 3/8-in. (340-mm) casing shoe.

[8]In Appendix B of Rowley and Carden, 1982, the BHA is often listed as including the HWDP. We use instead the more conventional drilling terminology, which defines the BHA as everything below the HWDP—i.e., the equipment used for drilling and/or reaming.

Rotary drilling of the 12 1/4-in.-diameter hole continued until July 24, when, at a depth of 6444 ft (1964 m), a tool joint on a drill collar twisted off. Drilling came to a halt while a two-day fishing operation was carried out to recover the rest of the BHA.

A variety of TCI bits (12 in all, for 17 bit runs) were employed during this drilling sequence, which, except for occasional washouts of the drill collars and two brief retrieval operations, was the least troublesome period of drilling for either EE-2 or EE-3. This portion of the hole was surveyed approximately every 60 ft (20 m). The instantaneous drilling rate varied from 4 to 20 ft/h (1.2 to 6 m/h). The BHA components, the boxes, and especially the pin ends of collars, were routinely inspected. Drilling and related operations for this portion of the hole took 26 days.

At the new bottom-hole depth of 6444 ft, however, the inclination of the borehole was 10° from vertical and the azimuthal direction was trending toward the northwest (N58W), as had happened with the previous boreholes GT-2, EE-1, and EE-2. As mentioned earlier, this drift appears to result from the natural characteristics of the rock mass at these depths. To achieve the proper direction relative to the trajectory of EE-2, therefore, the hole would have to be turned toward the northeast. (This next step in the drilling program, aimed at turning the borehole to about N80E and raising the inclination to 35°, would be significantly delayed when, during off-bottom reaming at a TD of 10 528 ft, a twist-off of the 5-in. [127-mm] drill pipe led to an extended—and unsuccessful—retrieval attempt. Eventually, it would also lead to a problem-plagued sidetracking of the hole from a kickoff point of 9444 ft.)

Directional Drilling

When drilling resumed on July 26, at a depth of 6444 ft, only angle-building or angle-maintaining BHAs were used for both rotary and motor runs. The BHAs and motor types are shown in Table 5-5.

Table 5-5. Typical motor and bottom-hole assemblies used in the EE-3 borehole

Bit or hole diameter, in. (mm)	Motor type	Typical BHA	Remarks
12 1/4 (311)	Baker PDM	Motor, float sub, bent sub, orienting sub, 8-in. Monel drill collar, ten 8-in. drill collars, jars.	Used at temperatures below 200°C (depths less than 10 000 ft [3000 m]).
	Maurer turbodrill	Turbodrill, float sub, bent sub, orienting sub, 8-in. Monel drill collar, thirteen 8-in. drill collars, jars.	Used at higher temperatures (above 200°C).
		Turbodrill, float sub, bent sub, orienting sub, two 6 3/4-in. (171-mm) Monel drill collars, three 6 3/4-in. drill collars.	Used in very crooked hole below 10 300 ft (3200 m).

Table 5-5. (Continued)

Bit or hole diameter, in. (mm)	Motor type	Typical BHA	Remarks
12 1/4 (311)	Dyna-Drill PDM	Motor, bent sub, float sub, orienting sub, two 8-in. Monel collars, five 8-in. collars, jars.	Used during sidetracking attempts, 9300–9800 ft (2840–2980 m).
12 1/4 (311)	Dyna-Drill PDM (bent housing)	Motor, Dyna Flex or bent sub, orienting sub, two 6 3/4-in. Monel drill collars, four 6 3/4-in. drill collars, seven 8-in. drill collars, jars.	Used during sidetracking attempts, 9300–9800 ft.
8 3/4 (222)	Maurer turbodrill	Turbodrill, float sub, bent and orienting sub, two 6 3/4-in. Monel collars, five 6 3/4-in. drill collars, jars.	Used for eight directional corrections below hole-diameter-reduction point at 10 800 ft (3290 m).

Source: Rowley & Carden, 1982

For the initial two runs, magnetic single-shot orienting tools were employed, without a steering tool, in an attempt to orient the down-hole motor—a Baker PDM—such that the azimuth of the hole would be rotated while the inclination increased only slightly (changing azimuth at a low inclination greatly facilitates correction). During drilling, a magnetic single-shot survey was taken as each 30-ft joint of pipe was added to the drill string.

On the first run, the Baker motor torqued up and stalled repeatedly and had to be withdrawn after drilling only 76 ft. The second Baker PDM performed better (drilled 129 ft), but the inclination increased too sharply, to 14 3/4° from the vertical, while the azimuth changed little. During the latter part of the third directional drilling run with a PDM, the continuous-readout EYE steering tool was used. Following this run, the inclination was still 14 3/4°, but the azimuth, at N37W, was not changing rapidly enough for the 304 ft (92 m) of depth and four days of effort.

Over the next two weeks, another seven drilling runs were carried out, deepening the hole to 7482 ft (2281 m) and changing the azimuth to N47E—but the inclination decreased, to 7°. After a rotary reaming assembly had been run into the hole to return the gauge to 12 1/4 in., drilling was suspended on August 12, at a depth of 7542 ft (2299 m), and the rig was put on standby for five days because all the drilling funds had been expended. This hiatus was used for routine inspection of the drill string, replacement of the main drive shaft on the rig drawworks (a severe fatigue crack had developed), and inspection of other components of the hoisting equipment.

Rotary drilling began again on August 20, 1980, to increase the inclination while monitoring the azimuthal drift of the hole. By the time a depth of 7845 ft (2391 m) had been reached, the inclination had increased substantially, to 13 1/4°, but at the same time the azimuth had rotated to the north, from N83E to N46E—a change of 37° in about 300 ft (90 m). Because this change in direction jeopardized the position of EE-3 with respect to EE-2, directional drilling was resumed—now with a test run of a new, high-temperature Dyna-Drill (a 7-in. [178 mm]-diameter "DynaTurbine" motor); but steering-tool problems restricted the test run to about 11 ft (to a depth of 7856 ft).

In a sequence of nine motor runs over the next 11 days, the trajectory of the hole was corrected to N88E, 17 1/4° at a depth of 8407 ft (2562 m), reached on September 4. This sequence was followed by two more Dyna-Drill tests, both of which failed because of equipment problems.

Next came eight rotary drilling runs, for which either an angle-maintaining or a moderate-angle-building assembly was employed. At a depth of 9728 ft (2965 m) the trajectory was N72E, 26 3/4°. Because the inclination was increasing too quickly, the load on the bit was reduced, which dropped the angle back 1 3/4°, to 25°, at 9924 ft (3025 m).[9]

With downhole motors not available at this point, rotary drilling continued for two more bit runs. On October 2, 1980, with the borehole at a depth of 10 017 ft (3053 m) and on a trajectory of N72E, 24°, circulation was almost totally lost—probably caused by the flow of pressurized drilling fluid into one or more open joints within the lower reaches of the Phase I reservoir region. At this time in late 1980, Run Segment 5 (the 9-month flow test discussed in Chapter 4) was still under way. With the EE-1 injection pressure at 1250 psi and the GT-2 production backpressure only 170 psi, the pressure within the open joints of the reservoir would have been no higher than 1000 psi—whereas the pressure of the drilling fluid was between 1500 and 2000 psi.

A cement-bond log was run to evaluate the bonding between the cement and the 13 3/8-in. (340-mm)-diameter casing. The results showed that the bottom 230 ft (70 m) of the tag-cemented casing string—from 2552 ft up to about 2320 ft—was well bonded through and *above* the massive loss zone in the Sandia Formation at about 2380 ft. (Note: The interpretation of this part of the cement-bond log was no doubt in error, since it is highly improbable that the loss zone had been sealed off.) The cement-bond log

[9]Note: In a few cases—this is an example—different sections of the Rowley and Carden report give different numbers for depths, trajectories, etc. When unable to reconcile numbers given in the text with those in Table III and in Appendix B, we used the numbers shown in Appendix B.

also showed that the 1410- to 1837-ft (430- to 560-m) interval, which had not been cemented, had no bonding; and that the cement circulated to the surface above the stage collar at 1403 ft was only partially bonded.

By now a Dyna-Drill PDM was again available, and two runs were attempted; but the bottom-hole temperature proved to be too high for the elastomer components of the motor, causing it to lock up. Two Maurer 7 3/4-in. (197-mm)-diameter turbodrills were then enlisted for the resumption of directional drilling. The first Maurer run deepened the borehole to 10 116 ft in 5 hours, but also increased the inclination to 27°—a too-rapid increase that resulted in a severe dogleg (3° per 100 ft). Following a rotary reaming run, a further directional drilling run was initiated, but the Maurer turbine locked up after advancing only 7 ft and had to be pulled. The next two turbodrill runs were also problem-plagued: the hole was deepened by only 34 ft while the inclination remained unchanged at 27° (but the hole azimuth drifted back slightly to the north, to N67E). Two more rotary reaming runs were alternated with Maurer angle-building turbodrill runs to further increase the inclination. These runs took the hole depth to 10 334 ft (3150 m), but the net increase in inclination was only 1/4° (the azimuth of the borehole, however, had now rotated 16° farther to the north—to N51E).

On the next Maurer turbodrill run (October 13), the EYE steering tool—unbeknownst to the wireline operator—jammed in the downhole seating assembly, 170° away from its proper orientation. The turbodrill was thus severely misoriented on the next angle-building run, and instead of building angle actually *decreased* it, back to 24 3/4°. This decrease of 2 1/2° over a distance of only 44 ft translated to a dogleg severity of over 5 1/2° per 100 ft. Figure 5-9 makes starkly evident the problems caused by the directional drilling of EE-3.

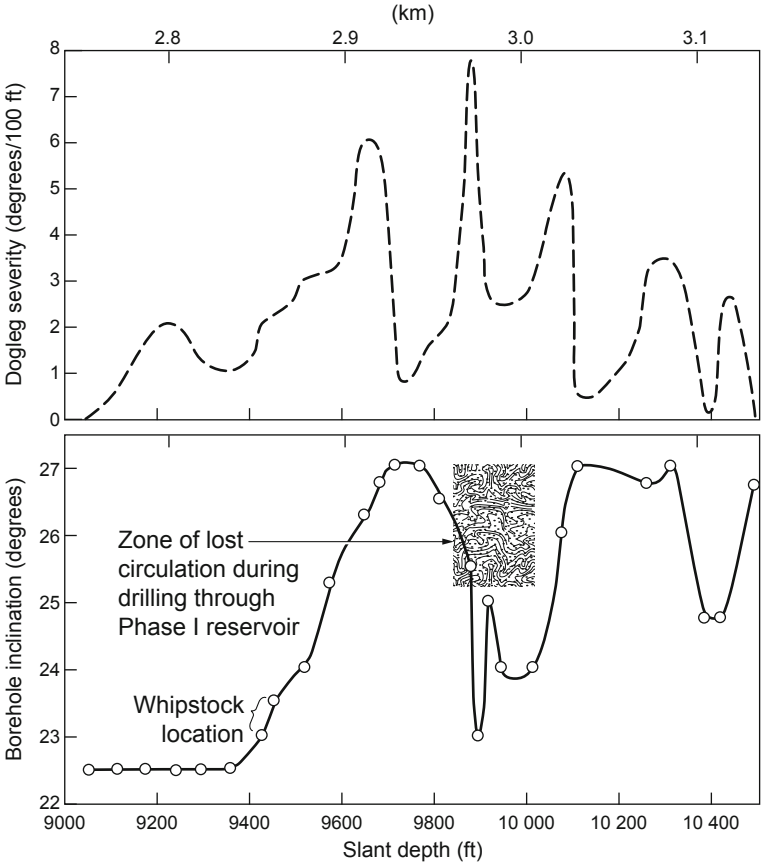

Fig. 5-9. Dogleg severity and variations in inclination over the 9000- to 10 500-ft (2700- to 3200-m) depth interval in EE-3. Also shown is the zone of lost circulation encountered during drilling through the Phase I reservoir region, which extended down to at least 10 017 ft.
Adapted from Rowley and Carden, 1982

When the BHA was brought up and inspected on the rig floor, it was discovered that wear of the components had caused the latch-in orienting sleeve on the steering tool to become jammed 170° away from the key pin in the orienting sub. (The geometry of the BHA was such that a misorientation of this kind would be extremely unlikely if component wear were routinely checked for—which should be done by the wireline operator as part of the procedure of multiple engagement and re-engagement of the latch-in device on the surveying tool.)

Note: In retrospect, it is clear that directional drilling should have been discontinued at this point, and further Maurer turbodrill runs should have waited until the borehole had been reamed out with a stiff, angle-maintaining rotary drilling assembly.

Another turbodrill run, aimed at regaining angle and reaming out the very crooked section of hole that had been produced by the severe oscillations in inclination (see Fig. 5-9), encountered extremely tight hole conditions. The borehole was deepened to 10 417 ft (3175 m), but with no change in trajectory. The first reaming assembly, with its 6-point near-bit reamer, could not be advanced through the very crooked interval and had to be replaced with a more limber assembly having a 3-point near-bit reamer. However, while reaming was under way at a depth of 10 372 ft (3161 m), a twist-off of the 5-in. (127-mm) drill pipe occurred. The free pipe—75 stands plus two joints of 19.6-lb/ft (29.2-kg/m), grade E drill pipe—was successfully retrieved. It appeared that the break was in the pipe body, about 2 ft (0.66 m) below a coupling, and that the threads in the lowermost steel drill collar in the BHA had been stripped. Following the retrieval operation, a reaming/drilling assembly was used to ream the hole back down to 10 417 ft. Directional drilling then continued with three Maurer turbodrill runs interspersed with rotary reaming runs in an effort to open up the very tight borehole. These runs succeeded in returning the borehole inclination to 26 1/4° at a depth of 10 528 ft.

On October 28, a second—and this time disastrous—twist-off occurred in the drill string at 7070 ft (2155 m). It is likely that this twist-off was a direct consequence of the severe borehole drag caused by the rapid changes in inclination described above. Because the borehole was being reamed with the bit *off bottom* at the time of the twist-off, it was assumed that the BHA had fallen to the bottom of the hole (then at 10 528 ft)—in which case not only could it be badly jammed into the hole, but there could be a considerable amount of bent or buckled drill pipe above it. When the drill pipe above the twist-off was finally fished out, the break was found to be very jagged and located just below a coupling. At this point, the "fish" included about 2300 ft of 5-in. drill pipe, six joints of HWDP, drilling jars, another nine joints of HWDP, two 6 3/4-in. drill collars, a crossover sub, a 3-point (string) roller reamer, another crossover sub, another 6 3/4-in. drill collar, a third crossover sub, a 3-point (near-bit) roller reamer, and a 12 1/4-in. TCI bit.

The next 48 days would be occupied with fishing operations to attempt to retrieve the massive fish. The effort would not only cause a major interruption in drilling but would ultimately be unsuccessful (further, in the process other pipe and equipment used in the retrieval attempts would be lost in the hole as well).

Free-point surveys showed that the region of the borehole in which the BHA was stuck coincided with the location of the upper (string) reamer—about 45 ft above the bit, which had landed with great force at the bottom of the hole. The drill pipe itself was not stuck, and fishing operations succeeded

in bringing up all of it, as well as the six joints of HWDP positioned above the drilling jars; but the fish parted in the middle of the jars, leaving nine joints of HWDP and the BHA still in the hole.

On November 1 the drill pipe was firmly attached to the top joint of HWDP, and with a single back-off shot all nine remaining joints of HWDP were unscrewed from the top of the BHA and removed from the hole. An attempt was then made to free the BHA, but the result was disastrous. As the drill pipe—firmly attached to the top drill collar of the fish—was simultaneously pulled hard and jarred, the drill pipe parted again, at a depth of about 2360 ft. Under the sudden force applied to the Kelly by the elastically rebounding drill pipe, the Kelly wedged in the rotary table and broke, damaging the swivel, cables, and hoisting block. Now unconstrained, the 2360-ft section of drill pipe, with the Kelly on top, fell back into the hole and lodged (within the 13 3/8-in. casing) alongside the section of drill pipe still attached to the BHA. Fishing in this "double-parked" situation (which was verified by tagging and a free-point survey) now became very difficult and delicate. Finally, after nine days of judicious backing off and jarring, joint by joint the entire 2360-ft section of drill pipe was loosened and removed—leaving the rest of the pipe with its top at about 2360 ft.

The task of retrieving the BHA, grapple, fishing jars, and drill pipe still in the hole was complicated by the presence of debris from the fishing operations that had fallen down the hole and was blocking the threads on the top box connection of the drill pipe. A special external cutting tool was used to cut the pipe at about 2405 ft, in the middle of the next joint (1 1/2 joints below the top of the drill pipe); the 1 1/2 joints were then removed, allowing most of the rest of the drill pipe (about 6775 ft) to be backed off to a depth of 9180 ft (2800 m).

At this stage, it was decided to change out the entire string of 5-in. drill pipe being used for the fishing operations—first, because of the nature of the pipe failure (twist-off): the break was very jagged, and numerous extremely deep corrosion pits were visible on the pipe's inner surface; and second, because the pipe had already seen more than 3000 hours of hard drilling in the EE-2 borehole. The 5-in. pipe was delivered to the rig contractor (Brinkerhoff-Signal Drilling Co.) and replaced with a string of 4 1/2-in. (114-mm)-diameter pipe.

Note: Considering the very difficult and expensive fishing operations under way at this time, the decision to use a smaller-diameter—and thereby inherently weaker—string of drill pipe would turn out to be an unfortunate one.

On November 23, after the 4 1/2-in. drill pipe had been picked up and run into the hole, fishing operations recommenced. A screw-in sub was attached to the top of the remaining 5-in. drill pipe at a depth of 9180 ft (this pipe was still connected to the fishing jars and grapple, which in turn were firmly attached to the stuck BHA), but jarring had no effect. During an attempt to

torque up the screw-in sub, a cracked thread in a pin caused the new drill pipe to twist off at a connection at about 3550 ft (1080 m). Finally, a deep back-off at a depth of 10 150 ft (3094 m) was successful in removing all of the 4 1/2-in. drill pipe above the screw-in sub, as well as a portion of the old 5-in. drill pipe below, down to a depth of 10 150 ft. The fish remaining in the hole now consisted of seven joints of 5-in. drill pipe, the old fishing jars and grapple, and the BHA.

Further jarring succeeded in moving the fish upward about 5 ft, but then the fishing jars, having been "soaking" in the high-temperature environment near the bottom of the hole for 35 days, gave out. The action taken next was ill-considered: torque was applied to the string in an attempt to back off (unscrew) the top drill collar from the rest of the BHA. But the fishing jars, not being designed to transmit much torque, twisted off. The top half, along with the seven joints of 5-in. drill pipe, were removed—leaving 140 ft (43 m) of fish in the hole, with its top at 10 383 ft.[10] The fish now consisted of the original BHA, the grapple attached to the box-end of the uppermost drill collar in the BHA, and the twisted-off lower portion of the fishing jars (a 3 3/4-in. [95-mm]-diameter mandrel made of hardened chromium steel). After several attempts to grapple the top of the mandrel, a lead impression block was run in; it confirmed that the mandrel was lying against the borehole wall.

At this point, it was judged that further grappling or milling attempts had a low probability of success. And having now lost a total of 48 days to the fishing effort, the drilling supervisors decided to sidetrack the borehole and drill around the stuck BHA. In hindsight, this decision was probably a mistake, considering that the final attempt at jarring had at last succeeded in moving the BHA up 5 ft, and had the jars not failed, the fishing operation might well have been successful. The very short, stout mandrel that formed the bottom part of the twisted-off jars was screwed into the grapple, which in turn had a firm grip on the uppermost 6 3/4-in. drill collar in the BHA; the mandrel could not possibly have been more than just "softly" lying on the bottom of the 12 1/4-in. hole, and would have been fairly easy to wash over with a quality overshot/grapple.

What appears to have been the real problem was inadequate drilling supervision. Of the 48 days of fishing, only 12 were actually spent attempting to pull out the BHA (the other 36 days were spent on unrelated

[10]The source document (Rowley and Carden, 1982) reports different depths for the top of the fish in different places (10 375 ft on p. 15; 10 338 ft in Appendix A; 10 388 ft in Fig. 3). After a careful analysis of the available information, we conclude that, given the borehole depth of 10 528 ft, the length of the fish (140 ft), and the fact that the fish was moved up 5 ft on Dec. 6, the top would have to be at 10 383 ft. The number in Fig. 3 (showing the depth before the fish was moved up 5 ft) is thus correct; and we assume that the number in Appendix A was simply a typographical transposition from 10 383 to 10 338.

twist-offs and other pipe failures, and their associated fishing operations). It seems likely that with some additional perseverance the BHA could have been retrieved, saving the project upwards of $2 million in subsequent—and mostly futile—sidetracking attempts. (At the same time, it is likely that pressure from the Laboratory's HDR Program Office to "get on with the job" was a factor in the decision to abandon the fishing effort.)

Sidetracking of the EE-3 Borehole

It took over three months to sidetrack the EE-3 borehole around the fish lodged at the bottom of the original hole (the top of the fish was at 10 383 ft). However, most of the activities engaged in during this period were fruitless, owing at least in part to questionable direction from the HDR Program Office. Because the Project leaders were unwilling to abandon the hard-won gains in borehole inclination—built up over the preceding several months of directional drilling—they insisted on sidetracking from the *high side* of the steeply inclined (26°–27°) EE-3 interval between 9760 and 9900 ft.

The sidetracking plan developed was a variation of the technique that had been successful in twice sidetracking GT-2 at similar depths (GT-2A and GT-2B)—namely, underreaming, i.e., enlarging the borehole diameter (used only for GT-2A) and then strategically placing cement plugs to aid in diverting the drilling path. Both sidetrackings of GT-2, however, had been initiated from the low side of the hole (gravity thus working in favor of the sidetracking). The EE-3 borehole was a very different story: its much greater inclination meant that sidetracking from the high side of the hole would be working *against* gravity! Thus, in the case of EE-3, this sidetracking approach led to a lengthy series of failures, correction attempts, and further failures: repeated placing of cement plugs, underreaming, and numerous attempts at directional drilling.

Finally, on February 22, the cement-plug approach to the sidetracking of EE-3 was abandoned in favor of using a cemented-in steel whipstock. A 10 3/4-in. whipstock had been ordered for the 12 1/4-in. drilled hole and was now on hand. Preparatory to setting it in place, the cement was drilled out to a depth of 9500 ft (2896 m). Following a temperature survey and cooldown of the borehole, the whipstock was run in with 30 ft of anchoring tailpipe below. The whipstock was equipped with a 10-ft curved slide to accommodate a 12 1/4-in. (311-mm) bit, and the wedge angle was set to drill at an azimuth of about N40E, off the high side of the hole. The whipstock was successfully cemented in place with its top at 9444 ft (2879 m) and the top of the cement "anchoring plug" at 9200 ft. After a 4-day cure the plug was tagged at 9123 ft, and drilling to 9270 ft with the 12 1/4-in.-diameter, steel-tooth bit showed the cement to be hard.

As drilling out of the cement proceeded, the bit encountered some junk. Two runs with tapered and flat-ended mills, followed by four magnet runs, cleared this metal from the hole.

Drilling off the whipstock began with 15 joints of HWDP and a BHA consisting of a 12 1/4-in. TCI bit, one 6 3/4-in. (171-mm) drill collar, and jars. About 15 ft was drilled in 15 1/2 hours, at bit loads of 5000–15 000 lb. When this drilling produced increasing amounts of granitic cuttings, a 12 1/4-in.-diameter angle-building assembly was run in. Over the next three days, drilling progressed another 97 ft (29.6 m). The rate of penetration (8–9 ft/h) and the bit weight (45 000 lb) confirmed that granitic rock was being drilled. On March 22, 1981, after 101 days of effort, the EE-3 sidetracking operation was finally completed.

Note: The failure of the initial sidetracking attempts, and the need to resort to a whipstock, were due entirely to the stipulation that the borehole be drilled out the high side. Such a stipulation is called for only in very special—and therefore rare—circumstances, and in fact was not necessary for EE-3. The sidetracking operation could probably have been completed in a few days if it had been initiated from the low side of the borehole, as had proved successful for both GT-2A and GT-2B. Any loss of inclination could easily have been recovered in a few days of directional drilling (in future drilling operations, preserving hole inclination while accessing an HDR reservoir would almost never be an issue). In the great majority of cases, a low-angle kickoff—without a whipstock—is the preferred approach. It is not only quicker and much less expensive, but it does not leave the original borehole forever unusable, plugged with cement and junk. However, successful low-angle sidetracking in granitic rock does require an experienced directional driller.

The first valid compass survey in the sidetracked hole below the whipstock was at a depth of 9516 ft (2900 m) and indicated a trajectory of N73E, 24°. A second compass survey, at 9518 ft, yielded the same readings. However, several earlier (and questionable) compass readings—influenced by the steel in the whipstock and in the 30-ft tailpipe anchor—were causing some concern that the sidetracking may have been to the left side of the hole instead of to the right. For this reason, it was decided to continue drilling to the next drill-pipe connection (at a depth of 9558 ft), then withdraw the bit and position a MINIRANGE magnetometer proximity tool (Jenson, Inc.) at 9491 ft (2893 m) in the sidetracked hole. This tool would enable determination of (1) the direction from the steel tailpipe in the old borehole toward the instrument location and (2) the normal distance from the tailpipe to the instrument location. The readings taken indicated that at a depth of 9491 ft, the direction from the tailpipe toward the magnetometer was indeed as desired at N90° ± 5°E, and the distance between the tailpipe and the magnetometer was 30 ± 6 in. A multishot gyroscopic survey was also done in the new hole, the results of which confirmed its direction with respect to both the whipstock and the original borehole.

Between March 27 and April 3, 1981, four drilling runs were carried out by alternating motor and rotary assemblies. For the first, a PDM equipped with an EYE steering tool was used to directionally drill 73 ft (22 m), to a depth of 9631 ft. During this run, the steering tool indicated an inclination increase of about 1° and a turn to the east of 7 1/2°. Next, an angle-building assembly with a 6-point, near-bit reamer was used to drill ahead to 9729 ft. Another PDM run then took the borehole to a depth of 9771 ft (2978 m). Finally, a rotary drilling run deepened the hole another 113 ft, to 9884 ft (3013 m). Single-shot surveys were conducted at two depths during the fourth run. At a depth of 9753 ft (2973 m) the trajectory readings were N78E and 24 1/2°, and at 9805 ft (2988 m) they were N77E and 24 3/4°.

With the trajectory data indicating a possibility that the sidetracked leg could intersect the original EE-3 borehole (which at 9728 ft had shown a reading of N72E, 26 3/4°), especially given the observed tendency of the hole to drift toward the north, the drilling of the next few hundred feet could be critical. For this reason, additional surveys were carried out—with both a gyroscopic multishot tool and a tandem magnetic multishot tool—across the whipstock and into the sidetracked leg. These surveys were plagued with instrument and operational problems, and only one (a tandem magnetic multishot survey) was considered valid. But because it generally confirmed the previous results from the MINIRANGE proximity-tool survey (indicating that the new leg would not intersect the original hole), the decision was made on April 4 to drill ahead with an angle-building assembly.

Orienting the Sidetracked EE-3 Borehole with Respect to EE-2

The next 30 days were spent orienting the sidetracked EE-3 borehole above EE-2, by establishing an inclination of 35° and a direction that would be parallel to that of EE-2 over the depth interval 10 600–10 800 ft. From a depth of 9884 ft, four rotary angle-building runs deepened the borehole to 10 226 ft (3117 m), while increasing the inclination by 6 3/4° (to 31 1/2°) and slightly rotating the hole back to the north (to N74E).

A sequence of six Maurer turbodrill runs followed, interspersed with rotary reaming and drilling runs, and on May 4 the 12 1/4-in. portion of the borehole was completed to a depth of 10 791 ft (3289 m), corresponding to a TVD of 10 504 ft (3202 m). During the Maurer runs, the inclination of the borehole was increased from 31 1/2° to 34°, but its direction was allowed to drift back to the north by almost 20°. The final trajectory was N55E, 34°. (From these results, it appears that the turbodrills were not as effective as conventional rotary directional-drilling assemblies, either at building angle or maintaining azimuth.)

The next task was to reduce the diameter of the borehole from 12 1/4-in. to 8 3/4 in. (22.2 cm). A 20-ft (6-m) transitional section was drilled with a 9 7/8-in. (251-mm) bit. A trajectory reading taken near the bottom of this 20-ft section—N54E, 34 3/4°—was very close to the previous reading at

10 791 ft, and both compared very favorably with the trajectory of the underlying section of the EE-2 borehole at a depth of 11 576 ft (N54E, 34 1/2°).

Drilling of the 8 3/4-in. Section of the EE-3 Borehole

The plan for drilling the 8 3/4-in.-diameter borehole through the intended Phase II reservoir region called for straight-hole rotary drilling with a very stiff, angle-maintaining BHA, and for single-shot surveying every 60 ft. Drilling was to be interrupted only if the azimuth and/or inclination varied by more than the specified tolerances from those of the corresponding underlying portion of EE-2. This drilling would end up consuming 93 days, because of several problems (including yet another extended fishing operation and remedial actions to reduce hydrogen sulfide in the drilling-fluid reserve pits).

The first run with an angle-maintaining BHA and an 8 3/4-in. bit began at a depth of 10 811 ft (3295 m). After steady drilling for about 310 ft, the slick line used for the single-shot surveys broke while being withdrawn and fell to the bottom of the hole. To recover the slick line, the drill string had to be pulled out, but in the process it became jammed at a depth of 6300 ft (1920 m), in the 12 1/4-in. portion of the hole. Retrieval of the slick line and dislodging of the BHA took four days.

The diagnosis was that a "keyseat" had formed in this zone; the 6 3/4-in. (171-mm)-diameter couplings on the drill pipe had worn a vertical groove into the high side of the borehole wall that was sufficiently deep to ensnare a BHA drill collar or reamer. Later examination of the BHA revealed deep scrape marks on the top part of the uppermost 3-point reamer, lending support to the keyseat diagnosis. The keyseat zone was drilled and reamed out, and a string reamer was added to the BHA so that reaming could continue during drilling. A moderately strong, rotary angle-building assembly was then used to drill to 11 454 ft (3491 m), at which depth single-shot surveying showed a borehole trajectory of N50E, 33 1/4°.

A second drill string was put into service at this point, so that the one that had been in use could be inspected (significant time and money were saved by having a second string of drill pipe on hand, because drilling did not have to be interrupted for inspections). The original drill string was found to have one cracked pin on the E-grade pipe and eight on the S-grade pipe.

The second drill string consisted of about 100 joints, or approximately 3000 ft, of E-grade drill pipe on the bottom of the string (E-pipe, being more fatigue-resistant, was better suited to the higher temperatures at depth) and 250 joints of high-strength, S-grade pipe at the top (where pulling loads are greater and a drag of 100 000 lb in excess of pipe weight was not infrequent). The string weight at this time was about 250 000 lb.

On May 15, the next drilling run—again with an angle-building assembly—took the hole depth to 11 595 ft and attempted to correct the loss in inclination of the previous run; surveying over the 141 ft (43 m) of

new drilling showed a gain in inclination of 1 1/2° in the first 67 ft (20 m), increasing to 2 1/2° by 137 ft (42 m). The trajectory was N50E, 35 3/4°. A 30-hour drilling run with an angle-building assembly then deepened the hole to 11 926 ft (3635 m)—a rate of 11 ft/h—but with no change in the direction or inclination of the borehole. At this point, it was becoming clear that downhole-motor corrections would be required to turn the hole direction more toward the east.

The first correction run was begun with the smaller (5 3/8-in. [137-mm])-diameter Maurer turbodrill. After just 25 ft had been drilled, at a low bit load of 5000 lb, the bit apparently "locked up" and the run had to be terminated. When the bit was inspected, the cones showed severely ground surfaces, indicating that the turbodrill had been "spinning" the bit rapidly on the bottom of the hole. A reaming and drilling assembly in an angle-maintaining configuration then got stuck twice—probably because sulfur-reducing chemicals (added to the reserve pits to reduce dissolved hydrogen sulfide) had compromised the lubricity of the drilling fluid. A further attempt at reaming and drilling was difficult, encountering very high torque and drag, but did manage to deepen the borehole to 12 079 ft (3682 m). In a test run, to evaluate the drilling-fluid conditions, the drag force was found to be 120 000 lb over string weight. On May 25, on the advice of the drilling-fluid specialists, the borehole and rig tanks were cleaned out, the annulus was flushed, the west reserve pit was emptied and recharged, and the east pit was emptied (the west pit would be used alone while the east pit was being cleaned).

Drilling continued the next day, and at a depth of 12 100 ft (3690 m) the borehole trajectory reading was N53E, 36°. Two more turbodrill directional runs, reaching a depth of 12 576 ft (3833 m) on June 3, altered the trajectory toward the east—to N72E, 37°.

After a four-day hiatus during which the reserve pits were again cleaned out, repaired, and reconfigured, drilling operations were resumed on June 8. The stiff, angle-maintaining assembly encountered some high-torque and tight-hole conditions, but in general progress was smooth; problems lessened as the concentration of the lubricity additive increased and the hole cooled down. At a depth of 12 895 ft (3930 m), the borehole was found to have a trajectory of N66E, 37 1/4°. A further azimuth correction was needed, but the attempt was plagued with wireline, cablehead, and turbodrill problems. A new EYE steering tool specially designed for high temperatures was ordered from California, and in the meantime drilling went forward for another three days with a rotary angle-maintaining assembly. On June 17 a depth of 13 365 ft (4074 m) was reached, just 568 ft shy of the final TD of 13 933 ft (4247 m). Surveying in EE-3 at this depth indicated a trajectory of N76E, 36°—close to the final reading obtained in the EE-2 borehole below at 14 962 ft (N79E, 35°).

Note: The EE-3 effort could just as well have been halted at this point; drilling of the additional 568 ft would consume another seven weeks of rig time but in fact make no difference to the ultimate development of the Phase II reservoir.

The drill string, which by now had accumulated 100 hours of rotating time, was pulled up for inspection, and the alternate string was put into service. A 64-arm-caliper inspection of the 13 3/8-in. casing showed no additional wear. With the intent of turning the borehole a little farther to the east, one more turbodrill run was initiated; but the drilling assembly could not reach bottom because of tight-hole conditions. Therefore, a reaming run was made, beginning at a depth of 13 280 ft (4048 m). After just a short distance, with the bit at 13 330 ft (4063 m)—35 ft (11 m) above the bottom of the hole—*the drill string parted at a depth of 6500 ft*. This twist-off was a surprise, as the string had just been inspected and no excessive torque or drag had been experienced. When the drill pipe was retrieved, examination revealed that the cause of the twist-off was failure of the threads on the pin end of the drill-pipe connection at this location.

Retrieval of the rest of the drill pipe, HWDP, and the BHA took 45 days. The process began with a free-point survey, which indicated that the drill string was essentially free down to the BHA. The planned approach was to unscrew the upper part of the drill string, remove it, and replace it with S-grade drill pipe. But because the high temperatures made it difficult to work with free-point and back-off-shot tools above the BHA, on June 26 perforations were cut in the HWDP at 12 216 and 12 915 ft, allowing water to be circulated down through the drill pipe and up the annulus to cool the hole.

The next day, two joints of HWDP were successfully unscrewed and the E-grade drill pipe above it all removed. The drill pipe was only slightly bent, raising hopes that the BHA had not jammed in the bottom of the hole. A fishing assembly with heavy fishing jars was then run into the hole. However, jarring was unsuccessful—probably because the remaining 25 joints of HWDP above the BHA were cushioning the impact of the jars. There was no alternative but to remove as much of the HWDP as possible.

After several failed back-off attempts, a pipe-severing service (Jet Research Center, Houston, Texas) was called in to cut the HWDP. A premature firing at 13 088 ft (3989 m), apparently triggered by high temperatures affecting the detonator, did not succeed in cutting the HWDP. Then, on June 30, a second jet severing tool fired properly at a depth of 12 953 ft (3948 m), in the fifth joint of HWDP.

When an attempt to latch onto the HWDP with overshot grapples failed, a mill was employed to face off the top tool joint of the HWDP; but the grapples still would not hold. Then, during another milling run, the drill string twisted off again, at a depth of about 5200 ft (1585 m). Overshot grappling did succeed in removing the milling assembly. The next day, the keyseat

zone between 6500 and 6700 ft (1980 and 2040 m) was reamed (some tightness had been noted in this zone as the milling assembly was being pulled up through it), and the drill string was changed out and inspected.

Meanwhile, field engineers and chemists were attempting to clean up and control high hydrogen sulfide levels in the two reconfigured reserve pits (a very large increase—to as high as 40 ppm—had been detected in one of them; 10 ppm is considered a critical level). The rig tanks were filled with clean water and used for the circulating fluids while the reserve pits were being cleaned, which took three days. A hose and jet nozzle were used to apply a strong biocide to the pit bottom, which brought hydrogen sulfide production to an acceptable level (below 5 ppm).

Following two final milling runs to clean the coupling and expose the 4 1/2-in. (114-mm)-outside-diameter section of the HWDP, the problems with setting the overshot grapples were resolved and the remaining HWDP and the BHA were at last pulled from the hole.[11] Ten magnet and junk-basket runs were then carried out, interspersed with milling and bit runs (both steel-tooth bits and TCI bits were used to "stir" the remaining debris), to clean out the bottom of the hole. After nine days of these operations, a final steel-tooth-bit run verified that the bottom of the hole was clean.

On August 1, 1981, drilling of the 8 3/4-in.-diameter hole resumed with a stiff, angle-maintaining assembly. With the hole depth at 13 494 ft (4113 m), the drill string twisted off at 9683 ft (2951 m). As before, failure of a pin thread was found to be the culprit. Fortunately, this time the BHA was on bottom when the twist-off occurred; the grapple latched onto the top of the drill pipe on the first try, and the fishing jars loosened the entire assembly with little effort, allowing it to be pulled out. The procedure took only one day. Before drilling began again, the drill string was inspected joint by joint on the rig floor, which turned up two pins with cracked threads. These were replaced.

Drilling continued with only one further problem: the drilling jars washed out and leaked, and had to be replaced. Drilling then proceeded steadily for another four days, until the bit torqued up at 13 933 ft (4247 m). This bit had drilled 439 ft (134 m) in 34 1/2 hours—an absolutely outstanding penetration rate of *12.7 ft/h* (4.8 m/h) considering the hardness of the rock, the inclination of the borehole, and the high-temperature environment of the hole. Because the 13 933-ft TD of the EE-3 borehole (corresponding to a calculated TVD of 13 048 ft) was now already *deeper* than the planned one (13 000 ft TVD) and the trajectory (N73E, 34 1/2°) was close to the planned one (N80E, 35°), it was decided to stop drilling at this point.

[11]It is interesting to note that this time, after 35 days' exposure to the 260°C static borehole temperature, the heavy-duty hydraulic drilling jars were still operating properly.

The Final Position of EE-3 Relative to EE-2

The EE-3 drilling plan was completed in 461 days with the target parameters closely approached. The largest deviations were (1) a slightly larger vertical spacing—about 1300 ft (400 m)—in the very upper portion of the intended reservoir region (the spacing fell within the target range of 1200 ± 50 ft for the rest of the region); and (2) a lateral displacement of EE-3 with respect to EE-2 of about 180 ft (60 m) at the EE-3 TVD of 13 048 ft, as estimated from magnetic single-shot survey data. The final relative positions of the two boreholes, and the magnitudes of the deviations of EE-3 from the target parameters, are illustrated in Figs. 5-10 and 5-11 (in terms of TVD) as surveyed after the completion of drilling.

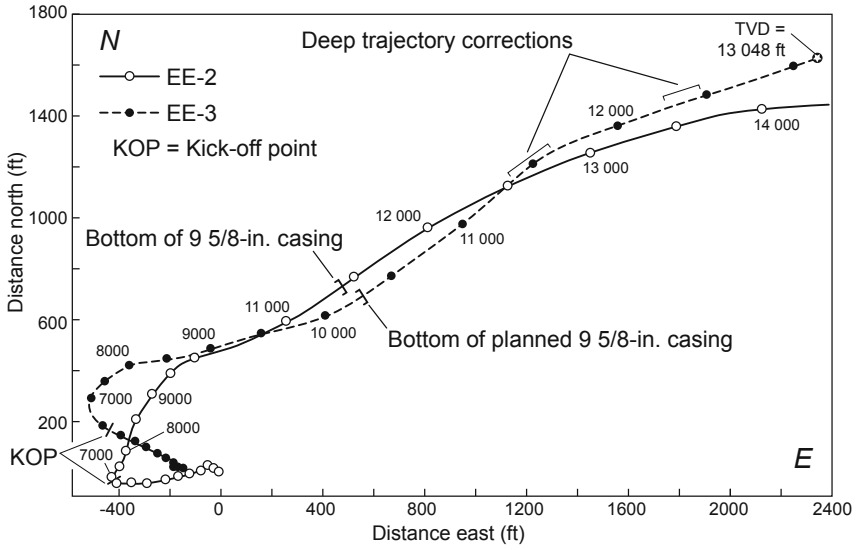

Fig. 5-10. Plan view of the relative trajectories of the EE-2 and EE-3 boreholes. (Depths are TVD.)
Adapted from Rowley and Carden, 1982

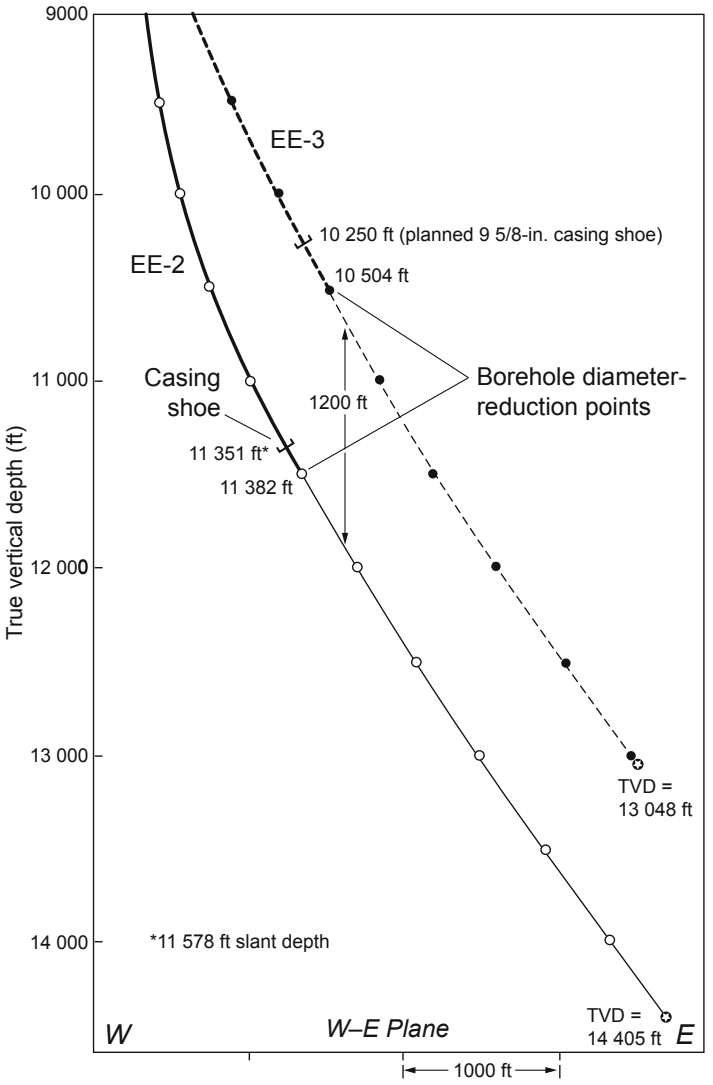

Fig. 5-11. Trajectories of the EE-2 and EE-3 boreholes projected onto a west–east vertical plane, showing the vertical separation between the two boreholes.
Adapted from Rowley and Carden, 1982

Completion of the EE-3 Borehole

The EE-3 TD of 13 933 ft/TVD 13 048 ft (4247/3977 m) was reached on August 7, 1981. The final 18 days of operations were spent completing EE-3 to serve as the production well for the planned two-well, Phase II HDR system. Central to this task was the running and stage-cementing of a string of 9 5/8-in. (244-mm) production casing, from the surface to a depth of 10 374 ft (10 250 ft TVD).[12]

Pre-Casing Operations

In preparation for running and cementing of the casing, the borehole was cleaned and conditioned. A significant amount of black "gunk"—thermally degraded Torq-Trim friction reducer mixed with drill cuttings and other residue—was coating the borehole walls and had trapped cuttings on ledges, crevices, and along the low side of the hole. The initial cleaning consisted of two 3200-gal. polymer–bentonite mud sweeps (to wash as much of the residual drill cuttings as possible out of the hole) followed by a detergent solution. Then, a field-fabricated 8 3/4-in. scraper assembly was run into the hole and cycled up and down across the lower (8 3/4-in.) section of the borehole. With the scraper assembly on bottom, 27 000 gal. of detergent solution was pumped into the hole.

Next, preparations began to install a cement plug, to ensure that when the casing was later cemented in place, the cement would not flow down the inclined borehole below the casing shoe by displacing the lower-density water. (Nevertheless, this is exactly what would happen to this first cement plug!) The bottom of the plug was to be placed at about 10 900 ft, a short distance into the 8 3/4-in. portion of the hole, which began at 10 811 ft. A temperature log run by the Los Alamos Instrumentation Group showed a static borehole temperature of 198°C at 11 000 ft, with a temperature recovery rate of 0.6°C/h. This information was forwarded to the cementing engineers at Dowell, for use in testing cement samples and calculating the amount of retarder to be added.

The drill pipe was run in open-ended to about 10 900 ft, and 2440 gal. (9200 L) of 16.5-ppg cement was pumped downhole. The cement slurry was then displaced from the drill pipe with water, the pipe was withdrawn from the hole, and the cement plug was left to harden for 18 hours. When a 12 1/4-in. steel-tooth bit was run into the hole to face off the cement plug, it reached 10 783 ft (8 ft above the bottom of the 12 1/4-in. portion of the hole) without tagging any cement. This meant that the cement plug had displaced the water in the borehole and had slid down into the 8 3/4-in. portion of the hole. While the bit was maintained at 10 783 ft, the hole was cooled by a 6-hour circulation to prepare for additional logging. Returns reaching the surface contained fine sand but no cement.

[12]Nowhere in the literature is there an indication of how this casing depth was selected.

The pipe and BHA were pulled out of the borehole, and the Los Alamos Instrumentation Group ran a repeat temperature log. It was followed by a Schlumberger suite of temperature-sensitive logs, run upwards from 10 800 ft to 3000 ft, that included gamma ray, compensated formation density, compensated neutron, and one-arm caliper (all but the caliper log were run to obtain baseline data for use following cementing of the casing, to test for any significant pockets of water that may have been bypassed by the cement). When the logging tools were recovered, they and the bottom 100 ft of logging cable were coated with black gunk. Schlumberger then ran a borehole geometry log (two-independent-arm caliper and dip-meter surveys), beginning around 9500 ft (2900 m) and proceeding upward to 5900 ft (1800 m), at which point the tool failed. This equipment too, when withdrawn, was found coated with black gunk, and there were traces of black gunk on the bottom 1510 ft (460 m) of logging cable.

The Los Alamos temperature survey tool was then rerun, between the surface and a depth of 10 800 ft (3290 m). At that depth, the poor response of the tool suggested that the probe had become plugged and thereby insulated from the borehole environment. The tool was moved up and down the hole in an attempt to flush off any accumulated material, but to no avail. When it was pulled out of the hole, the same black gunk was found to be coating the sonde and plugging the thermistor flow passages. The tool was cleaned and then run downhole again. This time it recorded a temperature-recovery rate of 4°C/h at 7300 ft (2225 m), and a temperature of 185°C and recovery rate of 0.5°C/h at 10 700 ft (3260 m). The probe was then lowered further, to sound for the cement plug. It bottomed at approximately 10 810 ft (3295 m). When once again withdrawn from the hole, it was heavily coated with black gunk.

On August 12, a repeat cement plug was placed through open-ended drill pipe positioned at a depth of 10 777 ft. This composite cement plug, "engineered" on the basis of the previous Schlumberger caliper logs, consisted of 1500 gal. of 16.5-ppg cement, followed by 2800 gal. of a lower-density, 11.3-ppg cement slurry containing 252 ft^3 of expanded perlite (intended to prevent "density overturn"), and finally 130 gal. of 16.5-ppg cement. The plug was successful. After a nine-hour wait, it was tagged at 10 215 ft and faced off to a depth of 10 400 ft. Two 3200-gal. polymer–bentonite mud sweeps followed, to clean the hole of remaining cement cuttings.

Preparations then began to run the casing—including the installation of casing jacks, with sub-base and supports, on the cellar floor underneath the rig structure; these would be used for tensioning of the casing after the first-stage cementing.

Running of the 9 5/8-in. Production Casing

Given the higher bottom-hole temperature measured in EE-2 (317°C instead of the anticipated 275°C), and consequently the likelihood of a higher mean reservoir production temperature, the design of the production

casing for EE-3 was critically reviewed and subsequently modified. The original casing specifications—40 lb/ft, grade S-95, and N-80 with buttress-thread connections—were upgraded to 47 lb/ft, grade P-110, and patented VAM connections designed to minimize the potential for joint failure during tensioning. A further reason for the selection of the thicker-walled P-110 casing was to provide a greater margin against collapse or buckling during reservoir production and greater resistance to wear and corrosion. (However, the drilling supervisors evidently did not take into account another factor: geochemical analysis of the dissolved gases in the reservoir fluids had revealed significant amounts of hydrogen sulfide. The grade S-95 steel, although not as hard as the grade P-110, is more corrosion-resistant and more resistant to the adsorption of hydrogen. Its replacement with grade P-110 steel meant that the new casing would be more prone to hydrogen embrittlement at the grain boundaries of the steel microstructure.) The casing was inspected for defects, both in the material and in threads and couplings. All joints received Amalog IV (AMF Tuboscope) special end-area and full-length drifting inspections, after which fifteen joints (5.3%) were rejected. The float shoe, float collar, and stage collar received black-light, end-area, and full-dimensional inspections.

Once the casing-handling and torque-turn-monitoring equipment had been assembled and installed on the rig floor, the production casing was finally picked up and run in the hole. The casing shoe (with the float collar just above it) was landed at a depth of 10 374 ft (3162 m), and the stage collar was installed in the casing string such that its final position was at 7281 ft (2218 m). While the first of two 53.3-lb/ft, L-80 landing joints was being run in, the string lost weight—it apparently had come to rest on an obstruction in the hole. With the attachment of a cementing head to the top of the string, the rig pumps easily washed the string through the obstruction. The other landing joint was run in without difficulty.

The next step was to stretch-test the casing string. When the 380 000-lb pull force initially on the rig's drawworks (the weight of the casing string less the frictional lift provided by the borehole) was increased to 434 000 lb, the casing rode up out of the hole only 10 1/2 in. (27 cm). A force of 500 000 lb brought about a movement of 24 in. (61 cm). When the pull force was returned to 380 000 lb, the casing retreated 28 in. (71 cm) into the hole—4 in. (10 cm) farther than its original position—probably because of a change in hole friction during this pipe-reciprocating exercise.

Stage Cementing

The 9 5/8-in. casing would be cemented in two stages: first, the bottom 3093 ft of casing, between 10 374 ft and the top of the stage collar (7281 ft); and second, a section of about 4280 ft above the stage collar. The formulation to be used for the first stage was a special Class H, high-temperature

cement mixture designed for superior strength and low permeability. For the second stage, a lightened cement would be placed in the annulus above the stage collar, to extend upward to about the 3000-ft (914-m) depth. Approximately 450 ft of borehole (outside the 9 5/8-in. casing and below the 13 3/8-in. casing) would be left uncemented to relieve any buildup of annulus pressure caused by heating during production.[13] This two-stage strategy meant that

1. the uppermost 3000 ft of the 9 5/8-in. casing would be uncemented —and thus unsupported—for about 2550 ft within the 13 3/8-in. casing and about 450 ft within the 12 1/4-in. drilled hole below the casing (because the water level in the annulus between the two casing strings rose to only about 1700 ft, the remainder of the annulus to the surface was filled with air);
2. the section of the casing in the mostly vertical portion of the borehole (from 3000 ft to 7281 ft) would be laterally supported with lightened cement; and
3. the lowermost section of the casing, over the inclined portion of the borehole below 7281 ft, would be strongly laterally supported with high-density cement (this extra strengthening afforded protection against the buckling that could result from thermal expansion during production).

Once the cement had set, a tension load of about 900 000 lb (40×10^5 N) would be exerted on the top 3000 ft of the 9 5/8-in. casing, to prestretch it enough to compensate for about one-half of the expected thermally induced compressive stress (with a hold-down force of about 450 000 lb, the welded, sealed wellhead was designed to contain the potential thermal growth within this unconstrained length of casing when, during reservoir production, it went from tension into compression).

The first stage of cementing began with a 34 000-gal. preflush of water (the pH increased to 12 by the addition of caustic soda) and an 800-gal. spacer of fresh water mixed with 1.2% D-28 retarder. Then 3500 gal. (13 400 L) of 10.5-ppg pozzolan scavenger cement slurry—288 sacks of pozzolan mixed with 2400 gal. (8900 L) of fresh water and 1.2% D-28 retarder—was pumped into the casing. Next, 2100 gal. (7900 L) of 16.6-ppg cement slurry was pumped in, consisting of 950 sacks of Class H cement, 6050 gal. (22 900 L) of fresh water, 40% silica flour, 40% 100-mesh silica sand, 2% bentonite, 0.75% D-65 turbulence enhancer, 0.6% L-10 and 1.2% D-28 retarders—a volume calculated to be 25% in excess of the amount needed to fill the annulus between the float shoe and the stage collar.

[13]Of course, considering the numerous holes and splits near the bottom of the 13 3/8-in. casing, which provided ample communication between the annulus and the loss zones in the Sandia Formation, pressure buildup should hardly have been a concern.

Next, the wiper plug was released from the cementing head and displacement water was pumped down the casing. The volume needed to displace the cement out of the casing and up the annulus to the stage collar had been calculated as 31 500 gal. (119 000 L); but because the system pressure had risen to 3300 psi (22.8 MPa), the most water that could be pumped in was 29 500 gal. When the casing pressure was released, about 400 gal. of water flowed back out of the casing, indicating that the check valves in the float collar and float shoe were holding. It was estimated that about 1700 gal. (6400 L) of cement remained in the bottom 650 ft (200 m) of casing.

The stage-collar-opening bomb was dropped, and 40 minutes later the pumping of 80 gal. of water at a pressure of 1200 psi (8.3 MPa) opened the stage collar. To flush any residual cement above the stage collar up and out the annulus, the rig pump circulated water down the casing and through the stage collar until cement was detected at the surface, and then until the return water became clear. A temperature survey followed: the tool was run down inside the casing to a (wireline) depth of 7282 ft (2220 m), where it encountered the stage-collar bomb (which was blocking the casing), confirming its location. The tool was pulled up to 7275 ft (2217 m), at which depth a 2-hour dwell measurement yielded a temperature of 138°C and a recovery rate of 0.1°C/h. A period of 72 hours was allowed for setting of the cement.

Note: A cement-bond log run several months later, after completion of the borehole, would find the top of the stage cement in EE-3 at 5300 ft—considerably lower than the planned depth of 3000 ft. The literature offers no explanation for this discrepancy.

The hydraulic casing-tensioning jacks were now activated by high-pressure fluid pumped from a Dowell frac truck, plumbed into the jacks' piping system. A hydrostatic test of the piping system was first run to 15 000 psi (103 MPa), then the wellhead slips were adjusted and the hydraulic system and casing jacks were tested. Next, the casing jacks were attached to the upper landing joint of casing and were cycled up and down five times to stretch the casing and work the neutral point (where the pipe was neither in tension nor compression) down to about 6440 ft (1960 m), with about 3 ft (0.9 m) of stretch retained. Finally, the wellhead slips were set in the casing head.

The cement for the second stage, a perlite-lightened cement slurry, was tested and mixed by Dowell personnel; the volume was carefully calculated, from the caliper log, to just fill the annulus to the 3000-ft (914-m) depth—about 4280 ft (1305 m) above the top of the first stage. After the borehole had been flushed with 840 gal. (3180 L) of highly alkaline (pH-12) water, followed by an 840-gal. spacer of fresh water containing 2% D-28 retarder, 16 100 gal. (61 000 L) of slurry was pumped down

the casing. The rubber top wiper plug was then released and displaced with 21 700 gal. (82 200 L) of water having a pH of 11–12. An increase in the pumping pressure to 3100 psi (21 MPa) indicated that the plug had reached the stage collar; when the surface pressure was released and only 210 gal. of water flowed back, and then all flow ceased, it was clear that the stage collar had closed.

The upper 3000 ft of casing (above the second-stage cemented zone) was now further pre-tensioned. Three loading cycles, the last of which attained 885 000 lb_f (3.94×10^6 N), sufficed to stretch the casing an additional 5 ft (1.5 m); added to the 3 ft of stretch achieved following first-stage cementing, the total casing stretch was now about 8 ft (2.5 m). The wellhead slips were set in the casing landing spool, and the top joint was cut off 5 ft (1.5 m) above the wellhead. When the jacks were lowered, the measured loss of casing stretch was only a little over an inch.

The cement was allowed to set for 72 hours, after which the wiper plug and the cement remaining in the casing above the stage collar were drilled out with a steel-tooth bit. Following high-viscosity-gel sweeps to clean out the cement cuttings, the cement plugs below the casing shoe were drilled out from 10 397 to 11 241 ft (3169 to 3426 m). Soft cement—and considerable amounts of black gunk—were encountered, prompting a second gel sweep of the hole. Cement-bond logs showed possible weak bonding between 10 082 and 10 296 ft (3073 and 3138 m) and good bonding elsewhere. But these results turned out to be unreliable because of improper centering of the logging tool, and new logs would be needed before the start of fracturing operations.

The final cleaning consisted of washing and reaming down to TD (13 933 ft) with an 8 1/2-in. (216-mm) bit, two flushings with a pH-12.5 solution, and a clean-water rinse. The EE-3 borehole was completed on August 25, 1981 (Fig. 5-12).

Unfortunately, as discussed in detail below (see *The "Incomplete" Completion of EE-3*, p. 312), no attempt had been made to validate the EE-3 casing setting depth of 10 374 ft. Although the casing and cementing programs were very well engineered, they did not take into account the possible presence, below the selected casing setting depth, of low-pressure joints associated with the Phase I reservoir. Nor was there any "contingency plan" for such a possibility.

Finally, the completion plan did not call for pressure-testing the casing shoe after cementing—a standard procedure in borehole completions.

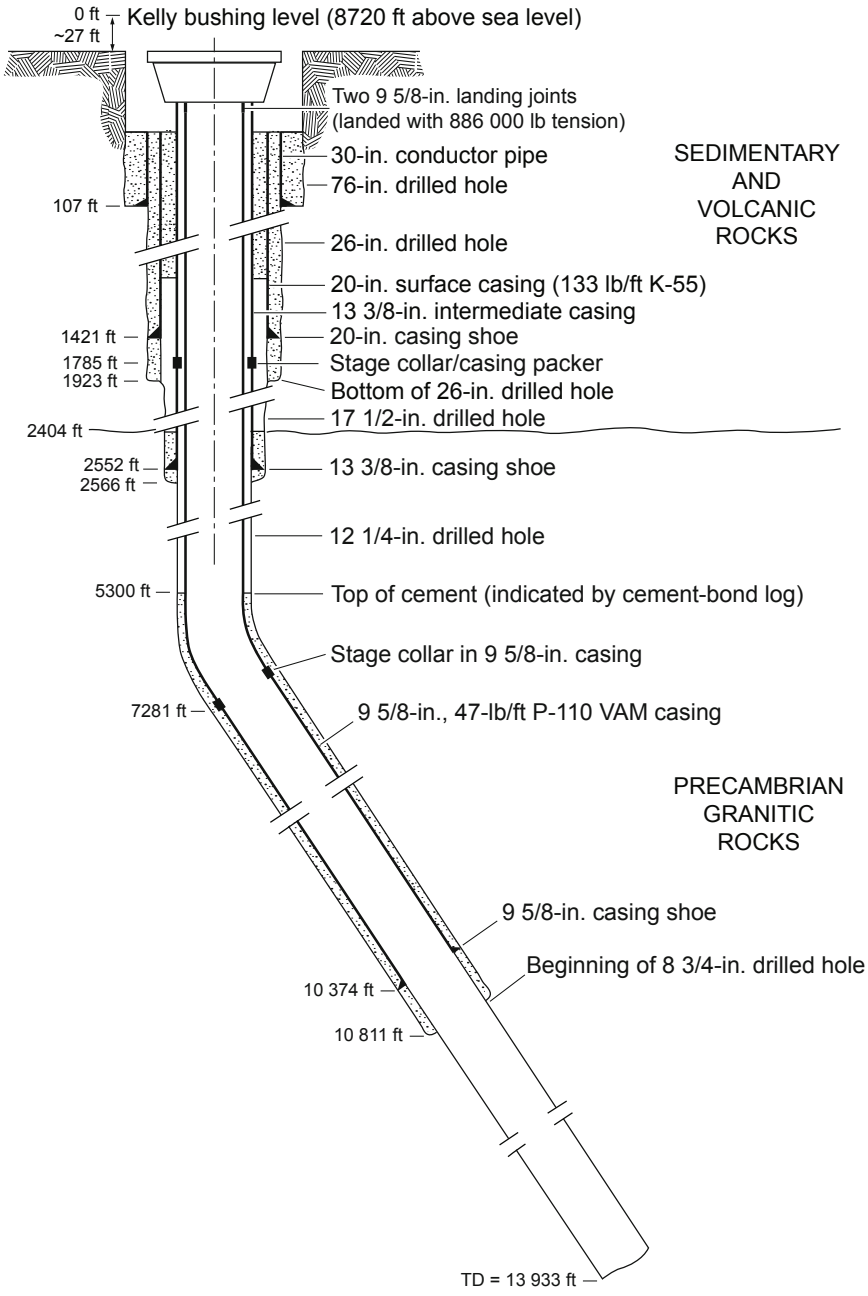

Fig. 5-12. Diagram of the completed EE-3 borehole following running and cementing of the 9 5/8-in. casing.
Adapted from Rowley and Carden, 1982

Equipment and Materials: Performance in the EE-3 Borehole

Rotary Drilling Assemblies Used in the Crystalline Basement

As was the case for EE-2, most of the drilling of the EE-3 borehole in the crystalline basement was done with rotary drilling equipment incorporating TCI button bits. The hole was stabilized and reamed with 6-point and 3-point roller reamers (smooth-faced TCI rollers could be installed when wall contact was desirable for stabilization, and knobby TCI roller-cutters could be installed for reaming). These reamers are very effective in granitic rock, and their rotating rollers also act as bearings between the BHA and the borehole wall.

In addition, all of the rotary BHAs included a near-bit roller reamer to keep the hole from narrowing too rapidly as the bit wore down in the very hard and abrasive drilling environment. If, during directional drilling, the inclination of the borehole needed to be increased, a standard "fulcrum"-type angle-building assembly was used (but these assemblies typically caused the borehole trajectory to drift toward the north at unpredictable rates).

The section of the 12 1/4-in hole between 2552 ft (the bottom of the 13 3/8-in. casing) and 6444 ft was drilled with angle-maintaining assemblies. The drilling plan called for this section to be straight, and the upper portion was; but the lower portion deviated somewhat toward the northwest because of heterogeneities in the crystalline rocks. Even though the angle-maintaining assembly was very stiff, bit load had to be reduced to keep the inclination from increasing too quickly. By the 6444-ft (1964-m) depth—the kickoff point for directional drilling—the inclination had reached 10°.

At the kickoff point, downhole motors were employed to change the azimuthal direction of the borehole from northwest to northeast. Because the TCI bits on these motors wore and lost gauge very rapidly, it was almost always necessary to use rotary reaming assemblies to bring the hole back into gauge. These reaming assemblies were also very stiff, angle-maintaining assemblies (allowing a similar stiff assembly, if needed, to be used directly in the next rotary drilling run).

Following the sidetracking of EE-3, angle-building and downhole-motor runs were alternated, the angle being controlled via a single 6-point reamer (it was assumed that an angle-maintaining assembly was no longer necessary in the 12 1/4-in. portion of the hole). Below 10 200 ft (3109 m), however, where the inclination had to be increased more quickly, the 6-point reamer was replaced with a 3-point reamer (with an extension sub between the bit and the bottom reamer). Unexpectedly, this assembly did not increase the angle by more than 1 1/2°/100 ft, comparable to the rate in EE-2 at similar depths—illustrating again the effect of variations in the fabric of the Precambrian basement on the progress of directional drilling. Even so, the alternating turbodrill and angle-building runs achieved a final inclination of 34 1/2° and an azimuth of N73E at a drilled depth of 13 933 ft.

For the most part, the rotary drilling assemblies used in EE-3 performed as designed, but the rates at which they changed inclination were neither predictable nor easy to control.

Downhole Motors

The performance of the directional-drilling assemblies used in EE-3 is summarized in Table 5-6. The major reasons directional runs were aborted were, in order of frequency, failure of the steering tool; wearing of the bit; leaking of the float valve (causing the motor to become plugged); and failure of the motor. Difficulty starting the motor was also a problem occasionally, even when the motor was properly oriented. In EE-3, the cause of this problem was usually a too-tight hole (because of sharp directional changes or insufficient reaming). In many cases the solution was to ream to bottom with the motor, or to begin motor drilling in a series of short runs (a bit-length each) while rotating the azimuth in small increments until the motor was correctly oriented.

Table 5-6. Performance of directional drilling* assemblies used in the EE-3 borehole

Motor type	Diameter of motor, in. (mm)	Total number of runs attempted	Number of runs drilled	Average run length, ft (m)	Average rate of penetration per run, ft/h (m/h)	Average duration of run (h)
Maurer T7	7 3/4 (197)	17	14	43.3 (13.2)	12.7 (3.9)	3.4
Maurer T5	5 3/8 (137)	8	5	59.3 (18.1)	28.2 (8.6)	2.1
Navidrill PDM	8 (203)	10	9	62.2 (19.0)	14.8 (4.5)	4.0
Dyna-Drill PDM	7 3/4 (197)	8	8	59.6 (18.2)	10.8 (3.3)	5.5
Baker PDM	6 3/4 (171)	5	4	98.5 (30.0)	7.0 (2.1)	14.0

*excludes sidetracking operations

Source: Rowley & Carden, 1982

As shown in the table, the three PDMs performed about equally well. The Baker motor, which ran the longest, averaged a drilled distance equal to three joints of drill pipe—considerably longer than that achieved by the Maurer turbodrill. Having the lowest rpm and highest torque characteristics of the three, the Baker motor delivers longer bit life; on the other hand, its lower rpm translates to a lower penetration rate.

The Maurer high-temperature turbodrills in general operated very satisfactorily. The larger, 7 3/4-in.-diameter motors, which were used in the 12 1/4-in.-diameter hole, were successful in 14 of 17 drilling runs; of the three failures, two were caused by float-valve problems that resulted in plugged bearings, and one by stalling of the motor under tight-hole conditions.

The smaller, 5 3/8-in.-diameter Maurer turbodrills, which were used for eight directional drilling runs in the 8 3/4-in.-diameter section of the borehole, performed very well. (These tools had been tested in EE-2 as well as in the laboratory, with a view to employing them in EE-3.) The last three of the eight runs had to be aborted, but it was because of failures of the EYE steering tool. Had these runs succeeded, the deepest part of the hole would probably have been maintained within the specified lateral tolerances. Once it became clear that excessive bit wear, bit liftoff, and "runaway" turbine speeds could be controlled with a high bit load (20 000–25 000 lb), operation of the turbodrill was stable and reliable. The rapid flat wear on the bit cones that had been caused by the turbodrill spinning off bottom—as though the bit had run up against a high-speed grinding wheel—was no longer encountered when bit load was increased. Further, although problems had been anticipated in keeping the bit load consistent and in controlling the speed of the turbodrill, these did not materialize. A steady rate of penetration was maintained at rotational speeds of 350–450 rpm.

Drilling Fluids System

The drilling fluids system used for EE-3, including methods for cooling of fluids, use of additives, and settling of cuttings, was based on the experience with the earlier boreholes (GT-2, EE-1, and EE-2). A large reserve pond, having a surface area of approximately half an acre, was used to cool the fluid as it exited the borehole and to allow cuttings to settle. The large surface area cooled the water effectively, but it also enhanced exchange of oxygen; for this reason, large quantities of oxygen scavenger (ammonium bisulfite) were added to the water before it was pumped downhole, to reduce the oxygen content and thereby the potential for corrosion. To further reduce this potential, a basic pH (9.5–10.5) was maintained. Scaling was controlled with a phosphonate compound that removed the cations available for precipitate formation. Monitoring via corrosion coupons (material samples exposed to drilling fluids) showed that these methods did keep corrosion to a minimum.

Drilling-fluid-related problems experienced during drilling in the crystalline basement arose mainly from the extreme abrasiveness of the rocks being drilled and the high temperatures encountered (up to 280°C). In addition, there was a modest amount of fluid loss when the EE-3 trajectory crossed several open joints that had previously been pressure-stimulated in the deeper region of the Phase I reservoir. The combination of the inclination of the hole (as great as 35° from vertical), the use of plain water as

the primary circulating fluid, the large volume of fluid, and the abrasiveness of the basement rocks created special problems with excessive torque. Reducing friction on the drill string and the BHA was extremely important under these conditions.

Several methods of friction reduction were evaluated and tested. The best candidate appeared to be a biodegradable, water-soluble chemical. Several types were tested in the laboratory, only two of which were found suitable for downhole testing (an additional constraint being the high temperatures to which the substance would be subjected). Torq-Trim II, a mixture of modified triglycerides and alcohols, performed the best, but this chemical was also susceptible to thermal degradation; at higher temperatures (greater than about 190°C), it was effective only temporarily and had to be continually replenished. With its use, wear on the drill string and on surface equipment was reduced, and higher loads could be placed on the cutting surfaces of the bit. When thermally degraded, the Torq-Trim formed a thick residue that combined with drill cuttings and other residue to form a heavy, black "gunk" that coated the BHA, the logging tools, and the borehole walls. To reduce buildup of the black gunk, a surfactant (detergent) was used to emulsify it, after which the hole was flushed with water.

Drill Pipe and Drill Collars

During the drilling of EE-3, the number of drill-string failures and twist-offs (the parting, separation, or breaking of a joint of drill pipe by torque or tension) was four times higher than during the drilling of EE-2.

Fifteen drill-string failures occurred that do not fit the traditional definition of twist-offs. These were "washouts," all but one of them in the threaded-connection areas of drill collars in the BHA. (A washout is the slow erosion of the metal in the threaded connection by pressurized drilling fluid: fluid enters a crack in the thread and progressively erodes the metal in the pin or box until, under either tension or torque, the connection finally breaks). Four such washouts necessitated fishing operations. The one non-drill-collar washout was in a joint of drill pipe.

Five true twist-offs occurred during drilling operations, compared with none during the drilling of EE-2. It was the second of two twist-offs in the body of the 5-in. (127-mm) drill pipe that led to the longest of the EE-3 fishing operations (and, when the fishing was unsuccessful, to sidetracking of the borehole). Following this second twist-off, the 5-in. pipe—which was fatigued from its use in both EE-2 and EE-3—was withdrawn from the hole. Examination of the two breaks in the pipe revealed severe corrosion pitting, and detailed post-failure analysis pointed to fatigue as the cause of the breaks. The other three twist-offs occurred in the 4 1/2-in. (114-mm) drill pipe that replaced the 5-in. drill pipe; all three were caused by cracking of the threaded pins on the tool joints.

Finally, two failures were caused by tension on the drill pipe that caused it to pull apart. The first was a failure in the body of a joint of 5-in. drill pipe, at loads well below the API minimum tensile strength—which is typical of weakening due to corrosion. Thirty-one days were lost to the retrieval operations necessitated by this failure. The second involved a tool joint on the 4 1/2-in. pipe that failed as a connection was being made: apparently the threaded pin on the upper section of drill pipe cracked and the connection pulled apart—again at loads far below the API-specified minimum.

In an attempt to prevent further drill-string failures in EE-3, two remedial actions were taken: first, the drill pipe was inspected every 30 days or 500 rotating hours, whichever came first; second, a complete, spare 4 1/2-in. drill string was procured and maintained on site so that drilling could continue with one string while the other was being inspected. The latter practice saved 4 1/2 days of the 5–6 days' downtime usually required for drill-string inspection. In addition, with more time available, the inspection could be done more carefully, increasing the likelihood that problems would be detected. A further measure, taken during the final bit runs, was inspection of the pins and boxes of each drill-string joint as it was being added. Three cracked pins were discovered in this way.

The higher frequency of drill-string failures in EE-3 was probably due in part to the accumulative fatigue of the 5-in. drill pipe (from earlier operations) and in part to the greater number and severity of doglegs (Fig. 5-13). Sharp s-curving, such as that created in the 6500- to 7200-ft (1980- to 2195-m) interval and in the 9700- to 10 500-ft (2960- to 3200-m) section of the original EE-3 borehole, was particularly bad. (Once a borehole in crystalline rock has become crooked, tight spots can be alleviated but straightening by reaming is nearly impossible.)

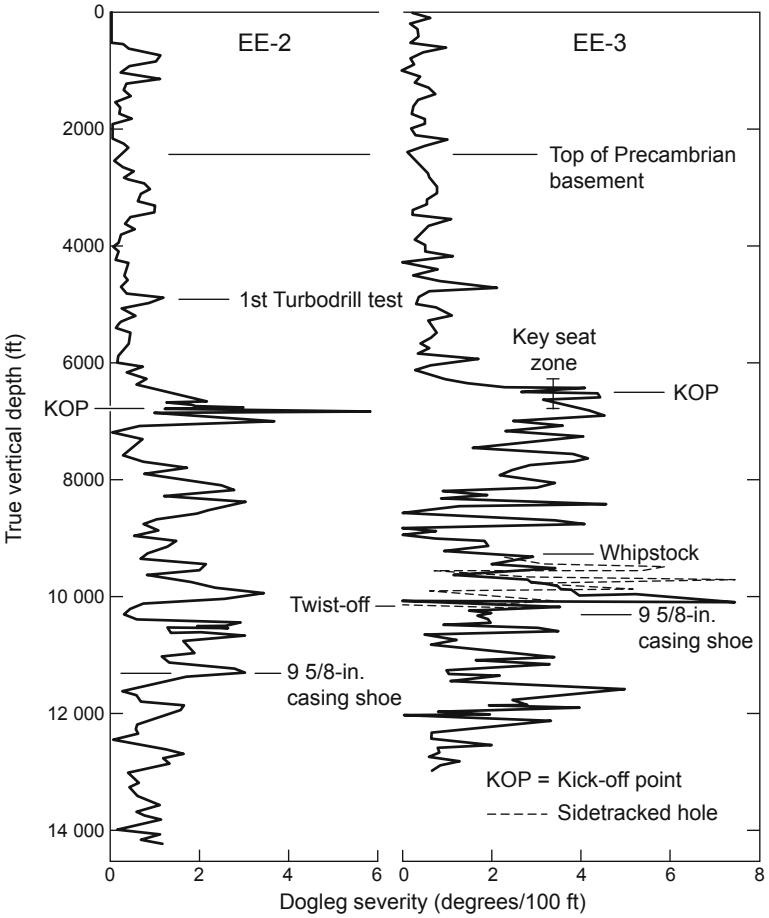

Fig. 5-13. Severity of doglegs in EE-3 vs that in EE-2.
Source: Rowley and Carden, 1982

Elastomer Seals

The elastomer seals used did not withstand high temperatures well. Many of the seals in components of the BHA failed or degraded rapidly at temperatures greater than about 165°C, leading to numerous equipment failures. One of the most frequently encountered failures of this type involved the seals in near-bit float (check) valves. These valves are usually included in a float sub to prevent backflow of drilling fluids and cuttings up the inside of the drill pipe, as can happen when a joint of pipe is added to the drill string. If float valves fail because of high temperatures, cuttings can be carried back up into the BHA, often plugging the downhole motor or the drill collars. Clearing of such plugging usually cannot be done by the rig pumps,

but requires withdrawal of the BHA, a trip to a distant repair shop, disassembly, cleaning and rebuilding of the motor, and rerigging of the steering tool—an expensive and time-consuming process.

During the drilling of EE-3, elastomer seals in float valves were replaced with test seals made of a material resistant to high temperatures. After testing of several prototypes from various elastomer suppliers, an EPDM (ethylene-propylene-diene monomer) seal gave good results in the Los Alamos autoclave for 30- to 40-h simulated rotary-drilling runs and for 3- to 5-h simulated turbodrill runs—both at temperatures of at least 280°C. In addition, a method was developed for tandem installation of float valves—one in the top turbodrill sub and one in a float sub above the turbodrill—to provide redundancy in the case of seal failure.

Corrosion Control Additives

Efforts to control corrosion were complicated by several factors: the high temperatures, the high torque and drag, and the large volumes (630 000 gal. [2 380 000 L]) of circulating fluid needed for cooling. Corrosion was successfully mitigated through the use of an oxygen scavenger (ammonium bisulfite) and maintenance of a basic pH (10–11).

In the later stages of the EE-3 drilling operation, the sulfur compounds added to the drilling fluid to control corrosion created another problem: when the sulfur combined with anaerobic bacteria in the bottom slime of the reserve pits, hydrogen sulfide was generated. The conditions in the reserve pits—low oxygen content, warmth, organic residues (from the friction reducer and gel sweeps) were ideal for the growth of these bacteria. To solve the problem, the pits were dredged, treated with biocides and iron sponge, and thereafter strictly monitored (including hydrogen sulfide levels and pH of the fluids).

Observations from the Drilling of the EE-3 Borehole

Sidetracking in Basement Rock

The diverting of the borehole around the deep fish in EE-3 (at about 10 400 ft) made abundantly clear that it is very difficult to sidetrack an inclined borehole in granitic rock if sidetracking from the high side of the hole is mandated (as it was in EE-3, to retain a high-angle trajectory). In this regard, oil-industry drilling experience proved to be of little use—and may even have been detrimental: it took more than three months for the contract drillers to realize that for high-side kickoffs in hard granitic rock, drilling off of cement plugs is the wrong approach. The result was not only wasted time, but the loss of several million dollars.

Drilling out the high side may work well in the soft to medium-hard sedimentary formations in which most oil drilling takes place; but it is ill-advised in crystalline basement rock, particularly if the angle of departure

from the original borehole is critical. In the case of EE-3, the requirement to drill from the high side was both unreasonable and unwarranted: this borehole could easily have been sidetracked out the *low* side—without the use of a whipstock—just as GT-2 had twice been successfully sidetracked at about the same depth. In addition, with the technique used in GT-2 there would have been little (if any) loss of inclination. Directional drilling could have been employed to realign the diverted borehole with the trajectory of the abandoned portion.

Drilling Through Severe Lost-Circulation Zones

The best of the then-available methods for handling severe losses of circulation—rapidly drilling ahead without returns and then running casing as soon as possible—was employed during the drilling of EE-3. However, as executed, it was not a "polished" procedure. The contract drilling supervisors had adequate knowledge (from the earlier drilling of boreholes GT-2, EE-1, and EE-2) of the first significant loss zone in the Madera limestone, at about 1900 ft, and for that reason they planned to control the sloughing and swelling of the clays and shales above this zone by casing them off before circulation was lost. The plan was to set the surface string of 20-in. casing just above 1900 ft, to cover these unstable sedimentary intervals while full returns were still being achieved. And in fact they managed to drill the 26-in. hole to 1923 ft with full circulation before the loss zone opened up at 1894 ft, with massive and uncontrollable lost circulation; but through a series of errors in execution of the plan, the surface casing string ended up at a depth of only 1580 ft—much higher than intended. As a result, almost 300 ft of soft shale and siltstone was left exposed, to cave and swell as drilling proceeded (without returns) through the Sandia Formation and then about 200 ft into the granitic basement.

Note: Expandable metal liners, such as those now available from Weatherford, would have offered an even better solution to sealing off the zones of severe lost circulation in the Madera and Sandia formations. The two principal loss zones above the granitic basement could have been sequentially "cased off" full-diameter with short lengths of expandable liner, avoiding the more hazardous method of drilling ahead without returns. For example, the 20-in. casing could have been set at about 1880 ft and then a 17 1/2-in. bit used to drill through the higher loss zone until the "bottom fell out of the hole." The subsequent placement of a short (40–50 ft) section of expandable liner, extending below the bottom of the 20-in. casing, would have covered and sealed the loss zone, restoring full circulation. The deeper loss zone, at about 2380 ft, could have been sealed off in the same way, allowing the hole to be drilled ahead into the crystalline basement with full returns. In addition, use of expandable metal liners would have allowed a much better cement job, because the cement could be circulated all the way from the bottom of the 13 3/8-in. casing up into the 20-in. casing.

Time Spent in Drilling-Related vs Remedial Operations

As shown in Table 5-7, the two major problems encountered during the drilling of EE-3—fishing (occasioned by failures of the drill pipe or of the BHA) and sidetracking (which became necessary when extensive fishing operations could not retrieve 140 ft of the BHA)—occupied 235 days, over half of the 461-day EE-3 drilling campaign.

Table 5-7. Time spent on principal activities during the drilling of EE-3

Activity	Incremental time (%)	Cumulative time (%)
Drilling-related		
Drilling	12.1	
Tripping drill pipe	15.1	
Reaming	2.6	38.4
Directional drilling	2.9	
Pipe inspection	1.5	
Circulating and surveying	4.2	
Remedial operations related to		
Sidetracking	21.2	
Fishing	22.2	
Lost circulation	1.2	50.2
Failures of directional-drilling tools	3.8	
Fluids system problems	1.8	
Casing-related		
Running casing	1.6	
Circulating to cool	1.5	5.5
Cementing	2.4	
Logging		1.2
Other activities		4.6

Phase II Drilling: Summary and Conclusions

Directional Drilling Program

The drilling of the deeper portions of the Phase II boreholes represented, up to that time, the most significant directional drilling program ever undertaken in hot, crystalline basement rock. At the same time, a review of the literature on these drilling campaigns makes it apparent that they had been allowed to become ends in themselves. Statements such as "first time directional drilling in deep, hot granitic rock had been accomplished" appear frequently, as if accomplishments of this kind were principal objectives of the HDR Project—which they most certainly were not. Seeing the very tight tolerances on the drilling of EE-3, one would assume that the designers of the effort were fully knowledgeable concerning the jointed

crystalline basement in the deep reservoir region, but this was not the case. It should be noted that almost 2 1/2 years and some $19 million had been devoted to the drilling of these two very difficult boreholes. And as discussed in the following chapter, had EE-2 instead been drilled essentially vertically, the target temperature (275°C) could have been attained in half the time and at a much lower cost—without affecting the ultimate development of the Phase II reservoir.

Drilling Supervision

The most outstanding issue with the drilling of the Phase II boreholes was the less-than-capable drilling supervision. The contract managers assigned to the Project by the consulting firm (which underestimated the complexity of the operation) did not have the necessary technical background and were not adequately experienced in such complex drilling operations. A number of the miscalculations and poor decisions that ensued had serious consequences:

- Because of the error made when adding up the joint lengths of the 13 3/8-in. intermediate casing string in EE-2, when the casing landed hard on the bottom of the hole, the drilling managers believed it to be 100 ft short of bottom (and thus mistakenly interpreted the hard landing as an encounter with an obstruction). Worse, an error in simple addition was not even checked for; instead, the casing was repeatedly rammed into the bottom of the hole, to force it through the "obstruction," until it collapsed. It is not known to this day when the mistake in addition was finally recognized.
- Once it was realized that the situation with the collapsed casing was becoming untenable, remedial action should have been taken: an additional casing string should have been run and cemented in place. It was not, primarily because of the HDR Program Office's lack of knowledge (due to lack of drilling experience) of this common and proven technique for handling severe hole problems. As a result, nearly all subsequent drilling operations in the crystalline basement portion of EE-2 were rendered much more difficult.
- The Laboratory had previously developed methods for sidetracking in deep, hard crystalline rock and had already used these methods successfully—twice—in GT-2. The failure to understand and make proper use of these methods, and instead to employ oilfield techniques suitable only for softer sedimentary formations (repeated attempts to sidetrack off of cement plugs) resulted in the loss of over two months of effort and close to $2 million.
- A number of tool-joint failures and/or twist-offs—several of which led to very lengthy fishing operations—are attributable to an inadequate drill-pipe inspection program (inspections should have been more frequent as well as more comprehensive).

Drilling Fluids Program

The drilling fluids program used during Phase II, which followed directly from that developed for GT-2 and EE-1, was based on the assumption that plain water would be less costly than mud-based drilling fluids. In retrospect, this decision was not altogether appropriate and should have been re-examined—in light of both the drilling fluids technology then available (early 1980s) and the actual results from the drilling of the Phase I boreholes. (This decision too reflected the contract supervisors' lack of experience with drilling in hot, hard rock.)

Given the following observations, it appears that a better choice would have been a mixture of clays (bentonite and other higher-temperature clays) in conjunction with a mud cooler, to cool the drilling fluid at the surface before reuse.

1. The fineness of the drill cuttings indicated that a considerable amount of regrinding of the cuttings was taking place at the bottom of the hole before they were eventually circulated to the surface.
2. The excessive wear on the near-bit reamers also indicated considerable regrinding of cuttings.
3. Upon petrographic examination, the very fine cuttings appeared to have been hydrothermally altered, suggesting to Laboratory geologists that a number of altered fractured zones had been drilled through, particularly in the deeper parts of EE-2. In contrast, petrographic analyses of drilling chips from the later (1985) redrilling of the lower portion of EE-3, referred to as EE-3A—for which mud-based drilling fluids were used—revealed no such hydrothermal alteration; in addition, the drilling chips were much larger than those from EE-2. This evidence strongly suggests that the EE-2 cuttings were hydrothermally altered *during* the actual drilling process rather than originating from hydrothermally altered zones in the basement rock.

The inherent advantages of a mud-based drilling fluids program, particularly for cleaning the hole, had long been recognized in the oil industry and would have markedly facilitated the task of directionally drilling the Phase II boreholes. The cuttings would have been much better suspended in the high-viscosity drilling mud, and thereby transported to the surface almost at the annular velocity of the fluid, preventing most of the regrinding that resulted from accumulation of the cuttings at the bottom of the hole (and the consequent severe wear on the near-bit stabilizers and other components of the BHA). In addition, the cuttings would not have remained at the bottom of the hole long enough to undergo the *in situ* hydrothermal alteration that so confused the geologists and thus led to erroneous conclusions.

Besides reducing equipment costs (fewer reamer runs would be needed before drilling ahead, and reamer assemblies would need less frequent replacement), a mud-based drilling fluid, with its natural lubricity, would also have reduced the wear and abrasion of the drill string so evident

during the drilling of EE-2 and EE-3 (and by thus eliminating the need for Torq-Trim, it would also have eliminated the "black gunk" problem).

The "Incomplete" Completion of EE-3

The way in which EE-3 was completed—precluding any use for the borehole other than that of a low-pressure production well—would drastically alter attempts to develop the Phase II reservoir.

In August 1981, following the drilling of EE-3, the HDR Project management's view of how the Phase II reservoir would develop was uniformly optimistic: A series of vertical "fractures" would be sequentially driven from EE-2 to intersect EE-3 above. In other words, the prevailing view was based on the same strategy that had *not* worked during development of the Phase I reservoir—the only HDR "data point" then available. Despite the failure of the numerous attempts to connect EE-1 to GT-2 (or GT-2B) by hydraulic fracturing during Phase I, it was still assumed that the Phase II reservoir would develop in line with the presupposed theory. Thus, EE-3 was completed as a high-temperature production well, involving several stages of cementing and sequential tensioning of the casing that ruled out any alternate use. A less "robust" *temporary* completion would have allowed for other options. For example, it would have enabled EE-3 to serve as an injection well or to be used for repeated pressure-stimulation of the envisioned joint connections from EE-2 (to reduce the near-wellbore outlet impedance)—which would have made the next several years' work much easier.

Further—and most important—the decision to set the bottom of the casing at 10 374 ft did not consider the possibility that open joints from the Phase I reservoir might extend below that depth—even though the partial loss of circulation only about 350 ft higher up had alerted the drilling supervisors to this possibility. It would have been relatively easy to pressure-test the region below the planned casing setting depth *before* proceeding with the completion: a Lynes inflatable packer rated for moderate temperatures and pressures was available, and had it been employed, the presence of a low-pressure joint connection to the borehole below 10 374 ft would have been quickly revealed. The EE-3 casing could then have been set deeper!

Alternatively, EE-3 could have been completed simply with a scab liner and frac string, which could be replaced or modified later to allow stimulation of EE-3.

With the completion of the Phase II drilling program, after almost two and a half years of work, the stage was finally set for the sequential hydraulic fracturing tests in EE-2 that, it was anticipated, would create multiple hydraulic connections between the two boreholes.

Chapter 6

Attempts to Create a Deeper Reservoir, Redrilling of EE-3, and Completion of the Phase II Reservoir

With the very difficult task of directionally drilling the lower portions of the EE-2 and EE-3 boreholes complete, in early 1982 the critical next step in the development of the Phase II reservoir began. Recall that at this time, the theory that a penny-shaped, vertical hydraulic fracture could be created in jointed basement rock still held sway with the HDR Project management (although many of the Project staff had by then abandoned it). This, of course, was why the lower portions of EE-2 and EE-3 had been inclined 35° from the vertical by costly and time-consuming directional drilling, with EE-3 terminating about 1200 ft vertically above EE-2. Mort Smith, in his Abstract for the 1982 Annual Report (HDR 1983b), stated that "During Fiscal 1982, emphasis in the Hot Dry Rock Program was on development of methods to produce the hydraulic fractures required to connect the deep, inclined wells of the Phase II system at Fenton Hill."

One of the most profound lessons that would be learned from the HDR Project is that it is extremely difficult to establish flow communication between two already-drilled boreholes by hydraulically fracturing between them. It is far better to develop a large pressure-stimulated region near the bottom of one borehole and *then* drill the second borehole through the seismically delineated region to establish the flow connections for the HDR reservoir (Brown, 1990a).

Summary: The Development of the Phase II Reservoir

The events covered in this chapter—the attempts to create an open, jointed reservoir region connecting the Phase II boreholes, by sequentially pressure-stimulating each; the eventual redrilling of the EE-3 borehole to intersect the EE-2 stimulated region; and the brief flow testing of the completed Phase II reservoir—are the most significant of the HDR Project. These experiments and flow testing revealed the major features of the deeper HDR reservoir and represent by far the steepest part of the "learning curve" in HDR reservoir engineering.

On the basis of the joint structures encountered during development of the Phase I reservoir, it was assumed that the principal joints in the Phase II region, just below, would have the same orientation—essentially vertical and striking northwest (the "Phase II assumption"). But this was a mistaken assumption. The principal—i.e., the more continuous—joints in this deeper region were actually significantly inclined from the vertical and therefore had much higher opening pressures.

The project managers were convinced (on the basis of the "penny-shaped fracture" theory) that with sufficient pumping, hydraulic fractures could be opened deep in EE-2 and then driven vertically upward to intersect EE-3.

D.W. Brown et al., *Mining the Earth's Heat: Hot Dry Rock Geothermal Energy*,
DOI 10.1007/978-3-540-68910-2_6, © Springer-Verlag Berlin Heidelberg 2012

After two failed attempts using inflatable packers, a scab liner was cemented deep in EE-2 and several pressurizations (Expts. 2011, 2012, and 2016) were carried out in the 447-ft open-hole interval below the liner. Although no hydraulic communication was established with EE-3—even after the injection of almost 1.3 million gal. of water during Expt. 2016—there were seismic indications that a large, pressure-stimulated region had been created around and above the bottom of EE-2. In section view, the poorly located microseismic events were concentrated in a relatively thin tabular region dipping to the west at about 45° and passing *below* the bottom of EE-3.

In June 1982, what would prove to be a significant error was made by project management: After only three weeks of serious testing of the bottom of EE-2, they decided to sand up and abandon some 3300 ft of the lower section—which had been so difficult and expensive to drill. In a hurry to achieve a connection by whatever means, they decided to abrogate the carefully conceived plan for developing the reservoir by methodically isolating, and then pressurizing, higher and higher regions of the EE-2 borehole. Instead, they carried out three increasingly large stimulation tests in EE-2, from just below the casing shoe at 11 578 ft (the only interval of the open hole that could be easily isolated without the use of either inflatable packers or another cemented-in liner). The top of this interval was isolated by both the cement behind the casing and a high-temperature casing packer set just above the shoe, while the bottom was isolated by the top of the sand plug at 12 060 ft (later raised to 11 648 ft—leaving only 70 ft of open hole).

In December 1983 the last of these tests, referred to as the Massive Hydraulic Fracturing (MHF) Test, created a very large, ellipsoidal volume of induced seismicity (referred to as a "seismic cloud"). Unfortunately, one of the major axes of this cloud was essentially co-linear with the trace of the EE-2 borehole, and the growth of the cloud toward EE-3—the direction of the minor axis—was minimal. Thus, none of the numerous joints pressure-dilated during the MHF Test intersected the EE-3 borehole above. Indeed, because these joints were nearly aligned with the boreholes, it turned out that EE-2 and EE-3 had been drilled in the worst possible direction for hydraulic "fracturing" to establish a connection between them. (Of course, had it been known at the time that the pressure-opened joints would be inclined rather than vertical, the boreholes could have been drilled vertically—which not only would have improved the chances for a connection, but would have been easier and cheaper.)

A large stimulation test (Expt. 2042) carried out in EE-3 in May 1984 also failed to connect the boreholes. Finally, from April through June of 1985, EE-3 was directionally redrilled through the MHF Test seismic cloud, and good flow communication through the nascent Phase II reservoir was at last achieved.

Hydraulic Fracturing Tests Near the Bottom of EE-2

The information on this period is adapted from HDR Geothermal Energy Development Program (1983b) and Matsunaga et al. (1983).

Preliminary Operations

In November 1981, in preparation for fracturing operations in EE-2, a cleaning rig (Brinkerhoff-Signal rig No. 78) was mobilized to remove the thick coating of "black gunk"[1] that had accumulated on the walls of the borehole below about 5000 ft. Two treatments with a commercial detergent, followed by a Hydrojet wash with fresh water, removed this coating and left the hole clean.

During January and February of 1982, pressurization tests were carried out to measure the permeability of the very long open-hole intervals in EE-2 and EE-3 and to identify any open joints. Experiment 2003 (January 6, 1982), conducted at a nominal pressurization rate of 9 gpm, showed EE-2 to be extremely tight: wellhead pressures of up to 2070 psi (14.3 MPa), maintained for 2 1/2 hours, produced an infiltration loss of only about 30 gal. In contrast, pressurization of EE-3 (Expt. 2006) to a maximum of 1480 psi (9.9 MPa) opened (or reopened) a joint at 10 394 ft, just below the casing shoe at 10 374 ft, leading to a rapid loss of water into the Phase I reservoir region. Temperature logging revealed that this joint extended downward along the borehole about 240 ft, suggesting an essentially vertical feature.

Note: This zone of fluid loss just below the casing shoe in EE-3 would create a number of problems in the months ahead. As noted in Chapter 5, the production casing string in EE-3 should never have been landed so close to the Phase I reservoir region. Because circulation had been almost totally lost at a depth of 10 017 ft during the drilling of EE-2 (October 2, 1980), and there was no assurance that the joints pressure-stimulated within the Phase I reservoir did not extend down another 400 ft or so, the region around the proposed EE-3 casing landing depth—about 10 400 ft—should have been pressure-tested *before* the production casing was run.

Fracturing Attempts with Lynes Inflatable Packers

On the basis of the extensive pressurization testing carried out during the development of the Phase I reservoir, it was assumed that a similar pressure-stimulation environment would exist near the bottom of EE-2 (from about 14 900 to 15 100 ft)—i.e., that moderate pressures (about 2500 psi) would suffice to initially open the most favorably oriented joints in this region.

[1]This material was mainly the thermal-degradation products of an organic lubricant added to the drilling fluid, combined with entrained fragments of rubber from drill pipe protectors, drill cuttings, and metal particles.

Thus, the plan was to employ Lynes inflatable packers to investigate the hydraulic fracturing behavior of the rock mass surrounding the bottom of the EE-2 borehole and then to establish hydraulic communication with the EE-3 borehole above.

First, a commercial Hydrojet tool (usually used to sever casing) was used to "notch" the EE-2 borehole 17 ft off bottom (at 15 272 ft). This circumferential notch was intended to serve as an initiation point for a hydraulic fracture, but there is no evidence that it actually affected subsequent fracturing behavior.

On May 2, 1982, after the EE-2 borehole had been cooled by circulating water through the drill pipe, the first Lynes packer test took place. With the center of the packer element at 14 981 ft, the 9-gpm Kobe pump was used to inject fluid at pressures that increased in steps to 1700 psi. The 19-gpm Big Kobe pump was then used to continue pumping. With a total of 225 000 lb of string weight holding the packer down, the pressure was further increased—reaching between 2700 and 2800 psi. At this point, it appears that the shear-pinned bull plug at the bottom of the packer assembly blew out; the shut-in pressure dropped to 2250 psi. There was no indication that any joint opening had taken place at the >2700-psi pressure within the 308-ft packed-off open-hole interval below the packer. Pumping was then resumed—until annular[2] bypass flow at the surface indicated packer failure. When the packer was recovered from the borehole, inspection revealed major blow-out damage on the lower part of the packer element.

The second Lynes packer test was conducted on May 6, after the hole had undergone further cooling by circulation. For this test the packer was centered at 14 989 ft (8 ft deeper than for the first test). With 130 000 lb of string weight holding down the packer, the annulus above was pressurized to about 2000 psi. When the injection pressure reached 4550 psi, after 22 minutes of pumping, the packer failed—as evidenced by a very significant annular flow and a rapid decrease in injection pressure. There was no evidence, either seismic or in pressure behavior, of the opening of a joint in the open-hole interval, despite pressures reaching at least 4500 psi.

Even though measures had been taken to cool the borehole from an initial temperature of 327°C, the wall temperature at the bottom of EE-2 was still high enough to damage the rubber packer materials. In addition, it was

[2]Throughout this chapter, the term "annulus" or "annular" refers to the space between the tubing being used for pressurization (frac string or drill pipe) and the surrounding borehole wall or deep 9 5/8-in. production casing, whichever applies. Where a different annulus is referred to, it is specified as such. During the HDR Project at Fenton Hill, annular bypass flows, or annular leaks—flow into the annular space—were encountered repeatedly.

now apparent that pressures higher than those for which the packers were designed would be required to hydraulically fracture the borehole. For these reasons, the use of inflatable packers was discontinued. Subsequent attempts to hydraulically fracture the lower part of EE-2 would be carried out with a much better mechanical sealing assembly: a cemented-in scab liner.

Fracturing Attempts with a Cemented-in Scab Liner

On May 11, after the bottom of EE-2 had been backfilled with a mixture of sand and bentonite, a 4 1/2-in.-diameter, 292-ft-long liner was run in and landed at 14 842 ft, 447 ft off bottom. The liner was then cemented in, the cement remaining in the liner bore was drilled out, and the sand mixture was washed out to bottom. The top of the liner was fitted with a polished bore receptacle (PBR) into which a mandrel—equipped with a seal assembly and installed at the end of the drill pipe or pressure tubing—could be inserted. With this high-pressure yet movable[3] coupling, the PBR assembly would enable the open-hole interval below the liner to be isolated and pressurized from the surface without affecting the pressure in the annulus above the liner.

For the cementing of the liner, two cement formulations were tested in a Laboratory autoclave under simulated downhole conditions. These tests showed that the kinetics of setting and curing were sensitive not only to temperature at the time of emplacement but also to the rate of temperature recovery after emplacement. A Class H cement formulation with 40% silica flour exhibited the better performance and was then field-tested: a small batch was pumped to the appropriate depth in EE-2 and retained in a section of pipe until it had set and cured. The cement performed satisfactorily during pumping, and when it was later brought up out of the hole and examined, its properties were found to be adequate. The liner was successfully cemented with this formulation (Fig. 6-1).

[3]The seal assembly could move up and down within the long PBR, compensating for tubing and drill-pipe expansion or contraction during injection or pressurization.

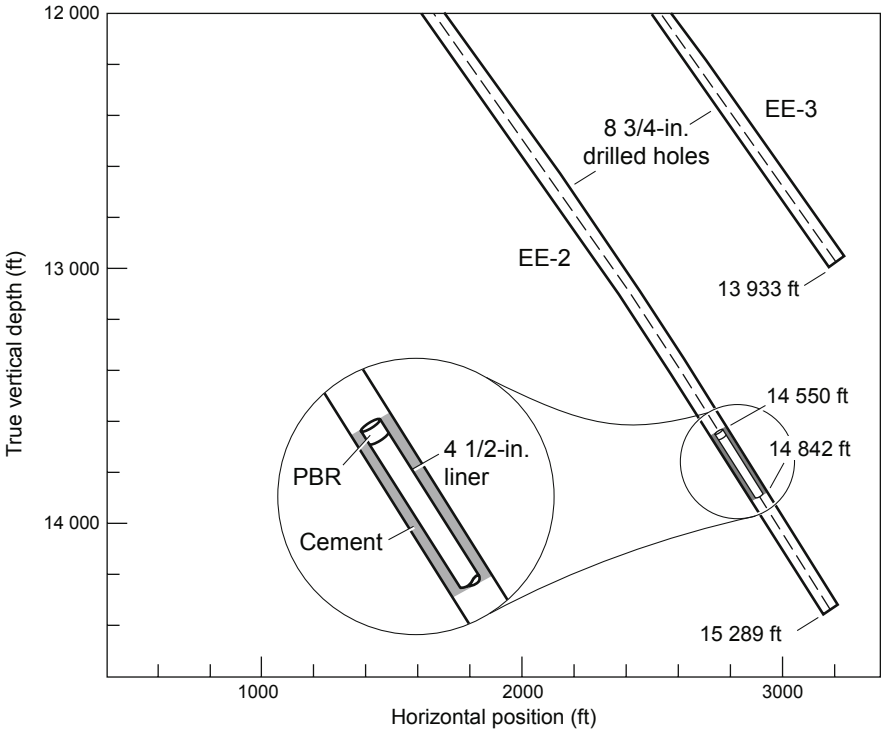

Fig. 6-1. The cemented-in scab liner assembly used to isolate the bottom 447 ft of the EE-2 borehole for Expts. 2011, 2012, and 2016 (vertical section projected onto N55E plane).

On May 30, 1982, the hydraulic fracturing experiments began with Expt. 2011. A Dowell pump truck was employed to gradually pressurize the open-hole interval below the liner at a rate of about 0.4 BPM. At the same time, to reduce the differential pressure across the PBR seal assembly, the annulus above the liner was pressurized to about 2000 psi with the Big Kobe pump. During the initial pressurization, the most favorably oriented joints first accepted fluid at about 4500 psi, then reached an injection-pressure equilibrium at 5500 psi (the pressure required to extend pressurized joints at a low injection rate). Following numerous shut-ins due to pumping equipment problems, the injection rate was finally stabilized at about 5 BPM (200 gpm) and thereafter continued for about 11 hours—until further problems with the pumping equipment forced an end to the experiment. During this time, 3300 bbl (140 000 gal.) was injected at pressures up to 7200 psi and injection rates up to 6.3 BPM. The seismicity produced during Expt. 2011 is shown in Fig. 6-2.

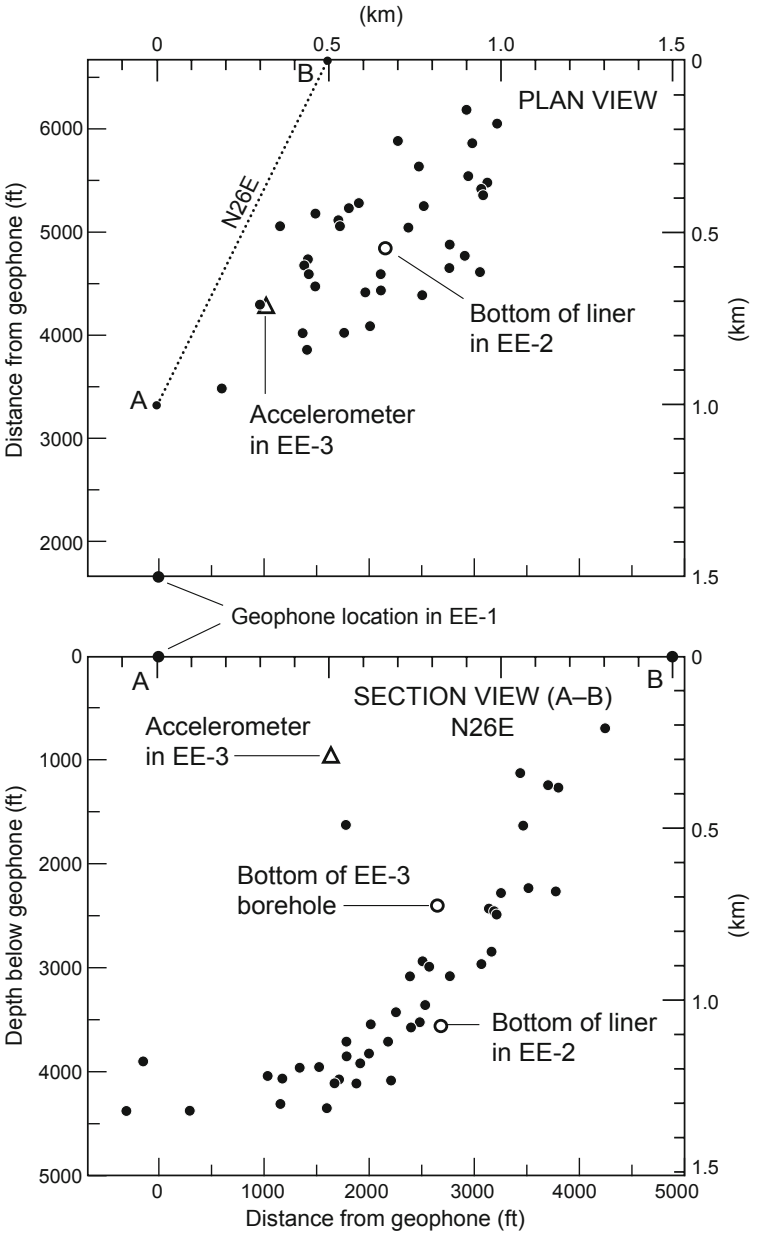

Fig. 6-2. Locations of microseismic events recorded during Expt. 2011 by a triaxial geophone at a depth of about 9600 ft in EE-1.
Source: HDR Project data archives

In plan view, this seismicity appears as a northwest-trending "blob" surrounding the EE-2 injection interval. In the accompanying section view, with the events projected onto a N26E-striking vertical plane (corresponding to the dotted line A–B in the plan view), the seismicity appears distributed in an arcuate pattern having its center at about the geophone location in EE-1.[4]

The next experiment, No. 2012, began at 10:00 on June 4 and continued through shut-in at 2:00 the following day. It involved a much larger volume of fluid (19 700 bbl, or 830 000 gal.) than that injected during Expt. 2011, as well as a chemical friction reducer, pumped in from a blender truck, to allow injection rates of 10 BPM or more without exceeding the pumping pressure limit. Because the PBR seals had withstood a differential pressure of over 5000 psi during Expt. 2011 without leaking, it was decided not to pressurize the annulus, but instead to leave it open and to monitor it. After beginning at 5 BPM, the injection rate was stepped up to 8 BPM and then to 11 BPM, at an injection pressure of 6000 psi. Friction reducer was added to the injection fluid at this point, and after 4 1/2 hours of pumping—at 14:30—the injection rate was increased to 20 BPM at a pressure of about 6200 psi.

Microseismic events began to be detected at about this same time (it was postulated that the prior 4 1/2 hours had been simply a period of aseismic reinflation of the region stimulated during Expt. 2011). The locations of the events are shown in Fig. 6-3, in both plan and section views (the latter, a projection onto a vertical plane striking N72E). Oddly, at these higher rates of injection the located events were more sparse than during the lower-rate injection of Expt. 2011, with some of the events occurring below the EE-2 injection interval—indicating growth in that region (see the section view). It is possible that the lower number of locatable events was due to poorer coupling of the geophone package[5] in EE-1 during this experiment than during Expt. 2011.

---

[4]This particular distribution pattern was later referred to by Rob Jones, then of the Camborne School of Mines in the UK, as an "error banana"—which it may well have been. When Bob Potter re-analyzed the seismic data from a later experiment (see discussion of Expt. 2018 and Fig. 6-7), he asserted that the first microseismic events must have occurred very near the borehole wall and just below the casing, because this was the region of lowest stress, wherein one would expect joints to begin opening. On that basis, he derived a correction for the calibration of the vertical geophone in EE-1, which yielded a tighter "clustering" of the microseismic event locations. If one were to re-analyze the Expt. 2011 microseismic data using that approach, it is likely that in the section view the event locations would appear "collapsed" into a more confined region around and above the bottom of EE-2.

[5]With its single locking arm, the geophone package in EE-1 could rotate in different directions during different deployments in the borehole—resulting in better or poorer coupling to the borehole wall.

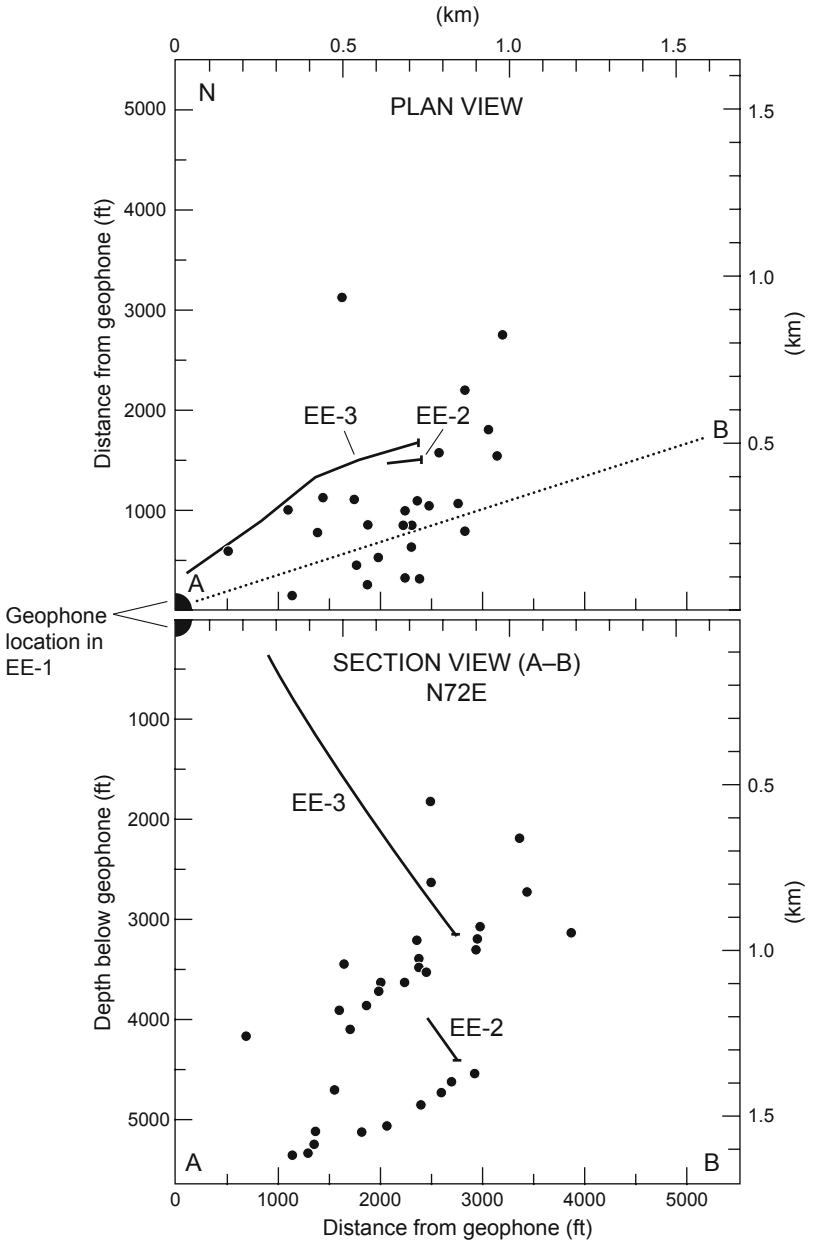

Fig. 6-3. Locations of microseismic events recorded during Expt. 2012 by a triaxial geophone at a depth of about 9600 ft in EE-1.
Adapted from HDR, 1983b

Also at about this time (14:30), a bypass flow developed at the surface, issuing from the annulus above the 292-ft cemented-in liner. Over the next two hours, this flow rapidly increased to about 18 gpm, then remained at that level for the remainder of the test. This bypass flow was very troubling and caused considerable discussion among the HDR Project staff and the drilling engineers. Not only did it call into question the cemented-in-liner approach to hydraulic stimulation, it cast doubt on the feasibility of further pressure stimulation of the open-hole interval below the scab liner.

Note: To those HDR staff familiar with rock mechanics and the behavior of jointed rock as observed during the Phase I experiments, it appeared probable that the flow was originating from the stimulated region below the liner; that is, it was working its way around the liner through a network of joints. The drilling engineers had no experience with joint flow of this nature and instead wanted to attribute it to flow through the cement or through a micro-annulus between the liner and the cement. However, such a micro-annulus (which is usually the result of long-term cement shrinkage) would have been very improbable this soon—particularly with the liner being pressurized and *expanded* against the cement during the injection period. Further, bypass flow through poor cement or through such a micro-annulus would have been cold, whereas temperature logging showed this flow to be warm.

The cumulative total duration of Expt. 2012 was more than 15 hours, with one 8-minute interruption caused by a pump-truck problem. The injection rate during the last 6 hours was about 30 BPM, at an injection pressure averaging 6600 psi (oscillating somewhat because of variations in injection of the friction reducer). At the end of this test, the wellhead was shut in at a pressure of 5200 psi, but the annular bypass flow was allowed to continue at about 18 gpm (had the annulus been shut in as well, the pressure buildup could have led to problems with the casing). By the next morning (Sunday, June 6), the pressure had dropped to 4600 psi—mainly owing to the venting of the stimulated region via the bypass flow.

Since some of the Dowell pumping equipment was still on site, a further pumping test (Expt. 2015) was planned to investigate the pressure integrity of the liner. The morning of June 6, with the annulus open but outflow controlled by a throttling valve, injection began at a rate of about 5 BPM. After just 25 minutes, there was a sudden drop in the injection pressure, from 6400 to 5400 psi, and a concomitant sharp rise in the pressure of the flowing annulus (just upstream of the valve), which almost doubled, from 1500 to 2800 psi. Pumping was stopped at once, which abruptly dropped the annulus pressure to 1800 psi, while the shut-in pressure declined more slowly to 4700 psi (close to its pre-injection level of 4600 psi). The rate of the annular bypass flow—as estimated by the pump truck operators—was by now about 1 BPM (between 40 and 50 gpm), twice what it had been during Expt. 2012.

Three possible explanations for the development of the bypass flow were discussed. To explore these, as well as the situation concerning the integrity of the liner, a meeting was held on June 7. Hugh Murphy's unpublished notes from that meeting summarize the main points:

1. Some staff suggested the possibility of a seal failure in the PBR assembly, but there was little if any evidence for this. For example, temperature logs taken before and after the development of the bypass flow showed a sharp temperature rise, which would not be indicative of seal leakage.

2. Others still wondered whether the liner cement had failed. But George Cocks and several others at the meeting, who had been involved with the careful design and placement of the liner cement, were extremely skeptical that it could have failed so early, and in such a way. In particular, the downhole temperature data argued against this possibility, because flow traveling via that route would have been cold.

3. The most logical explanation was that a hot flow path had opened up around the liner during Expt. 2012, through a network of interconnected joints in the stimulated region. The temperature data would be entirely consistent with such an occurrence. The consensus was that the liner was still viable but had been somewhat compromised by this bypass flow. (Note: Any pressure stimulation effort in deep, jointed crystalline rock involving a cemented-in scab liner or tag-cemented casing would be susceptible to an occurrence of this type, if the stimulation eventually opened a flow path to the much-lower-pressure annulus above the cement.) To the HDR lexicon would hereafter be added the term "frac-around"—to describe such a bypass flow.

The consensus of those at the meeting was that the liner had been somewhat compromised by this bypass flow but was still viable. The decision was therefore made to again attempt to connect EE-2 with EE-3 by stimulating the region below the EE-2 liner—this time with an even greater volume of injected fluid and at rates up to 30 BPM—despite the continuing frac-around flow.

The final stimulation of the region below the liner, Expt. 2016, began on June 20 and lasted 24 hours. Following a 4-hour cooldown period at an injection rate of 5 BPM, the rate was increased to 30 BPM and the pumping pressure—again with the aid of injected friction reducer—was maintained at about 7000 psi for 3 hours. But over the next 11 hours, the test was plagued by repeated pump failures. Finally, steady injection conditions were re-established at 30 BPM and 7000 psi and were maintained for the last 5 hours of the test. A total of 1.29 million gal. was injected into the region below the scab liner, but still there was no evidence of flow communication with EE-3. Experiment 2016 was terminated on June 21, with the stimulated region shut in at an initial pressure of 5400 psi.

During this final experiment below the liner, the bypass flow started at a very low rate, reached 20 gpm in 8 hours, then leveled out at about 50 gpm in two more hours. Such a return to a previous rate of flow as the stimulated region reinflates, but without a flow "runaway," is very indicative of joint flow—and definitely not of seal failure. It boosted confidence in the conclusion that the bypass flow was through an interconnected set of joints in the pressure-stimulated region surrounding the liner. Further, it suggested that at least a portion of the joints in this region were aligned *along* the trajectory of the EE-2 borehole.

The locations of the microseismic signals recorded during Expt. 2016 are shown in Fig. 6-4, in both plan and section views. The microseismicity is much more dense than that during Expt. 2012, even though the amount of injected water was not much greater. (It is possible that better coupling of the geophone in the EE-1 borehole during this experiment—translating to better P- and S-wave arrivals for many of the microseismic events—was responsible.) Figures 6-3 and 6-4 make clear the dilemma facing the Project. The large volumes of fluid injected into EE-2 had produced an extensive "cloud" of seismic events, representing a large stimulated region surrounding the EE-2 injection interval and extending eastward. As shown most clearly in Fig. 6-4, this region was inclined to the west at about 45° and passed *below* EE-3. In other words, even repeated and extended hydraulic stimulation, at very high pressures and injection rates, had failed to connect two boreholes in close proximity to one another.

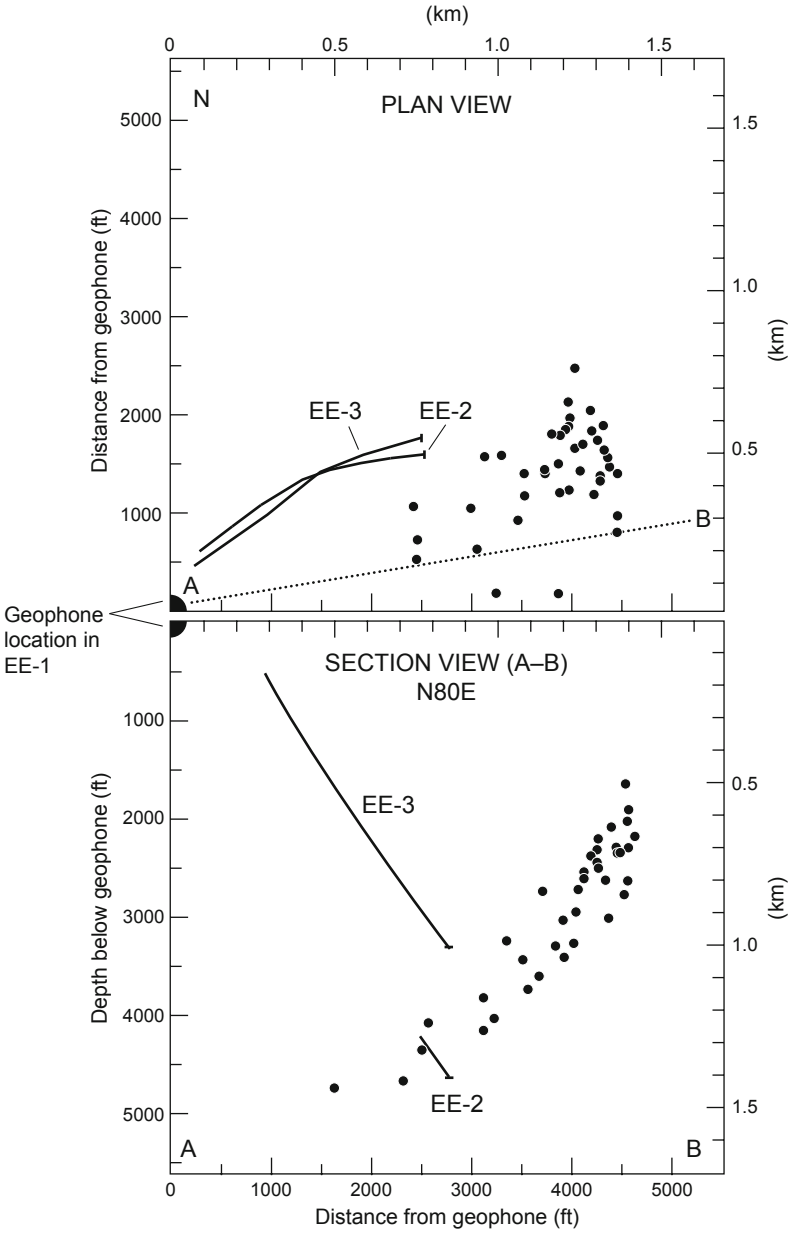

Fig. 6-4. Locations of microseismic events about halfway through Expt. 2016, recorded for one hour (12:30–13:30 on June 20, 1982) during the first steady-state period. The wireline-deployed triaxial geophone was positioned at a vertical depth of 9635 ft in EE-1.
Source: HDR Project data archives

It was at this stage that several HDR staff proposed an alternative strategy: that EE-3 be drilled ahead, with no directional drilling to maintain angle (i.e., that the hole be allowed to gradually "droop" under the influence of gravity), to intersect the pressure-stimulated seismic region surrounding the bottom of EE-2. If this strategy had been pursued, it probably would have succeeded in connecting the two boreholes, saving the Project over three years of effort and millions of dollars. In addition, the HDR reservoir thus created would have been an even deeper one, with a mean temperature of over 300°C. The suggestion was not well received, however, because the Project was under pressure from DOE Headquarters to quickly achieve a flow connection between the two boreholes.

A hiatus in Project spending for field operations at this time could have served as an opportunity to "step back," examine the favorable seismic interrogation situation presenting itself, and then proceed with a concerted effort to understand the structure of the deep basement rock being pressurized. This effort could have included

- developing a Dewar-protected or temperature-hardened geophone package, to be placed in EE-3 (in the middle of the seismic cloud);
- deploying a geophone package in the granite at about 2400 ft in GT-1;
- improving the coupling of the geophone package in EE-1 by adding an aligning system to prevent the locking arm from being positioned near the low side of the tool (this system would consistently align the geophone package such that the locking arm was pushing it firmly against, rather than lifting it off, the low side of the hole).

Expt. 2016 could then easily have been repeated, with much more satisfactory results (at least in terms of accurate location of microseismic events). With three separate geophone stations receiving unique P- and S-wave arrival signals, a travel-time algorithm[6]—rather than the one-station hodogram method—could have been used to locate each event. Such an effort, which would have been a truly scientific one, would have paid handsome dividends for the future of the HDR Project. Instead, unfortunately, the only plan was to carry out further hydraulic fracturing attempts—in the continuing hope that the *next* one would succeed in establishing a flow connection between the two boreholes.

---

[6]This algorithm is based on P- and S-wave arrivals at three separate stations (a total of six signals). Because only four arrival times are needed to determine the spatial coordinates (x, y, and z) and the time coordinate (t, or time of event), the algorithm enables any given event to be located in both space and time with up to two levels of redundancy. It would later be used for locating the seismicity produced during the MHF Test, by which time the hodogram approach had finally been deemed unreliable and abandoned.

Hydraulic Fracturing Tests Below the Casing Shoe in EE-2

Because of the pressure from DOE Headquarters, the failure to achieve a flow connection to EE-3 from deep in EE-2 posed a very difficult problem for the Project management. Stimulating a higher interval in the open-hole portion of EE-2 was not an option because the unexpectedly high injection pressures ruled out the use of inflatable packers. In addition, given the trajectories of the two boreholes (see Fig. 5-11), it appeared that if a west-dipping stimulated region could be created from just below the EE-2 casing shoe, it "couldn't miss" intersecting EE-3 *somewhere* along the long open-hole section. The Project managers thus reasoned that with the casing shoe at 11 578 ft in EE-2 affording a good upper seal, sanding up the bottom of the borehole would create a favorable injection interval and geometry for expeditiously connecting EE-2 to EE-3. They therefore took the drastic step of abandoning (at least temporarily) most of the open-hole interval in EE-2—sanding up all but about the top 400 ft—with the hope of effecting a flow connection.

The information in this section is based on HDR Geothermal Energy Development Program (1985), Matsunaga et al. (1983), and Hoffers (1983).

Initial Testing: Expt. 2018

The plan was to fill the bottom 3300 ft of EE-2 with sand, leaving about 400 ft of open hole between the top of the sand plug and the bottom of the final EE-2 casing string at 11 578 ft. Thus, in a sequence of sanding-up operations, the EE-2 borehole was backfilled to a depth of 11 935 ft. Over the next week or so, as the sand settled, the top of the plug dropped to 12 060 ft. The open-hole interval to be tested was now 482 ft, which would be pressure-isolated by running a casing packer on drill pipe and installing it a safe distance above the casing shoe (protecting most of the 9 5/8-in. casing from over-pressurization during the high-pressure stimulations to follow).

On July 17, after two separate Baker casing packers had set prematurely and been fished out, an Otis hydraulic-set, retrievable steam packer, with a 49-ft-long (5 1/8-in. outer diameter) slick joint inserted into its bore, was run in on drill pipe and positioned in the casing at 11 335 ft (243 ft above the casing shoe). The frac head was then rigged up on the drill pipe, and for the next two hours the Otis technician attempted to activate the packer-setting mechanism, but met with problems. Unknown to the rig crew, during these attempts the jay-latch keeping the slick joint attached to the packer was inadvertently released. When the drill pipe was pulled up several tens of feet, there was no drag—which normally would indicate that the packer had not set.

Assuming that the packer was still attached to the drill pipe, the crew pulled all the drill pipe out of the hole to inspect the packer. They found the slick joint and jay-latch attached, but no packer! Perhaps it had in fact set properly? After careful inspection to ensure the integrity of the slick joint and jay-latch, a "mule shoe" was installed at the bottom of the slick joint and the

assembly was run back into the hole. With the aid of the mule shoe, the slick joint was inserted into the bore of the packer and jay-latched in. Finally, the annulus was pressurized to 2200 psi—which both confirmed the integrity of the packer's inner seals and showed that the packer had set successfully. The jay-latch was then released; the slick joint could now move freely up and down within the packer to compensate for the thermal contraction of the drill pipe during the upcoming injection of cold water. Lastly, Dowell was rigged up for pumping and the geophone package was installed in EE-1.

The injection phase of Expt. 2018 finally began the afternoon of July 19, 1982, at an initial injection rate of 2 BPM, and continued for about 9 1/2 hours (Fig. 6-5). The injection pressure increased very rapidly to 4750 psi, then "rolled over" to an asymptote at 5500 psi. Judging from past experience, this behavior represented the opening of one or more of the lowest-opening-pressure joints exposed in this previously untested interval in EE-2. The absence of any pressure overshoot upon initial fluid acceptance suggests that the joint-filling material had a vanishingly small tensile strength. Further, the subsequent pressure rise to 5500 psi suggests that the joint(s) started to dilate and accept fluid at 4750 psi, after which the pressure continued to rise (as the asperities progressively lifted off) until the joints were fully dilated and extending at a constant pressure of 5500 psi. When adjusted for the frictional pressure loss in the 3 1/2-in. drill pipe, the full opening pressure of the joints would be 5300 psi—implying that the joints were inclined.

Although higher-than-expected injection pressures had been observed deep in EE-2 during the injection testing of Expts. 2011, 2012, and 2016, it was not until Expt. 2018 that the significance of the *injection impedance* "jelled." This is the impedance associated with the level of pressure required to "pry open" the most favorably oriented set of joints. For the Phase I reservoir region, in which the first-opening joints were essentially vertical, the opening pressure was in the range of 1500–2000 psi. For the Phase II reservoir, however, the opening pressure was considerably higher—indicating that the first-opening joints were significantly inclined from the vertical; and it is the joint inclination that explains the higher injection impedance.

After about 50 minutes an annulus leak developed; but the test continued, first with the injection rate increased to 7 BPM and then, with friction reducer added, to 12 BPM at 7200 psi. Three hours into the test the annulus flow was measured at 3/4 BPM, and over the next four hours it increased to 1 3/4 BPM.

Experiment 2018 ended abruptly on July 20 with the failure of the 3 1/2-in. drill pipe, which was being used as a frac string. As fluid began flowing through the split in the drill pipe and into the annulus between the drill pipe and the deep casing string, there was a sudden increase in backside pressure. Pumping was immediately stopped, and both the backside and the drill pipe were vented. Temperature logging located a failure in the drill pipe at a depth of 2590 ft—a 2-ft-long crack, about 0.05 in. wide. The consensus was that this was a stress-corrosion crack caused by dissolved H_2S in the injected (recirculated) fluid. The total amount of fluid injected during Expt. 2018 was 240 000 gal.

The failure of the frac string can be seen in Fig. 6-5. Also discernible is the effect of the friction reducer, which was added to the injection fluid starting at 17:40 on July 19. The injection pressure, which had been rising up to this time, began to drop sharply as the injection flow rate was further increased. Most of the ups and downs in the injection pressure and flow rate plots beyond 17:40 were due to the erratic addition of friction reducer.

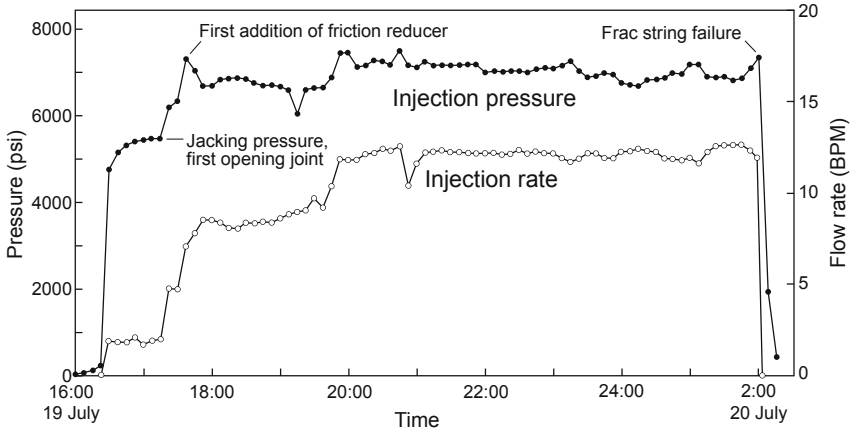

Fig. 6-5. Injection pressure and injection rate during Expt. 2018, the first pressurization of the upper 482-ft open-hole interval in EE-2 (isolated between a casing packer—set in the 9 5/8-in. casing above the shoe at 11 578 ft—and the top of the sand plug at 12 060 ft).
Source: Matsunaga et al., 1983

In the absence of a flow shut-in during this experiment, the next-best method of determining the extension pressure of the principal joints was to solve for this pressure from the injection rates and pressures of two different, near-steady-state pumping intervals during which friction reducer was used. The extension pressure thus calculated was about 5800 psi—but with a considerable margin of error because the computation assumes a constant effect from the friction reducer (in fact, the effect was highly variable).

Another significant feature of this experiment was the almost constant final "pressure plateau" of 7100 psi at an injection rate of 510 gpm (12 BPM) during the last 6 hours—indicating a very orderly process of extension of the pressure-stimulated region. The extension pressure was being controlled by the highest-opening-pressure joints, which were manifolding flow to the dilating joints in the surrounding rock mass.

Following Expt. 2018, temperature logging identified three distinct zones of fluid acceptance (Fig. 6-6). All three were in the upper 240 ft of the open hole and probably were discrete joints—whereas no joints were opened below that. In retrospect, it is surprising that there were *no* favorably oriented joints intersecting the lower part of the open borehole!

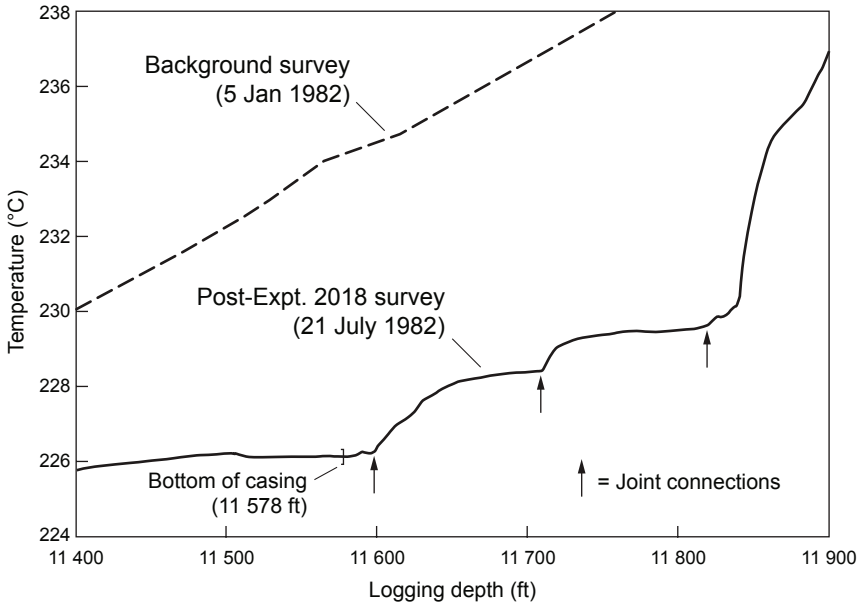

Fig. 6-6. Temperature survey in EE-2 immediately following Expt. 2018, showing three distinct zones of fluid acceptance in the upper part of the open-hole interval: at 11 600 ft, 11 710 ft, and 11 820 ft. Depths are as recorded in the logging van.
Source: Hoffers, 1983

Figure 6-7a shows the first five hodogram-determined event locations recorded during the early part of Expt. 2018 (17:10 to 17:40, during which time the injection rate was increased from 80 gpm to 300 gpm—see Fig. 6-5). The first of these seismic events was recorded after the injection of only 80 gal. into EE-2—which, Bob Potter asserted, meant that it *must* have occurred very close to the previously unpressurized EE-2 borehole (rather than hundreds of meters away, as shown in Fig. 6-7a). For this reason, Potter applied a multiplier to the output of the vertical geophone, varying its value until this first event's location came very close to the EE-2 borehole. The resulting multiplier was 3.4 (Hoffers, 1983), suggesting that the quality of the coupling of the vertical geophone was less than 1/3 that of the horizontal ones (not unreasonable, considering the single, and rather weak, locking arm). As shown in Fig. 6-7b, this correction, which brought the first event (solid dot) to within about 30 m of the borehole, shifted the small cluster of events in Fig. 6-7a 300 m deeper and 200 m to the south—almost half the distance from the geophone package indicated by the raw hodogram data!

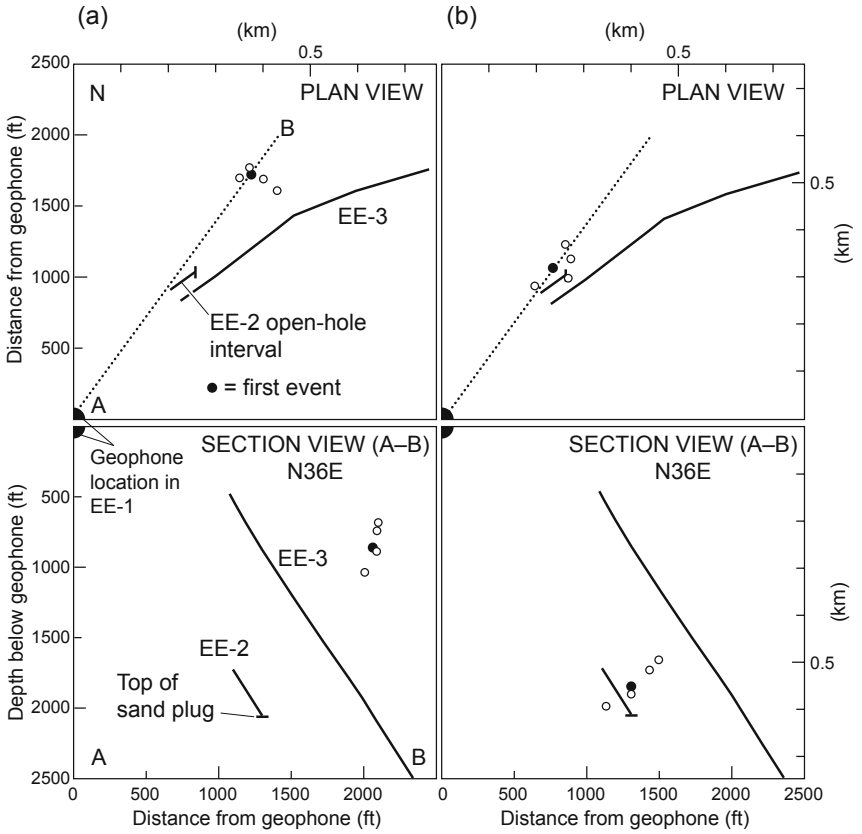

Fig. 6-7. Hodogram-derived event locations during the early part of Expt. 2018, with a triaxial geophone package located at a cable depth of 9670 ft in EE-1: (a) raw locations, shown in both plan and section views; (b) corrected locations. Source: Hoffers, 1983

Although Potter's hypothesis seemed reasonable, the very significant relocation of the Expt. 2018 microseismic data left the Project staff very concerned. What if such a correction factor had been applied to the hodogram-derived microseismic locations for the much deeper injection tests below the cemented-in liner (Expts. 2011, 2012, and 2016)? How reliable was the inferred 45°-dipping seismic cloud that had "missed" the bottom of EE-3 (Fig. 6-4), leading the Project management to abandon most of EE-2 and retreat to a stimulation interval just below the casing shoe? In Fig. 6-8, the corrected microseismic pattern for Expt. 2018 is shown in relation to the broadly diffuse pattern of microseismicity generated during Expts. 2012 and 2016. It is not difficult to conclude that if the deeper seismicity had been correctly located, the events would probably have clustered more around the EE-2 injection interval.

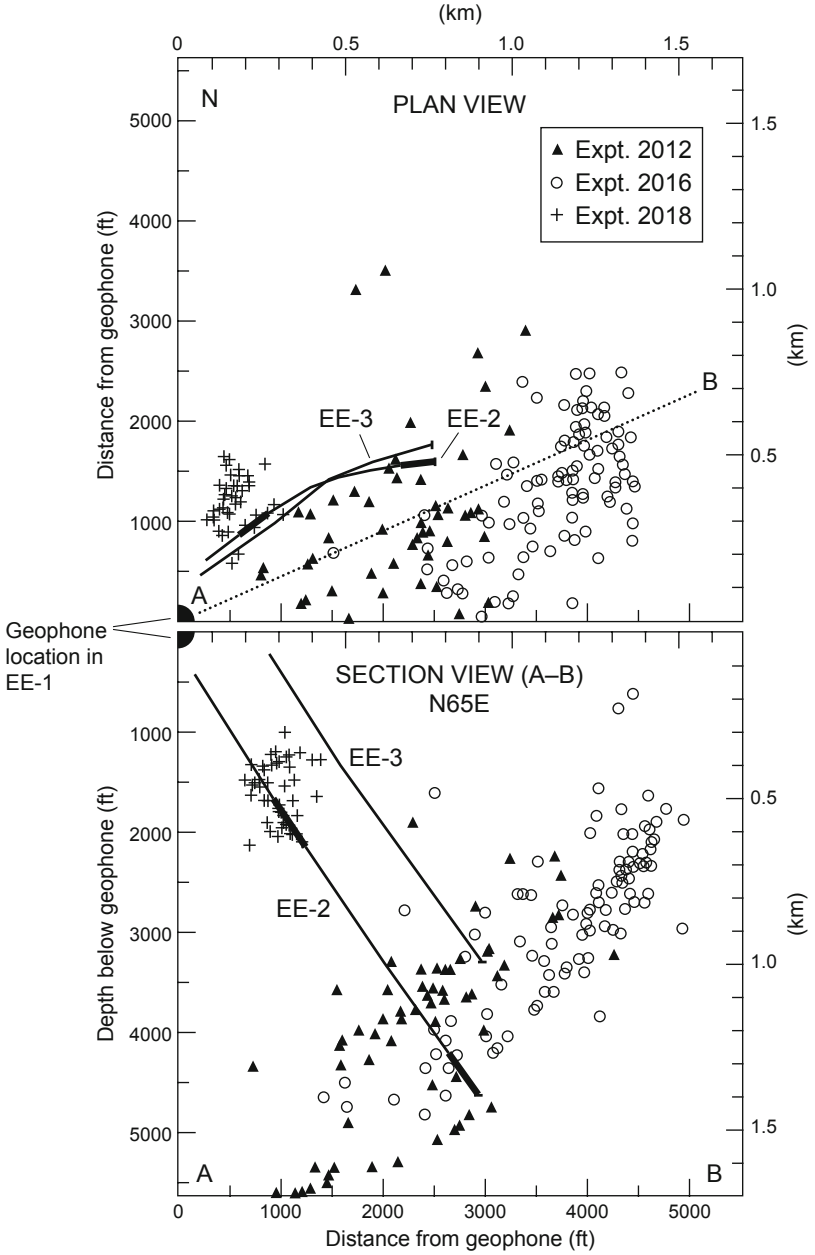

Fig. 6-8. Locations of microseismic events recorded during Expt. 2018 (corrected) compared with those recorded during Expts. 2012 and 2016 (uncorrected), shown in plan and section views.
Adapted from HDR, 1983b

InfoNote

The hodogram method was first used at Fenton Hill to locate pressure-induced microseismicity occurring reasonably close to, and not too far above or below, the geophone station (see Chapter 3). In contrast, the microseismicity produced during Expts. 2012 and 2016 occurred far below the geophone station, presenting a new complication: an inordinate reliance on the signals received by the vertical geophone—which renders the deeper event locations shown in Fig. 6-7 somewhat questionable. This new complication calls for further explanation of the hodogram method.

As described by Fehler (1984), the hodogram (particle-motion) method uses the difference between the S- and P-wave travel times to obtain the distance from the microseismic event to the geophone station, and the particle motion in three dimensions to determine the direction to the event. However, plotting of the first cycle or so of particle motion is strongly dependent on how effectively each of the seismic axes in the geophone package is coupled to the borehole wall. Typically, the coupling of the vertical geophone was considerably less effective than that of the two horizontal geophones (see discussion of Fig. 6-8). This coupling problem was one of the main incentives for the development, by the HDR Instrumentation Group (ESS-6), of a downhole detonator tool to calibrate the geophones.

The Microseismic Analysis Review Panel felt that the travel-time method of locating microseismic events (which requires multiple geophone stations) is superior to the hodogram method because the travel-time method is less affected by rock heterogeneity and instrumentation coupling problems (Fehler, 1984). The travel-time method would therefore be used for the MHF Test (December 1983) and all subsequent pressure-stimulation tests.

The Otis casing packer, which had been retrieved from the borehole late on July 20, was now reinstalled for a second attempt to pump into the open-hole section of EE-2 (Expt. 2019). But another drill-pipe failure brought a halt to this experiment after only 11 300 gal. had been injected in 55 minutes of pumping—begun at 2 BPM. Once again, a very sharp rise in the backside pressure (to 3700 psi) indicated the pipe failure.

Because of the failures of the 3 1/2-in. drill pipe, at midnight on July 29 the drill rig was placed on standby until a more capable frac string could be obtained.

Experiment 2020: Larger Injection Below the EE-2 Casing Shoe

On September 19, 1982, with a replacement string of 4 1/2-in. drill pipe and a 4 1/2-in. high-pressure casing string (to be used as the frac string)[7] on hand, the drill rig was reactivated. A new top for the sand plug having been tagged at 11 994 ft, there now remained 416 ft of open hole below the EE-2 casing shoe.

Following several false starts with casing packers (a Baker and an Otis), on September 29 a reworked Otis steam packer was run into the hole on the drill pipe and set in the casing at a depth of 11 262 ft. The drill pipe was then tripped out of the hole and laid down. Next, the 4 1/2-in. casing/frac string was run in, with a slick-joint/mule-shoe assembly on the bottom; guided by the mule shoe, the slick joint was stabbed into the Otis packer and the packer was pressure-tested, completing the preparations for Expt. 2020.

Experiment 2020 was designed as a very large volume and high-pressure re-stimulation of the EE-2 open-hole interval (first stimulated during Expt. 2018). The injected volume would be up to 1 million gal., over four times as large as that of Expt. 2018. Following a cooldown phase of 2 1/2 hours at 5 BPM, the flow rate would be increased in steps, to 10 BPM and then to 20 BPM. The main part of the test would be conducted at a maximum injection pressure of 7000 psi. With the addition of friction reducer, the projected injection flow rate was 32 BPM (Brown, 1982a; Brown et al., 1982). This rate—much higher than the 12-BPM injection rate reached under similar conditions during Expt. 2018—was achievable because of the larger flow area provided by the 4 1/2-in. frac string.

Just before the start of Experiment 2020, a triaxial geophone package was deployed at 9400 ft in EE-1[8] and the Laboratory's newly developed high-temperature, slim-line detonator tool was run deep into EE-3 and successfully fired twice to calibrate the package. This direct calibration had the twofold purpose of determining (1) the "station corrections" (measured P- and S-wave velocities across a reasonable representation of the actual reservoir rock) for the EE-1 station, and (2) the sensitivities of the three separate axes of the geophone package—which unfortunately varied for each deployment, depending on the quality of coupling to the borehole wall.

---

[7]The casing obtained made a much better frac string because of its higher pressure rating (in addition, casing is generally freer of the surface damage to which drill pipe is subjected, from handling tools, etc.). In spite of such advantages, the contract drilling supervisors tended to use the drill pipe as the frac string because it was easier to handle. Drill pipe was already racked in the derrick in 90-ft "stands," whereas casing had to be picked up off the pipe racks joint by joint, by a casing crew using special handling equipment, then after use unscrewed joint by joint and returned to the racks—a time-consuming operation.

[8]This location in EE-1 would be used for geophone recording during all subsequent reservoir testing.

Experiment 2020 began on the evening of October 6 and lasted almost 12 hours, during which time 844 000 gal. of water was injected. The experiment ended abruptly when one of the collars on the frac string failed—again attributed to stress-corrosion cracking. To control the annulus pressure, the annulus was vented, initially at a rate of about 1/2 BPM; but after pumping was stopped and the frac string shut in, the annulus vent rate continued to increase. It took nearly 24 hours to reinstall the blow-out preventer, tubing head, and "christmas tree," and to install a vent line at EE-2. Finally, on the morning of October 8, venting of the reservoir through the 4 1/2-in. frac string began; but another two days passed before the vent pressure was low enough to start long-term venting, allowing further work to be done at EE-2. (The venting would last through the following January.)

InfoNote

Hydraulic fracturing operations in EE-2 had an unexpected result: the production of large quantities of gas, probably dissolved in the fluids contained within the network of joints in the crystalline basement (which are somewhat more permeable than the surrounding matrix rock). The gas was made up mainly of carbon dioxide but also hydrogen sulfide (about 60 ppm) and trace amounts of other species. Their presence posed not only safety problems (gas could erupt during rig and logging operations, referred to as "kicks," and the vented hydrogen sulfide could be toxic if concentrated), but also corrosion problems. The series of failures of drill pipe and casing collars that had repeatedly prevented long-term injections were all due to stress-corrosion cracking—from dissolved hydrogen sulfide abetted by carbonic acid (dissolved carbon dioxide). All such failures so far investigated involved high-strength steels having tempered-martensite microstructures, and all appear to have originated at indentations produced by handling (with elevators, tongs, slips, etc.). It is reported that as little as 1 ppm of hydrogen sulfide can lead to sulfide stress-corrosion cracking in high-strength steels.

The profiles of the injection pressure and injection rate during Expt. 2020 are shown in Fig. 6-9. During the first 2 1/2 hours, the Expt. 2018 stimulated region was being reinflated at an injection rate of 5 BPM and a pressure of about 5400 psi. This injection behavior essentially replicated that of the early part of Expt. 2018 (Fig. 6-5)—the joint connections to the stimulated region still exhibiting a high injection impedance.

During the latter part of the experiment, the injection rate reached about 34 BPM at 6700 psi, somewhat higher than what had been predicted (on the basis of an "effectiveness factor" of 65% for the friction reducer). The fluctuations in the injection flow profile reflect repeated problems with the pumping equipment, particularly during the last six hours of this test.

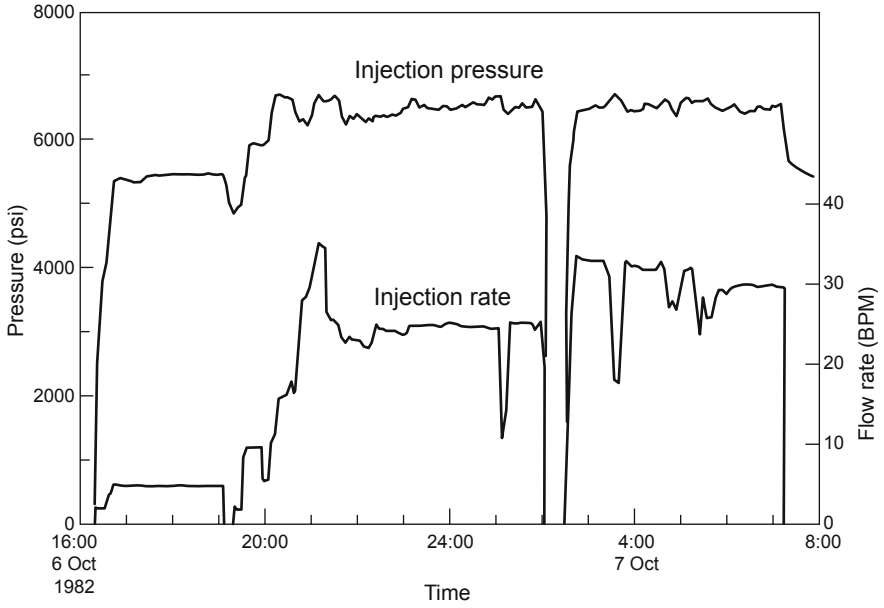

Fig. 6-9. Injection pressure and injection rate at EE-2 during Expt. 2020. Source: HDR, 1985

As planned, at 2:00 on October 7, after the injection of 486 000 gal. (1840 m^3) in 9 1/2 hours, the flow was shut in for about half an hour. This shut-in, one of the most significant features of Expt. 2020, allowed the joint-extension pressure to be *measured directly*, on the basis of the pressure profile for the first minute or so (Fig. 6-10). From the previous steady-state injection-pressure level of 6360 psi, the shut-in pressure rapidly stabilized at 5500 psi. (With friction reducer, the measured pressure loss in the 4 1/2-in. frac string at 34 BPM was 860 psi.) It is unfortunate that this direct method of measuring the extension pressure of the joints that controlled the Phase II reservoir was not used extensively during other injection testing of the reservoir region.

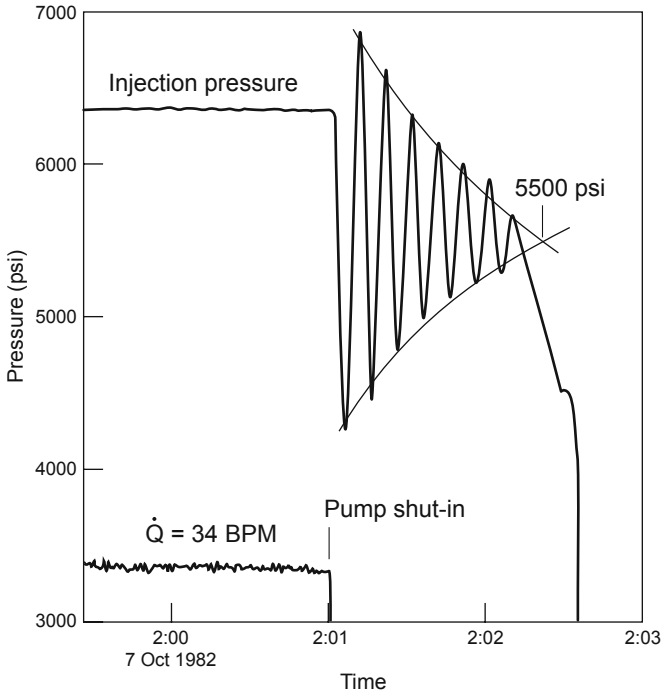

Fig. 6-10. Pressure profile during the first minute of the Expt. 2020 flow shut-in (2:01 on October 7, 1982).
Source: HDR Project data archives

Figure 6-11 displays the seismicity recorded during the last half of Expt. 2020. The seismic pattern is similar to that recorded for Expt. 2018 in that it is concentrated around—and along—the injection interval in EE-2, but it is somewhat more extensive, particularly in the north–south direction (as seen in the plan view). At the time, the seismic cloud was reported to be in the form of an ellipsoid, one of its major axes oriented north–south and its minor axis oriented perpendicular to the trace of the EE-3 borehole (roughly east–west). Although the seismicity appeared to have approached the EE-3 borehole, there was no indication of flow communication.

The volumetric nature of this cloud suggests that an array of pre-existing natural joints had been reopened, producing a three-dimensional reservoir (rather than a tabular one, as would have resulted from the creation of several *en echelon* "fractures"). This seismic pattern showed that a much larger fluid injection would be required to extend the seismic region perpendicular to EE-2 (along the direction of the minor axis), to intersect EE-3.

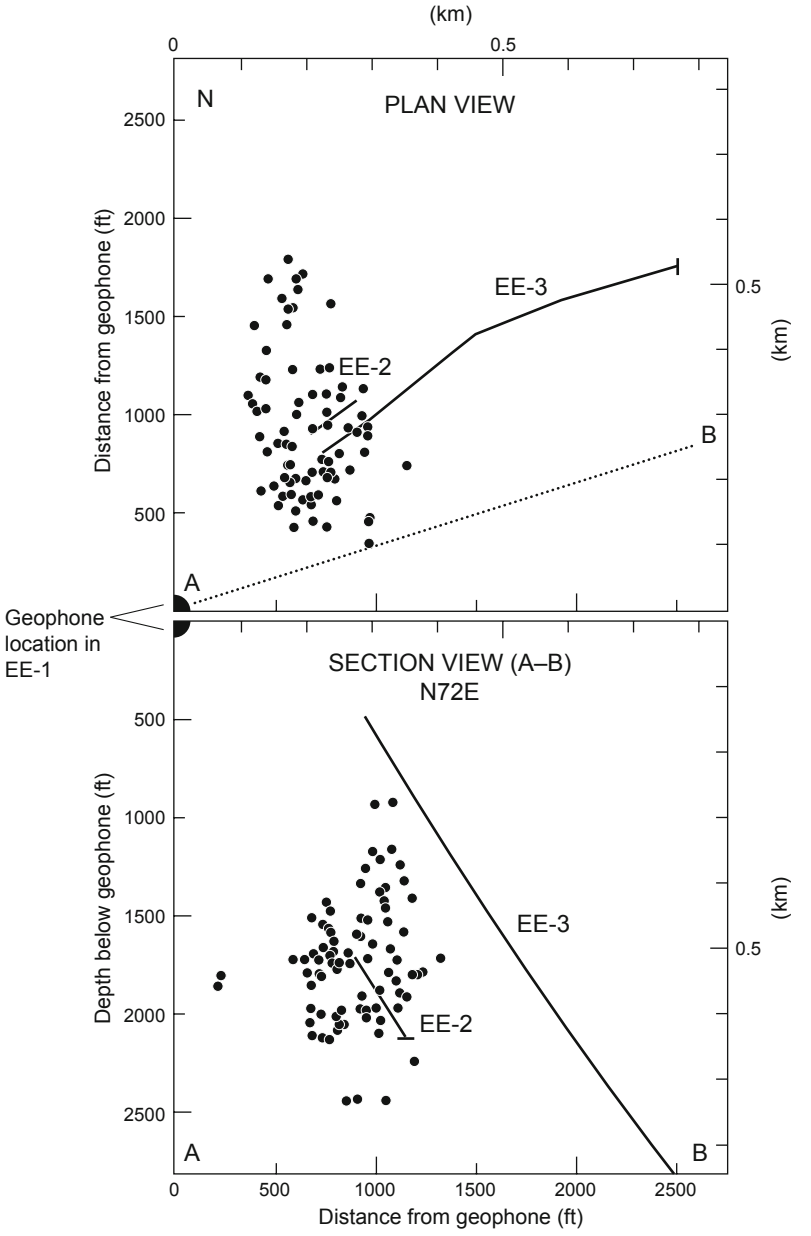

Fig. 6-11. Locations of microseismic events recorded during the last half of Expt. 2020 (from 1:00 to 7:00 on October 7), by a triaxial geophone at a depth of 9400 ft in EE-1.
Source: HDR Project data archives

Late on October 9, after the casing crew's equipment and the lay-down machine had been rigged up, the upper portion of the 4 1/2-in. frac string was pulled from the EE-2 borehole. It was found that a coupling had split lengthwise, leaving 49 joints in the hole below. The 4 1/2-in. drill pipe was picked up, and a string of fishing tools (with a grapple and overshot on the bottom), was run into the hole; it tagged the top of the fish—the lower portion of the frac string—at 9370 ft. The fish was then removed; attached to its bottom end was the slick joint that had been inserted into the Otis packer. It took two more days of fishing to retrieve the Otis packer, then another three days to fish out the Baker packer (the failure of this packer had necessitated the setting of the Otis packer just above it). At noon on October 17, after the EE-2 borehole had been cleared down to the top of the sand plug, the rig was placed on standby.

The Connection Conundrum

The fact that Expt. 2020 had failed to achieve a flow connection between EE-2 and EE-3 (possibly by not creating a large enough stimulated region) left the Project staff in a real quandary. Some, thinking that the stress concentration surrounding the low-pressure EE-3 borehole might have been an obstacle to achieving a flow connection, proposed repeating Expt. 2020 in EE-2 while at the same time pressurizing EE-3. Others, especially among Project management, believed the problem was that the volume of water injected into EE-2—"only" 844 000 gal.—had simply been too small to achieve a connection. (The corollary claim, that injection pressures and/or flow rates even higher than 34 BPM and 7000 psi were needed, had generally been debunked.) But an injection of the massive volume thought necessary by the second camp could have been attempted only with a frac string more resistant to the downhole chemical environment. (Because of ongoing indecision on the part of Laboratory management, such a string—5 1/2-in., C-90 tubing—would not be ordered until May of 1983—7 months later!)

Without the means to carry out a massive injection in EE-2, almost everyone was now clamoring to *do something in EE-3*—but what?

For any significant injection into EE-3, a major cause for concern was the string of 9 5/8-in. production casing run in August 1981, when EE-3 was completed. The top 3000 ft of this casing had been left uncemented, probably because the integrity of the surrounding 13 3/8-in. casing (set at 2552 ft) was somewhat in doubt. Because this borehole was slated to be the production well for the two-well circulation loop, the top 3000 ft of the casing had been tensioned to 80% of its yield strength to accommodate subsequent thermal expansion during hot fluid production. Thus, to now consider injection operations in EE-3, which would cool the casing and create tensile thermal stresses that might result in its separation, was unnerving to say the least. However, a strategy that might overcome this potential problem—

without resorting to the expensive operation of releasing the tensile load on the casing—was to heat the water before injection. Calculations showed that pre-heating the water to 70°C or more posed little risk to the casing.

The injection of a large volume of water (up to 1 million gal.) at such temperatures would have required a sizable and quite elaborate pre-heating system. However, a "hot-oiler" (a truck- or skid-mounted heating unit, available from oilfield service companies) could be used for injected volumes up to about 200 000 gal. An injection so limited probably would not open a joint network extensive enough to reach EE-2, but could create one suitable as a "target" for later pressure-stimulation from EE-2 (and in any case a larger target than the EE-3 borehole!)

But even if this strategy could overcome the casing problem, the fact remained that any effective stimulation program in EE-3 would require high-pressure injection—which was precluded by the presence of the low-pressure joint exposed at about 10 394 ft, just below the casing shoe (identified by pressurization testing during Expt. 2006 in February 1982).

Note: In retrospect, considering the problems at EE-3, there was no certainty that this borehole could become an effective production well for the hoped-for two-well HDR circulation system (and, in fact, it never would!). The best course of action at this juncture would have been to *re-engineer* the completion of the EE-3 borehole to improve flexibility. The drill rig could have been skidded over EE-3, the 9 5/8-in. casing released at the surface, and then a string of 7 5/8-in. casing run in and cemented across the open joint below the 9 5/8-in casing shoe. This strategy would have eliminated the major deficiencies at EE-3 while maintaining good logging capability, and would not have been any more costly or time-consuming than the "evolving" strategy that actually was used. Moreover, it would have provided a much better EE-3 "platform" for subsequent high-pressure testing of the potential reservoir region.

On November 8, an experiment (Expt. 2023) was carried out to evaluate the difficulties of injecting large amounts of heated water into EE-3. With no drill rig over EE-3, rental pumping and water-heating equipment were used to inject about 930 bbl of water, heated to 65°C, straight down the 9 5/8-in. casing and into the low-pressure joint just below the casing shoe—mainly at an injection rate of 6.5 BPM and a pressure of 1820 psi. This injection proceeded with little difficulty, despite very cold outdoor temperatures. (As expected, the low-pressure joint accepted water in a manner similar to that seen during numerous injections into the Phase I reservoir—indicating the connection of this joint to that low-pressure region). The successful injection of heated water indicated that a deeper region of the EE-3 borehole could be stimulated without creating severe casing problems. Thus, in late November, the Brinkerhoff-Signal rig No. 78 was skidded over EE-3.

Hydraulic Fracturing in EE-3

After the drill rig had been rigged up, the 4 1/2-in. drill pipe was run into the hole. A series of sand plugs were then pumped in, to greatly reduce the available open-hole interval. On November 30, with eight plugs having been placed, the top of the sand was tagged at 11 768 ft. Unfortunately, the operation that followed was based on the misconception that the joint just below the casing shoe could be sealed with lost-circulation material—even though previous experience had shown that no technique, including this one, was effective in sealing off pressure-opened joints in basement rock. A 150-bbl mixture of bentonite, barite, and lost-circulation material was pumped into the hole and "squeezed" into the joint at a pressure of about 2500 psi. This effort completely failed, and left a number of "bridges" of lost-circulation material in the borehole that had to be washed out.

A succession of plans were developed for connecting EE-3 with the Expt. 2020 seismic cloud. All of these involved hydraulic fracturing in a deeper part of the EE-3 borehole—bypassing the open joint at 10 394 ft, just below the casing shoe.[9] (At this time, nearly everyone within the HDR Project believed that with a sufficiently robust injection, there was at least a *chance* of connecting EE-3 to the Expt. 2020 stimulated region.)

For the first injection (Expt. 2024), a redesigned Lynes inflatable packer was run into the hole on drill pipe and set at a depth of 11 415 ft, leaving a 353-ft open-hole interval below. However, when the injection pressure reached 2030 psi (after only 21 minutes of pumping), the packer failed—as evidenced by flow out the annulus.

For the next experiment, a 4 1/2-in. scab liner would be installed in EE-3, as had been successfully done at the bottom of EE-2. But this liner would be much longer—1283 ft. To ensure that it would be well cemented, two additional sand plugs were placed in EE-3, up to a depth of 11 389 ft. On December 8 the liner (including a liner hanger and PBR on top) was run into the hole on drill pipe and set on top of the sand plug. The liner hanger was then landed inside the 9 5/8-in. casing, 228 ft above the casing shoe at 10 374 ft, and the liner was cemented in place up to about 10 850 ft. Unfortunately, the completion engineering was poor: the liner was not cemented all the way up into the 9 5/8-in. casing. If it had been, the low-pressure joint connection at 10 394 ft would have been sealed off, precluding many later problems (including the collapse of the liner just above the cement-supported interval, due to high annular pressure during the gas-laden venting of EE-3 following Expt. 2025).

After a 24-hour wait for the cement to harden, a 2 1/8-in. drill-pipe extension was used to drill out the liner and then wash the sand out to a depth of 11 770 ft. Three days later the top of the sand was tagged at 11 770 ft. Figure 6-12 shows the configuration of the EE-3 borehole in preparation for Expt. 2025.

[9]This low-pressure joint entrance in EE-3 appeared to be connected to the deepest part of the Phase I reservoir.

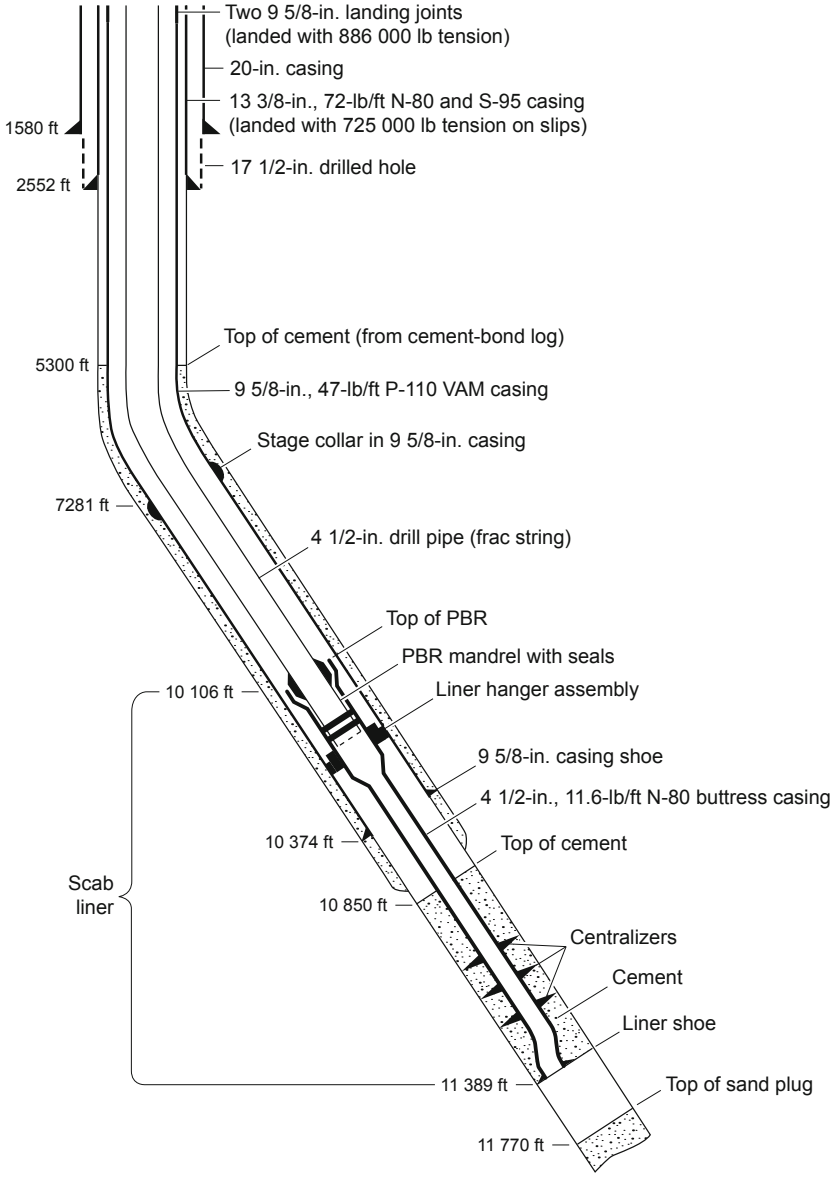

Fig. 6-12. Configuration of the EE-3 borehole with a cemented-in scab liner, just before Expt. 2025.
Adapted from HDR, 1985

Experiment 2025: High-Pressure Injection into EE-3

Experiment 2025—the pressurization of the 381-ft open-hole interval between the bottom of the liner and the sand plug—began on December 13. It lasted about two days, met with many problems, and ended with the failure of the 4 1/2-in. drill pipe, inappropriately being used as the frac string. (Note: The higher-pressure-rated 4 1/2-in. casing was on site at the time and *should* have been used as the frac string for this very important high-pressure injection. The few hours saved in pipe-handling was vastly outweighed by the six months of inactivity that followed the failure of the drill pipe—time that, with an intact frac string, could have been used for invaluable testing of a significant, pressure-stimulated region.)

Early on the first day of Expt. 2025, at an injection flow rate of 2 BPM (5 L/s), the backside pressure started to rise as the injection pressure approached 2600 psi; when attempts to bring it down failed, pumping was stopped. The diagnosis was that faulty or damaged seals in the PBR assembly were allowing leakage into the annulus (the leak was much too small to have been caused by a frac string failure). The next day, following repeated exercising of the seals in the PBR assembly, the leak was brought under control at 13 gpm with the annulus vent pressure maintained at about 900 psi. Injection was recommenced at 2 BPM and increased in steps to 7 BPM over the first hour, then rapidly increased to 20 BPM and held at that rate for about another 2 1/2 hours at an average injection pressure of 6600 psi. (During injection, the rate of the annulus leak declined further, to less than 4 gpm.)

The injection impedance during Expt. 2025 remained high, reflecting those of Expts. 2018 and 2020.

As shown in Fig. 6-13, after about 3 1/2 hours and the injection of some 3600 bbl (580 000 L) of hot water, the injection pressure suddenly dropped. When the annulus pressure was checked, it was found to have abruptly equalized with the borehole pressure—indicating that the frac string had failed. Pumping was halted and venting began.

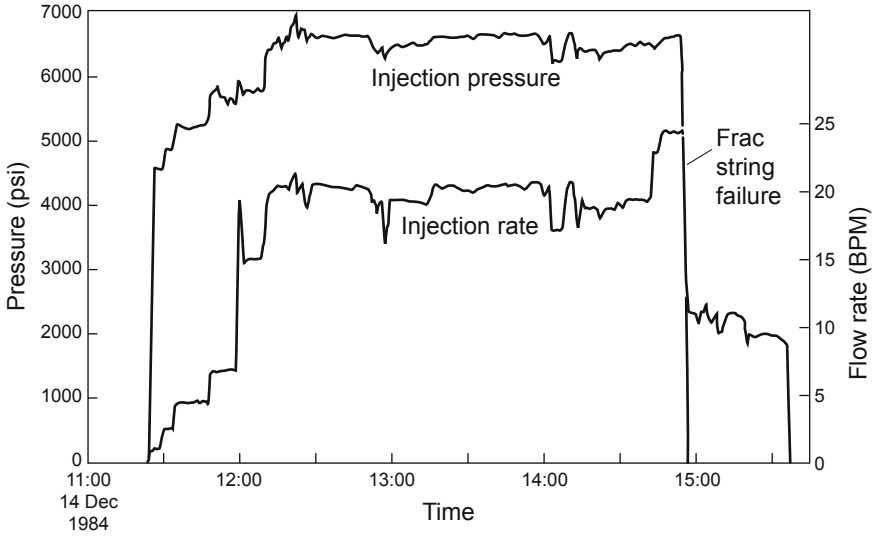

Fig. 6-13. EE-3 injection pressure and flow rate on the second day of Expt. 2025 (December 14, 1982).
Adapted from HDR, 1985

The pressure plateau at about 4600 psi in Fig. 6-13, at the initial injection rate of about 1 BPM, indicates that the first joint in this previously untested interval of the borehole opened at this pressure (somewhat lower than the initial joint-extension pressure measured in EE-2 during Expt. 2018—5500 psi). Over the next hour, the injection pressure increased in close correlation with the step-wise increase in injection rate, suggesting the possibility of other joint openings.[10]

Post-Expt. 2025 temperature logs indicate the presence of joint inlets at 11 155, 11 188, and 11 254 ft (TVD) over about the first 100 ft of the 381-ft open-hole interval. It is possible that not only the first but all three of these joints opened at the initial pressure of 4600 psi; or that the other two opened only as the injection pressure was further increased. This temperature evidence for the opening of multiple joints in the pressurized interval was one of the most significant features of Expt. 2025. It also parallels that seen during Expt. 2018, when three joints were opened across the upper part of the open-hole interval in EE-2 (see Fig. 6-6).

A total of some 150 000 gal. of water was injected into the open-hole interval below the scab liner during this experiment, which produced a

[10]During several previous injection tests, joint-opening pressure plateaus had been observed in the rapid first phase of borehole pressurization—but no obvious additional plateaus were observed as injection rates increased.

number of seismic signals (the hodogram method was still being used to determine event locations). The 1983 annual report (HDR, 1985) devoted one paragraph and one figure to Expt. 2025, but offered no comment on the induced seismicity. Fortunately, an unnumbered internal Laboratory memorandum (Pearson et al., 1982) provides a summary plot of these signals, shown in Fig. 6-14. It is evident that the seismicity clusters around the EE-3 borehole, starting from near the bottom of the injection interval, and appears to reach almost halfway to EE-2.

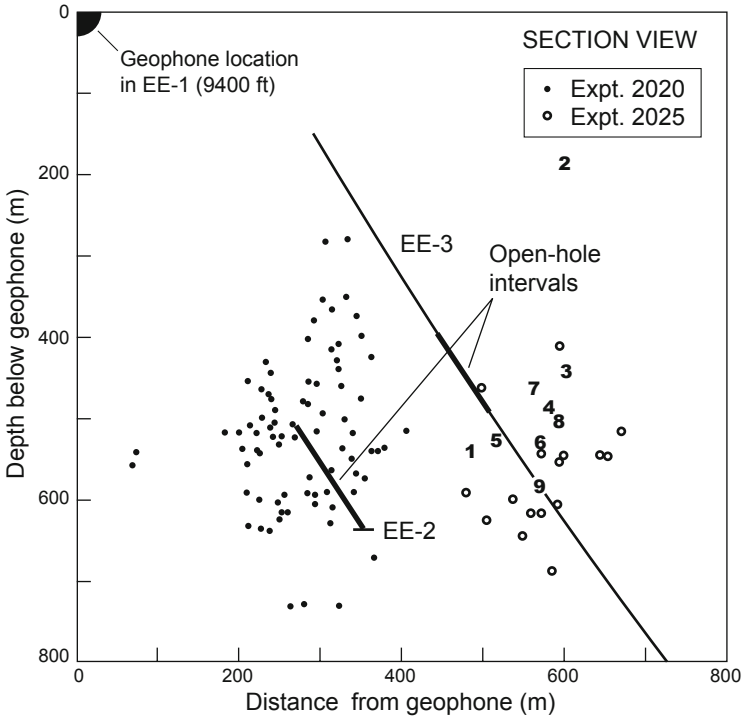

Fig. 6-14. Section view (projected onto N60E plane) of a selected set of the microseismic events recorded during Expt. 2025. The locations of these events are corrected by recalibration of the hodogram signals to place the first few events close to the injection interval. The first nine events are represented by numbers rather than open circles, signifying the order of their occurrence (note that the anomalous location of No. 2 may be the result of a computational error). For comparison, the seismicity generated during Expt. 2020 is also shown.
Adapted from Pearson et al., 1982

An examination of the two seismicity plots in Fig. 6-14 reveals an intriguing phenomenon. The Expt. 2025 seismic cloud appears to be "pushed down" to the very bottom of the EE-3 injection interval—as if the dilation of the rock mass produced by the 844 000-gal. injection of Expt. 2020 in EE-2 had exerted pressure on the nearby region surrounding the EE-3 open-hole interval, preventing the joints in that region from being opened by the Expt. 2025 pressurization (a relationship that becomes evident only through observation of both seismic clouds in concert).

Recent re-analysis of the data has made clear that the joints stimulated during Expt. 2025 would never have been able to connect to the open joints within the Expt. 2020 stimulated region, because that region was enclosed within a "stress cage"[11]—an annular zone of hyper-compressed rock resulting from the expansion of the inner pressure-dilated volume. This zone extended out some distance *beyond* the seismic cloud shown in Fig. 6-11 and imposed an additional closure stress on the potential connecting joints.

Note: Experiment 2025 also gave rise to the development of an additional seismic network. It was inspired by the clear seismic signals recorded on a geophone placed in the granite at the bottom of exploratory borehole GT-1, about 1 1/2 miles north of the Fenton Hill site. With GT-1 as its focal point, the new "Precambrian Seismic Network" would comprise several geophones positioned near the Precambrian surface but radially displaced from the Fenton Hill site. This network would add considerably to the location accuracy of the microseismicity generated during the forthcoming MHF Test.

Another Drill Pipe Failure

On December 15, after EE-3 had (with some difficulty) been vented down, a temperature log was attempted; but when the temperature tool could not be worked past the bottom of the PBR, it was withdrawn and the logging equipment was rigged down. Next, the frac head was removed from the top of the drill pipe (leaving the drill pipe open to the atmosphere), and the flow lines were rigged down. But as the fluid pressure dropped, without warning the sudden release of dissolved gas caused the well to "blow out" through the open drill pipe. An attempt was made to pull the drill pipe out of the PBR, but the borehole started flowing on both sides (bore and annulus), releasing large amounts of gas. The Kelly was picked up and attached to the drill pipe, the Hydril rams were closed, and fluid was pumped down the drill pipe to "kill the well." The next three days were spent trying to recover the drill pipe, during which time dissolved CO_2 was causing EE-3 to repeatedly "unload."

[11]This stress cage is analogous to the circumferential hoop stress that develops in the rock surrounding a pressurized borehole.

The drill pipe failure—in a section of pipe some 1770 ft below the Kelly bushing—had been caused by a 28-in.-long axial split in the body of the pipe, about 7 ft below the box end. This was the sixth catastrophic failure of high-strength pipe in five months of injection testing. Table 6-1 summarizes these six failures; but no words can convey the sense of "malaise" and frustration experienced by the Project staff because of the inability of "off-the-shelf" high-strength tubular steels to perform adequately in this chemically hostile environment.

Table 6-1. Stress-corrosion failures of high-strength drill pipe and casing

Date	Pipe type and location	Material	Approximate depth of failure (ft)
20 July 1982	3 1/2-in. drill pipe, near the box end	S-135	2590
24 July 1982	3 1/2-in. drill pipe, near the box end	S-135	2540
27 July 1982	3 1/2-in. drill pipe, in slips area below box	S-135	5550
7 Oct 1982	4 1/2-in. casing collar	P-110	9250
10 Oct 1982	4 1/2-in. casing collar	P-110	9370
17 Dec 1982	4 1/2-in. drill pipe, 7 ft below the box end	S-135	1770

Cracks in several of these failed tubulars were examined both visually and with a scanning electron microscope. The type of damage observed at the grain boundaries of such austenitic steels is often referred to as "hydrogen embrittlement." All of the failures seemed to originate at indentations in the steel resulting from the use of elevators, tongs, or slips. Because as little as 1 ppm of H_2S can cause sulfide stress-corrosion cracking, it was assumed that this was the failure mechanism.

After the failed joint had been removed from the string, the drill pipe was run back into the hole and stabbed into the PBR. The next three days were spent working to get the gas situation under control and to "stabilize" the borehole: the gas-saturated fluid was circulated out by repeatedly stabbing the drill pipe into the PBR, pulling it out again, and then circulating water down the drill pipe and back up the annulus. Finally, the drill pipe was tripped out of the hole and laid down, and the 4 1/2-in. casing was picked up, run into the borehole, and stabbed into the PBR. On December 20, after the wellhead had been installed, EE-3 was shut in and the drill rig was placed on standby. (The rig would end up being furloughed for over five months, while a new 4 1/2-in. frac string of a corrosion-resistant, low-alloy steel was being procured for use in EE-3.)

The failure of the December 1982 effort to connect EE-3 to the Expt. 2020 seismic zone led to the replacement, in early 1983, of the Fenton Hill HDR Project management team. John Whetton, the HDR program manager and Earth and Space Sciences (ESS) deputy division leader, was understandably unhappy with the team's inability to achieve a flow connection between the two boreholes and was looking for new leadership—as well as a new technical thrust.

The EE-2 and EE-3 Stimulated Regions Display Similar Joint Characteristics

The pressurization data for Expts. 2018 and 2020 in EE-2 and Expt. 2025 in EE-3 (Figs. 6-5, 6-9, and 6-13) exhibit one important feature that was not well recognized at that time. In all of these experiments, there was a common extension pressure—close to 5500 psi—that appears to represent the jacking pressure for the set of essentially continuous, "principal" joints having the highest opening pressures within each of the two stimulated regions. The pattern of interconnectivity within both regions was one of internal "manifolding" of high-pressure fluid from these principal joints to the lower-opening-pressure joints, which were discontinuous and truncated. It is intuitively obvious that if *any* of the sets of lower-opening-pressure joints had been continuous, they would have continued to extend at lower pressure; and in that case they—rather than the higher-pressure joints—would have controlled the growth of the stimulated region.

As these figures show, any attempt to increase the pressure within the stimulated region above 5500 psi by pumping at higher rates would simply have made the region grow faster but at a constant pressure. The lower-opening-pressure joints could not have been extended beyond their truncated ends, but—being hyper-dilated at the 5500-psi extension pressure for the principal set of joints—would still have stored large volumes of fluid.

Unfortunately, the inclination of the principal joints was more or less aligned with the trajectories of both EE-2 and EE-3 (i.e., dipping to the east) and thus offered little opportunity for growth in the orthogonal direction from EE-2 towards EE-3, or vice versa. This alignment is best seen in the section view of Fig. 6-8 (the seismic data for Expt. 2018, represented by the upper-left cluster of events). It was therefore becoming apparent that additional hydraulic stimulation had only a slim chance of connecting EE-2 and EE-3.

Fiscal Year 1983—A Frustrating Year for the Project

Although reorganized, the HDR Project leadership would be unable to make much progress given the "hand that they had been dealt." The plan had been to continue the high-pressure testing of EE-3. However, the new 4 1/2-in. frac string to be used for this testing was not scheduled for delivery until May—which would leave only five months in the fiscal year. (Note: Even with the new frac string finally on hand, the plan for EE-3 would not materialize: a collapse of the unsupported pipe just above the cemented-in portion of the scab liner would lead to five weeks of unsuccessful fishing and ultimately to the rig being placed on standby for the rest of the fiscal year.)

Meanwhile, interest in a much larger injection into EE-2 had persisted following Expt. 2020, but only in May of 1983 would a new 5 1/2-in. frac string be ordered for that purpose.

As detailed in *Phase II Drilling: Summary and Conclusions* at the end of Chapter 5, the completion of EE-3 had not been done properly, and this was the cause of many of the problems that followed. If only the selected open-hole interval had been pressure-tested *before* the production casing was set (which would have revealed the presence of the low-pressure joint, mandating a deeper setting depth for this casing), almost a year of fruitless effort could have been averted.

One of the few things accomplished during this time was the daily measurement, by Dan Miles, of the post-Expt. 2020 shut-in pressure at EE-2 during the summer and early fall of 1983 (see Fig. 6-15 below).

Temporary Suspension of Operations

The many and frequent problems encountered with the tubular goods during the fracturing experiments (problems caused by the unexpectedly high reservoir-stimulating pressures in a chemically corrosive downhole fluid environment) had finally forced a decision to suspend operations at the end of 1982. Despite the disappointment of this interruption in the experiments, the work in microseismic mapping was continued and made impressive progress. A large statistical sample of the microseismic events produced during hydraulic stimulation was obtained and mapped. Unfortunately, these analyses did not strongly verify the *volumetric* nature of the stimulated regions, which could have helped guide and direct the forthcoming MHF Test in EE-2. However, they revealed a distinct *absence* of evidence that vertical features in the stimulated regions (Expts. 2018, 2020, and 2025) were extending. This fact should have dealt the final blow to the flawed notion that a penny-shaped fracture could be created and then extended vertically through heterogeneous crystalline rock containing an array of weakly cemented—but sealed—joints. (Nevertheless, Mort Smith and several others never did abandon the theory.)

On May 3, 1983, the drill rig that had been in place over EE-3 was reactivated. The plan was to continue pressurization testing in EE-3 with the new 4 1/2-in., L-80 frac string. First, the old 4 1/2-in., N-80 casing (frac string) that had been left in the borehole at the end of 1982 was pulled out and laid down. But when a small mill was run in on drill pipe to clean out the cemented-in scab liner, an obstruction was encountered at 10 833 ft, 17 ft above the top of the liner cement.[12] It appeared that during the first episode of hole unloading through the drill pipe at the end of Expt. 2025, the liner had collapsed—probably as a result of the very large pressure differential between the fluid-filled annulus and the almost empty bore of the drill pipe.

Note: The cumulative venting behavior observed in the wake of Expt. 2025 demonstrated that there was still a good high-pressure flow connection at EE-3, through the obstruction at 10 833 ft and down into the pressure-stimulated region. But the Project managers did not believe that this connection was adequate for continued injection testing, because it would not permit full-diameter logging. This judgment was an unfortunate one; injection testing of this region could have proceeded with slimline temperature logging and would have had very beneficial results. Moreover, with the new frac string, EE-3 could then have served as a good-to-excellent production borehole for the upcoming MHF Test, obviating the need for the prolonged, difficult, costly—and ultimately only marginally successful—workover effort.

A very difficult fishing operation ensued at EE-3, which lasted from May 5 to June 18. During this time, the PBR (inside the 9 5/8-in. casing, at 10 106 ft) and the liner hanger were recovered; then the liner, consisting of 4 1/2-in., buttress-thread N-80 casing, was removed down to the collapsed joint—a slow and careful operation in which a combination of inside and outside cutters was used to recover about 120 ft of pipe at a time. After repeated cutting, milling, and fishing steps, the top of the remaining liner (a threaded collar at a depth of 10 890 ft) was only 57 ft above the point of collapse.

On May 18, twenty joints of the new 4 1/2-in. L-80 casing, with a PBR on top, were successfully screwed into this top collar. The connection was then pressure tested—first with the rig pumps and then by Dowell—and shown to be pressure-tight. But when an OWP[13] collar locator was run into the liner, it could not get past an obstruction at 10 895 ft (wireline depth). A 3 1/2-in. mill was run in on smaller-diameter drill pipe to clear the obstruction, after which the borehole was checked down to 11 450 ft (as far as the smaller drill pipe would reach). The 4 1/2-in. drill pipe was then withdrawn from the hole and laid down, followed by the smaller-diameter drill pipe. Finally, on May 20, most of the remaining 4 1/2-in. L-80 casing—which

[12]Fig. 6-12 shows the top of the liner cement and other details of the EE-3 liner.

[13]Oil Well Perforators, Inc., Casper, Wyoming.

would serve as the frac string—with a redressed seal assembly on bottom, was run into the borehole. The next morning, the seal assembly was inserted into the PBR (but the frac string was not pressure-tested at this time).

First "Sideshow" Experiment in EE-3—Expt. 2028

Experiment 2028 took place on June 22. This "nitrogen blanket" experiment was designed to test whether, by replacing the water in the upper part of the annulus (outside the frac string) with nitrogen, the rate of heat transfer from the casing to the frac string could be decreased enough for cool water to be safely injected—obviating the need for pre-heating.

In preparation for this experiment, the seal assembly was pulled out of the PBR again. Nitrogen was then injected into the annulus at high pressure, which displaced the water and caused it to flow back up the 4 1/2-in. frac string. When the seal assembly had been reinserted into the PBR, the annulus was shut in and the annular fluid level was logged (inside the frac string) by OWP. After repeated injections of water and nitrogen into the pressurized annulus, the water level was finally stabilized at 5900 ft.

During the next part of the experiment, an OWP temperature tool was "parked" at a depth of 4000 ft for continuous recording. A Dowell pump truck was used to pump water down the frac string for 1 1/2 hours at a constant rate of 1 BPM. The initial injection pressure of 5500 psi (at 9:00) rose to 6050 psi in 10 minutes, slowly dropped back to 5500 psi in the next 10 minutes, then finally leveled out at 5300 psi (at 9:30) and remained there for about 1 hour. During this pumping interval, the screw-in connection to the collar at the top of the liner stub appeared to be pressure-tight up to at least 6000 psi. A full-depth slimline temperature log followed, as well as an annular fluid-level log that showed the level still at 5900 ft; then the OWP temperature tool was again parked at 4000 ft.

Pumping with the Dowell truck recommenced at 12:13. The beginning rate of 1 BPM was slowly increased to 8 BPM at an injection pressure of 5500–5600 psi. Two hours later, at 14:13, the annulus pressure suddenly rose to 3450 psi, indicating a serious leak somewhere. Pumping was shut down, the temperature tool removed, and Expt. 2028 prematurely terminated.

The temperature measurements during this experiment showed that the injection of nitrogen did reduce heat transfer significantly, but only enough to allow a decrease of about 15ºC in the temperature of the injected water. In other words, pre-heating would still be necessary.

Because the Expt. 2025 stimulated region had been reinflated with the injection of about 40 000 gal. of water, the frac string had to be vented down before any other operations could take place. Concurrently, the nitrogen in the annulus was vented, through the rig's choke manifold. Then the annulus had to be refilled with water. To determine the location of the leak, a combined temperature/collar-locator log was run by OWP, which revealed that the leak was at the screw-in connection, at a depth of about

10 890 ft. (It would later be found that the collar at the top of the liner stub had pulled away from the rest of the liner, apparently because of cooling-induced thermal contraction of the injection piping).

Work began the morning of June 23 to pull the frac string from the borehole and lay it down on the pipe racks. This task complete, the drill pipe—with a setting tool installed on its lower end—was run in. Once the PBR had been tagged, the setting tool inserted, and the J-lugs inside the PBR engaged, the whole liner tie-back assembly was pulled from the borehole. Attached to its bottom were the screw-in joint and the separated 4 1/2-in. casing collar.

More Fishing in EE-3

The next two weeks were spent in a reasonably successful effort to re-establish a pressure-tight connection at the top of the cemented-in liner in EE-3. Throughout these operations, the interval below the liner (stimulated during Expt. 2025) was producing large amounts of gas—mostly CO_2—that had to be dealt with almost continuously and severely hindered progress.[14]

On July 4, 1983, following a series of washover and outside cutting operations (and a final "clean-up" run with a skirted, flat-faced mill that removed another 9 in. of pipe), the top of the remaining liner was at a depth of 10 897 ft. Twenty joints of the new 4 1/2-in. L-80 casing were then used to extend the scab liner upward into the 9 5/8-in. casing. Fitted with a "temporary" overshot casing patch and grapple on the bottom, this extension was slipped over the top 3.3 ft of the liner stub. (A special high-temperature casing patch, designed to withstand high stimulation pressures, was on order but delivery was not expected for several months.)

After the 4 1/2-in. drill pipe had been pulled from the hole and laid down, the 4 1/2-in. L-80 frac string, with a repaired seal assembly on bottom, was picked up, run into the hole, and stabbed into the PBR on top of the scab liner. As a final step, the annulus was filled with sepiolite mud and corrosion inhibitors to protect the 9 5/8-in. casing. This "completion," although not ideal, would enable EE-3 to serve as a production well if the planned MHF Test in EE-2 finally succeeded in connecting the two boreholes.

On July 8 the drill rig was furloughed again and would remain inactive until mid October.

[14]The ongoing production of large amounts of gas strongly suggests that by far the largest source of this gas was the connate fluids contained within the mineralized joints that had been reopened during Expt. 2025—not the pore fluid in the very tight (permeability in the nanodarcy range) rock surrounding these joints.

Second "Sideshow" Experiment in EE-3—Expt. 2033

The purpose of Expt. 2033 was to stimulate the lower portion of the Phase I reservoir region by injecting heated water down the EE-3 *annulus* (outside the frac string) and through the low-pressure open joint just below the casing shoe—the one that had caused so many problems in the past. The primary objective of activating the joints in this low-pressure region was to generate enough seismic signals to test how the vertical geophone stations in GT-1 and PC-1 would work in concert with the triaxial geophone at 9400 ft in EE-1.[15] A couple of months later, these stations would be added to the deep triaxial geophones in EE-3 and GT-2, to constitute the seismic network for the MHF Test in EE-2.

The GT-1 and PC-1 geophones were located near the Precambrian surface, as part of the new "Precambrian Network"—a supplementary seismic network designed to enhance lateral control of the microseismic event locations recorded during the MHF Test, mainly by the two deep geophones in EE-1 and EE-3. The geophone in PC-1, at 2148 ft, was about 250 ft above the Precambrian surface at Fenton Hill (the intervening rock being vuggy Madera limestone), but was deep enough to be largely unaffected by the problems encountered with the surface seismic instrumentation. The geophone in GT-1 was at 2460 ft—nearly 400 ft into the Precambrian basement in Barley Canyon—and was totally unaffected by these problems. (The nine 1-Hz, vertical-component surface stations installed in 1978 for Phase I testing, which were located on a radius of about 2 miles [3.2 km] from the EE-1 wellhead, were susceptible not only to surface noise but to severe attenuation of the signals, which had to pass through the thick layers of volcanic and sedimentary rocks above the Precambrian surface.)

Other objectives were (1) to more clearly delineate the boundary between the low-pressure (Phase I) and high-pressure (Expt. 2025) stimulated regions, by mapping the seismicity in this lower Phase I reservoir region and comparing it with the seismicity generated by stimulation of the joint network during Expt. 2025; and (2) to observe the venting behavior of the lower Phase I reservoir region.

Experiment 2033 began on September 27, 1983, with the drill rig on standby over EE-3. The injection of 197 000 gal. of heated water generated sufficient microseismic signals to test the seismic network, and at the same time enabled the demonstration of an enhanced travel-time algorithm for locating individual events. (Because the seismic signals received at PC-1 were not

[15]In the summer of 1983, PC-1 was drilled 4260 ft southeast of EE-2 as the first of two deep seismic observation holes. PC-1 was about 2200 ft deep and bottomed in hard Paleozoic limestone, just above the granite surface. The later drilling of a second hole, PC-2, due west of the EE-2 location, would complete the Precambrian Network (GT-1, PC-1, and PC-2).

of sufficient quality, the algorithm was based on triangulation from P- and S-wave signals received at the GT-1 geophone and the deep geophone stations in EE-1 and EE-3).

This experiment also yielded the following findings for the two ancillary objectives:

1. The lower portion of the Phase I reservoir region was seen to extend downward to within about 260 ft of the upper boundary of the high-pressure EE-3 seismic cloud generated during Expt. 2025.
2. Venting of the low-pressure Phase I region (just below the casing shoe in EE-3) proceeded at about 50 gpm (3 L/s) with the borehole at atmospheric pressure. A significant volume of fluid was returned from this confined region (the actual amount was not measured).

Measurements in EE-2: The Shut-in Behavior of the Expt. 2020 Reservoir

As mentioned earlier, following the pipe failure that ended Expt. 2020 (October 7, 1982), the reservoir was continuously vented for nearly four months (through January 1983). The next six months were occupied with a sequence of small, low-pressure injection tests, vent-down periods for logging, and shut-ins. Then, beginning in mid July 1983, EE-2 was shut in for an extended period of time. Within the first few minutes of this extended shut-in, the pressure rose to 648 psi. What ensued, over the next 73 days, was a "self-pumping" of the reservoir, eventually reaching a pressure of 1270 psi.

This pressure buildup confirms that a residual pressure-dilated region still existed at the time of Expt. 2025 (only 9 weeks after Expt. 2020)—one that was surrounded by a stress cage, as discussed earlier (and shown in Fig. 6-14). In other words, this region was *totally confined* within an impermeable body of hot crystalline rock.

The pressure buildup curve is shown in Fig. 6-15. If this curve is extrapolated to infinite time using the Muskat technique,

$$P\infty - P(t) = e^{-at},$$

where $P(t)$ is the buildup curve and a is an arbitrary constant, the equilibrium reservoir shut-in pressure reaches about 1450 psi (10 MPa)—the opening pressure for the apparently very large array of vertical joints oriented essentially orthogonal to the direction of the least principal earth stress (N111E).

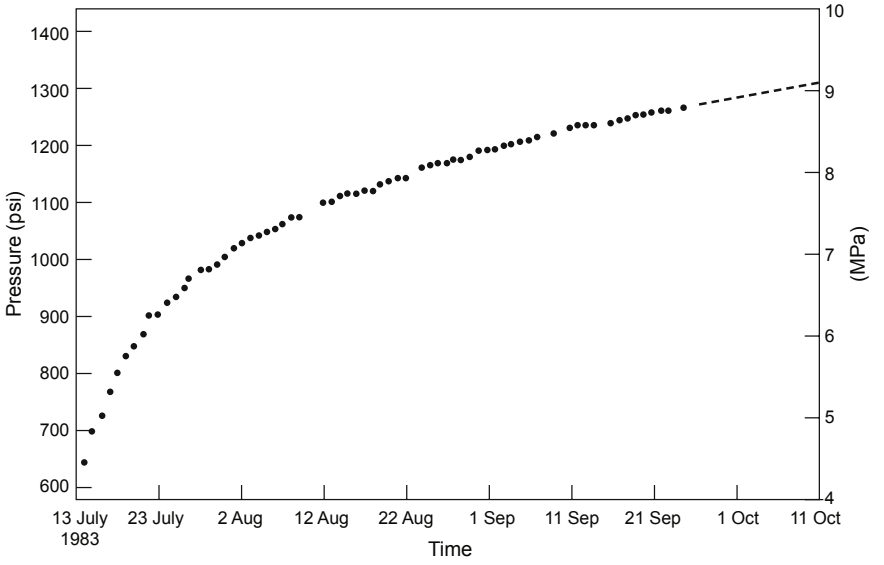

Fig. 6-15. Pressure buildup in EE-2, beginning about 10 months after Expt. 2020 and lasting 73 days, due to self-pumping within the enclosed reservoir region.
Source: Brown, 1989b

This pressure-buildup behavior implies, first, that a large and pervasive source of pressurized fluid was still "locked" within the reservoir, even a year after Expt. 2020. Second, this fluid probably originated from numerous still-open joints with an internal equilibrium pressure of about 1450 psi. And third, because the pressure buildup was so very slow, one can infer that the flow paths from the principal joints (i.e., the *manifolding* joints) to these numerous fluid-storing smaller joints were highly impeded (i.e., held tightly closed) at these low reservoir pressures. Moreover, it seems probable that the self-pumping observed at the shut-in EE-2 borehole would have occurred at the reservoir boundaries as well—which implies that the perimeter of the Expt. 2020 stimulated region was tightly closed. An open perimeter would never have allowed the reservoir to internally self-pressurize!

The Massive Hydraulic Fracturing Test: Expt. 2032

Mapping of the microearthquakes that occurred during the several hydraulic pressurization experiments in EE-2 and EE-3 revealed a picture of ellipsoidal seismic clouds, centered close to the injection intervals in the two boreholes and inclined to the east at roughly the same angles as the borehole trajectories. The clouds extending from the upper injection interval in EE-2

(Expts. 2018 and 2020) were subparallel with and close to the cloud later generated during Expt. 2025 (by stimulation of the interval below the scab liner in EE-3)—at least judging from the data obtained via hodogram, the seismic location method being used at the time. It had been postulated that if these two zones of activity exhibited significant overlap (unfortunately they did not), the likelihood would have been high that additional stimulation would result in a hydraulic connection.

A concomitant hypothesis, championed by the few remaining adherents to the penny-shaped fracture theory, was that a high-pressure and high-volume injection into an even more restricted interval of EE-2 (only about 70 ft) could drive upward one or more vertical hydraulic "fractures," *across* a set of already opened inclined joints, to intersect the EE-3 borehole. Restricting the injection interval to 70 ft would facilitate this effort, by isolating the uppermost of the three borehole joint connections activated during Expt. 2018 (see Fig. 6-6).

It was for these less-than-compelling reasons that a "massive hydraulic fracturing"—higher rate and much larger volume—operation was planned, to enlarge the zone of seismic activity surrounding the restricted injection interval just below the casing shoe in EE-2, and thereby (it was hoped) expand the network of stimulated joints between the boreholes. The basic plan for the MHF Test was based on experience gained from Expt. 2020.

On the recommendation of a group of industrially experienced experts, assembled as a Workover Operations Review Committee (HDR, 1985), in mid September the plan for the MHF Test was modified as follows:

- The maximum injection rate was increased from 20 to 40–50 BPM (friction reducer would be used to enable such an increase, the ultimate rate being determined by the maximum injection pressure of 7000 psi [47 MPa]).
- The injection interval was reduced from about 400 ft to only 70 ft.
- Finely-ground calcite was to be injected as a fluid-diverting agent (to plug up some of the secondary flow paths opened during Expt. 2020).

Between 4 and 6 million gal. (15–23 million L) of water—a volume up to six times greater than in any previous high-pressure stimulation—would be injected into EE-2 over a period of 2 to 3 days. A higher pumping rate (80 BPM) and injection pressure (8000 psi) were advocated by some, but were ruled out for monetary as well as technical reasons. In retrospect, an injection rate of only 20 BPM (as originally planned) would have been sufficient to effectively create the Phase II HDR reservoir, and would have been simpler and less expensive.

The information in this section is augmented by information from the following reports: Dreesen and Nicholson (1985); House et al. (1985); and HDR Geothermal Energy Development Program (1985 and 1986c).

Preparations

In addition to the Precambrian Seismic Network (Fig. 6-16), the preparations for the MHF Test included the construction of a number of other facilities and supporting systems, development of tools, and work on the EE-2 site and borehole.

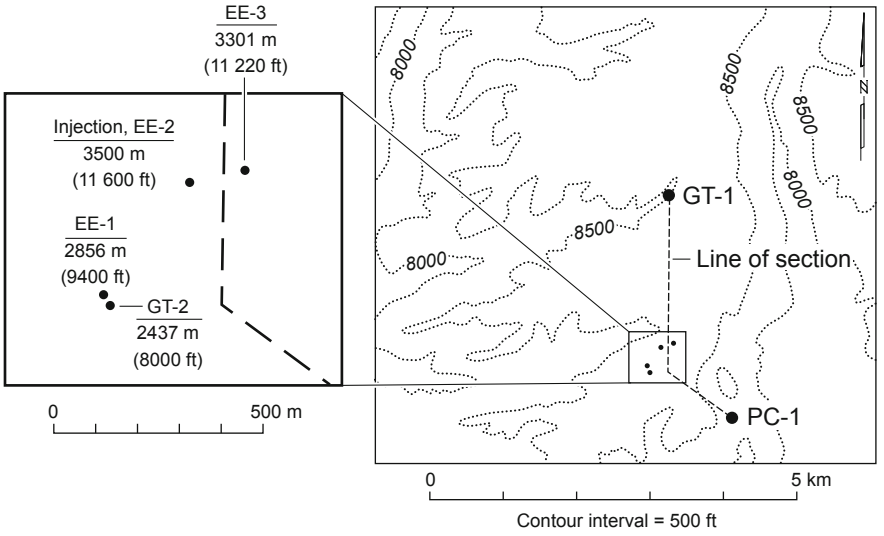

Fig. 6-16. Map view of the seismic network for the MHF Test, showing the locations of the Precambrian Seismic Network geophone stations (GT-1 and PC-1) and the deep seismic stations. All geophone depths shown in meters are true vertical depths; those shown in feet are equivalent slant depths (measured along the borehole).
Adapted from HDR, 1986c

Five-Million-Gallon Pond and Supporting Equipment

In contrast to previous fracturing tests at Fenton Hill, for which above-ground (rental) water-storage equipment was used, the greater water requirements of the MHF Test would be supplied by a large, specially constructed, in-ground pond. Construction of this pond began in August 1981 and was completed in July 1982. Designed to hold 5 million gallons, the pond measured 200 ft by 250 ft and sloped to a depth of 23 ft. It was lined with a reinforced rubber (polyester and nylon) lining placed on a bed of sand, and was covered with a similar material. The pump house for this pond was equipped with two pumps, to transfer water into the surface circulating system through a buried, 150-psi ductile iron pipe. (This pipe was also connected into the above-ground, 500-bbl rectangular water storage

tank—see Fig. 4-6.) During Fiscal Year 1983, the 5-million-gal. pond was filled to capacity; over 3 million gal. was commercially hauled water and the rest came from the on-site water well.

Slimline Downhole Instrumentation

The months preceding the MHF Test saw a concerted effort to develop two slimline, high-temperature tools for use inside the 4 1/2-in. frac string in EE-3. The first of these was a highly sophisticated, triaxial geophone package that, to this day, has no equal in the commercial logging industry. This tool was designed to operate not for hours but for *days* in the hostile (high-pressure and high-temperature) environment at 11 200 ft in EE-3, where the temperatures reached almost 240°C. Instead of the time-sensitive Dewars or heat sinks normally used for thermal protection of electronics and instruments, this slimline geophone package incorporated high-temperature components having very long operating lifetimes.

The second slimline, high-temperature tool was a multi-detonator sonde that would provide acoustic signals from a known, fixed location deep in EE-3 to calibrate the geophone packages deployed in adjacent boreholes. This tool incorporated a collar locator for correcting cable-depth measurements, and a high-temperature geophone for obtaining a time-zero firing signal. This detonator tool was successfully tested in borehole environments at temperatures in excess of 270°C.

Note: Almost from its beginning, the HDR Project had operated at or beyond the limits of existing downhole technology with regard to equipment, instruments, and experimental techniques (see the Appendix for a complete discussion of the large array of downhole tools and sensors developed by the Laboratory for the HDR Project). This proved to be particularly true for downhole seismic instrumentation, the principal reservoir diagnostic technique.

Preparation of the EE-2 Site and Borehole

On November 2, orders were given to skid the rig back to EE-2, and by November 8 it was in place. After the blow-out preventer had been installed and rigged up (to preclude anticipated problems with dissolved gas), the 4 1/2-in. drill pipe was picked up and run in the hole with an 8 3/4-in. bit on bottom. At a depth of 5400 ft, the borehole was circulated for 70 minutes to clear the fluid of dissolved gas. The drill pipe was tripped in farther, to 7770 ft, at which depth a gas "kick" stopped further operations. After extensive circulation, the bit was tripped in farther still, until the top of the sand plug was tagged at 11 996 ft, 418 ft below the casing shoe. A number of logging runs and a casing scraper run (on drill pipe) were then done.

On November 17, the EE-2 borehole was further backfilled through drill pipe: four separate bentonite and sand slurries were pumped in, at intervals of several hours (to allow the sand to settle). The final depth for the new top

of the sand plug was 11 648 ft—leaving a 70-ft open-hole interval below the casing shoe for the MHF Test. The 4 1/2-in. drill pipe was then pulled from the hole.

Installation of the Otis Casing Packer

The packer selected to protect the EE-2 production casing from full pumping pressure during the MHF Test was an Otis steam packer equipped with a retrievable, 40-ft-long slick joint having an outer diameter of 5 1/8 in. and an inner diameter of 4 in. A packer of this type had been successfully used during Expt. 2020, at surface pressures up to 7000 psi—80% of its rated pressure—and had performed well for an injection period lasting about 15 hours at rates up to 32 BPM (until the frac string failed—see Fig. 6-13). At the time, there had been a kind of "superstition" among the Los Alamos personnel working with Otis on the design of this packer, that over extended pumping periods the injection pressure would slowly creep up. In fact, this belief was unfounded—*no data* supported it. The joint behavior discussed earlier (in the sidebar *The EE-2 and EE-3 Stimulated Regions Display Similar Joint Characteristics*) directly counters such a belief, as do the reservoir[16] data shown in Figs. 6-9 and 6-13 (both for near-constant-pressure injections of around 1 million gal. into the same rock mass that would be further stimulated during the MHF Test).

As part of the collaboration with Otis, a retrievable "control" packer was also developed, to be installed in the casing *below* the steam packer. Its principal component was an integral check valve—known as a "foot valve"—designed to prevent pressurized back-flow from the reservoir. In the event of a high-pressure leak in the steam packer (a major concern for the MHF Test), this safety feature would shut off the reservoir back-flow, permitting the steam packer to be replaced. In addition, it would enable any part of the frac string or other component downstream of the surface master valves to be repaired without venting-down of the reservoir. And most important, in the event of a blow-out at the surface, the foot valve would activate immediately, well before the master valves could be closed by hand.

On November 20, the Otis control packer was given a test run. After it had been set at a depth of 2000 ft, a pressure-check of the foot valve showed no leakage. But the next day, when the control packer was run back in and set at its final depth of 11 358 ft, it released prematurely and was

[16] At this time (just before the MHF Test) there was no "reservoir" in the truest sense, because no hydraulic connection had been established between the boreholes (that would happen almost two years later, during Expt. 2059, when the MHF stimulated region was finally connected to borehole EE-3A). The term "reservoir" as used here, then, should be understood as a pressure-stimulated region that would later become a true reservoir.

found 460 ft higher up in the hole. The design was reworked to prevent this problem (unfortunately, because several months would have been needed to implement the change, in the end the control packer was not installed for the MHF Test—a *big* mistake!). But the premature release of the control packer sounded an alarm with respect to the steam packer: might it too release prematurely? In an effort to head off such an occurrence, the packer was shipped to a machine shop in Farmington, NM, for a "field" modification. (Note: It is not known why the control packer was not modified in the same way!)

For a couple of days the borehole was circulated with the rig pumps to cool it down, and several logs were run. On November 27, the refurbished Otis steam packer was run in on drill pipe and set at a depth of 11 297 ft (281 ft above the casing shoe). To test whether the setting was successful, the drill pipe was used to pull up on the packer with 65 000 lb of force and then to push down on the packer with 60 000 lb of load. In neither case was there any perceptible movement of the packer, indicating that it had set properly. The drill pipe was unlatched from the packer and tripped out of the hole, the jay-latch was removed, and a special assembly (including a short slick joint with a vented joint below) was attached, for pressure-testing of the packer. The drill pipe was tripped back into the hole, and after the special assembly had been stabbed into the packer, Dowell successfully pressure-tested the packer by pumping into the 70-ft EE-2 injection interval at pressures up to 4000 psi (essentially using the Expt. 2020 reservoir as a high-pressure "plug": the 4000-psi pressure was lower than that required to open the joint network). Finally, the drill pipe and testing assembly were pulled from the hole and the drill pipe was laid down.

Figure 6-17 shows the downhole configuration for the MHF Test in EE-2, with the Otis steam packer, slick joint, and associated hardware in relation to the casing and the open-hole injection interval.

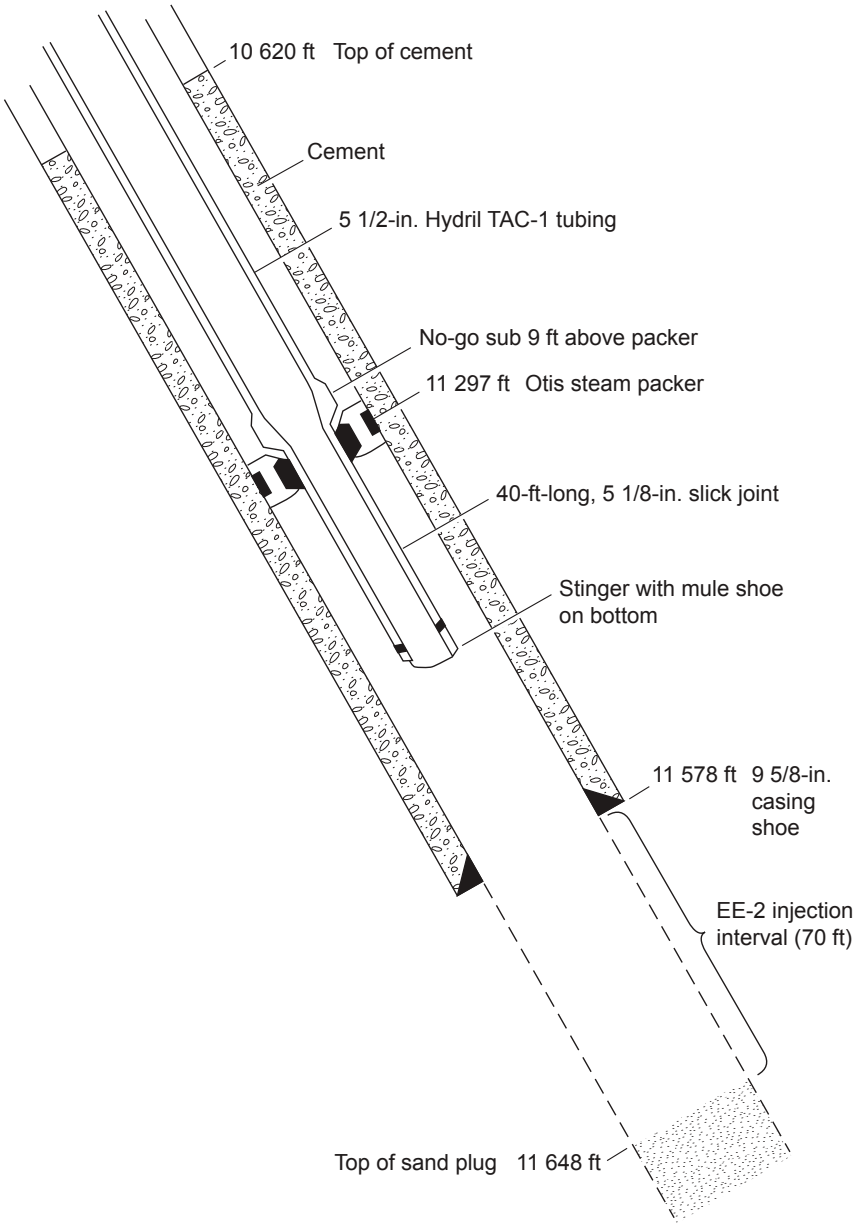

Fig. 6-17. The downhole configuration of the EE-2 borehole for injection during the MHF Test.
Adapted from Dreesen and Nicholson (1985)

Installation of the Frac String

The new, low-alloy-steel 5 1/2-in. (20 lb/ft, C-90) frac string for the MHF Test in EE-2 had been received almost a month earlier. This specially fabricated tubing, fitted with integral TAC-1 Hydril tool joints, was the first fully adequate frac string used in the Fenton Hill stimulation efforts. It was run into the hole on November 28, with the 40-ft-long slick joint for the Otis packer and a mule shoe on bottom. The slick joint was stabbed 31 ft into the packer, leaving 9 ft for thermal expansion if the borehole had to be back-flowed. Between the frac string and the slick joint was a special no-go (locator) sub, to limit the upward movement of the packer if it became dislodged. At the surface, the frac string was fitted with tandem master valves below a frac head consisting of two "crosses"—a 10 000-psi-rated, multiple-inlet manifold for the injection operations.

Pre-Pump Test

On November 30, the packer and frac string were pressure-tested. A Dowell pump truck was employed to inject 95 000 gal. of water into the Expt. 2020 reservoir at rates varying from 1 to 8 BPM and pressures up to 6000 psi (Fig. 6-18). During the first 1 1/2 hours, at an injection rate of 1 BPM, the injection pressure leveled off at about 3250 psi—considerably lower than the 5400-psi joint reopening pressure plateau at the beginning of Expt. 2020 (Fig. 6-9). This behavior suggests that the residual fluid volume of the *connected* joint network remaining after the long-term venting of the Expt. 2020 reservoir was very small—about 3800 gal.

The injection rate was then stepped up to 2 BPM for 1 hour. Near the end of this period, the injection pressure rose to nearly 5000 psi, replicating the levels observed during the early stages of Expts. 2018 and 2020. Although it was not recognized at the time, this evidence for a continuing high injection impedance suggests that there was no significant self-propping (by shear slippage) along the near-borehole joint connections to the reservoir—even after the very large injection of 844 000 gal. during Expt. 2020.

This test, which effectively subjected the packer to 90% of the projected maximum bottom-hole injection pressure at 80% of the maximum cooldown for the MHF Test, showed that the frac string and the packer were functioning properly. Throughout the test, the annulus pressure was maintained between 1500 and 2000 psi by the injection of water during cooldown and back-flow during thermal recovery. The volumes of injected and back-flow water matched those anticipated for a closed, leak-free annulus.

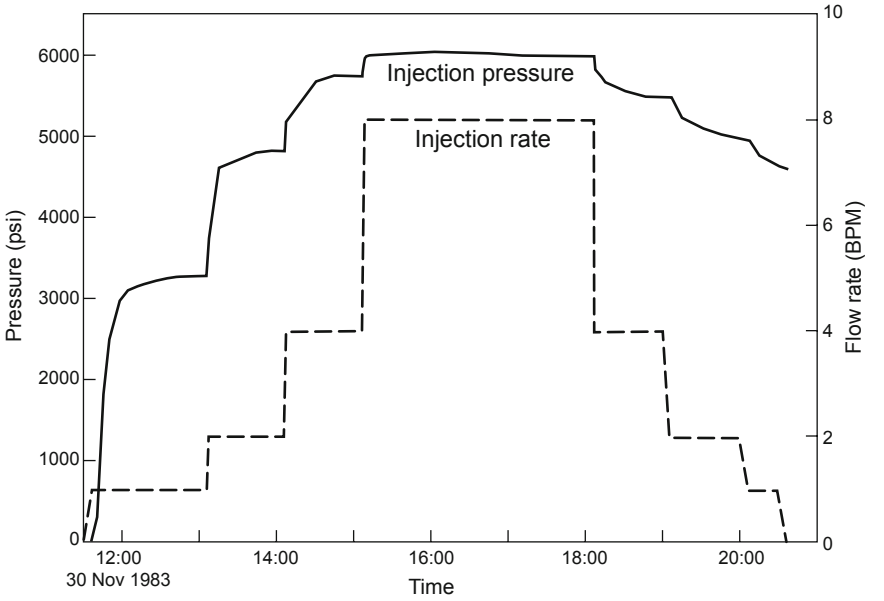

Fig. 6-18. Injection-rate and injection-pressure profiles recorded during the Pre-Pump Test (November 30, 1983).
Source: Murphy, 1984

Figure 6-18 also reveals something very significant: the clearest measurement yet of the true value of the opening pressure for the principal (i.e., the flow-controlling) joints in the Expt. 2020 reservoir—5500 psi.[17] This value is obtained from the pressure asymptote at the end of the 4-BPM injection plateau near the end of this test (at about 19:00, following some 7 hours of injection—by which time the frac string was fully cooled down and both the single joint entrance from the borehole and the several interconnecting joints to the Expt. 2020 reservoir were thermally dilated).

Pumping Equipment

Fourteen pumping units and twenty-one auxiliary support units were mobilized for the MHF Test, making the area of the site west of EE-2 quite crowded (Fig. 6-19). A blender and an industrial transfer pump were tied into the main 12-in. transfer line from the 5-million-gal. water storage pond, which discharged into two 1600-bbl storage tanks. The blender was

[17]In the discussions of injection testing in this chapter, the terms "joint-opening pressure" and "joint-extension pressure" have been used more or less interchangeably—because, except for the very smallest of joints, the pressure required to extend the undilated ends of resealed joints is very close to that required to jack them open (Murphy, 1984).

used to inject a dry friction reducer into the main supply flow (unlike the pre-hydrated liquid chemicals used in previous experiments, this friction reducer would be hydrated in-line). A flow rate of 40 BPM was thought to provide sufficient residence time for the hydration to take place, at a temperature of 0°C, and for fluctuations in concentration to be evened out. In addition, a second blender was deployed to add finely ground calcium carbonate to the injection fluid as a "diverting agent" (to plug the joints having smaller openings), thereby enhancing, it was hoped, the chances that one or more major joints could be driven upward to intersect EE-3. In total, 220 000 lb of 300-mesh (0.05-mm) calcium carbonate would be injected into EE-2 during the MHF Test.

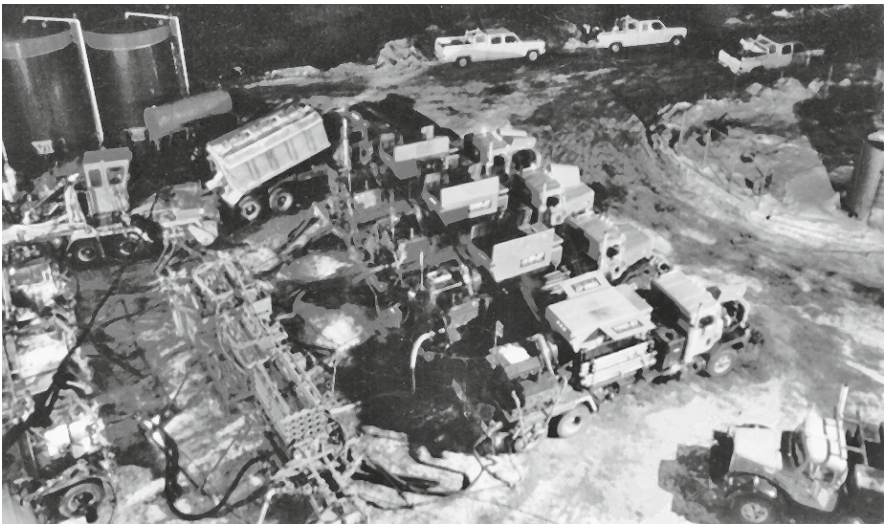

Fig. 6-19. Dowell equipment deployed around EE-2 for the MHF Test. Source: HDR Project photo archives

A minimum of 13 000 HHP was needed for moderate loading of the pumping equipment and to allow sufficient time for routine maintenance of and repairs to the pumps. Two high-pressure manifolds, each with a blender and sand truck containing fluid-loss additive, were located on the suction side; and fourteen high-pressure pumping units were installed on the discharge side. The small size of the area available for the pumping system was a source of concern, but this equipment plus a nitrogen pump (nitrogen was used to pressure-test lines under the extreme winter temperatures), two fuel tanks, a light plant, and a pump control bus were successfully assembled within its confines. However, only half of the equipment was accessible for repair or replacement, if needed, during the MHF Test, and neither the frac head nor the majority of the high-pressure lines were visible from the control bus.

Pulsation-Induced Fatigue of High-Pressure Lines

Pulsation of the high-pressure lines, frac head, and tubing over a prolonged period of pumping can cause fatigue and failure of the injection system. But because of cost and the difficulty of obtaining them in time, no pulsation dampeners were installed on the discharge side of the pumps. Instead, alternative measures were developed to minimize pulsation: (1) suction-side dampeners were to be properly charged and valved; (2) the suction system was to be operated at the optimum pressure; (3) the suction hoses between the pumps and manifolds would be short; and (4) flow rates in the high-pressure lines would be limited.

Four high-pressure injection lines—two from each manifold attached to the pump trucks—were run up to the rig floor and hooked into two 4 1/16-in. (103-mm), 10 000-psi (67-MPa) crosses on the frac head, with Laboratory-furnished companion flanges. Each line was pressure-tested with the nitrogen pump to 8000 psi (54 MPa).

Last-Minute Preparations

Early on December 6 a number of final preparations began, most of them carried out by Dowell personnel. All the pumps and engine drives were checked one last time; the connections of the pumps to the two high-pressure manifolds and the four high-pressure lines connecting these manifolds to the frac head were given a final checkout, then pressure-tested to 8000 psi with nitrogen; a cement pumper equipped with displacement tanks was tied into the annulus between the frac string and the casing, to measure the injection and back-flow volumes required to maintain the annulus at 2000 psi throughout the MHF Test; the 14 Dowell pump trucks were connected up to the two 1600-bbl water-storage tanks supplied from the 5-million-gal. pond; Laboratory personnel deployed and calibrated the deep geophone packages in EE-1, GT-2, and EE-3 (Fig. 6-20) (downhole seismometers were already in place in GT-1 and PC-1); and the Data Acquisition Trailer (DAT) monitoring systems were given a final checkout. The very last activity was a comprehensive safety meeting with all the Laboratory personnel actively involved in the MHF Test as well as the Dowell supervisors (the meeting room was full!).

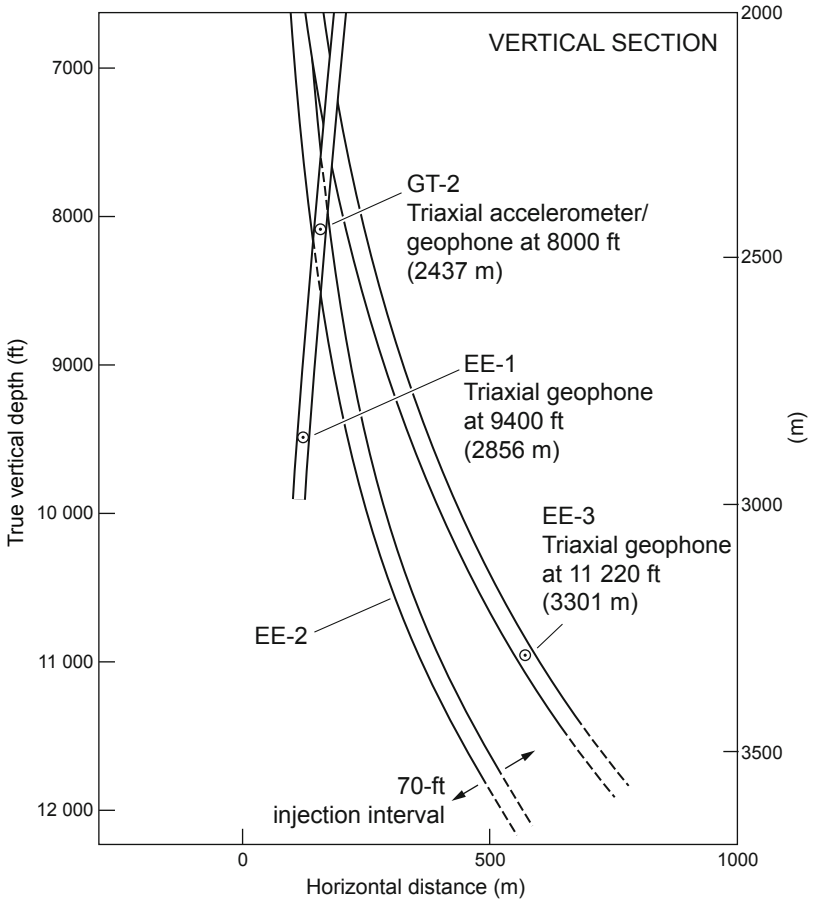

Fig. 6-20. Section view of the deep seismic array used for the MHF Test, projected onto a N45E plane. All geophone depths shown in meters are true vertical depths; those shown in feet are slant depths (measured along the borehole).
Source: HDR Project data archives

Note: The principal seismic stations used to determine event locations during the MHF Test were the geophone in GT-1 and the deep geophones in EE-1 and EE-3. The deep geophone in GT-2 served as a backup. The seismicity recorded at PC-1 was not often used because of problems with signal attenuation and the need for a rather large station correction, as determined from calibration shots run in EE-3 just before the start of the MHF Test (the slimline high-temperature detonator tool, although not available for Expt. 2033 in September, was finished just in time for the MHF Test).

Retrospective: The MHF Test Was Premature

After a quarter century of reflection, it is obvious that the MHF Test should not have been carried out in early December 1983. Pressure from the DOE to "finally" achieve a flow connection between the two boreholes, in addition to an extremely tight funding situation, precipitated the decision to go forward with the test—in the face of a number of limitations and obstacles that should not have been ignored:

- The winter weather was simply horrible that first week in December, with heavy snowfall.
- Because of time and cost constraints, pulsation dampeners for the 14 injection-pump discharge lines had not been obtained.
- The control packer and foot-valve assembly (a "safety" packer for installation just below the Otis steam packer in case of packer failure or surface blow-out) was not available because of insufficient time to have the borehole locking mechanism re-worked at the factory.
- The second deep borehole for the Precambrian Seismic Network had not yet been drilled.
- Time was too short for the backside pump truck to be relocated well away from the congestion near the drill rig.

Even so, the MHF Test went forward—with the result that a blow-out occurred that severely damaged the EE-2 borehole. In fact, the damage was so severe that EE-2 had eventually to be redrilled, at considerable added expense. In addition, yet another DOE advisory panel dictated both the drilling methodology and the trajectory of the new "leg" of the borehole relative to the original hole.

Had the MHF Test instead been delayed until the following spring, many of these limitations and obstacles could have been overcome, the blow-out could have been averted, and the HDR Project could have saved considerable time and money.

The MHF Test: The Largest Injection Ever

As discussed earlier, the injection interval for the MHF Test in EE-2 was the reduced (70-ft) open-hole region between the casing shoe at 11 578 ft and the new top of the sand plug at 11 648 ft (see Fig. 6-17). Pumping began at 16:00 on December 6, 1983, and except for a few brief interruptions continued for 61 hours. A total of 5.6 million gal. (21 000 m^3) of water, containing small amounts of friction reducer and a finely ground, calcium-carbonate diverting agent, was injected through the packer into this short interval. The pumping rate became erratic early on, fluctuating between 26 and 43 BPM at a pressure of 7000 psi (48 MPa), which was attributed to inconsistent additions of friction reducer.

Early during the test, the 1-million-gal. surface pit next to EE-2, water from which was being commingled with water from the pond, was emptied to make room for vent-back water in the event of a downhole failure. Injection at a pumping rate of about 40 BPM, as dictated by the injection pressure limit of 7000 psi, was subsequently achieved and lasted for the remainder of the pumping period.

Figure 6-21 shows the variations in injection flow rate and pressure during the MHF Test. Except for some erratic behavior during the first 18 hours, the MHF Test settled into a fairly uniform pattern with a maximum injection rate of 43 BPM at 7000 psi.

Note: The injection pressure *did not* creep up at the maximum injection rate of 43 BPM during the 2 1/2 days of the MHF Test (as erroneously stated in some reports) but remained constant at about 7000 psi.

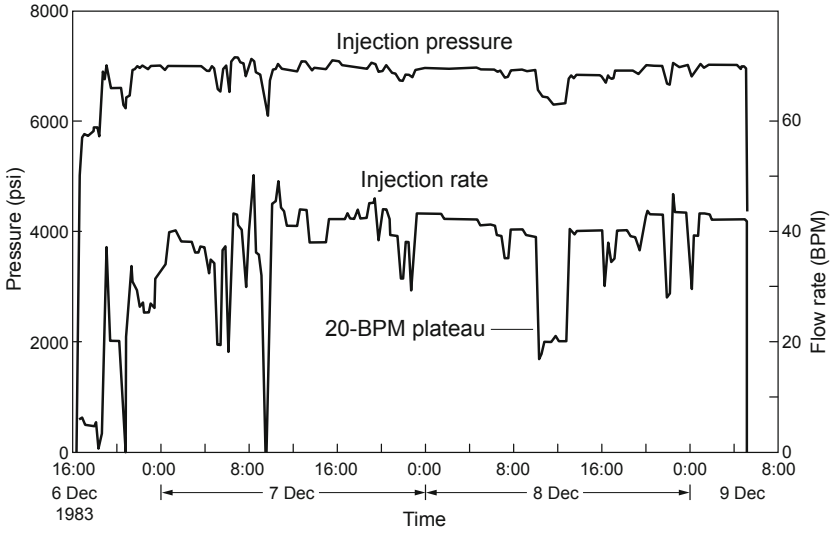

Fig. 6-21. The surface injection-rate and injection-pressure profiles during the 2 1/2 days of the MHF Test in EE-2.
Source: Dreesen and Nicholson, 1985

The brief (2 1/2-h) injection-rate plateau at 20 BPM on December 8 reflects what would have been seen throughout the MHF Test had it been conducted at this originally planned rate (had the DOE-appointed outside advisors not prevailed). From 10:30 to 13:00 on December 8, *without* the use of any friction reducer, the injection pressure averaged about 6300 psi, about 800 psi above the joint-opening pressure of 5500 psi measured during the Pre-Pump Test. The only measurement of the joint-extension pressure during the MHF Test itself was done about 2 hours after the test began; at that point, at the end of the 5-BPM injection (Fig. 6-21), the measured value was 5770 psi—close

to the 5500-psi value (but somewhat elevated because the 2 hours of low-flow injection would not have allowed for adequate cooldown).

The 61-hour pumping period saw nine failures of high-pressure pumps, of which two were caused by washouts of heads, one by loss of a power end, one by a broken tie rod, and one by a blown-out pump plunger. These failures resulted in an estimated 190 hours of downtime of individual pumping units. Routine maintenance, service, and minor repairs accounted for another 56 hours of pump downtime.

Many of the pump failures occurred when the pumps were being operated at rates *exceeding* those recommended for long-term, continuous operation or for keeping discharge pulsation at a minimum. For the first 18 hours pulsation was minimal; over the next 16 hours it increased intermittently and after that occasionally became severe. For the last 26 hours it was kept at moderate levels for the most part, by modifying the pumping rate or changing out pumping units. But discharge pulsation *was* the eventual cause of a flange failure at the frac head and the blow-out that followed.

A Blow-out at the Frac Head

The MHF Test came to an abrupt end at 5:10 on the morning of December 9, when vibration-induced metal fatigue caused one of the two threaded companion flanges[18] on the lower cross of the frac head to fail, leading to a catastrophic blow-out of the very large reservoir. Venting of high-temperature fluid through the 5 1/2-in. frac string reached an estimated rate of 5000 gpm as pieces of rock and cement were being spewed out of the flange in the direction of the backside pump truck. Personnel in that area were forced to abandon their stations. Despite the peril, the rig supervisors—with Bob Nicholson leading the way—were able to get onto the rig floor and close the master valves below the frac head, just three minutes after the blow-out began. The reservoir was thus effectively shut in and the EE-2 borehole was stabilized—for the moment. (The maintenance of this "under-control" shut-in condition for the next several months, to enable multiple studies of the reservoir, would have been very desirable; unfortunately, that would not be the case.)

Still No Connection to EE-3

At the time of the blow-out, a total of 5.6 million gal. (21 000 m^3) of water had been pumped into the one joint connection with the 70-ft open-hole interval of EE-2—probably the largest-volume high-pressure injection ever carried out in North America.[19] Previous experiments at Fenton Hill having been limited by mechanical failures, injection volumes had never exceeded 1.3 million gal.

---

[18]These companion flanges had been supplied by the Laboratory.

[19]Even if the blow-out had not occurred, the MHF Test would have come to an end within a few more hours, because the on-site water supply had been nearly depleted by the massive injection.

Despite the massive, high-pressure injection, there was *no* evidence of a flow connection with EE-3. As in the case of Expt. 2025, only later would it become clear that a stress cage similar to the one that surrounded the Expt. 2020 reservoir—but much larger and more pervasive—was developing in the hyper-compressed rock mass surrounding the MHF Test dilated region. This stress cage continued to grow and extend during the test, isolating the reservoir from the adjacent low-pressure jointed region surrounding EE-3. (All that was noted at the time was that about two-thirds of the way through the MHF Test, large amounts of gas, particularly carbon dioxide, began issuing from EE-3. It was postulated that as the stimulated region continued to pressure-dilate—and thereby volumetrically expand—it progressively compressed the region adjacent to EE-3, "squeezing" out some of the gas-laden fluid filling the EE-3 joints opened during Expt. 2025.) Following the MHF Test vent-down, the stress cage was reduced but still present, maintained by residual fluid pressurization and the additional dilation resulting from the propping-open of a number of joints by pressure-spalled rock fragments.

Pressure Spallation of Joint Surfaces from Rapid Venting

Following the 3-minute blow-out, the rig floor was covered to a depth of 4–6 inches with a layer of fine calcite (remnants of the diverting agent[20]) mixed with and overlain by chunks of the casing cement and fragments of rock.

The ejected rock fragments were typically thin in one dimension, and most appeared to have come from the surfaces of joints opened near the injection interval (which would have been highly thermally dilated during the 61 hours of cold-water injection and would not have reclosed quickly—allowing time for the ejection of some fragments into and up the frac string). Other fragments would have been trapped within the closing joints as the rapid venting drastically reduced the pressure in the borehole—becoming in effect "spallation propping" and holding open the critical near-borehole joints that exhibit such an inordinate influence on the reservoir flow impedance (and, thereby, productivity).

Studies by George Cocks (reported in Murphy, 1984) found that the surfaces of the rock fragments were "freshly fractured and rather angular." Further, Cocks reported that of the 50 rock fragments he examined, only 6 appear to have come from the surface of the borehole. It is postulated that the pressure "soaking" of the joint surfaces for 61 hours of high-pressure injection allowed fluid to permeate several millimeters into the very low permeability rock matrix adjacent to the joint surfaces—creating a region of high pressure within the interconnected microcrack fabric. When the blow-out caused a sudden release of the fluid pressure in the joints, the trapped

[20]The anecdotal evidence suggests that the calcite diverting agent, rather than selectively plugging the smaller joints, actually "gummed up the works" in general. It was one of numerous techniques adopted from the oil industry that proved to be a complete failure (nevertheless, a diverting agent would be used again later).

fluid in these adjacent high-pressure regions (especially in microcracks aligned with the joint surfaces) would have induced pressure spallation of these surfaces, akin to thermal spallation.

InfoNote

The 61-hour MHF Test represents only one "cycle" of a potential multiple-cycle "treatment" that could be implemented routinely to increase reservoir productivity. After a significant period of time for "pressure-soaking" of the joint surfaces, pressure spallation would be induced by very rapidly venting high-pressure fluid from the reservoir through the cooled near-borehole region surrounding the injection interval. The rock spalls thus produced, by "propping" the joints open, would reduce the near-wellbore outlet impedance of the production wells in a new (or reactivated Fenton Hill) HDR system, thereby increasing reservoir productivity. With reservoir productivity remaining the principal issue to be addressed in a commercial demonstration of HDR, pressure-spallation propping offers a heretofore unrecognized technique. Its effectiveness would be verified in April 1985, before the Initial Closed-Loop Flow Test (ICFT): during Expt. 2052 (reservoir inflation and injection testing of EE-2), the low-pressure injection impedance would show a significant decrease from the equivalent impedance indicated before the MHF Test (see Fig. 6-18).

Collapse of the Casing

During the 3-minute blow-out, the pressure in the inner annulus (between the frac string and the 9 5/8-in. casing)[21] increased from 2200 to 2650 psi. After the master valves had been closed, continued heating of this shut-in annulus by the hot fluid filling the frac string caused the pressure to keep rising, but the now tired crew in the control bus failed to notice. The Laboratory staff person in the DAT charged with monitoring the annulus pressure was also "asleep at the switch": unaware of the rapidly rising pressure, he did not instruct the crew that had been forced to abandon the backside pump to return to the area once the master valves were closed, to blow down the annulus to 2000 psi. (A relief valve had been installed on the backside line, but it either failed to open or opened insufficiently to accommodate the flow.) Three minutes after closure of the master valves, the annulus pressure—now at 3200 psi—burst the safety rupture disk on the annulus vent line at the wellhead. The sudden release of the pressure in the annulus allowed the hot fluid within it to rapidly boil and "geyser," in turn causing the pressure to drop precipitously (to a final value of less than 200 psi absolute).

[21]This annulus, outside the pressurization string, is commonly called the "backside." For clarity, in EE-2 it is henceforward referred to as the "inner annulus" because following the blow-out, the annulus outside the 9 5/8-in. production casing ("outer annulus") also became a factor as it began venting at the surface.

The pressure differential created between the high-pressure, dilated region surrounding EE-2 and the now very low pressure, steam-filled annulus is estimated to have reached as high as 9000 psi. It was enough to dislodge the steam packer and push it upward about 9 ft, until it engaged the lugs on the no-go sub (Fig. 6-17). At the same time, the pressure differential between the 9 5/8-in. casing and the annulus (the outer surface of the casing was effectively pressurized to over 5000 psi by several dilated joints obliquely intersecting the borehole) caused the casing to collapse onto the frac string in at least two places. It would be found later, during an assessment of the damage to the borehole (mainly Expt. 2036), that the frac string had been severely indented by the collapsed sections of casing and was clamped inside the casing at depths of 10 740 ft and 10 900 ft.

Multiple-Path Venting of the Reservoir

After the rupture disk had burst and relieved the pressure in the inner annulus, the boiling and geysering in this confined space should have slowly tailed off with no other consequences. Instead, the annulus outflow *continued to increase*. This outflow—obviously from the pressurized reservoir—was being channeled into the annulus through splits in the collapsed casing.

The crew first rerouted the annular flow through the rig's choke manifold, allowing the reservoir to continue venting via this secondary flow path. Then, to enable the shut-in frac string to vent to the choke manifold as the primary flow path, they replaced the broken companion flange with an intact one from the upper cross of the frac head, closed the isolation valve between the upper and lower crosses, reopened the master valves below the frac head, and began a controlled vent-down of the reservoir through the frac string.

Just as the master valves were reopened and reservoir vent flow from the frac string started through the choke manifold, thermal expansion caused the frac string to begin rising through the blow-out-preventer stack. As the frac string continued to rise, one of the chains attached to the derrick legs to stabilize the frac head broke and the remaining chain was bending the very stout, 5-in. landing joint to the side. (The frac string would eventually rise a full 5 ft above the rig floor, confirming that the steam packer had been displaced upwards—taking up the entire 9-ft thermal expansion allowance—and had engaged the lugs on the no-go sub.) Fearing that the landing joint would burst, the rig crew increased the flow through the frac string in an attempt to rapidly reduce the surface venting pressure, now at about 5000 psi. The ensuing high-rate vent-down of the MHF Test stimulated region continued for 36 hours. The replumbing to channel flow from both the frac string and the inner annulus through the choke manifold kept the blow-out under control, but during this period the surface temperature of the vented water rose as high as 227°C.

The replumbing work had scarcely been completed when a new complication arose: the outer annulus—above the 11 578- to 10 620-ft region of tag-cemented 9 5/8-in. casing—was now venting as well. Overpressure had caused the rupture disk protecting this annulus to burst. (It would later be determined that a frac-around of the tag cement, by flow from one or more joints connected to the high-pressure reservoir, was responsible for the overpressure.) Not only was the reservoir venting what appeared to be steam via this third path, but reservoir vent-back was also flowing from the outer annulus into the Phase I reservoir, through splits in the 13 3/8-in. casing, and recharging that low-pressure region. Although not specifically mentioned above, this frac-around in fact represented the failure of the tag cement used in the EE-2 completion. It is estimated that before it was all over, more than half the water that had been injected during the MHF Test was vented back.

Analysis of Seismic Data

A superb seismic data set was obtained from the MHF Test, which would be analyzed and re-analyzed over the following years. These data would be used for determining, first, the orientation and extent of the pressure-stimulated region (perhaps the most important information provided by the MHF Test was that a very large pressure-stimulated region of jointed basement rock was clearly delineated by the boundaries of a "cloud" of microseismic activity) and, later, the orientations of some of the joints stimulated within that region. The multiple applications of such data highlights the great importance of seismic interrogation of HDR reservoirs—destined to be the operator's "eyes and ears" for the development of future HDR reservoirs—and the need for further development of this critical diagnostic tool.

InfoNote

In the not-so-distant future, microseismic data from a modest initial stimulation (recorded both by near-surface geophones and by a triaxial geophone at the bottom of the injection borehole) will be used to preliminarily determine the orientation of the reservoir. On the basis of that orientation, surface locations for the two production boreholes will be established, and the boreholes will be drilled to appropriate positions—one above each end of the elongated initial reservoir. A geophone package will then be placed at the bottom of each production borehole, and a much larger reservoir stimulation will be carried out. The seismic data recorded will guide "mid-course" corrections to the drilling trajectories for best accessing the two ends of the final reservoir.

Seismic monitoring of the MHF Test began shortly after the start of injection and continued for about 84 hours. Because the region being pressure-stimulated initially was the same as the Expt. 2020 stimulated region, it was essentially aseismic for about the first 10 hours, reflecting reinflation. Then, as the envelope of the Expt. 2020 dilated region started to expand, the level of microseismicity began to increase rapidly.

Although the growth of the MHF Test stimulated region was followed in real time, through application of the hodogram method to the triaxial signals received at the geophone installed in EE-1, this approach was abandoned after the MHF Test and would never be used again. It was replaced by a methodology whereby the inversion of the arrival times (P- and/or S-wave) at the two Precambrian Network stations and the three deep geophone stations (see Figs 6-16 and 6-20) was used to accurately locate the individual microseismic events generated during the MHF Test. In addition, the surface network of nine 1-Hz, vertical-component geophones received a very sparse set of large seismic signals (large enough to reach the surface with sufficient resolution on at least one station). Only about 10% of the most energetic of these signals were used for fault-plane solutions and to ascertain displacement directions for these larger events. Digital data from the downhole geophones represented about 1800 seismic events. All of the data were recorded on analog magnetic tape (15-ips Ampex tape recorders). Seismic ray paths to the downhole geophones in EE-1, EE-3, GT-1, and GT-2 were entirely within the basement rock and were assumed to be straight. In contrast, ray paths to the surface stations and, to a lesser extent, to the more distant borehole instrument located in PC-1, were distorted by the lower-seismic-velocity sedimentary and volcanic rocks that overlie the Precambrian surface. Arrival times were picked from digital seismograms with a precision of 1 ms, which implies an optimal spatial resolution of 6–10 m.

The seismic velocities used—5.92 km/s for P and 3.50 km/s for S—were obtained from detonator calibration experiments. Slight variations from assumed constant velocities were compensated for through station corrections, obtained from detonator calibration experiments and from a suite of well-recorded events within the pressure-stimulated region. The fact that individual station corrections amount to only a few percent of the travel times to the stations supports the constant-velocity assumption. The only exception was the outlying downhole station PC-1; its position some 200 m above the granite, in a sedimentary formation, was responsible for considerable delays in both P and S arrival times relative to the constant velocity, which necessitated corrections as large as 10%.

Of the 1800 events recorded during the MHF Test, 844 were located and digitized with computed spatial errors of less than 50 m (the precision of relative locations is estimated to be 10–20 m and that of absolute locations 50–100 m). This subset of recorded MHF Test seismicity is shown in Fig. 6-22. The magnitudes of these events ranged from –3 to 0 on the expanded Richter Scale.

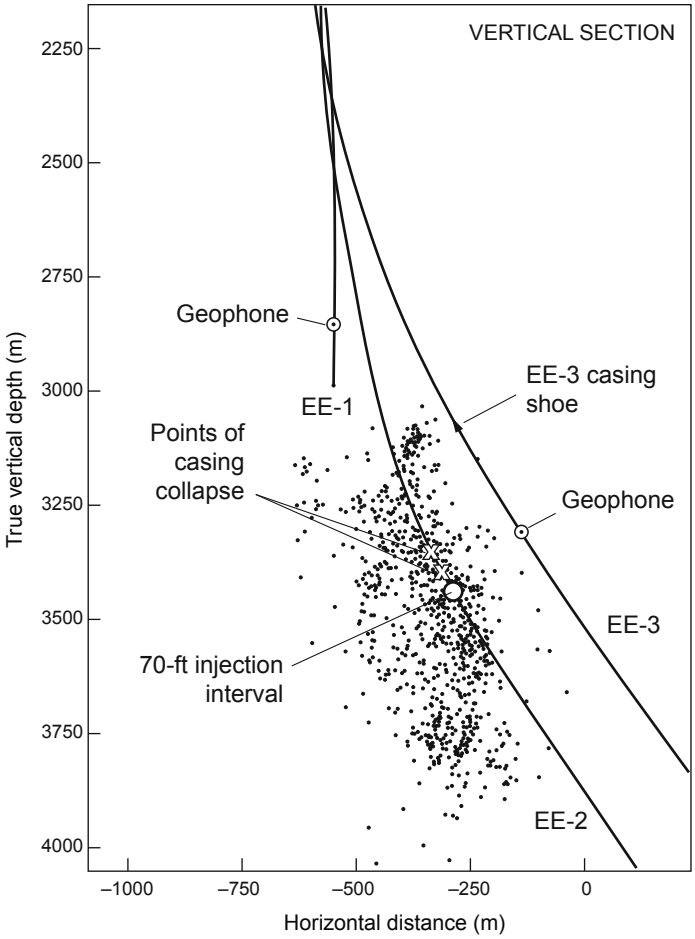

Fig. 6-22. A vertical view of the 844 microseismic events having spatial errors of less than 50 m, plotted on a N70E cross section. The close proximity of this "cloud" of events to the deep geophones in EE-1 and EE-3 is evident. Also shown is the 70-ft injection interval in EE-2 (bounded at the top by the casing shoe and at the bottom by the sand plug).
Source: HDR Project data archives

The most pronounced feature of this figure is a large, seismically active region surrounding EE-2. In striking contrast to the short injection interval, the seismicity extends upward along the borehole for at least 500 m—above the top of the tag cement, to a vertical depth of about 3100 m (corresponding to a slant depth of 10 200 ft). A second notable feature is the almost total lack of seismicity around the target borehole, EE-3. Finally, the downward extension of the seismic region, to more than 300 m below the top of the

sand plug, demonstrates the futility of using sand plugs to control the growth of a reservoir region consisting of multiple interconnected joints.

The known points of casing collapse indicated in the figure are at slant depths of 10 740 ft and 10 900 ft (there may have been others as well). Because both of these points are well within the microseismic cloud, it is probable that these collapses were due to the pressure exerted on the casing by highly pressurized open joints intersecting the borehole at these depths.

Observation: If these open joints could have been produced at the surface via the inner annulus, the Phase II reservoir could have been completed in a counter-flow configuration, through EE-2 alone. A one-well HDR production concept of this type—employing insulated injection casing—was written into the original HDR patent by Don Brown (Potter et al., 1974); however, a disastrous confirmation of that idea, as provided by the MHF Test, was hardly foreseen!

Figure 6-23 shows the seismic activity recorded during the injection phase of the MHF Test, in three orthogonal views. Because there were so many well-located microseismic events, the shape of the microseismic cloud is most clearly depicted by density plots of these events, in 10-m^3 blocks. Particularly in the (c) view (toward the west), the cloud appears to contain "pockets" of seismic activity.

The three views of the MHF Test stimulated region shown in this figure confirm that the MHF Test expanded the envelope of the Expt. 2020 seismic volume. As seen in the plan view (a) of Fig. 6-23, the seismic events recorded during the MHF Test most definitely do not exhibit a simple planar distribution. They form a roughly ellipsoidal volume dipping 70° to the east and extending about 900 m in the N16W direction, with an inclined height of about 800 m and an average thickness of about 200 m. Given the spatial accuracy of 10–20 m for the microseismic events, this thickness is obviously not an artifact of imprecision in the event locations. The vertical W–E section view (b) and the S–N section view (c) show the extent—about 800 m vertically and 900 m horizontally—to which activity and, presumably, pressure-opened joints, spread nearly symmetrically away from the injection interval.

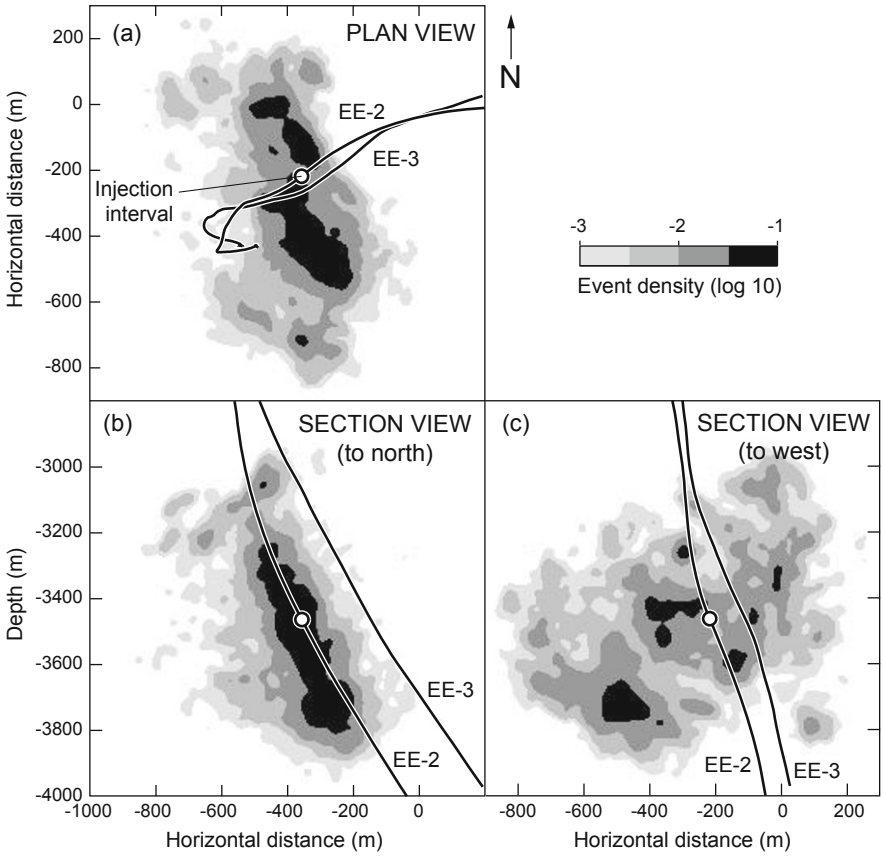

Fig. 6-23. Density plots of microearthquakes detected by downhole seismic instruments during the injection phase of the MHF Test: (a) plan view; (b) west–east vertical cross section viewed toward the north; and (c) south–north vertical cross section viewed toward the west. The depth axes are relative to the ground surface, and the distance axes relative to a site survey reference point. The open circle represents the short injection interval in EE-2.
Source: Scott Phillips, EES Division, Los Alamos National Laboratory (2008)

The Volumetric Nature of HDR Reservoirs

The seismic cloud associated with the MHF Test appears to have expanded rather monotonically. As a means of quantifying its growth, the seismic volume was computed at four times over the course of the test. The results of these computations, made by Bob Potter, are shown in Fig. 6-24. This plot clearly shows that the reservoir created during the MHF Test was volumetric in nature and *not* composed of a few parallel linear features (as

postulated by some). It also shows that the seismic volume of the reservoir is directly proportional to the amount of water injected. From this observation, one can draw a very important inference: To create even larger HDR reservoirs, one need only pump at high pressure for longer periods of time.

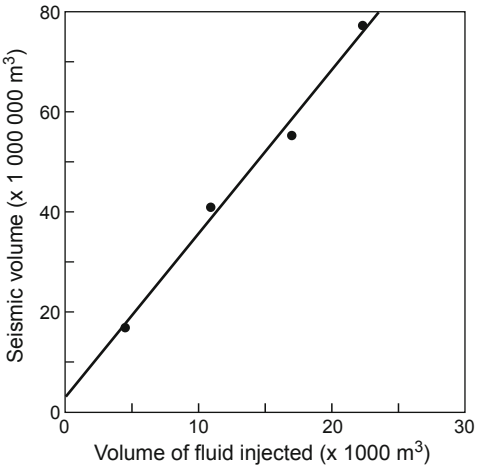

Fig. 6-24. Linear relationship between the seismic volume of the reservoir and the volume of injected fluid, as determined from microseismic event location data during the MHF Test.
Source: Brown, 1995b

Fault-Plane Solutions

During the MHF Test, over 700 microseismic events were recorded at one or more of the nine surface stations and simultaneously on the two downhole Precambrian Network stations. A small subset of these events—those energetic enough to be recorded on all nine surface stations—were used to study focal mechanisms (the Precambrian Network signals were not used).

The first motions of all 69 of these events show both compressions and dilatations, and although their patterns exhibit great diversity, all are consistent with shear-slip fault-plane solutions. Only 26 of the 69 events (those with magnitudes close to zero on the Richter Scale) provided enough first-motion data for well-constrained fault-plane solutions to be calculated (by means of the maximum likelihood method of Dillinger et al., 1972). Nineteen of those solutions correspond to one or the other of the two typical solutions shown in Fig. 6-25. The difference between the two is traceable entirely to the change in sign of the first motion at a single station (which, in Fig. 6-25, lies in the southeast quadrant of each solution).

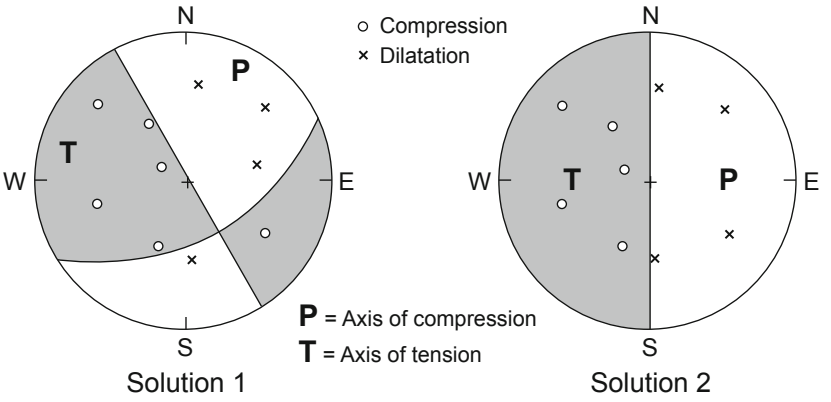

Fig. 6-25. Composite fault-plane solutions (lower-hemisphere, equal-area projections).
Source: House et al., 1985

The two solutions have in common a near-vertical nodal plane that strikes almost north–south. Recall that the strike of the seismic cloud produced during injection was N16W (Fig. 6-23a) and the dip about 70° east (Fig. 6-23b). This nodal plane is subparallel to the orientation of the seismic cloud, which suggests that it may be a dominant fault plane of the microearthquakes and that the earthquake fault surfaces may be *en echelon*. In addition, for both solutions in Fig. 6-25 the T axis trends roughly east–west and is in reasonable accord with the regional stress observations of Aldrich and Laughlin (1984). Cash et al. (1983), having obtained fault-plane solutions nearly identical to these on the basis of data from two experiments spatially separated by about 1000 m, proposed that the dramatic difference in slip direction between the two solutions might be attributable to spatial differences in the stresses associated with the nearby Valles Caldera complex. This explanation cannot be called upon to account for the difference in the fault-plane solutions for the MHF Test, however, because the events on which the latter are based were not spatially separated.

Intuition vs Geophysics: A Critical Reassessment of the MHF Test Seismic Analyses

Mike Fehler, using his "three-point-method"[22] and a statistical analysis of the results, identified the "predominant" joint sets stimulated during the injection phase of the MHF Test (Fehler, 1989). These are shown in Table 6-2.

[22]This method was based on his assertion that any three microseismic events define a plane in space (Fehler, 1984).

Table 6-2. Planes of the predominant joints identified via the three-point method (all angles in degrees)

Average depth (m)	Strike	Dip	Number of events
3383	N31W	74E	130
3738	N90E	27N	35
3165	N29W	67W	50
3548	N7E	67E	81
3594	N29E	60W	28

For the joints to have been "identified" through analysis of the microseismic data set implies that each group of three events consisted of well-located events (that is, having not only a very pronounced S-wave arrival, but also a distinguishable P-wave arrival). The question, however, is—does location of the joints whose orientations are most favorable for shear displacement add to our insight regarding the fluid connectivity throughout the stimulated region? Unfortunately, in the case of the Phase II reservoir, the answer is no. The joints that control fluid connectivity across this stimulated region are the continuous, manifolding joints—as revealed by the flow behavior of the reservoir. This set of principal joints truncates all lower-opening-pressure joints. The seismic data, in combination with previous test data, provide some clues regarding the orientation of these principal joints:

1. The trace of the seismic cloud in plan view (Fig. 6-23a) shows that these joints must have a strike of about N16W.
2. The well-measured reservoir joint-opening pressure of 5500 psi (e.g., from the MHF Pre-Pump Test) indicates that these joints would have a dip of about 45° to the east.[23]

That no north-striking, 45°-east-dipping planes were located by the three-point method raises questions about the suitability of this approach for determining the significant joint structures within a pressure-dilated region such as the Phase II reservoir. However, a re-analysis of the MHF Test data set by Roff et al. (1996), using a clustering technique and waveform amplitude ratios, does reveal several joints with an eastward dip close to 45°. What is certain, then, is that the science of HDR seismology is still evolving. (Most of the DOE funding for this effort at Los Alamos was stopped in the late 1980s.)

[23]This 45° eastward dip obtains if one bases the calculation on a vertical stress of 8300 psi (above hydrostatic) at a depth of 12 000 ft and an associated horizontal stress of about 1400 psi. The contravening solution, a 45° dip to the west, is precluded because it would have guaranteed flow connections to EE-3—as can be seen from the vertical trace of the borehole positions shown in Fig. 6-22.

Deficit in Seismic Moment

Fehler and Phillips (1991) note that the total moment of all events recorded by the surface seismic network was only 0.1% of that expected (on the basis of McGarr's [1976] work relating seismic moment to the volume of fluid injected). Fehler concludes that even with a computational margin of error underestimating the seismic moment by a factor of 10, the level of seismicity accompanying the MHF Test was still very low. Therefore, at least 99% of the injected volume must have been accommodated by *aseismic tensile fracturing*. From the seismic perspective, aseismic tensile fracturing would imply the pressure-opening of a set of joints within the MHF Test stimulated region that were oriented approximately orthogonal to the direction of the least principal earth stress. These joints would therefore be the lowest-opening-pressure joints in the stimulated region, would be hyper-inflated at the reservoir extension pressure of about 5500 psi, and would account for a large fraction of the water storage.

MHF Test "Post-Mortem"

The huge volume of fluid that was injected during the MHF Test and the number and distribution of seismic events indicate that a very large system was created; the amount of return fluid and the rate of return indicate that this system was tightly sealed at the boundaries and well connected; and the high rate of energy production during the rapid vent indicated that heat could be extracted efficiently from the jointed reservoir rock. Unfortunately, because of specific mistakes made in its execution, the MHF Test not only failed to exploit the potential of this expanded reservoir region, but it set the entire Project back greatly. Upon reflection, *any one* of the following actions could have spelled success for the MHF Test and protected the very valuable EE-2 borehole.

- Despite pressure to get the test under way quickly, time should have been taken to rework the control packer and install it below the Otis steam packer.
- The scientist assigned to monitor the pressure in the inner annulus should have been alert enough to notice the sudden rise in the annulus pressure. Quick action to lower it would at least have averted the collapse of the casing.
- The team assigned to the backside pump truck should have returned to their stations following the blow-out, once the master valves had been closed and the frac string shut in. (If the inner annulus had been vented down to 2000 psi, the casing would not have collapsed.)
- The injection rate should have been limited to 20 BPM, which would have markedly reduced the pump-driven vibrations at the frac head and probably would have prevented the blow-out. It would also have lengthened the test, allowing for more efficient rotation of the crews and improving their ability to cope with unforeseen events.

- The test should have been halted after the injection of 4 million gal. (by that point it should have been evident that no amount of injected water would achieve a connection).

The Condition of EE-2: Preliminary Investigations

Immediately following the MHF Test, all that was known with certainty was that the stimulated region had vented via three distinct flow paths: the inner annulus, the frac string, and the outer annulus (between the 9 5/8-in. casing and either the 13 3/8-in. casing or—below the latter casing—the borehole wall). It appeared that a mixture of steam and water had been vented through the first two of these paths, and dry steam through the third. It should be noted that the venting of the reservoir via this third path gave rise to some confusion: even though there had been a previous instance of such bypass flow (around the 292 ft of cemented-in liner deep in EE-2, which developed during Expt. 2012 in June 1982), the frac-around of nearly 1000 ft of cement was surprisingly long. Originating from the injection interval below the casing shoe at 11 578 ft, the flow must have traveled through a network of pressure-dilated joints within the reservoir and eventually into the outer annulus above the top of the cement at 10 620 ft.[24]

In addition, a change in the venting behavior of the Phase I reservoir was observed about this time: before the MHF Test, the Phase I wellbores had been inactive, with subhydrostatic water levels between 900 and 1800 ft; following the test, GT-2 began producing water at a rate of 1–2 gpm and EE-1 began producing large quantities of gas mixed with water. This change indicated that this upper reservoir was being recharged by high-pressure fluid vented through the outer annulus during the blow-out and subsequent vent-down, most probably via a joint entrance opened from the EE-2 borehole.

On December 15, with the reservoir vent-down essentially over, the draw works and rig pumps were used for a series of tests to assess the condition of the EE-2 borehole. The findings may be summarized as follows:

1. The frac string was stuck in the borehole at an overpull of up to 70 000 lb. The depth at which it was stuck, based on a rough calculation from pipe stretch vs. load (uncorrected for temperature), was in the vicinity of 10 300 ft.
2. After 10 hours of pumping at a rate of 6 BPM (a total of ~150 000 gal.), the rig pumps were able to pressurize the inner annulus to only 2000–2200 psi. No pumping-related flow returns up the frac string were

[24] As described in Chapter 5, the Project managers, in their desire to complete EE-2 quickly and to save money, abandoned the elaborately designed cementing plan for the 9 5/8-in. production casing at the last minute and instead tag-cemented only the bottom 1000 ft. As shown in Fig. 5-4, the actual tag-cemented length of casing was only about 960 ft—adequate in the minds of those who thought the Phase II reservoir would be developed with a set of essentially vertical "hydraulic fractures."

observed (confirmed by a fluorescein-dye tracer test), which indicated *no* flow communication between this annulus and the frac string. However, both the inner annulus and frac string were in good communication with the MHF Test stimulated region.

3. After 3 hours of pumping at a rate of 3 1/2 BPM (a total of 26 000 gal.), the frac string could be pressurized to only about 1500 psi, with no flow returns up the annulus.

4. A run with a Homco sinker-bar/collar-locator tool having a 1 7/8-in. outer diameter showed that the frac string was open to a depth of at least 11 300 ft, i.e., nearly to its lower end, and well below the known points of collapse. No attempt was made to log below the frac string with the Homco tool (because of the danger involved with bringing the tool back up from the casing into the smaller-diameter frac string above); but it was apparent—and would later be confirmed by injection pumping—that the borehole was open all the way into the reservoir, and therefore that the reservoir could be repressurized via the frac string.

The pressurization behavior showed that (a) both the frac string and the inner annulus were "pressure-tight"; and (b) both were in direct flow communication with the high-pressure reservoir—the frac string via the short (70-ft) injection interval below the casing shoe, and the annulus via splits in the collapsed 9 5/8-in. casing (that is, flow was coming directly from the high-pressure reservoir, via the joints intersecting the outer annulus[25] at 10 740 and 10 900 ft, thence into the inner annulus through the splits in the casing).

This reservoir reinflation behavior is significantly different from that observed during the MHF Pre-Pump Test (Fig. 6-18), when a pressure of nearly 5000 psi was required to pump into the Expt. 2020 reservoir at only 2 BPM. The long period of pressure "soaking" during the MHF Test (61 hours), followed by the very rapid vent-down, had drastically altered the injection flow characteristics—in ways that were not yet understood.

The Condition of EE-2: Further Investigations (Expt. 2036)

The next few weeks were spent trying to understand what had occurred at the end of the MHF Test, and further assessing the damage to the borehole. Experiment 2036, carried out from January 17 to 21, 1984, consisted of several low-pressure injection tests with the rig pumps, through both the inner annulus and the frac string (Brown et al., 1984). The January 19 injection test (through the annulus) reinflated the MHF Test stimulated region; Figure 6-26 shows the last two pumping sessions of that test, plotted against the natural log of elapsed time. Like that observed a month earlier, this reinflation behavior is significantly different from that of the Pre-Pump Test (Fig. 6-18).

[25]Because there was cement in this part of the outer annulus, the flow was prevented from traveling up the annulus and out at the surface; the resultant buildup of pressure in this confined space is what led to the collapse of the casing.

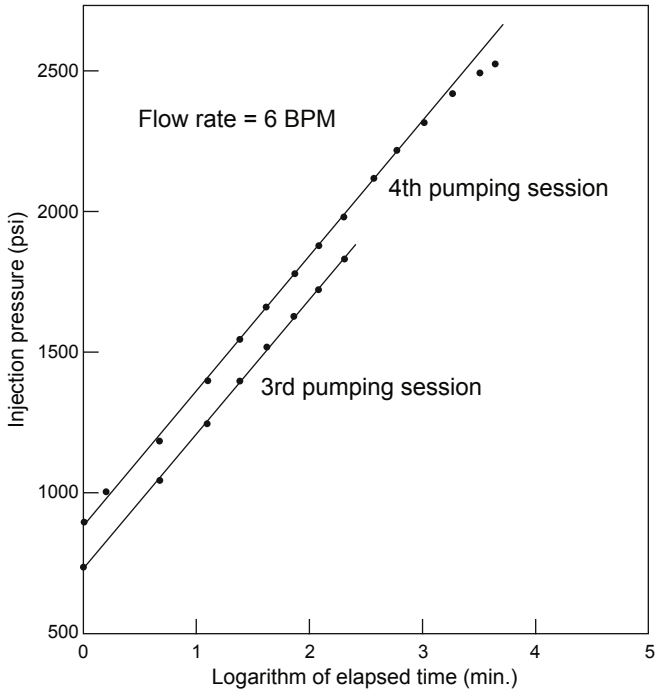

Fig. 6-26. Expt. 2036: Reinflation, through the inner annulus, of the MHF Test stimulated region (January 19, 1984).
Source: HDR Project data archives

It appeared that the region being reinflated—the collapsed network of flow paths that remained after the complete vent-down following the MHF Test—was now a highly permeable region; its residual fluid volume, as indicated by the amount of fluid injected at low pressure, was at least 150 000 gal. (2.7% of the 5.6 million gal. originally injected for the MHF Test).

During the annulus injection, logging in the frac string with a slim-line temperature tool—past the location of the Otis steam packer at 11 297 ft—showed that the frac string was open to at least the 2-in. diameter of the tool. The temperature logs confirmed that there were two fluid entrances from the annulus into the reservoir: a minor one at 10 740 ft and a major one at 10 900 ft (Fig. 6-27). Further, injecting into the annulus at up to 2800 psi (see Fig. 6-26) showed that there was no bypass flow around the Otis packer.

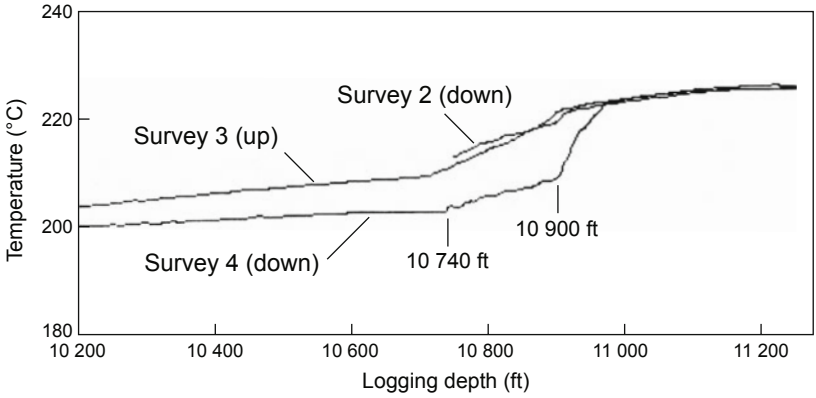

Fig. 6-27. Temperature surveys in EE-2 (January 19, 1984). Depths are as recorded in the logging van.
Source: HDR Project data archives

On January 20, logging was done inside the frac string by Dresser (with their "freepoint" tool) to determine exactly where the pipe was stuck inside the collapsed casing. This log showed that the pipe was free in the borehole to a depth of 9350 ft; at 9400 ft it had 40% movement, and at 10 000 ft no movement. The tentative conclusion was that the 10 000-ft depth represented another point at which the casing had collapsed onto the frac string (earlier calculated as around 10 300 ft). But this could not be confirmed, and in fact a companion temperature log did not show a split in the casing at this depth. It may be that the frac string was simply "corkscrewed" inside the casing and being rigidly held at this spot.

The injection of a radioactive tracer into the inner annulus during Expt. 2036 demonstrated that there were no flow exits through the 9 5/8-in. casing between 1600 ft and 2500 ft, dispelling the notion that over this depth interval the annulus was somehow connected to the low-pressure loss zone above the crystalline basement. In addition, the tracer results showed that the casing was intact down to a depth of 10 500 ft, confirming what had been found earlier: that the inner annulus was not in direct communication with the frac string but only with the high-pressure reservoir, via splits in the casing adjacent to the joints at 10 740 ft and 10 900 ft (the shallower of these being still 120 ft below 10 620 ft, the top of the cement in the outer annulus). Further, tracer testing showed that the outer annulus was *not* in communication with the inner annulus, confirming that the cement formed an effective seal between the two.

Most interesting, the testing of Expt. 2036 revealed a significant change in the injection impedance of the joint connections to the reservoir. This impedance was much lower than expected, given the considerably higher values seen previously in EE-2 (Expts. 2011, 2012, 2016, 2018, and 2020).

This change—much lower pressures for the same injection rate—signaled that a new phenomenon was being observed. As described earlier, the blow-out that ended the MHF Test had caused pressure spallation of the joint surfaces. Some of the resulting rock fragments became trapped within the joints connecting the borehole to the reservoir, propping them open.[26]

Project Assessment and a Return to EE-3

Given the extensive damage to EE-2 caused by the blow-out at the end of the MHF Test, no further testing of the reservoir through EE-2 was deemed appropriate. In particular, the frac string bore—narrowed by the indentations created by multiple collapses of the surrounding casing—permitted only slimline temperature logging across the upper part of the reservoir (down to about 11 300 ft).

At this juncture, then, the focus of Fenton Hill operations turned to EE-3 as a last hope of achieving a reservoir flow connection between the two boreholes. However, a number of complications beset the plans for renewed injection operations in EE-3:

- The uncertain condition of the cemented-in scab liner in EE-3
- The barely marginal "completion" of EE-3, which left the frac string with a low-pressure connection into the Phase I reservoir region—via the annulus above the scab-liner cement and the low-pressure joint intersecting the borehole at 10 394 ft, just below the 9 5/8-in. casing shoe (at 10 374 ft)
  (In July 1983, after Expt. 2025 and before the drill rig was skidded to EE-2 for the MHF Test, a *temporary* unsealed casing patch had been slipped over the stub-end of the cemented-in, 4 1/2-in. scab liner in EE-3—at about 10 900 ft—and connected to the surface via the 4 1/2-in. frac string. This patch was unnecessary, because any connection to EE-3 could have been produced directly through the casing.)
- The condition of the 9 5/8-in. production casing
  (This final casing string had originally been tensioned to 885 000 lb_f for service as a production casing, under the plan that EE-3 would be the HDR production well. Because of the magnitude of the injection contemplated—2 million gal.—the heated-water technique used for Expt. 2025 would not be feasible; this time the tension on the casing would need to be released.)

[26]The fact that rock fragments from the reservoir were ejected during the blow-out lends credence to this conclusion. Although in the past some geoscientists had asserted that self-propping (resulting from shear slippage along pressure-stimulated joints in an HDR reservoir) would result in significant impedance reduction, such a phenomenon was never observed at Fenton Hill. The data show that self-propping of the joints near the EE-2 injection interval due to shear slippage was minimal. Had there been significant self-propping, an impedance reduction would have been observed following the 844 000-gal. injection of Expt. 2020.

On the positive side, the region stimulated during the MHF Test was somewhat closer to the EE-3 borehole (Fig. 6-23) than the region stimulated during Expt. 2020 (Fig. 6-11). (Unfortunately, at the time the presence of the extensive and very pervasive stress cage surrounding the MHF Test stimulated region was not recognized; this stress cage would prevent any joint interconnection.)

On January 24, the EE-2 wellhead was secured and preparations began to skid the rig back to EE-3.

Further Repairs at EE-3

As summarized at the end of Chapter 5, the completion of EE-3 had been poorly designed. Not only had the 9 5/8-in. casing been set too high, but the well was completed solely as a production well—precluding injection or stimulation of potential deep reservoir regions—a limitation that created ongoing problems when Project plans shifted.

January 31, 1984, saw the start of renewed operations at EE-3. The 4 1/2-in. frac string was pulled and laid down, the drill pipe was picked up, and the PBR, tie-back string, and temporary casing patch were pulled from the hole. Next, casing jacks were used to try to release the high level of tension on the 9 5/8-in. production casing. But the attempt had to be aborted when the jacks failed, leading to a 5-week furlough of the drill rig. The rig was reactivated on March 14, with the arrival of repaired casing jacks and a Dowell pump truck to pressurize them.

Three attempts were made to grapple and then lift the casing, with the aid of various inside spears. After much effort and a number of tool failures, a Tri-State spear finally worked and the 885 000 lb_f of casing tension was released. (Even with the tension fully released, the casing was expected to exceed its rated minimum yield stress at full injection cooldown. But because the casing was supported by cement, the risk of a catastrophic failure was considered to be minimal: the yield stress would be distributed, and therefore the rated elongation of the steel would not be exceeded.) Then, with a back-off shot, the top ±100 ft of casing was removed from the hole. New casing was screwed into the top section of remaining casing and torqued to 13 000 ft-lb.

The Otis high-temperature outside casing patch that had been ordered was now on hand, and on March 19 it was attached to a length of 5 1/2-in. tie-back string with a PBR on top and run in on drill pipe. But the connection made to the top of the 4 1/2-in. scab-liner stub leaked upon pressure testing. (Note: No attempt was made to repair or replace the Otis casing patch, even though an adequate patch would have saved the next four weeks of effort.) With an adequate connection to the scab liner essential for high-pressure injection at EE-3, a highly convoluted composite connection was finally patched together. It included a 4 1/2-in. Otis casing packer set *inside* the scab liner and attached to the tie-back string by a length of 2 7/8-in. tubing; a floating

internal/external seal mandrel; and a 4 1/4-in. PBR above the seal mandrel.[27] The Brinkerhoff-Signal rig No. 78 was furloughed on April 19, and by May 4 had been dismantled and removed from Fenton Hill.

Experiment 2042

This injection test in EE-3, which would be considerably larger than Expt. 2025 (but at only one-third the injection rate) had a twofold objective: to effect a connection with the MHF Test stimulated region, and to further investigate the seismic characteristics of the extended joint system initially created below the cemented-in liner during Expt. 2025. It was scheduled to begin on May 15, 1984, and to last about four days. The injection zone would be the same as that of Expt. 2025: the open-hole interval between the liner shoe at 11 389 ft and the sand plug at 11 770 ft.

Attempting a Connection

The rate of flow for this injection test would be limited to 10 BPM (rather than the 20 BPM used during Expt. 2025), mainly because of the complexity of the final connection to the scab liner in EE-3, which restricted the flow path. In addition, by this time it had finally been recognized that the injection *rate* affected only the *rate of growth* of the stimulated region and had very little to do with joint dilation and, thus, with the potential for achieving a flow connection. On the basis of previous experience, the injection pressure at 10 BPM was estimated to be 6000 psi, about 500 psi above the joint-opening pressure of 5500 psi.

The 4 1/2-in. frac string was run back in, inserted into the PBR on top of the rebuilt and reconfigured scab liner assembly, and pressure-tested. Then a wellhead having a working pressure of 10 000 psi was installed on the top of the frac string, and two 3-in., 15 000-psi lines were run from the cross on the wellhead to a single 3-in. injection line at ground level. To this line were connected four high-pressure (3000-hydraulic-horsepower) triplex pumps, each supplied by a single 4-in. suction hose. Three Los Alamos vent-down lines were installed: one from one side of the cross, one from the inner annulus, and one from the annulus outside the 9 5/8-in. casing. These lines were tied via a choke manifold into a 10-in. gas-venting system.

The suction system consisted of two 100-bbl tanks supplying a blender that discharged into the four suction hoses and then through turbine meters connected to a 7-in. common manifold. The suction tanks were kept full, and backside Kobe pumps were installed to maintain the inner annulus at 1000 psi.

---

[27]The authors' attempt to reconstruct the twists and turns of this workover effort from the daily drilling reports, 25 years after the fact, was an exercise in futility. (The later temporary completion of the borehole, in preparation for Expt. 2042, would be equally convoluted—as may be verified by even a cursory look at Fig. 1 of Dash et al., 1984.)

Injection began on May 15, and as shown in Fig. 6-28, the rate quickly reached 8 BPM at a pressure of about 6000 psi (40 MPa). It soon became apparent that there was a significant frac-around flow connection from below the liner to the annulus above, but at a low rate relative to the injection rate. From the confined annulus, this bypass flow entered the low-pressure joint connection below the casing shoe and then made its way into the Phase I reservoir region, maintaining the annulus pressure at between 1400 and 1700 psi during Expt. 2042. By reducing the differential pressure across the complicated connection to the liner, the frac-around flow eliminated the need for the backside pumps to pressurize the annulus. The rate of this liner bypass flow was never measured (which would have required venting of the annulus at the surface).

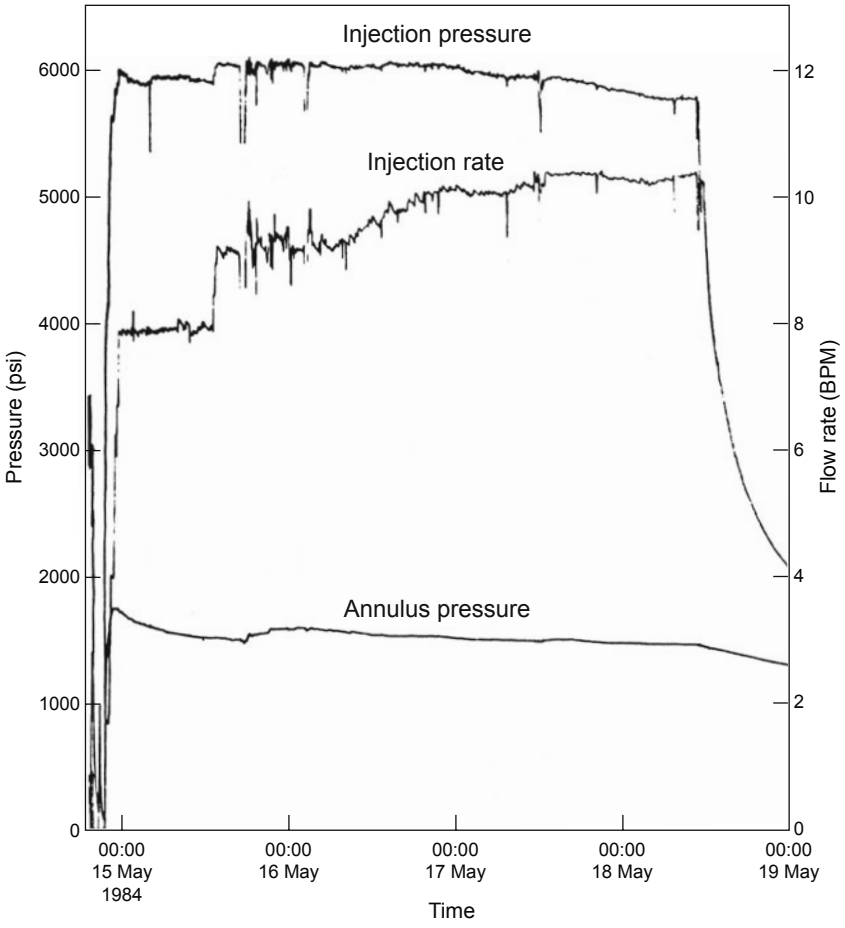

Fig. 6-28. Pressure and flow-rate history for Expt. 2042 in EE-3.
Source: Dash et al., 1985b

Over the next few days, the 6000-psi pressure was held relatively constant while the injection rate was gradually increased. Near the end of the experiment, the injection flow finally reached the planned rate of 10 BPM (420 gpm or 26.5 L/s). Very little can be concluded from this behavior given the continuing bypass flow—at an unknown and probably varying rate.

Unfortunately, Expt. 2042 is notable because of the important parameters that were *not* measured:

- What was the steady-state joint-extension pressure in the stimulated region?
- What portion of the injection flow went into the reservoir, and what portion went via the liner bypass (frac-around) into the lower part of the Phase I reservoir?

Had the first parameter been measured, it would also have provided the actual frictional pressure loss in the frac string for the 10-BPM injection rate at the end of the test (which would have allowed the frac-around flow rate during the entire test to be calculated through simple flow modeling). The temporal variation of the second parameter, the flow split, could then have been determined. (The reason for not venting the annulus—even at the end of the test—was probably to avoid raising the pressure differential across the several seals in the composite connection to the scab liner.)

Near the end of Expt. 2042, the injection pressure was 5740 psi and the rate 10 BPM. The injection fluid was plain water, except for a 7-hour interval May 16–17, when a 4-lb/1000-gal. slurry of sepiolite mud (a diverting agent, similar to the fine calcium carbonate used during the MHF Test) was injected in an unsuccessful attempt to reduce the rate of flow of the frac-around.

Expt. 2042 was relatively trouble-free. Unfortunately this also meant that, with no periods of total pump shut-down, there were no opportunities for measuring the joint-extension pressure (but even if there had been, the measurement would have been compromised by the liner bypass flow).

Despite the magnitude of the injection into EE-3, there was absolutely no pressure response at the shut-in EE-2 borehole—i.e., no hydraulic communication.

Pressures recorded during subsequent pumping tests, which were carried out periodically over the next four months, showed no evidence of leakage in the patch assembly. Further, no damage was detected in the 9 5/8-in. casing from the severe cooldown and resultant tensile loads exerted during this test.

Investigating the Seismic Characteristics of the Expt. 2042 Joint System

A network of downhole seismic stations provided information on the locations of microearthquakes produced during Expt. 2042. The deepest of these stations were in EE-1 (at 9400 ft) and EE-2 (at 11 300 ft). The other stations were at depths of 2460 ft in GT-1; 2148 ft in PC-1; and 8000 ft in GT-2. In addition, the array of nine surface seismic stations recorded signals from the larger microearthquakes. The monitoring network was in operation during the entire injection period (nearly 72 hours) and registered about 1300 events. The locations of these events were calculated, on the basis of data from the five downhole stations, by inversion of the arrival times of signals. Only the most reliable of the calculated locations—a total of 830 events—were plotted; these are shown in Fig. 6-29.

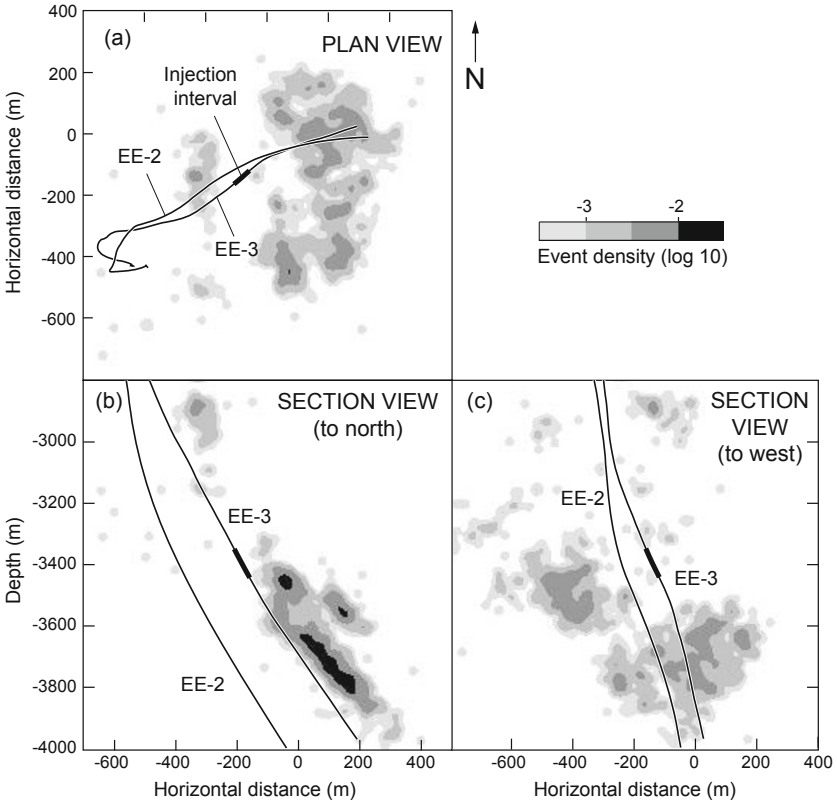

Fig. 6-29. Locations of microearthquakes recorded during Expt. 2042: (a) plan view; (b) west–east vertical cross section viewed toward the north; and (c) north–south vertical cross section viewed toward the west.
Source: Scott Phillips, EES Division, Los Alamos National Laboratory (September 2008)

Focusing on (b)—the seismicity projected onto a west–east vertical plane as viewed to the north—one sees that the vast majority of the events recorded during Expt. 2042 occurred *above* the trace of EE-3. The Expt. 2042 seismic cloud is less steeply inclined (at about 55° to the east) than that of the MHF Test, shown in view (b) of Fig. 6-23. A residual zone of hyper-compression, or stress cage, obviously still surrounded the MHF Test stimulated region, even five months after the MHF Test and the ensuing reservoir depressurization. This residual stress cage was deflecting the Expt. 2042 seismicity away from this region—analogous to what had occurred during Expt. 2025, but on a much larger scale. The MHF Test stimulated region was still significantly dilated, partly because a large amount of fluid was still stored in the lowest-opening-pressure joints (see the discussion related to Fig. 6-15 above), and partly because a number of joints had been irreversibly propped open by pressure-spalled rock fragments.

The results of Expt. 2042, added to those of Expt. 2025, demonstrated that there was no possible way of connecting EE-3 to the MHF Test stimulated region *except* by redrilling EE-3 into it! But because the longer-range objectives of the Project included production of the Phase II reservoir under high-backpressure operating conditions at EE-2, it was decided to delay the redrilling of EE-3 until the EE-2 borehole could be repaired.

First Attempt to Repair the EE-2 Borehole (October 15–December 18, 1984)

As described in detail in Chapter 5, the 13 3/8-in. (340-mm) intermediate casing had suffered damage during and following its placement at a depth of 2593 ft (790 m) in EE-2. To enable this borehole to be used for development of the Phase II reservoir, a 9 5/8-in. (244-mm) casing string had been installed to a depth of 11 578 ft (3529 m) and the bottom 960 ft of the annulus between the casing and the borehole had been tag-cemented (up to about 10 620 ft), with the remainder left uncemented. Later, during preparations for the MHF Test, a special-alloy, 5 1/2-in. frac string and a high-temperature casing packer were installed in EE-2 to protect the 9 5/8-in. casing from the very high MHF Test injection pressures (expected to be in the range of 6000 psi).

As discussed above, following the MHF Test the condition of EE-2 was assessed on the basis of (1) the reservoir vent-down behavior; (2) the results of the December 15 injection testing with the rig pumps, into both the frac string and the inner annulus; (3) the observed change in the venting behavior of the Phase I reservoir; and (4) the results of Expt. 2036.

The picture that emerged from this assessment was as follows:

- The 9 5/8-in. casing had collapsed onto the frac string in at least two places, at depths of 10 740 ft and 10 900 ft.
- Both the frac string and the inner annulus were in direct flow communication with the high-pressure reservoir—the frac string through the 70-ft injection interval below the casing shoe, and the annulus through the splits in the casing at 10 740 ft and 10 900 ft.
- The outer annulus was also connected to the MHF Test stimulated region, probably through other joints within the high-pressure reservoir that intersected the uncemented portion of this annulus above the top of the cement at 10 620 ft. (As mentioned above, the flow paths through the jointed reservoir and around the tag-cemented casing in EE-2 gave new meaning to the term *frac-around*—circumventing a nearly 1000-ft length of cemented casing!)
- The high-pressure venting of the MHF Test stimulated region into the outer annulus had opened a low-pressure entrance into the older Phase I reservoir. (In May of 1985, injection testing and temperature logging would locate this entrance at 9800 ft.)

The EE-2 repair operations began in mid October and lasted through December 18, 1984. The workover/drilling rig was supplied by Brinkerhoff-Signal Drilling Co. of Denver, CO. Because of the problem presented by the outer annulus, a major stipulation was that this annulus flow path from the reservoir be sealed off. The plan was to first remove the frac string almost down to the depth of the upper casing collapse (10 740 ft); next, perforate the casing; then inject cement into the outer annulus above the top of the existing cement at 10 620 ft; and, last, complete the borehole anew to allow high-pressure injection or production.

The operation to remove the frac string went rather smoothly down to 10 718 ft, when time was taken out to replace the top 902 ft of the 9 5/8-in. casing to repair a near-surface leak. The casing was perforated at 10 600 ft, but when adequate circulation could not be established at that depth, it was perforated again at 10 550 ft.

Next, a bridge plug was installed inside the stub of the remaining frac string (which was held firmly by the collapsed casing at 10 740 ft) and the casing was backfilled with 23 ft of sand, to a depth of 10 695 ft. A cementing packer was then landed at a depth of 10 292 ft, with a tailpipe extending down to 10 424 ft, 126 ft above the perforations. Finally, on November 15, 1000 gal. of cement was pumped through the packer and tailpipe, most of which flowed through the perforations at 10 550 ft and up into the outer annulus. This amount—estimated to fill about 200 ft of the annulus—brought the top of the cement to a level later measured as 10 378 ft. But it would have been prudent to use additional cement to seal off more of this annulus from the high-pressure reservoir, given the likelihood that an extended period of high-pressure operation could give rise to

an even longer frac-around. (With its top at just 1200 ft above the casing shoe at 11 578 ft, the existing tag cement provided a meager barrier against the joint-opening pressure exerted by a stimulated region already some 2500 ft high and centered around the casing shoe.)

Note: Eleven years later, in 1995, a frac-around of the tag-cemented production casing deep in EE-3A would bring a halt to the Long-Term Flow Test (LTFT)—and within months to the termination, by the DOE, of the Laboratory's HDR Project.

After the cementing packer had been pulled from the hole, the casing was successfully pressure-tested to 2400 psi, confirming that the cement had sealed both the outer annulus and the perforations. With this principal objective of the EE-2 repair operation achieved, the borehole could have been re-completed by drilling out the cement, cleaning out the sand on top of the frac-string stub at 10 718 ft, removing the bridge plug, setting an Otis steam packer just below the deeper set of perforations at 10 600 ft, and running the 5 1/2-in. frac string back in. But instead, a second—and more extensive—cement job was already in the works, to seal the outer annulus up to a depth of about 6500 ft. It had been planned in the belief that flow from the high-pressure reservoir could still travel via this annulus to the loss zones higher up, in the 1900- to 2400-ft depth interval (which was not the case: these loss zones were already sealed off from the inner annulus by casing, and from the reservoir by the cement job through the perforations at 10 550 ft). This much larger cement job was aimed at a problem that did not exist, and it would have a very poor result.

Note: This would have been an excellent time for radioactive-tracer mapping, by a commercial logging company, of any flow paths originating near the top of the plugged frac string at 10 718 ft (the still-intact 9 5/8-in. casing could have been pressurized with the rig pumps while the tracer was released deep in EE-2).

On November 16, following five failed attempts, the casing was finally perforated with ten shots over a 3-ft interval, at a mean depth of 9100 ft. Six days later, after a number of false starts, a cement retainer[28] was set at 8892 ft and 7350 gal. of cement was pumped through the retainer, to force it through the perforations and into the outer annulus. Unfortunately, when a valve on the cementing head was opened (after a wait of more than

[28]A cement retainer is a special type of packer equipped with a check valve that can be opened by a stinger on the bottom of the drill pipe to allow cement to be pumped through it. When the stinger is pulled up and out of the retainer, the check valve closes, preventing the cement from being pushed back up into the casing by the differential pressure created by the weight of the cement in the annulus.

two hours for the cement to set), it was found that the drill pipe was on a vacuum, signaling a major problem with this second cement job.

The short sand plug at 10 695 ft should have prevented any cement from flowing out below that depth; but instead, the borehole was found to be full of cement where it should not have been—below the perforations at 9100 ft. The cement was drilled out to 9356 ft, and the casing was then pressure-tested to 3000 psi. In 25 minutes, the pressure dropped 450 psi, implying that the perforations had not been completely closed off.

When the cement below 9356 ft was drilled out, it was found to extend all the way down to 10 650 ft. The conclusion seemed inescapable that almost all the 7350 gal. of cement injected had gone on down the hole instead of out the perforations and up the outer annulus. Given a calculated volume of about 5000 gal. for the casing between 9100 ft and 10 650 ft, the question was, where did the rest of the cement (2000+ gal.)—and the water previously filling the casing below the cement retainer—go? No doubt the answer is that both were forced through the splits in the 9 5/8-in. casing and out into the joints intersecting the borehole at 10 740 ft and 10 900 ft. Just before being displaced with water, the cement filled the drill pipe plus approximately 650 ft of casing; the pressure at the bottom of such a column of 16.6-lb/gal. cement would have created a net pressure differential across the 23-ft sand plug of at least 4000 psi—more than enough to have washed all the sand and cement down and out through the casing tears at 10 740 ft and 10 900 ft, thence into the joints at those depths.

These joints, then, must still have been open and directly connected to the high-pressure reservoir. They were able to accept the cement because they were being held open by rock spalls (from the MHF Test blow-out), as can be inferred from the fact that on December 15, at a rate of 6 BPM, injection pressures of only 2000–2200 psi were required, whereas during Expt. 2020 injection pressures were over 5000 psi. (It appears that the rapid vent-down of the reservoir through the inner annulus, like the vent-down through the frac string, resulted in near-outlet pressure spallation.)

On November 30, with the cement cleared to 10 650 ft, the hole was circulated clean and then pressure-tested with the rig pumps. When the pressure did not build up, even at full pumping rate, it seemed evident that the second cement job had failed not only to seal the outer annulus but also to plug the perforations in the casing at 9100 ft, thereby seriously degrading the pressure integrity of the casing.

The hole was cleared of cement and debris down to the top of the remaining 5 1/2-in. frac string at 10 718 ft. But time and budget constraints then brought an end to the "repair" effort in EE-2 (including further attempts to remove the rest of the frac string and casing packer). Of the more than six weeks spent, almost half had been taken up by the two cementing operations to seal off the outer annulus from the high-pressure reservoir—the first quick and

successful, the second lengthy, unnecessary, and unsuccessful. In addition, unfortunately, when the casing was perforated at 9100 ft for the second cement job, a bypass flow path was opened from inside the 9 5/8-in. casing; this path would carry flow through these perforations, up the outer annulus, through splits in the 13 3/8-in. casing, and finally into the shallow aquifers on top of the Precambrian surface.

The drilling supervisors were now forced to focus on the main task of making EE-2 functional as the production well for future reservoir flow testing. First, to restore flow communication with the high-pressure reservoir, the bridge plug would have to be removed from just inside the top of the remaining 621 ft of 5 1/2-in. frac string at 10 718 ft. To form a transition from the top of the frac string to the 9 5/8-in. casing, seven joints (291 ft) of 7-in. casing were made up and run into the hole on drill pipe, in a liner-hanging configuration (the top end equipped with a liner sleeve to be used with a liner setting tool). The bottom end was fitted with a 3-ft-long, tapered "mule-shoe" guide (7-in. outer diameter and 5 3/4-in. inner diameter), designed to slip over the top of the frac string; however, it was not equipped with any type of seal. The transition casing was then washed and rotated about 2 ft over the top of the frac string and released.

Next, a "plug-plucker" assembly attached to the end of 12 joints of small-diameter drill pipe (2 7/8 in. with a tool-joint diameter of 3 1/4 in.) was run in on the bottom of the standard drill pipe. The slips on the bridge plug were milled off, and the assembly was pulled from the hole—but sans the bridge plug. Over the next eight days, various techniques were tried, at deeper and deeper depths, to recover the plug (which obviously was slipping down inside the remaining frac string). Eventually the bridge plug lodged at around 11 285 ft and was completely "milled up." Now the small-diameter drill pipe was able to move freely up and down inside the frac string (past the two points of casing collapse), all the way down to the Otis steam packer at 11 297 ft. On December 12, with a new bottom-hole assembly and more small-diameter drill pipe, the hole was circulated clean to 11 642 ft—just 6 ft above the top of the sand/barite plug at 11 648 ft. It was now possible for EE-2 to be logged with the Laboratory's 3 1/4-in.-diameter temperature tool as far as the bottom of the MHF Test stimulation interval.

On December 14, a new Otis steam packer was run into the hole on drill pipe (along with an assembly that included a tie-back bushing to connect to the top of the 7-in. transition casing at 10 419 ft, a crossover sub, and a packer-setting tool). After the tie-back receptacle on top of the transition casing had been engaged, the packer was landed with its top at a depth of 10 401 ft (*above* the perforations at 10 550 and 10 600 ft). The packer seal against the casing was then pressure-tested to 2500 psi for 30 minutes; there was no pressure bleed-off.

Next, the drill pipe was removed from the hole and laid down, and the now-repaired 5 1/2-in. frac string was run in with a slick-joint assembly on bottom, which was worked into and through the seal assembly on the Otis packer. Finally, the inner annulus above the packer was again pressure-tested—successfully—to 2500 psi. This test was followed on December 18 with further pressure testing, by Dowell, under more controlled conditions: the annulus was cycled to 2500 psi at least ten times, the pressure bleeding off to about 2100 psi between cycles. During this operation, which lasted over two hours, the injection of about 450 gal. of water was required to repeatedly attain the 2500-psi annulus pressure. (All this water was lost, probably through the perforations at 9100 ft; although temporarily closed off, apparently this region was never tightly sealed.)

The Status of the EE-2 Borehole at the End of 1984: Summary

The perception that the EE-2 borehole was in poor condition would significantly affect preparations for the Initial Closed-Loop Flow Test (ICFT) and ultimately lead to the redrilling of this borehole (the EE-2A "leg"). In reality, EE-2 provided full high-pressure access to the upper part of the reservoir region created by the MHF Test, by two paths—both connected to the new section of frac string. The first flow path was through the 7-in. transition casing, the 621 ft of the original frac string (clamped tightly within the 9 5/8-in. casing at the two zones of casing collapse), the 9 5/8-in. casing that extended from the deeper Otis packer at 11 297 ft to the casing shoe at 11 578 ft, and, finally, 64 ft of open hole (down to 11 642 ft). The second flow path was through the 7-in. transition casing, around the slip-over—but unsealed—connection to the stub of the old frac string at 10 718 ft, into the inner annulus, and then into the reservoir through the joints connected to the splits in the casing at 10 740 ft and 10 900 ft.

In addition, the fact that the inner annulus *above* the Otis steam packer was not pressure-tight would be inconsequential for high-pressure production via EE-2, because this annulus was isolated from the production flow by the packer.

Finally, the borehole could be logged with 3 1/4-in.-diameter tools all the way down to the top of the sand plug at 11 642 ft, which meant in particular that the upper 1200 ft of the reservoir could be temperature-logged.

Given all these factors, EE-2 was still a "working borehole," suitable as a production well for any forthcoming flow test initiated from a redrilled EE-3. Even so, those involved with the EE-2 repair operations mistakenly viewed this borehole as a potentially "leaky" one.

Redrilling and Pressure-Stimulation of EE-3

As stated earlier, the Project staff had concluded that their one remaining option for achieving hydraulic communication between EE-2 and EE-3 was to sidetrack EE-3 and directionally drill it through the deeper, central portion of the MHF Test seismic cloud. The trajectory for this drilling program, as determined by Don Brown, is shown in Fig. 6-30.

The information in this section is adapted from HDR Geothermal Energy Development Program (1987), Schillo et al. (1987), and the daily drilling reports.

Sidetracking of EE-3 (EE-3A)

Early in 1985, the Brinkerhoff-Signal workover/drilling rig positioned over EE-2 was skidded to EE-3 for the first stage of redrilling. The new drilling trajectory had been selected to (1) penetrate the densest parts of the MHF Test seismic cloud, (2) be easy to redirect toward other nearby seismic "clusters" if the first 600 ft of drilling failed to achieve adequate hydraulic communication with EE-2, and (3) minimize both the amount of directional drilling and the severity of borehole curvature.

The new leg of the borehole was to be initiated at a depth of about 9300 ft, where the orientation of EE-3 was N77E, 22 1/2°. The sidetracking would exit EE-3 to the right, and as drilling proceeded, the inclination would slowly be dropped to 11° as the azimuth was rotated 67° (to the right), around to S36E.

To prepare for the sidetracking, a 68-ft-long window was cut in the 9 5/8-in. casing (9285–9353 ft), and then the 9293- to 9330-ft depth interval of the exposed 12 1/4-in. drilled hole was underreamed to a 16-in. diameter, creating a modest 2-in. ledge for the kickoff.

After three "half-hearted" attempts to sidetrack off the ledge with 8 1/2-in. TCI bits—none of which succeeded—the drilling supervisors resorted to cementing-in a whipstock.[29] The casing window was lengthened by 20 ft, to 9373 ft, to accommodate a packstock (a whipstock assembly with a packer on bottom). Over the next three weeks (and at a cost of about $350 000), the hole was prepared; the packstock was installed on the lower stub of the casing, with its top at 9349 ft; drilling off the whipstock began; the hole was reamed; the BHA became stuck and twisted off; fishing retrieved the BHA; and—finally—the hole was drilled ahead about 100 ft, to 9470 ft.

[29]Eight years earlier a competent directional driller, using smaller-diameter (7 7/8-in.) bits, had successfully sidetracked GT-2 twice (GT-2A and -2B) in very hard granitic rock, by drilling off ledges on the low side of the 9 5/8-in. borehole—without using a whipstock. The success of these kickoff operations clearly involved a high degree of "art"—including the selection of the appropriate bit type and size.

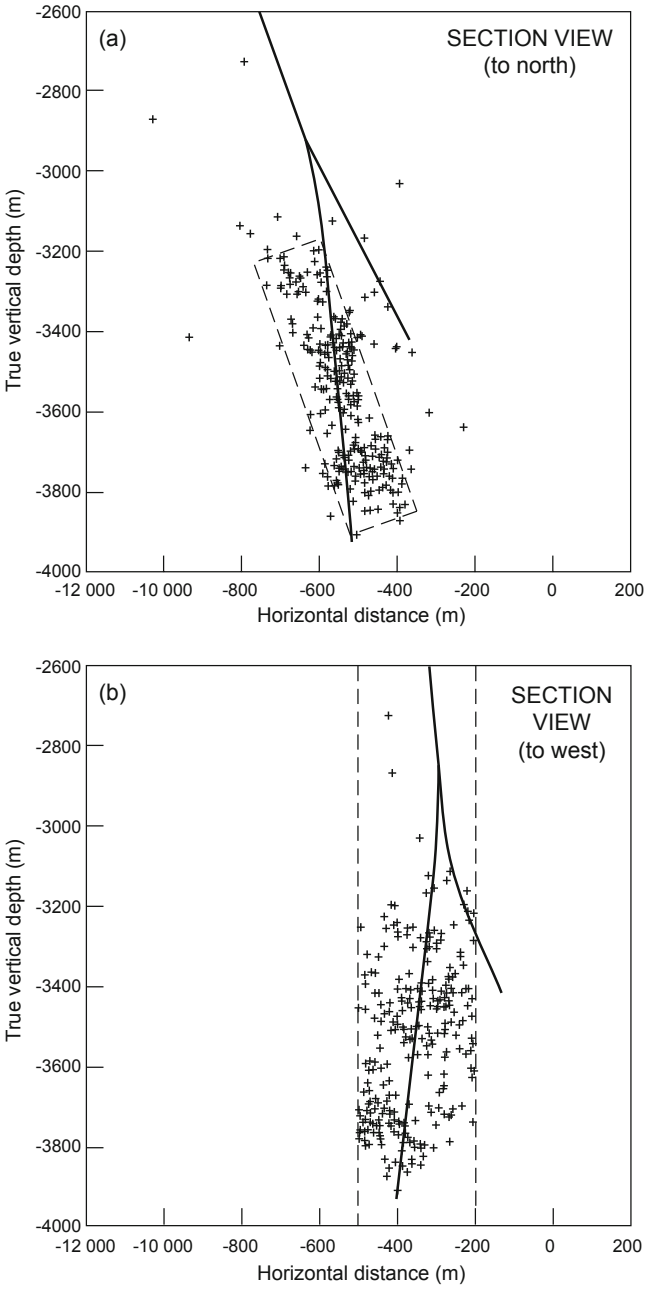

Fig. 6-30. Planned EE-3A drilling trajectory through the MHF Test seismic cloud: vertical sections viewed (a) toward the north and (b) toward the west. Source: HDR Project data archives

In March 1985 the Brinkerhoff-Signal workover/drilling rig was dismissed, and a larger drill rig (the Big Chief Drilling Co. rig #47) was mobilized to complete the drilling of EE-3A. On April 3, a TCI bit was run in to clean out the new borehole and drill it ahead. The next day, a Dyna-Drill run began turning the borehole to the right. For the first time at Fenton Hill, a high-temperature, clay-based drilling fluid (mud) was used for drilling in the hot granitic rocks. This fluid, a sepiolite and bentonite system with lignite and caustic soda, was designed to reduce drag, corrosion, torque, and abrasion; to improve hole cleaning; and to reduce the recirculation of cuttings, which had caused excessive wear on previous bottom-hole assemblies when plain water was used as the drilling fluid.[30] From a reading of N88E, 14° on April 10—at a depth of 10 026 ft—the trajectory of EE-3A was turned to S71E, 15° on April 17, at a depth of 10 841 ft.

Reinflation of the Reservoir Through EE-2—Expt. 2052

Before drilling proceeded below 10 841 ft, to take EE-3A through the deeper part of the MHF Test seismic cloud, the reservoir was reinflated through EE-2 (with the Laboratory's newly acquired positive-displacement "super-pump," capable of injection at a rate of 100 gpm and pressures up to 5000 psi). Referred to as Expt. 2052, the reinflation began on April 16, 1985, and lasted almost two weeks. Some 1.4 million gal. of fluid was injected into the MHF Test stimulated region—up to that time second only to the amount injected during the MHF Test. The injected fluid was tagged with a chemical tracer (boron), to enable detection in the EE-3A drilling fluid returns, but because of the huge volume of the reservoir when inflated, the tracer was below the threshold for detection during the drilling of EE-3A.

This experiment yielded two major findings:

- The injection impedance (as reflected by the pressure required to inject at a certain flow rate) was—like that of Expt. 2036—much lower than those observed earlier in EE-2 (Expts. 2011, 2012, 2016, 2018, and 2020, and the MHF Pre-Pump Test).
- Almost all the injected fluid was flowing into the Phase II reservoir through the joints at 10 740 and 10 900 ft, rather than out the bottom of the borehole below the casing shoe.

Experiment 2052 began at an injection rate of 115 gpm. To the surprise of many, the injection pressure started out very low and increased very slowly (mirroring the behavior seen during Expt. 2036): over the first 15 hours of pumping, it rose to only 1860 psi—reflecting a much lower injection impedance than seen before the MHF Test. In particular, during the Pre-Pump Test (see Fig. 6-18), the pressure rose to nearly 5000 psi for an injection rate of only 2 BPM (84 gpm), indicating that none of these earlier injections,

[30]This change in drilling fluid yielded drill cuttings that were a geologist's dream—the longest dimension typically over 1/4 in., which made petrographic analysis much easier.

including the very large one of Expt. 2020, had induced any significant "self-propping" (due to shear displacement) of the pressure-stimulated joints connecting the EE-2 borehole to the body of the reservoir.

Temperature logging showed that nearly all of the injected fluid was exiting the EE-2 borehole, not at the bottom—as had been expected—but through the joints responsible for the casing collapses at the end of the MHF Test, at 10 740 ft and 10 900 ft. (Apparently the short MHF Test injection interval below the 9 5/8-in. casing shoe was now completely plugged with fill.) The markedly lower injection impedance combined with the lack of evidence for shear-slippage propping strongly supports the conclusion that these joints had been propped open by pressure spalls during the violent vent-down of the reservoir at the end of the MHF Test.

Early in Expt. 2052, a sharp "break-over" in the pressure curve, at 1460 psi, provided another clear indication of the opening pressure for the joint set having the lowest opening pressure in the reservoir. This additional finding of Expt. 2052 confirmed the earlier evidence that these tensile-opening joints were almost exactly orthogonal to the least principal earth stress,[31] explaining why they had no significant seismic signature during the MHF Test.

By noon on April 20, after the injection of 417 000 gal., the injection pressure had risen to only 1900 psi, showing conclusively that the portion of the reservoir closest to EE-2 was now readily accessible to the injected fluid through the splits in the 9 5/8-in. casing—that is, more than 800 ft above the MHF Test injection interval (11 578–11 648 ft).

First Lynes Packer Test in EE-3A—Expt. 2049

While Expt. 2052 was still ongoing in EE-2, preparations began for Expt. 2049 in EE-3A. The drilling mud was displaced from the borehole with water, then the drill pipe was tripped out and the length of each stand measured. It was discovered that an extra joint of pipe had been picked up, apparently during the Dyna-Drill run on April 4—which meant that the depth of the borehole was 10 875 ft, not 10 841 ft.

Experiment 2049 was planned as the first test of the completely redesigned Lynes high-temperature/high-pressure inflatable packer. To conduct it as a "mini-frac" test with only a modest amount of fluid injection, the open-hole interval would be restricted to only a few tens of feet. On April 19, a Lynes packer was set at a depth of 10 830 ft, leaving a 45-ft injection interval above the bottom of the borehole at 10 875 ft.

The first injection (240 gal.) lasted only 6 minutes, at a rate of 1 BPM, and opened a joint near the bottom of the interval at a pressure of 3640 psi. The extension pressure for this joint reached a maximum of 4440 psi

[31]This pressure of 1460 psi, with a warm column of fluid in EE-2, was about 200 psi higher than the injection pressure in GT-2 with a cold column of fluid, when the least principal earth stress was measured in February 1976 (see Expt. 114 in Table 3-12, Chapter 3).

(an overshoot of 800 psi) in one minute, then over the next two minutes—until pump shut-in—decayed to 4240 psi. The joint shut-in pressure then slowly dropped, and after 18 minutes leveled out at 3640 psi, the same as the joint-opening pressure.

The second injection, at a rate of 2 BPM for 11 minutes, brought a rise in the pressure to 4500 psi. Since a choke had been installed just above the packer, it could not be determined whether the joint being extended, at double the earlier flow rate, was the one already opened near the bottom of the interval, a different one, or both. Pumping was again shut in, then resumed at a rate of 4 BPM for 8 minutes. This time the joint-extension pressure rose to 4600 psi. Finally, when the interval was pressurized once more, at a rate of 6 BPM, the joint-extension pressure rose again—to 4800 psi.[32]

During this experiment the annulus was also pressurized, to reduce the pressure differential across the packer. But the presumedly simple task of quickly pressurizing the annulus with the rig pumps turned out to be a very significant injection (5000 gal.), which unexpectedly opened up a low-pressure joint above the packer that accepted a high volume of flow. Later located at 10 260 ft, this joint appeared to be connected to the lower portion of the Phase I reservoir (not unlike the one below the casing shoe in EE-3—at 10 394 ft—that had previously caused so much trouble). Thus, not only was the maximum annulus pressure achieved far below the desired 2000 psi (only 570 psi), but this joint would also complicate subsequent stimulation tests by hindering pressurization of the annulus above the packers.

With a total injection of 5600 gal. over 3 hours, Expt. 2049 was a successful test of the redesigned Lynes packer.

Continued Drilling Brings Signs of Hydraulic Communication with EE-2

On April 21, an oriented core was cut from 10 875 ft to 10 880 ft with a Dowdco PDC core bit (8 1/2-in. outer diameter, 4-in. inner diameter). The 33-in.-long core was recovered in two pieces that were separated by a significant joint, striking NNW–SSE and dipping 43° to the WSW (Levy, 2010).

Drilling over the next three days took the hole to a depth of 11 127 ft; surveying at 11 086 ft showed a trajectory of S53E, 14°. The final Dyna-Drill run—188 ft in just under 17 hours—was completed on April 25. (Note: Of particular interest for any subsequent HDR drilling program, this mud motor survived a downhole [static] rock temperature of 233°C!) At the new depth of 11 315 ft, the hole trajectory was S30E, 9 1/2°. On April 27 the borehole was reamed to bottom—necessary following the Dyna-Drill run—then over the next two days it was rotary-drilled ahead, with a TCI bit, to 11 593 ft.

[32]The 560-psi difference between the initial joint-extension pressure (4240 psi) and the final one (4800 psi) may have been due entirely to the increasing pressure drop across the choke and the increasing frictional pressure loss in the drill pipe as the injection rate was raised from 1 to 6 BPM.

On April 30, following a bit run to 11 600 ft to clean the hole and drill up or recover lost bearings and carbide buttons left on bottom, a second core was cut from 11 600 ft to 11 615 ft with a Smith hybrid 7 7/8-in.-diameter core bit having four roller cones (cutting a 3-in.-diameter core). About 11 ft of core was recovered. A hole survey at 11 615 ft showed the EE-3A trajectory as S32E, 9°.

A temperature log run the next day in EE-3A showed a very significant anomaly at 11 440 ft—a 20°C temperature spike. This was the first evidence of hydraulic communication between the two boreholes: hot fluid from EE-2 was entering EE-3A at this depth, at a rate of about 15 gpm. The low-pressure joint entrance at about 10 260 ft, responsible for the annular fluid loss during Expt. 2049, was also identified.

Experiment 2057

On the morning of May 2, with the borehole at a depth of 11 615 ft, a second Lynes inflatable packer was set at 10 841 ft, leaving an injection interval of 774 ft that spanned the first EE-3A production zone at 11 440 ft. The sparse data on this experiment (obtained from the driller's log) are given in Table 6-3. The experiment ended at 22:51, when the packer failed—as evidenced by significant bypass flow into the annulus. Only a modest amount of microseismic activity was detected from the reservoir during this experiment. When the packer was recovered on May 3, it was in good shape except for some damage to the jay-latch and the loss of the outer rubber seal element, which had been left in the hole. The nearly 5 hours that this packer lasted, at temperatures approaching 200°C and a differential pressure close to 4500 psi (without pressurization of the annulus), was a world record for inflatable packers at that time.

Table 6-3. Experiment 2057: injection into first EE-3A production zone at 11 440 ft (May 2, 1985)

Time interval (h)	Pressure (psi)	Rate (BPM)
18:13–19:00	4550	6.1
19:00–20:00	4540	6.1
20:00–21:00	4530	6.1
21:00–22:00	4500	6.2
22:00–22:51	4470	6.2

It is tempting to conclude that this injection flow was all entering the single joint intersecting EE-3A at 11 440 ft. Further, the joint-reinflation pressures shown in Table 6-3 are similar to those of Expt. 2049, which—with an inline choke installed above the packer—showed an injection pressure of 4800 psi at 6 BPM.

The final phase of Expt. 2057, a temperature log run on May 3, revealed two minor zones of fluid acceptance, at 10 880 ft and 11 000 ft (in addition to the major one at 11 440 ft).

More Signs of Hydraulic Communication with EE-2

As EE-3A was deepened following Expt. 2057, a stronger flow—about 25 gpm in total—was observed coming from three joints intersecting the borehole: at 12 000 ft, 12 100 ft, and 12 150 ft. Drilling was suspended on May 9, at a depth of 12 203 ft. By the next day, the EE-3A surface outflow had increased to 30–40 gpm, and by May 12 to about 60 gpm. The borehole orientation, at 12 163 ft, was N44E, 9°.

On May 14, following a five-day hiatus for rig repairs, a third Lynes packer was run into the hole and landed at about 11 500 ft—below the two minor zones of fluid acceptance identified by the temperature logging of May 3, and just below the joint at 11 440 ft. Unfortunately, the packer did not inflate properly, then became stuck in the borehole. Nearly two weeks of fishing operations ensued (the packer was finally retrieved on May 26), and during this period—on May 20—the drill-rig pumps were used to inject water into EE-3A. Almost immediately there was a rise in pressure in the shut-in EE-2. Given these portents of success, a high-pressure stimulation test (Expt. 2059) was planned for EE-3A.

The First Successful Connection: Expt. 2059 (May 1985)

During this experiment, EE-2 would for the first time serve as a production well. However—as shown by temperature logging associated with Expt. 2052—the short open-hole interval below the EE-2 casing had become plugged with mud and sediment. To clear it, a 1-in. coil-tubing rig was mobilized; but instead of setting up to drill and wash out the collected sediment using reverse circulation, the drilling managers brought in a nitrogen truck (hoping to speed up the cleanout operation by unloading the borehole from several successively deeper positions).

Unfortunately, this cleaning operation was neither well conceived nor well executed, coming on the heels of several reservoir pressurization tests through both EE-2 and EE-3A. The pressure-stimulated region surrounding EE-2 (up to about the 10 200-ft depth) would have been at some modest pressure *above* hydrostatic. Thus, when the coil-tubing unit delivered pressurized nitrogen at a rate of 750 scfm, the nitrogen rapidly displaced the fluid from both the frac string and the region below the Otis steam packer—causing the pressure inside the 9 5/8-in. casing below the packer to fall considerably below hydrostatic. As had happened 18 months earlier, the large inward pressure differential from the reservoir caused the 9 5/8-in. casing to collapse at a depth of about 10 512 ft, this time onto

the 7-in. transition casing below the packer. In the process, the coil tubing was ensnared. (This second episode of casing collapse would not be discovered until much later, however [see Chapter 7]—though attempts at logging in EE-2 with 2 1/8-in.-outer-diameter slimline tools encountered an "unexplained" obstruction within the 7-in. transition casing at this depth.) The nitrogen injection did clear a large amount of mud from EE-2, but the first period of high-flow production would undoubtedly have accomplished the same thing.

Circulation of a solution of soap and cold water cooled the well and finally enabled the stuck coil tubing to be removed. But the damage had been done: what had been a "reasonable" EE-2 production well situation—enabling access by slim-line logging tools well into the Phase II reservoir (see *First Attempt to Repair the EE-2 Borehole*, above) and production capacity up to pressures of at least 2500 psi—was now compromised. Moreover, high-backpressure production of EE-2 would probably not have been necessary for the planned LTFT, because the joints connecting the reservoir to the EE-2 production interval were already propped open with rock spalls generated by the rapid depressurization of these joints at the end of the MHF Test (DuTeau and Brown, 1993). In other words, had it not been for the botched attempt to clean out the wellbore, EE-2 would have been in usable condition for both the ICFT and the LTFT.

The only positive outcome of this otherwise colossal mistake would be the later identification of at least one of the joints responsible for the venting of the high-pressure reservoir through the outer annulus following the MHF Test blow-out. This joint intersected the borehole at the depth of the casing collapse (about 10 512 ft), more than 200 ft above the highest joint intersection identified earlier (10 740 ft).

Experiment 2059, carried out on May 27 and 28, was aimed at stimulating the flow connections observed below 11 537 ft during the redrilling of EE-3A—most particularly those in the depth interval 12 000–12 150 ft. On May 28, with EE-3A still at a depth of 12 203 ft, a fourth Lynes packer was run in on 4 1/2-in. drill pipe and set successfully at a depth of 11 537 ft, in an interval of the borehole that appeared, from a caliper log, to be reasonably smooth. The injection interval would be 666 ft long, from 11 537 ft to 12 203 ft. Over a period of 20 hours, 423 000 gal. of water was injected, mainly at rates of 6.2 and 9.6–10 BPM (16 and ~26 L/s) and injection pressures varying from 4740 psi (at 6.2 BPM) to 5900 psi (at 10 BPM), as shown in Fig. 6-31.

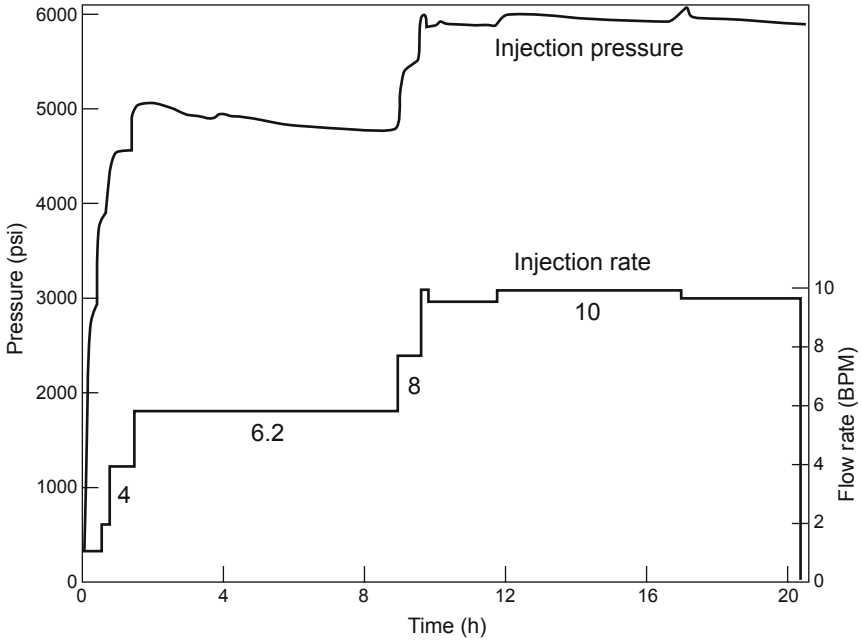

Fig. 6-31. Pressure and flow-rate history for Expt. 2059 in EE-3A. Source: Kelkar, 1985

Pressure rose rapidly at EE-2, and after two hours of pumping, the wellhead valve was opened and water flowed out. The flow was small at the outset, but as the well was repeatedly surged (shut in for a short time and then rapidly vented), flow steadily increased. When the flow rate had reached about 160 gpm (10 L/s), the experiment was stopped—and the celebration began! (See Fig. 6-32.) The measured flow impedance was 27 psi/gpm (3 MPa/L/s)—already only twice that measured for the Phase I reservoir after several months of operation and a number of high-pressure stimulations—and this transient value would certainly drop considerably with continued operation.

After 20 hours of injection, Expt. 2059 came to a very orderly end, with no pipe or packer failures. Pumping was simply stopped at 20:19, and then the EE-3A wellhead was shut in. The 423 000 gal. of fluid injected was not nearly enough to refill the Phase II reservoir, which had been created by the 5.6-million-gal. injection of the MHF Test.

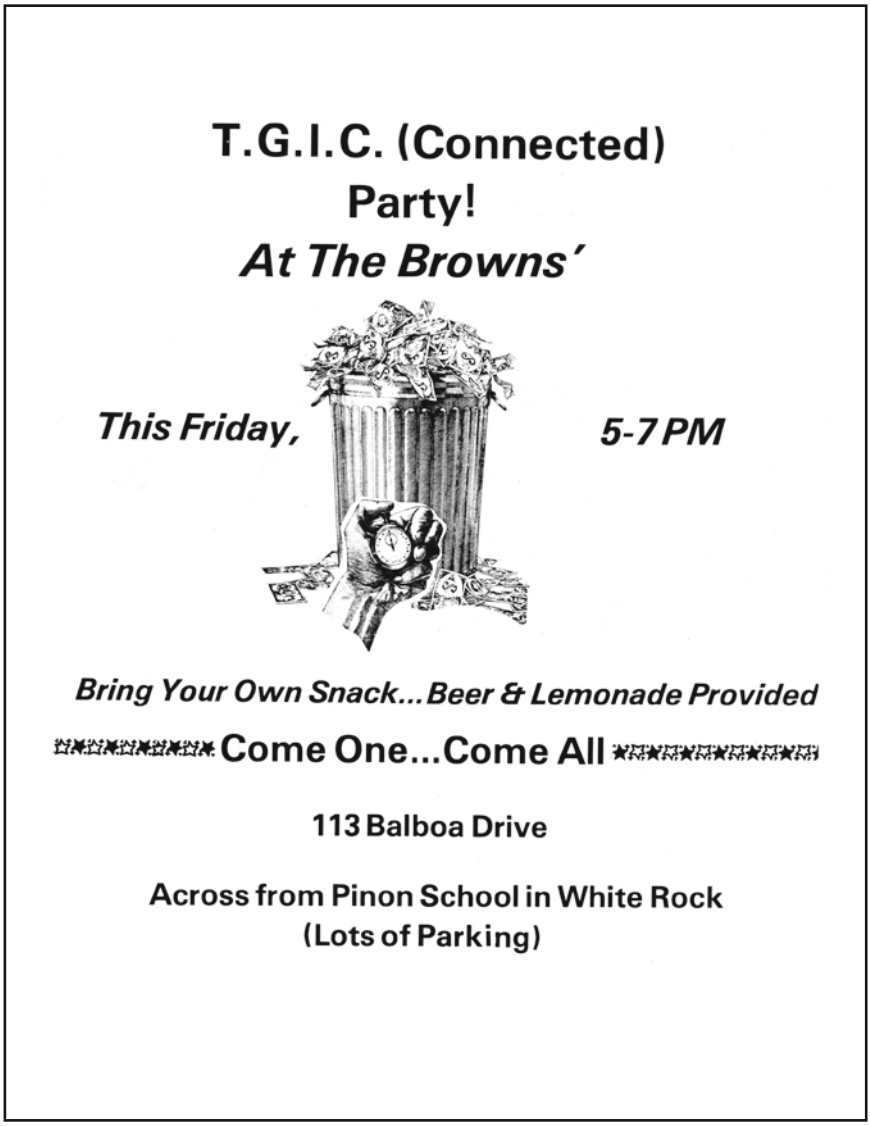

Fig. 6-32. The invitation to the "Connection Party" held on May 31, 1985. (TGIC = Thank God It's Connected!)

Temperature surveying in EE-3A on May 30 showed that several new joints had been stimulated during Expt. 2059 and were carrying flow into the reservoir. Figure 6-33 compares the profile from this survey with the background temperature profile of May 10. The principal fluid entrances are clearly visible—at 11 730 ft and 11 930 ft—as are several smaller fluid entrances below these.

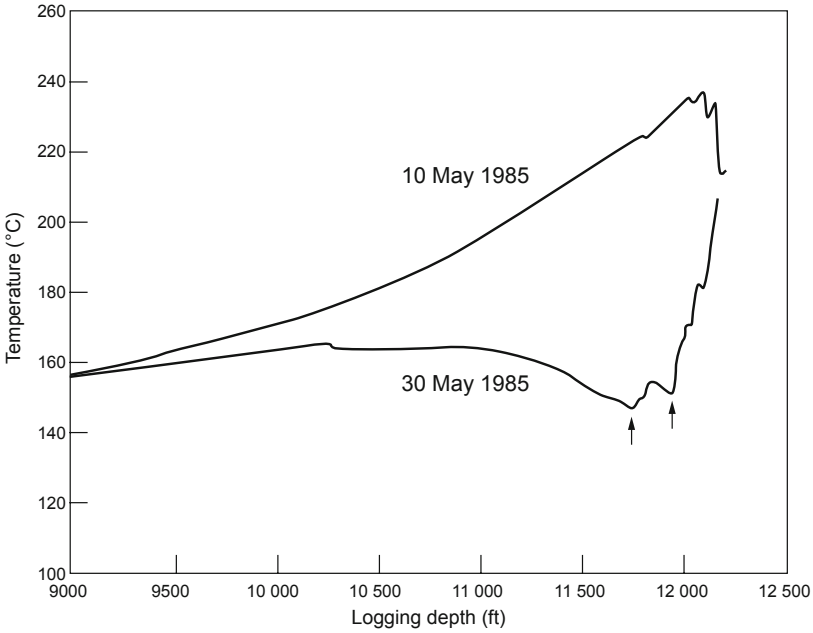

Fig. 6-33. Comparison of temperature profiles before and after Expt. 2059. Depths are as recorded in the logging van.
Source: HDR Project data archives

Seismically, Expt. 2059 was a dud—which should have been expected, because the amount of fluid injected was not nearly sufficient to fill, let alone extend, the reservoir. During the 20 hours of injection into EE-3A, only 20 microseismic events were captured on the newly acquired Biomation seismic signal digitizers. Only three of those events were eventually located—all within 100 m (330 ft) of EE-3A, at vertical depths ranging from 3300 to 3800 m (10 800 to 12 500 ft).

Final Stage of Drilling in EE-3A

Before the final stage of drilling could begin in EE-3A, the remains of the third Lynes packer, which had been pushed all the way to hole bottom before Expt. 2059, had to be fished out. On June 8, with this task complete, drilling proceeded and reached a TD of 13 182 ft (a TVD of 12 926 ft) on June 19, 1985. This drilling stage in granitic rock averaged about 12 ft/h (an overall rate of more than 100 ft/day) at an average cost of $240/ft. It included two additional coring runs with 7 7/8-in. Smith hybrid core bits: 12 412–12 438 ft and 12 439–12 459 ft.

All in all, the redrilling of EE-3 in deep, hot granitic rock was accomplished with very few problems and represented a significant achievement for that time.

Examination of all four oriented cores from EE-3A revealed that the joints in the Phase II reservoir have substantially different orientations from those in the Phase I reservoir above: whereas the latter are predominantly near-vertical, striking in a wide range of directions, the former are inclined in the 30°–60° range.

Experiment 2061

The deepest stimulation of EE-3A (Expt. 2061) was carried out June 29–July 2, between 12 555 ft and the bottom of the hole at 13 182 ft. Seismically this experiment was very energetic, because a new array of joints was being opened. But it failed to connect this deepest stimulated region in EE-3A to EE-2—which should not have been puzzling: As shown in Fig. 6-34, almost all of the region being stimulated was below the MHF Test seismic cloud, but obviously affected by the compressive stress cage surrounding the MHF Test stimulated region. This stress cage held potential connecting joints tightly closed, "deflecting" the newly developing seismicity downward (as had occurred during Expt. 2042) and preventing any flow communication.

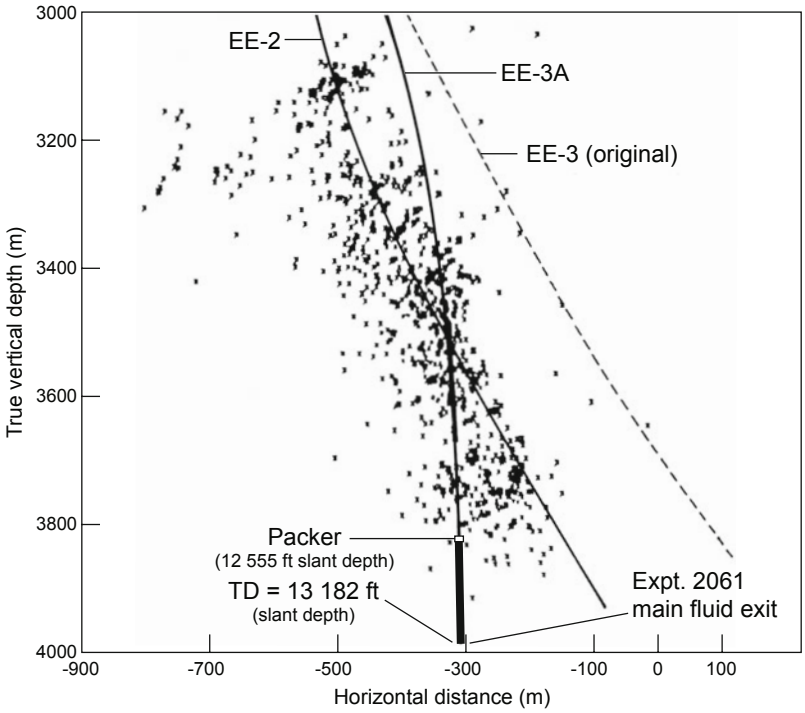

Fig. 6-34. The trajectory of EE-3A superimposed on the seismicity generated during the MHF Test (viewed to the north).
Adapted from HDR, 1987

The injection-pressure and flow-rate profiles during the 62 hours of Expt. 2061 are shown in Fig. 6-35. A total of 1.38 million gal. was injected into EE-3A at an average rate of 8.8 BPM. Examination of the initial 8-hour-long injection plateau of June 30, at a rate of just over 5 BPM, reveals that the injection pressure was still rising at the end of this plateau, reaching a final value of 5850 psi just before the flow rate was increased again. Correcting for the 410-psi pressure loss in the drill pipe and choke at this flow rate, one obtains a joint-inflation/extension pressure of 5440 psi—very close to the 5500-psi values previously measured for the Phase II reservoir.

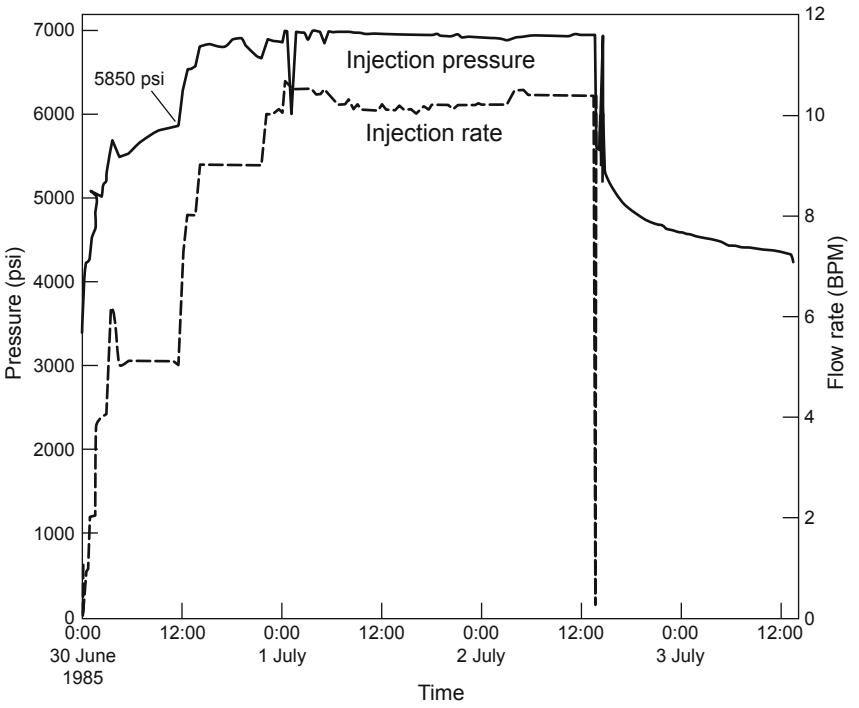

Fig. 6-35. Injection-pressure and flow-rate history for Expt. 2061. Source: Dash et al., 1985a

Comparison of the Expt. 2061 injection-pressure behavior and seismic "signature" with those of Expt. 2020 led to an epiphany in our understanding of HDR reservoir development and "flow access." Except for minor variations in pressure, these two experiments look identical (Figs. 6-9 and 6-35). In other words, in both cases a new reservoir region was being created (that of Expt. 2061 was directly adjacent to the MHF Test stimulated region, but the two were *separate*).

As indicated by the temperature profiles for this experiment (Fig. 6-36), almost all the flow exited the EE-3A borehole at the very bottom (13 182 ft), but small amounts exited through six other outlets (joint intersections) between 12 600 and 13 100 ft. All of these data indicate that Expt. 2061 had pressure-stimulated a region just outside the MHF Test stress cage.

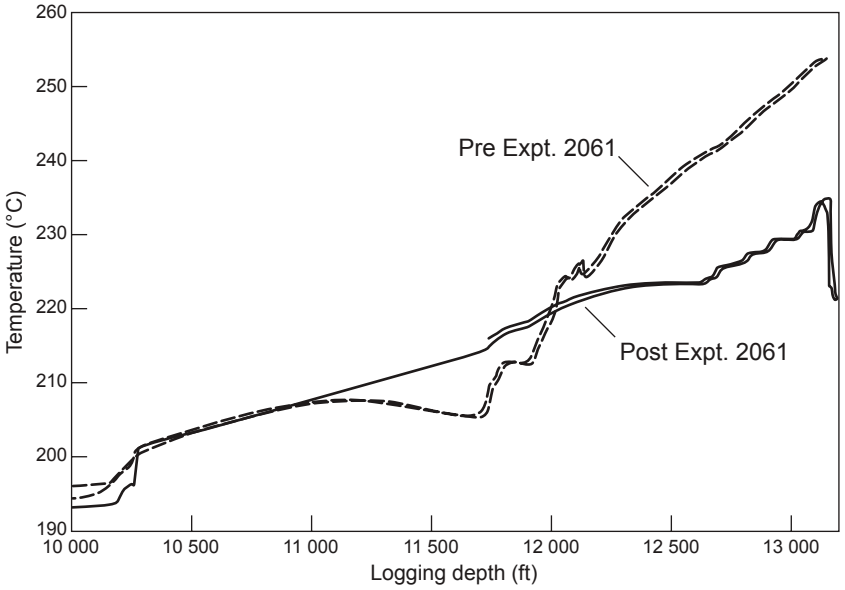

Fig. 6-36. Temperature profiles in EE-3A before and after Expt. 2061. Depths are as recorded in the logging van.
Source: Dash et al., 1985a

Seismic activity was pronounced during Experiment 2061, and many events were large enough to be detected at the surface. Later in the experiment, the locations of the events migrated downward (Fig. 6-37) in a manner similar to that seen during Expt. 2042. However, as seen in the view toward the north, a dense cluster of events in the upper portion of the Expt. 2061 seismic cloud appears to be nearly coincident with a deeper cluster produced during the MHF Test (see Fig 6-22)—which is perplexing, because there was absolutely no indication of flow communication with EE-2.

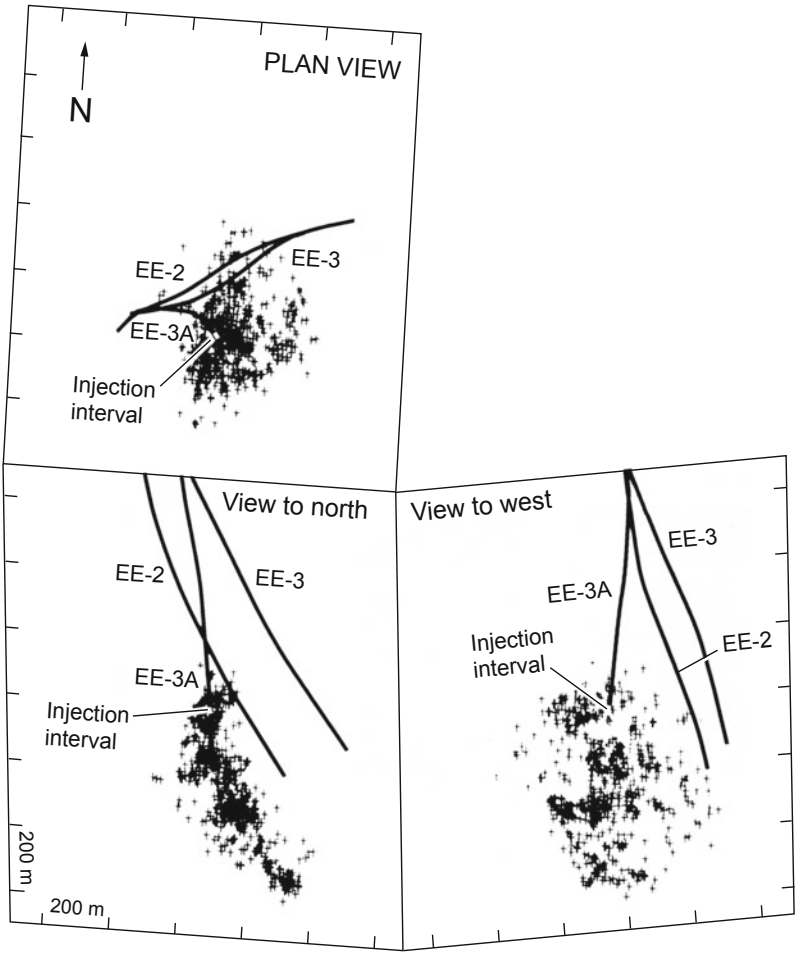

Fig. 6-37. Seismicity generated during Expt. 2061.
Source: HDR, 1987

Experiment 2062

Experiment 2062, the second experiment to succeed in connecting the two boreholes across the MHF Test stimulated region, was performed July 18–20, 1985. In preparation for this experiment, the EE-3A borehole was sanded back from its final drilled depth of 13 182 ft to 12 561 ft, to close off flow access to the deeper region—below the Phase II reservoir—stimulated during Expt. 2061. On July 18, a Lynes inflatable packer was run in on drill pipe and set at a depth of 11 976 ft. The 585-ft stimulation interval thus created overlapped to some extent the Expt. 2059 stimulated interval (11 537–12 203 ft).

Experiment 2062 lasted 84 hours; a total of 1.52 million gal. was injected into EE-3A, at an average rate of 7.2 BPM. This experiment improved the flow connections to EE-2 across the Phase II reservoir by activating several other previously stimulated joints. It was also evident that the main EE-2 connection to the reservoir was now via the inner annulus (instead of the original EE-2 injection interval below the casing, which by this time was totally plugged with sediment).

Because previously opened connecting joints were being reinflated during Experiment 2062, seismic activity was much more moderate (one event every 10 to 15 minutes) and the number of events detected at the surface was much smaller than during the previous experiment (Expt. 2061).

The injection-pressure and flow-rate profiles for Expt. 2062 are shown in Fig. 6-38.

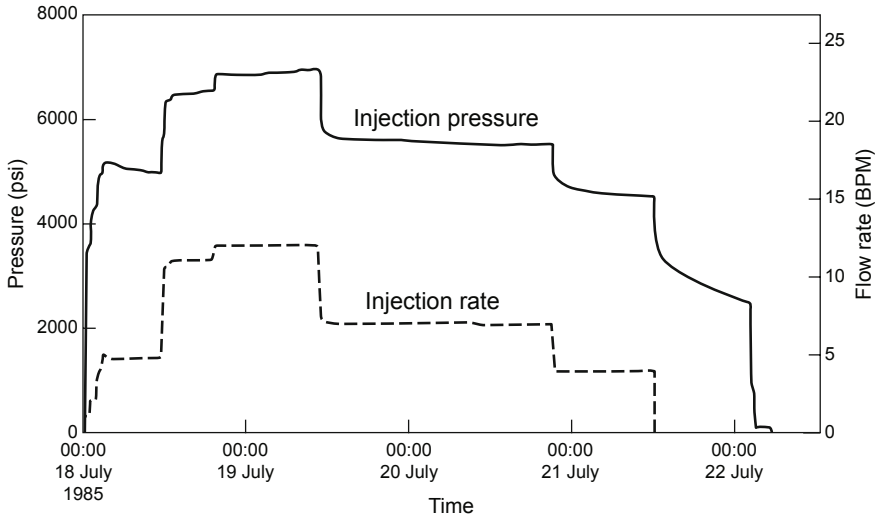

Fig. 6-38. Injection-pressure and flow-rate history for Expt. 2062. Source: Robinson et al., 1985

If one compares this injection-pressure profile with those for Expts. 2020 and 2061 (Figs. 6-9 and 6-35), it is clear that Expt. 2062 was simply reinflating the Phase II reservoir by repressurizing previously stimulated joints. As seen in Fig. 6-38, near the end of the experiment, at a flow rate of 4 BPM, the injection pressure leveled off at about 4400 psi—far below the joint-extension pressure of 5500 psi. Thus, the injection of over 1.5 million gal. of water accomplished nothing more than a reinflation of the Phase II reservoir (with no further growth).

This experiment did, however, provide the best measure yet of the true reservoir joint porosity at an inflation pressure of 4400 psi. Using the 2σ seismic reservoir volume of 130 million m^3 and a fluid volume of 1.5 million gal. within the open network of joints, one obtains a porosity of 0.44×10^{-4}.

Figure 6-39 shows the EE-3A temperature profiles before and after Expt. 2062. The principal joint entrance was at about 12 000 ft, and secondary entrances are visible at 12 050 ft and 12 300 ft.

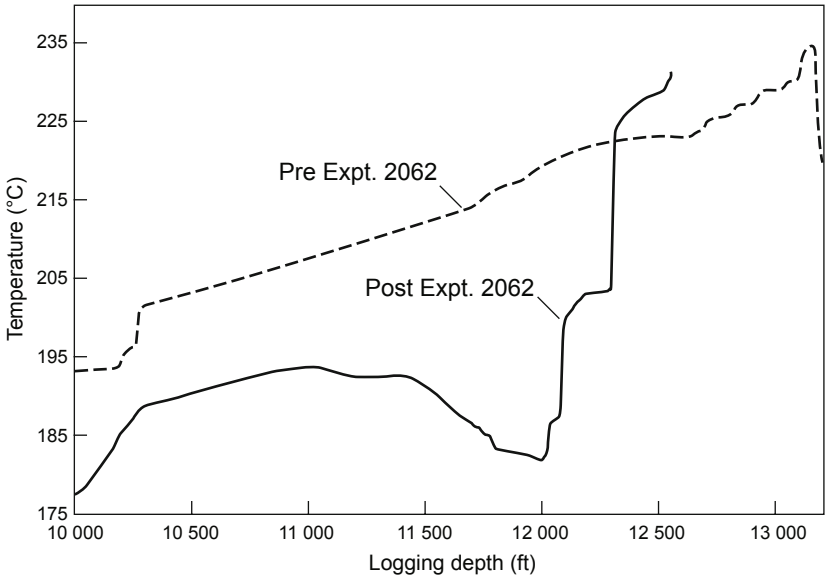

Fig. 6-39. Temperature profiles in EE-3A before and after Expt. 2062. Source: Robinson et al., 1985

Experiment 2066—A Seismic Anomaly

Given the success of Expt. 2062 in improving the reservoir flow connectivity between EE-3A and EE-2, the Project staff re-examined the results of Expt. 2061, which had not achieved a flow connection. The six small fluid entrances shown in Fig. 6-36 were intriguing, because they possibly offered the opportunity of opening several deeper—and hotter—reservoir flow connections from EE-3A. Experiment 2066, carried out January 30–February 1, 1986, was an attempt to open one or more of these potential connections. The sand was washed out of the bottom of EE-3A, then the borehole was sanded back up to a depth of 12 850 ft (drill pipe measurement).

A Lynes inflatable packer—the last one to be used at Fenton Hill—was set at 12 350 ft, in one of the few remaining good sections of the EE-3A

borehole (apparently, pressure spallation was taking its toll on the borehole surface following several cycles of pressurization). The open-hole stimulation interval thus isolated was 500 ft long. (Note: Following Expt. 2066, the Lynes packer could not be recovered from the borehole and was abandoned in place, with some associated piping extending up to 12 272 ft. To make sure that the Expt. 2066 interval was sealed off from the upper part of EE-3A, a barite plug and then a sand plug were placed on top of the packer assembly, with the top of the sand at 12 235 ft.)

Some 996 000 gal. of water was injected during Expt. 2066, at an average rate of 7.5 BPM. The injection-pressure and flow-rate profiles are shown in Fig. 6-40.

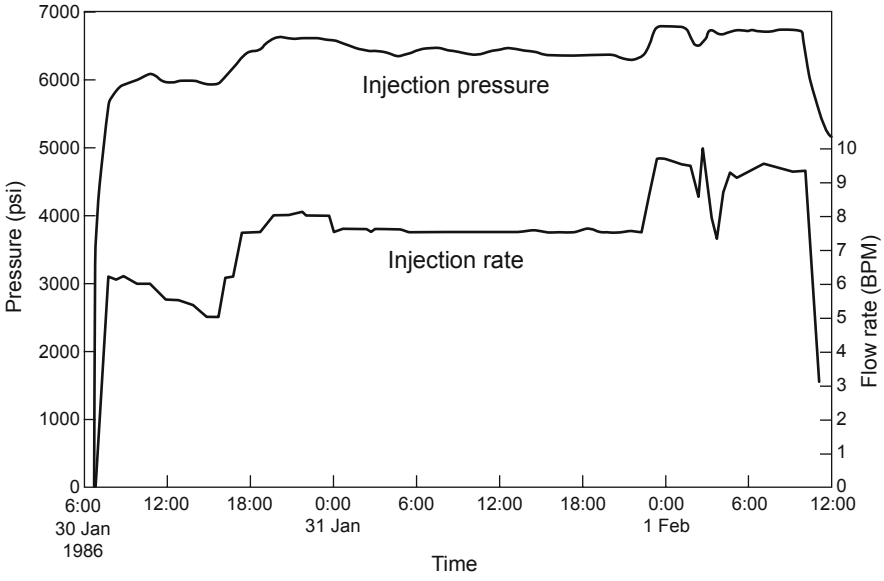

Fig. 6-40. Injection-pressure and flow-rate history for Expt. 2066.
Source: HDR Project files

The similarity of this pressure profile to that of Expt. 2061 (Fig. 6-35) suggests that a previously unstimulated rock mass was now being pressurized. However, this new region was in very close proximity to the Phase II reservoir, rather than below it as was the case for Expt. 2061. In fact, as shown in Fig. 6-41, a good portion of the Expt. 2066 seismicity fell essentially on top of the lower part of the MHF Test seismicity.

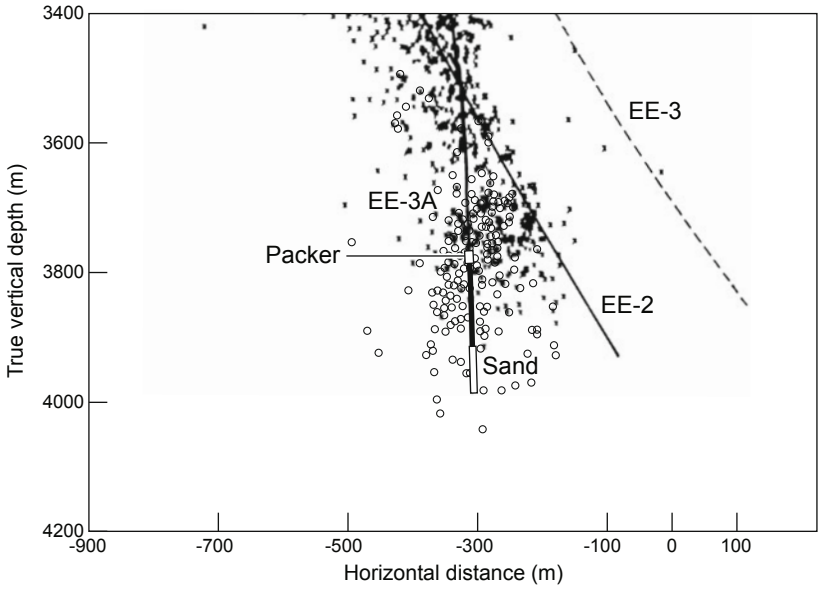

Fig. 6-41. The seismicity generated during Expt. 2066 (open circles) compared with the lower part of the seismicity generated during the MHF Test (viewed to the north). The trace of the Expt. 2066 injection interval is visible near the bottom of the figure, between the packer and the sand plug. Adapted from HDR, 1987

This figure illustrates the "seismic anomaly" of Expt. 2066: how could two large seismic regions fall essentially on top of one another without flow connectivity between them? Given the limited scope of Expt. 2066, this question can be answered only partially, on the basis of the related information that is available. Apparently, for the MHF Test stimulated region, the well-connected joints within the body of the reservoir did not extend all the way to the edge of the microseismic cloud. Although the seismic events at the cloud's edge were undoubtedly produced by the action of high-pressure water along the periphery of the extending reservoir, the joints in that region do not appear to be well connected to the "body" of the reservoir.

The most likely explanation is as follows: When the Phase II reservoir was initially created during the MHF Test, the joints at the periphery of the expanding reservoir were extending at a pressure of about 5500 psi. By the time of Expt. 2066, this reservoir region had deflated and those peripheral joints were being held tightly shut by a closure stress of several thousands of psi. The mechanics governing how the growing Expt. 2066 stimulated region could extend into the periphery of the previously pressure-opened MHF Test region is an issue that only a sophisticated coupled analysis could resolve. (This analysis would explore the interactions between the changing

fluid pressure and stress fields surrounding a set of joints extending into a previously stimulated region, with its previously altered stress field—a very good topic for a Ph.D. dissertation in rock mechanics!)

Only several years later, during static reservoir pressurization testing (Expt. 2077 in 1990—see Chapter 7) would it become clear that with lower reservoir-operating pressures—in this case more than 3000 psi lower than the joint-opening pressure—a large portion of the reservoir periphery was being held tightly closed, severely inhibiting fluid access to these peripheral regions.

The "seismic anomaly" depicted in terms of cumulative locations in Fig. 6-41 is illustrated from a different perspective in Fig. 6-42: the temporal variation of the focal depths for the induced seismicity during Expt. 2066. This distribution shows that although nearly all the events occurred below a depth of 3600 m (12 000 ft), they showed some downward growth only during the first half of the experiment, then stabilized in the second half. (Other seismic data plots—not shown—indicate that the Expt. 2066 seismic cloud showed some growth toward the south.)

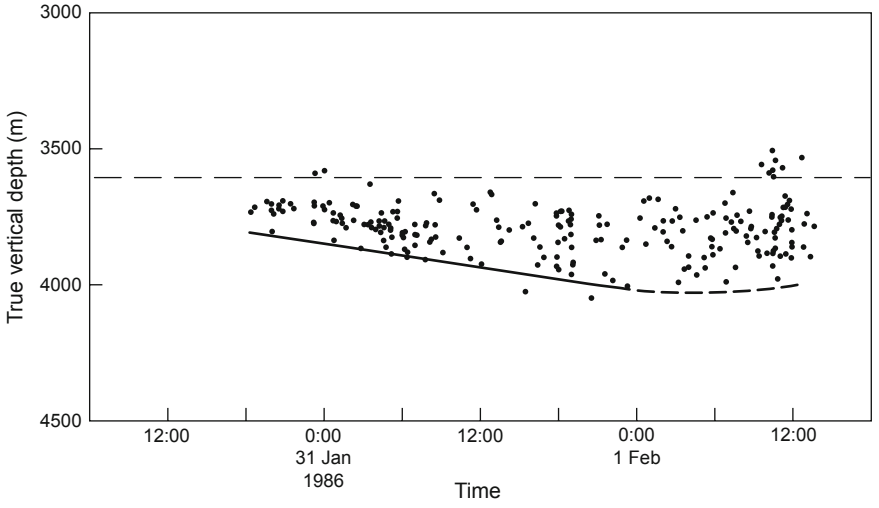

Fig. 6-42. Temporal variation in the focal depths of the microseismic events located during Expt. 2066.
Source: HDR Project files

Fenton Hill "Resurrected"—A Near-Term Possibility?

As discussed earlier, it was observed at Fenton Hill that the outer boundary of the seismic cloud lies beyond that of the circulation-accessible portion of an HDR reservoir, which occupies a somewhat smaller volume. Thus, it is possible to drill a production borehole into a seismically defined "reservoir region" but miss the circulation-accessible reservoir, so that no flow communication is achieved. In attempting to connect a borehole to an HDR reservoir, therefore, the dilemma is: Where should one drill to best access the circulation-accessible reservoir volume? Although seemingly simple, all of HDR reservoir engineering hangs on this question. If the reservoir cannot be connected back to the surface, there is no HDR system at all! And because the residual stress cage surrounding a pressure-stimulated HDR reservoir poses a substantial obstacle to the establishment of production flow, this issue is far from a trivial one. The very valuable lessons about HDR reservoir completion learned from Expts. 2059, 2061, 2062, and 2066 need to be kept firmly in mind.

Obviously, the EE-3A borehole penetrated the circulation-accessible volume of the Phase II reservoir during both Expts. 2059 and 2062, as evidenced by the paucity of seismicity and the very gradual rise in reservoir inflation pressure (Figs. 6-31 and 6-38). In the event that the Phase II reservoir at Fenton Hill can be brought back on line in the near future, it will be necessary to drill two new production wells near the ends of the seismically delineated reservoir region, to complete the HDR circulation system. Ideally, there would be a method of determining the boundaries of the circulation-accessible reservoir, so as to eliminate the risk of having to redrill these new production wells. Unfortunately, to our knowledge no such method yet exists; the best strategy at this time is to *drill well inside the seismic cloud*.

How can one tell whether a production well has been drilled into or outside the circulation-accessible reservoir? If injection pumping is very "stiff"—as it was during Expts. 2061 and 2066 (Figs. 6-35 and 6-40), the production well has been drilled *outside* the circulation-accessible HDR reservoir. (This same injection behavior was seen earlier, in Expts. 2018, 2020, and 2025—see Figs. 6-5, 6-9, and 6-13, which show the injection pressure very rapidly rising to the joint-extension pressure level of 5500 psi.) If injection pumping is "soft," as exemplified by the inflation behavior during Expts. 2059 and 2062 (Figs. 6-31 and 6-38), the production well has been drilled *inside* the circulation-accessible HDR reservoir, and the injected fluid is simply reinflating the region stimulated during reservoir creation.

Completion of the EE-3A Wellbore (May 1986)

The completion of the EE-3A borehole was poorly conceived, unnecessarily complicated, and eventually a failure. Following the deepening of EE-3A to 11 615 ft, a temperature log had shown that the top of the Phase II reservoir was at least as high as 11 440 ft (the highest point of fluid communication from the pressurized Phase II reservoir found during the drilling and testing of EE-3A). Further, there was a low-pressure joint entrance at about 10 260 ft (which should have been cemented-off but never was). Given this knowledge, EE-3A should have been completed such that the portion of the borehole below 11 440 ft remained open to injection and the portion above 11 440 ft was sealed off with good cement—up into the 9 5/8-in. casing and across the "loss" zone at 10 260 ft.

But the completion of EE-3A (designed by a contract drilling engineer with input from several HDR staff) was instead as shown in Fig. 6-43: A cemented-in 5 1/2-in. liner and a 4 1/2-in. tie-back string of special L-80 tubing were installed, with a PBR assembly on top of the liner and a matching mandrel (with seals) on the bottom of the tie-back string. This approach was probably driven by worries about thermal contraction imposed on the pipe during cold injection; but thermal contraction could have been better dealt with by cementing-in a full-length string of 7-in. casing (as would later be done for the completion of EE-2A in late 1987).

Further, this completion specified that the liner would be tag-cemented only over its bottom 860 ft (11 810 to 10 950 ft). During the development of the Phase II reservoir, several liners had been tag-cemented from the surface in the conventional way (cement pumped down the drill pipe, through the liner, and then back up the annulus). Despite these past successes, an untried (at least at Fenton Hill) technique of tag cementing was decided upon. First, the borehole was sanded back to 11 810 ft; next, the liner was lifted up off the sand plug as the cement was pumped down through the drill pipe and out the liner (which was fitted on bottom with a cement shoe incorporating a check valve), forming a long "plug" of cement on the bottom of the hole. The liner was pulled up out of the cement plug, then lowered back down—but unfortunately, the cement "flash-set" before the liner could be lowered all the way to 11 810 ft. Its bottom end stopped at 11 436 ft. With the top of the cement at 10 950 ft, 1665 ft of the open borehole above it was left uncemented—up to 9285 ft (the bottom of the 9 5/8-in. casing, which had been cut in preparation for the sidetracking).

Note: As shown in Fig. 6-43, *following* the completion of EE-3A, temperature logging identified the intersection of a high-pressure joint—at 10 840 ft—emanating from the high-pressure Phase II reservoir. Although it would not be clearly manifested until the ICFT, when a small (3- to 4-gpm) annular bypass flow developed between the tie-back string and the 9 5/8-in. casing (see Chapter 7), the presence of this joint suggests that the Phase II reservoir extended at least as high as 10 840 ft.

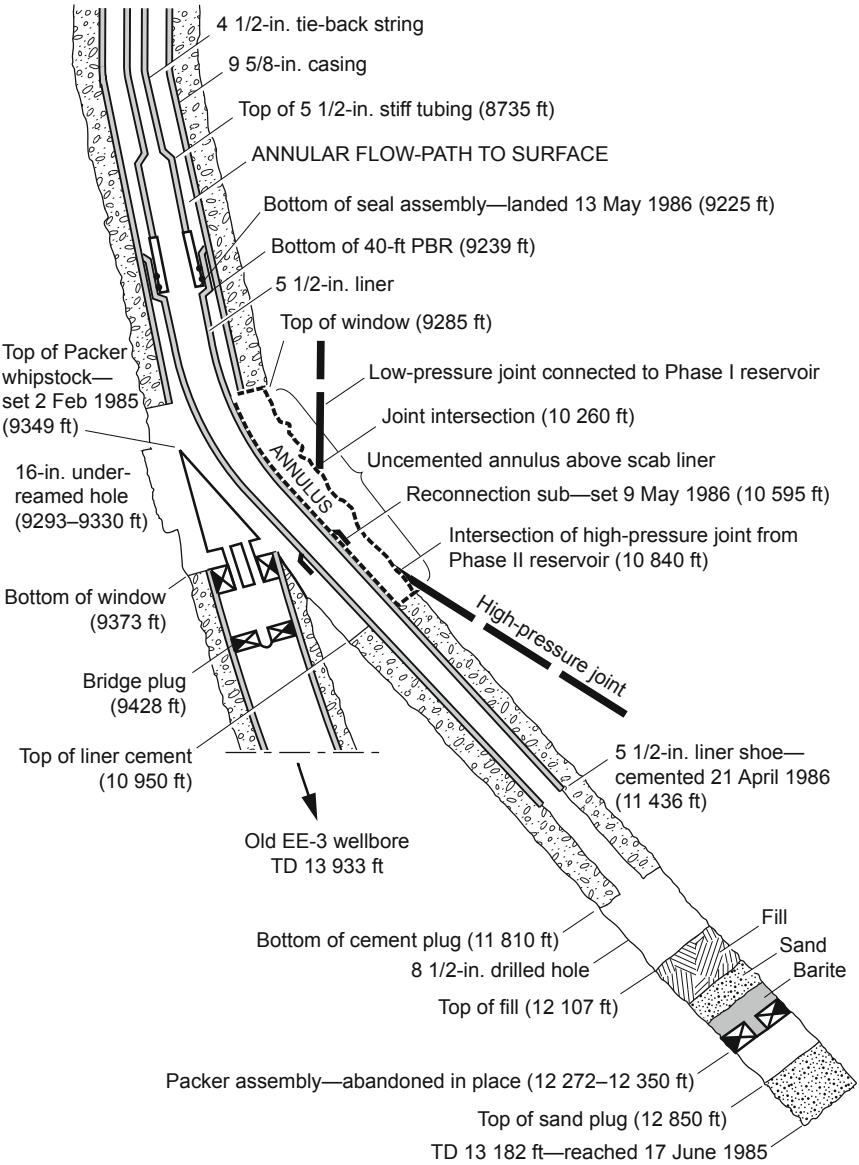

Fig. 6-43. Completion of the lower part of EE-3A.
Source: HDR Project files

A cement-bond log run after the 5 1/2-in. liner had been drilled out and the sand plug removed down to a depth of 12 235 ft showed that the seal between the bottom of the liner at 11 436 ft and a depth of about 10 950 ft was good; the liner was judged to be satisfactory for the upcoming ICFT. At the same time, it is important to remember that the open annulus between the cement at 10 950 ft and the 9 5/8-in. casing at 9285 ft (labeled ANNULUS in Fig. 6-43) acted as a manifold, connecting the high-pressure frac-around of the cemented portion of the EE-3A liner to the low-pressure joint at 10 260 ft—and thereby connecting this annulus to the Phase I reservoir.

The Completion of the Phase II Reservoir: A Summary

Figure 6-44, a comparison plot of three temperature logs performed in EE-3A following Expts. 2059, 2061, and 2062, provides a "picture" of the development of the Phase II reservoir connections to EE-3A.

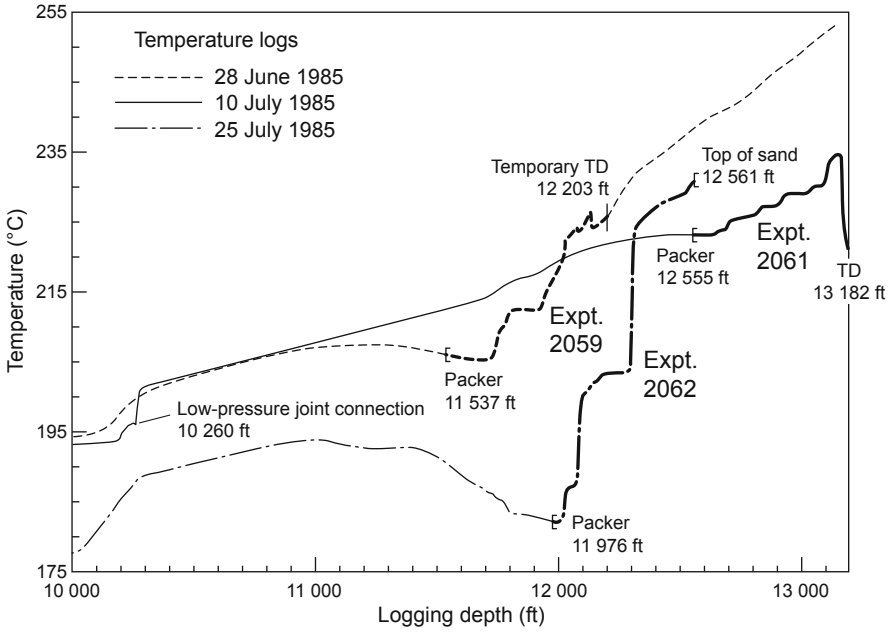

Fig. 6-44. Temperature logs in EE-3A following Expts. 2059, 2061, and 2062 (the thicker segment of each curve denotes the experimental interval). Source: HDR Project data archives

The connections developed during Expt. 2059 are seen at depths of 11 730 ft and 11 930 ft, while the major connection developed during Expt. 2062 was at about 12 000 ft, just below the packer setting depth (11 976 ft). The deepest connection was the one developed during Expt. 2062, at 12 300 ft. Note that the temperature log for Expt. 2061 shows a complete absence of reservoir connections below 12 555 ft, but shows clearly the low-pressure joint connected to the Phase I reservoir (at 10 260 ft), opened when the annulus above the packer was again pressurized with the rig pumps.

Finally, as can be seen in Fig. 6-43, the completion of EE-3A resulted in a very limited injection interval. Only the short section from 11 436 ft to the top of the fill at 12 107 ft—a total of about 670 ft—was now available for flow connections into the body of the high-pressure Phase II reservoir. Since a horizontal connection model is irrelevant for the multiply jointed and interconnected Phase II reservoir, a much greater range of depths should have been provided. Both temperature logging and tracer testing several years later, during the LTFT, would show that the injection-cooled region surrounding EE-3A extended not only to the physical bottom of the borehole, but below it: most of the injected fluid was exiting EE-3A near the bottom of the open-hole interval.

Chapter 7

Initial Flow Testing of the Phase II Reservoir, Redrilling of EE-2, and Static Reservoir Pressure Testing

The demonstration of flow connectivity between the redrilled EE-3A wellbore and the EE-2 reservoir zone (Expts. 2059 and 2062) made it clear that a viable HDR system had finally been established, although that stage of the Fenton Hill HDR Project took about five years (1980–1985)—much longer than originally anticipated. Throughout that period, Germany and Japan contributed both funds and manpower to the effort. The Germans withdrew from the Project at the end of 1985, but the Japanese maintained a presence through the following year. In early 1986, they began pressing strongly for the thermal and flow characteristics of the HDR system to be evaluated.

But the lower part of the EE-2 wellbore had twice sustained casing damage. The first episode took place immediately following the MHF Test in December 1983. Repair work done in the fall of 1984 (see Chapter 6) did succeed in restoring EE-2 to a usable condition, with a high-pressure flow connection clear down to the top of the sand plug, then at 11 642 ft; but EE-2 was also open to the Phase II reservoir through high-pressure joints connected to splits in the casing at 10 740 ft and 10 900 ft. The second episode of casing collapse, in May 1985, rendered wireline logging in the lower part of the wellbore impossible—but at the time the reason for the logging problems was unknown (this further damage to the casing would not be discovered until November of 1986, 18 months later).

At this juncture, then, the most reasonable option for testing the Phase II reservoir was to make EE-2 the production well and EE-3A the injection well.

Summary: The Initial Closed-Loop Flow Test, Second Attempt to Repair EE-2, Redrilling of EE-2, and Extended Static Testing of the Phase II Reservoir

The Initial Closed-Loop Flow Test (ICFT) greatly enhanced our knowledge of the Phase II reservoir, providing information critical for establishment of operating parameters for the later Long-Term Flow Test (LTFT—see Chapter 9). In addition, the ICFT demonstrated, for the first time, the significant power-producing potential of an HDR reservoir: the achievement of a sustained thermal power production of 10 MW heralded a future three-well strategy that could enable output levels of 20 MW or more, with minimal water loss.

D.W. Brown et al., *Mining the Earth's Heat: Hot Dry Rock Geothermal Energy*,
DOI 10.1007/978-3-540-68910-2_7, © Springer-Verlag Berlin Heidelberg 2012

Following the ICFT, a second attempt was made to repair the regions of collapsed casing at 10 740 ft and 10 900 ft in the EE-2 wellbore. It was during these operations that the second episode of casing collapse, which had taken place in May 1985 at 10 512 ft, was finally discovered. Given its condition at that time—with three regions of collapsed casing, sections of pipe stuck at various depths, and unsealed perforations in the casing at 9100 ft—the wellbore was deemed practically beyond repair. The consensus was that redrilling would be the best solution, by sidetracking EE-2 from just above the highest damaged section and drilling along a trajectory close to that of the original borehole. This undertaking turned out to be a major one, consuming most of the (continually shrinking) HDR budget during 1987–1988; but it was essential to provide a competent production well for sustained flow testing during the LTFT.

The redrilling operation was very successful, and in June of 1988, after preliminary flow testing, the new EE-2A wellbore was completed. An extended static pressure test of the reservoir concluded this pre-LTFT period. It yielded valuable insights regarding the water-loss behavior of a tight HDR reservoir under conditions of constant pressurization. Following this period, the focus of the work at Fenton Hill turned to construction of a permanent surface plant (described in Chapter 8).

The Initial Closed-Loop Flow Test

It was mainly under pressure from the Japanese, who were eager to see a closed-loop flow test of the Phase II reservoir while they were still part of the Project, that the 30-day ICFT took place in the late spring of 1986 (May 19–June 18). But its design and execution at this time meant the postponement of many necessary repairs and improvements to the surface facilities, and to the EE-2 wellbore, the unsound condition of which made it usable only as a production well. Although the reservoir had been created during the MHF Test and then developed as an HDR circulating system by the redrilling of EE-3A through the microseismic cloud, the ICFT was the first experiment specifically designed for the production of energy from the Phase II reservoir. The information in this section is based mainly on the comprehensive report on the ICFT published by Dash et al. (1989).

Envisioned as a precursor to a long-term (ca. 1 year) flow test, the ICFT had two principal objectives:

- To demonstrate that significant amounts of power could be produced from the Phase II reservoir on a sustained basis

- To quantify the characteristics of the reservoir, as a basis for establishing operating parameters for the LTFT

Ancillary ICFT objectives aimed at gathering the information needed to design a productive LTFT were the following:

- To measure important system parameters (such as flow rate, impedance, water loss, and microseismic activity) at two quasi-steady-state injection-pressure levels: moderate and high
- Through tracer experiments, to determine fluid dispersion and estimate the through-flow fluid volume of the reservoir (the volume of fluid flowing through the network of interconnected joints at a selected time) at each of the two injection-pressure levels

By the time of the ICFT, both the injection and production wells had undergone considerable reworking. In Well EE-3A, the open-hole interval extended from the bottom of the scab liner at 11 436 ft to the top of the fill at 12 107 ft, and included a number of joints—at least four and possibly as many as eight—pressure-opened during Expts. 2059 and 2062. This interval had last been pressurized in July 1985, during Expt. 2062. (Expts. 2061 and 2066, injection tests carried out in EE-3A in early 1986, opened up joints in a region below the Phase II reservoir; neither test achieved any discernible connection to Well EE-2.) Thus, Well EE-3A had been essentially quiescent for some 10 months before the start of the ICFT.

The configuration of the EE-2 wellbore at the time of the ICFT is shown in Fig. 7-1. The portion of the open-hole interval stimulated during the MHF Test extended 70 ft, from the casing shoe at 11 578 ft to a sand plug at 11 648 ft (the 6 ft of debris in this interval had been washed out during Expt. 2059).

The figure also shows the zones of casing collapse. The first episode (at the end of the MHF Test in December 1983, when the casing collapsed—and split—at 10 740 ft and 10 900 ft) opened the inner annulus to the high-pressure reservoir via the two pressure-stimulated joints at these depths; but it also damaged the 5 1/2-in. frac string and obstructed logging into the MHF Test interval. Logging access was restored during repair operations in December of 1984, after which an Otis steam packer was set at 10 401 ft. The injection testing that followed revealed a continuing flow connection from below the packer to the high-pressure reservoir through the splits in the casing. The second episode of casing collapse took place in May of 1985, when the 9 5/8-in. casing collapsed onto the 7-in. transition casing below the Otis packer, once again obstructing logging into the MHF Test interval. But this collapse would remain undiscovered until 1986, several months after the ICFT.

Figure 7-1 also shows the locations of the remedial cementing operations described in Chapter 6 and the intersections of the high-pressure joints at 10 740 ft and 10 900 ft, identified during Expt. 2052 (pressurization of the Phase II reservoir through EE-2 during the drilling of EE-3A).

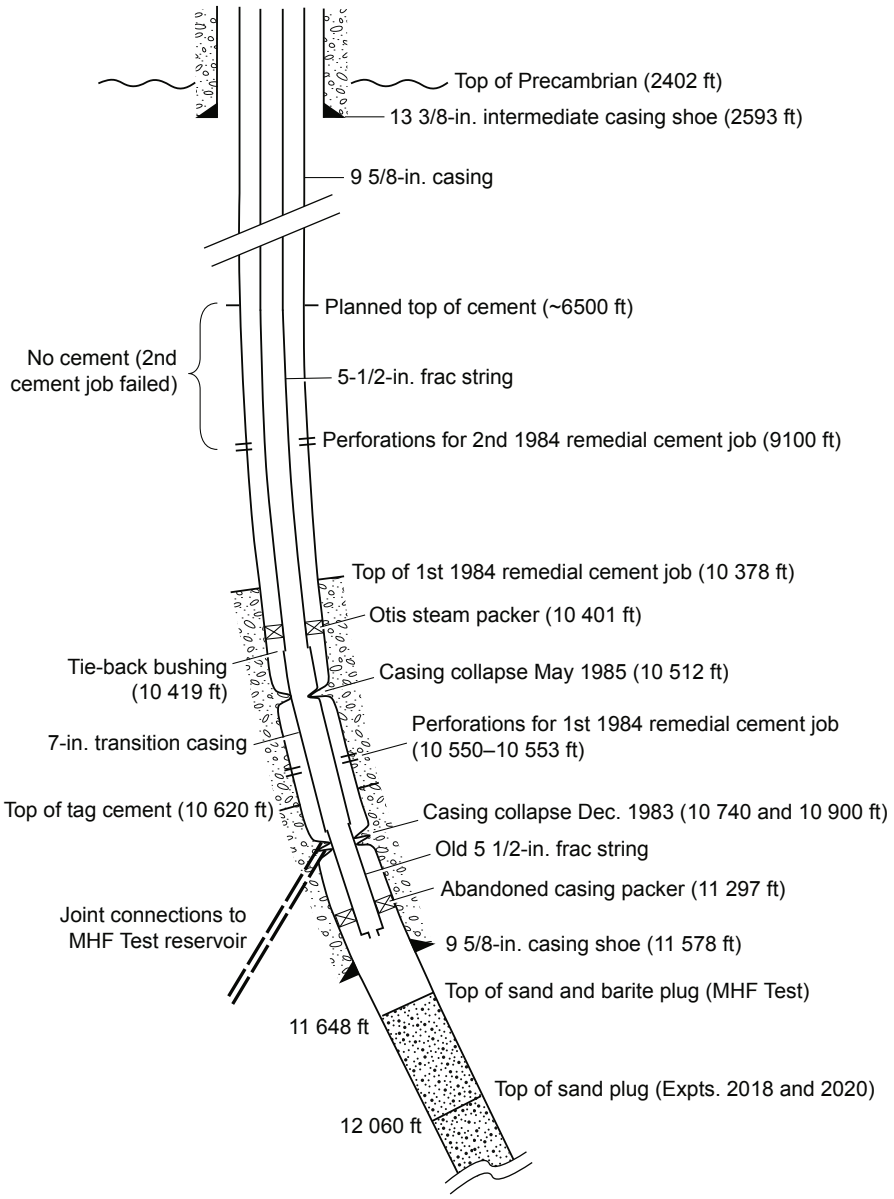

Fig. 7-1. Configuration of the EE-2 wellbore during the ICFT. Adapted from Dreesen et al., 1989

The Surface Facilities

The temporary, experimental surface facilities constructed for the ICFT included the EE-2 and EE-3A wellheads, the diagnostics and reservoir production flow-control sections (up to the air-cooled heat exchanger), the makeup-water system, the main (rental) circulating pumps, the chemical-sampling system, and a venting system connected to both wellheads that would separate contained gas in solution from the fluid. These facilities, shown in Fig. 7-2, incorporated much of what would eventually be the surface plant for the LTFT—the preliminary design for which was also completed during the period leading up to the ICFT.

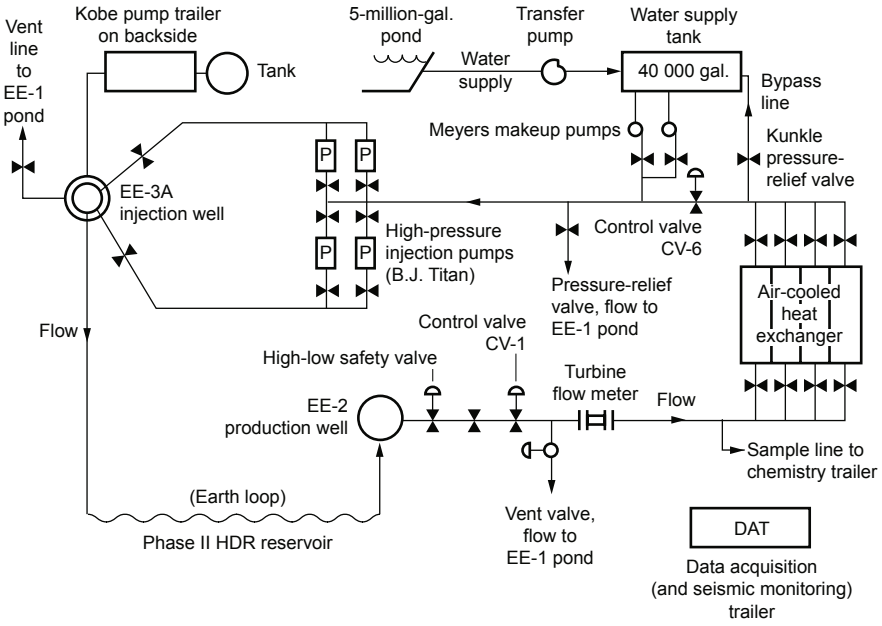

Fig. 7-2. Schematic diagram of the surface facilities for the ICFT. Source: HDR, 1989a

The surface piping that joined these various components was divided into six zones, according to pressure rating.[1]

Zone 1 consisted of the short section of high-pressure pipe between the EE-2 wellhead (API-rated at 10 000 psi) and the high-low safety valve

[1]To avoid confusion, the piping shown in Fig. 7-2 is greatly simplified. The surface facilities at Fenton Hill developed gradually, over many years, and included a multitude of piping networks and interconnections that could not possibly all be represented.

(rated at 5000 psi). This zone included the wellhead master valve, wing valves, and 15 000-psi-rated hammer union pipe and pipe fittings. The high-low safety valve automatically shut in the well if the EE-2 production pressure exceeded 700 psi (to protect downstream components rated for lower pressures) or dropped below 250 psi (to prevent flashing of the production fluid).

Zone 2 comprised the piping between the high-low valve and control valve 1 (CV-1). The latter valve was rated at 1500 psi and had a 3000-psi working pressure at 400°F; its function was to drop the pressure from Zone 2 to an operating level safe for Zone 3 whenever necessary—as during high-backpressure experiments and while the strainer was being cleaned.

Zone 3 consisted of the components between CV-1 and control valve 6 (CV-6, rated at 600 psi). The piping for the heat-extraction system—part of this zone—was constructed in 1982. The forced-draft, air-cooled heat exchanger, which was equipped with finned tubes, was rated for a working pressure of 2500 psi at 500°F but was hydrostatically tested several times to 2800 psi. Zone 3 piping was also protected by a 1.5-in. × 2.5-in. Kunkle pressure-relief valve having a 0.5-in.^{2} nozzle. This valve could handle flow from the EE-2 well at all specified rates as long as the water had been cooled by the heat exchanger (hot fluid could convert the nozzle to two-phase operation, choking the flow at about 1–2 BPM). The Kunkle valve was set at 600 psi for all the experiments except those high-backpressure experiments during which CV-1 was not used.

Zone 4 encompassed all of the system downstream of CV-6, including the Meyers makeup pumps, and terminated at the suction inlet manifold to the B. J. Titan pumps. This low-pressure zone was protected with a pressure-relief valve, set at 250 psi. The piping included 4-in. Schedule 40 and 160 pipe, 3-in. Schedule 80 and 160 pipe, and 6-in. Schedule 40 and 80 pipe. The rest of the zone was equipped with Schedule 80 and 160 pipe.

Zone 5 comprised the piping between the 5-million-gal. pond and the 40 000-gal., open water-supply tank (this tank provided the suction for the Meyers makeup-water pumps).

Zone 6—possibly the most critical—consisted of the high-pressure contract piping through which water was injected into the reservoir via Well EE-3A. Supplied by the B. J. Titan Co., the piping was rated for a working pressure of 15 000 psi and consisted of 3-in. pipe with hammer unions, valves, etc., feeding the EE-3A wellhead (API-rated at 10 000 psi). The system was assembled around a suction-and-discharge-manifold trailer and four truck-mounted frac pumps that were remotely controlled from a control van. Instrumentation in another van monitored temperature, pressure, and flow (in BPM). Other components of Zone 6 were double 4-in. suction lines and 3-in. discharge lines, used with remotely operated wing valves on the wellhead; and a 2-in. vent line to the EE-1 pond.

Critical components of the surface piping were anchored with precast, concrete safety blocks, about 40 in all.

Circulation Components

The surface portion of the closed-loop circulation system included several important components that had been installed for earlier flow testing:

- The 12-MW, air-cooled, high-pressure heat exchanger (and associated piping) procured and installed in 1977 for flow testing of the Phase I reservoir
- The 5-million-gal. pond, which was constructed before the MHF Test in 1983
- The two Meyers high-pressure, makeup-water pumps
- The 40 000-gal. water supply tank

The lower-pressure production piping—firmly mounted on concrete blocks for stability and security—carried the hot water from the EE-2 wellhead to the air-cooled heat exchanger and then back to the inlet of the injection pumps. Control valves, strainers, sampling ports, makeup-water lines, and a number of flow-monitoring or metering devices were located at various points in the loop. Much of this auxiliary equipment would become part of the permanent surface plant constructed for the LTFT (see Chapter 8).

Data Acquisition and Control

All the monitoring and control functions of the loop, except those directly concerned with the injection pumps or the fluid chemistry, were performed in a data acquisition trailer (DAT). Signals from temperature, pressure, and flow monitors at various points in the loop were received in the DAT, and all data was processed and stored by equipment located there. Commands to change operational conditions could be issued from the DAT, both manually and automatically. In the event of conditions outside the specified range of operating parameters, an alarm would sound, and in certain cases the system would shut down automatically. A small sample line was located between the heat exchanger and the injection pumps, to carry samples of cooled fluid from the loop for immediate analysis in the chemistry trailer, from which both water chemistry and tracer returns were monitored.

Seismic Instrumentation

Seismic monitoring during the ICFT was extensive, carried out via three separate seismic detection networks. The first was the array of nine surface stations installed in 1978 for the Phase I testing, located on a radius about 2 miles (3.2 km) from the EE-1 wellhead. The second was the three-station "Precambrian Network": one geophone package installed near the bottom of the GT-1 borehole in Barley Canyon (at a depth of 2460 ft, nearly 400 ft into the Precambrian granite); and two packages, each at a depth of about 2100 ft, in the PC-1 and PC-2 boreholes (which bottomed in the dense limestone overlying the Precambrian basement rock). The Precambrian Network stations were located approximately equidistant from one another, along the circumference of a circle 1 mile (1.6 km) in radius centered on the

EE-1 wellhead (and thus also centered around the Phase II reservoir). The third network, the wireline-deployed, triaxial geophone package at 9400 ft in EE-1, was much closer to the Phase II reservoir than any of the other seismic detectors. The surface and Precambrian seismic networks were monitored continuously (from the DAT) over the term of the ICFT, but because of temperature limitations the deep triaxial geophone package in EE-1 was deployed only during four periods of high-pressure injection (ranging from 12 to 51 hours), when significant seismic activity was anticipated.

Wellbore Temperature Measuring Equipment

Background (pre-test) and post-test temperature measurements in both wellbores were conducted with Los Alamos logging equipment, as had been done during the Phase II reservoir development experiments. Because of the high wellhead pressures during the ICFT, temperature logging was handled by commercial oil services companies. For logging in EE-3A during high-pressure injection, a grease-injector control head and lubricator combined with a small-diameter electric cable were used; the production well was logged with a small-diameter slick line and a high-temperature Kuster sonde.

Operational Plan

As noted earlier, because of the condition of the EE-2 wellbore in the reservoir region, the original plan to use it as the injection well was changed; it would instead become the production well. The direction of fluid flow employed during the ICFT and all subsequent circulation testing of the Phase II reservoir, thus, would be the opposite of that first envisioned: cold water would be injected into EE-3A and hot water would be returned to the surface via EE-2 (and, later, EE-2A—the redrilled EE-2).

In the interest of expediency—given the long lead times needed to procure reliable, high-quality injection pumps—four service-company frac pumps were rented for the ICFT (despite their rudimentary controls and marginal long-term performance capabilities; this type of pump was designed almost exclusively for short-duration pumping—less than 1 day).

A number of different operating modes were planned for the ICFT, primarily based on varying the injection flow rate and pressure, and the backpressure at the production well. These modes included

- a start-up (reservoir reinflation) mode lasting several days, during which the injection rate would be increased in a number of steps with the production well shut in;
- an open-loop, gas-purging mode lasting 2 days, during which gas dissolved in the reservoir fluid would be circulated out;
- two closed-loop HDR power-production modes (at moderate and high injection pressures and flow rates), during which makeup water would be added as required;

- a vent mode, which would be implemented several times during reservoir production—for example, to flush the system with fresh water or to further purge gases[2] from it;
- a final reservoir shut-in mode, during which the reservoir pressure decay would be monitored.

Start-up Mode: Reinflating the Reservoir

The ICFT (also known as Expt. 2067) began on May 19, 1986, with EE-2 initially shut in. The 40 000-gal. supply tank was filled with water from the 5-million-gal. pond and the makeup-water pumps were started. After the lines had filled with water, the high-pressure injection pumps were brought on line to begin inflating the reservoir in a series of pressure steps. The main results of this step-rate test are shown in Table 7-1.

Table 7-1. Step-rate injection testing of EE-3A (May 19, 1986)

Start time	Flow rate, BPM (L/s)	Injection pressure at end (psi)
16:12	1.7 (4.5)	4060
17:36	3.3 (8.7)	4380
18:49	4.1 (10.9)	4520
20:00	7.4 (19.6)	4990

At 20:18, a small pressure response was seen at the shut-in EE-2. Constant-rate injection, at 4.5 BPM (11.9 L/s), began at 21:15.

Open-Loop Circulation

When the reservoir was sufficiently inflated—i.e., the increase in pressure extended all the way from the inlet side to the outlet side, as evidenced by a consistent pressure rise in EE-2—the system was put into an open-loop circulation mode for 2 1/2 days. During this time, injection had to be shut in several times because of equipment problems as the reservoir was purged of start-up gas (N_2).[3]

[2]Entrained gases proved to be a particularly vexing problem during the ICFT, with venting often required to get rid of them; interestingly, during the LTFT a few years later, no such problems would be encountered (probably because most of these gases had been expelled during the ICFT).

[3]Nitrogen was injected along with water into the EE-3A wellhead to "clean out" the joint flow paths connected to the deep production interval in EE-2. The theory was that as the production fluid neared the surface and the N_2 came out of solution, the buoyant "lift" in EE-2 would be increased and create a surging effect.

Closed-Loop Circulation

Finally, late on May 22, the vent flow to the pond was closed off, flow was directed continuously to the heat exchangers, and the first of the two main pressurized-circulation, closed-loop segments of the ICFT began. Hot water produced from Well EE-2 was piped to the heat exchangers for cooling, then combined with makeup water (drawn as needed by the makeup pumps, from the water supply tank) and fed to the high-pressure injection pumps for reinjection into the reservoir via Well EE-3A. During this first power-production segment (May 22–June 3), injection flow rates and pressures were both moderate (4.0–4.3 BPM [10.6 –11.4 L/s] and about 3900 psi [27 MPa], respectively). Two brief periods of high injection flow and high pressure (about 6.8 BPM and 4500 psi) were interposed about halfway through the segment.

The second segment began on June 3 and lasted until June 18. The injection flow rate and the pressure were both high: a flow rate of 6.8 BPM (18 L/s), with one brief excursion to 10 BPM (26.5 L/s), and an injection pressure of about 4500 psi. At the end of the second segment, injection was terminated and the reservoir was shut in.

ICFT Results

During the 30 days of the ICFT, the system was operated 24 hours a day. A total of 9.76 million gal. (37 000 m^3) of water was injected, of which 6.15 million gal. (23 300 m^3) was produced hot water that had been cooled and then reinjected.

Unfortunately, the rental pumps either required maintenance or failed completely a number of times during the 30-day test, leading to multiple brief shut-ins of the injection well. Thus, the hoped-for staged flow test, with two steady-state segments, essentially turned into two nominal-injection-rate tests, each consisting of a series of injection-pressure transients interrupted by flow shut-ins. Only a few brief periods of what could be considered close to steady-state reservoir operation were actually achieved; and the desired near-constant levels of injection pressure for the two flow segments were only marginally achieved. Further, because of the problems with the rental pumps, injection flow rate had to be used as the primary control parameter rather than injection pressure (of course, the injection flow rate—in tandem with the degree of reservoir inflation and, to a lesser extent, the reservoir injection impedance—determines the injection pressure at any point in time).

For the production well, the backpressure was maintained at a fairly constant level of between 200 and 500 psi (1.4 and 3.4 MPa), ensuring single-phase flow from the well and through the heat exchanger. The flow rate and temperature of the produced fluid were determined partially by the degree of reservoir inflation, partially by the backpressure, and partially by the hydraulic and thermal interactions that took place as the fluid passed through the reservoir rock.

The two curves of Fig. 7-3 are profiles of the injection pressure and injection flow rate over the course of the ICFT (these were drawn from 15-minute, time-averaged data points, so that most of the 18 brief shut-ins of the system are not shown).

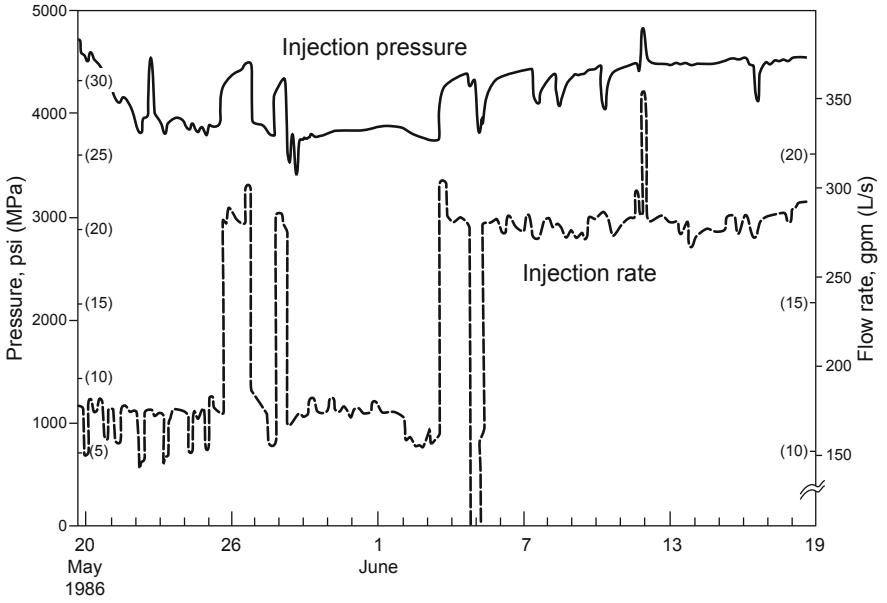

Fig. 7-3. Pressure and flow rates at the EE-3A wellhead during the ICFT. Source: Dash et al., 1989

Circulation Performance

Figure 7-4 charts the general course of three important circulation parameters over the duration of the ICFT. As can be seen, during the first (moderate-flow/moderate pressure) segment of the ICFT, the production flow rate increased gradually, while the production temperature rose rapidly to about 190°C. Water loss declined rapidly during this segment, to a final value of about 30%. At the beginning of the second segment, water losses increased sharply at the higher injection pressure and flow rate, then again declined, reaching a final value of about 30% at a very significant production flow rate of 220 gpm at 200°C.

Note: The "water-loss" shown in this figure is actually a composite loss, derived simply by subtracting the production flow rate from the injection flow rate. As such, this "loss" number includes at least two categories of stored reservoir fluid that, being recoverable from the reservoir region, are not actual losses: (1) the fluid required to inflate the existing (previously

stimulated) joint network; and (2) the fluid stored in newly opened joints, i.e., during reservoir extension. Only fluid that flows from the pressurized reservoir region to the far field is actually a water loss; but that loss could not be independently determined given the difficulty of quantifying the two categories of storage.

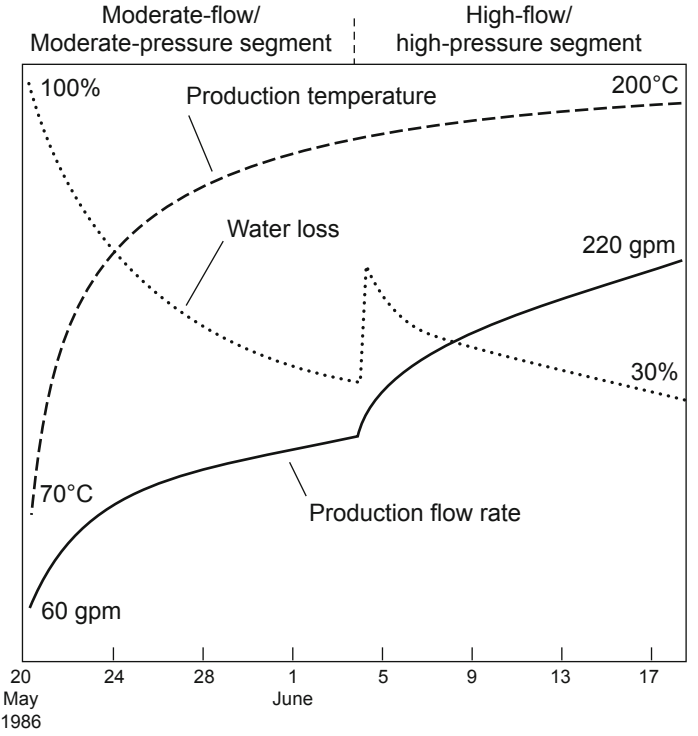

Fig. 7-4. Production temperature, production flow rate, and percent water loss during the ICFT.
Source: HDR, 1993

Most of the increase in the production flow during the first closed-loop segment of the ICFT was undoubtedly due to the decreasing rate of fluid storage in the dilating joints within the region pressure-stimulated during the MHF Test. Seismic surveillance showed that there was no reservoir growth at the boundaries during this segment. The simultaneous increases in the production flow rate and the water-loss rate at the beginning of the second closed-loop segment were due, of course, to the higher injection flow, which raised the pressure level within the reservoir. Although much of this additional flow went into the further pressure-dilation of existing joints and—as evidenced by the strong seismic activity—to the opening of new joints, a

significant portion showed up as increased flow at the production wellhead. Once the existing and newly opened joints had become fully dilated at the imposed higher reservoir pressure, and the rate of further joint-opening had leveled off, the water-loss rate resumed its gradual decline. Unfortunately, the conditions of the second segment of the ICFT, with continuous enlargement of the pressure-stimulated region, made it impossible to evaluate just how low water losses might fall were the reservoir not expanding.

Figure 7-4 also shows that the production temperature increased over the course of the ICFT, attributable in large part to heating of the production wellbore early in the test. The higher flow rate during the second closed-loop segment of the test meant less time for the fluid to cool as it traveled up the production wellbore.

If one considers only the issue of productivity, the data of Fig. 7-4 demonstrate that higher injection pressures do lead to greater reservoir productivity—but at the cost, at least temporarily, of higher "water losses" as the reservoir grows. In fact, in such a transient mode of operation, in which pressures at the reservoir periphery are high enough to extend existing joints or induce the opening of new ones (as indicated by renewed seismic activity), not only are water losses initially excessive but almost all aspects of reservoir performance become more difficult to assess.

Power Production

The rate of power production—a function of production temperature and flow rate—increased with time over both the moderate-flow/moderate pressure and high-flow/high-pressure segments of the ICFT, eventually reaching about 10 MW_{th} (Fig. 7-5). In the figure, the numerous shut-in periods have been removed to smooth the curve and make the overall trends more evident.

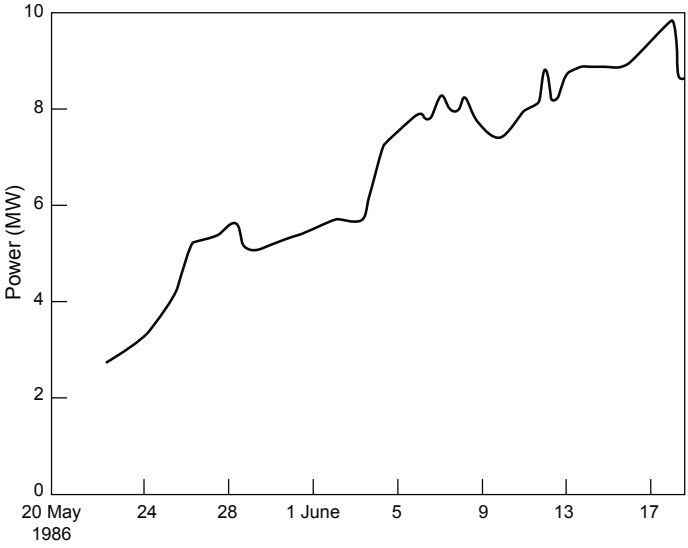

Fig. 7-5. Rate of power production increase with time during the ICFT.

Table 7-2 summarizes the operating conditions and resultant power production during a selected period of quasi-steady-state operation near the end of each test segment. (Note: the Laboratory's injection flow measurements, obtained from an in-line turbine flow meter, were recorded in gpm.)

Table 7-2. Operating conditions during two quasi-steady-state periods representing the two segments of the ICFT

Operating conditions	Moderate-flow/ moderate-pressure period (1–2 June 1986)	High-flow/ high-pressure period (18 June 1986)
Injection		
Flow rate, gpm (L/s)	179 (11.3)	290 (18.3)
Pressure, psi (MPa)	3890 (26.8)	4570 (31.5)
Temperature, °C	18.5	16
Production		
Flow rate, gpm (L/s)	135 (8.5)	214 (13.5)
Pressure, psi, (MPa)	351 (2.4)	500 (3.4)
Temperature, °C	173	190
Rate of water loss, gpm (L/s)	44 (2.8)	76 (4.8)
Thermal power production, MW	5.6	9.8
Flow impedance, psi/gpm (MPa per L/s)	26 (2.9)	19 (2.1)

One feature of reservoir performance shown in this table is striking: The increase in flow rate with increasing pressure is more than linear. A 17 1/2% increase in injection pressure between the moderate and high-pressure segments gave rise to a 62% increase in flow rate (from 179 to 290 gpm). This reservoir behavior is probably closely related to the nonlinear manner in which the joints dilate as they are pressurized.

The ultimate objective of all HDR research and development work is, of course, power production. The power generation data in the table for the high-pressure (seismic) segment of the ICFT are particularly promising in this regard—and even more so considering that during that time, water losses were substantial owing to reservoir growth in the region not accessed by the production wellbore.

If the ICFT Had Reached Steady-State Operation, the Ultimate Produced Power Would Have Been Considerably Higher

The ICFT, unfortunately, never achieved steady-state operation, as is clearly shown in Fig. 7-4. True steady-state flow conditions would probably have been reached in another month or so if the test had continued. Particularly during the second segment, the production flow rate was still increasing quite rapidly, and would probably have reached about 260 gpm in a few more weeks. Similarly, the percentage water loss appeared to be falling toward 20% in the same period of time—even in the presence of continuing reservoir growth to the south—and this decline would no doubt have continued. Finally, the production temperature would probably have topped out at about 210°C. Taken together, these trends imply an ultimate power production level of about 14 MW—a significant achievement!

The shape of the Phase II HDR reservoir had been clearly revealed by the MHF Test seismic cloud (see Fig. 6-23, plan view), but only following the ICFT did it become clear what a profound influence this elongated shape could have on the power production potential of the reservoir; and, consequently, that the most efficient way to operate this reservoir would be to drill another production well near the southern end of the reservoir, to access fluid in this previous "backwater" region (far removed from the EE-2 production well). In addition, the lower-pressure regions surrounding the two production wells would greatly reduce the tendency toward further reservoir growth, even at injection pressures exceeding 4600 psi.

In light of current knowledge, it is a reasonable assumption that had a second production wellbore been in place, power production during

the second half of the ICFT would have been roughly twice that actually observed (about 20 MW_{th}). This is enough energy to produce several MW of electricity, even at the modest thermal-to-electric conversion rates achievable at geothermal temperatures. An electric production facility of this size would be ideal for a small community or a modest industrial facility. (At the same time, the second production well would capture most of the water otherwise lost, and would act as a "pressure-relief valve," virtually eliminating the seismic activity that characterized the high-flow/high-pressure segment.)

Perhaps the most important result of the ICFT, then—although not fully appreciated at the time—was the demonstration that practical amounts of power could be generated from an HDR system.

Seismic Observations

As illustrated in Fig. 7-6, it was during the high-pressure segment of the ICFT that the vast majority of seismic events were recorded. In fact, the few events detected during the moderate-pressure segment occurred during or shortly after the two brief high-pressure excursions. These data provide strong evidence that the seismic volume of the reservoir was stable during the moderate-flow/moderate-pressure segment of the ICFT, but was undergoing significant growth throughout the high-flow/high-pressure segment.

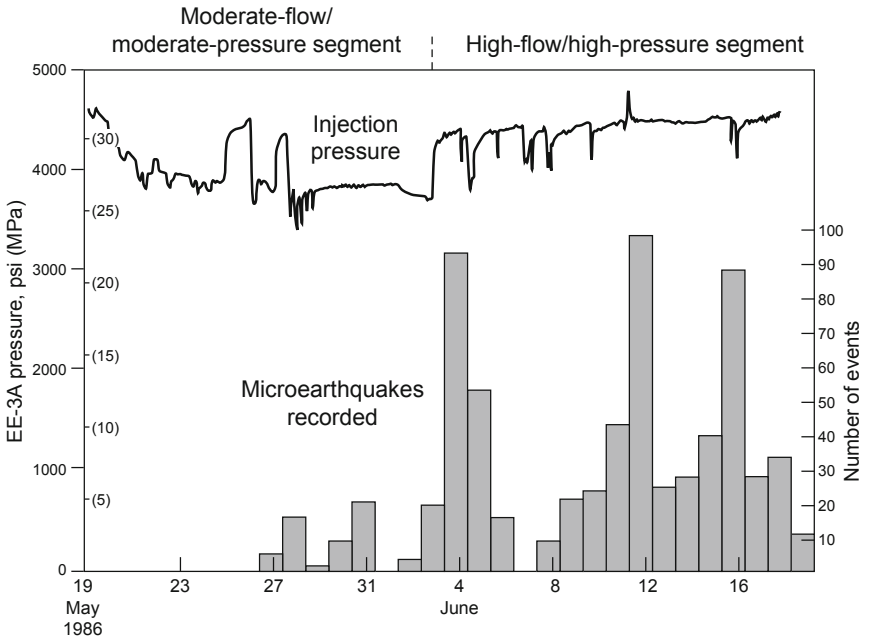

Fig. 7-6. Correspondence between injection pressures and microearthquake occurrences over the course of the ICFT.
Source: Dash et al., 1989

The spatial pattern of the seismicity observed during the latter half of the ICFT (shown in planar view in Fig. 7-7) indicates that reservoir growth took place in the stagnant region beyond the injection well, on the side of the reservoir farthest from the low-pressure region surrounding the production well. Figure 7-7 also shows seismic events recorded during the MHF Test, which originally created this reservoir. Whereas the events of the MHF Test are more or less symmetrical around the injection wellbore (which at the time was EE-2), those of the ICFT are highly asymmetrical; the few visible in the region near the injection wellbore (EE-3A) were all recorded during the shut-in at the end of the test.

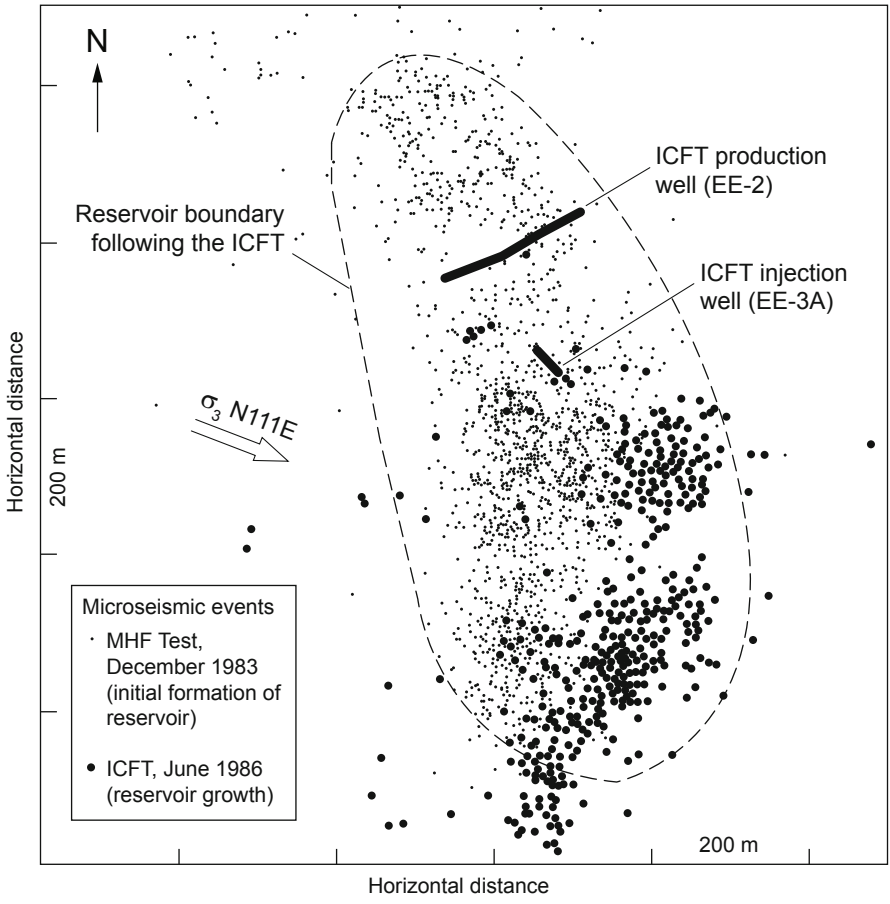

Fig. 7-7. Distributions of seismic events during the MHF Test, the high-pressure segment of the ICFT, and the shut-in following the ICFT. The direction of the least principal earth stress (σ_3) is also shown.
Source: Brown, 1995b

One objective of the LTFT (see Chapter 9) would be to circulate fluid through the reservoir at the highest pressure possible without causing reservoir growth. By demonstrating circulation under both aseismic and seismic conditions, the ICFT provided invaluable guidance for selecting the optimum injection conditions for the LTFT.

Hydraulic Characteristics of the Reservoir

During the ICFT, the principal experimental parameters—injection flow rate and pressure at EE-3A, production flow rate and backpressure at EE-2—were measured continuously. Changes in the relationships among these parameters provided the basis for investigating a number of reservoir hydraulic characteristics.

When injection was initiated in Well EE-3A, after the long period of quiescence that preceded the ICFT, the reservoir did not begin accepting fluid until the pressure reached about 2500 psi. Corrected to conditions of steady-state injection (a cold column of fluid in the injection borehole rather than the initial warm column), this initial joint-opening pressure would be closer to 2200 psi (15.2 MPa). According to pressure-profile analyses carried out later, during the LTFT, this joint-opening pressure was the second lowest observed during Phase II reservoir testing[4] (the lowest being 1450 psi [10 MPa]—see Fig. 6-15 and the related discussion).

At the end of the ICFT, the Phase II reservoir was shut in to study the pressure decay of the reservoir. As soon as the injection flow stopped, eliminating the frictional pressure loss in the frac string at EE-3A, the pressure dropped by about 300 psi—to 4200 psi (29 MPa). This shut-in pressure then was constant over the next 7 minutes. It represented the opening pressure for the set of joints in the expanding reservoir having the highest opening pressure—those that were actively extending to the south at the end of the ICFT. In contrast, during the MHF Test and other experiments (2018, 2020, 2025, and 2042) carried out near the depth of the casing shoe in EE-2, a joint-extension pressure of about 5500 psi was found for the "manifolding" joints (see Chapter 6). This 1300-psi difference dramatically points out the heterogeneity of the "expanded" Phase II reservoir region, and the difficulty of knowing just what joints are extending in what part of the reservoir region.

[4]The 2200-psi/15.2-MPa joint-opening pressure was determined from an analysis of pressure-curve inflection data obtained during several constant-flow-rate inflations and shut-ins; it is the pressure at which the first identifiable set of joints within the Phase II reservoir (those most favorably oriented with respect to the least principal earth stress) starts to jack open. For this set of joints, 2200 psi/15.2 MPa appears to be the internal pressure required to just balance the joint-closure stress.

Note: The inability of the injection pressure to exceed 4600 psi (at 6.9 BPM) during the second segment of the ICFT may also explain why the reservoir was not actively extending to the north; in that region, a pressure of 5500 psi had previously been required for joint extension.

By the end of the first day of shut-in following the ICFT, the pressure had decayed to 3320 psi (22.9 MPa), principally because fluid losses were continuing at the periphery of the pressurized region. (As shown in Table 7-2, the rate of water loss to the far field at the end of the first segment of the ICFT, at an aseismic injection pressure of 3890 psi that produced no reservoir growth, was about 44 gpm [calculated as the difference between the injection and production flow rates].)

At the beginning of the ICFT, the pressure in the production well began to be affected by the injection pressure about 4 1/2 hours after pumping began. It then rose steadily for several more hours, at a rate of about 1.4 psi/min, until it reached the range of the imposed backpressure. (The backpressure was typically maintained in the range of 200–500 psi, to keep the system flow single-phase; but there were many exceptions to this strategy—such as during venting, gas kicks, and shut-ins.) As shown in Fig. 7-8, which compares injection and production flow rates in the two wells during the ICFT, production flows increased even when the injection rate was held constant for extended periods.

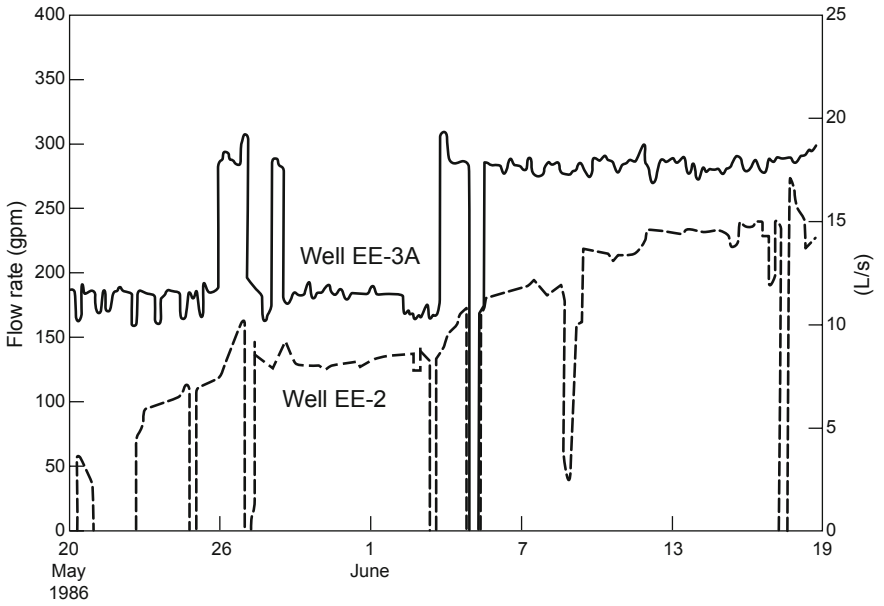

Fig. 7-8. Flow rates during the ICFT: Well EE-2 vs Well EE-3A.

In the first few days of the ICFT, the reservoir near-wellbore inlet impedance declined sharply. By the end of the moderate-flow/moderate-pressure segment, it had dropped from an initial value of 6.6 psi/gpm to essentially zero (0.02 psi/gpm), as shown in Fig. 7-9, with a resultant overall system flow impedance of 26 psi/gpm (see Table 7-2). (Note that this overall impedance is greater than the 24-psi/gpm flow impedance achieved *before* the redrilling of GT-2, during the initial attempts to develop the Phase I reservoir.) The cause of the drop in the near-wellbore inlet impedance, which was most rapid during the first week, was no doubt thermal contraction of the rock in this region as cold water was continually injected into the reservoir, effectively dilating the joint openings.

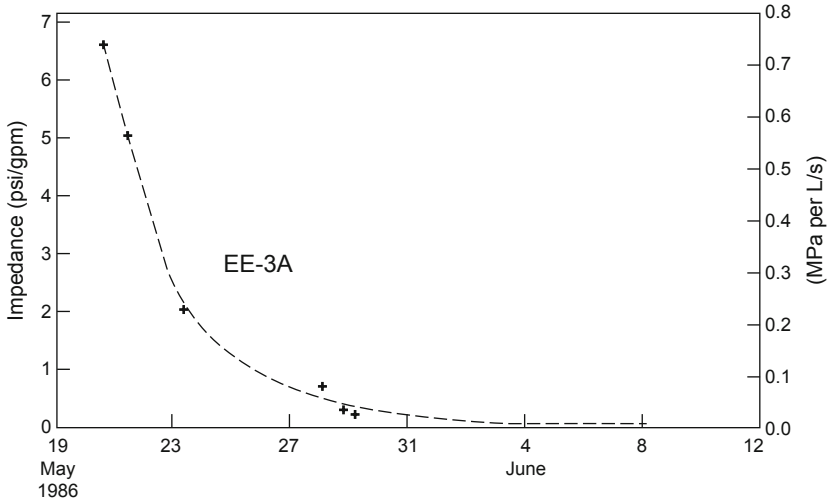

Fig. 7-9. Rapid decrease in the near-wellbore inlet impedance during the early phase of the ICFT.
Source: Dash et al., 1989

By the end of the high-flow/high-pressure segment of the ICFT, the overall reservoir flow impedance had decreased to about 19 psi/gpm (Table 7-2). This further reduction is probably due to the higher mean pressure within the reservoir during this segment and the consequent increase in joint dilation. In fact, with the injection flow rate and pressure both constant, the production flow rate continued to gradually increase with time—suggesting that the flow impedance across the body of the reservoir was continuing to decline as the reservoir, at this higher injection pressure, became more fully inflated.

Another consequence of the continued reservoir inflation and pressure redistribution was an increase in the differential pressure between the production wellbore and the reservoir region surrounding it. Physically, the

principal determinant of the near-wellbore outlet impedance is the variation in the joint-closure stress—the stress normal to the joint surface minus the fluid pressure within the joint—in the reservoir rock immediately adjacent to (probably within 15 ft of) the production borehole. This closure stress, which increases rapidly as flow from the reservoir converges radially toward the production well, depends on the local state of stress in the rock mass—as modified by (1) the compressive hoop stress at and just adjacent to the borehole wall and (2) the rapidly decreasing pressure of the fluid as it flows across this zone from the high-pressure reservoir to the lower-pressure production borehole. The result is a progressive pinch-off of the flowing joints. The degree of this pinch-off determines the magnitude of the near-wellbore outlet impedance.

As noted above and shown in Fig. 7-4, the overall rate of water loss, including water stored within the reservoir and water diffusing outward from the reservoir boundaries, declined consistently during the first (non-extensional) half of the ICFT. It can be inferred from Fig. 7-4 that if the injection pressure had remained the same during the second half of the ICFT (no more than 3900 psi), the rate of water loss would have continued to decline. But the increase in injection pressure from 3900 to 4500 psi led to considerable new reservoir growth, mainly downward and to the south (on the opposite side of the reservoir from the production well, EE-2). The result was a marked increase in the overall rate of water loss, most of which was accounted for by additional storage of water in newly opened joints. The percent water loss given in Fig 7-4 would translate to a fourfold increase in the rate (from 44 to 175 gpm) and a total amount of water "lost" during the ICFT of 13 700 m^3 (3.4 million gal.). Almost half of that amount (6480 m^3 [1.7 million gal.]) was accounted for by storage within the inflated joints of the reservoir—see *Reservoir Through-Flow Fluid Volume (Based on Tracer Data)*, below, and the Note preceding Fig. 7-4.

Thermal Studies

Three temperature profiles were obtained from the 9000- to 12 300-ft depth interval in the EE-3A wellbore: the first on May 15, shortly before the start of the ICFT, under shut-in conditions; the second on June 23, five days after the ICFT; and the third on August 28, several months later (Fig. 7-10).

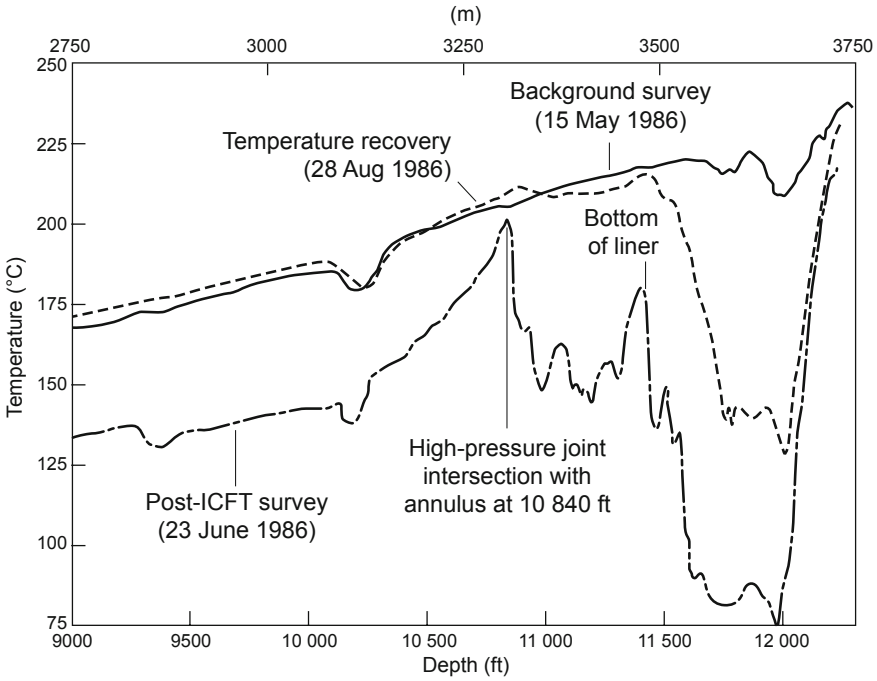

Fig. 7-10. Comparison of three temperature surveys in EE-3A, the injection well (one pre-ICFT background survey and two post-ICFT surveys). The top of the Phase II reservoir is shown at 10 840 ft.
Source: Dash et al., 1989

To properly interpret these profiles, one should review the results of the MHF Test conducted in late 1983 (Chapter 6) and Fig. 6-43 (completion of the lower part of EE-3A). Of the MHF Test results, those pertaining to the region surrounding the injection well (at that time, EE-2) are particularly significant: microseismic evidence of joint openings, pressure and temperature data, the zones of casing collapse, and other information show that the actual high-pressure injection interval extended much higher than the short (70-ft) open-hole interval between the bottom of the casing and the top of the sand plug. It appears that one or more east-dipping joints that were closely aligned with the borehole acted as injection "manifolds," providing paths for the pressurized fluid to flow up behind the casing and out into the rest of the reservoir. Because of the severe casing collapse episodes in EE-2, no temperature survey was done following the MHF Test; but if one had been done, it would probably have yielded a profile similar to that of the post-ICFT survey of June 23 in EE-3A (that is, it would have indicated that a number of pressurized joints were intersecting the EE-2 borehole behind the liner).

As shown in Fig. 6-43, the liner was landed at a depth of 11 436 ft in Well EE-3A and was cemented up to 10 950 ft, leaving an uncased open-hole injection interval of about 670 ft between its lower end and the top of the fill at 12 107 ft. In Fig. 7-10, the most significant feature is the very pronounced temperature depression of the June 23 survey, which reflects cooling by the injected fluid below the bottom of the liner (between 11 436 ft and the deepest—and most prominent—joint intersection, at about 12 000 ft).

The June 23 survey shows, further, that the region from the bottom of the liner up to 10 840 ft was also affected by the cold, pressurized fluid injected into the open-hole interval below the liner. A small portion of this fluid was flowing *upward* around the liner, through one or more joints connected to the high-pressure reservoir, and then emptying into the annulus above the liner cement (see Fig. 6-43). Each of the temperature depressions along that interval (behind the liner) probably represents a pressure-dilated reservoir joint within the upper margin of the Phase II reservoir, associated with this upward flow (evidence of a developing liner frac-around).

Another feature of the June 23 temperature log is significant: the top of the Phase II reservoir in the vicinity of the EE-3A wellbore is clearly shown to be at 10 840 ft: the uppermost extension of the pressure-stimulated joint network. Thus, the open-hole interval above the liner cement at 10 950 ft was exposed to the very upper portion of the high-pressure Phase II reservoir. This exposed interval was probably the source—via the high-pressure joint at 10 840 ft—of a small (3–4 gpm) annulus bypass flow that would persist for the next nine years. However, because of the compressive hoop stress at the borehole wall and the low annulus pressure at the surface (no more than a few hundred psi), there was no significant communication from the high-pressure reservoir into the lower-pressure annular region above 10 950 ft (until a disastrous flow breakthrough in July 1995—see Chapter 9).

InfoNote

It will be helpful, at this point, to recap the annular flow situation at EE-3A. The high-pressure reservoir exhibited multiple (inferred from Fig. 7-10) joint connections to the annulus above the liner cement (identified as ANNULUS in Fig. 6-43). But in addition, the annular flow channel outside the tie-back string and inside the 9 5/8-in. casing (see Fig. 6-43) was directly connected to the surface. This flow channel could be completely shut off at the surface, where a throttling valve had been installed; but such a shutting-off would not affect the ANNULUS, which remained in direct communication with the old Phase I reservoir via the low-pressure joint intersecting EE-3A at 10 260 ft. In other words, with the annular flow channel to the surface shut in, the Phase II reservoir could still vent directly into the old Phase I reservoir via the open ANNULUS!

Such a situation would not have existed if the EE-3A completion had been done properly—with cement circulated all the way up into the 9 5/8-in. casing and completely filling the ANNULUS.

For thermal studies in EE-2, the production wellbore, three temperature logs were run to a depth of 10 450 ft (unfortunately, temperature information could not be collected from the production interval itself, owing to the damage in this wellbore).[5] The first log was run nine days after the start of the ICFT, the second shortly after the end of the ICFT, and the third several months later (Fig. 7-11). As was shown in Fig. 7-4, the surface production temperature increased continuously over the span of the ICFT as the production wellbore warmed and in-transit thermal energy losses decreased. Comparison of the three logs indicates that once circulation was halted, the formation began to quickly return to its former temperature profile, and by about five months later essentially all the thermal effects of circulation had dissipated.

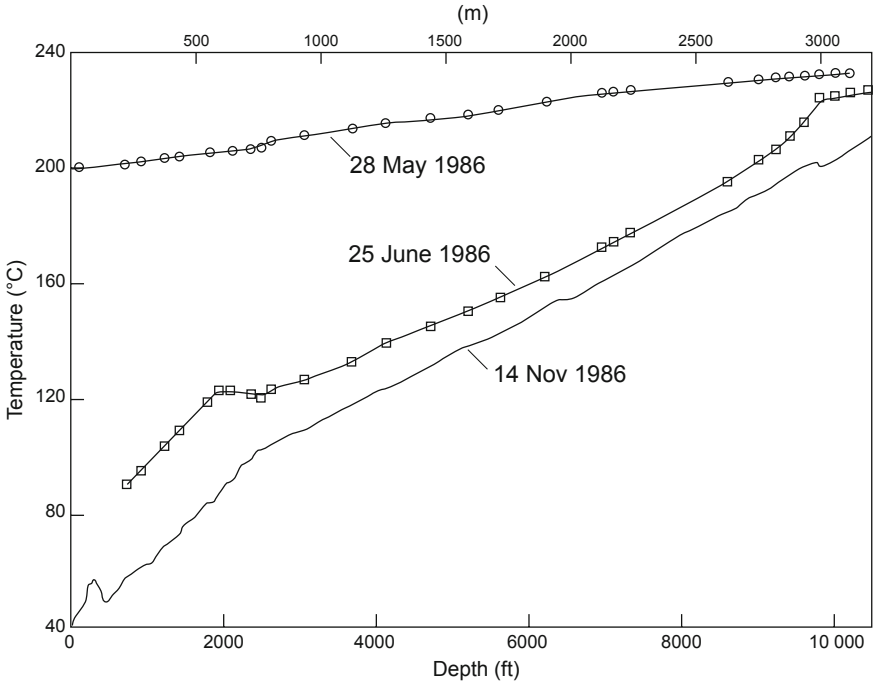

Fig. 7-11. Temperature surveys carried out in Well EE-2 (via Kuster recorder) during and immediately following the ICFT, vs temperature survey done (with Los Alamos equipment) five months post-ICFT.
Source: Dash et al., 1989

[5]Although the casing collapse at 10 512 ft had not yet been discovered, the "unknown obstruction" it presented to logging was thought to lie at roughly 10 550 ft. Logging was therefore not attempted below 10 450 ft, leaving a 100-ft safety margin.

Reservoir Through-Flow Fluid Volume (Based on Tracer Data)

Two tracer tests were conducted during the ICFT, the first on May 30 (during the moderate-flow/moderate-pressure segment) and the second beginning on June 13 (well into the high-flow/high-pressure segment). Radioactive bromine, in the form of ammonium bromide—which has a half-life of only a few days—was used for both. The results of these tests are displayed graphically in Fig. 7-12.

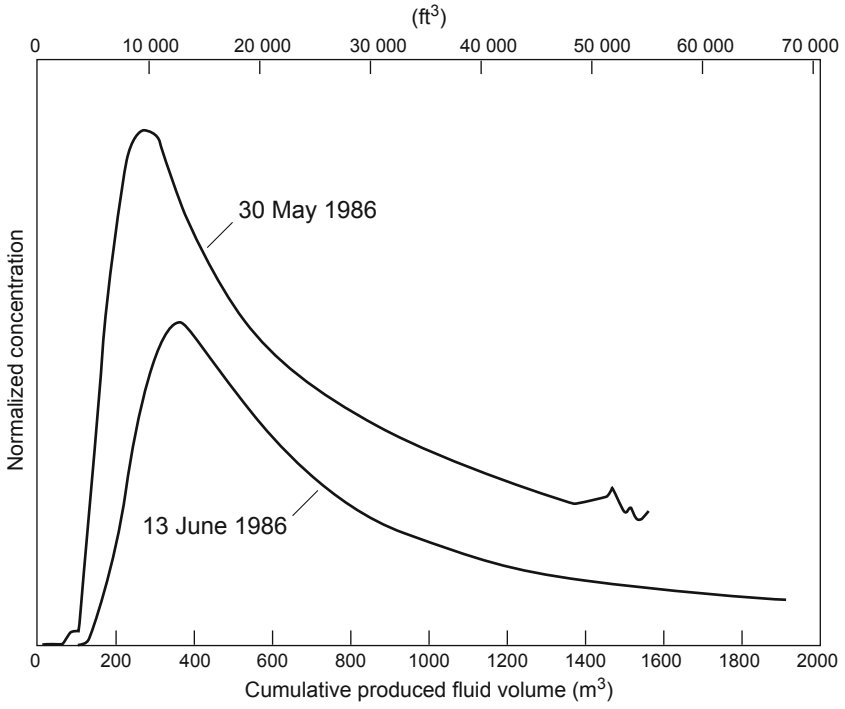

Fig. 7-12. Residence-time distribution curves for the two radioactive-tracer experiments carried out during the ICFT.
Source: Dash et al., 1989

Note that the second tracer test shows a longer time to initial return, a later peak return point, and a smaller total tracer return than the first tracer test. These differences are consistent with a significantly greater reservoir through-flow fluid volume at the time of the second test. In fact, calculations indicate that the integral mean (fluid) volume of the reservoir—a measure of its fluid storage—increased from 2200 to 8500 m^3 (78 000 to about 300 000 ft^3) over the period between the two tracer tests. In other words, much of the water thought to be "lost" during this period was actually going into storage within the pressure-dilated reservoir. This conclusion was further supported when the reservoir was vented at the end of the ICFT:

almost half the 13 700 m^3 (3.4 million gal.) of water previously earmarked as "lost" returned to the surface as vented fluid (approximately 6480 m^3). At least a portion of that fluid may have been stored within the jointed and sealed, but slightly permeable, rock mass at the reservoir periphery (through pressure diffusion to the far field, particularly during the high-pressure segment of the ICFT) and then returned when the boundary pressure gradient was reversed during venting of the reservoir.

Geochemistry of the Circulating Fluid

The essence of the geochemistry results from the ICFT is captured in Fig. 7-13.

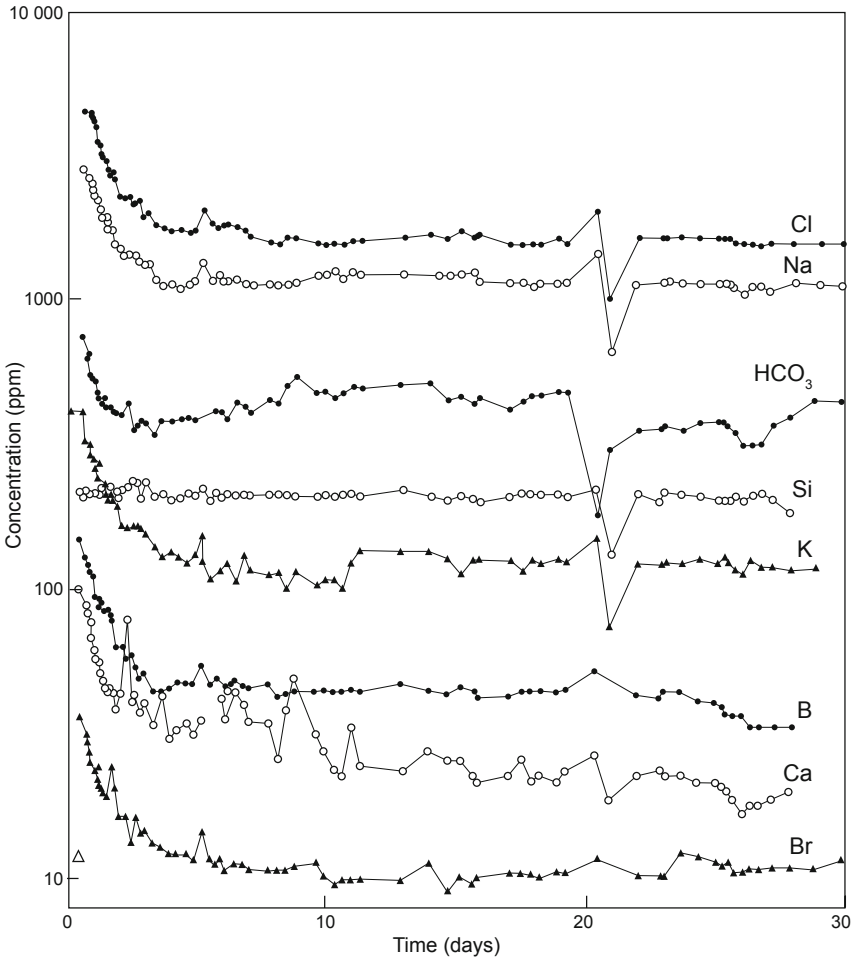

Fig. 7-13. Variation in the concentrations of the major dissolved species in the production fluid during the ICFT.
Adapted from Dash et al., 1989

Of the major dissolved species detected in the production fluid, all but silica saw a rapid drop in concentration as the ICFT proceeded and soon reached equilibrium levels. This behavior is that of inert, nonadsorbing species that either were already present in the injected water or were derived from pore fluid within the joint-filling material. As the injected fluid gradually swept the pore fluid from the opened joints, the concentrations of these species in the produced fluid were initially high; then, after about a week, they generally declined to near the levels in the injected fluid.

In contrast, the concentration of silica remained almost constant throughout the ICFT—a behavior indicative of a reactive species. It appears that unlike the other major species, the silica was coming from the granitic rock itself (rather than pore fluid), through dissolution of quartz from the hot surfaces exposed along the opened joints. This inference is supported by the silica geothermometer temperature, which was almost constant at a level of 250°C during the ICFT.

Typical concentrations of various species in the production fluid a few days into the ICFT, when the total dissolved solids level had reached a state of approximate equilibrium, are shown in Table 7-3. The concentration of dissolved solids in the fluid was very low during the ICFT—only about a tenth that of seawater. In fact, it did not differ markedly from the concentration that would be found some years later, during the LTFT. At consistently low concentrations such as these, dissolved solids should not present a problem for the operation of an HDR system.

Table 7-3. Typical ion concentrations (sample collected on Day 6 of the ICFT)

Ion	Concentration (ppm)
Arsenic	0.6
Boron	48
Bromine	11.5
Calcium	42
Chlorine	1814
Fluorine	10.4
Iron	2.1
Bicarbonate	408
Potassium	114
Lithium	23.4
Sodium	1180
Silica	452
Sulfate	183
pH	5.79
Total dissolved solids	4300

The only gas found in any significant amount was carbon dioxide. As shown by its concentration profile over the duration of the ICFT (Fig. 7-14), it was present at a level of about 0.9% at the beginning of the test, which is believed to be its concentration in the pore fluid. Note that as the pressure was increased in the second half of the test, there was a short-lived jump in concentration—perhaps due to a temporary rise in the proportion of pore fluid in the produced water as new joints were opened by the higher pressure. By the end of the ICFT, the carbon dioxide concentration had declined to 0.1%–0.2%. (Interestingly, during the LTFT carbon dioxide levels in the circulating fluid would average 0.2%–0.3%, close to those predicted by the ICFT data.)

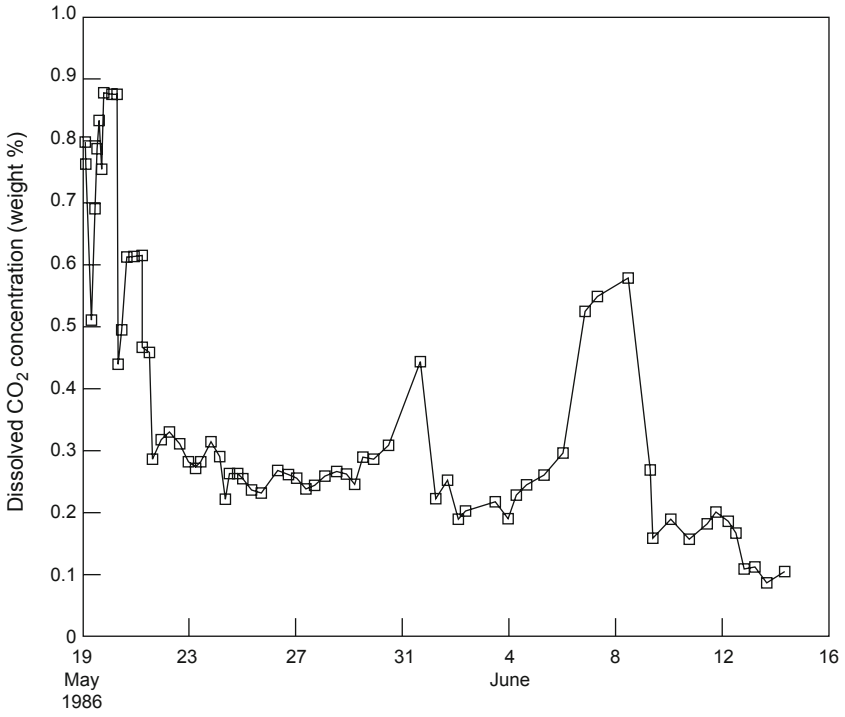

Fig. 7-14. Concentration of dissolved carbon dioxide in the production fluid during the ICFT.
Source: Dash et al., 1989

ICFT Summary

The ICFT, the first extended circulation test of the Phase II HDR system, was carried out with a surface system put together largely on an *ad hoc* basis using rented and temporary equipment. The test itself was plagued with operational problems (most related to the rental injection pumps) that

led to more than a dozen unscheduled shut-ins—the majority, fortunately, very brief. In spite of these difficulties, the ICFT produced a wealth of new information that would prove invaluable in the design and operation of the LTFT. In particular, seismic data from the ICFT shed light on the pressure threshold below which seismic growth of the reservoir would not be induced—knowledge that would enable the LTFT to be run from the very beginning at the highest possible aseismic injection pressure. These data also demonstrated the important role that the production well plays as a pressure sink in an HDR reservoir, giving rise to the recognition that multiple production wells are essential if an HDR energy production system is to operate at maximum productivity. Further, the ICFT generated data on the hydraulic, thermal, water-loss, and geochemical behavior of the Phase II reservoir that significantly advanced our understanding of HDR systems—not only at Fenton Hill, but for future systems elsewhere.

Finally, the most significant result of the ICFT was the thermal power production achieved: an impressive 10 MW. At the time, some detractors argued that this level of output was not really meaningful because of the high injection pressures (over 4500 psi), which caused an undesirable expansion of the reservoir in the "stagnant" region farthest from the production well. In reality, the achievement of this level of power production only in the region of wells EE-3A and EE-2 has profound implications: had a second production well been in place on that far side of the reservoir, it not only would have prevented reservoir growth but would have doubled the output! It is estimated that with two production wells, 20 MW_{th} could have been produced from the Phase II reservoir for a significant period (reservoir modeling suggests at least 20 years). It is clear, then, that in 1986 the ICFT unequivocally demonstrated the technical feasibility of the HDR concept.

Well EE-2: Second Repair Attempt, Redrilling, and Testing (November 1986–June 1988)

When the ICFT ended, most of the HDR team believed that the production well, EE-2, was unsound. In fact, at that time they were not even aware of the extent of damage caused by the bungled coil-tubing cleanout operation associated with Expt. 2059. As they were soon to discover, during that operation a second episode of casing collapse had taken place, at a depth of 10 512 ft.

The following information, on the second repair attempt, redrilling, and flow testing of Well EE-2, is based mainly on the HDR Geothermal Energy Development Program (1988b), Birdsell (1988, 1989) Brown (1988b), Dreesen et al. (1989), and Fenton Hill Operations Daily Log Book No. 3.

Second Attempt to Repair Well EE-2

Following the completion of the ICFT in June of 1986, both wells were shut in at the surface until late September to observe the slow decay of the reservoir pressure. Then the remaining fluid was vented through Well EE-2. During the observation period, some of the HDR Project staff incorrectly assumed that a portion of the fluid venting from the reservoir was flowing up into the Phase I reservoir, although no such flow path had been identified.

The contract for the Big Chief Drilling Company rig #47, originally taken out in 1985 for the redrilling of EE-3, was extended so that the rig could be skidded over to EE-2. After it was in place, the 5 1/2-in. frac string and the Otis steam packer (at 10 401 ft) were removed from the hole. However, the 7-in. transition casing connecting the packer to the top of the remaining section of old 5 1/2-in. frac string at 10 718 ft did not come out with the packer, but was left in the hole. Fishing operations began to retrieve it, and on the third attempt the tie-back bushing, which had connected the transition casing to the bottom of the packer, was removed from the hole along with two joints of the transition casing. Inspection revealed that the bottom joint of the recovered transition casing had also partially collapsed. From these observations it was inferred that the 9 5/8-in. casing had collapsed over an interval that extended down to 10 512 ft (the point of most severe collapse of the 7-in. transition casing), and that the remaining portion of the 7-in. casing was caught inside it. On November 26, two Dia-Log casing inspection logs confirmed this inference: the 9 5/8-in. casing had collapsed onto the 7-in. transition casing, causing it to in turn collapse inward. The nature of the "obstruction" encountered at 10 512 ft more than a year earlier, during attempts at logging below the casing packer, was thus finally explained.

Two attempts were made to mill out the collapsed region of the 7-in. casing, but without success: apparently the distorted pipe was forcing the mill to one side, such that on the second attempt it ground holes through both the 7-in. casing and the surrounding 9 5/8-in. casing, and finally penetrated the borehole wall. Regaining logging access into the Phase II reservoir through EE-2 now appeared problematical at best.

Although a short flow test indicated that the milling operations had not significantly affected fluid circulation through the reservoir or up the EE-2 wellbore, the condition of the well was obviously precarious. In fact, the consensus was that it would not survive the anticipated LTFT. Repair operations were suspended, and in January of 1987 a panel of experts was convened by the U. S. DOE to work with Los Alamos personnel in exploring options for returning Well EE-2 to service. They were briefed in detail on EE-2's current condition: three regions of collapsed casing; 621 ft of the "old" 5 1/2-in. frac string still in the hole (extending from just above the collapse at 10 740 ft down to the deeper—abandoned—casing packer at 11 297 ft); five joints of 7-in. transition casing stuck in the wellbore above the old 5 1/2-in. frac string; and milled holes in the casings (at about 10 510 ft, near the top

of the stuck 7-in. transition casing). The recommended option was that the well be sidetracked from a point above the highest zone of collapsed casing and redrilled through the Phase II reservoir.

Note: Part of the redrilling plan was to complete the new wellbore (EE-2A) for both hot fluid production *and* a modest amount of cold water injection (if needed to further open the joints connecting EE-2A to the body of the reservoir).

Sidetracking and Redrilling of Well EE-2

The seismic data obtained from the MHF Test suggested that the optimum sidetracking trajectory for EE-2 would be one that substantially increased the separation between the injection and production wells. Redrilling in this way would access more of the pressure-stimulated reservoir region, thereby significantly improving our understanding of methods for enhancing reservoir flow and power production. The DOE-assembled panel, however (possibly none of whom actually knew what an HDR reservoir in basement rock looked like), feared that a redrilled leg at some distance might miss intersecting the open joints initially pressure-stimulated during the MHF Test. They insisted that the new leg be drilled at a distance of no more than 100 ft from the existing wellbore (and that over the open-hole portion—11 578 to 11 648 ft—it be within a 50-ft radius).

Thus, rather than using the best available picture of the reservoir geometry in the vicinity of EE-2—the seismic data—to determine the redrilling path, the DOE panel forced the 100-ft constraint upon the HDR Project.

The Big Chief Drilling Company rig already on site for the second repair attempt was retained for the redrilling and completion job. Having a draw works, mast, and substructure rated for a 1.5-million-lb pull, this rig was overrated for the EE-2A work; but its large capacity had proved valuable several times during the redrilling of Well EE-3.

The drilling plan, modeled after that used to successfully drill EE-3A, featured (1) large-diameter (5-in.), moderate-strength drill pipe to eliminate twist-offs; (2) carefully designed bottom-hole assemblies (BHAs) and bits to improve the accuracy of directional drilling and length of bit runs; and (3) a high-temperature sepiolite/bentonite drilling fluid to keep the hole clean, thereby increasing the rate of penetration.

The selected kickoff depth for sidetracking was 9725 ft, about 800 ft above the highest region of collapsed casing. Field work began in early September 1987, with three cementing operations to plug back and completely seal off the borehole below about 9800 ft—both inside and outside the 9 5/8-in. casing. Once this now-abandoned lower portion of the borehole had been well sealed, the casing was perforated over the 9546- to 9550-ft interval and a Baker retrievable cement packer was set at 9166 ft. Then 1000 gal. of cement was injected behind the casing to stabilize and support it just

above the kickoff point. On September 17, the cement was drilled out down to 9889 ft. (About six weeks later, a cement-bond log would show that the cement had filled the annular space from 9500 ft to 9225 ft.)

The next eight days were spent milling a window through the casing from 9688 to 9747 ft. Next, to prepare for placing a cement plug across the window, the casing interval between 9755 and 9885 ft was cleared of milling debris with the drill bit and washed clean; then the section up to 9742 ft was backfilled with sand. On September 28 a 730-gal. cement plug was placed through open-ended drill pipe, filling the window, the annular space outside the window, and the casing above it, to about 9520 ft.

The stage was now set to close off the remainder of the upper casing annulus. The region of casing between 6470 and 6476 ft was perforated, a cement retainer was set at 6326 ft, and 20 000 gal. of lightweight cement was injected through the perforations, filling the annulus up to the loss zones on top of the Precambrian surface at 2400 ft. This operation finally accomplished what much time and effort had failed to do during the first EE-2 repair attempt—the troublesome annulus leak outside the casing was now fully sealed. Only the portion of the annulus between 9500 ft and the perforations at 6470–6476 ft remained uncemented.

With this large cement job complete, the cement retainer and the small amount of cement on top of it were drilled up, allowing the drill bit to be run on down the hole to 9520 ft, where hard cement was encountered. The center of the cement plug across the window in the casing was now drilled out, with an 8 1/2-in. rock bit on a very stiff drilling assembly, to 9748 ft; then the sand was washed out down to 9875 ft. But when the "dummy" whipstock locator assembly was run in the well, it could not be worked through the window interval because of debris. After this interval and the inside of the casing stub (at 9747 ft) had been "conditioned" with a bit and roller reamers, a second run was made, but the locator failed to set properly on the lower casing stub. Finally, a section mill was run in to mill 1 ft off the casing stub. On the next run, the locator assembly successfully tagged the stub.

On October 7 and 8, the whipstock/packstock assembly was run in the hole on drill pipe. The packstock was slipped about 6 ft inside the stub of the 9 5/8-in. casing, the whipstock was oriented, and the packstock was locked into place. Limber BHAs fitted with 8 1/2-in. insert bits were used for the first 40 ft of drilling off the whipstock (October 9–10) from a kickoff depth of 9725 ft. First the hard cement that remained in the window was carefully drilled through, a distance of 17 ft; then a second bit was used to drill 23 ft out into the granitic rock, completing the kickoff.

Figure 7-15, the configuration of EE-2 just after the initiation of side-tracking, shows the window in the casing, the position of the whipstock, the first 40 ft of the new EE-2A leg, and the plugged and abandoned lower portion of EE-2.

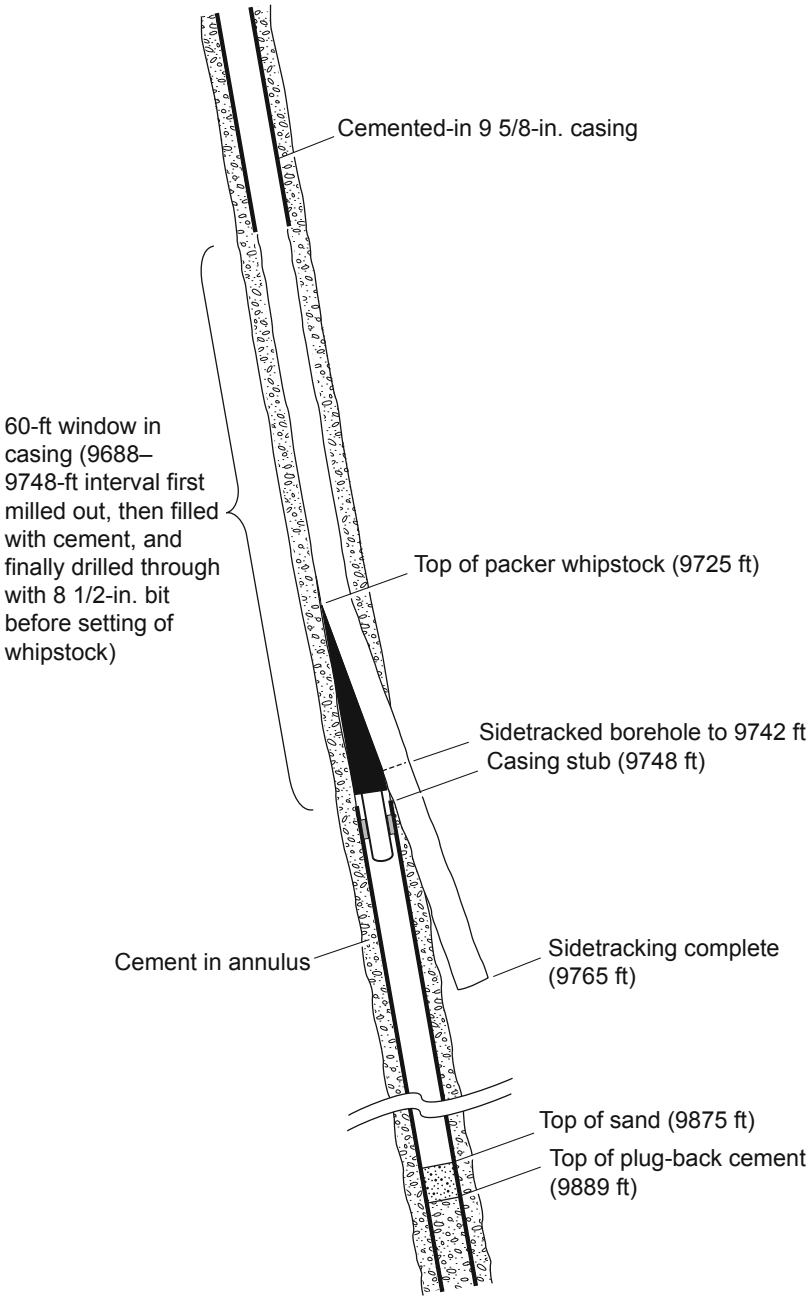

Fig. 7-15. Configuration of the EE-2 wellbore just after the initiation of sidetracking (to 9765 ft).
Adapted from Dreesen et al., 1989

At 9742 ft, the measured inclination was 13 1/2°. By October 15, the new EE-2A leg had reached 9960 ft and the inclination had been increased to 14 3/4°. To keep the trajectory true, the borehole was turned toward the south by means of a positive-displacement-motor (PDM) assembly. By October 17, the drilled depth was 10 149 ft. Magnetic compass single-shot surveys had been done on every drill pipe connection near the kickoff point and on every second or third connection thereafter. When a multi-shot gyroscopic survey was run to verify the accuracy of the single-shot azimuth readings, the location obtained was within 11.5 ft of that given by the single-shot readings.

From October 18 to November 2, the reservoir was pressurized through Well EE-3A and inflated to 2200 psi (15.2 MPa) above the hydrostatic pressure. As EE-2A penetrated the Phase II reservoir, the top of the reservoir was indicated by evidence of flowing joints (changes in flow, pH, and concentrations of carbon dioxide and other dissolved chemical species measured by mud and geochemistry logs). It was calculated to be at a depth of 10 840 ft—the same as that found for the top of the reservoir in the vicinity of Well EE-3A, by temperature logging (see the June 23 survey of Fig. 7-10).

On October 26 EE-2A reached a depth of 11 009 ft, at which point surveying showed the trajectory to be N70E at an angle of 24 3/4°, very close to that planned. The drilling fluid was then displaced with water and the drill pipe was removed. Another two days of temperature logging, sampling of bottom-hole fluids, and flow testing followed, after which drilling was resumed. The injection pressure in Well EE-3A was reduced several times as more joints were intersected, to protect the reservoir without overdiluting the drilling fluid.

On November 11, Well EE-2A was drilled to its final depth of 12 360 ft, some 300 ft below the apparent bottom of the Phase II reservoir (to allow for a "rat hole" to collect debris that otherwise could block the lowest producing joints). Logging revealed fourteen reservoir flow connections over a 1200-ft interval (10 840–12 030 ft), with a major set of deep, flowing joints located near 12 000 ft.

The sidetrack drilling campaign went extremely well. All drilling targets were achieved, including the recommendation of the DOE panel that the wellbore be within a 50-ft radius of the very short (70-ft) open-hole portion of Well EE-2. (The redrilling never deviated more than 25 ft from its target trajectory, and over the total Phase II reservoir interval—10 840 ft to 12 030 ft as observed in EE-2A—the actual surveyed separation distance was within 100 ft.) A magnetic multishot survey at 12 030 ft located the hole bottom as within 18 ft of that projected by the single-shot surveying. There were no twistoffs, and no fishing jobs were required. And although other activities—hole surveying, tripping the drill string in and out to change bits, etc.—added significantly to the total time of the

operation, the project was completed within the time and cost estimates. From initial sidetracking, the hole was drilled 2595 ft (791 m) in less than 30 days. The successful drilling fluids program contributed to the high average penetration rate: when the drill bit was rotating, the rate of penetration was an impressive 10.5 ft/h! Even at the averaged rate of 90 ft/day, drilling proceeded two and one-half times faster than the rate at which Well EE-2 had originally been drilled.

Preliminary Flow Testing (Expt. 2074)

Expt. 2074, a 7-day reservoir flow test with injection into EE-3A, took place December 2–9, 1987, following the successful redrilling of EE-2A (Birdsell, 1988). The principal objective of this flow test was to assess the reservoir flow connections to EE-2A, via tracer testing and temperature logging. In addition, the experiment included gamma-ray logs, three-arm-caliper logs, and seismic monitoring. Because the Phase II reservoir was essentially deflated when the flow test began, the EE-3A injection pressure and flow rate reflected a transient reinflation of the reservoir over the 7 days—yielding very little reservoir flow information. Only 28% of the injected tracer was recovered at EE-2A, suggesting the presence of many long-residence-time flow paths. Few seismic events were recorded (the injection pressure never reached the joint-extension pressure of 5500 psi).

One of the most significant findings of Expt. 2074 was evidence of flow from the reservoir that was bypassing the cemented-in liner in EE-3A. This frac-around flow was shunting high-temperature fluid upward around the liner through a network of joints that, at that time, were highly impeded.[6] Figure 7-16 shows the temperature log run on January 21, 1988 (Brown, 1988b), which confirmed this frac-around flow as well as the location of the principal reservoir flow inlet near 12 000 ft. Also indicated in this figure is the temperature depression reflecting low-pressure flow into the Phase I reservoir region via the joint opening at 10 260 ft (see the discussion of this leakage path in the section *First Lynes Packer Test in EE-3A—Expt. 2049*, Chapter 6).

[6]This network of joints was near the upper boundary of the Phase II reservoir and appeared—like other joints at the periphery—to be fluid-accessible but not well flow-connected to the body of the reservoir. Later, however, as the LTFT proceeded in mid 1995 (see Chapter 9), this flow path would suddenly "open up"—probably as the reservoir pressure-field slowly extended into this boundary region, opening the individual joints episodically rather than continuously. (The Expt. 2020 region had been further expanded in the same way during the MHF Test, as clearly shown by the microseismic data.)

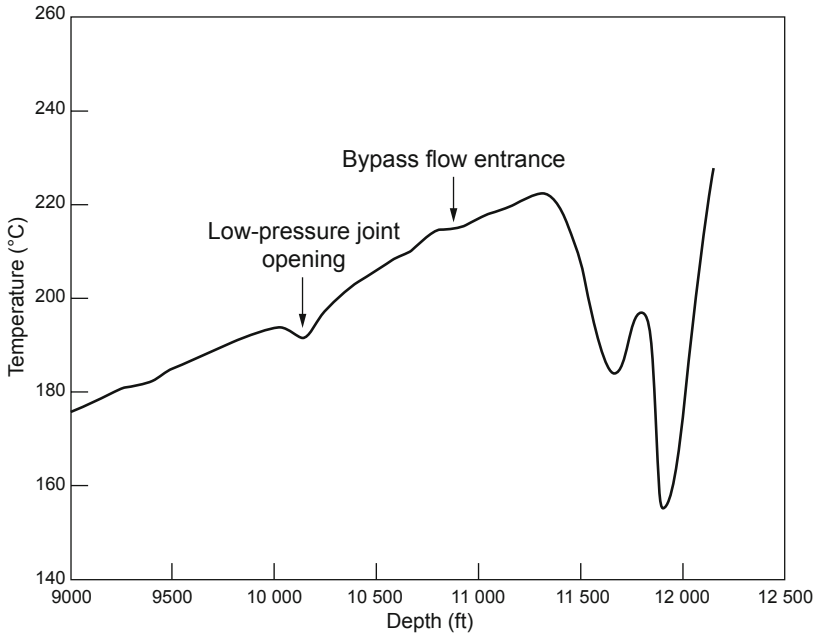

Fig. 7-16. Temperature survey run in Well EE-3A on January 21, 1988, showing the liner bypass flow entrance.
Source: Brown, 1988b

Note: The "frac-around" of the liner testifies to the poor completion of EE-3A nearly two years earlier, which was probably the most costly mistake made at Fenton Hill. Later, in mid 1995, that completion would fail totally, leading to the DOE's termination of the Fenton Hill HDR Project. If, following the completion of EE-2A, the drill rig had been skidded back over EE-3A and the well had been re-completed (with casing cemented all the way to the surface, as would be done for EE-2A in May of 1988—see below), there would have been little reason for the termination, in "mid-stream," of a very successful HDR Project.

Completion of the EE-2A Wellbore

The completion of EE-2A was to be different from that of any other wellbore at Fenton Hill: the wellbore was to be cased from just above the Phase II reservoir all the way to the surface, and the casing would be cemented over its entire length.

The plan was to first backfill the reservoir interval with sand (to prevent cement from invading any of the pressure-stimulated joints); then to run and cement-in a liner from the top of the sand into the 9 5/8-in. cased hole; and, finally, to run and cement-in a "tie-back" casing string from the top of the liner to the surface. The liner was already on site: a string of 7-in., 35-lb/ft, C-90 VAM casing, purchased in 1984 for the original EE-2 but never run. The tie-back string—a 7-in., 32-lb/ft, C-95 casing with premium MSCC connections—would be specially manufactured by Nippon Steel. (Because the lead time from ordering to delivery of this casing was 6 months, the drilling rig was furloughed in the meantime.)

The rig was reactivated on May 16, 1988. Following multiple logging runs and televiewer surveys of the entire open-hole interval below the window, to ensure that it was still in good condition, the reservoir production section was covered by filling the hole with sand to 10 775 ft. Then the liner was run in the hole on drill pipe and hung off the 9 5/8-in. casing with a liner hanger, putting its top some 190 ft above the window and its bottom at 10 770 ft (5 ft above the sand plug). The polished bore receptacle (PBR), intended to serve as the interface with the tie-back string, was installed with its top at 9499 ft, 91 ft above the liner hanger at 9590 ft. The liner was then cemented in place.

The next step in completing the wellbore would have been running of the tie-back string; but with all the cementing equipment on site, it was decided to first cement the uppermost 850 ft of the annulus between the 13 3/8-in. casing and the 9 5/8-in. casing, to protect the latter from excess thermal stresses during upcoming flow testing (this annulus had been left uncemented when the top 902 ft of 9 5/8-in. casing was replaced in 1984—see Chapter 6).

First, a plug was built up in the annulus outside the 9 5/8-in. casing: a quantity of frac balls, gravel, and sand was dropped into the annulus on top of the 11 3/4-in. screw-in sub that had been installed at 920 ft in 1984. Next, the casing was perforated at a depth of 855 ft and the cement that remained above the liner hanger (from 9269 ft to 9499 ft) was drilled out with an 8 1/2-in. bit. A solid rubber wiper plug was then pushed down inside the casing with drill pipe and positioned just below the perforations. Finally, cement was pumped in through the perforations. The operation was only partially successful: cement-bond logs indicated that the cement rose only to a depth of 214 ft. Therefore, after the residual cement and the wiper plug inside the 9 5/8-in. casing had been drilled up, on May 25 the 9 5/8-in. casing was perforated again—this time from 210 to 212 ft—so that immediately following cementing of the 7-in. tie-back string to the surface, the annulus could be cemented as well.

Three days later, a run with a 5 3/4-in. bit drilled the cement out of the top 1100 ft of the 7-in. liner, and then a mill run dressed off the PBR at the top of the liner assembly. On June 1, the 7-in. tie-back casing, with a tie-back stem (PBR mandrel) on bottom, was run into the hole; but the tie-back stem could not be made to engage the PBR. After several attempts at engagement, the tie-back casing was cemented—with the stem simply resting on top of the PBR—with a combination of low- and high-density cement (6650 linear ft of low-density cement on top, the remainder high-density cement). At the surface, cement was first circulated out the annulus between the 7-in. casing and the 9 5/8-in. casing, and then (through the perforations at 210–212 ft) out the annulus between the 9 5/8-in. casing and the 13 3/8-in. casing.

Cement-bond logs indicated a good cement density over most of the cemented interval and in all of the critical regions—such as around the PBR at the bottom of the tie-back casing and near the surface. The liner was tensioned, set in the wellhead grips, and cut to length; secondary wellhead seals and a blowout-preventer were installed; the cement was drilled out with a 5 3/4-in. bit; and the sand in the bottom of the hole was washed out.

By mid June the EE-2A wellbore had been completed, as shown in Fig. 7-17. Both the drilling and the completion work were accomplished within budget and on schedule.

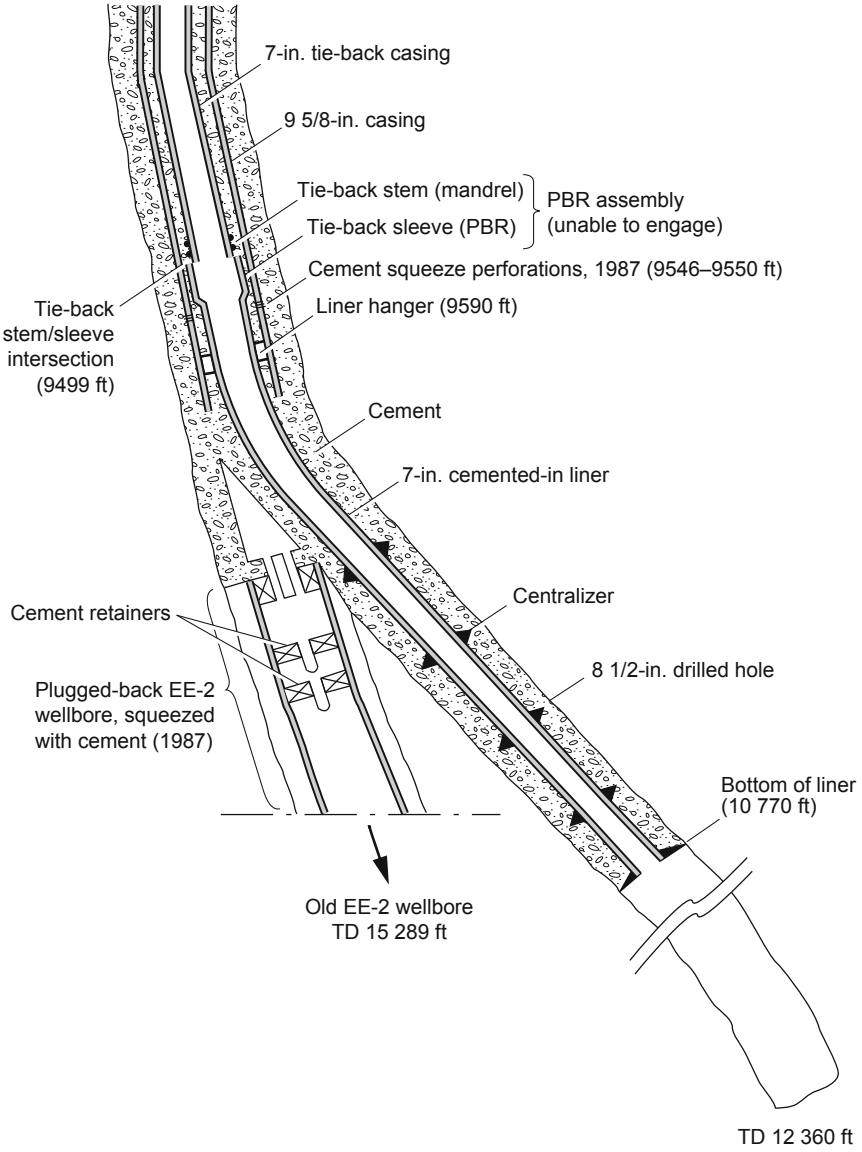

Fig. 7-17. Well EE-2A as completed in June 1988.
Adapted from Dressen et al., 1989

Post-Completion Injection Testing in EE-2A (Expt. 2076)

Preliminary pressure testing had demonstrated the integrity of the 7-in. liner at 2500 psi. In June 1988, the integrity of both this liner and the tie-back string were further assessed: during Expt. 2076, which lasted just 6 hours, nearly 50 000 gal. of water was injected at rates of 1–15 BPM and corresponding wellhead injection pressures of 1500–4300 psi (10–30 MPa) (Birdsell, 1989). This brief test led to three significant conclusions regarding EE-2A:

- The liner and tie-back string appeared to be pressure-tight to at least 4300 psi.
- The joints identified during the earlier testing of the redrilled section (Expt. 2074) were still present and flowing.
- At comparable pressures, almost twice as much fluid could be injected into the reservoir via the redrilled EE-2A wellbore as via the EE-3A wellbore—which suggested that residual joint propping (due to pressure spallation from the MHF Test in late 1983) not only still existed, but extended outward from the old EE-2 wellbore into the region traversed by EE-2A. The implication is that for future development of HDR reservoirs, a controlled (but very rapid and energetic) venting of high-pressure fluid from the reservoir through each production well in succession—similar to what occurred in an uncontrolled way at the end of the MHF Test—could be an effective means of reducing the very critical near-wellbore outlet impedance (pressure spalls derived from the joint surfaces providing spallation-propping).

Modifications to the EE-2 Wellbore: Summary

The sidetracking, redrilling, and completion of EE-2A were a complete success. These operations represented the culmination of the Fenton Hill HDR drilling experience, and stand to this day as an example of superlative design, engineering, and operations supervision. They resulted in a production well that was structurally sound and provided excellent access to a number of fluid-carrying reservoir joints. This wellbore was to perform flawlessly during all subsequent testing of the Phase II HDR system.

This success, along with the previous achievement of redrilling the EE-3A wellbore, show that HDR drilling should no longer be viewed as high-risk and overly difficult. With good planning, sufficient lead time to order the proper equipment, and, most important, excellent rig supervision—especially the ability to adjust to changing conditions—a drilling project can be undertaken with only moderate risk even in a difficult, high-temperature drilling environment such as Fenton Hill. Note too that the average penetration rate during the redrilling of EE-2A (a total of 1940 ft) in deep, hot granite was 10.5 ft/h, which in 1988 dollars translated to an extremely reasonable cost of $188 per foot.

A New Concept of Reservoir Rock Volume

Over the years, as the HDR geothermal energy concept has been researched, several different methods of characterizing the rock volume of the reservoir have evolved. As described in Chapter 4, the first of these was the *seismic volume*, which is based on the hypothesis that only hydraulic pressurization can induce joint slippage, thereby generating microseismic shear events. Thus, the seismic volume is the rock volume contained within the envelope of the cloud of microseismic events, and based statistically on either a 1σ or 2σ standard deviation of the event locations. It represents the volume of the rock mass pressure-stimulated during injection operations.

The second reservoir rock volume, introduced as a concept in Chapter 4 and amplified upon in Chapters 6 and 7, is the *circulation-accessible volume*. Smaller than the seismic volume, this volume is characterized as the volume of reservoir rock accessible to the circulating fluid during power production or flow testing. The reservoir testing described in Chapter 6 made it apparent—as would the upcoming Expt. 2077 (static reservoir pressure testing)—that this rock volume is strongly pressure-dependent. There is no known method for measuring the circulation-accessible rock volume, although the volume of the *fluid* that circulates through this rock volume (the through-flow fluid volume) can be measured—for a given reservoir pressure—via chemical tracer techniques. For the rock volume itself, an *estimate* can be arrived at—but only on the basis of an *assumption* regarding the pressure-dependent reservoir joint porosity.[7] During Expt. 2077, a third concept of the rock volume of the reservoir would be developed, through a method of characterization devised and tested under static (non-flowing) pressurization. This volume, called the *fluid-accessible volume*, comprises both the circulation-accessible volume and the zone near the periphery of the reservoir where fluid has permeated into the joint extensions. It is thus slightly larger than the circulation-accessible rock volume at any given reservoir pressure, and appears to offer a reasonable analog to the latter—but one that can be measured through static reservoir pressure testing.

[7]The reservoir joint porosity is defined as the ratio of the volume of fluid within the pressure-dilating joints to the volume of the rock mass. This porosity is to be distinguished from the always-present microcrack porosity (the ratio of the volume of fluid within the interconnected network of microcracks to the volume of the matrix rock). The microcrack porosity is very much smaller than the joint porosity.

Extended Static Reservoir Pressure Test (Expt. 2077)

With the EE-2A production wellbore complete, and thus the underground portion of the Phase II HDR system ready for the LTFT, attention turned to construction of the surface plant (described in Chapter 8). Because it would not be possible to carry out experiments requiring circulation through the reservoir while the surface plant was being built, an extended series of pre-LTFT reservoir pressure tests was planned to (1) assess peripheral water loss over an extended period, under non-flowing conditions and at two pressure levels; and (2) determine the fluid-accessible reservoir volume at a moderate pressure (15 MPa). These tests were designed to use low-volume pumps and related equipment already on hand. The information on this experiment is abstracted from Brown (1991 and 1995b).

Known as Expt. 2077, this extended static reservoir pressurization lasted from late March 1989 through December 1990.[8] With EE-2A shut in, water was injected into the EE-3A wellbore to pressurize the reservoir to a target level; then the injection rate was reduced to maintain the pressure (± 25 psi, as measured at the EE-2A wellhead) and adjusted—by alternating pumping periods with shut-in periods—to just offset the peripheral water loss at that pressure. This procedure was carried out a number of times, for several different target pressures. (For this experiment, pressures were specified in integer MPa rather than psi, to accommodate the many foreign observers of this experiment.) Expt. 2077 also offered an opportunity to address the concerns voiced first by personnel from the AEC, then ERDA, then the DOE, and finally by the Japanese and Europeans—that reservoir water losses could prove to be a severe constraint on commercialization of the HDR technology. (For a *confined* HDR reservoir, these concerns were experimentally shown to be unfounded.)

In Figure 7-18, pressure plateaus are visible at 7.5, 15, and 19 MPa. The four 15-MPa (2176-psi) plateaus were implemented to observe the decline in the rate of water loss with time at this pressure level. The dip in the pressure decay curve during July and early August 1990 represents the interval during which the pressure reached its lowest point, followed by rapid reinflation—which provided important information on the partitioning of fluid storage between the network of joints and the microcracks in the matrix rock of the reservoir.

[8]Following Expt. 2077, the Phase II reservoir would remain shut in for 12 months (until December 1991, when the surface plant was essentially complete). During this time, the small (about 2.6 gpm) "backside" reservoir vent at EE-3A would cause the shut-in reservoir pressure to slowly decay—from about 2500 psi to 2270 psi by the beginning of Expt. 2078A (Dec. 2, 1991).

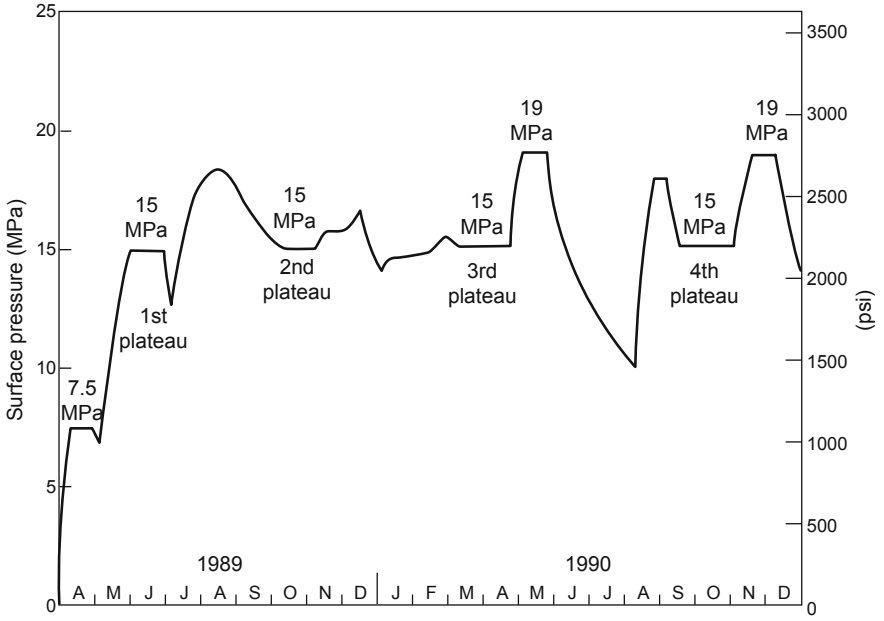

Fig. 7-18. Pressure profile of the Phase II reservoir during the 21 months of Expt. 2077.
Source: Brown, 1991

Water Loss Trends

The results of Expt. 2077 showed clearly that the water loss from a *confined* HDR reservoir region, created by pressure-opening a previously sealed joint structure within a deep region of hot crystalline basement rock, can be very small. Figure 7-19 depicts the rate of water loss observed at a pressure of 15 MPa during the 17 months of static reservoir testing between June 1989 and October 1990. (Note: Although construction of the surface plant was going on at the same time as this experiment and created a number of difficulties in controlling pressures, the *average* pressure during this 17-month period was about the same as that during the four 15-MPa pressure plateaus.)

InfoNote

Until this experiment, many "experts" worldwide had been convinced that no such large region of the deep crystalline basement could be maintained at a pressure level up to 10 MPa above the measured least principal earth stress (8.6 MPa) without spontaneous hydraulic fracturing and subsequent rapid pressure loss! (For further information on this subject, see Brown, 1999.)

Following an initial inflation period of about 14 days, during which water was being injected at a pressure of 15 MPa and stored in pressure-dilating joints within the body of the reservoir (represented by the shaded area in Fig. 7-19), the water-loss rate declined linearly with the natural logarithm of time. This observation implies two-dimensional diffusion from the reservoir boundaries (no significant water loss in the vertical direction), which is consistent with the flattened ellipsoidal shape of the reservoir indicated by the seismic data. During the latter part of the test period, the water-loss rate appeared to be approaching a constant value of about 2.1 gpm—suggesting that with extended pressurization, water loss transitions to spherical diffusion from a point source. It is interesting to note that by the end of the fourth pressurization at 15 MPa, the pressure on the Phase II reservoir (a volume of pressure-stimulated rock measuring close to 0.13 km^3) was being maintained by a flow less than that from a typical garden hose.

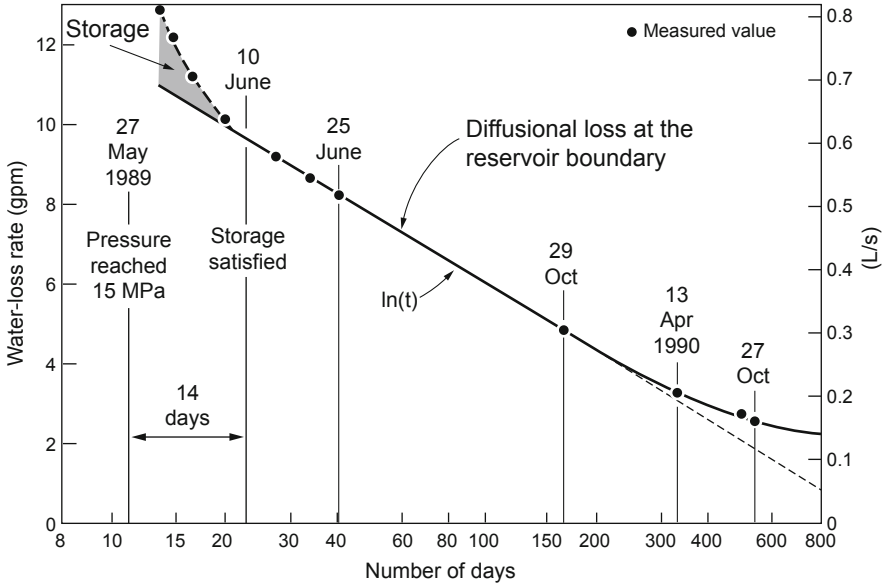

Fig. 7-19. Water-loss rate vs log (time) during the 15-MPa pressure plateaus of Expt. 2077 (diffusion of pressurized water to the far field).
Source: Brown, 1995b

The Fluid-Accessible Reservoir Volume

As noted above, the through-flow fluid volume of the reservoir was based on the use of chemical tracers to measure the steady-state volume of fluid flowing through the reservoir. But calculation of the corresponding rock volume, the circulation-accessible reservoir region, required an *assumed* overall reservoir joint porosity. Unfortunately, as became apparent with pressure testing, the porosity of the reservoir is pressure-dependent and, even more to the point, is almost impossible to measure in a global sense. Then, Expt. 2077, which was a steady-state operation *in toto*, provided a unique opportunity. With the reservoir shut in, a strictly mechanical method was developed for measuring the true *fluid-accessible reservoir volume* (a method that is especially useful because the volume of hot rock available for heat transfer can be measured before any actual reservoir power production; if this volume is found to be too small for the intended purpose, it can be increased by additional hydraulic stimulation).

First, postulate a region of crystalline rock that is "fractured" on all scales—from interconnected microcracks through large, pressure-stimulated joints (which definitely appears to be the case for the deep crystalline basement at Fenton Hill). If this region were to be pressurized in such a way that the fluid contained in the cracks and joints—whatever their size—was in pressure equilibrium at the beginning and end of a pressure rise, then the only material that would be compressed (ignoring the compressibility of the contained water, because the overall porosity of the rock mass is so small—0.01% or less) would be the mineral constituents of the rock matrix between cracks, e.g., quartz, feldspar, and biotite crystals. The corresponding decrease in volume (ΔV) of the rock matrix between the initial and final pressure levels (ΔP) would be equal to the amount of fluid that would need to be injected to raise the pressure in the *confined* reservoir by the amount ΔP.

In other words, the "mechanical" method arrives at the fluid-accessible reservoir volume by measuring the decrease in volume of the rock mass within the reservoir region between two different steady-state pressure levels, achieved within such a short time span that the small diffusional losses from the boundaries of the reservoir can be neglected. This method is based on (1) a linearly elastic compressibility equation, given in Table 7-4 along with the initial and final pressure levels; (2) the amount of injected fluid (which is equal, but opposite in sign, to the decrease in the volume of the rock mass); and (3) the *in situ* bulk modulus. The last, which was determined from the seismically measured compressive- and shear-wave velocities for the reservoir rock, compares very favorably with laboratory measurements on dry granite samples under high confining stress. (Also listed in this table, for comparison, are the seismic reservoir volumes based on two Gaussian distributions of the microseismic events.)

The fluid-accessible reservoir volume probably provides the most relevant measure of the effective volume of the reservoir, because only hot rock that is in close proximity to the pressurizing fluid can contribute to thermal energy production.

Table 7-4. Determination of the fluid-accessible reservoir volume

Pressure increment (ΔP)	7.5 to 15 MPa
Decrease in volume of rock mass (ΔV) (equal to the amount of injected fluid needed to raise the pressure by ΔP)	2715 m^3
Bulk modulus for rock mass (K)	55 GPa
Fluid-accessible reservoir volume: $\mathbf{V = K \frac{\Delta V}{\Delta P}}$	**20×10^6 m^3**
Seismic volume (1σ—67% of events)	16×10^6 m^3
Seismic volume (2σ—95% of events)	130×10^6 m^3

A Major Caveat

Although not expressly stated, a major caveat in the mechanical modeling of the dilation of the reservoir as a function of pressure, shown in Table 7-4, is that a constant-strain boundary condition is assumed to surround the reservoir region. This is obviously fallacious. It should be clear that if the interior of the jointed reservoir is pressurized, the sealed boundary regions would also be affected. This premise constitutes the basis for the concept of a *stress cage* surrounding the pressure-stimulated reservoir (see Chapter 6). If one were to pressurize a deep borehole in granitic rock, one would expect the borehole to expand in reaction to the imposed pressure, creating a compensating compressive hoop stress in the surrounding rock. If the borehole were filled with sand—which would also be compressed—the borehole wall would still react in the same way (as if the sand were not present). Obviously, the interconnected joint network within the Phase II reservoir cannot be represented simply as an array of sand grains; but how could one best allow for the effects, in the surrounding sealed rock mass, of inflating an ellipsoidal, open-jointed reservoir region?

The answer to this question is probably best left for Professor Dan Swenson and his students at Kansas State University. Professor Swenson has developed the most sophisticated 2-D, discrete-element mechanical model for the pressurized deformation of the open-jointed crystalline basement—the GEOCRACK model—which has been validated by Fenton Hill data. (Investment in such a project would be a very worthwhile use for some of the U. S. DOE's geothermal funding.) A quantitative representation of the above problem could be modeled with GEOCRACK and provide a good answer. The authors would hazard a guess that if the concomitant compression of the boundary regions is taken into account, the fluid-accessible rock volume could increase as much as twofold—but this is only a *guess*.

Fluid Partitioning Between Joints and Microcracks

When fluid is circulated through a network of interconnected joints in an HDR reservoir at a pressure above the minimum joint-opening pressure, the joints provide multiple pathways for the rapid movement of fluid from the injection well to one or more production wells. In contrast, microcracks and/or pores in the matrix rock primarily store pore fluid, which after a considerable lag time comes into pressure equilibrium with the pressurized fluid in the adjacent joints. The pore fluid, therefore, does not mix in any significant way with the injected water that is transported across the reservoir (if it did, one would have a commercial hydrothermal reservoir without the need for hydraulic stimulation!).

From a reservoir power production standpoint, it is important to understand how the pressurizing fluid gets partitioned between joints and microcracks at various reservoir operating pressures. This partitioning determines how the reservoir rock will be affected geochemically by the transpiration of the pore fluid within the microcrack network, which may help in ascertaining the optimal method of reservoir power production. Expt. 2077 provided valuable information about fluid partitioning through two episodes of slow deflation of the reservoir followed by rapid reinflation: once at a pressure level of 10.5 MPa (below the 15-MPa joint-opening pressure for the Phase II reservoir at Fenton Hill), and once at a pressure above 15 MPa.

The lower-pressure test took place a little over a year into Expt. 2077. Following the first 19-MPa pressure plateau (see Fig. 7-18), the reservoir was shut in for 11 weeks; during the last five weeks of this shut-in, the surface pressure declined from 1750 to 1420 psi (12 to 9.8 MPa), at a rate averaging about 8.9 psi/day (Fig. 7-20). This decline was due almost entirely to the very small reservoir bypass flow path to the surface at EE-3A, via the annulus between the tie-back string (the EE-3A injection string, which was shut in during this time), and the 9 5/8-in. casing. The water loss from this bypass flow—about 2.6 gpm—was being carefully monitored.

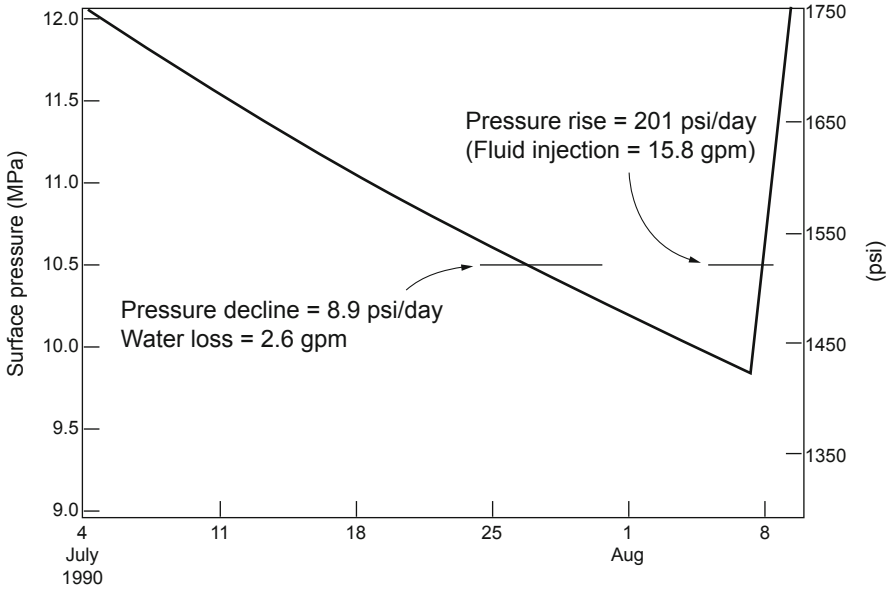

Fig. 7-20. Low-pressure (10.5 MPa) slow deflation–rapid reinflation test in the injection well (EE-3A).
Source: Brown, 1991

Reinflation of the reservoir through EE-3A began in early August, with the Big Kobe pump, at a rate of 19 gpm and a starting pressure of 1420 psi (9.8 MPa). The net rate of injection was 15.8 gpm[9]—six times higher than the water-loss rate during shut-in. But initially, the reservoir pressure rose at an anomalously high rate: 201 psi/day, more than 20 times faster than it had declined during the last weeks of the shut-in. Because this test was designed to elucidate the storage behavior of the rock mass when the 15-MPa pressure-stimulated joint set was essentially re-closed, the deflation–inflation characteristics of the reservoir were analyzed at a pressure of 10.5 MPa (above the least principal earth stress of 8.6 MPa[10]). At this pressure, the joint sets having opening pressures above 15 MPa were tightly closed.

The obvious explanation for the anomalous high rate of pressure increase at the onset of pumping was that the reservoir joints, even though closed, were still at least two orders of magnitude more permeable than the network of interconnected microcracks within the rock blocks. During the very slow

[9]That is, a pumping rate of 18.4 gpm minus the 2.6-gpm rate of water loss from the EE-3A annulus.

[10]This value is based on the Phase I measurement of 8.6 MPa (see *State of Stress within the Phase I Reservoir*, Chapter 4).

deflation of the reservoir, stored fluid was flowing out both from the microcracks and from the joints, in a very nearly pressure-equilibrated manner. However, upon subsequent rapid reinflation, almost all the injected fluid went into partially pressure-dilating the closed network of permeable joints. It would be expected that within less than a day after the start of reinflation, only a very small amount of the injected fluid, even as the pressure increased, would have been able to penetrate the surfaces of the large rock blocks making up the body of the reservoir. From the data shown in Fig. 7-20, it was determined that at pressures below the minimum joint-opening pressure, 73% of the outflow was produced from fluid stored in the microcrack fabric of the rock blocks and only 27% from that in the network of joints. This result—which is counterintuitive for a jointed HDR reservoir—correctly implies that the flow impedance of pressure-dilated joints that have re-closed is quite high. This has been confirmed experimentally: attempts to circulate the reservoir below about 15 MPa have been unsuccessful.

In November 1990, a second slow deflation–rapid reinflation test was carried out, to further investigate the partitioning of reservoir fluid storage (Fig. 7-21). This time, a mean reservoir pressure *above* the 15-MPa initial joint-opening pressure was used: 16.4 MPa (2380 psi).

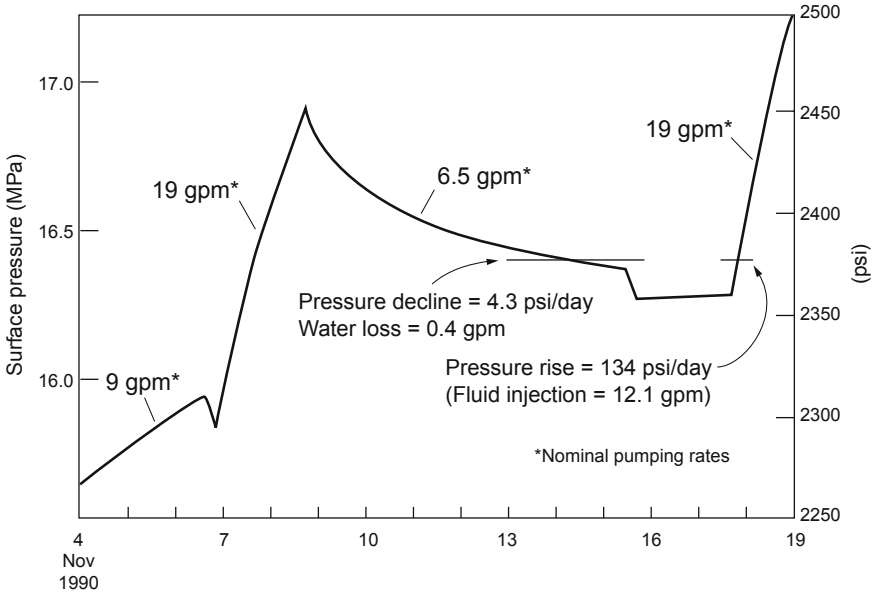

Fig. 7-21. High-pressure (16.4 MPa) slow deflation–rapid reinflation test in the injection well (EE-3A).
Source: Brown, 1991

This "high-pressure" test took place under less-than-ideal conditions. With the preparatory work for the LTFT going on at EE-3A, injection with the Big Kobe pump unfortunately could be carried out only occasionally. It can be inferred from Fig. 7-21 that had another week or so of injection been possible, at a rate of 6.5 gpm, the reservoir pressure would have leveled out at about 16.3 MPa. At this pressure level, the permeation loss rate would have been 3.9 gpm, just balancing the 6.5-gpm injection rate minus the 2.6-gpm annulus leakage rate at EE-3A. Extrapolating from this permeation loss rate and the permeation loss rate at the end of the fourth 15-MPa pressure plateau (2.57 gpm, the last data point shown in Fig. 7-19), one would obtain a permeation loss rate of 4.3 gpm at 16.4 MPa.

A close look at Fig. 7-21 reveals that by November 14, after the rate of injection had been reduced to 6.5 gpm, the reservoir pressure was declining very slowly (4.3 psi/day)—indicating a very slight net "negative" injection of –0.4 gpm (a water loss). The result was a pressure change per fluid storage change of –10.2 psi/day/gpm. Similarly, during the rapid reinflation on November 17, the pressure was increasing at 134 psi/gpm at a net injection rate of 12.1 gpm, resulting in a pressure change per fluid storage change of +11.1 psi/day/gpm.

Within the accuracy of the above analyses, the magnitude of the pressure change per fluid storage change during slow deflation (–10.2 psi/gpm/day) is essentially the same as that during rapid reinflation (+11.1 psi/gpm/day). In other words, these experimental results show that at an average reservoir pressure of 16.4 MPa, there is no longer any appreciable difference in reservoir behavior between slow deflation and rapid reinflation, as there was at a mean pressure of 10.5 MPa (Fig. 7-19). It therefore appears that at pressures above 15 MPa, almost all the pressure-dependent change in fluid storage takes place in the open joints within the pressure-stimulated reservoir region (i.e., pore fluid storage is unaffected—essentially decoupled from pressure changes within the jointed reservoir region).

Even though Expt. 2077 was conducted mainly to fill a time gap when more complicated experiments were not possible, it provided information about reservoir behavior that would serve as good guidance for the conduct of the LTFT; in addition, it increased our overall understanding of pressurization and fluid storage phenomena in open-jointed HDR reservoirs. These insights, together with the demonstration via the ICFT of the suitability of the reservoir for routine energy production and the redrilling of Well EE-2A, set the stage for the upcoming definitive test, the LTFT.

Chapter 8

The Surface Plant for the Long-Term Flow Test

Following the ICFT, work began to complete the design and installation of a permanent surface plant for the Long-Term Flow Test (LTFT), which was planned as a realistic demonstration of the viability of HDR technology under conditions closely approximating those of a commercial HDR power facility. The major difference was that no power would be produced (the thermal energy brought to the surface during circulation would simply be wasted to the atmosphere). The decision not to produce power was based on the following considerations:

1. The addition of power-production equipment would considerably increase the cost of the plant.
2. Concurrent operation of an electricity-generation unit would draw resources, time, and expertise from the primary goal of extracting thermal energy.
3. The ability to convert geothermal energy to electricity was already well established in the commercial sector.

Design of the Facilities

The LTFT surface plant included the above-ground parts of the HDR circulation loop, external equipment important to the operation of the loop, installations for chemistry and seismic monitoring, and miscellaneous structures. Many of these facilities had been built for the ICFT (carried out in May of 1986—see Chapter 7); then, between 1987 and 1991, new components were designed and constructed. The design took into consideration not only the use of existing facilities, but also of government surplus components and commercially available equipment. These facilities and components were evaluated, tested, repaired if necessary, and otherwise brought up to the standard to which the LTFT surface plant was being built. Because the plant had to be erected around the two existing Phase II wellbores and the large heat exchanger already in place at the site, its configuration was not the most compact possible. At the same time, it was designed for high reliability without sacrificing the flexibility and control needed for operation in different modes. The plant was constructed in compliance with all the codes and standards that applied to commercial power facilities at the time. In particular, the pressure vessels and piping were designed to conform to the ASME Boiler and Pressure Vessel Code and to the ANSI Power Piping Code, respectively.

Two parameters were of particular importance in the design of the surface plant: the anticipated reservoir water-loss rate under long-term operating conditions, and the maximum allowable surface injection pressure (the maximum pressure that could be applied without inducing reservoir growth).

D.W. Brown et al., *Mining the Earth's Heat: Hot Dry Rock Geothermal Energy*,
DOI 10.1007/978-3-540-68910-2_8, © Springer-Verlag Berlin Heidelberg 2012

Early on, long-term water losses had been a concern because high loss rates would have been a major impediment to development and implementation of the HDR concept. It was already clear, however, that water lost from a confined, pressurized HDR reservoir consists only of water from the reservoir boundaries that permeates into the surrounding, lower-pressure rock mass. Near the end of Phase I reservoir testing in late 1980, the measured water loss was just 7 gpm—much lower than any recorded for an HWR (hot wet rock, or marginal hydrothermal) reservoir worldwide.

Note: The tightness of the Phase II reservoir had been established during Expt. 2077 (March 1989–December 1990—see Chapter 7). By the end of 17 months of pressure testing at 15 MPa (2200 psi), the rate of water loss from the confined Phase II reservoir was close to 2.1 gpm.

To ensure consistent measurements of water loss (as well as of fluid volume, impedance, heat extraction, and power production), it would be essential to keep the size of the reservoir constant; that is, the volume of stimulated rock that constituted the active reservoir region would be maintained by keeping the injection pressure below the seismic threshold (seismicity being the indicator of renewed reservoir growth). The maximum allowable pressure for aseismic circulation was selected to be 3960 psi (27.3 MPa), on the basis of findings from the ICFT: the first segment of that test, at a final injection pressure of 3890 psi, was essentially aseismic, whereas the second segment, at a pressure of 4570 psi, was highly seismic (see Chapter 7, Table 7-2 and Fig. 7-6). The essentially aseismic operation of the LTFT would later confirm the validity of this seismic threshold selection.

At the same time, to provide for unexpected events—as well as an opportunity to investigate a wider range of operating conditions—the surface plant was designed to enable operation at water-loss rates and injection pressures somewhat higher than those anticipated during steady-state operation.

The rate of flow through a pressure-dilated HDR reservoir is a function of the differential pressure across the reservoir in concert with the overall reservoir flow impedance, as controlled by the injection and production pressures. Conversely, for a given injection rate, the pressure-dependent reservoir flow impedance determines the injection pressure. The production backpressure is regulated by a combination of manual- and pneumatic-control choke valves. Depending on demand, the makeup-water pumps operate singly or in parallel to maintain a suction flow rate at the injecton pump equal to the selected injection flow rate.

Figure 8-1 is an aerial photograph of the Fenton Hill HDR Test Site as it appeared in 1992. The large pond in the woods, visible at the upper left of the photo, was the property of the HDR Project; the trailers in the upper center of the photo belonged to the U. S. Forest Service. The paved highway serving the facility is just out of view at the extreme lower left of the photo, near the site entrance.

Fig. 8-1. The Fenton Hill HDR Test Site, 1992 (view toward the west). Source: HDR Project photo archives

The components making up the surface plant would perform several major functions. They would (1) develop the pressures required for circulation of water through the reservoir; (2) remove the thermal energy from the hot geothermal fluid; (3) measure the temperature, pressure, and flow rate of the production fluid and control the production well backpressure; (4) remove any gases and solids from the fluid; and (5) add makeup water to the process stream, just upstream of the injection pump.

Figure 8-2 is an aerial photograph of the surface flow loop as completed in 1991, with major components identified. The backpressure-regulating station (located under a metal framework) was the "heart" of the surface flow-control system. During pressurized, closed-loop operation it provided feedback control of the backpressure at EE-2A; and during testing and open-loop operation it regulated the pressure of the fluid coming from the wellhead. In addition, flow rate and pressures were measured at this station. (To ensure accuracy, the fluid production temperature was measured in an insulated enclosure, as the fluid exited the production well.[1]) The tall structure in the upper right of Fig. 8-2 is the logging tower over the EE-1 borehole (the principal downhole seismic station was located in EE-1, at a depth of 9400 ft).

[1]With 5000-psi wellhead equipment, one does not attempt to use temperature wells!

The surface flow loop was designed for automated operation, via a high-speed data acquisition and control system (housed in the Data Acquisition Trailer, or DAT, the building closest to the highway, shown at the top of Fig. 8-2) that simultaneously collected operating information. Using a PC-based computer with commercial software, the control system enabled the loop to be operated unmanned for extended periods and provided for automated shutdown in the event of a deviation from normal operating conditions.

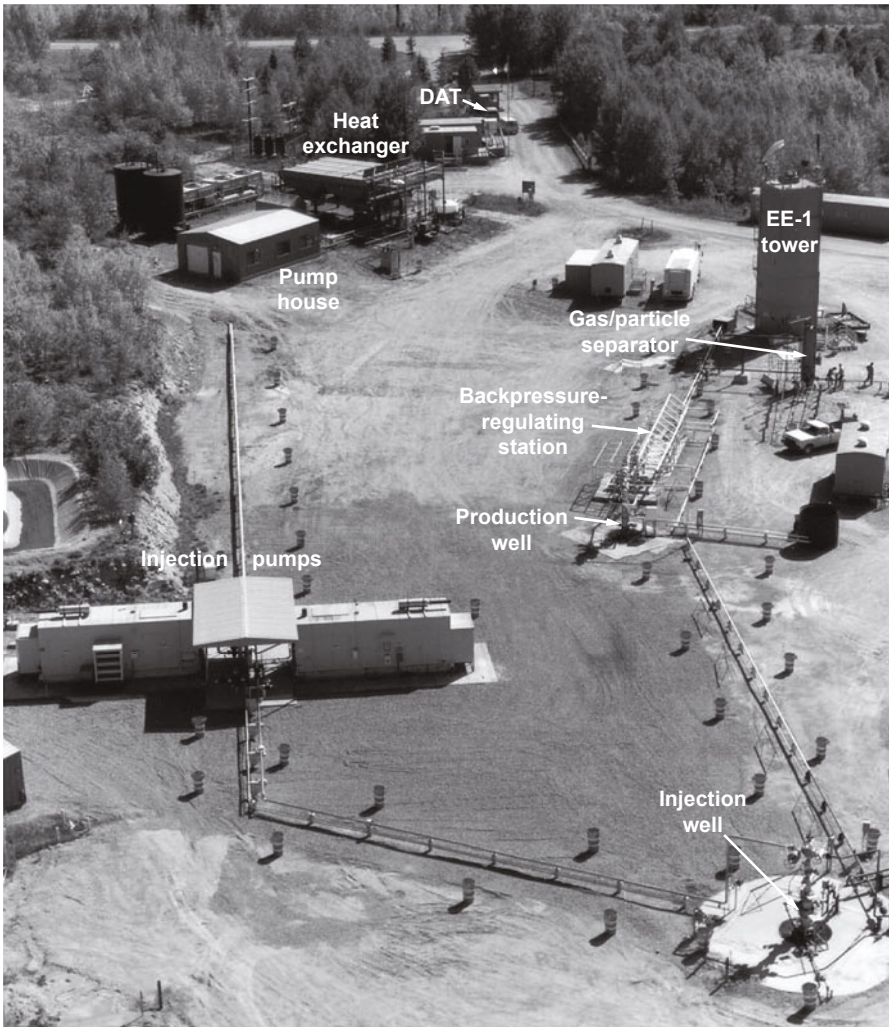

Fig. 8-2. Surface flow loop at the Fenton Hill HDR Test Site, 1991 (view toward the east).
Source: Duchane, 1994c

Figure 8-3 is a flow diagram of the major closed-loop test components. The order of operations was as follows: One or the other of the injection pumps (which were housed in soundproof buildings) would pump water into the reservoir via the injection well (EE-3A); the water would circulate through the reservoir under high pressure, and would exit the reservoir at high temperature via the production well (EE-2A); the produced fluid would pass through the flow-monitoring and backpressure-regulating station, then through the gas/particle separator for removal of any free gas and suspended solids; next, the fluid would flow through an air-cooled heat exchanger; and finally, with makeup water added from the pump house, it would be reinjected.

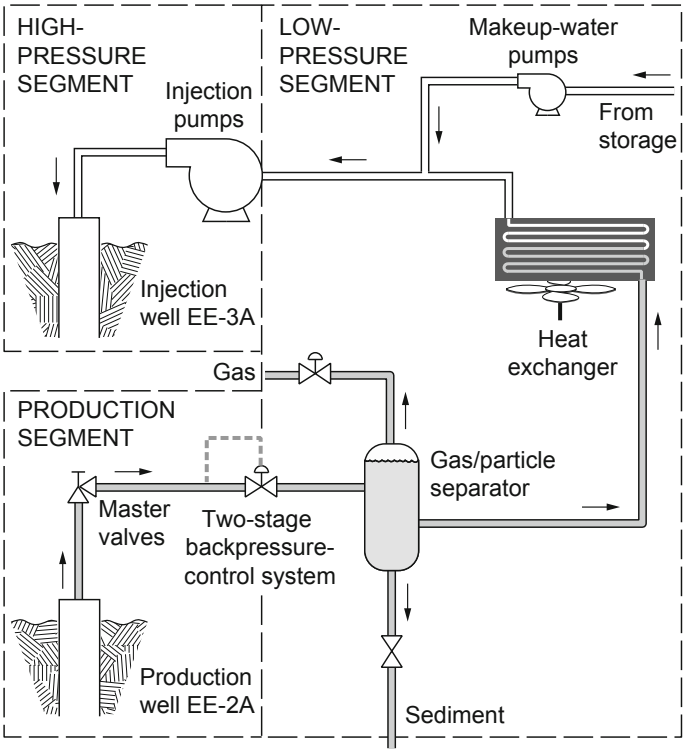

Fig. 8-3. Layout of the closed-loop portion of the Phase II surface facility. Adapted from Ponden, 1991

From a mechanical design standpoint, the plant can be envisioned as comprising three segments, as shown in the figure:

- The high-pressure segment
- The production segment
- The low-pressure segment

High-Pressure Segment

This segment consisted of the injection wellhead, the injection pumps, and piping dedicated to the novel functions of HDR technology: injection of water into a confined geothermal reservoir at pressures high enough to open joints that would normally be closed; and circulation of that water across the HDR reservoir through the interconnected array of opened joints, thence up the production wellbore.

Injection Wellhead (EE-3A)

Figure 8-4 is a schematic drawing of the high-pressure injection wellhead assembly. The central, 4 1/2-in.-diameter injection tubing (shown as the tie-back string in Fig. 6-43), with the attached 5 1/2-in. liner, extended down to the beginning of the open-hole section of the wellbore at 11 436 ft (3486 m). As a major control point for high-pressure fluid being pumped through the reservoir, the EE-3A wellhead was equipped with numerous valves, ports, and instruments that served a variety of functions related to fluid control, measurement, safety, and logging. This wellhead enabled the circulating fluid to be directed down into the reservoir or, during testing of the surface system, to be sent to the production wellhead via a bypass line. A special valve at the top of the wellhead allowed logging to be carried out while the system was under pressure. (All of the valves at this wellhead that controlled the circulation of fluid were replaced in 1990, as part of the preparations for the LTFT.)

For safety purposes, two master valves were installed on the wellhead—the upper one rated at 5000 psi and the lower one at 10 000 psi—to contain any overpressure that might inadvertently be applied to the injection string (the planned LTFT injection pressure was only 3960 psi). Additional pressure-relief valves and side outlets were employed for the various annuli between casing strings, as shown in the figure. As mentioned several times earlier, because of the frac-around of the poorly cemented liner at EE-3A, fluid from the reservoir continued to flow from the annulus outside the injection tubing, exiting the wellbore through the backside flow line.

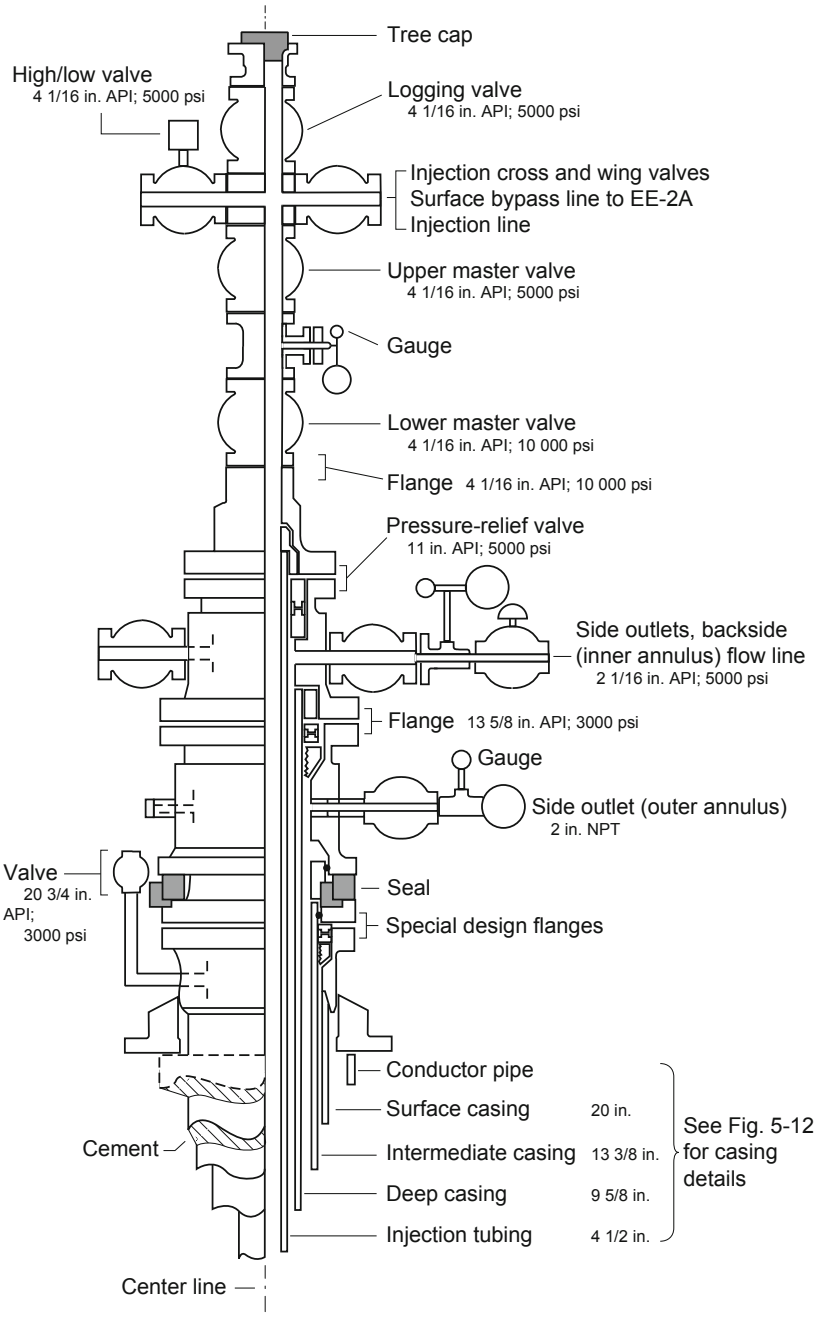

Fig. 8-4. High-pressure injection wellhead assembly (Well EE-3A). Left: exterior view; right: cutaway view.
Based on an HDR Project drawing by D. S. Dreesen, 1992

Injection Pumps

The injection pump was the "driver" of the HDR circulation system. It provided the motive force for moving fluid at high pressure into the wellbore, forcing the fluid through the pressure-propped open joints, and after considerable natural and imposed pressure reduction, returning the fluid to its own inlet chamber. In developing specifications for the pump, pressurization capability and fluid-transfer capacity were important considerations; but the deciding factor was the ability to tolerate a very high fluid pressure—up to 1100 psi (7.5 MPa) at its inlet, so that the entire HDR circulating system could be run as a pressurized, closed loop. Unfortunately, at the time, no manufacturers of centrifugal pumps could guarantee a mechanical seal sufficient for meeting those suction-pressure specifications.

After an evaluation in 1989 that considered experimental, operational, and economic issues, and a review of products from several manufacturers, plunger-type pumps were chosen over centrifugal pumps for this high-pressure application. A pair of 5-cylinder reciprocating pumps (Fig. 8-5) was purchased from Ingersoll-Rand (IR) Corporation. Having two pumps would enable them to be operated alternately, provide a backup capability, and allow for pump maintenance without the need to shut down LTFT operations.

The reciprocating pumps were essentially similar to pumps produced by IR for petroleum-reservoir fracturing and water-flooding applications, but were specially engineered for the particular requirements of the HDR Project: the higher pressures and longer periods of sustained operation that were anticipated, as well as the unique characteristics of the geothermal fluid. Each cylinder moved in its own block—cast from Nitronics 50, a high-strength steel alloy—with the bore machined to tight tolerances. These blocks, produced by a subcontractor to IR, typically were quenched rapidly in water after casting; but at the request of Los Alamos, IR directed that the blocks for these particular pumps instead be air-cooled to relieve any thermal stresses in the cast metal. All parts that would be in contact with geofluids were made of corrosion-resistant materials: Nitronics 50 stainless steel for the pressure-boundary parts, and Inconel (another special type of stainless steel) for the valves.

Each pump was powered by a 520-hp Caterpillar diesel engine via an automatic transmission that permitted a considerable range of operating conditions. The pump–transmission–driver assembly was skid-mounted and housed in a sound-attenuating enclosure to reduce noise. Each unit and its housing—which together weighed about 70 000 lb (32 000 kg)—was firmly anchored to a 10 ft × 28 ft (3.0 m × 8.5 m) concrete pad embedded in the local tuff bedrock. In addition, pulsation-dampening devices were installed on the pumps to reduce vibration in adjacent parts of the loop. The pumps could produce flow rates in the range of 84–336 gpm (5.3–21.2 L/s). Operated alternately, each would run for a period of 250 hours (the recommended operating period between oil changes for their diesel-engine drivers). A 10 000-gal. (38 000-L) diesel fuel tank was located in a plastic-lined berm near the pumps.

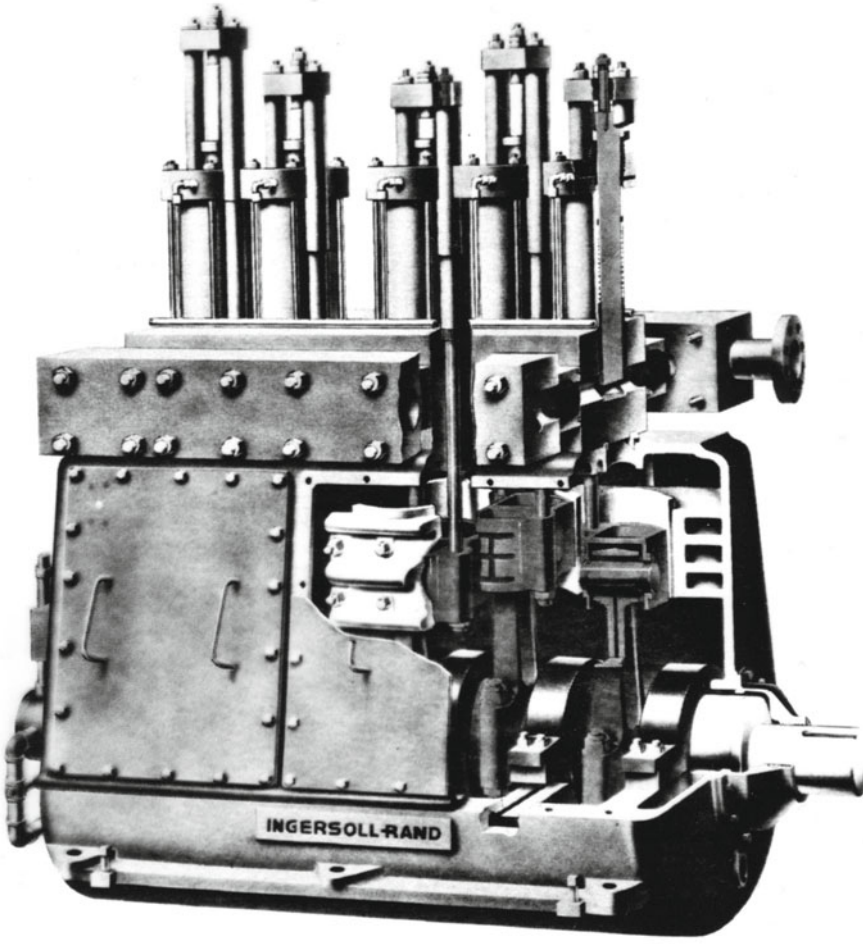

Fig. 8-5. Ingersoll-Rand 5-cylinder reciprocating pump.
Source: HDR, 1993

The failure of *both* injection pumps within a period of two days, after only a few months of operation (see Chapter 9), would be a major setback for the Fenton Hill HDR flow-testing effort. Following an unsatisfactory attempt to substitute other pumps—first smaller pumps that had been used in earlier experiments and then a rented plunger pump—a high-pressure centrifugal pump would be rented from the REDA Pump Co. (Fig. 8-6). This unit, built specifically for the Fenton Hill HDR application, was a 200-stage pump driven by a 350-hp electric motor and incorporating new sealing technology; it was designed for continuous operation at the high suction pressures and flow rates needed for full-scale reservoir circulation. Despite initial problems with the electrical hookup, the pump would provide

excellent service, maintaining the desired level of injection flow rate until operations were suspended (because of a funding shortfall). Only following a two-year hiatus would a new centrifugal pump be purchased from REDA; it would operate, like its predecessor, nearly trouble-free for the remainder of the LTFT.

Fig. 8-6. The REDA centrifugal pump.
Source: REDA Pump Company brochure, 1992

High-Pressure Piping

Several hundred feet of high-pressure piping connected the injection pump to the injection well. This section of the loop was fabricated from nominally 4-in. (100-mm), type 304L stainless steel pipe having an inner diameter of just over 3 in. (75 mm). (Carbon steel pipe was not used because, to meet the 5000-psi [34-MPa] maximum working-pressure standard, the inner diameter would have had to be very small—far too small to accommodate the flow velocities required during injection at anticipated rates.)

The high-pressure piping was connected to the two injection pumps via a manifold system that enabled fluid entry from either pump or simultaneously from both. Because of its length, the pipeline was mounted on rollers several feet off the ground to allow for thermal expansion. It was tied into the injection wellhead at a point about 12 ft (3.7 m) above ground, via an elbow (designed to further relieve stresses resulting from thermal expansion and contraction) positioned a few feet from the wellhead. This design would prove to be a problem-free one during LTFT operations at Fenton Hill.

Production Segment

This segment had the same pressure rating as the high-pressure segment (5000 psi). It consisted of the production wellhead and the adjacent backpressure-regulating station.

As shown in Fig. 8-7, the configuration of the production wellhead was similar to that of the injection wellhead: it was equipped for logging during production or for receiving flow directly from the injection wellhead via a surface pipe that bypassed the reservoir (for testing of the surface system). It was fitted with an array of valves, outlets, and gauges similar in general to those on the injection wellhead but with variations specific to the process of high-pressure fluid production. Unlike the injection well, the production well was cased and cemented full-depth (see Fig. 7-17). Except for the lower master valve, all the valves controlling the circulation of fluid at this wellhead were replaced in 1990, as part of the preparations for the LTFT.

From the production well, the geofluid flowed through either arm of a redundant choke manifold that maintained the desired backpressure at the production well. This two-stage backpressure-control system was a major control point for the circulation of fluid through the reservoir. It consisted of a manually adjusted choke valve (used for the first stage of pressure control), a strainer assembly designed to remove particulates as small as 50 μm from the circulating fluid, and a feedback-controlled automatic throttling valve that further increased the backpressure. The piping in this segment was designed for operation at pressures of up to 5000 psi (34 MPa).

Thermal stress was anticipated at the outlet of the production wellbore, because (1) temperature changes of over 100°C could be expected in the 10 770 ft (3283 m) of production casing as the system went from dormant (geothermal gradient) to full circulation (hot); and (2) it was known that the cement within the wellbore, which normally would have minimized thermal expansion, had suffered some deterioration. With this in mind, the outlet piping from the production wellbore was designed to expand up to 2 1/2 in. (6 cm). But this degree of allowance for expansion would quickly prove to be insufficient, and early in the LTFT the piping would be redesigned to incorporate an expansion elbow capable of accommodating 6 in. (15 cm) of growth.

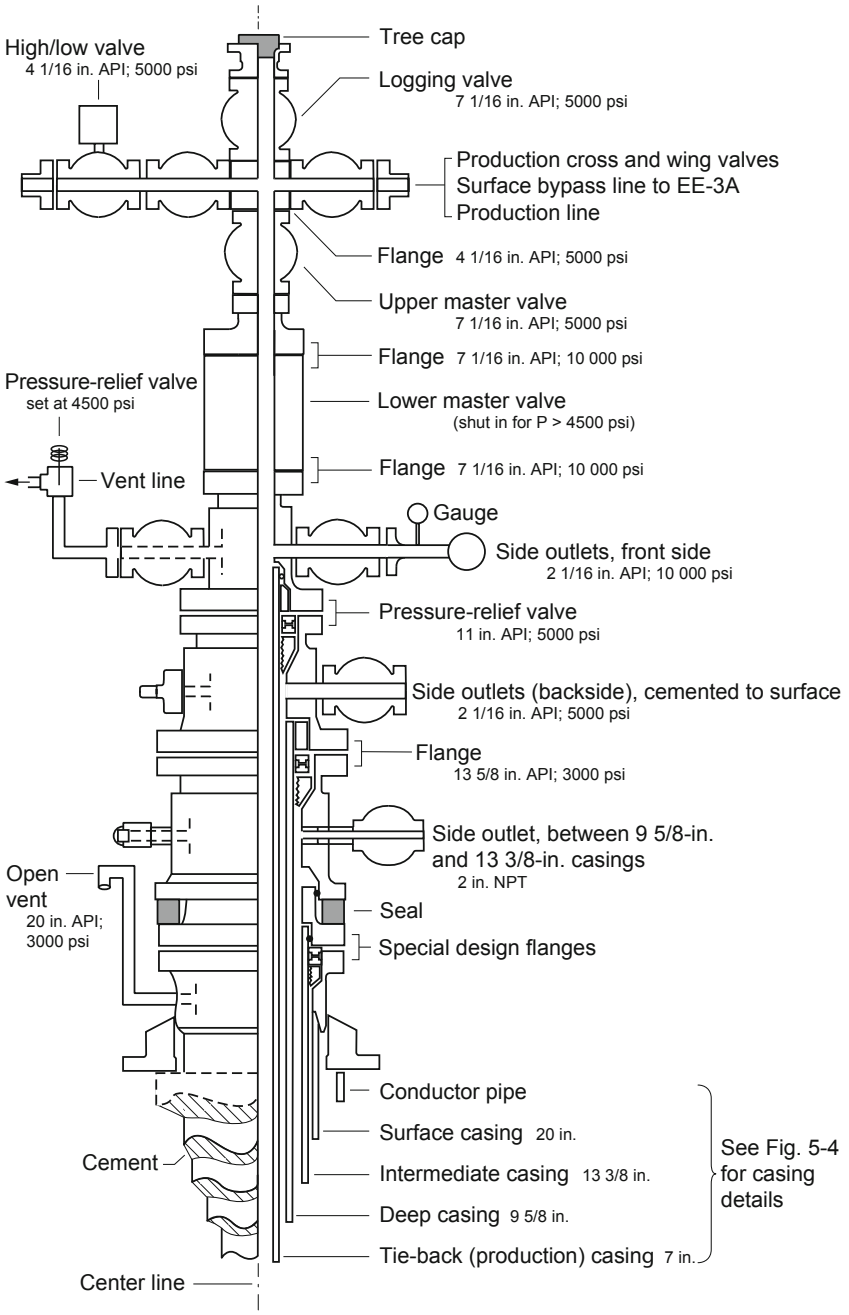

Fig. 8-7. Production segment: production wellhead assembly (Well EE-2A). Left: exterior view; right: cutaway view.
Adapted from Dreesen et al., 1989

Low-Pressure Segment

This segment comprised the gas/particle separator, the heat exchanger, the pump house, and the interconnecting piping. The fluid coming from the production segment flowed sequentially through these components, then (with makeup water added at the pump house) was routed to the inlet of the injection pump. The pressure in this segment was determined by the production flow rate and the combined flow impedance of the included equipment (primarily the heat exchanger) and the connecting piping, which were constructed primarily of carbon-steel materials having a maximum design pressure of 1100 psi (7.5 MPa).

Gas/Particle Separator

This unit was located just downstream from the backpressure-regulating station (see Fig. 8-2) and therefore received very hot fluid during circulation. The separator was built and installed in conformity with the ASME Boiler and Pressure Vessel Code. It was designed to separate any free gases (at up to 350 lb/min [160 kg/min]) and suspended solids (at up to 3 lb/min [1.4 kg/min]) from the circulating fluid via a cyclonic process. Because it was pressurized to the same level as the other parts of this segment of the loop, the separator would remove only those gases whose concentrations exceeded their solubility limits in the geofluid at that pressure. (The separator would never be taxed to anywhere near its capacity, however.)

Heat Exchanger

The heat exchanger had been in use periodically at Fenton Hill since 1976, when it was purchased from the Yuba Heat Transfer Company for testing of the Phase I reservoir. This air-cooled unit was designed to extract geothermal power—essentially the same function that commercial geothermal power plants perform when exploiting natural (hydrothermal) hot water resources. Modular in design, it contained four separate bundles of finned, ASTM A-214 carbon-steel cooling tubes, each with a cooling capacity on the order of 5 MW.[2] For circulation testing, in fact, the heat exchanger was larger than needed; during the LTFT, typically only one of the four bundles would be used at any given time.

Because of the age of the unit and the susceptibility of the cooling pipes to corrosion, several of the tubes were removed and inspected during construction of the surface plant. The inspections turned up iron-carbonate scale deposits, probably resulting from the interaction of dissolved carbon dioxide with the mild steel of the heat exchanger tubes. When the scale was

[2]Some references may cite a capacity of 20 MW per bundle, or 80 MW total. The original order called for a unit that size, but because of budget cutbacks in 1975, the unit actually purchased was much smaller.

removed from the test specimens, the walls turned out to be sound: degradation of the wall material was negligible. On the basis of this evaluation, the decision was made not to clean or replace the tubes.

Improvements were made to several other parts of the heat exchanger in preparation for the LTFT: the motor control unit for the fans was modernized to provide more reliable operation and bring it into compliance with the latest code for the operation of large electrical equipment; the operation of the louvers was automated; and the four valves controlling the inlet flow to the tube bundles were replaced.

Makeup-Water Pumps

Downstream from the heat exchanger was the pump house (see Fig. 8-2), in which were installed two types of makeup-water pumps: high-pressure, low-volume Roto-Jet pumps and low-pressure, high-volume Meyers pumps. There were two of the centrifugal Roto-Jet pumps, each driven by a 50-hp motor and capable of delivering 37 gpm (140 L/s) against a pressure head of 1000 psi (6.8 MPa). These pumps would be used during closed-loop circulation when the HDR system was under pressure. It was expected that once steady-state reservoir circulation had been established, with water losses projected to be only in the range of 10–20 gpm, a single Roto-Jet pump would suffice.

The Roto-Jet pumps were controlled by an electronic duplex logic circuit designed to automatically activate the second pump whenever the demand exceeded the capacity of a single pump. This logic circuit would prove to be somewhat troublesome, causing several shutdowns. Eventually, the electronic controls were modified so that the system would automatically restart after brief power outages, such as those attributable to the Roto-Jet pump circuitry. Despite overall satisfactory performance, the Roto-Jets would prove to be expensive to maintain (in particular because of ongoing problems with erosion of components).

The second type of pump, used for simply filling the reservoir or for open-loop operations, was a conventional, high-volume Meyers pump. Four of these were installed in the pump house and plumbed into the loop. Each pump was capable of supplying water at a rate in excess of 100 gpm.

Low-Pressure Piping

The low-pressure segment of the loop contained the several hundred feet of piping between the choke assembly and the inlet of the injection pump. This section of piping was designed for operation at pressures up to 1100 psi (7.5 MPa). It routed the produced fluid from the outlet of the flow-monitoring and backpressure-regulating station, through the gas/particle separator, under a service road, and into the inlet manifold for the heat exchanger. Piping from the heat exchanger outlet then delivered the cooled fluid to the pump house, where makeup water was added as required. The

fluid discharging from the pump house was now at the suction pressure for the injection pump—the lowest pressure in the closed circulation loop (the so-called low-side pressure)—and at the appropriate flow rate.

As mentioned above, the rather circuitous route of the low-pressure piping stemmed from the need to connect the wellbores of the deep system via the heat exchanger without moving that massive piece of equipment. The piping was made of carbon steel, much of it salvaged from earlier operations. Before being used for the LTFT, it underwent both mechanical and radiographic inspection, which showed the overall condition to be good (a few welds did not meet specifications and had to be redone). A short distance downstream of the gas/particle separator, an elbow was built into the piping for protection against thermal expansion.

It should be stressed that the surface loop for an HDR power plant is unique: it differs from all other types of geothermal power plants in that it is a pressurized flow loop associated with a pressurized reservoir. The lower the parasitic pressure losses in the surface equipment, the better—because higher losses would increase the pumping power required. For the LTFT, for instance, the pressure rating of the low-pressure segment would ideally be greater than 1400 psi, enabling the production fluid to be fed to the injection pump at a pressure not much lower than the controlled backpressure of 1400 psi. However, the heat exchanger (which had been installed before Phase I testing and before high-backpressure operation was envisioned), was not capable of operation at these higher pressures. This limitation unfortunately precluded a more desirable, higher-fluid-pressure operating condition for the LTFT.

Automated Control and Monitoring System

The operations of the surface plant could be controlled automatically via a Dell 486 computer in the DAT. The software used, DMACS (Distributed Manufacturing and Control Software), was a commercial product marketed by Intellution of Norwood, MA, USA. The computer was interfaced, via an optical-fiber network, with three other on-site computers: a backup computer in the DAT, a large-display terminal in the operations building, and a unit in the chemistry trailer. This arrangement permitted personnel in any of the three buildings to view operating parameters in real time, implement changes in the control parameters, or call up historical data. (These functions could also be performed remotely by telephone via a modem connection.) The system was password-protected to prevent unintentional or unauthorized changes.

Figure 8-8 shows the data-acquisition and control points in the surface loop. Overall system balance was extremely important because of the potential for "feedback" effects during closed-loop operation. For example, the amount of pressure from the low-pressure side of the loop, at the inlet

to the injection pump, is additive to the pressure generated by the pump; that is, a cumulative pressure results that is greater than that produced by the injection pump alone. That greater pressure, if unregulated, could lead to increases in both the injection pressure and the injection flow rate, thereby boosting the production flow rate and, in turn, the low-side system pressure—and so on. The pressure delivered by the injection pump is normally controlled by adjusting the flow rate, but is also affected by the overall reservoir flow impedance (which is a function of the reservoir pressure and the production well backpressure). To facilitate control, pressures and flow rates would be checked regularly during the LTFT, at a number of points in the loop—as would the production temperature, which, along with the production flow rate, determines the productivity of an HDR system.

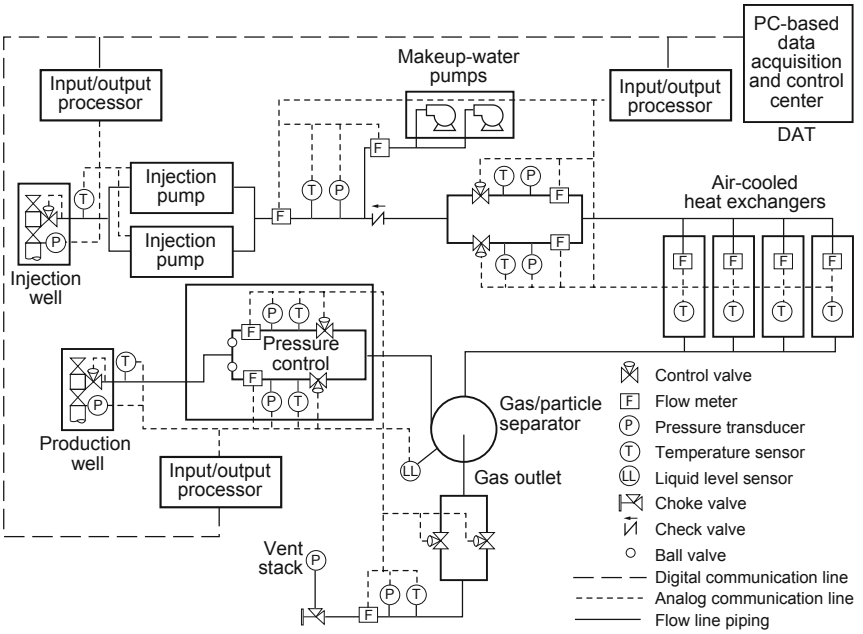

Fig. 8-8. Schematic of the data acquisition and control system. Adapted from Ponden, 1992

When not used specifically to provide an elevated level of backpressure on the production well, the throttling valves at the outlet of the production well would function as outlet-flow-control valves. By maintaining pressure in the low-pressure side of the loop at a level that would preclude flashing of the hot production fluid, these valves would prevent scaling, cavitation, and other problems related to two-phase fluid flow. Another parameter that was monitored and controlled was the water level in the water storage tanks that supplied the makeup-water pumps. Finally, there were a number of control points that

could be used during startup or shutdown, for safety checks, or in special situations such as out-of-range conditions (which automatically triggered alarms).

Flow could be vented from several points in the loop. In addition, from the injection wellhead the "injected" fluid could be pumped directly across to the production wellhead instead of through the reservoir—an option that was especially useful during testing of the surface loop. From the production wellhead, fluid could be vented to the storage pond adjacent to the loop, either (1) directly from the wellhead (hot fluid); (2) from the pump house, after passage through the heat exchanger (cooled fluid—a more desirable option); or even (3) just before entry into the injection wellbore. The temperature at the heat exchanger was controlled by adjusting the positions of the louvers that directed air over the tubes. Automated operation of the heat exchanger's cooling fans served primarily to ensure that rapid on–off cycling would be avoided.

Although the system was fully automated, the programmed control points could always be overridden manually. A HI/HI–LO/LO alarm mechanism was set so that the first "out-of-bounds" signal would simply set off an alarm, but a further deviation from programmed conditions would actually shut the plant down (during manned operations, the initial alarm alerted on-duty personnel to take corrective action, and thereby avert a shutdown).

In warm weather, automated system shutdowns could deactivate the system completely by closing valves and turning off fans and pumps. In the winter, however, when freezing conditions could be expected, the outlet control valves could be left partially open to allow a 10- to 15-gpm (40- to 60-L/s) flow of heated water to be produced from the reservoir, directed through the production and injection lines to keep key components from freezing, and then vented to the pond. Because of the residual pressure in the reservoir, such a standby low-flow venting status could be maintained for weeks or even months (though such long-term usage would not prove to be necessary).

Ancillary Facilities

A number of support facilities were needed to keep the surface plant running, collect important data, and manage the overall operation. Electricity was obtained from the Jemez Mountains Electric Coop, the local power supplier. During summer thunderstorms or winter snowstorms, power outages could and did occur—and would prove to be a major cause of inadvertent system shutdowns over the course of the LTFT. These support facilities and equipment included the following:

On-site Water Well

The 450-ft (140-m)-deep water well drilled in 1976 would continue to supply water for all domestic and loop operations throughout the LTFT. Its nominal production rate was 100 gpm.

Water Storage Ponds

The two water storage ponds on the site would provide storage and venting capacity during the LTFT. The larger pond (5-million-gal. capacity) was located about 300 ft (100 m) south of the surface loop (see top left area in Fig. 8-1). Water from this lined, covered pond was pumped via an underground pipeline to the storage tanks behind the pump house (visible just to the left of the pump house in Fig. 8-2).

The smaller storage pond (Fig. 8-1, near the center), which had a capacity of about 1 million gal., contained primarily water vented from the circulation loop. Because such water could contain a few parts per million arsenic (as well as a number of other minerals), dissolved gases such as carbon dioxide, and small amounts of hydrogen sulfide, the pond was upgraded in 1990, before the start of the LTFT. It was further excavated and graded, after which a narrow trench was dug down the middle. It was then lined, including the trench, with 30-mil, polyvinyl-chloride plastic. Perforated pipe was installed in the trench on top of the liner, running the length of the pond. Finally a second liner, of XR-5 (a material with superior resistance to ultraviolet radiation), was added. This upgrade—double lining plus a pipe to collect any fluid that might escape through the inner liner, so that it could be pumped out and properly disposed of—was done in accordance with standards approved by the New Mexico Oil Conservation Division.

Buildings

The four buildings essential to operation of the loop were the operations building, the DAT, the pump house, and the chemistry trailers. (All of these buildings except the pump house and the second [smaller] chemistry trailer were in service during the Phase I operations.)

Operations Building

Located outside the loop just beyond the small pond (see Fig. 8-1), the operations building served as the site's administrative center. As mentioned above, all loop functions could be monitored and controlled from this building as well as from the DAT. For the LTFT, the building's conference room was equipped with a large-screen television that could display a diagram of the loop and the current flow rates, temperatures, and pressures at the injection and production wellheads (displayed in boxes beside their icons and updated every few seconds). It could also display historical data graphically.

Data Acquisition Trailer

The DAT, the control center for the loop, housed the master computer by means of which loop operations were monitored and controlled, the computer hardware and software for receiving and processing seismic data, and the media for storing all the operating and surveillance data as it was generated. (Most of the equipment that had earlier been installed in this trailer, for monitoring of the Phase II pressure-stimulation experiments, had by now been upgraded, disabled, or removed.)

Pump House

This small insulated building, which was located between the heat exchanger and the injection pumps, contained the six makeup-water pumps (two high-pressure Roto-Jets and four high-volume Meyers pumps) and a number of control valves. The two 2000-gal. (7600-L) storage tanks behind the building were often referred to as the "frac tanks," because they had originally been used to store water for the "fracturing" (pressure-stimulation) experiments.

Chemistry Trailers

The chemistry trailer used during Phase I operations and expanded during Phase II (in Fig. 8-2, the long trailer beyond—and partially obscured by—the tall logging tower over EE-1) remained in its original location beside the main site road and adjacent to the water well. For the LTFT operations, a second, smaller "chem trailer" was stationed physically within the loop, between the two wellbores (the small trailer visible just to the right of the metal framework over the production-flow-monitoring and backpressure-regulating station in Fig. 8-2). This small portable building contained the instruments that automatically monitored the pH, oxidation/reduction potential, and conductivity of the circulating fluid (a small geofluid sidestream of about 0.5 gpm [0.03 L/s] was diverted to these instruments; collection of the gaseous components from this sidestream, and their periodic measurement, were both done automatically). Sulfide-ion and oxygen levels were monitored offline by species-specific electrodes. The trailer also contained a small benchtop laboratory area and filtering equipment for collection of fluid samples, which would be sent to the main chemistry trailer for elemental analysis by inductively coupled plasma (ICP) spectroscopy.

Seismic Monitoring Network

Only part of the seismic monitoring network established for the Phase II hydraulic-stimulation operations would be used during the LTFT; the plan was to instrument the three downhole (Precambrian Network) seismic stations for radiotelemetric reporting to the central computer in the DAT. These three stations were the single-axis geophones installed in GT-1 (Barley Canyon) at a depth of 2570 ft; in PC-1 (Lake Fork Canyon) at

2450 ft; and in PC-2 (Lake Fork Mesa) at 1900 ft. In addition, on occasion a 3-axis geophone would be deployed at a depth of 9400 ft in the EE-1 borehole, which was extremely close to the reservoir, to pick up very minor seismic activity or even system "noise" created by the movement of the fluid through the open joints of the reservoir. (Unfortunately, budgetary constraints prevented the Project from supporting even a part-time seismologist for the LTFT.)

Miscellaneous Equipment and Structures

A number of surge tanks, miscellaneous equipment, and storage structures were located on the site (see Fig. 8-1). Other structures enclosed the Phase I wellbores (the large square tower visible near the center of Fig. 8-1 enclosed the EE-1 wellhead, and the shorter tower south of EE-1 enclosed the GT-2 wellhead). Also on the site were trucks, a small bulldozer for grading and snow removal, and a large crane procured in 1991.

Environmental and Safety Controls

A variety of environmental and safety measures were put in place to govern work at the site. These included an established safety program with regular meetings, an operational readiness review (conducted by an independent committee before the start of the LTFT), and a site-wide environmental surveillance plan, as well as guidance on how to respond in unexpected or emergency situations. Particular attention was paid to the potential for releases of deadly hydrogen sulfide gas: warning signs were placed in strategic locations, and alarmed detectors were installed at sites where escaping gas could present a significant danger. In addition, a number of portable detectors were procured. No doubt owing at least in part to careful compliance with these precautions, no significant environmental or safety problems arose during the LTFT.

Chapter 9

Long-Term Flow Testing of the Phase II Reservoir

In the wake of initial Phase II reservoir testing and the ICFT, fundamental questions about the commercial potential of HDR technology remained to be answered. How reliable is power production from an HDR reservoir? What might be the longevity of such a reservoir? To answer these questions, and to demonstrate that geothermal energy could be extracted on a sustained basis, more extensive testing would be required. The Long-Term Flow Test (LTFT) for the Fenton Hill Phase II reservoir was designed to simulate as closely as possible the conditions under which a commercial HDR power plant might operate.

From its very beginning, the HDR Program had as its overriding goal to demonstrate that the heat-mining concepts developed at Los Alamos could be applied to extract useful amounts of energy from the vast, non-hydrothermal HDR resource. As described in Chapter 4, the small, Phase I HDR research reservoir had been flow-tested extensively between 1978 and 1980. With those accomplishments as a foundation, all the work on the larger, Phase II reservoir was conducted with an engineering-scale demonstration of HDR technology in mind. As the HDR Program at Los Alamos was scaled back in the 1980s, therefore, the remaining effort was directed almost totally toward the LTFT. Essential information for the design of the LTFT was derived from the results of the ICFT and of Expts. 2074 and 2077 (see Chapter 7).

The information in this chapter is derived primarily from reports of the Hot Dry Rock Geothermal Energy Development Program (1993 and 1995), Brown (1994b, 1995a, and 1996a), Brown and DuTeau (1993), and Duchane (1995b and 1996c).

Development of the Operating Plan

On September 9, 1986, several months after completion of the ICFT, the Los Alamos HDR Program Office issued a memorandum that set forth two principal goals for the LTFT:

1. Improve reservoir performance—specifically, reduce both flow impedance and water losses
2. Operate the reservoir at various steady-state conditions, up to an undefined maximum flow rate

The memorandum described only a generalized operating plan for the LTFT. That plan was somewhat ambivalent about the details of the test protocol, stating in one instance that "continuous loop operation during a reservoir improvement sequence of experiments is not necessary or desirable," while

D.W. Brown et al., *Mining the Earth's Heat: Hot Dry Rock Geothermal Energy*,
DOI 10.1007/978-3-540-68910-2_9, © Springer-Verlag Berlin Heidelberg 2012

in another place presenting a diagram for a 9-month continuous test period under undefined operating conditions.

Over the next year, these two goals matured into the following set of six goals, as paraphrased from the Program's Annual Report for 1987 (HDR, 1989b):

1. Determine the thermal characteristics of the reservoir, including power vs time, extractable heat, and thermal stress effects
2. Determine the time-varying hydraulic characteristics of the reservoir
3. Study the operating characteristics of the system
4. Confirm the usefulness of various reservoir diagnostic techniques
5. Verify and refine analytical reservoir models
6. Provide a database useful for the creation of additional HDR reservoirs

With these goals as a basis, a more detailed operating plan was formulated, which included experiments designed to meet multiple scientific and engineering objectives. For example, tests were proposed to maximize reservoir productivity and severely stress the HDR reservoir. The plan called for three quasi-steady-state flow stages, at successively greater rates of injection, until the maximum operating rate was reached. The first two stages would each last 30 days, while the third stage—circulation at the highest possible aseismic pressure—would last 9 months. During the first month of the third stage, some additional experiments would be carried out:

- A backpressure study to assess the effects, on the production flow rate, of variations in the pressure maintained at the outlet of the production well.
- The first of four stress-unlocking experiments, during which the production well would be shut in and the injection pressure increased briefly to very high levels (up to 5000 psi [34.5 MPa]). These four experiments, to be spaced about two months apart, were designed to induce additional joint-opening and thereby improve reservoir productivity. They were expected to produce some seismicity but also to progressively enhance aseismic flow when steady-state operating conditions were resumed.

The plan also called for tracer experiments at key points during the three flow stages and regular seismic monitoring, especially during the stress-unlocking experiments.

The LTFT would be concluded with a 2-week cyclic experiment to demonstrate the operation of the system in a "huff–puff" (inject–produce) mode. During each 24-hour cycle, water would first be injected and stored in the reservoir at increasingly higher pressures for 12 hours, then extracted and produced at decreasing pressures over the next 12 hours.

As is usually the case in designing a complex experiment, it was difficult to achieve a balance between the desire to obtain as much information as possible, through reservoir testing under a variety of conditions, and the need to obtain basic, straightforward data that would provide a solid foundation for further HDR development.

The HDR Program's external advisory committee, known as the Program Development Council (PDC), consisted of representatives from relevant industrial, academic, and government organizations. The industrial members, in particular, had continually stressed the fundamental importance of the LTFT to the future of HDR. During meetings held in June 1988 and in March 1990, the PDC pushed hard for "getting on with the LTFT." At the same time, they found the 1987 operating plan (HDR, 1986b) too complicated, and argued for a simple testing protocol that would provide unambiguous answers to key questions. Declining budgets, too, were forcing a rethinking of the plan. By the time of the July 1991 meeting of the PDC, when the surface plant had been constructed and other preparations for the LTFT were nearing completion, the plan presented by the HDR Program Office had been revised to the following components:

1. A one-month preliminary circulation period, to evaluate the state of the HDR system and determine parameters for subsequent testing. This period would also include a brief evaluation of the effects of maintaining a high backpressure at the outlet of the production well.
2. One month of steady-state circulation at the highest possible aseismic injection pressure, to determine the best performance that could be expected of the existing reservoir under benign operating conditions; and to obtain data regarding water consumption during circulation in a non-growth mode.
3. A long (8- to 10-month) period of steady-state circulation, under seismic conditions of moderate reservoir growth, to ascertain the system's maximum sustainable energy production capability. This test phase, by taxing the thermal capacity of the reservoir, would provide data from which the useful thermal lifetime of the reservoir could be estimated.

In addition, some "enhancements" to the plan were included, to be implemented if the LTFT could be continued beyond one year:

- Continuation of the 8- to 10-month steady-state operation for up to 9 additional months.
- A single stress-unlocking experiment at a maximum injection pressure of 4500 psi (31 MPa), followed by a two-week period of steady-state circulation to assess its effectiveness in increasing the productivity of the reservoir.
- An additional month of steady-state operation at the highest possible injection rate, to (a) ascertain the maximum productivity obtainable from the reservoir and (b) simulate, to the extent possible, the operation of an HDR system with multiple production wells. (Multiple production wells would ostensibly provide additional pressure sinks for the circulating fluid and thereby permit aseismic injection at much higher pressures.)
- A month-long cyclic experiment entailing a 12-hour injection/12-hour production schedule similar to that proposed in the 1987 LTFT plan.

Like previously proposed protocols, this new plan called for extensive tracer testing and seismic monitoring throughout the test period. In the eyes of the Los Alamos staff, it responded to concerns expressed by the PDC by incorporating a longer period of truly "steady-state" operation (albeit under seismic conditions to maximize reservoir productivity). It was designed to test the Phase II HDR reservoir under rigorous conditions—which, it was hoped, would bring about measurable thermal drawdown of the reservoir while maximizing opportunities to collect important scientific data.

The PDC, led by its industrial members, still found this approach to the LTFT too complex. They urged instead a straightforward test that would provide fewer, but much less ambiguous, answers to questions about the viability of HDR for the practical production of useful amounts of geothermal energy. They argued that any evidence of thermal drawdown, or lack thereof, that might be observed under conditions of continuing reservoir growth would be very difficult to interpret.

The LTFT was therefore redesigned one last time, to something much more akin to a simple demonstration that the Phase II reservoir could provide reliable energy in a routine manner. The test conditions would represent those that could be replicated in an HDR production plant. The LTFT plan that was adopted by the PDC may be summarized as simply,

> *Bring the reservoir to the highest possible aseismic pressure and circulate water through it under steady-state conditions for as long as possible.*

Over the next several years, although the spirit of this operating strategy was adhered to, unanticipated events were to impose a number of modifications.

Preliminary Flow Tests

In the fall of 1991, with construction of the surface plant essentially complete, a series of brief flow tests were planned to ensure that the system was fully capable of the sustained operation the LTFT would require. (Well EE-3A was still serving as the injection well, with the same injection interval used since the ICFT in 1986.) These tests were carried out between December 1991 and March 1992. Three of them were production flow tests, significant data for which are summarized in Table 9-1.

Table 9-1. Preliminary flow tests

	Test 1 4–6 December 1991	Test 2 5–7 February 1992	Test 3 2–13 March 1992
Operating parameters at close of test period			
Injection pressure, psi (MPa)	3700 (25.5)	3872 (26.7)	3756 (25.9)
Injection flow rate, gpm (L/s)	86 (5.4)	114 (7.2)	111 (7.0)
Production backpressure, psi (MPa)	2210 (15.2)	1537 (10.6)	1494 (10.3)
Production data at close of test period			
Temperature, °C	154	177	180
Production flow rate, gpm (L/s)	74 (4.7)	101 (6.4)	95 (6.0)
Water loss rate,* gpm (L/s); %	9.7 (0.6); 11	11.4 (0.7); 10	7.3 (0.5); 7
Thermal power production, MW	2.7	4.2	4.0
Calculated flow impedance, psi/gpm (MPa per L/s)	20.1 (2.2)	22.9 (2.5)	23.8 (2.6)

*net after taking into account the bypass flow around the cemented-in liner in the injection wellbore.

Test 1 (also known as Expt. 2078A) marked the first time in about four years that water had been circulated through the Phase II HDR reservoir. The test was preceded by two days of pressurization, during which the reservoir was inflated from 2284 to 3111 psi (15.8 to 21.4 MPa). Because the purpose of this first flow test was simply to evaluate the surface plant and ensure that continuous circulation was possible, the operating conditions were conservative: the final injection pressure of 3700 psi (25.5 MPa) was somewhat lower than that employed in the first (non-reservoir-growth) part of the ICFT five years earlier. The temperature reached, 154°C, was well below the known temperature of the reservoir. Water losses were small at 11%, as would be expected under such conservative conditions. Overall, this initial test demonstrated in a forthright manner the viability of the surface plant and its adequacy for long-term flow testing. (It also brought to light a number of minor problems, which were corrected before testing proceeded.)

Test 2 was designed to evaluate both the reservoir and the surface plant under typical operating conditions. It revealed a number of points at which simple engineering refinements could improve the performance of the surface plant. It was followed by two additional short flow tests (not documented in Table 9-1)—one for evaluating an emergency procedure to protect the surface equipment from freezing in the event of unanticipated winter shutdowns, and one for evaluating the response of system controls to unexpected power outages.

Originally only two preliminary flow tests had been scheduled, and following these the LTFT proper was begun in early March 1992. But circulation had to be halted after only 11 days because of greater-than-anticipated expansion of the production piping (indicated by excessive upward movement at the wellhead). The production wellhead piping was redesigned, and an additional stress-relief bend (often referred to as an "expansion loop") was installed in the line near the wellhead to accommodate an expansion of 6 in. (15 cm). Regular inspections of the casing showed that following the redesign, the piping typically lifted 2–3 in. (5–8 cm) off its support, but the stress-relief bend virtually eliminated the danger of pipe failure. The 11 days of circulation in March became by default a third preliminary circulation test, Test 3.

During the last three days of Test 3, the reservoir had essentially reached steady-state operation—except for the temperature of the production fluid, which had continued to rise at an average of 0.4°C/day (Fig. 9-1). The produced thermal power at the end of 10 days, when the surface injection temperature was 21°C, was 4.0 MW.

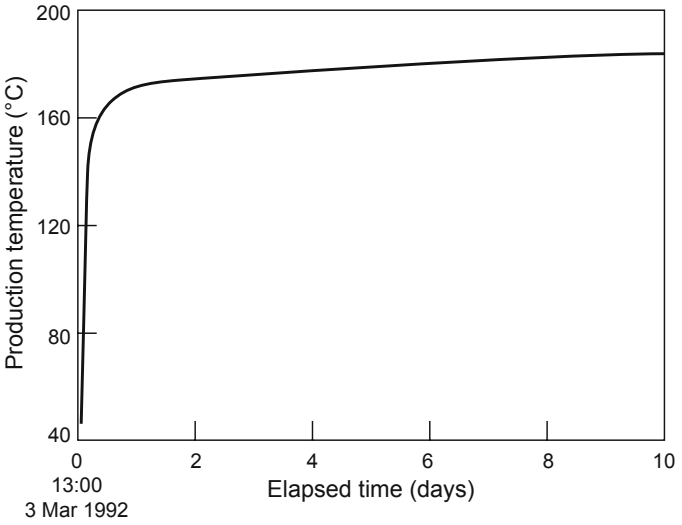

Fig. 9-1. Temperature of the production fluid during pre-LTFT Test 3 (March 1992).
Source: Brown, 1992

Performance of the Surface Facilities During the Pre-LTFT Tests

Overall, the automated surface plant operated smoothly and without major problems throughout the pre-LTFT flow tests.

By the close of these tests, the 5-cylinder reciprocating pumps had each been subjected to approximately 700 hours of operation since their arrival at Fenton Hill in December 1990. The only mechanical problem encountered was a defective crank bearing in one of the pumps, which caused some trouble early in the test period; the pump was quickly repaired by the manufacturer and returned to service. On-site inspection of the pumps uncovered heavy wear on the sealing surfaces of the discharge valves and the suction valves, but this did not seem to affect hydraulic performance.

The gas/particle separator was found to effectively remove undissolved gases from the production flow. Such gases were produced less frequently and over shorter intervals during the pre-LTFT tests than during the ICFT. There was very little sediment. As an example, less than 1 g of sediment was removed from the separator following one of the 3-day circulation tests.

A minor problem was encountered with the makeup-water system; it was remedied by redesign of the control logic and the installation of additional control equipment.

The Long-Term Flow Test: Operations (1992–1995)

The LTFT can be considered as having extended from April 1992, when sustained circulation was initiated, until circulation was permanently halted in July 1995. Figure 9-2 is a generalized timeline of the operations carried out at Fenton Hill over this period.

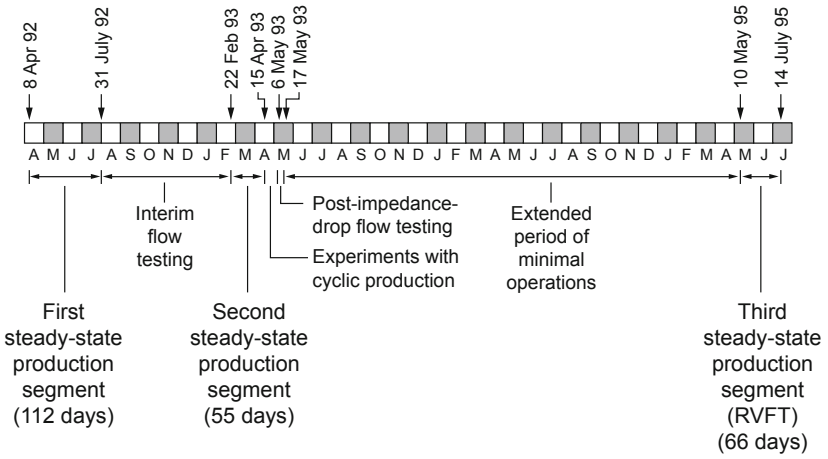

Fig. 9-2. Timeline of LTFT operations at Fenton Hill (April 1992–July 1995).

The LTFT plan approved by the PDC had been to conduct a one-year continuous flow test; but unforeseen mechanical and financial problems imposed a more fragmented testing regimen over a more protracted test period. As illustrated in the figure, by the time circulation testing came to a full halt in mid July 1995, three major, steady-state production segments had been carried out: early April–late July 1992 (112 days); mid February–mid April 1993 (55 days); and May–July 1995 (66 days). In total, these segments amounted to almost 8 months of operation. In addition, several brief experiments were carried out to evaluate cyclic production (both surging and load-following); and a number of short flow tests were conducted during otherwise nonproductive intervals, bringing the total time of circulation through the reservoir to about 11 months.

First Steady-State Production Segment: April–July 1992

After the installation of an expansion loop and other minor system modifications to compensate for the wellhead growth (expansion of the production piping) observed during the preliminary Test 3, water was injected into the reservoir on April 7, 1992. The next day, April 8, circulation was begun. The operational goal was to maintain continuous circulation for a period of one year. Injection pressure was maintained at the highest level that would not cause joint extension (approximately 3960 psi [27.3 MPa]), and the backpressure at the production well was kept at 1400 psi (9.7 MPa); these levels were designed to pressure-dilate the deep joint connections to the production borehole while preventing the boiling of the superheated water and keeping dissolved gases in solution. Everything ran smoothly for nearly four months, the two high-pressure injection pumps operating on an alternating basis, ten days each at a time with oil changes every 250 hours. (The fact that no microearthquakes were detected during this test period indicates the absence of additional joint openings or extensions—i.e., of further reservoir growth.)

Then, unexpectedly, at the end of July both the injection pumps failed within two days of one another, forcing a shutdown. The problem was traced to leakage of circulating fluid into the pumps' oil reservoirs. Inspection revealed hairline cracks in almost all the cylinder blocks of both pumps, rendering them unusable. A committee of materials experts from several institutions was convened to review the pump design and to carry out metallurgical evaluations and stress analyses. The conclusion finally reached was that the microstructure of the Nitronics 50 stainless steel used for the cylinder blocks was not homogeneous but contained a sigma phase in the alloy (possibly a result of the slow, air-cooling annealing procedure used during manufacture, which—at the Laboratory's insistence—had been substituted for rapid quenching in an effort to minimize residual stresses). To verify the effectiveness of rapid cooling, the Los Alamos Materials Technology group carried out a heat-treatment experiment in which one of

the defective components was heated to 1122°C and then rapidly cooled by oil quenching. When the component was cut into sections and examined microscopically, the sigma phase was found to be significantly reduced—suggesting that rapid quenching (as had been specified by Ingersoll-Rand) was preferable.

In spite of its premature termination, this first steady-state test segment was extremely successful in almost every technical aspect. With the exception of a few minor quirks, which were corrected, the surface plant performed as planned. Perhaps the most significant technical accomplishment was that only 10 days after the start of circulation, the surface equipment was performing so well that it was possible to put the plant in an automatic, "unmanned" operational mode for the weekend. However, a brief electrical power "glitch" occurred the next evening—Sunday, April 19—provoking an automatic shutdown that resulted in 15 hours of lost production (this shutdown feature and all the other automated control and safety systems performed as designed). Flow was reinitiated early Monday morning, when operating personnel returned to the site.

Unfortunately, the first few weeks of operation saw several more electrical glitches, during both manned and unmanned periods. Finally, the electrical controls were redesigned to prevent random power interruptions of a few seconds or less from totally shutting the plant down. The redesign was successful: unmanned operations—at first over weekends and then every night as well—soon became the rule.

Over the course of the first steady-state production segment, the system functioned more and more smoothly. Numerous diagnostic tests were also conducted during this period. Circulation was maintained more than 95% of the time, and production rates and temperatures were extremely stable. It appears that, had the injection pumps not failed, circulation could have been maintained indefinitely.

Interim Flow Testing: August 1992–February 1993

When the injection pumps failed, a backup pump was enlisted so that pumping could resume. The primary goal during this period—known as the Interim Flow Test, or IFT[1]—was to keep the reservoir pressurized and maintain circulation, thus preserving the integrity of the reservoir and, in turn, the ability to resume testing once the injection pump problem had been resolved. In addition, maintaining circulation allowed a modicum of data to be collected.

Injection resumed on August 13 and production on August 20, at somewhat lower flow rates than during the first steady-state test segment (the backup pump had neither the capacity to inject at the high levels desirable for the LTFT nor the quality of construction for long-term operation).

[1]For more information on the IFT, see Brown and DuTeau, 1993.

In early October, the backup pump "died of old age," with a cracked cylinder head. The reservoir was shut in for about four weeks, until an oilfield-type, high-pressure, high-capacity piston pump could be leased and installed. Flow testing began again on October 28, 1992; but the leased pump (known in the industry as a "mud pump"), which was designed to circulate drilling fluids containing additives with some degree of lubricity, suffered repeated failures as its rubber piston seals eroded. A redesign of the pistons and seals managed to prolong the pump's life into early January 1993, allowing additional data to be collected. When this pump too died, the reservoir pressure began to decline rapidly (by injecting into EE-3A, the pump had maintained a flow of about 18 gpm [1.1 L/s] from the production wellhead and through the surface loop to keep the equipment from freezing). A small backup pump was then brought on line to continuously inject fluid at 19 gpm to keep the pressure of the reservoir from dropping too drastically. It was used for about a week, beginning January 19, until a new rental pump (already on order from the REDA Pump Company of Bartlesville, OK) was delivered. The REDA pump, which was installed on January 25, was fundamentally different in design from the failed injection pumps: centrifugal rather than piston, and powered by electricity rather than diesel fuel. Although the new pump had a narrower operating range than the piston pumps and was more expensive to run because of the electric drive, it proved to be simpler to operate and maintain.

The IFT included two higher-backpressure flow tests, conducted in December 1992. These tests were designed to assess the extent to which production well backpressures higher than the nominal 1400 psi (used during the first steady-state segment of the LTFT) would degrade performance. With the injection pressure maintained at 3960 psi, two "off-design" backpressures were specified: first 2200 psi and then 1800 psi. Near the end of each flow test, operating conditions close to true steady-state were established, and operating parameters were measured on the date when those conditions were the most representative. The "data points" thus obtained followed a 2200-psi backpressure "plateau" of about 10 days for the first test (December 10), and an 1800-psi "plateau" of 17 days for the second test (December 27).

The resulting production flow rates were 84.6 gpm and 90.5 gpm, respectively (Table 9-2). Compared with the production flow rate of 89.7 gpm near the end of the first steady-state production segment (see Table 9-3, below), these results represented a flow reduction of only about 4% at 2200 psi, and essentially no change at 1800 psi.

In all, the IFT lasted nearly 7 months, maintaining pressure on the reservoir and enabling several flow experiments to be carried out, which yielded valuable operational and diagnostic information. Operations during the IFT are summarized in Fig. 9-3. Not depicted in the figure are the frequent, brief pump shut-ins that interrupted circulation (even at the reduced injection rates and pressures, the temporary injection pumps were not adequate to the task).

Table 9-2. Reservoir flow performance under conditions of higher backpressure during the IFT

	Date of measured performance	
	10 December 1992 Nominal 2200-psi backpressure	27 December 1992 Nominal 1800-psi backpressure
Injection		
Flow rate, gpm (L/s)	116.2 (7.33)	113.1 (7.14)
Pressure, psi (MPa)	3963 (27.32)	3962 (27.32)
Production		
Flow rate, gpm (L/s)	84.6 (5.34)	90.5 (5.71)
Pressure, psi (MPa)	2201 (15.18)	1798 (12.40)
Temperature, °C	177.1	182.8

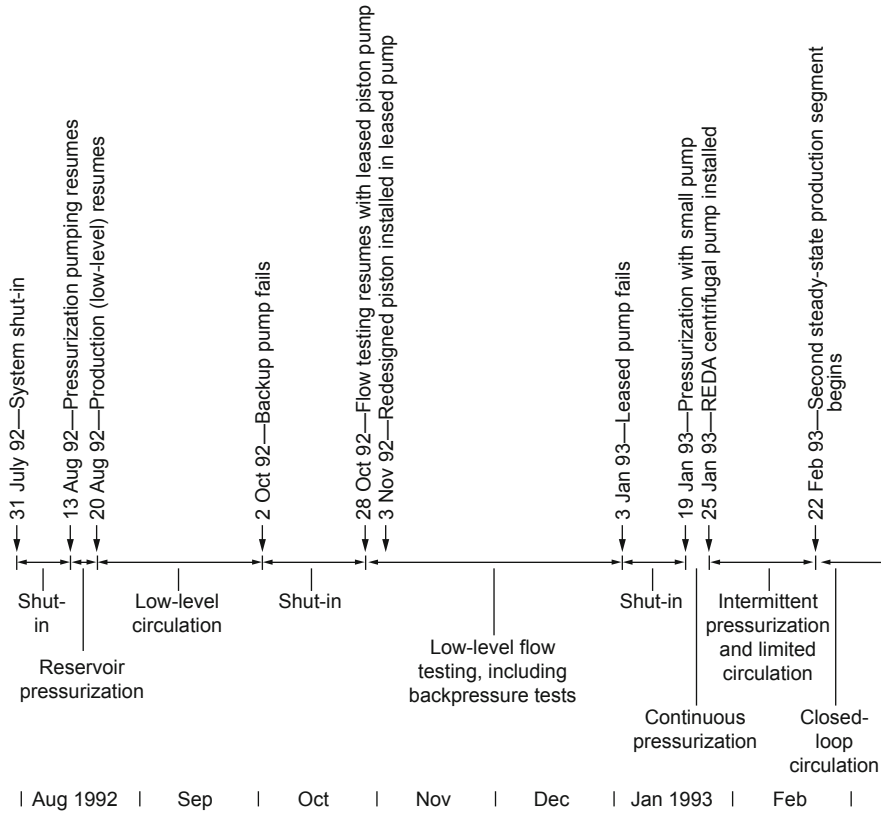

Fig. 9-3. Schedule of operations during the IFT (July 31, 1992–Feb. 22, 1993).

Second Steady-State Production Segment: February–April 1993

The second period of continuous circulation began February 22, 1993. Because the reservoir had been maintained under pressure during the almost 7 months since the first steady-state segment, similar operating conditions were rapidly re-established. The only problem encountered during this test segment was related to the much greater electric power requirements of the REDA pump. The problem was so persistent that in late March the pump manufacturer was called in, and the system was shut in for 44 hours while larger underground electric cables and auxiliary components were installed. The system was then restarted, and operations continued with no further technical problems through April 15. During the early stages of this test segment, circulation had been maintained about 85% of the time; but after the electrical problem was corrected, the system remained on line 100% of the time. (It is important to note that there were no problems with the pump itself during this entire test period—only with its power supply.)

Although continuous circulation under the desired conditions was achieved for only 55 days, the second steady-state production segment demonstrated that even after many months of intermittent operation, an HDR system could be rapidly returned to steady-state conditions—provided the reservoir had been kept pressurized. During this segment, much was learned about the system through the flow tests, logs and other measurements, and a number of special experiments. It is especially significant that the operational difficulties were confined to the surface components and the supply of electricity to the site. Not only was the reservoir heat-extraction loop essentially problem-free, it demonstrated an important capability to undergo repeated shutdowns and restarts without damage or significant changes in operating characteristics. It was now clear that the HDR reservoir at Fenton Hill was resilient enough to tolerate the kinds of technical problems routinely encountered in the operation of a commercial facility.

The reservoir operating conditions for the first and second steady-state production segments of the LTFT are summarized in Table 9-3. The most striking feature is how similar those conditions were. The only significant change was in the rate of water loss, which dropped from 12.5 gpm to 6.8 gpm, reflecting the additional time that the reservoir pressure had been maintained.

Table 9-3. Operating conditions: first and second steady-state production segments of the LTFT

	Period of measured performance	
	21–29 July 1992 First steady-state production segment	12–15 April 1993 Second steady-state production segment
Injection		
Flow rate, gpm (L/s)	107.1 (6.76)	103.0 (6.50)
Pressure, psi (MPa)	3960 (27.29)	3965 (27.34)
Production		
Flow rate, gpm (L/s)	89.7 (5.66)	90.5 (5.71)
Pressure, psi (MPa)	1401 (9.66)	1400 (9.65)
Temperature, °C	183	184
Net water loss*		
Rate, gpm (L/s)	12.5 (0.79)	6.8 (0.43)
% of injected rate	11.7	6.6

*after taking into account injected water returned to the surface via the annular flow path in EE-3A.

The First Experiment with Cyclic Operation: "Surging" the Production Flow

As mentioned above, a number of short, unplanned interruptions of system operations occurred during the first two steady-state production segments, and particularly during the period between them. These interruptions turned out to have some value: they were instructive concerning what to expect upon restart and prompted the implementation of highly standardized restart procedures; they provided opportunities for testing of the automated shutdown systems; and they furnished other useful reservoir operating data. Certainly, they proved that unanticipated shutdowns could be handled and recovered from rapidly.

It was noted that fluid production declined slowly and consistently with time during the steady-state circulation segments; but immediately following each of the unplanned production shut-ins, it jumped back to near its original level before again beginning a slow decline. This behavior inspired the investigation, in the spring of 1993, of a technique for restoring productivity following these long, slow declines. Referred to as "surging," it is based on the long-held thesis that cyclic operation—periodically shutting in the production well and then rapidly opening it again—might help maintain (or even slightly increase) the steady-state flow rate from an HDR reservoir.

To test this thesis, a 3-day cyclic surging experiment was designed that employed brief daily shut-ins of the production well, each followed by a release, or surging, of the production flow. This experiment took place April 15–17, 1993, immediately following the second steady-state production segment, during which the production flow had been slowly declining.

While injection was maintained at a steady rate of 103 gpm (6.5 L/s) and an injection pressure of 3960 psi, the production well was shut in for 25 minutes each morning, then surged. As expected, when the production flow rate was measured near the end of each day (following the re-establishment of steady-state flow conditions), it showed an increase of about 1% (Fig. 9-4).

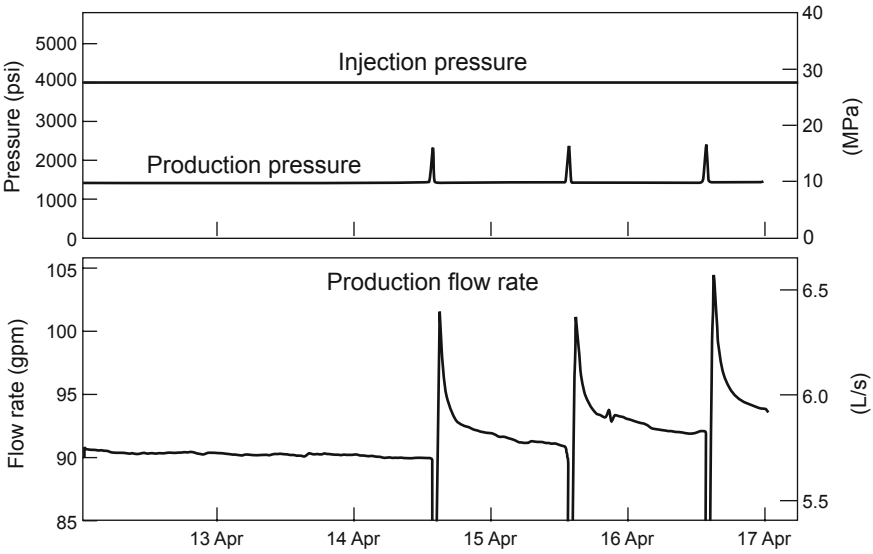

Fig. 9-4. Injection pressure, production pressure, and production flow rate during the first surging experiment (April 15–17, 1993).
Source: DuTeau, 1993

The corresponding increase in power production for the last cycle (over that for the previous 48 hours) was 2.6%, as shown in Fig. 9-5. Although this trend would no doubt have leveled off over time, the experiment proved that brief, regular production wellbore shut-ins can help maintain the productivity of an HDR system. (A second surging experiment, essentially replicating this one, would be carried out two years later, in June of 1995.)

At the end of the three-day surging experiment, both wells were shut in and, because of budget constraints, preparations began to return the rental pump. Fortuitously, REDA decided that the pump was not needed immediately and offered the HDR Project an extra month of use, rent-free. The pump was returned to service at once, to maintain reservoir pressure, while an even more important experiment was being designed.

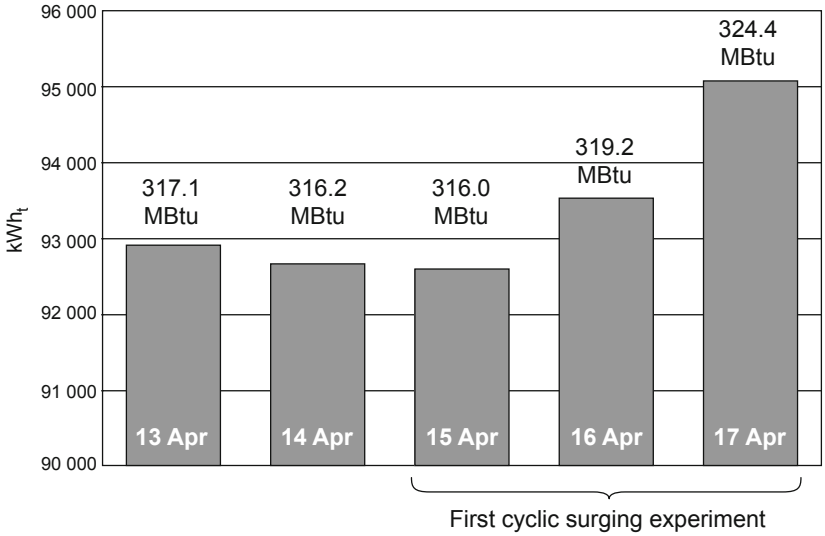

Fig. 9-5. Enhancement of energy production during the first surging experiment (April 15–17, 1993).
Source: DuTeau, 1993

InfoNote

For an HDR reservoir, "surging" is accomplished by shutting in production while continuing injection. The shut-in causes the pressure deep in the production well to rise rapidly to the pressure level of the nearby reservoir. With the cessation of flow from the body of the reservoir to the region near the production wellbore, the pressure in this region rises as well, approaching that of the body of the reservoir. This increase in pressure in turn causes additional fluid to be "stored" in the overpressured joints connected to the production wellbore. When the flow is subsequently released, it *surges* at high velocity through these now hyper-dilated joints, clearing them of accumulated debris and modestly increasing steady-state production.

Surging had been used before at Fenton Hill. For example, following the redrilling of EE-3A, it was used to clean out/open up the joint connections to the production borehole (see the section on Expt. 2059 in Chapter 6).

The First Load-Following Experiment

On May 4, 1993, a first investigation of cyclic "load-following" production was begun. (For this first experiment, unfortunately, the level of back-pressure specified for the production well during the "steady-state" intervals was very high, which unnecessarily restricted reservoir productivity.)

A second—and much more definitive—load-following experiment would be carried out two years later, in July 1995, near the end of the third steady-state production segment.

The reservoir operating strategy known as load-following involved partially venting the stored fluid near the production wellbore for a few hours each day, by significantly reducing the production well backpressure during that period. The vented fluid would then be replaced (i.e., the reservoir would be recharged) during the remainder of the daily operating cycle, by increasing the injection flow rate somewhat above the previous steady-state rate. The aim was to show that HDR power production could be increased temporarily to meet peak-period demand—and that such temporary increases could be *scheduled*. Load-following was seen as potentially having both production and marketing advantages: The enhanced power production could be used to meet a portion of the peak-power needs of a nearby electric utility, which would provide much higher value power than the equivalent baseload production.

This first load-following experiment continued for three daily cycles, with continuous injection at about 100 gpm. The production-well backpressure was very high (3000–3300 psi) and, maintained for 16 hours, limited production flow to about 25 gpm (1.6 L/s)—just enough to prevent freezing of surface loop components in the event of very cold weather. At the end of the 16-hour period, the backpressure was drastically reduced for 8 hours, which led to a significant increase in flow (averaging 140–150 gpm for the first two cycles).

The pressure and flow-rate behavior of the reservoir are shown in Fig. 9-6. Assuming that flow rate is a reasonable analog for power production, 8 hours at 145 gpm followed by 16 hours at 25 gpm results in a daily average flow rate of 65 gpm—much less than the nominal 90–100 gpm production rate under "steady-state" conditions. Although this clearly does *not* represent an improvement in overall reservoir performance, the level of backpressure selected for this experiment—pressure that would be released when the production well was opened—turned out to be excessive. A *programmed* reduction in backpressure, from a somewhat lower level (and for a shorter period of time than 8 hours), appeared to be a better approach to load-following. Nevertheless, the very significant increase in production flow rate for 8 hours each day provided a "taste" of what was possible with this mode of operation.

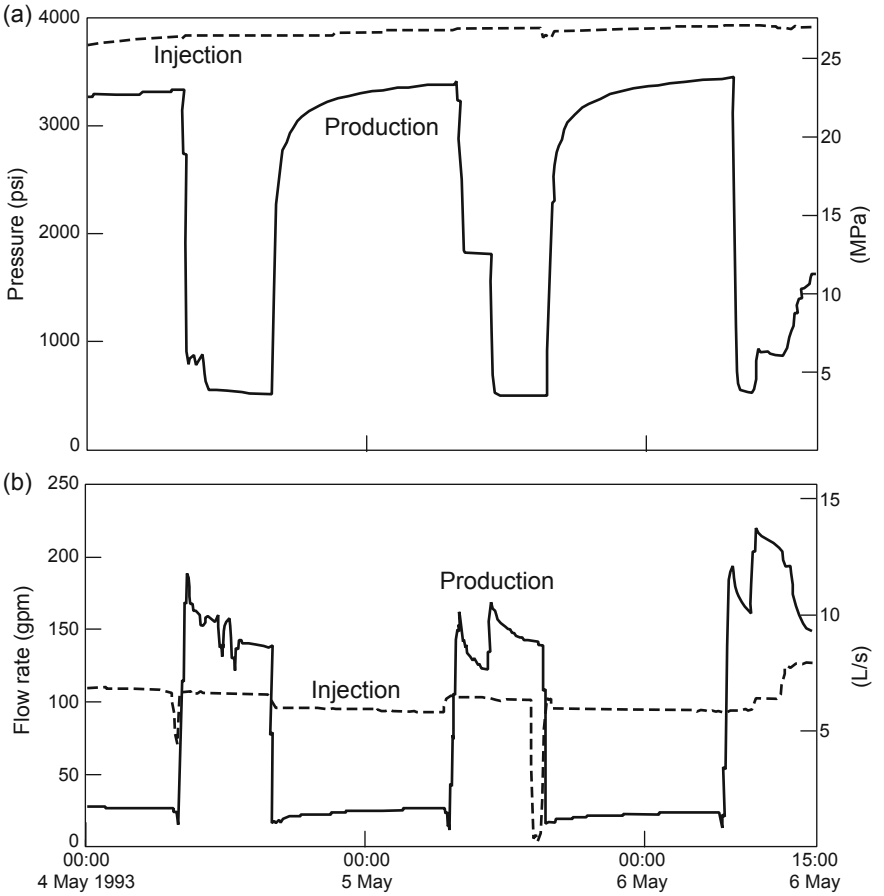

Fig. 9-6. The first load-following experiment (May 4–6, 1993): (a) injection and production pressure profiles and (b) injection and production flow-rate profiles.
Source: Brown and DuTeau, 1995

After the second cycle, as shown in the figure, other events intervened. Near the beginning of the third cycle, reservoir flow impedance dropped significantly, as evidenced by an increase of about 30% in the production flow rate (from 165 to 220 gpm). This impedance drop occurred within less than one minute. The increase in flow began to taper off, but this event was completely unexpected. At the same time, it was not unlike the flow enhancement observed following over-pressurization of the reservoir during the SUE (in December 1980, at the end of the nine-month flow test of the Phase I reservoir—see Chapter 4). In both cases, it appears that the somewhat higher pressures within the reservoir released contact points between

certain rock blocks, allowing local movement on associated joints and the opening or shifting of one or more flow channels. The dramatic reduction in flow impedance meant that more water was transported into the production wellbore; but because the open-hole portion of the wellbore was not logged, no information was obtained regarding the source of the additional flow—whether it was an existing open joint or a newly opened one. (Note that the flow increase was not accompanied by the seismic activity typically observed when an HDR reservoir is strongly pressure-stimulated.)

The greatly increased production flow made it impossible to pump water at a rate high enough to keep the injection pressure at the standard 3960 psi (27.3 MPa). Even with the pump running at its maximum rate of 130 gpm (8.2 L/s), the injection pressure reached only 3860 psi (26.6 MPa). Had it been possible to maintain the injection pressure at 3960 psi (27.3 MPa), the flow rate would have shown an even greater net increase over the 103 gpm seen at the end of the first steady-state production segment (see Table 9-3). (Typically, the higher the injection pressure, the lower the impedance in the body of the reservoir.)

Following the sudden impedance drop, the system was returned to steady-state operation. Injection and production were continuous for the next 11 days so that the reservoir's behavior could be observed. Except for the lower injection pressure, all control parameters matched those of the second steady-state production segment. As shown in Table 9-4, the temperature of the produced fluid rose about 6°C (this rise had to be entirely the result of the more rapid transport of the hot fluid up the wellbore, as logging to the bottom of the production wellbore casing showed no change in the temperature of the fluid where it entered the casing). The flow rate tapered off from its initial high level but still remained about 30% higher than during the second steady-state production segment a few weeks earlier.

Table 9-4. Operating conditions before and after the sudden impedance drop (May 1993)

	Second steady-state production segment (April 1993)	After impedance drop (May 1993)
Injection		
Flow rate, gpm (L/s)	103 (6.5)	130 (8.2)
Pressure, psi (MPa)	3960 (27.3)	3860 (26.6)*
Production		
Flow rate, gpm (L/s)	90 (5.7)	124 (7.8)
Pressure, psi (MPa)	1400 (9.7)	1400 (9.7)
Temperature, °C	184	190

*maximum pumping pressure attainable after the impedance drop and increase in flow.

On May 17 the wells were shut in and the pump was returned to REDA. Figure 9-7 shows the pressure and flow profiles between the time of the impedance drop and the cessation of circulation.

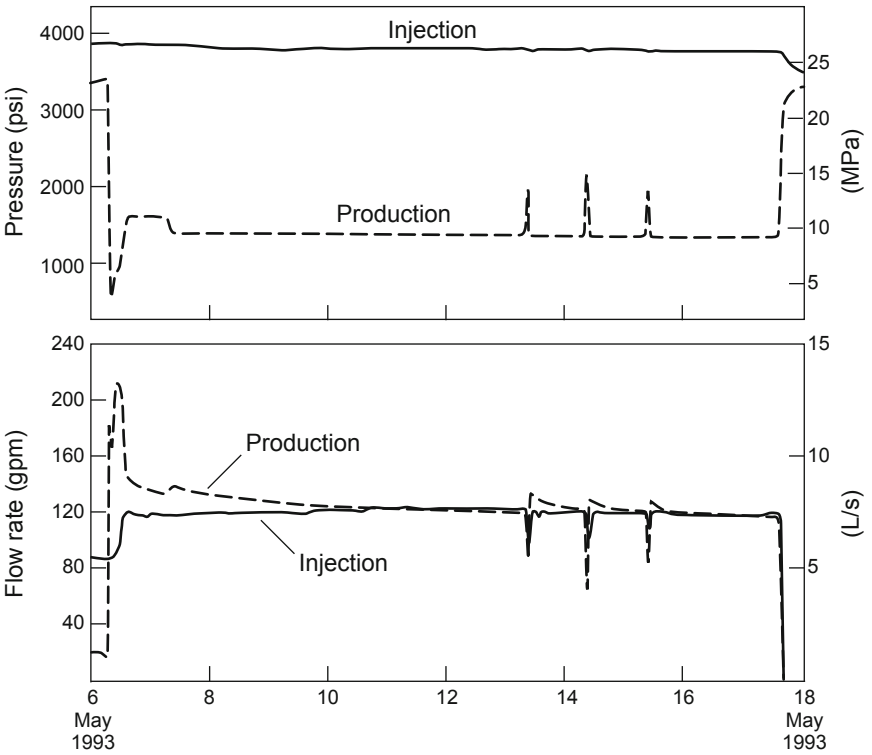

Fig. 9-7. Pressure and flow profiles following the sudden drop in impedance of May 6, 1993. (The three pressure spikes between May 12 and May 16 were due to brief shut-ins.)
Source: Brown, 1993b

Note: Impedance reduction had long been a goal of the HDR Project. Unfortunately, a funding shortfall for fiscal year 1993 prevented a more detailed investigation of the large impedance drop at the end of the second steady-state production segment. Had it been possible to fully explore this singular event, the insights gained might have led to practical impedance-reduction technologies for commercial HDR systems. But it would be two years before the resumption of flow testing, by which time the reservoir conditions had partially reverted to those obtaining before the impedance drop.

Extended Period of Minimal Operations: May 1993–May 1995

The period between May 17, 1993 (following the first load-following experiment) and May 10, 1995 saw a shutdown of two full years, during which no reservoir flow testing took place in the conventional sense. This long hiatus in the HDR Project was the result of a continued severe lack of funding. Figure 9-8 shows the decline in funding for the last 10 years of the HDR Project.

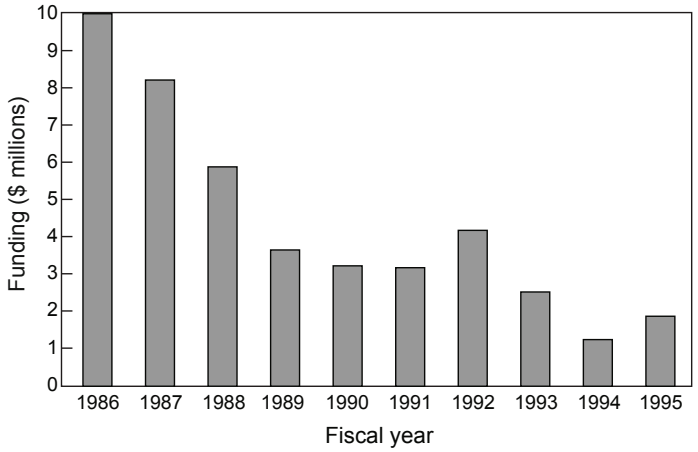

Fig. 9-8. HDR Project funding for the last ten years (1986–1995).

Although Los Alamos Project staff saw the choking-off of funding as the DOE's attempt to bring an end to the Fenton Hill HDR experiments, they persevered. By eliminating most of the scientific studies and surviving on a very limited budget, they managed to carry out a number of interesting and useful experiments during this two-year period (Fig. 9-9).[2]

After the wells had been shut in, the surface throttling valve was activated to close off the EE-3A annular flow path to the surface (see Fig. 6-43) and the reservoir pressure was simply left to decay naturally. During this time, the reservoir fluid was venting, through one (or more) high-pressure joints emanating from the Phase II reservoir, into the Phase I reservoir region via the deeper, open annulus flow connection (ANNULUS in Fig. 6-43).

[2]In addition, they even saved enough money to purchase the REDA injection pump that the Project so desperately needed!

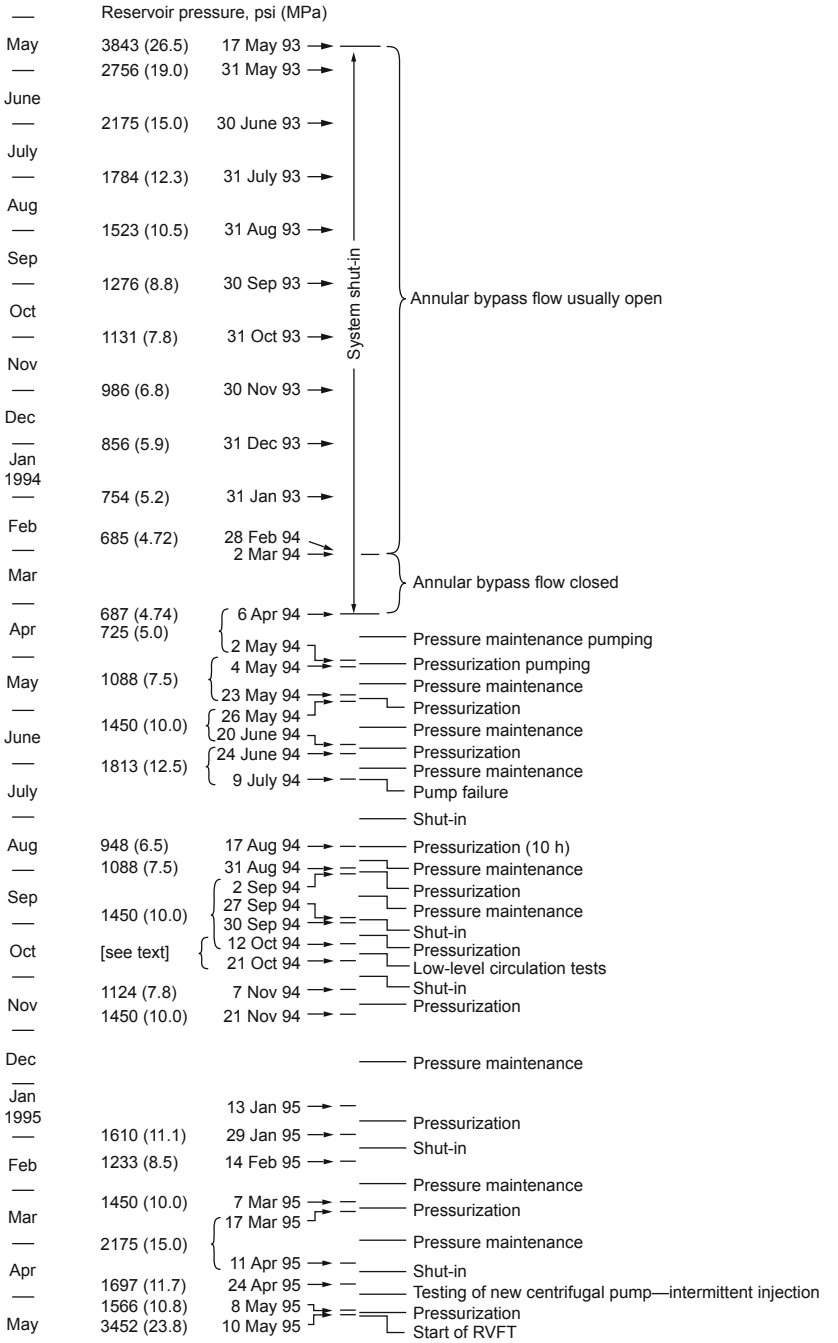

Fig. 9-9. Activities during the extended period of minimal operations (May 1993–May 1995).

During the winter of 1993–1994, the annular flow path to the surface was reopened to keep the wellhead from being damaged by freezing. By the end of February 1994, the reservoir pressure (as measured at EE-3A) had declined to 685 psi (4.72 MPa). In early March, in an attempt to find the source of a temperature anomaly noted during logging, the annular flow path to the surface was once again closed off, for 34 days, so that more precise data could be collected. During that period the reservoir pressure actually increased slightly, to 687 psi (4.74 MPa), in spite of the fact that no water had been injected from the surface—a clear sign that water was flowing back into the reservoir from the overpressured periphery.

On April 6, 1994, the Roto-Jet makeup-water pumps were used to inject enough fluid to increase the reservoir pressure to 725 psi (5 MPa). A pressure management study began on May 2. The Big Kobe pump was used to continuously inject about 19 gpm (1.2 L/s) of water at higher pressures than the Roto-Jets could attain, to increase the reservoir pressure further. On May 4, after 50.5 hours of pumping and the injection of 56 000 gal. (212 000 L) of water, the pressure reached 1088 psi (7.5 MPa). It was held at this level until May 23, when continuous pumping was resumed. Three days later, after 79 hours of pumping and the injection of 83 500 gal. (316 000 L) of water, the pressure reached 1450 psi (10 MPa) and was held at this new plateau until June 20. Finally, a further episode of continuous pumping—105 000 gal. (398 000 L) of water over 95.5 hours—increased the pressure to 1813 psi (12.5 MPa). This level was maintained through July 9, when injection had to be stopped because of a pump failure.

A rental pump capable of injecting water at a rate of 28 gpm (1.8 L/s), but having limited working pressure, was procured shortly thereafter. By August 16 the pressure of the reservoir had dropped to 948 psi (6.5 MPa), and the next day the new pump was deployed to raise it to 1088 psi (7.5 MPa). Then, beginning on August 31 and lasting 36.5 hours, an injection of 61 820 gal. (234 000 L) at a rate of about 28 gpm succeeded in raising the pressure to 1450 psi (10 MPa)—a level that had been reached only after 79 hours and 83 500 gal. (316 000 L) with the Big Kobe pump injecting at 19 gpm. Moreover, the 1450-psi reservoir pressure was maintained for 41 days (including a 3-day shut-in in late September) simply by injecting fluid for a few hours each day.

On October 12, low-level circulation testing (matched to the injection capability of the rental pump) was begun, to evaluate the performance of the reservoir under "off-design" conditions. The first circulation test lasted until October 16, with an average production rate of 23.5 gpm (1.5 L/s), when inclement weather forced a 29-hour shut-in. During a second test, from October 17 to October 21, the average production rate was 21.5 gpm (1.4 L/s). During the two tests, injection pressures averaged 2453 and 2474 psi (16.9 and 17.1 MPa), respectively, and backpressures were maintained at 1100 psi (7.6 MPa) and 1200 psi (8.3 MPa), respectively.

The reservoir pressure was then allowed to decline, and the now-repaired Kobe pump was reinstalled. Except for a short period of injection (7 hours) on November 3, the system remained shut in until the morning of November 7. Pumping then recommenced with the reservoir pressure at 1124 psi (7.8 MPa), and sufficient fluid was injected to raise the pressure to between 1305 and 1450 psi (9 and 10 MPa); periodic injections of fluid maintained the pressure at this level or higher for the next six months, until May of 1995. The pumping schedule tended to be erratic over this period, partly because of the vagaries of the weather and, later on, because a new pump was being brought on line, necessitating some modifications to the loop.

Third Steady-State Production Segment (Reservoir Verification Flow Test): May–July 1995

In May 1995, renewed flow testing of the Phase II reservoir began after a two-year hiatus. After a couple of days of fluid injection to increase the pressure in the reservoir, full circulation was begun on May 10. This third segment of steady-state operation, known as the reservoir verification flow test (RVFT), was designed to (1) verify whether the system could be brought back to the operating conditions in effect at the end of the preceding steady-state production segment (and, in particular, determine whether the flow behavior brought about by the sharp impedance drop of two years earlier had persisted through the intervening time period); and (2) collect circulation data that would be important for the industry-led HDR project then being envisioned.

A new REDA pump, similar to the one that had been rented in 1993 for the second steady-state production segment but with 218 rather than 200 centrifugal stages, was purchased for the RVFT. To minimize procurement and operating costs, the new pump was powered not electrically but by a diesel engine scavenged from one of the defunct reciprocal injection pumps. The REDA pump design was remarkable for its simplicity and reliability. Like the rental unit, this new pump was virtually trouble-free, but shutdowns were scheduled periodically for oil changes and other routine maintenance on the diesel drive.

Figure 9-10 shows the four operational stages of the RVFT.

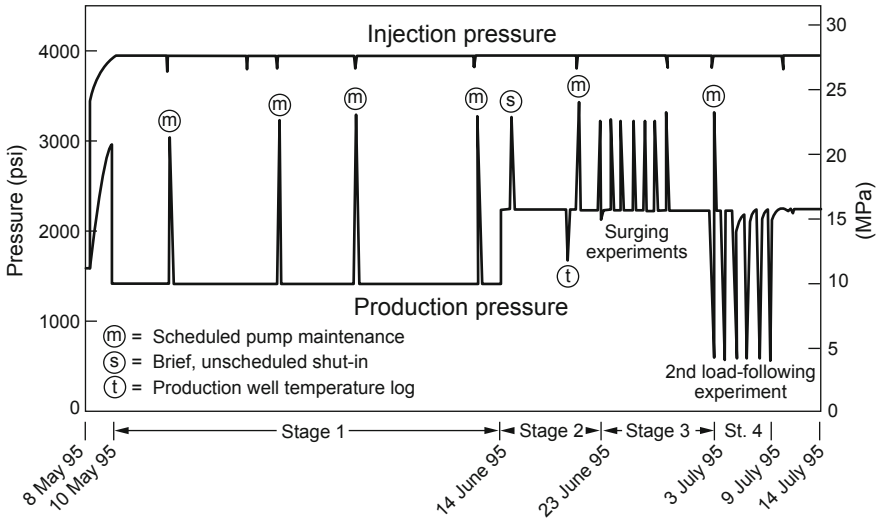

Fig. 9-10. Operational stages of the third steady-state production segment (RVFT), May 10–July 14, 1995.
Source: Duchane, 1995a

Over the 35 days of Stage 1, operating conditions essentially identical to those of the first two steady-state production segments were gradually re-established.

On June 14, Stage 2 of the RVFT began: the backpressure of the production well was increased about 50%, from 1400 to 2200 psi (9.5 to 15.2 MPa), replicating the conditions of the backpressure experiment carried out in December 1992, during the IFT. The effect was to reduce the circulation driving pressure[3]—the net pressure difference between the injection and production surface pressures—by about a third, from 2560 to 1760 psi (17.7 to 12.1 MPa) (Table 9-5). Interestingly, the decline in fluid production was only about 10%. From an economic standpoint, it remains to be determined whether or not decreasing the driving power required to pump fluid through the reservoir under the higher backpressure conditions would compensate for the somewhat lower rate of fluid production. But further investigation of this strategy's potential for increasing the net productivity of HDR systems is certainly warranted—particularly considering the benefits of a two-well production system, which enables the reservoir to be circulated at a significantly higher mean pressure level.

The reservoir operating conditions during the first two stages of the RVFT are presented in Table 9-5.

[3]This differential pressure is what causes fluid to flow across the reservoir.

Table 9-5. Reservoir operating conditions during stages 1 and 2 of the RVFT

	Third steady-state production segment (RVFT)	
	Stage 1 (May 1995)	Stage 2 (June 1995)
Injection		
Flow rate, gpm (L/s)	127 (8.0)	120 (7.6)
Pressure, psi (MPa)	3960 (27.3)	3960 (27.3)
Production		
Flow rate, gpm (L/s)	105 (6.6)	94 (5.9)
Pressure, psi (MPa)	1400 (9.7)	2200 (15.2)
Temperature, °C	184	181
Circulation driving pressure, psi (MPa)	2560 (17.7)	1760 (12.1)

A comparison of the reservoir operating conditions for Stage 1—the re-establishment of steady-state circulation after two years of shut-in—with those after the significant drop in flow impedance in May 1993 (see Table 9-4) is interesting and revealing: following the impedance drop, the production flow rate was 124 gpm, up from 90 gpm just one month earlier. Then, during Stage 1 of the RVFT, the production flow rate was 105 gpm—intermediate between the 90 gpm measured before the impedance drop and the 124 gpm after it. In other words, it had fallen, but not back to the level seen before the impedance drop. This suggests that the additional (or re-arranged) reservoir flow path(s) opened in May 1993 still persisted to some extent two years later.

Another revealing comparison is between Stage 2 of the RVFT, when the nominal backpressure was 2200 psi (Table 9-5), and the 2200-psi backpressure test of the IFT (Table 9-2): The production flow rate of 94 gpm during Stage 2 of the RVFT was 11% greater than the 84.6 gpm achieved during the IFT—again reflecting the persistence of the effects of the impedance drop two years earlier.

In terms of water loss, the two-year reservoir shut-in at low pressure took its toll! Obviously, during stages 1 and 2, the reservoir periphery was being repressurized with a higher level of diffusional flow—resulting in a loss rate even greater than that in July 1992, at the end of the first steady-state production segment (12.5 gpm—see Table 9-3).

The Second Surging Experiment

Stage 3 of the RVFT began on June 23: the production well was shut in for 25 minutes every morning for six days, while all other operating parameters remained unchanged—replicating the operational mode of the first surging experiment carried out two years earlier. The result was also essentially the same as that of the first surging experiment: a very slight increase in production flow rate, which then tailed off. The results of the two surging experiments clearly show that the simple strategy of briefly shutting in the production well on a daily basis can increase the overall production rate slightly.

The Second Load-Following Experiment

On July 3, 1995, the fourth and final stage of the RVFT began. This 6-day experiment was the second test at Fenton Hill of the load-following concept, designed to induce and temporarily sustain a large increase in the production flow rate. Being much more comprehensive than the first experiment with load-following in 1993, it became known as *the* Load-Following Experiment and generated the most important data of the third steady-state production segment (Brown, 1996a).

Throughout the experiment, the injection pressure was maintained at 3960 psi (27.3 MPa). Production was once again cyclic: each day, the backpressure was maintained at 2200 psi (15.2 MPa) for 20 hours; it was then reduced, in a programmed manner, for 4 hours to maintain an increase in the production flow rate 60% above its normal level. This process required human control at the outset, but by the third cycle it was fully automated. The backpressure was programmed to drop to about 500 psi (3.4 MPa) by the end of the 4-hour period. (The backpressure profile required to maintain a steady level of production over the 4-hour period of enhanced flow was determined and regulated by the plant's automated control system.)

Figure 9-11 presents data from the last two days of the Load-Following Experiment, showing (1) that for 4 hours each day, a large and constant increase in production flow—and power production—was achieved by a programmed reduction in the production well backpressure; and (2) that the reservoir could be "refilled" during the subsequent 20 hours by a modest increase in the injection flow rate. In other words, by alternating between a baseline level and the enhanced level achieved through periodic venting of fluid stored near the deep production interval, it would be possible to tailor power production to match increased utility power demands during high-use periods.

A Disastrous Annular Breakthrough at EE-3A

On July 6, near the end of the sixth cycle of the Load-Following Experiment, the annular bypass flow at EE-3A abruptly increased fivefold—from a rate of 6–7 gpm to about 35 gpm—greatly aggravating the water-handling and storage problems at the site. Fluid was more aggressively bypassing the cemented-in liner through a high-pressure joint (or joints), connected to the annulus *above* the liner, that had suddenly opened further. This frac-around was disastrous. It not only ended the LTFT, but would shortly lead to the shutdown of the entire HDR Project.

An appeal was made to DOE Headquarters to fund a remedial cementing operation, which would have involved perforating the 5 1/2-in. liner just above the liner cement at 10 950 ft (see Fig. 6-43 in Chapter 6), then injecting cement into the annulus and up into the 9 5/8-in. casing to a depth of about 9250 ft. But despite the modest cost of such an operation, the appeal was denied.

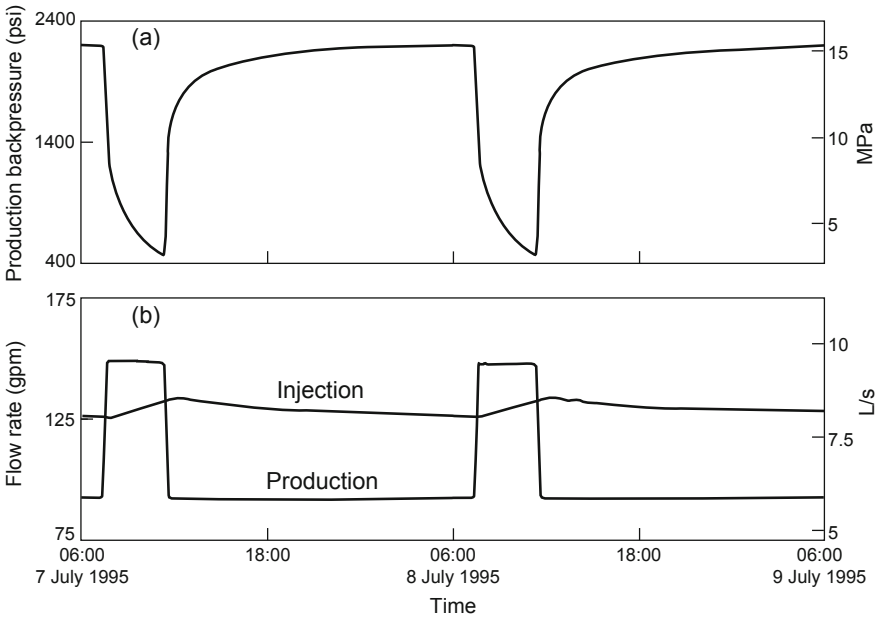

Fig. 9-11. Operating data from the last two days of the Load-Following Experiment (Stage 4 of the RVFT): (a) production backpressure, and (b) injection and production flow rates.
Source: Brown, 1996a

On July 7 the RVFT flow conditions were re-established. The EE-3A bypass flow, then at 30.2 gpm, decreased only slightly (to 25 gpm) over the next week. Reservoir circulation was discontinued on July 14, ending HDR operations at Fenton Hill.

The RVFT lasted a total of 66 days. During this entire period, there were no unintentional shut-ins of production. Some scheduled shut-ins of the production well were part of the experimental plan, as were brief (2-hour) shutdowns of the injection pump once every two weeks, to change the oil in its diesel-powered driver.

Tracer Studies

At various times before, during, and just after the LTFT, tracers were added to the circulating fluid at the injection well and subsequently collected from the production fluid. The tracer recovery profile provides a useful picture of the behavior of the fluid as it circulates through the reservoir. Tracers were

also used to investigate the annular bypass flow around the scab liner in the injection wellbore. There are, however, a number of factors that could potentially interfere with the performance of the tracers—such as chemical reactions, thermal degradation, adsorption of the tracer on reservoir rock or wellbore surfaces, and recirculation of unrecovered tracer. Despite these obstacles, not to mention budget limitations, tracer studies played an important role in elucidating the behavior of the HDR reservoir during the LTFT.

Sodium fluorescein, the chemical tracer most commonly used in geothermal systems (because its fluorescence is so intense that it can be detected at part-per-billion levels) was employed the most often. It has the added advantages of being cheap, easy to obtain, and generally recognized as environmentally benign. But fluorescein also has a significant disadvantage: at temperatures above about 200°C, it slowly decomposes, making it difficult to obtain quantitative measurements in very hot geothermal systems. To compensate for this disadvantage, at Fenton Hill the more thermally stable tracer p-TSA (para-toluene sulfonic acid) was frequently used in conjunction with fluorescein. Many of the conclusions discussed in the *Results* section below are drawn from tests that employed both tracers. Other tracers with specialized properties were evaluated as part of the HDR Project (Birdsell and Robinson, 1989), but funding limitations precluded the use of these more exotic tracer materials for reservoir testing during the LTFT.

The results of tracer tests are typically evaluated in terms of the following parameters (note that fluid volumes stored in dead-end or other nonflowing open joints within the reservoir are not considered; tracers measure only fluid volumes in active pathways between the inlet and the outlet of the reservoir):

1. First-Arrival Volume or Time: The volume of fluid circulated from the initial entry of the tracer into the reservoir to its first appearance at the production well, or the time elapsed during circulation of that volume.
2. Integral Mean Volume: The total volume of all flow paths carrying fluid from the injection to the production wellbore (derived by computing the integral of the tracer return curve). Because the point of complete tracer recovery must be obtained by extrapolation of the long tail of the curve, this volume can only be approximated.
3. Modal Volume: The volume of produced fluid from the time of tracer injection to the point of maximum tracer recovery. This is a more precise measurement than the integral mean volume, but it includes only the relatively low impedance flow paths, which route the fluid the most rapidly and directly.
4. Dispersion Volume: The volume represented by the tracer return curve at 75% of its maximum height. Although this point is somewhat arbitrary, the volume thus obtained provides a measure of the dispersion of the tracer and, by inference, of the complexity and variety of the flow paths through the reservoir.

Each tracer test provides a "snapshot" of the reservoir at the time of tracer passage. On the basis of these semi-quantitative data, important reservoir properties can be estimated: fluid volume, extent of contact with rock surfaces, complexity of fluid pathways, etc. Tracer data can be even more valuable when several tests are carried out sequentially and the results are combined to obtain a picture of reservoir changes over time (when combined in this way, the data are "normalized" to compensate for test-related variables, such as differences in production flow among the various tests and transit times down and up the wellbores). Such data formed the basis for several important conclusions regarding reservoir performance during the LTFT.

The Long-Term Flow Test: Results

The LTFT lasted 39 months, of which more than 27 were downtime—most of that accounted for by the two years of noncirculation (1993–1995). In all, the system was operated in a circulation mode for only a little over 11 months. Even so, the results obtained from these limited operations achieved the Project's primary goal: to demonstrate the viability of HDR technology for reliable and predictable sustained energy production. They also provided valuable information with respect to secondary objectives, such as maximizing the energy output of an HDR system and understanding its performance.

With respect to applying specific lessons learned from the ICFT (see Chapter 7), perhaps the only deviations were (1) that the flow rate was typically maintained at 87–103 gpm (5.5–6.5 L/s)—much lower than the rate of 200–250 gpm (12.6–15.8 L/s) recommended after the ICFT; and (2) the number of injection zones was not increased. The higher flow rates simply were not possible during the LTFT without inducing seismicity. And, at that point in the HDR Project, further high-pressure reservoir stimulation was deemed not to be appropriate.

Performance of the Surface Plant

The high-pressure piping performed well and showed no problems over the course of the LTFT. The expensive gas/particle separator, which could remove 130 000 scf (3700 m^3) per day of gas and 170 lb/h (77 kg/h) of solids, was never taxed to anywhere near its capacity, and from an engineering standpoint, proved not to be necessary. Dissolved gases (mainly carbon dioxide) were found in the circulation fluid at concentrations of about 3000 ppm, but at the typical operating pressures of 300–600 psi (2–4 MPa) in the production part of the surface loop, these gases stayed in solution. Very little solid material was brought up the production wellbore during steady-state operations (in fact, the solids removed over the entire test period, in both the strainers and the separator, could be measured in ounces rather than pounds).

The makeup-water pumps' electronic duplex logic circuit caused several shutdowns. Shortly after the LTFT was initiated, the electronic controls were modified to automatically restart pumping in the event of a brief power outage shutting down the units. Although hydraulically and mechanically the pumps worked satisfactorily, erosion of pump components proved to be a problem over the term of the LTFT. Because the Roto-Jets used to supply the makeup water were expensive to maintain, our experience indicates that a smaller version of the high-pressure REDA injection pump might provide a more practical method for injecting makeup water into the loop under pressure.

Finally, the failure of both the 5-cylinder reciprocating pumps early in the LTFT was a major setback, compounded by the fact that the only substitute reciprocating pumps that were immediately available were inadequate. However, the performance of the REDA centrifugal pumps—one rented for the IFT and the second steady-state segment, and the other purchased for the third steady-state segment—was fully satisfactory. All other components of the surface plant operated as anticipated. The automated control system permitted the plant to be operated routinely with no personnel on site, and all safety, standby, and automatic shutdown systems functioned reliably and effectively.

Steady-State Production

As described above, the Phase II HDR reservoir was tested under operating conditions simulating those of a commercial HDR plant, albeit at a power output lower than desirable.

Circulation data for the first two steady-state production segments (Table 9-3) and for Stage 1 of the RVFT (Table 9-5), all under similar operating conditions, show that over a span of about three years the production flow rate showed an overall increase while the temperature of the produced fluid remained about the same. As noted earlier, the increase in flow rate reflects the residual effects of the productivity "burst" that followed the dramatic impedance drop at the end of the first load-following experiment (May 1993). These results provide the basis for the most important conclusion drawn from the LTFT, namely:

> *HDR reservoirs can provide reliable and predictable energy for extended periods, even in the face of lengthy shut-ins or prolonged and complicated excursions from routine operating conditions.*

During the more than 11 months of circulation, there were no significant declines in productivity and no thermal drawdown was observed at the surface. In fact, it is likely that the Fenton Hill HDR plant, as configured at the end of circulation testing in 1995, could have continued to perform for years—perhaps even decades—into the future.

Production Well Backpressure Experiments

The most definitive picture of how backpressure influences reservoir production flow comes from the two higher-backpressure flow tests carried out during the IFT (data shown in Table 9-2). Figure 9-12 plots the production flow rates and the production backpressure data points from these flow tests, along with the 1400-psi backpressure data point measured near the end of the first steady-state production segment (Table 9-3). Although only three data points were obtained, it appears that changes in imposed backpressure in the 1400- to 2200-psi (9.7- to 15.2-MPa) range affected the production flow rate very little; and, by extrapolation, that 1400–2200 psi represents the optimal backpressure range for operation of the Phase II reservoir at Fenton Hill.

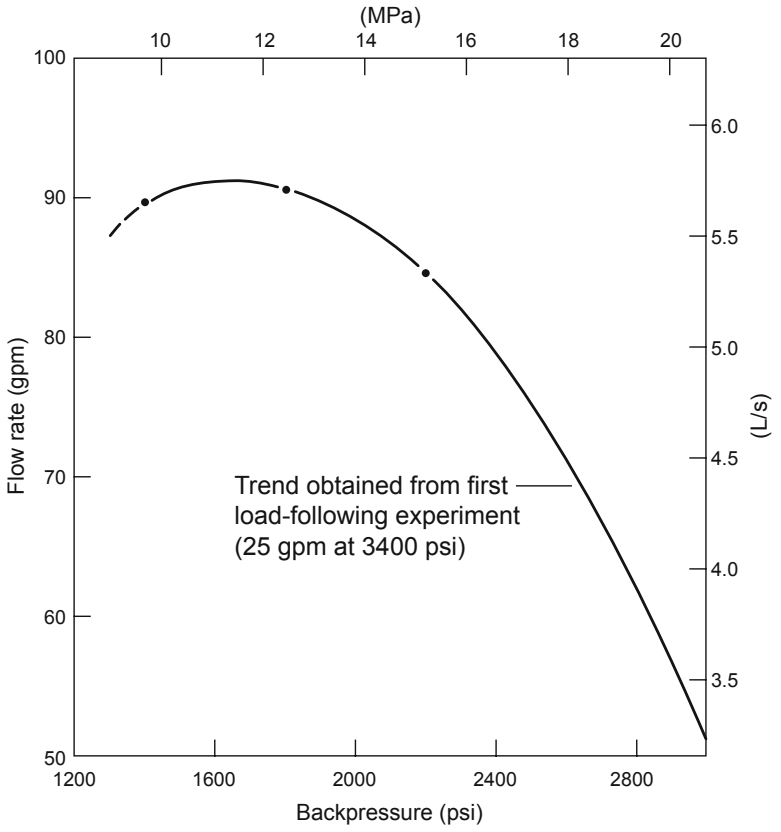

Fig. 9-12. Variation in production flow rate with changes in backpressure: IFT and first steady-state production segment.
Adapted from Brown, 1996a

The importance of controlling the backpressure on the production well, to maximize flow, has long been recognized. While having a throttling effect on fluid flow (reducing the circulation driving pressure), the maintenance of a high backpressure also increases the pressure within the fluid-carrying joints, partially counteracting the joint-closure stress in the region of the reservoir where the flow in those joints converges to the production wellbore. In contrast, if the reservoir is produced at low backpressure (just high enough to prevent boiling), the fluid-carrying joints are severely pinched off near the production borehole.

For an optimum production rate, then, the *reduction* in flow brought about by increasing the backpressure must be balanced against the *increase* in flow that results from further pressure-dilating the pinched-off joint connections to the borehole production interval, which reduces the near-wellbore outlet impedance.

Load-Following Revisited

The information in this section was drawn mainly from Brown, 1996a.

Along with the extended flow testing to characterize the steady-state performance of the Phase II reservoir, the most important component of the LTFT was the pair of cyclic (i.e., non-steady-state) load-following experiments of 1993 and 1995. The second of these was particularly significant, demonstrating irrefutably that HDR power is dispatchable in direct response to varying demand!

During the last cycle of the 1995 Load-Following Experiment, mean enhanced production was 146.6 gpm at 189°C for 4 hours, followed by 20 hours of baseload production averaging 92.4 gpm at 183°C (see Fig. 9-11). As shown in Table 9-6, this equates to a flow enhancement of 59% and a produced power increase of 65%. The time required for the power output to rise from the previous baseload condition to the peaking rate was about 2 minutes.

In other words, even though the operating conditions of this second experiment had not been optimized, a very significant power increase—65%—was achieved for a period of 4 hours each day, through a programmed decrease in the production well backpressure (from 2200 psi down to 500 psi, as shown in Fig. 9-11). This temporary decrease resulted in the venting of a portion of the hot, high-pressure fluid stored in the dilated joints near the deep production interval in EE-2A. Then, over the next 20 (off-peak) hours, these joints were reinflated by high-pressure injection. In the case of an HDR system associated with an electric generating plant and using excess off-peak power to reinflate the reservoir, this mode of operation amounts to a form of *pumped storage*.

Table 9-6. The Load-Following Experiment, last cycle

	Enhanced production (average over 4 hours)	Baseload production (average over 20 hours)	Overall production (average over 24 hours)
Injection flow rate, gpm	129.3	129.6	129.6
Production			
Flow rate, gpm	146.6	92.4	101.6
Temperature, °C	188.7	182.9	183.9
Thermal power, MW	6.12	3.72	4.11

The 24-hour overall average flow rate for the last cycle of the Load-Following Experiment, 101.6 gpm, represents an increase of 8% over the production flow rate for Stage 2 of the RVFT (94 gpm at a backpressure of 2200 psi—see Table 9-5). This translates to an equivalent overall power increase of 8% (uncorrected for the accompanying temperature increase, which would make it even larger). Viewed from another standpoint, the power levels shown in Table 9-6 imply a 10% gain over the 20-hour baseload level (4.11 MW/3.72 MW)—a very significant gain in power.

The results of the Load-Following Experiment provide just one example of the production flexibility and output enhancement that may be attainable from HDR systems on a sustained basis, through the application of novel production strategies.

Reservoir Engineering Studies

Water Loss

Figure 9-13 illustrates water-loss trends during the first two steady-state production segments of the LTFT (the principal data for these production segments are given above, in Table 9-3). Because those segments were separated only by the fairly brief IFT, this pattern of water loss is considered to be more representative of reservoir behavior than that seen during the third steady-state segment, or RVFT. Because the RVFT followed two years of reservoir shut-in, during which reservoir pressures declined to very low levels (similar to those observed before the start of previous circulations), water losses during the RVFT are not indicative of long-term system performance. These data confirm the conclusion reached in earlier static reservoir pressurization studies, namely, that under conditions of constant pressure the water-loss rate declines with time.

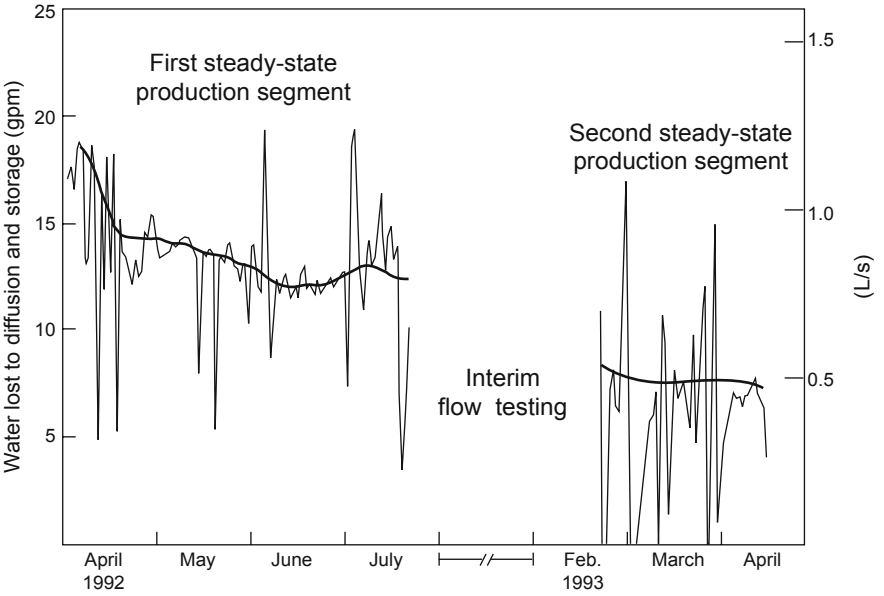

Fig. 9-13. Water loss trends during the first two steady-state production segments of the LTFT.
Source: Brown, 1999

These data reaffirm that water losses are governed by the level of reservoir pressure and the time that the pressure has been maintained, rather than by the circulation flow rate. Note in particular that water losses were smallest during the second steady-state production segment, after the reservoir had been maintained at high pressure for well over a year. Presumably, under constant pressure conditions, water from the high-pressure reservoir diffuses at a decreasing rate into the lower-pressure rock mass beyond the pressure-stimulated reservoir region. Experience at Fenton Hill not only supports such an assertion, but shows that the pressure diffusion rate is essentially independent of the circulation flow rate. On that basis it would be reasonable to expect that, in a commercial reservoir maintained at high pressures over a period of several years, the water-loss rate would decline to a very low level.

The extended period of minimal operations (May 1993–May 1995), when injection was suspended and the reservoir pressure was allowed to drop to just 685 psi (4.72 MPa), provides evidence of the fate of "lost" water. Pressure declines during that two-year period were attributed primarily to the frac-around of the scab liner in EE-3A (via joints intersecting the uncemented portion of the wellbore above the liner) and subsequent venting of the fluid at the surface—a much faster process than diffusion of fluid into the sealed rock mass at the periphery of the reservoir. The 34-day closure of

the annular flow path to the surface actually resulted in a slow increase in reservoir pressure (from 685 to 687 psi [4.72 to 4.74 MPa]). This increase was no doubt due to inflow of pressurized water from the surrounding rock mass, which would have become overpressured with respect to the reservoir as the reservoir was being slowly vented.

The pressure increase took place in spite of the fact that water was being lost to the Phase I reservoir—flowing via the annulus above the cemented-in liner into the low-pressure joint intersecting the EE-3A borehole at 10 260 ft. Recharge of the Phase I reservoir via this path had been suspected years earlier, in the spring of 1985, when one of the Phase I wellbores began to "belch" during shut-in; and by a pressure–flow response in both Phase I wellbores (see Chapter 6, Fig. 6-43 and the section *First Lynes Packer Test in EE-3A—Expt. 2049*, for supporting information on this joint connection). The volume of water possibly shunted to the Phase I reservoir was estimated at 50 000–100 000 gal. (200 000–400 000 L). During the 34 days of slowly rising reservoir pressure, the shut-in annulus pressure rose to 250 psi (1.7 MPa).

Of the several experiments conducted during the two-year extended period of minimal operations, two yielded significant data concerning water loss. At the end of August 1994, when the reservoir pressure was raised to 1450 psi (10 MPa), injection of fluid for a few hours each day maintained that level of pressure for 38 days (including a 3-day shut-in in late September). Typically, about 5800 gal. (22 000 L) of water was injected per day, of which some 4000 gal. (15 000 L) returned to the surface via the annular flow path between the tie-back string and the 9 5/8-in. casing. The net water loss to the far field (beyond the pressure-stimulated reservoir) was thus on the order of 1800 gal./day (7000 L/day), or *1.3 gpm* (0.08 L/s) at the 1450-psi (10-MPa) pressurization level. This was the smallest value yet recorded for the Phase II reservoir.

The second experiment began in November 1994. The pressure of the reservoir was again raised to and maintained in the 1300- to 1450-psi (9- to 10-MPa) range (this time with more erratic pumping, owing to the weather and construction activities at the site). Nonetheless, by early May 1995—after about 6 months on this intermittent schedule—the water-loss rate to the far field had declined even more, to about *0.9 gpm* (0.06 L/s).

Taken as a whole, the studies of water loss at Fenton Hill demonstrated that water use should not be a concern in HDR systems. In tight HDR reservoirs, water loss will continue to decline—and at a steadily decreasing rate—as the pressure in the surrounding rock mass approaches the pressure at the periphery of the inflated reservoir. In short, water loss in tight, confined HDR systems should be very low, and predictable.

Water loss in pressure-stimulated hydrothermal systems (sometimes referred to as hot wet rock, or HWR, reservoirs) has been widely studied in other countries and has been found to be much greater than at Fenton Hill.

At the Soultz HWR site in France, for example, a downhole pump was employed to pull water from the reservoir into the production well and thereby mitigate the water loss problem. Table 9-7 shows water loss from two HWR (unconfined) reservoirs compared with that from the HDR (confined) Phase II reservoir at Fenton Hill.[4]

Table 9-7. Water loss: HWR (unconfined) vs HDR (confined) reservoirs

Location	Type of reservoir	Injection pressure, psi (MPa)	Water loss (%)
Ogachi (Yamamoto et al., 1997)	Unconfined (HWR)	970 (178)	78
Rosemanowes (Richards et al.,1994)	Unconfined (HWR)	1710 (11. 8)	45
Fenton Hill (Brown, 1994a)	Confined (HDR)	3960 (27.3)	7

Impedance Distribution Across the Reservoir

Although the large impedance drop observed at the end of the second steady-state segment of the LTFT was unplanned, and the reasons for it are not well understood, important information about the impedance distribution within the Fenton Hill HDR reservoir was coming from other, incidental LTFT operations. As depicted in Fig. 9-14, within a few minutes of shutdown of the HDR system, a large rise in pressure was measured at the production well and a small decline in pressure was measured at the injection well. This initial behavior was followed by a period during which these pressure increases and decreases continued, but at a much slower rate, as the system crept toward pressure uniformity. This behavior implies that the flow impedance is concentrated near the production wellbore, rather than distributed uniformly across the reservoir. As discussed in more detail in the *Reservoir Modeling* section of this chapter, this nonuniform impedance distribution means that it may be possible to construct larger HDR reservoirs, with much more widely separated wellbores, without proportionately increasing the flow impedance.

Reservoir Joint Opening/Closing Pressures

The extended period of minimal operations (May 1993–May 1995), which followed the second steady-state production segment, provided a unique opportunity to observe the natural pressure decline of the dilated Phase II reservoir. As shown in Fig. 9-15, over the 135 days immediately following cessation of circulation, the pressure declined from 3400 psi (23.4 MPa) to 1250 psi (8.6 MPa) as stored water continued to vent to the surface via the

[4]The source for this table is *Geothermics* (August–October 1999). This entire special issue of the journal, entitled "Hot Dry Rock and Hot Wet Rock Academic Review," was devoted to these geothermal systems.

frac-around of the scab liner in the injection wellbore (with minor diffusion into lower-pressure regions beyond the periphery of the reservoir). The pressure decline followed the expected course, with the exception of two small inflection points, one at a pressure of 2100 psi (14.5 MPa) and one at 1500 psi (10.3 MPa). Magnified views of the curve around these points are shown in the insets to the figure.

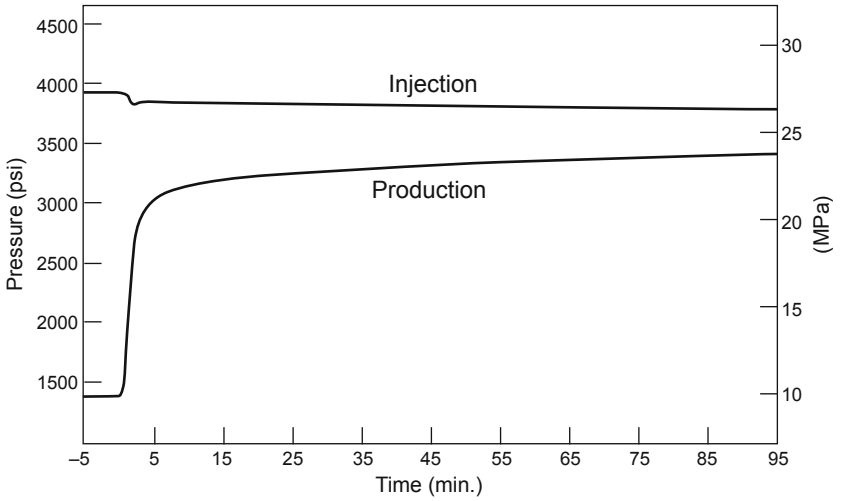

Fig. 9-14. Changes in surface pressures following shut-in of the HDR system. Source: Brown, 1994b

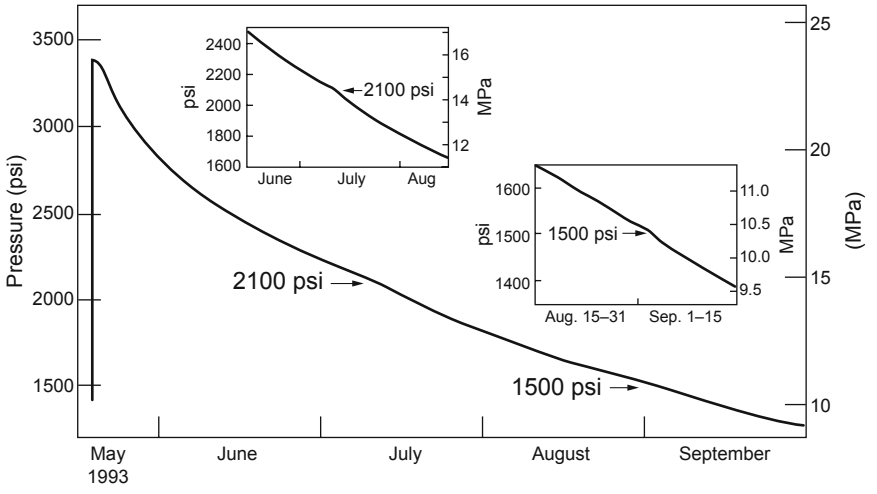

Fig. 9-15. Decline in production well pressure during 135 days of shut-in following the second steady-state production segment.
Adapted from HDR, 1995

These inflection points represent the opening pressures of two sets of joints. At each point, the pressure first flattened out for several days (reflecting the venting—at near-constant pressure—and then closing of the joint set) and afterwards resumed its decline. (The pressure decline was being controlled by the near-constant reservoir vent rate, which was in turn being mostly controlled by the frac-around, i.e., flow bypassing the scab liner deep in EE-3A.) This pressure behavior may be better understood by picturing *inflation* of the reservoir at a slow, but constant, rate of injection: the inflection points would be reversed, showing a period of leveling out in the pressure as each joint set was opened and then inflated at near constant pressure—the first set at about 1500 psi and the second at about 2100 psi.[5]

The Dominance of the Joints in Controlling HDR Reservoir Behavior

As first recognized during the stimulation and flow testing of the Phase I reservoir, and then confirmed during the stimulation and extensive flow testing of the Phase II reservoir, the interactions between the joints within the pressure-stimulated region control the deformational behavior of an HDR reservoir, which in turn determines the flow patterns. In other words, how the joints interact under pressurization—not the characteristics of the matrix rock—controls the deformation of the basement rock. The Young's Modulus, Poisson's ratio, and compressive strength of the rocks making up the crystalline basement are very similar, and influence deformational behavior only marginally. For this reason, laboratory studies on rock cores (or blocks) are of very little use.

Temperature Data: Production Well

The temperature stability of the production flow through the first two segments of the LTFT and the first stage of the RVFT was remarkable, as shown by the data in Tables 9-3 and 9-5. Even the minor temperature differences measured during the Load-Following Experiment (see, for example, Table 9-6) can be attributed to variations in the cooling effect of the production wellbore during transit of the circulating fluid: at higher flow rates, the shorter transit times would result in higher production temperatures at the surface. Thus, the higher temperature shown in Table 9-6 (188.7°C) was measured during the four hours of enhanced flow during which production rates reached 146.6 gpm (9.25 L/s), whereas the lower temperature (182.9°C) was coincident with the lower flow rate of 92.4 gpm (5.83 L/s).

In addition to the surface temperature measurements, logging was done periodically within the production wellbore to determine the temperature of the fluid at various depths. Data from six logs taken during the first year of the LTFT are presented graphically in Fig. 9-16.

[5]This joint-closing behavior had been observed previously during the testing of the Phase II reservoir, with pressure-inflection points at 22.4 MPa (3250 psi) and 10.3 MPa (1490 psi), as described in Brown, 1989b.

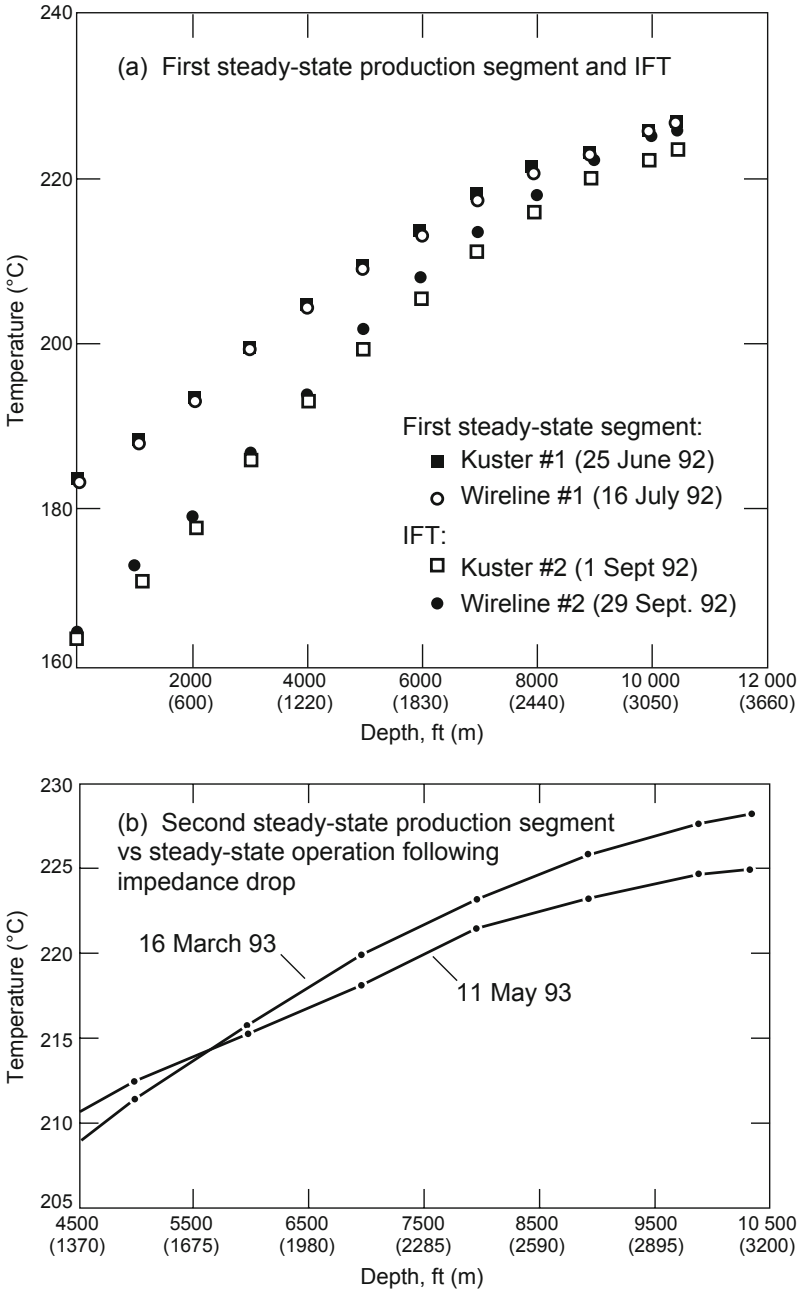

Fig. 9-16. Temperatures in the production well (EE-2A) during periods of circulation, 1992–1993.
Sources: HDR, 1993; HDR, 1995

As can be seen in Fig. 9-16a, the temperature curves from Kuster and wireline logs taken during the first steady-state production segment of the LTFT fall just about on top of each other. The logs taken during the IFT, while showing significantly lower temperatures at the surface (reflecting the lower flow rates of that period), are more steeply sloped at depth, approaching those of the first steady-state production segment. In fact, the wireline IFT log of September 29, at 10 400 ft, gave a mixed-mean temperature (average temperature of the total flow from all the producing joints) of 226°C—essentially identical to the wireline steady-state log of July 16, even though the IFT flow rate was only about two-thirds of the steady-state one (60 gpm vs 92 gpm). In other words, there appears to have been virtually no decrease in reservoir temperature over the 10-week interval between the logs.

The log of May 11, 1993 (Fig. 9-16b) was taken during the episode of significantly higher fluid production that followed the dramatic drop in flow impedance of May 6. As can be seen, this log shows a temperature at depth very close to those measured by the other logs represented in Fig. 9-16a and b—including that from the second steady-state production segment (March 16, 1993) just two months earlier. The log also shows that the temperature within the wellbore declined less rapidly as the fluid moved toward the surface, no doubt because of the increased rate of fluid flow up the wellbore following the sharp drop in impedance.

On several occasions, temperature logs were also taken in the open-hole portion of the production wellbore. Table 9-8 shows the temperatures measured at four specific depths (corresponding to known fluid-entry points) within this interval, by five logs taken over a three-year period.

Table 9-8. Temperatures at four fluid-entry points in the open-hole portion of the production wellbore (EE-2A), July 1992–July 1995 (°C)

Fluid-entry points	16 July 1992	29 September 1992	16 March 1993	22 June 1995 (corrected)	12 July 1995
Point A 11 840 ft (3608 m)	234.5	233.9	231.5	229.7	227.3
Point B 11 320 ft (3450 m)	233.4	232.9	232.4	230.6	229.2
Point C 10 990 ft (3350 m)	232.0	231.7	231.5	230.0	228.7
Point D 10 750 ft (3277 m)	228.2	228.1	227.8	227.3	226.4

These production-interval logs indicate a significant decline in temperature (about 7.2°C) at the deepest point, A, but a much smaller decline (less than 2°C) at the shallowest point, D, over the three years. It is important to remember that the time covered by these measurements included long periods of reservoir shut-in and low flow, even though the logs themselves were taken during high-production periods.

The open-hole temperature data for the four fluid-entry points, compiled from the log of July 16, 1992, are presented graphically in Fig. 9-17.

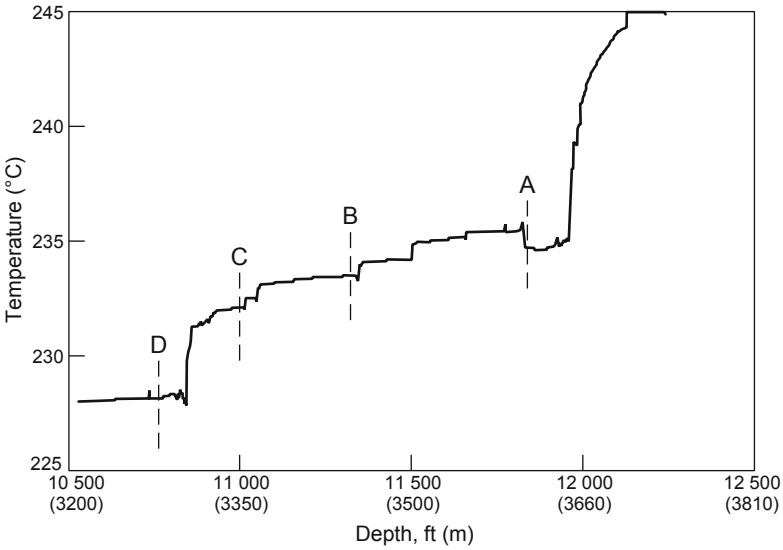

Fig. 9-17. Temperature profile through the open-hole portion of the production wellbore (EE-2A), July 16, 1992.
Source: Brown, 1994b

Figure 9-18 shows the temperature profile from October 12, 1993—one of two logs done during periods of no circulation. Because these temperatures were measured under conditions of thermal recovery—static rather than flowing—they cannot be compared directly with the temperatures recorded during flow testing (e.g., Fig. 9-17). They do, however, provide evidence that after flow testing stopped in May 1993, no significant overall temperature changes occurred in the open-hole region of the production wellbore. A final temperature log was taken in the production wellbore on October 18, 1995, several months after termination of the LTFT. It indicated that following cessation of production, temperatures in the portion of the wellbore above the production zone had decreased toward the pre-existing geothermal gradient. In addition, the temperature changes at the four fluid-entry points were less abrupt than those shown in Fig. 9-17, suggesting that after the several months of shut-in, thermally driven natural convection within the production interval had flattened out the previous temperature gradient.

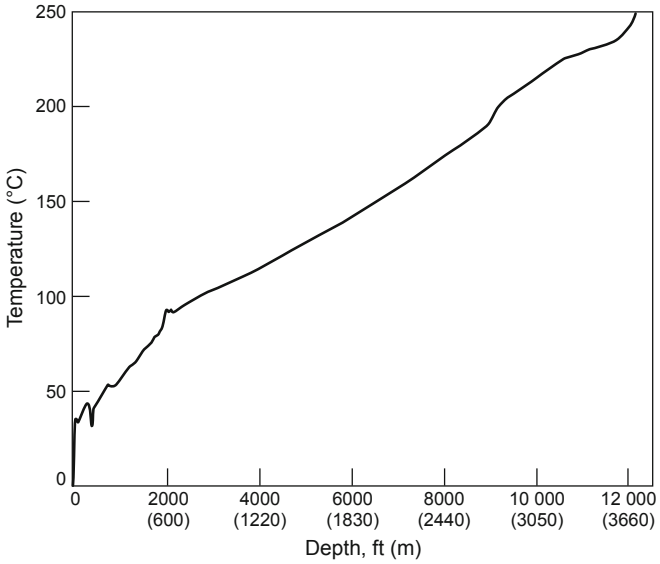

Fig. 9-18. Temperature profile in the production wellbore during shut-in (October 12, 1993).
Source: HDR Project data archives (Technical Status Report, October 1993)

Temperature Logging: Injection Well

Opportunities to assess the temperature within the injection wellbore were limited, because it was typically kept under very high pressure during circulation. The first LTFT temperature log in this wellbore was run on December 10, 1993, during the extended period of minimal operations that followed the second steady-state segment (Fig. 9-19); these data elucidate temperature drawdown in the injection zone of the reservoir over the first 13 months of flow testing. The logging was carried out almost 7 months after the cessation of circulation, which allowed the reservoir pressure to decline at its natural rate. The delay had two positive effects: first, pressure-control equipment already on hand could be used, avoiding the additional cost of a commercial survey done with a high-pressure, grease-injector control head and lubricator; and second, the tension in the injection wellbore tie-back string had time to relax, reducing the risk of well damage (which is inherent in any logging operation).

These temperature data essentially replicate those obtained in the injection well following the ICFT in 1986 (shown—with much greater detail in the curve—in the June 23 survey of Fig. 7-10). Clearly evident are the cooling effects of the frac-around flow below 10 800 ft, as well as the major reservoir flow entrance just above 12 000 ft. It is apparent that the major portion of the injected water exited the wellbore near the bottom of the open-hole interval, although the distribution of the flow from that

region into the body of the reservoir cannot be ascertained. Figure 9-19 also shows that—as would be anticipated—the temperature profile of the region behind the liner and tie-back string (to a depth of about 10 500 ft) paralleled the geotherm of the reservoir rock as it recovered from the radial cooling induced by the long period of cold-water injection during the second steady-state production segment.

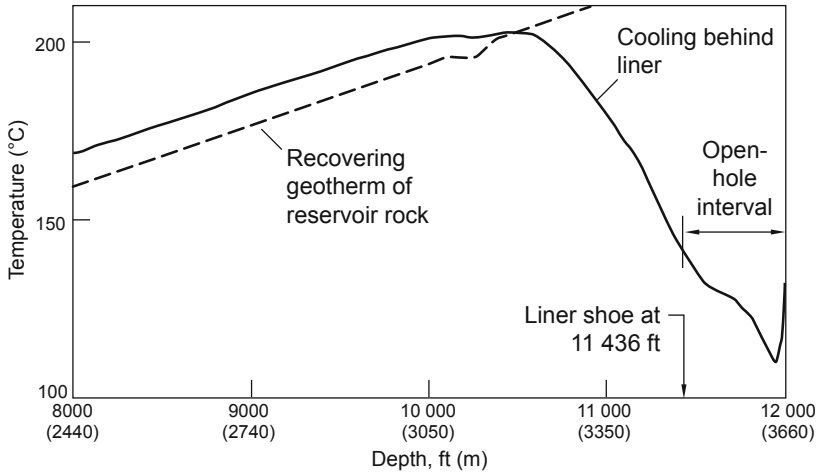

Fig. 9-19. Temperature profile in the injection wellbore during shut-in (December 10, 1993).
Source: Duchane, 1995a

Postulated Reservoir Segmentation and Connections to the Phase I Reservoir

The entire question of the segmentation of the Phase II reservoir was based on the observance of different pressure responses at EE-3A and EE-2A. This question and the related question of the apparent connections to the Phase I reservoir are answered by one simple scenario, shown in Fig. 6-43 of Chapter 6. The annulus above the scab liner in EE-3A was connected both to the Phase II reservoir (via the frac-around of the liner) and to the Phase I reservoir (via the low-pressure joint that also intersected this annulus). It was the breakthrough on July 6, 1995 that created a more direct connection between the two reservoirs. In other words, the Phase II reservoir was not segmented.

In the summer of 1995, additional evidence from post-LTFT temperature logs spurred further testing (even though it was essentially redundant) of the EE-3A frac-around. At the end of July the shut-in reservoir pressure, as measured at the production wellhead, stood at 2161 psi (14.9 MPa). During the ensuing two months, water was briefly injected into the reservoir in small amounts (accompanied by tracer testing) while the frac-around flow path—connected to the surface by the annular flow path—was alternately shut in and vented. The reservoir pressure continued to decline, reaching a

level of 1160 psi (8.0 MPa) by September 4 and about 812 psi (5.6 MPa) by the end of September. During these operations, the annulus pressure measured at EE-3A did not approach the reservoir pressure as measured at EE-2A—clearly showing that the pressure of the reservoir was only marginally related to the pressure of the deep ANNULUS (see Fig. 6-43).

Tracer and Geochemical Studies

The information in this section is drawn primarily from Birdsell and Robinson, 1988b, Rodrigues et al., 1993, and Callahan, 1996 (a more detailed discussion of the tracer findings may be found in these publications), as well as HDR Geothermal Energy Development Program monthly and annual reports, 1992–1995. (See also *Tracer Studies* in the section *The Long-Term Flow Test: Operations (1992–1995)*, above.)

Reservoir Fluid Pathways

Figure 9-20 shows normalized recovery profiles for three fluorescein tracer tests conducted during the first and second steady-state production segments and during the brief steady-state period that followed the impedance drop in May 1993. Also shown is a recovery profile for a p-TSA tracer test that took place at the same time as the first fluorescein test, and which confirms the fluorescein one. It can be seen that as circulation proceeded, the tracer took progressively longer to traverse the reservoir. The lengthening time to first arrival of the tracer at the production well is a clear indication that as time went on, the shorter flow paths were being closed off. The later peaks and broader shapes of the 1993 curves generally indicate that the modal and dispersion volumes were growing. (It is not possible to ascertain changes in the integral mean volume simply from casual observation of the curves.) These data leave no doubt that the HDR reservoir at Fenton Hill was a dynamic entity—i.e., that under conditions of steady-state circulation, the volume of hot reservoir rock accessible to the circulating fluids was continually increasing—a very good portent for future HDR power production!

The data in Fig. 9-21, from two p-TSA tracer tests, show recovery profiles during the first steady-state production segment—which yield important information about the nature of changes in the reservoir between May and July of 1992 (assuming no chemical degradation of the p-TSA). During that period, the integral mean volume of the reservoir increased by about 520 m^3 and water losses were some 3400 m^3 (Rodrigues et al., 1993). The tracer data suggest that about 15% of these "losses" (520 divided by 3400) actually consisted of increased fluid volume within the expanding network of fluid-carrying joints. Rough calculations of rock contraction caused by the cooling effects of the circulating fluid can account for about 190 m^3 of the growth in integral mean volume, implying that the remaining 330 m^3 reflected new joint openings. The other 85% of the water losses may be explained by pressure diffusion into the rock matrix beyond the periphery of the pressure-stimulated reservoir, and/or storage in further-opened but nonflowing, dead-end joints.

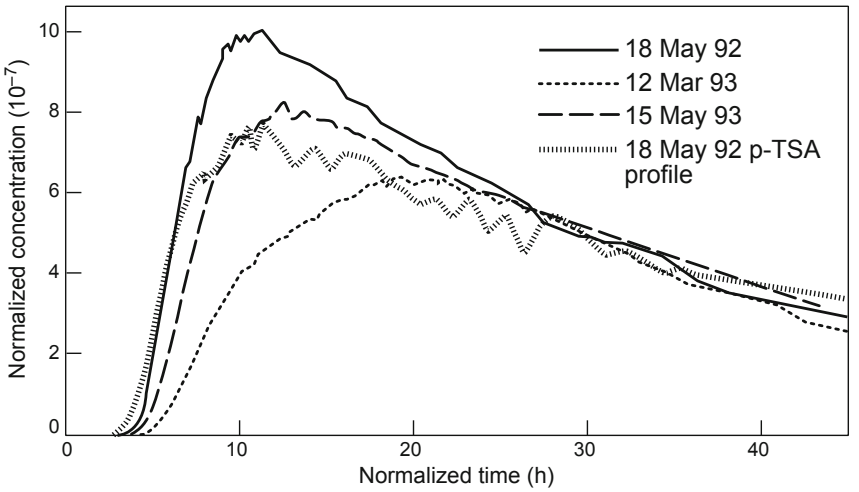

Fig. 9-20. Tracer recovery profiles during steady-state operation (1992–1993): three fluorescein and one p-TSA.
Source: HDR, 1995

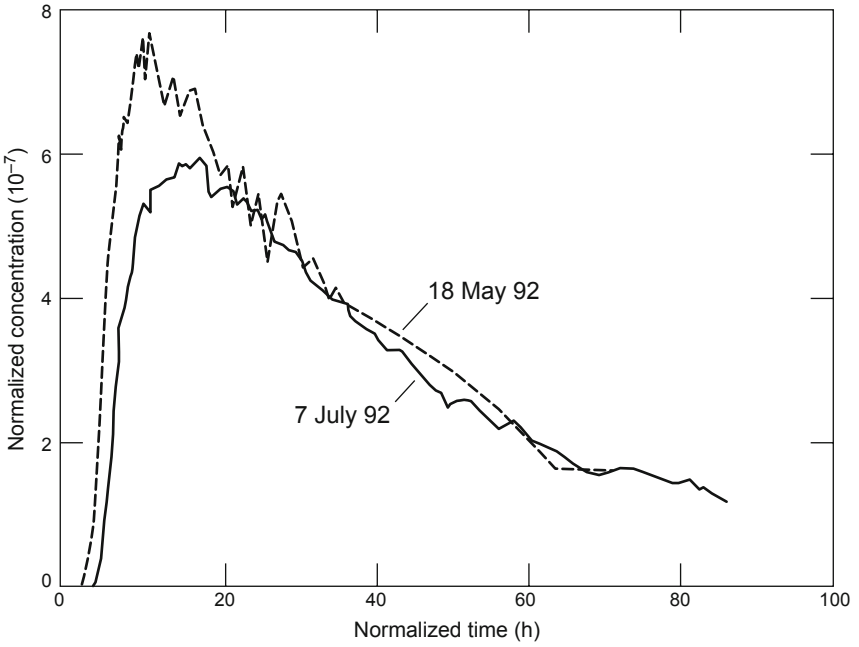

Fig. 9-21. Recovery profiles from two p-TSA tracer tests conducted during the first steady-state production segment.
Source: Rodrigues et al., 1993

Table 9-9 shows the operating parameters under which tracer testing was done. As noted earlier, the parameters during the second steady-state production segment of the LTFT essentially replicated those of the first segment, whereas later experiments, including the third steady-state segment, involved several variations. Reservoir volume information based on the data from these tracer tests are presented in Table 9-10.

Table 9-9. Operating parameters during various tracer tests of the LTFT

Date of test	Average injection pressure, psi (MPa)	Average production flow rate, gpm (L/s)	Average backpressure, psi (MPa)	Average water-loss rate, gpm (L/s)
18 May 1992 (First steady-state production segment)	3883 (26.8)	98.44 (6.2)	1408 (9.7)	13.47 (0.85)
12 April 1993 (Second steady-state production segment)	3968 (27.4)	90.67 (5.7)	1408 (9.7)	7.45 (0.47)
15 May 1993 (Steady-state following impedance drop)	3854 (26.6)	122.06 (7.7)	1408 (9.7)	-3.96* (-0.25)
6 June 1995 (Third steady-state production segment, Stage 1)	3968 (27.4)	104.94 (6.6)	1408 (9.7)	17.91* (1.13)
11 July 1995 (Steady-state, after Load-Following Experiment)	3968 (27.4)	93.05 (5.9)	2205 (15.2)	8.24 (0.52)

Based on Callahan, 1996

* Water-loss data were irrelevant during these test segments.

Table 9-10. Reservoir volumes* based on tracer tests conducted during various LTFT experiments

Date of test	Modal volume (m^3)		Dispersion volume (m^3)	Integral mean volume (m^3)		First-arrival volume (m^3)
	Fluor-escein	p-TSA	p-TSA	Fluor-escein	p-TSA	p-TSA
18 May 1992 (First steady-state production segment)	277	277	320	n.d.	2246	79
12 April 1993 (Second steady-state production segment)	477	511	658	6579	2034	124
15 May 1993 (Steady-state following impedance drop)	314	n.d.	358**	3558	n.d.	105**
6 June 1995 (Third steady-state production segment)	496	389	610	6565	1789	88
11 July 1995 (Steady-state after Load-Following Experiment)	478	357	743	8376	1630	111

Based on Callahan, 1996
n.d. = no data collected

*See *Tracer Studies* in the section *The Long-Term Flow Test: Operations (1992–1995)* for a discussion of the volume terms in this table.

**obtained from fluorescein data

The variability in operating conditions makes comparisons of the data from these several tracer tests more difficult, but some important observations can be made. As might be expected, the first-arrival volume continued to increase through the end of the second steady-state production segment, even though the integral mean volume actually decreased from its value of May 1992 (during the first steady-state segment). One could speculate that the reduced pressures and flows during the nearly 7 months of the IFT (August 1992–February 1993) led to relaxation and partial closure of the fluid-carrying joints. In fact, a tracer measurement from that period (September 1992), when the reservoir was being circulated intermittently, gave an integral mean volume of about 72 000 ft^3 (2044 m^3) (Rodrigues et al., 1993, Table II). This contraction from earlier larger volumes was attributed at the time to the lower operating pressures and flow rates during the IFT.

The tracer data of Table 9-10 clearly show the effects of the sudden drop in flow impedance in May 1993. The modal, integral mean, and first-arrival volume data all show sharp declines, indicating that fluid was traveling much faster through the reservoir. Apparently, the newly opened joint(s) transmitted fluid at such a high rate that other pathways were effectively cut off from the flow and thus did not come into play in the tracer measurements.

It is more difficult to ascertain from the available tracer data what changes took place in the reservoir over the two years of noncirculation (May 1993 to May 1995). Tracer data from 1995, however, showed a significant rebound in the modal, dispersion, and integral mean volumes since May of 1993, as well as a resumption of the increasing trend of the first-arrival volume. These data indicate that the shorter flow path(s) opened during the impedance drop of May 1993 had begun to close off again. In other words, it appears that the reversal in these trends effected by the drop in flow impedance was an anomaly.

At the time of the July 1995 tracer test, the reservoir was being operated in a load-following mode and the backpressure at the production well was higher than in early June. The modal and integral mean volumes (except for the fluorescein data in the case of the latter) showed slight decreases from the June test readings, probably as a result of the changes in operating conditions. Those changes make comparisons with tracer data from earlier periods somewhat ambiguous; but the 1995 data, like that from 1992–1993, show an increase in the dispersion volume with time, indicating the development of more complicated flow paths through the reservoir.

Tracer Data as an Indicator of Reservoir Temperature Trends

Figure 9-22 compares the June 1995 cumulative return curves for p-TSA and fluorescein with those of July 1995.

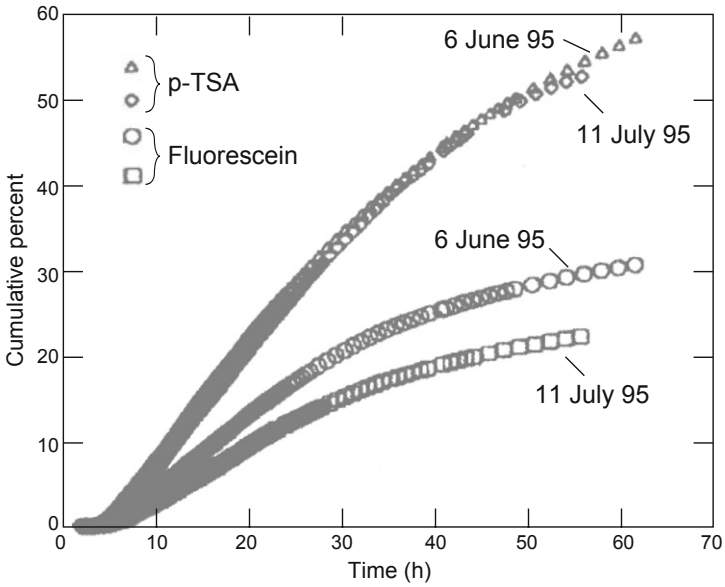

Fig. 9-22. Tracer recovery profiles, p-TSA and fluorescein, June 1995 vs July 1995.
Source: Callahan, 1996

Note that whereas the two tests are almost identical with respect to return volumes of p-TSA, the July test shows a definite decline in return of fluorescein. This difference cannot be explained by changes in reservoir flow pathways, because that should have affected the fluorescein and the p-TSA equally; nor were any significant changes observed in the fluid chemistry that might have affected the fluorescein. The only possible explanation is a difference in temperature—that is, the greater fluorescein degradation during the July test implies that the average temperatures encountered by the tracers as they traversed the reservoir were higher than a month earlier. This finding suggests, as do a number of others, that as circulation of fluid in an HDR reservoir continues, access to hot rock improves.

Geochemical Analyses and the Fresh-Water Flush

The chemistry of the circulating fluid was remarkably consistent over the entire term of the LTFT. As shown in Table 9-11, the concentrations of significant anions and cations in the produced water were similar during all three steady-state segments and did not change significantly even after the sudden impedance drop of May 1993. Far less than a kilogram of suspended solids was collected on the 50-µm strainers installed at the outlet of the production well; and the water was not particularly high in dissolved solids, being about a tenth as saline as seawater—a result that mirrors the circulation-fluid geochemistry measured during the ICFT in 1986. Most of the species were benign, but the levels of boron, fluoride, and especially arsenic, were high enough to make the recirculated water nonpotable.

Table 9-11. Concentrations of dissolved species in produced water during the LTFT (ppm)

	First steady-state production segment		Second steady-state production segment	RVFT Stage 1	RVFT Stage 4 (Load-Following Experiment)
Species	April 1992	July 1992	March 1993	May 1995	July 1995
Chloride	1220	953	1002	890	1160
Sodium	1100	900	899	839	1020
Bicarbonate	552	588	556	469	505
Silicate (as SiO_2)	458	424	402	419	445
Sulfate	285	378	342	328	385
Potassium	95	89	91	90	94
Boron	47	35	34	30	39
Calcium	19	18	17	13	15
Lithium	19	16	15	15	17

Table 9-11. (Continued)

	First steady-state production segment		Second steady-state production segment	RVFT Stage 1	RVFT Stage 4 (Load-Following Experiment)
Species	April 1992	July 1992	March 1993	May 1993	July 1995
Fluoride	14	17	13	15	15
Bromide	6.5	5	5.1	4.6	6.8
Arsenic	3.8	7.2	3.5	3.0	4.0
Iron	1.0	0.8	0.3	0.3	0.2
Aluminum	0.9	1.2	0.8	0.8	0.9
Ammonium	0.8	1.1	1.3	1.0	0.4
Strontium	0.8	0.8	0.8	0.6	0.8
Barium	0.2	0.2	0.2	0.1	0.1
Magnesium	0.2	0.1	---	---	0.1
Total dissolved solids	3845	3434	3387	3118	3713

Levels of dissolved gases were consistently below 3000 ppm, with carbon dioxide constituting more than 95% of the total. Hydrogen sulfide was present only in small amounts (typically less than 1 ppm). During closed-loop circulation, the pressure was high enough, even in the production side of the loop, to keep the small amounts of dissolved gases in solution so that they were not removed by the gas/particle separator. Like the dissolved solids, the gases appeared to quickly reach an equilibrium level in the circulating fluid.

From September 2 to 8, 1992, as part of the IFT (between the first and second steady-state production segments), the water that had been recirculated repeatedly through the reservoir was replaced with fresh water. This fresh-water flush (FWF) can be considered a type of tracer experiment, because the species present in the fluid being replaced, those in the fresh water replacing it, or those in both (by comparison of the concentrations) serve as tracers.

Table 9-12 shows the concentrations of major dissolved species in the fresh water at the beginning of the flush, in the produced fluid at the end of the flush, and in the produced fluid about three weeks thereafter. Note that except for calcium and magnesium, these concentrations were much lower in the fresh water than in the produced fluid. At the end of the FWF (September 8), the level of total dissolved solids in the produced fluid had dropped by about a third from those observed during the first steady-state production segment (Table 9-11). However, three weeks later the concentrations of individual species had recovered to levels similar to those seen during all other periods of closed-loop circulation.

Table 9-12. Concentrations of dissolved species during and following the FWF (ppm)

Species	Injected fresh water (2 September 1992)	Produced fluid	
		8 September 1992	28 September 1992
Chloride	101	615	1109
Sodium	54	569	935
Bicarbonate	259	430	419
Silicate (as SiO_2)	81	396	451
Sulfate	21	235	361
Potassium	10	53	94
Boron	1.9	18	40
Calcium	89	9.3	18
Lithium	0.7	8.7	16
Fluoride	0.5	15	14
Bromide	0.6	3.2	5.6
Arsenic	<0.1	2.7	3.4
Iron	0.5	0.3	0.5
Aluminum	0.2	1.3	0.6
Ammonium	0.1	1.1	1.3
Strontium	0.3	0.4	0.7
Barium	0.1	0.1	0.2
Magnesium	8.6	<0.1	0.1
Total dissolved solids	633	2358	3471

The FWF led to a number of insights. The mixing of fresh water into the circulating fluid alone would be expected to gradually reduce the concentrations of total dissolved solids and, proportionately, the concentrations of most individual species. Such a reduction was observed for most of the ions (sodium and chloride are good examples); but it did not take place as fast as tracer studies had indicated it should if mixing were the only mechanism at work. In addition, the decline in concentration of silicate was much smaller than expected, compared with the declines in total dissolved solids. Finally, the concentrations of calcium and magnesium did not show the increases expected, considering their higher concentrations in the fresh water. These findings imply that some other mechanism or mechanisms were influencing the chemistry of the fluid.

Figure 9-23 shows the normalized concentration-decline curves of boron, bromide, and chloride in the produced fluid over the course of the FWF compared with those anticipated (on the basis of a decline curve derived from p-TSA tracer data).

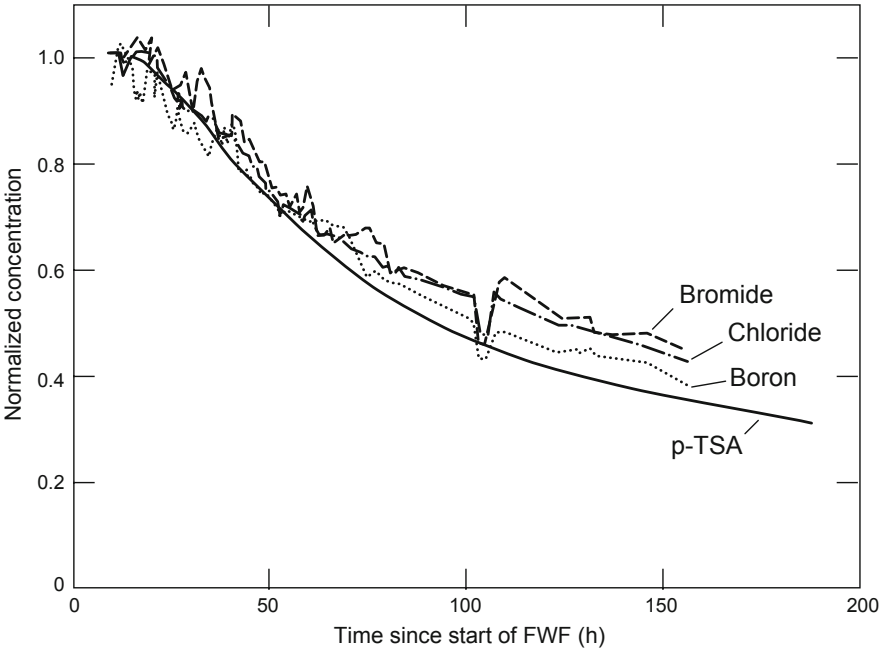

Fig. 9-23. Normalized concentration-decline curves for bromide, chloride, and boron during the FWF compared with a decline curve derived from p-TSA tracer data.
Source: Rodrigues et al., 1993

All three ions show smaller-than-anticipated declines, indicating a source within the reservoir. That source is almost certainly the pore fluid, since there are no minerals in the rock that could be the source for these species. The pore-fluid-derived concentrations of these species in the produced fluid can be calculated by comparison with the tracer-based decline curve. The results are shown in the first column of Table 9-13. The approximate concentrations of these species in pure pore fluid, as determined from samples taken during development of the HDR system, are shown in the second column of the table. The numbers in the third column, obtained by dividing the first column by the second, indicate that from 4% to 7% of the water produced during the FWF was derived from pore fluid.

Table 9-13. Pore fluid contributions* to produced water during the FWF

Species	Concentrations of pore-fluid-derived ions in produced water (ppm)	Ion concentrations in pure pore fluid (ppm)	Pore fluid in produced water (%)
Boron	12	178	7
Bromide	1.5	42	4
Chloride	274	5870	5

*primarily pore fluid within the original joint-filling material, not the rock matrix.

The concentrations of most of the other dissolved species also showed smaller-than-anticipated declines, but these are not so readily attributed to contributions by pore fluid to the produced flow. Some of these species may have sources in the reservoir rock. Silicate, which shows only a marginal decline in concentration, might be rapidly dissolved from quartz at temperatures existing within the Phase II reservoir. If the dissolution rate is fast enough, an equilibrium level of silicate (400–450 ppm) could even be reached in a single pass of fluid through the reservoir. Fluoride concentrations actually increased slightly during the FWF; although still not exceeding those typically found in the recirculated fluid, the higher levels in the produced fluid were unexpected and probably indicate that fluoride was being dissolved from minerals present in the reservoir rock.

The behavior of calcium and magnesium is perhaps the most fascinating. Although present in the fresh water at greater concentrations than in the water circulated during the first steady-state production segment, both showed declines in concentration in the FWF produced fluid. Undoubtedly the reservoir water contained higher levels of dissolved carbon dioxide than did the fresh water. Mixing of the two would have rapidly precipitated most of the injected calcium and magnesium ions—the most probable explanation for their low levels in the produced water.

The results from the FWF—particularly those for calcium and magnesium—must be taken in context. It should be remembered that an HDR system will invariably be operated in a pressurized, closed-loop fashion, minimizing the amount of makeup fluid needed. Extensive geochemical analyses at Fenton Hill have shown that dissolved gases and solids in the recirculated geofluid reached equilibrium levels within one to two weeks after the start of circulation and did not vary significantly thereafter. In addition, by preventing exposure of the fluid to oxygen, closed-loop circulation minimizes corrosion of the piping and casing in the pressurized sections of the system.

Ninety-two hours into the FWF, the injection pump unexpectedly failed. The automated control system then implemented a partial shut-in of the production wellhead, thereby increasing the backpressure and reducing

the flow rate. The effect was to temporarily reduce the flow impedance (see Fig. 9-24), which presented an opportunity for some unique measurements.

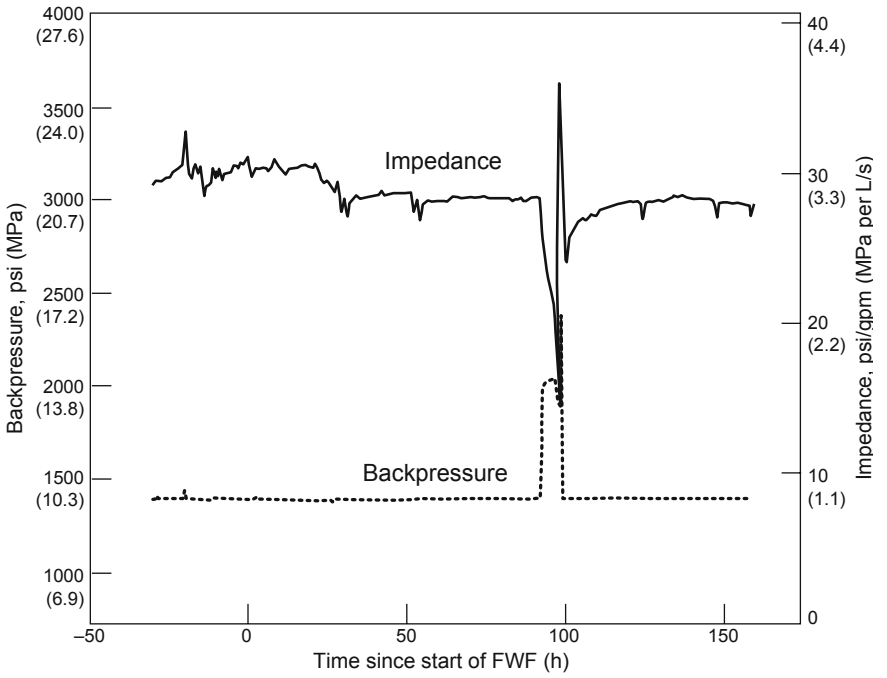

Fig. 9-24. Production well backpressure and calculated impedance over the course of the FWF.
Source: Rodrigues et al., 1993

Measurements of the changes in backpressure imposed by the automatic control system during this episode show a remarkable synchrony with changes in the conductivity of the produced fluid. As shown in Fig. 9-25, the six numbered points of the pressure curve closely mirror those of the conductivity curve—the rises in pressure bringing about decreases in conductivity until a subsequent decrease in pressure returned conductivity to its previous higher level. These findings suggest that the increased backpressure caused joints near the production wellbore to open, and over a period of several hours surges of fresher water entered the wellbore. These slugs of water began traveling upward, and when each reached the surface it was detected by the system's conductivity meter (the fresher water perhaps contained less pore fluid—and/or fewer ions derived from dissolved minerals—owing to its rapid escape from the body of the reservoir).

The time between each pressure change and its detection at the surface (as a change in fluid conductivity) corresponds to the transit time of the slug of water up the production wellbore.

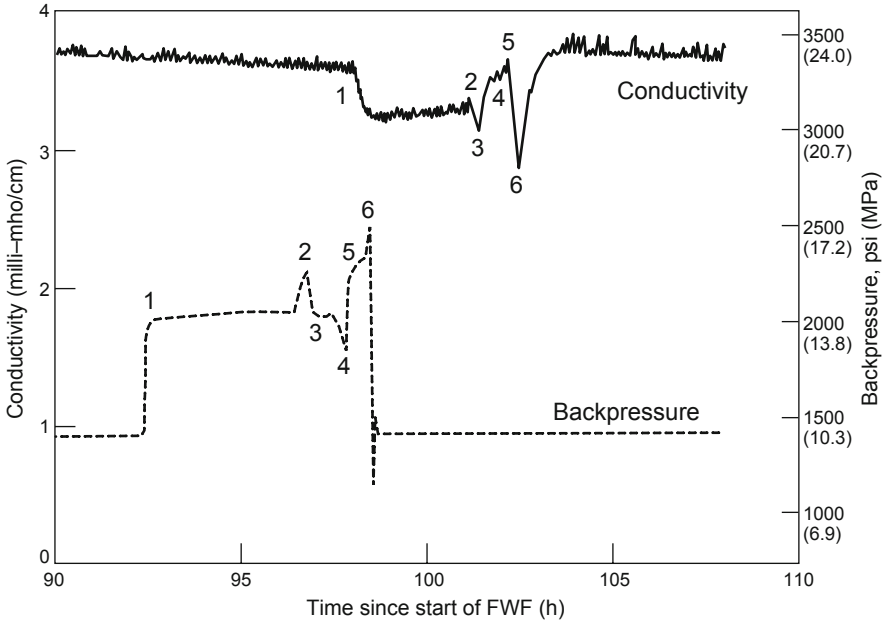

Fig. 9-25. Changes in the conductivity of the produced fluid in response to changes in backpressure during the partial shut-in episode of the FWF. Source: Rodrigues et al., 1993

Figure 9-26 shows the variations in transit time of fluid from five previously identified joints at different depths. Each numbered point locates one of the fresh-water surges by time of origin and transit time. Because transit times are a function not only of joint depth but of flow rate—which changed several times as the system was partially throttled and then reopened—the transit times of the six slugs of water (the six points in Fig. 9-25) ranged from 5.37 hours for the first one to 3.96 hours for the last one.

Note that all six points lie on or very near the transit-time profiles of the two uppermost joints—which suggests either (1) that these joints were preferentially opened as a result of the partial wellbore shut-in, or (2) that by the time of the shut-in, the fresh water had reached the outlets of the upper joints but not of the deeper ones. In either case, these data confirm that the upper joints play a very significant role in fluid transport through the reservoir, but reveal nothing definitive about the deeper joints.

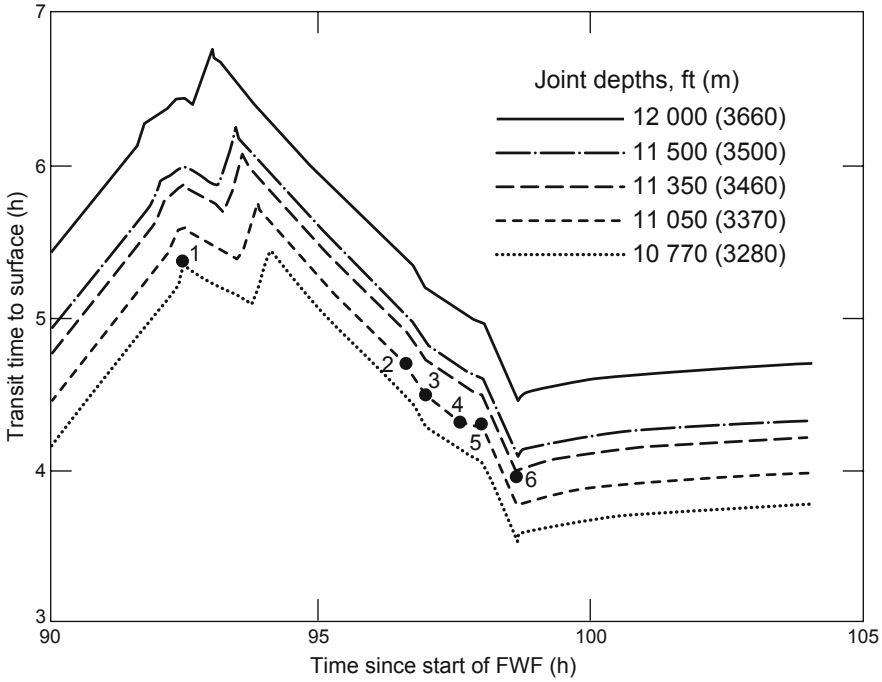

Fig. 9-26. Calculated transit times of water in the production well from joints at various depths. The lag times between changes in backpressure and corresponding changes in fluid conductivity are shown by the six points (which correspond to those in Fig. 9-25).
Source: Rodrigues et al., 1993

In sum, the results of the LTFT tracer tests and geochemical analyses, including the FWF, lead to the following conclusions:

1. The reservoir is dynamic in nature. Changes in tracer-return profiles from one test to another indicate that flow paths are continually changing—probably owing to localized cooling of joint pathways and consequent cooling of the circulating fluid, which increases its viscosity. The higher viscosity means greater resistance to flow, which redistributes the pressure within the reservoir and causes previously closed joints to open.
2. As the redistribution of flow paths proceeds, the fluid is continually accessing new, hot rock. Additional evidence for this process comes from geochemical data indicating the presence, in the production flow, of small but significant amounts of pore fluid (newly opened joints being the source) even after many months of circulation. This phenomenon has the important effect of extending the useful lifetime of the resource.

3. The sudden drop in flow impedance that occurred during the first load-following experiment (May 1993) involved the opening of one or more important new (and shorter) pathways through the reservoir. It demonstrated that manipulations of the pressure applied to the reservoir may, intentionally or unintentionally, significantly alter the flow conditions within the reservoir. The lesson is not only that operating strategies must be carefully designed and closely monitored, but that the reservoir can actually be "adjusted" through intentional application of pressure.

4. The geochemistry of the circulating water rapidly reaches an equilibrium. In reservoirs created in hard crystalline rock, such as the ones at Fenton Hill, the water can be expected to have total salinity levels well below that of seawater and therefore to be relatively noncorrosive.

5. The upper flow-producing joints contributed significantly to flow within the Phase II reservoir at Fenton Hill.

Seismicity During the LTFT

A major goal of the LTFT was to assess the performance of the Fenton Hill HDR system under conditions of maximum reservoir stability. For that reason, the LTFT was operated at injection pressures just below the anticipated threshold of seismic stimulation. Some seismic activity was observed, however, during the IFT—when the reservoir was maintained at a high level of pressurization but circulation was conducted only on an intermittent basis—and during the following months. The first seismic event was recorded very early on December 24, 1992, and 48 additional events were recorded through the end of May 1993. The correlations between these events and the surface pressures during this period are represented in Fig. 9-27.

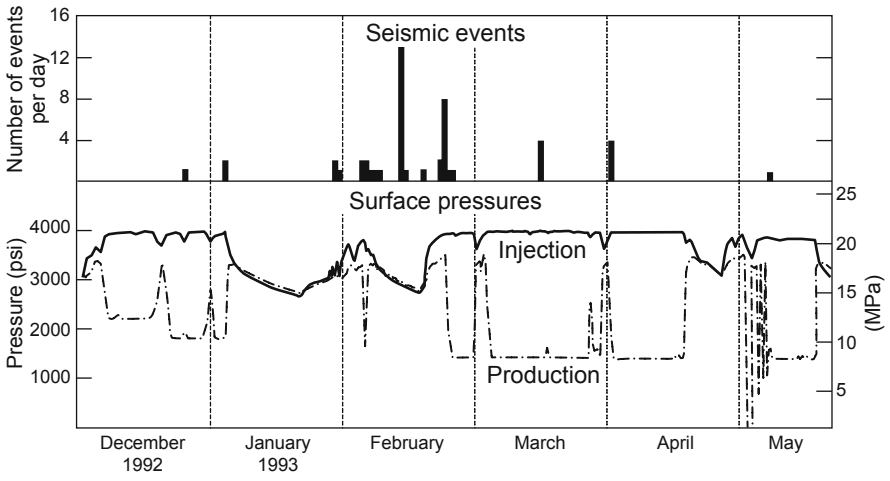

Fig. 9-27. Seismic activity and surface pressures during and following the IFT.
Source: HDR, 1995

It appears that, in general, seismic events occurred at times when surface production pressures were high—which correspond to periods when the system was shut in for one reason or another, and the reservoir (in the absence of an imposed pressure gradient between the injection and production wellbores) was equilibrating to a uniform pressure.

The locations of 31 of the 49 seismic events recorded during the IFT were reliably determined; all were found to have occurred at shallower depths and farther to the north than the large number of seismic events associated with the MHF Test of 1984 (which created the reservoir). But their locations did correlate closely with the seismicity observed during shut-in periods of the ICFT in 1986 (see Chapter 7). The ICFT seismic events were thought to possibly have been caused by "increased pressures in the production side of the reservoir after shut-in" (Dash et al., 1989). It is interesting to note that no significant seismic activity was associated with the sudden large drop in reservoir impedance in early May 1993, when the operating mode involved periodic shut-ins of the production wellbore.

In summary, aseismic conditions were the rule during the LTFT. The long aseismic periods of flow testing, the infrequency and relatively small number of seismic events, and the lack of a strong and consistent correlation between those events and imposed conditions imply that the observed seismicity was related to some long-term relaxation of the stresses created within the reservoir (or, perhaps more likely, near its boundaries) by the extended period of flow operations.

Reservoir Modeling Related to the LTFT

Reservoir modeling is essential to the successful operation of an HDR geothermal system; by predicting performance under various operational scenarios, modeling enables the system to be managed in a way that will maximize its productivity, useful lifetime, and economic return.

The results obtained from any model are, of course, only as valid as the input data. HDR models rely both on directly verifiable data (such as flow rate and production temperature) and on parameters that are not directly verifiable (such as the effective reservoir rock volume available for heat transfer, the distance between the fluid-carrying joints, the dimensions of the open joints, and the distribution of the fluid among the various joints). Parameters in the latter category are extremely important but poorly understood; in some cases, modeling results obtained by different methods vary dramatically, underscoring the difficulty of obtaining accurate input data. For example, calculation of the effective heat-transfer volume of the Phase II reservoir on the basis of purely geometric considerations yields a value of about 5 million m^3. That figure increases to 20 million m^3 if the volume is calculated on the basis of hydraulic considerations; 22 million m^3 when tracer data is the basis; and 28 million m^3 when a very conservative measurement of the geometric spread of seismic events observed during

reservoir creation is the basis. The ability to match modeled results to experimentally measured results (validating the model), then, increases the confidence level regarding the model's input data—which in turn increases the credibility of modeled results as a predictor of the future behavior of an HDR reservoir.

Early Models

A predictive model known as the Finite Element Heat and Mass (FEHM) model, developed at Los Alamos to measure fluid flow in a porous medium, was used to estimate temperature decline in the Phase II reservoir (as a starting point for modeling the behavior of the HDR system during the LTFT). Using an assumed reservoir volume of 16 million m^3, the FEHM model predicted a temperature decline of about 10°C over a span of 5 years, at a flow rate of 125 gpm (8 L/s). However, because the Phase II HDR reservoir was created in highly impervious rock in which flow is limited to a relatively small number of interconnected open joints, a model designed for flow in a porous medium could not be expected to yield very credible results.

Two models more relevant to HDR systems are the Los Alamos HDR Heat Model and the Stanford Geothermal Program (SGP) Model. The models are similar in that both are based on one-dimensional, heat-sweep flow of fluid through rock blocks, and both use total rock volume and joint spacing as the primary input variables. But they differ with respect to calculation methods and in that the Los Alamos model uses tracer-based data as part of its input. Before the start of the LTFT, Robinson and Kruger (1992) carried out experimental runs of both models in an attempt to predict the thermal performance of the Phase II HDR reservoir under the projected conditions of the LTFT. Their results indicated that at a flow rate of approximately 125 gpm, a decline in the temperature of the reservoir from 240°C to 210°C would take—depending on the model and on the initial assumptions—from just over 6 to nearly 11 years. In other words, both models predicted no discernible (judged to be at least 10°C) thermal drawdown over the anticipated two-year span of the LTFT.

The results of these early modeling efforts were encouraging, because all three models predicted that an LTFT lasting two years would not tax the reservoir sufficiently to produce an observable decline in the temperature of the produced fluid, signaling the probability of long useful lifetimes for HDR systems. But the results also indicated, disappointingly, that the duration of the LTFT would be too short to provide the insights into the nature of HDR reservoirs that can be obtained with certainty only through observance of the onset of thermal decline.

In early 1995, following the first two steady-state production segments of the LTFT, the SGP model was once again applied to the Fenton Hill system (Kruger, 1995). On the basis of the model's results, Kruger calculated that by the end of the second steady-state segment, only about 6% of the available heat had been removed from the Phase II HDR reservoir.

The GEOCRACK Model

By the early 1990s, a model designed specifically for the Phase II HDR reservoir was being developed at Kansas State University under the sponsorship of Los Alamos (Swenson et al., 1991). Known as GEOCRACK, this two-dimensional, fully coupled model simulates fluid flow in a pressurized, jointed reservoir. Joints and rock blocks are modeled through an iterative, finite-element method: solutions are first reached for the fluid flow and joint openings on the basis of initial input parameters, then iterations are performed whereby each fluid-flow solution becomes the input for the subsequent joint-opening calculation, and vice versa. The process is repeated until the two solutions converge.

In this way, the fluid flow in the joints is coupled to the rock deformation—the flow is dependent on the joint openings and, in turn, the joint openings are dependent on the applied fluid pressure. Nonlinear joint stiffness, elastic and thermal deformation of the rock blocks, and temperature-dependent viscosity of the fluid are included, as are two options for reservoir boundary conditions: displacements and surface tractions.

As the LTFT progressed, GEOCRACK was tested against data obtained from various experiments and was continually refined by, for example, adding flexibility to the dimensions of the rock blocks; introducing random blockages in the flow paths; taking into account the fluid lost via diffusion beyond the boundaries of the pressure-stimulated reservoir; and incorporating heat-transfer equations not originally included. By the end of the LTFT, GEOCRACK could accurately reflect observed LTFT results, including transient behavior and tracer responses. It could also provide information about the anticipated thermal performance of the reservoir over the longer term under a variety of operational conditions.

Early Results. The practical contributions of GEOCRACK to the LTFT began even before the start of the testing program. In 1991, GEOCRACK was used to simulate a proposed cyclic circulation study that entailed holding the backpressure of the production well at 2200 psi (15.2 MPa) for 16 hours, then reducing it to zero for 8 hours (HDR, 1993). The aim was to significantly increase production during each 8-hour part of the cycle by essentially running the production well "full open" (the backpressure valve fully open). The simulation showed that whereas the joints were maintained at their normal openings during the high-backpressure stage of each cycle, those nearest the production wellbore closed within a few minutes of initiation of the zero-backpressure stage (in response to the greatly increased joint-closure stress near and at the borehole wall). Closure of these joints effectively cut off the production wellbore from the large volume of pressurized fluid in the body of the reservoir, drastically reducing the rate of fluid production—when the goal was to increase it. This result, which is intuitively obvious after the fact, made it clear that in any cyclic production scheme, the backpressure on the production well must be high enough

to prevent the joint closure predicted by GEOCRACK. Researchers were quickly able to ascertain, from known stress conditions in the reservoir, that at Fenton Hill the lower boundary for such a backpressure would be between 1450 and 2200 psi (10 and 15.2 MPa). This understanding was to provide invaluable guidance on several occasions when cyclic operations were employed during the LTFT.

Further, GEOCRACK modeling provided additional insight into the importance of the major stress regimes in the Phase II HDR reservoir. During reservoir pressure testing, several slow venting episodes had enabled three major joint-closure stresses (for three different joint orientations) to be inferred, but these closure stresses were not well quantified. Then, during reservoir reinflation testing at low flow rates, joint openings at 2200, 3300, and 4000 psi (15.2, 22.8, and 27.6 MPa) were identified. It was not clear from the hydraulic data, however, which pair of these three joint-opening pressures controlled the interconnected joint flow during circulation. In early GEOCRACK simulations, use of the two lower opening pressures as pressure-boundary parameters did not yield a match between the modeled flow rate and the experimentally observed flow rate. But when the two higher opening pressures were used to define the pressure-boundary conditions, the model gave results that closely agreed with experimental flow values (HDR, 1993). Thus, the model contributed to the understanding that the relationship between the highest and the intermediate joint-opening pressures exerts a greater influence on overall flow than does the relationship between the intermediate and lowest joint-opening pressures.

Results Compared with LTFT Field Data. As noted above, GEOCRACK was continually modified to assure that the results obtained from it agreed with reality in those cases in which the phenomena could be verified by testing. This process served to increase confidence in the long-term but untested (and untestable, within the available funding limits and time frame) predictions of the model. Figure 9-28 shows just how well a GEOCRACK simulation matches actual LTFT field data on changes in surface pressures during shut-in. Figure 9-29 shows the match between several LTFT tracer return profiles and the GEOCRACK-predicted tracer return pattern. (In both figures, the error bars indicate the range of individual data points obtained through analysis of the model's results.) These two examples confirm the ability of GEOCRACK to faithfully simulate pressure and flow behavior during the LTFT.

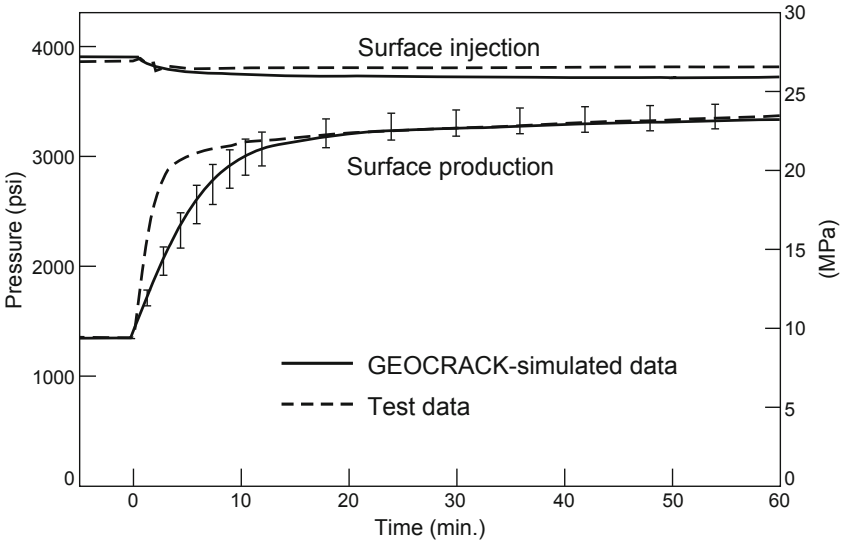

Fig. 9-28. Pressure responses upon shut-in of the injection and production wells: GEOCRACK-simulated data vs test data.
Source: Swenson et al., 1995

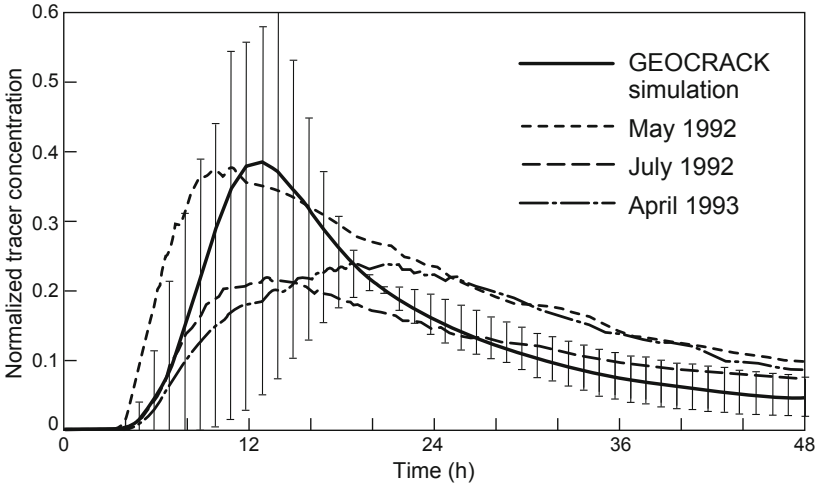

Fig. 9-29. GEOCRACK-simulated tracer data vs test data from the LTFT.
Source: Swenson et al., 1995

Predictions Concerning the Effects of Wellbore Spacing on Flow Impedance. Because GEOCRACK proved able to accurately simulate the impedance distribution within the reservoir (as indicated by the pressure changes shown in Fig. 9-28), the model was used to ascertain whether and how the spacing between the wellbores might affect flow impedance. Reservoir pressure profiles were modeled for two hypothetical HDR systems, one having a wellbore spacing of 200 m and the other a spacing of 400 m. (In the Fenton Hill Phase II system, the average separation between the wellbores at depth was roughly 100 m). One set of results from this modeling effort shows that if an HDR system having a wellbore separation of 400 m is operated at a flow rate 16% lower than the flow rate of a system having a separation of 200 m (84 gpm vs 100 gpm), the pressure variation between the injection and production wells of the two systems would be almost identical (Fig. 9-30).

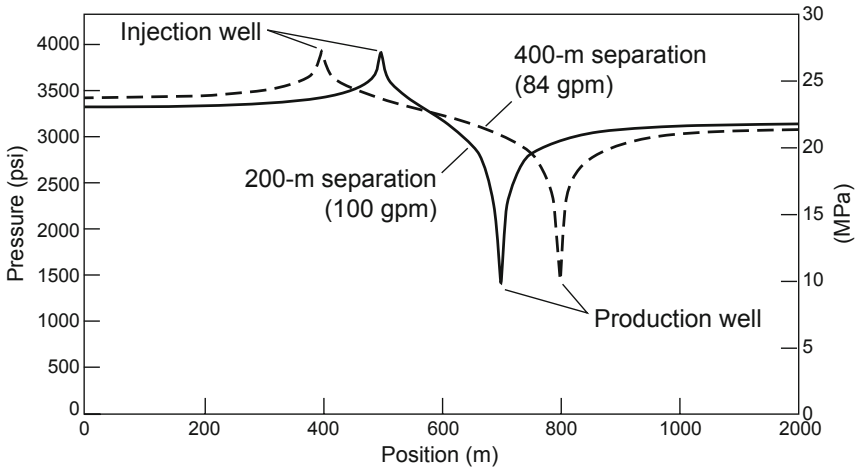

Fig. 9-30. GEOCRACK-modeled reservoir pressure profiles for two hypothetical HDR systems under the same conditions of injection pressure and production backpressure but with different wellbore spacings.
Source: Brown, 1994b

In other words, it should be possible to greatly increase the size of an HDR system (just a doubling of wellbore spacing would probably increase the volume of the accessible reservoir by a factor of four, and probably more) without increasing flow impedance significantly—which means that reasonable amounts of fluid could be circulated through HDR reservoirs much larger than the Phase II system at pressures attainable with currently available commercial equipment.

Predictions Concerning Future Thermal and Flow Behavior. During the two-year hiatus in LTFT flow testing (May 1993–May 1995), GEOCRACK was used to optimize the design of the cyclic-production test that demonstrated the load-following potential of the HDR system. Given the choice between a daily cycle consisting of (1) 16 hours at base level followed by 8 hours of enhanced production, and (2) 20 hours at base level followed by 4 hours of enhanced production, GEOCRACK simulations indicated significant productivity advantages with the 20/4 schedule. As described earlier, in the section on the third steady-state production segment, the Load-Following Experiment based on this operational plan was carried out in July 1995 with highly successful results (Brown, 1995b).

Because GEOCRACK permits the cooling front that develops from the inlet to the reservoir at the injection well to be mapped as circulation proceeds, the model can be used to design an energy production schedule that maximizes recovery of the available heat from an HDR reservoir. Like the other models employed to evaluate the LTFT, GEOCRACK predicted that no discernible temperature decline would be detected over the course of the LTFT; in fact, as shown in Fig. 9-31, GEOCRACK simulations indicated that even after 40 years of circulation (at the relatively low flow rate employed during the first two steady-state production segments of the LTFT), the temperature at the production well would not have declined significantly.

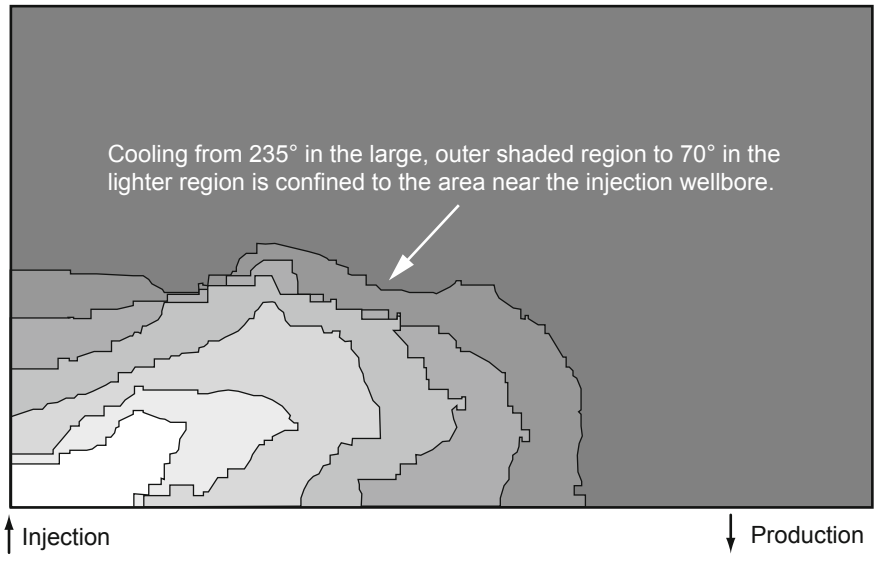

Fig. 9-31. GEOCRACK simulation of cooling contours within the Phase II HDR reservoir after 40 years of circulation at flow rates employed during the first two steady-state production segments of the LTFT.
Source: Duchane, 1995b

The injection pressure used during the LTFT was the maximum that could be applied without inducing reservoir growth, which necessarily limited the circulation flow rate. As shown in Fig. 9-32, a GEOCRACK simulation of reservoir performance several years into the future predicts that the flow rate through an HDR reservoir similar to that at Fenton Hill will begin to increase after about one year of operation even under constant injection conditions (Duchane, 1995b).

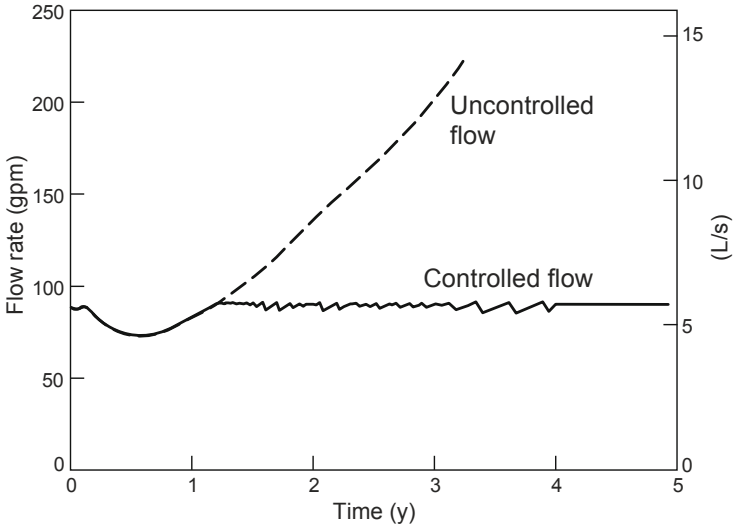

Fig. 9-32. GEOCRACK simulation of flow through the Phase II HDR reservoir, showing an increase in the rate of flow beginning after about one year if no flow control is imposed.
Source: Duchane, 1995b

If this projection is accurate, the flow rate would need to be controlled to prevent the system from reaching a short-circuit-like state wherein the production temperature would cool to below useful temperatures well before all the available thermal resource had been extracted. Unfortunately, the LTFT was not continued long enough to observe whether this predicted effect would indeed occur. Had the LTFT been sufficiently long, and had such a flow increase been observed, it may have been possible to induce a temperature decline at Fenton Hill after only a few years of circulation. Such a result would have gone a long way toward verifying or refuting the thermal-energy-extraction predictions derived by all of the models used to assess the Fenton Hill HDR reservoir. This example provides an excellent illustration of how important it is to couple a thorough understanding of reservoir characteristics with intelligent flow management if we are to make efficient use of HDR resources.

The LTFT was the culmination of the Los Alamos HDR Project. Although the technical goal of continuous production of energy for a full year was not achieved, the maintenance of circulation for a total of more than 11 months did demonstrate that energy could routinely be extracted from an HDR reservoir over an extended time period. Moreover, the intermittent shutdowns provided an unanticipated opportunity to evaluate the response of the HDR system to a variety of adverse circumstances that might reasonably be encountered during operation of a commercial HDR energy plant (notably, it was clearly demonstrated that the system could be rapidly brought back on line after long periods of nonproduction, regardless of whether reservoir pressure had been maintained in the interim).

The LTFT also showed that cyclic load-following production schedules could be employed to enhance productivity. With early tests providing the groundwork, straightforward cyclic production strategies implemented during the final stages of the LTFT (RVFT Stage 4) provided unambiguous evidence of the advantages of this technique, from both operational and marketing standpoints. It seems likely that when commercial HDR plants are eventually built, cyclic production schedules modeled after those proven effective by the LTFT will be employed to maximize overall efficiency.

Finally, the LTFT produced a wealth of experimental data that can be used to improve models—not only those designed to simulate HDR systems, but also those designed for hydrothermal (i.e., hot wet rock) faulted/jointed systems. As a result of the LTFT, a great deal more is understood about HDR systems now than was known in 1992. The LTFT brought significantly closer to reality the potential for HDR technology to become a major source of commercial energy for the 21st century world.

PART IV

Future Outlook for Hot Dry Rock

Chapter 10

The Future of Hot Dry Rock Geothermal Energy

As detailed in preceding chapters, the technical feasibility of HDR geothermal energy was clearly demonstrated at Fenton Hill, with the testing of two separate confined reservoirs. The major task now in view is moving this revolutionary new technology to its appropriate place in the world's energy supply mix. Obviously, technical feasibility is not enough: HDR must also be capable of supplying useful amounts of energy economically. For that requirement to be met, several issues—which have yet to be adequately addressed—will need to be resolved.

- Productivity: Can the thermal output of an HDR reservoir be increased through engineering strategies?
- Sustainability: What is the expected lifetime of a typical HDR system, and what are the best methods for extending it?
- Universality: Can HDR systems be developed virtually anywhere?

Once these remaining issues have been favorably resolved, it is a comparatively short step to the widespread establishment of commercial electric power plants drawing their thermal energy from HDR. And with their establishment—and realization of the unique advantages of fully engineered HDR systems—will certainly come incentives to further develop HDR technology. Many advanced scientific and engineering concepts that today have been only theoretically proposed will be explored through field testing and evaluation, and eventually implemented to make HDR even more economical. The following sections discuss possible approaches to resolving the remaining issues and describe some of these advanced concepts.

Enhancing Productivity

The Long-Term Flow Test (LTFT) at Fenton Hill produced thermal power on the order of 4–5 MW. The fluid was brought to the surface at about 180°C, and because conversion to electricity would be about 15% efficient at this temperature, the electric power production potential was only about 0.5 MW. This is much lower than the levels needed for HDR to be a practical source of power and justify the considerable investment in drilling and reservoir development.

During the initial flow testing (ICFT) of the Phase II reservoir in 1986, it was recognized that the single production well at Fenton Hill was accessing only one side of the elongate reservoir, which had developed symmetrically around the injection well from which it was created. During the second half of this 30-day test, the injection pressure was increased to about 4600 psi, which boosted steady-state thermal power production to

D.W. Brown et al., *Mining the Earth's Heat: Hot Dry Rock Geothermal Energy*,
DOI 10.1007/978-3-540-68910-2_10, © Springer-Verlag Berlin Heidelberg 2012

10 MW. The higher injection pressure also expanded the reservoir, which substantially increased net water consumption. But as shown in Fig 10-1, seismic data indicated that rather than being "lost," most of the water was going into expanding those regions of the reservoir where no production wellbore was present to serve as a pressure-relief valve. (Important note: later pressure testing confirmed that this enlarged Phase II reservoir remained fully confined.)

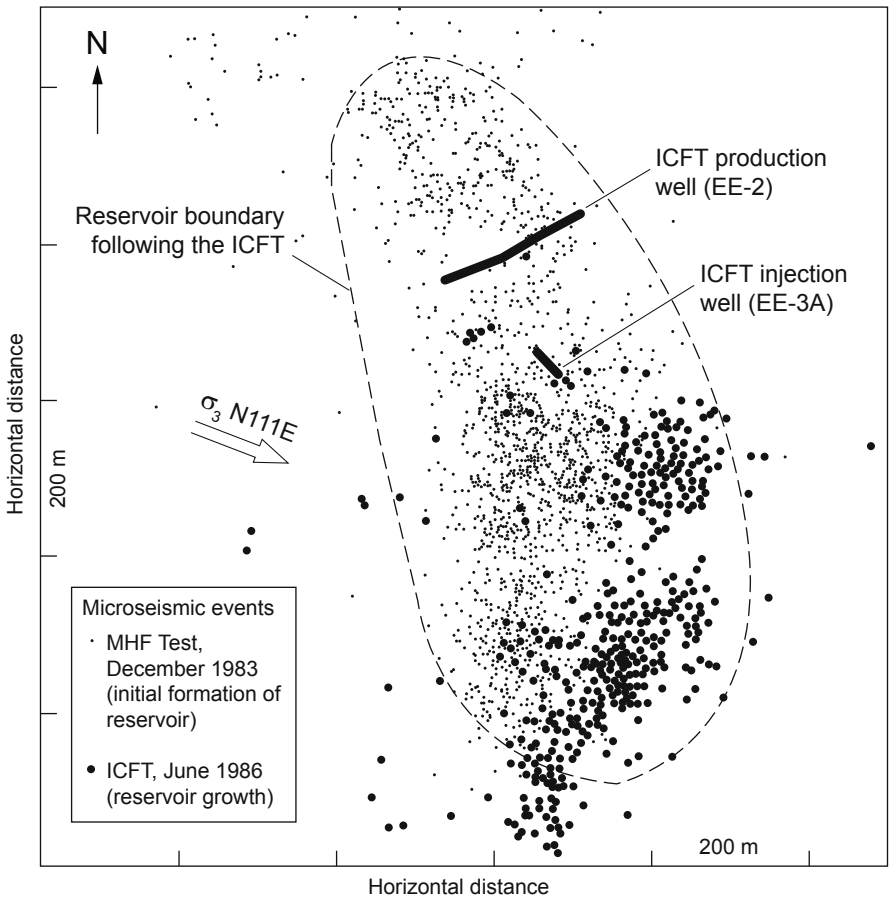

Fig. 10-1. Distributions of seismic events during the MHF Test and during the second half of the ICFT. The direction of the least principal earth stress (σ_3) is also shown.
Source: Brown, 1995b

The ICFT gave rise to two important, related observations:

1. A second production well on the stagnant end of the elongated reservoir could produce a substantial amount of additional fluid, increasing productivity.
2. A production wellbore on that side of the reservoir would provide pressure relief, enabling injection at considerably *higher* pressures without causing reservoir growth. The higher-pressure injection would in turn lead to higher flow rates in both production wellbores and a further rise in productivity. It is estimated that the productivity of the Phase II Fenton Hill HDR reservoir could have been increased to at least 20 MW_{th}—without a net water loss of more than 7–10 gpm from the confined reservoir region—simply by drilling a second production wellbore in an appropriate location. In brief, multiple production wellbores are the key to highly productive HDR systems. Properly implemented, this strategy is virtually certain to enhance productivity.

There are many other potential techniques for productivity enhancement that could be investigated through renewed flow testing of the deeper HDR reservoir at Fenton Hill. Examples are pressure cycling of the production wells and the drilling of deep laterals from each production well. Short (1000- to 2000-ft) laterals could be drilled immediately following the drilling of the production wells, and before they are completed. The targets of these laterals would be regions near the ends of the stimulated reservoir, where more production could be "captured." Since almost all of an HDR reservoir's flow impedance is concentrated near the production wellbores, increasing the number of production wells that pass through the reservoir region could significantly reduce the net flow impedance and thereby significantly increase productivity.

Extending the Lifetime of the System

The deeper Fenton Hill reservoir showed no signs of thermal drawdown over the 11-month period of the LTFT. In fact, as discussed earlier, tracer testing showed that the circulating water was continually accessing new areas of hot rock near the boundaries of the reservoir region. Modeling indicated that the 4-MW_{th} system at Fenton Hill could have been operated under the conditions of the LTFT for more than 30 years without any cooling at the production wellbore. (These conditions, however, as stated earlier, were not sufficient to achieve the levels of productivity required for a commercial HDR venture.)

All the evidence to date indicates that sustainability should not be a problem for HDR systems; but sustainable energy production can be convincingly demonstrated only by operating an HDR system for an extended period of time at a commercially practical rate of power production. Further, as shown by the work at Fenton Hill, the production

wells can intersect the dilated reservoir region at locations quite far from the injection well, because the resistance to flow is not primarily a function of the distance traversed by the fluid; rather, it is much more a function of the near-wellbore outlet impedance (the pressure of the circulating fluid declines sharply as the fluid nears the point of entry into the production wellbores). Given the several production variables involved, the best way to demonstrate sustainability is with long-term, continuous power production from an appropriately productive HDR reservoir.

Establishing the Universality of Hot Dry Rock

Obviously, the applicability of HDR technology to a wide variety of locations can be demonstrated only through its widespread implementation. As the value of the work at Fenton Hill was recognized, experiments were initiated in several other countries. However, none of these projects led to the creation of Fenton Hill-type HDR systems.

At Rosemanowes, in the British Isles, a reservoir was created with pressure stimulation, but in rock that was not hot enough to produce useful amounts of energy. In Japan, the two projects attempting to create HDR reservoirs were carried out in calderas, where hot rock was reached at relatively shallow depths. But in both cases the reservoirs were open rather than confined (i.e., not true HDR reservoirs) and were plagued with high water losses during periods of circulation. If the drilling had gone deeper—or better yet had been done elsewhere than in a caldera—hot competent rock would probably have been reached. At Soultz-sous-Forêts in eastern France, the European HDR project drilled into a hydrothermal region with naturally open faults and joints in the granitic basement. Their system was thus based on production of a combination of natural and injected fluid—now known as hot wet rock, or HWR. In Australia, an "HDR" reservoir was created in rock very similar to that of the Fenton Hill system (similar depth and rock temperatures). However, like the Europeans, the Australians encountered a granitic rock mass with natural hydrothermal flow in open joints. During their operations in the Cooper Basin in South Australia, they pressure-stimulated a region in which an overpressured brine containing a significant amount of dissolved gas fills these open joints.

Thus, even with these several projects having grown out of the Fenton Hill work, the universality of HDR has yet to be demonstrated.

For much of the Basin and Range Province of the western U. S., as well as broad expanses of the Great Plains east of the Rocky Mountains, the geological setting typically consists of several thousand feet of sedimentary rock overlying the crystalline basement. Except for those unusual areas where recent faulting has disturbed the basement rock, the geology is similar to that of Fenton Hill: free of open joints or faults. The basement rocks may be a melange of many types. As clearly shown at Fenton Hill, it

is not the type of basement rocks (predominantly igneous or metamorphic) that is important for HDR reservoir development, but the joint structures within them. For that reason, it should be possible to replicate the HDR reservoirs at Fenton Hill in literally tens of thousands of locations. The biggest unknown is how deep it might be necessary to drill into the basement to reach rock at temperatures suitable for HDR development (greater than about 150°C).

In summary, it appears that the two keys to widespread application of HDR technology are (1) drilling deep enough to reach suitable temperatures and (2) drilling into basement rock that is free of open joints or faults. Because the confining pressure on the rock mass targeted for reservoir development increases with depth, in general greater depth implies better reservoir confinement. And the absence of open joints or faults means low inherent rock porosity and permeability, which is critical to ensure that a pressure-stimulated HDR reservoir, at whatever depth it is created, will be confined.

Addressing the Remaining Issues

The key to advancing HDR technology is developing and operating larger and more productive reservoirs. A first step might be to establish a demonstration plant with two production wellbores. If this is done at Fenton Hill, the Phase II reservoir could be re-accessed and reactivated—work that could be undertaken with a high degree of confidence (because of the existing knowledge base) and at significantly lower cost than if HDR work has to be started at an entirely new location. Such an effort would be the most rapid and economical means of obtaining hard data regarding the issues of productivity and sustainability; in turn, these data would reinforce the case for moving forward at other locations. The issue of the universality of HDR will be resolved only as new systems are established in many other locations.

The problems associated with further HDR work at Fenton Hill are more administrative than technical. Approval for access to the site must be obtained, the required water rights secured, and environmental concerns addressed in detail. Because of the pristine nature of the area, any transmission of power from Fenton Hill would be limited to the capacity of the power lines already in place, and electricity would be generated only in that amount, plus the amount required to run the surface plant and injection pumps. Even under such conditions, with only limited power generation, a representative conversion-efficiency would be established that could serve as a baseline for projecting per-kilowatt-hour power costs for subsequent commercial operations at other sites.

Certainly, successful results from renewed flow testing of the deeper HDR reservoir at Fenton Hill would provide the strongest possible incentive for private investment in subsequent HDR facilities. But if it should prove impossible to reactivate Fenton Hill, a new site would have to be

found. It would need to meet several criteria with respect to surface as well as underground characteristics: a good thermal gradient and competent rock at depth (in which there is no evidence of recent faulting) will be important, but so will accessibility, proximity to a transmission line, a market for the power produced, and local political support. With either Fenton Hill or a suitable alternative site, it should be possible to build the first practical HDR power plant. Successful operation of this plant, proving that HDR is both a productive and sustainable technology, will establish its role in the energy market of the 21st century.

Future Innovations in HDR Technology

Once HDR has been recognized as a competitive source of abundant and clean energy, there will be strong incentives—including financial ones—to pursue the many innovative ideas and concepts that today exist only in the realm of speculation. A few of the major potential innovations are outlined below.

Advanced Drilling

By far the most expensive and risky part of developing an HDR system is the extensive amount of hard-rock drilling required to reach basement depths having suitable temperatures. Although deep drilling has been a vital technology in the oil and gas industry for many years, in that domain it is primarily used to drill through the sedimentary formations that harbor oil and gas. These rocks are by nature softer and easier to drill than the typical granitic basement rock. There has been little incentive to develop specific drilling equipment for hard rock, and of the new technologies proposed to date, only a few have undergone preliminary testing. But once the economic viability of HDR systems has been demonstrated, the drive to reduce drilling costs will create strong incentives to develop advanced drilling technologies and will draw investment funding to programs that today are struggling to find financing.

Load-Following and Pumped Storage

As discussed in Chapters 2 and 9, a cyclic experiment at the end of the LTFT clearly demonstrated that energy output from an HDR reservoir could be rapidly ramped up or down by simple changes in the backpressure applied to the production wellbore. Because electric power is more expensive when demand is high, this capability to quickly and easily adjust power production to meet changing demands has very significant economic advantages. In fact, this load-following potential may well be a key factor in making HDR a competitive energy source, and thereby expedite its widespread utilization.

A second strategy, related to load-following, is "pumped storage": the ability to temporarily store additional pressurized fluid by hyper-inflation of the reservoir. Injection is carried out at a steady rate, but the rate of production is lowered during periods of reduced demand, the accumulated difference being stored in the reservoir. A variant of this strategy would be to link HDR with another renewable but intermittent energy resource (such as wind power); by storing energy during off-peak hours, the intermittent resource is used more effectively. For instance, wind power could be harnessed during the evening to drive an auxiliary injection pump, thus effectively using the HDR reservoir as an "earth battery." Pumped storage techniques are already in use today at some hydroelectric plants; generators are kept running during the low-demand nighttime hours to pump water back behind a dam, thus ensuring sufficient hydroelectric power for the higher-demand daylight and early evening hours. An HDR reservoir used in pumped-storage mode could resolve the dilemma of how to exploit wind or solar energy when the wind isn't blowing or the sun isn't shining. Linkage with HDR could turn such "green" but intermittent energy resources into dependable, full-time power suppliers.

Treating Wastewater

To minimize water use in HDR power production, the approach most often considered is binary-cycle technology—continually recirculating the pressurized geofluid in a closed earth loop. With this technology, wastewater (if available in large amounts) could be used as a major portion of the system's circulating fluid—in the process becoming sterilized: Organic wastes typically found in municipal sewage, lumber- or paper-mill effluent, and other industrial wastewaters could potentially be decomposed as the water is superheated and subjected to enormous pressure in the HDR reservoir. If necessary, auxiliary agents such as oxygen could be added to the injected fluid to accelerate such processes.

The production of potable water is also a possibility. An open-loop HDR system could be employed, with wastewater making up part of the geofluid. The simplest such system would be based on flash technology: the portion of the geofluid converted to steam in the flash plant could be condensed and used as a fresh water supply, and additional wastewater could be added to the injected fluid to make up for the water lost through vaporization. (One drawback to this method, which would need to be resolved, is that dissolved minerals in the geofluid might become more concentrated with time, eventually leading to their deposition in the surface piping.)

An HDR reservoir, then, in tandem with producing electric power, could function as a source of clean water and a treatment facility for municipal or industrial wastewater.

New Circulation Fluids and Circulation Conditions

As HDR power plants become more and more widespread and the technology evolves, additional novel ideas will merit evaluation. An example is the use of fluids other than water as the circulating geofluid. One candidate that has already been suggested is supercritical carbon dioxide (Brown, 2000, 2003). Although its much lower mass heat capacity makes it a less effective heat-transfer medium than water, its much lower viscosity under typical HDR reservoir conditions means that the reservoir production flow rate would be substantially higher with supercritical CO_2 than with water—at least partially compensating for the lower mass heat capacity.

No environmental problems would be created by the leakage of small volumes of carbon dioxide into the tight rock mass surrounding the HDR reservoir (the gas being already present at depth in many locations); and in fact, "sequestering" some CO_2 in the rock by this means would remove modest amounts from the atmosphere, thereby contributing to the mitigation of global warming. At the same time, CO_2 could interact with the small amounts of water in the reservoir region, leading to the formation of potentially harmful carbonic acid (or other unanticipated effects). Because of the potential problems, much more research and development would be required before carbon dioxide could be used in an HDR system. No doubt as the HDR industry matures, ideas for other circulation mediums—water solutions or combinations of environmentally acceptable fluids—will emerge.

With advances in drilling technologies, it may become practical to reach rock at temperatures in excess of 374°C (at which temperature pure water becomes supercritical). As with carbon dioxide, the chemistry of supercritical water could pose problems in actual practice. But with an established and vibrant HDR energy industry, exploration of these and other promising ideas would become economically attractive and could make a good resource even better.

New Approaches to the Detection and Location of HDR-Associated Microseismic Events

As discussed in Chapter 6 (see *Deficit in Seismic Moment*), during the MHF Test at least 99% of the injected fluid volume must have been accommodated by *aseismic* tensile fracturing—i.e., joints opening in tension, with no measurable shear displacement. The still-unanswered question is: what were the locations and orientations of the lower-opening-pressure joints making up this very large array? Seismically speaking, without any means to answer that question from the data obtained during the MHF Test, the seismologists "missed the party"! Given that hindsight recognition, the next question is: how can we improve the situation? The obvious answer is to concentrate on the detection and location of microseismic signals

whose only significant component is the P-wave. The best approach would need to be developed by experts in nontraditional seismic analyses. For example, current work in identifying low-frequency earthquakes in non-volcanic tremor (e.g., Maceira et al., 2010) appears to hold promise as a new seismic method for analyzing HDR pressure-stimulation data.

Summary

The highest priority must be given to addressing the issues of HDR productivity, sustainability, and universality. Only when these important questions have been resolved will it be possible to establish HDR power plants that will be both profitable and environmentally superior. Once an industry based on HDR comes into being, investigation of the advanced concepts discussed above—and no doubt many others not yet even imagined—will proceed rapidly. As the 21st century progresses, HDR will play a bigger and bigger role in providing abundant, clean, and domestic energy for virtually all the nations of the world.

Appendix

High-Temperature Downhole Instrumentation

The development of the Phase II reservoir at Fenton Hill—hotter and deeper than the Phase I reservoir—involved drilling and well completion to over 15 000 ft (4600 m) in very hard crystalline rock; reservoir creation and extension by massive pressure stimulation; and extensive reservoir flow testing. These operations imposed requirements on equipment and materials seldom if ever called for in the oil and gas industry, or in conventional geothermal operations. The temperatures reached in the Phase II boreholes were significantly higher than those of Phase I (up to 320°C), as were the pressures needed to open and extend joints in the deep basement rock (on the order of 7000 psi [48 MPa]). In addition, directional drilling was extensively employed at Fenton Hill, where it was carried out for the first time in deep crystalline rocks. Finally, the downhole testing was of a unique, experimental nature—unlike anything attempted by the oil industry, the hydrothermal geothermal industry, or any other entities doing research on the Earth's crust.

As discussed briefly in Chapter 5, very few commercially available instruments could withstand the high temperatures and pressures of the downhole environment at Fenton Hill, even for brief periods. In many cases, either the instruments or the cablehead failed before the instruments even got near the depths at which the measurements were to be made. Although a few logging instruments developed for use in oil and gas wells (such as cement-bond logs and multi-arm casing-inspection calipers) proved to be either directly usable or modifiable for Phase II applications, it was clear that a unique suite of diagnostic instruments—capable of sustained residence in the severe downhole environment—was needed. Most of this instrumentation had to be specially designed, fabricated, and tested at Los Alamos. Developmental work in this critical area remained an integral part of the Fenton Hill HDR Project through August 1987. (Unfortunately, after that time the Laboratory no longer received DOE funding for this effort.)

It should be noted that several of the diagnostic logging tools developed over the years for the HDR Project were used as originally intended only during Phase I, for interrogating the reservoir region. By the early 1980s, when Phase II reservoir development was under way, what was understood about the pressure-stimulated region had evolved considerably. Whereas the Phase I reservoir was essentially a restricted (tabular) region comprising a few near-vertical, interconnected joints, the Phase II reservoir turned out to be a much larger, volumetric region comprising multiple interconnected joints—the flow-manifolding ones at a significant inclination. It became clear that tools such as the downhole injector/gamma-ray detector and the crosswell acoustic detector, designed when the reservoir was assumed to consist of a simple assemblage of direct flow paths, were not really appropriate for interrogating the much more complex Phase II reservoir.

D.W. Brown et al., *Mining the Earth's Heat: Hot Dry Rock Geothermal Energy*,
DOI 10.1007/978-3-540-68910-2, © Springer-Verlag Berlin Heidelberg 2012

Some of the design and fabrication of these specialized downhole instruments was done independently at the Laboratory and some in cooperation with, or by subcontract to, industrial manufacturers and other laboratories. The applications for these instruments fall into three major categories:

- Seismic interrogation of the reservoir region, to monitor its growth and geometry and to map major interior joint systems
- Characterization of the borehole and the reservoir (temperature, intersections of joints with the borehole, points of fluid entry or exit) and borehole diagnostics during drilling and completion
- Characterization of the physical properties of the reservoir rock and the geochemistry of the reservoir fluid

Much of the information in this Appendix is drawn from Dennis et al., 1985; HDR, 1985; Dennis (comp.), 1986; and Dennis, 1990.

Seismic Interrogation of the Reservoir Region

Accurate characterization of an HDR reservoir depends primarily on reliable measurements of the seismicity induced during pressure stimulation. If the precise locations of the microseismic signals are known, one can determine the envelope of the seismically active region (i.e., the reservoir region), as well as its three-dimensional orientation, as it develops over time. In addition, through analysis of the waveforms of the signals arriving at multiple stations, one can determine the location, orientation, and size of some of the joints having higher opening pressures (the opening of which is reflected by a significant S-wave component in the microseismic signal). For the Phase II reservoir, such measurements required geophones capable of remaining in the high-temperature environment for extended periods (for example, the MHF Test lasted almost three days, and during the ICFT seismicity persisted for *over two weeks*).

The Los Alamos-designed downhole **triaxial geophone detector** (Fig. A-1) detects microseismic (i.e., acoustic) signals generated by the movement of joints during the pressure stimulation that creates the reservoir region.

Signals generated by a seismic source generally comprise both compressional (P) waves, from normal joint dilation, and shear (S) waves, from the small displacements that typically occur on the higher-opening-pressure, inclined joints. The P-waves propagate through the media parallel to the direction of particle displacement (generally orthogonal to the joint or joints being dilated), whereas the S-waves propagate perpendicular to that direction (generally in the direction of joint slip, *if there is any*). Because P-waves travel faster through solid media than do S-waves, by knowing the medium and measuring the lag time between P- and S-wave arrivals, one can determine the distance to the source (polarization direction of P-wave arrival gives direction; polarization direction and S-minus-P lag time give direction and distance relative to the detector).

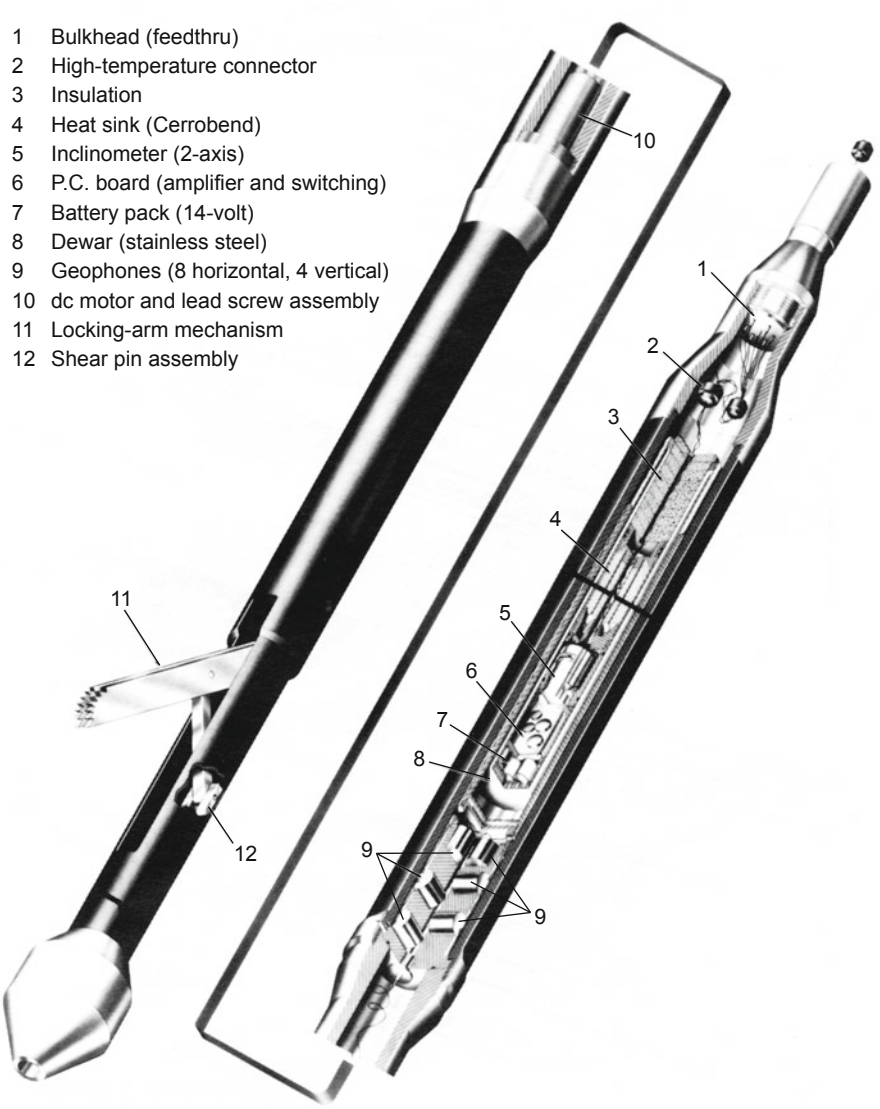

Fig. A-1. The standard high-temperature (275°C) triaxial geophone detector developed at Los Alamos.
Source: Dennis, 1990

The standard triaxial geophone detector is 68 in. long, has an outer diameter of 5 1/2 in., weighs 160 lb, and is rated for temperatures of up to 275°C and pressures to 15 000 psi. Each axis contains four 30-Hz geophones connected in series. The electronics are housed in a thermal-protection system

that combines a Dewar (controlled-environment enclosure) with a heat sink containing Cerrobend (an alloy having a low melting point); this protective system greatly increases downhole operating time and also allows use of low-temperature electronics. Acoustic coupling is improved by a one-arm locking mechanism, designed to press the instrument against the borehole wall. (The effectiveness of this coupling can vary, however, depending on the position the tool eventually takes after its natural rotation at the end of the cable.) A downhole signal-multiplexing unit—controlled through the surface data acquisition and control system—allows monitoring of other data, such as internal Dewar temperature, geophone orientation (through measurement of the slant angle of the borehole), and power supply voltage.

A smaller version of the standard triaxial geophone, the **slimline detector** (Fig. A-2), is designed for use inside drill pipe or tubing. It is 152 in. long, has a 3 1/4-in. outer diameter, weighs 52 lb, and is laboratory-tested to 275°C at pressures up to 15 000 psi. It uses two 30-Hz geophones connected in series and incorporates a high-temperature amplifier circuit, enabling it to remain in the downhole environment for many hours or even days.

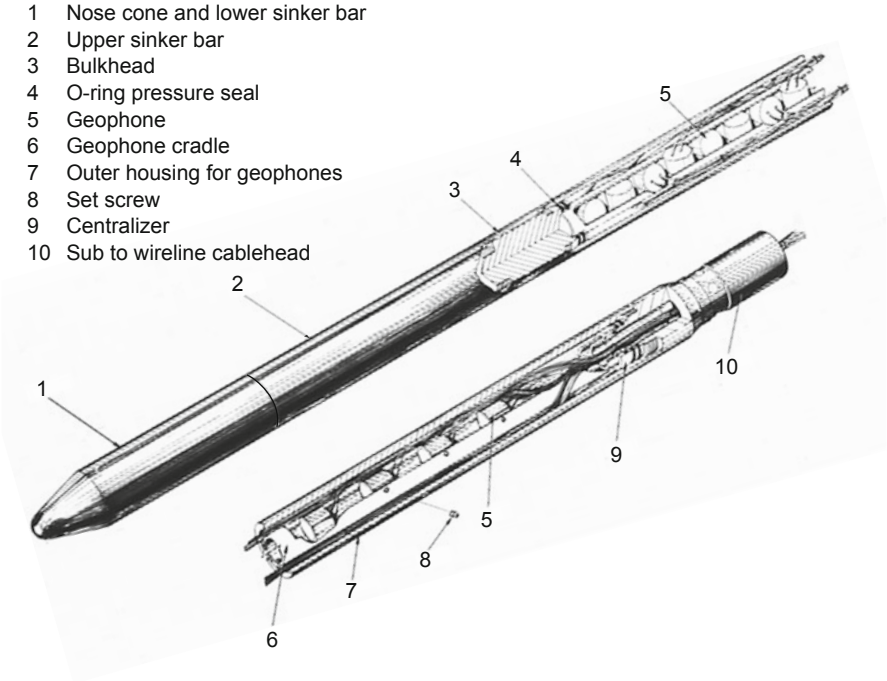

Fig. A-2. The slimline high-temperature (275°C) triaxial geophone detector developed at Los Alamos.
Source: HDR, 1985

A third type of geophone detector, the **Precambrian vertical detector**, is a much smaller unit rated for lower temperatures. Measuring 22 in. long × 2 1/2 in. in diameter and weighing only 20 lb, it contains four 4.5-Hz vertically oriented geophones connected in series. Several of these devices were positioned at depths of 2000–2500 ft, at or near the granitic surface, to form the "Precambrian Network."

All of these geophone detectors are calibrated through the use of **acoustic source detonators**. Detonators positioned at one or more known locations in one borehole provide explosive source signals, simulating those of seismic events occurring within the reservoir region. These signals are detected by geophones positioned at a "seismic station" at a selected depth in another borehole and used to calibrate that seismic station. The multiple-fire detonator can fire up to twelve sequential shots; its firing-module rack contains three detonator levels, each of which accommodates four exploding-foil detonators designed for high temperatures and high fluid pressures. A **slimline acoustic source detonator** was also developed, to run in drill pipe or tubing. It fires two detonators, and with an added front-end carrier to allow a larger explosive charge, can be used for a high-temperature string shot (i.e., a tool-joint backoff shot). Both the multiple-fire and the slimline detonators incorporate safety features to prevent accidental detonation during transit and handling at the surface.

Characterization of the Borehole and the Reservoir

Temperature Surveys

Temperature surveys at various depths in the borehole provide important data for characterization of the borehole and the reservoir. These data are the basis for determining points of fluid entry or exit from the borehole, thermal gradients, thermal drawdown, and recovery rates. In addition, they are often critical for other areas of investigation, as described below.

Temperature sondes are a major tool for characterization of both the borehole and the reservoir. By revealing anomalies and variations from the background temperature gradient, temperature logging is the most reliable indicator of the locations of joint inlets/outlets (which can be determined to within ±10 ft). For example, it was temperature information that ultimately enabled the composite flow geometry of the Phase I reservoir (shown in Chapter 4, Fig. 4-5) to be determined; and it elucidated many of the characteristics of the Phase II reservoir during extensive flow testing. From a diagnostic standpoint, temperature logging was also critical in "unraveling" some of the more bizarre borehole flow phenomena. For instance, when the borehole was shut in following the MHF Test, it was temperature logging that revealed that fluid was flowing back out of the high-pressure Phase II reservoir and upward through the borehole, then exiting (through breaks in the collapsed 9 5/8-in. production casing) into the much-lower-pressure Phase I reservoir region. Finally, it was through temperature logging that the disasterous frac-around of the EE-3A tag-cement completion was identified.

Another important task accomplished through temperature logs (in combination with caliper logs and analyses of drill cuttings) is identification of suitable areas for packer seating. By revealing points of previous fluid infiltration, temperature logging identifies areas that should be avoided as packer-seating sites.

The temperature sondes developed at Los Alamos employ a thin-walled, stainless steel thermistor probe having high accuracy and resolution. To provide accurate depth-correlation information for correcting cable depth, each sonde also incorporates a high-temperature collar locator (as well as, typically, a gamma-ray detector). The sondes were fabricated in various sizes (ranging in length from about 6 to almost 10 ft and in weight from 84 to 230 lb), all rated for temperatures of 350°C and pressures of 15 000 psi. The **slimline temperature/collar-locator tool** shown in Fig. A-3 is 112 in. long, has a diameter of 2.0 in., weighs 76 lb, and is rated for 350°C at 15 000 psi.

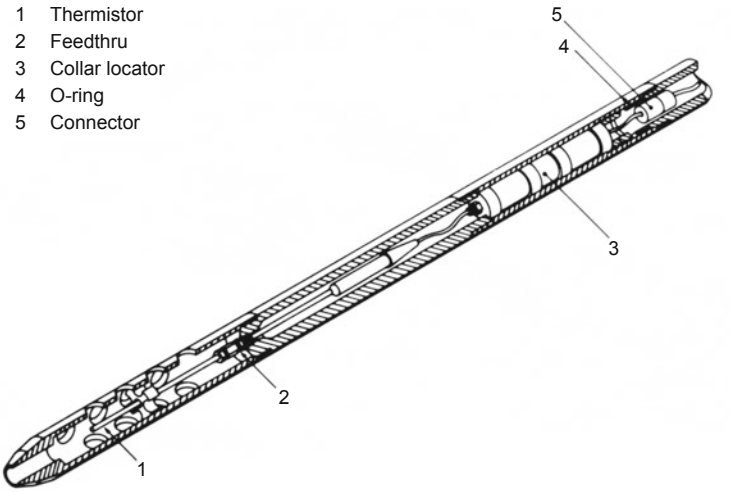

Fig. A-3. Slimline temperature/collar-locator tool.
Source: Dennis et al., 1985

Borehole Diagnostics

Because commercially available single- and dual-arm caliper tools proved inadequate for delineating the profile of an HDR borehole drilled in crystalline rock—easily missing ledges and washed-out regions of joint-filling material or borehole breakouts, any of which could cause a packer to rupture—the Laboratory developed a high-temperature, independently recording **multi-arm caliper tool** capable of measuring radii from 2.5 to 7 in. In several instances, this tool provided information on the geometry (strike and dip) of eroded joints intersecting the borehole. It was also useful for identifying regions of casing that were collapsed but still pressure-tight; or, in combination with temperature logging, for locating holes and tears in casing.

The original design was a three-arm tool that could be modified to have six independent arms; the arms were evenly spaced circumferentially and could be varied in length to measure hole diameters up to 30 in. Activated by a motor, the arms could be extended or retracted on command from the surface. They were retracted while the tool was run in, then extended to measure the area of interest, and finally retracted again for removal. The borehole radius measurements were converted to electronic output via a mechanical linkage, magnetic couplings, and high-temperature rotary potentiometers. To compensate for wear of the caliper pads, which could be significant on longer runs, both pre- and post-log calibrations were done. The caliper tool is rated for temperatures of 300°C and pressures of 15 000 psi (a combined rating that to this day exceeds that of any similar tool available from industrial logging companies). This tool measures 9 1/3 ft long × 3 in. in diameter and weighs 154 lb.

Development work on a very desirable instrument for borehole characterization, the **borehole acoustic televiewer**, began in the mid 1980s as a joint project between the U. S. and Germany.[1] This instrument, which would provide actual images of the borehole wall, was far along in the field-development stage when funding unfortunately was curtailed. The prototype device (Fig. A-4) was 14 ft long and 3 3/8 in. in diameter, weighed 225 lb, and was rated for a downhole temperature of 275°C and a pressure of 12 000 psi.

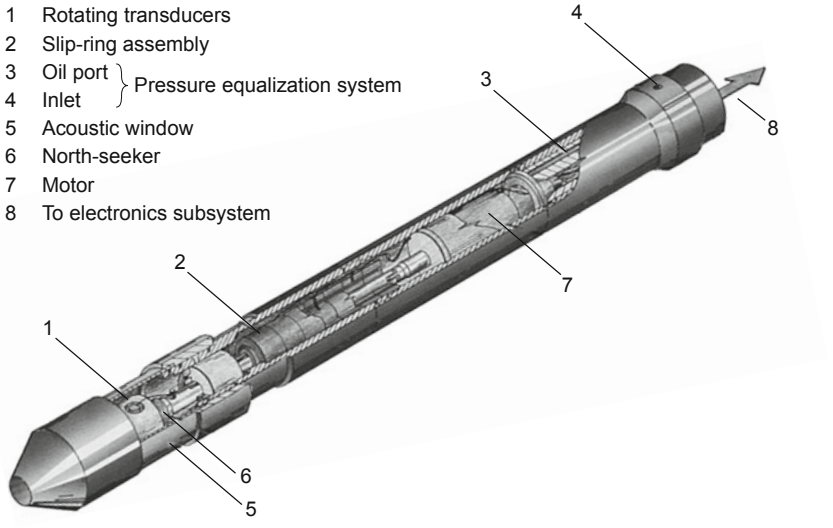

Fig. A-4. The borehole acoustic televiewer tool developed at Los Alamos. Source: HDR Project files

[1]A tool of the same general type, though analog and less sophisticated, was already being used by the USGS Water Resources Division in Denver, CO; but it was rated only for temperatures below 200°C and its availability was limited.

To facilitate field assembly and maintenance, the televiewer's construction was modular, consisting of an acoustic subsystem (to transmit and receive acoustic pulses) and a downhole electronics subsystem (to collect, process, and transmit data). The acoustic subsystem housed two piezoelectric transducers (crystals)—one 1.3 MHz and one 625 kHz—mounted 180° apart on a rotating head. The transducers were rotated in a silicon-oil-filled cavity by an ac synchronous motor at 360 rpm, with either one selectable as the operative transducer from the surface control unit.

The electronics subsystem incorporated a military-version microprocessor that would emit pulses as the tool was moved along the borehole wall, each pulse triggering the selected transducer to fire a shot. After each shot, the transducer would be reconfigured as a receiver for the reflected signal; then the electronics subsystem would measure the signal's amplitude and travel time and transmit the data (via the logging cable) to the surface. The surface control unit, which was constructed around a Siemens microprocessor system, recorded the data digitally on tape and displayed it on a color monitor. The output provided real-time information, at a logging rate of 10 ft/min, of the fine-grained topography of the borehole wall—such as the orientations of the various joints and induced thermal fractures intersecting the borehole, zones of stress-spalling induced by changes in pressure and/or temperature (borehole breakouts), and even the orientation of the gneissic fabric of the rock.

Had its development been allowed to proceed, this tool would have been a significant asset to the HDR Project. Because of its ability to transmit scans of the borehole, *potentially* in both pressurized and depresssurized modes, the borehole acoustic televiewer would have provided invaluable specific information on the orientations of the fluid-accepting joints and changes in their apertures with pressure. To this day, *in situ* information on the deformation mechanisms of rock masses remains the "holy grail" of rock-mechanicians, given that such data can never be obtained in above-ground laboratories, no matter how large.

In addition to interrogating the borehole wall, the televiewer would have provided superior information on other details of interest, such as areas of damaged casing, washouts, and ledges. But after having been successfully deployed in Well EE-2 in 1987, the televiewer was not developed further because the DOE felt that work on geophysical instrumentation was no longer part of the Laboratory's mandate.

Radioactive-Tracer-Based Diagnostics

Two tools developed in the earlier years of the HDR Project that were later discontinued because of environmental concerns are the downhole fluid injector and the downhole injector/gamma-ray detector.

The **downhole fluid injector** was used to inject tracers—mainly radioactive[2] but sometimes chemical (e.g., fluorescein dye)—into the borehole adjacent to a given fluid-accepting joint or set of joints. The intent was to circulate the tracer through the reservoir and then collect it in the effluent from the production well. In reality, however, attempts to flow tracers *across* the reservoir met with little success—both because the amount of tracer that could be injected by a downhole tool was too small, and because the tracers were quickly diffused as they flowed through the network of interconnected flow passages.

The injector measured about 10 ft long and 3 1/4 in. in diameter, weighed 175 lb, and was rated for temperatures up to 275°C and pressures of 15 000 psi. A cylinder at the lower end contained the fluid to be injected, while discharge ports and flapper-type check valves at the upper end prevented loss of fluid during insertion of the tool. When the desired depth was reached, a release mechanism was activated to discharge the fluid through openings at the cylinder's end cap.

The **downhole injector/gamma-ray detector** (Fig. A-5) combined a downhole fluid injector with an integral gamma-ray detector, the latter thermally protected in a Dewar equipped with a Cerrobend heat sink. This tool, which proved somewhat more successful than the downhole fluid injector, was used to inject a radioactive tracer (usually ^{82}Br) into an open joint and subsequently measure its return to the borehole. It could also be used to diagnose casing damage. With the tool positioned in the borehole adjacent to an open joint, the radioactive tracer would be released by activating a motor-propelled rod that smashed a quartz ampoule containing the tracer. The path of the tracer as it left the tool would be tracked by the integral gamma-ray detector.

This tool, however, like the downhole fluid injector, provided little information for reservoir characterization. The data it yielded was useful mainly for identifying intersections of flowing joints with the borehole or the locations of holes in the casing.

[2]The radioactive tracers, such as bromine (^{82}Br), were produced "in-house" at the Laboratory's test reactor.

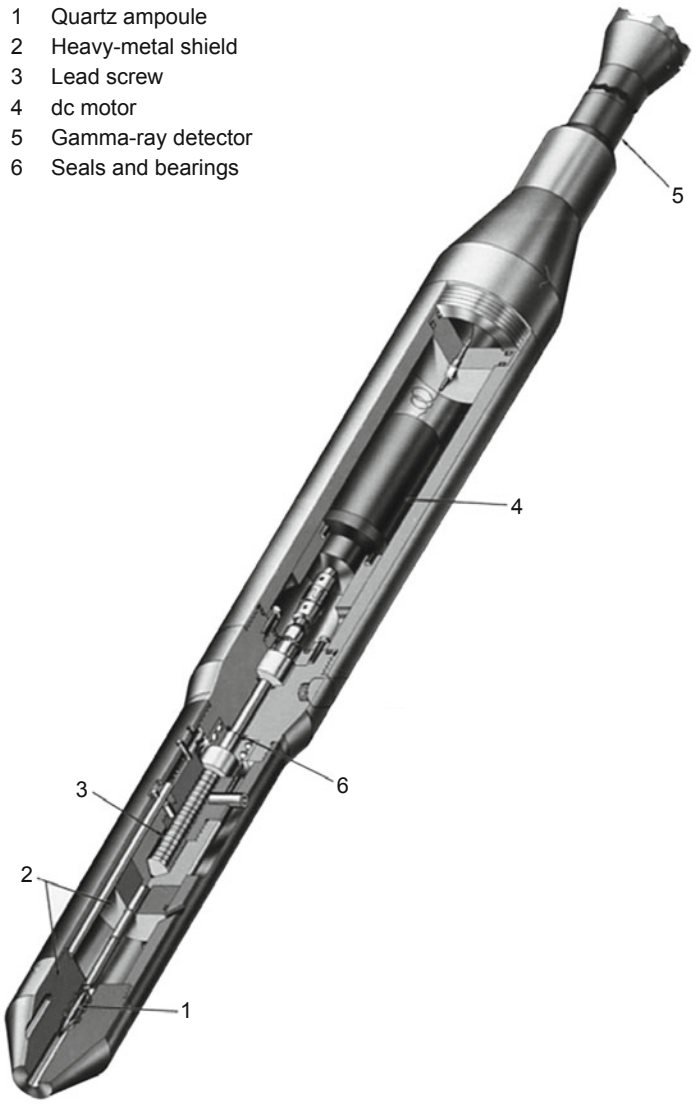

Fig. A-5. The downhole injector/gamma-ray detector developed at Los Alamos. Source: HDR Project files

Characterization of Physical Properties of the Rock Mass and Fluid Geochemistry

Determination of Elastic Properties

A viable method for determining the elastic properties of the rock mass between two boreholes is the **crosswell acoustic transceiver (CAT) system** (developed for interrogating the much smaller and simpler Phase I reservoir). The system comprises (1) a transmitter, deployed in one borehole, that generates an acoustic signal in a constant, repetitive, and controlled manner; (2) a receiver, deployed in a second borehole, that detects the arrival of the acoustic wave; and (3) a surface data acquisition and control system. The CAT is rated for temperatures of 250°C and borehole fluid pressures of 10 000 psi.

The transmitter component measures 17 ft long × 5 1/4 in. in diameter. It discharges a high-temperature capacitor through an SCR firing circuit to two magnetostrictive devices (scrolls) housed in an oil-filled cavity within a pressure-balanced TFE Teflon window. As the transmitter is moved from one position to another in the borehole, at comparable distances above and below the receiver component installed in the second borehole, it generates signals at a rate controlled by a computer in the surface system. The receiver component is 16 ft long and has a diameter of 5 1/4 in. It receives the acoustic signal from the transmitter via a piezoelectric crystal, housed in an oil-filled cavity within a pressure-balanced TFE Teflon window. The crystal converts the acoustic wave into an electrical signal that is transmitted to the surface via the logging cable. The signals from the receiver, which are recorded on magnetic tape, are stacked according to receiver depth (to reduce system noise)—thus producing, for each transmission path, the unique scan that defines that path. The characteristics of the medium through which the signals propagate are deduced from the character of the received signals and from their arrival times.

Geochemisty of the Reservoir Fluid

The acoustic tools described above under *Seismic Interrogation of the Reservoir Region* allow one to determine certain physical properties of the reservoir rock, such as P- and S-wave velocities, which allow the computation of "global" elastic moduli for the rock mass. To add to the data thus obtainable, a **borehole fluid sampler** was developed at Los Alamos, because chemical analysis of the connate fluids contained in the pore space within the joint-filling material as well as in the microcrack fabric of the rock—before their mixture with injected borehole fluids—reveals valuable geochemical information. Even though the development of this tool came too late for its potential benefits to be realized at Fenton Hill, some description is warranted. The sampler could take either two 270-cm^3 samples or a single 780-cm^3 sample. Mounted on the sample container is a valve that

stays closed until the sampler is in the desired downhole location, when it is opened by a miniature dc motor to allow fluid to flow in (but no reverse flow). This tool is about 7 1/2 ft long and 5 in. in diameter, weighs 229 lb, and is rated for a downhole temperature of 300°C and pressure of 15 000 psi.

Connection of Tools to the Logging Cable

All of the instruments described above transmit data to the surface facilities through an armored, multi-conductor logging cable, to which they are joined by an electromechanical coupling device, the **cablehead assembly**. The development of this high-temperature assembly (Fig. A-6) is one of the stellar accomplishments of the HDR Project's instrumentation initiative: it allows geophysical tools to stay on zone for *days* at a time.

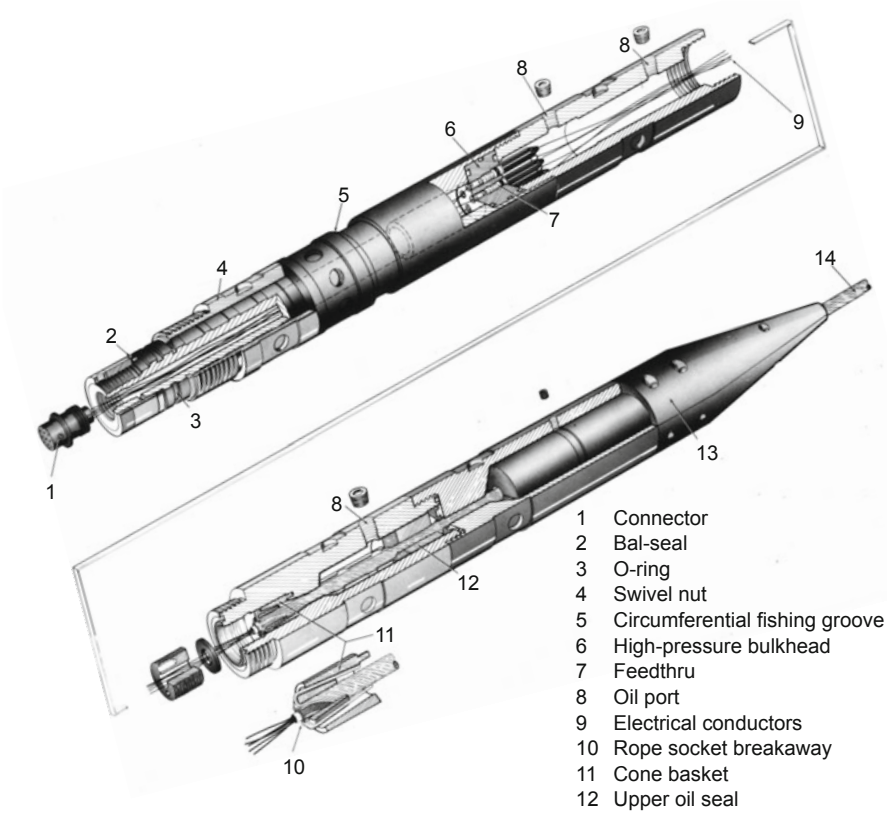

Fig. A-6. The Los Alamos-designed high-temperature, high-pressure cablehead assembly.
Source: HDR Project files

The cablehead assembly serves as (1) a water-tight chamber for the electrical conductors, ensuring their integrity by protecting them from borehole fluids; (2) a pressure-transition chamber between the high-pressure, high-temperature downhole environment and the low-pressure environment in the tool; and (3) a quick-release mechanism, allowing the tool to separate from the cable in the event the tool becomes stuck in the hole. In addition, the fishing bell housing contains a circumferential groove, providing a positive gripping area for overshot fishing tools to latch onto should the tool need to be retrieved from the borehole.

The ability of a downhole tool to reliably make measurements and transmit data depends partially on the quality of its connection to the logging cable. Unfortunately, the industry approach was often to get in and out of the hole as fast as possible, while obtaining a modicum of data. The cablehead assemblies produced with such a purpose in mind were not at all satisfactory for the HDR Project, which typically required a series of measurements over an extended period (up to 14 days for some geophone deployments during the ICFT). The high-temperature and high-pressure cablehead assembly developed at Los Alamos was designed to keep the high-pressure water from working its way up into the 7-conductor cable and eventually shorting out one or more of the conductors. It proved critical in obtaining many of the deep borehole measurements from the Phase II reservoir. Measuring 35 in. long and 2 1/8 in. in diameter, the cablehead assembly is rated for temperatures of 350°C and pressures of 15 000 psi.

The development at the Laboratory of downhole instrumentation having temperature capabilities far superior to those of commercially available instrumentation was one of the most significant accomplishments of the HDR Project's first 15 years.

The temperature logging tools were the "workhorses," providing information—both day and night—about borehole conditions, casing problems, and the locations of flow connections (essential for reservoir characterization). The high-temperature geophone packages also proved to be extremely valuable: without them, far less would be known about the complexity and the shape of the Phase II reservoir. Coupled with these tools, the superb cablehead assemblies, with their ability to withstand extreme temperatures and pressures, enabled downhole measurements for much longer periods than was possible with commercial logging tools.

Glossary

Acoustic ranging—A seismic technique used to determine the distance and *direction* from one borehole to another nearby borehole; signals generated by an acoustic source in the first borehole are received by a geophone positioned in the second borehole.

Backpressure—The reverse pressure (or throttling pressure) intentionally imposed on any portion of the circulation system *beyond* the surface injection pumps. Typically, backpressure is applied at the production wellhead to partially jack open the flowing joints connecting the body of the HDR reservoir to the production interval in the production well(s).

Backwater region—The region of the Phase II reservoir farthest from the production well, pressure-stimulated during the high-flow/high-pressure segment of the ICFT (1986). Flow into this region did not seem well connected to the production well, and the stimulation resulted in considerable reservoir growth to the south (see Fig. 7-7, p. 439).

Basement rock—The hard crystalline rock found beneath the layers of sedimentary and/or volcanic rock. In the western U. S., this rock is typically igneous or metamorphic, and often of Precambrian age.

Body impedance—The resistance to fluid flow through the body of a jointed and pressure-dilated HDR reservoir. This impedance is additive to the impedances connecting the body of the reservoir to the wellbores, such that:

Total flow impedance = body impedance + near-wellbore inlet impedance + near-wellbore outlet impedance.

(See also *Near-wellbore inlet impedance* and *Near-wellbore outlet impedance*.)

Borehole televiewer—An acoustic logging device, first developed by Los Alamos National Laboratory in the mid 1980s, for mapping irregularities in the borehole surface—many of which are associated with sealed joints (see p. 133 and the Appendix).

Circulation-accessible reservoir volume—The volume (or region) of the pressure-stimulated rock mass that is actually accessible to the pressurized circulating water. In a jointed HDR reservoir, this volume—which is dependent on the mean reservoir pressure—can theoretically be as large as the seismic volume; typically, however, it will be somewhat smaller than the seismic volume, because some of the higher-opening-pressure joints developed during the initial high-pressure stimulation will be too impeded to be effectively accessed by the lower-pressure fluid circulating through the reservoir.

Circulation driving pressure—The pressure applied to the fluid as it enters the injection wellhead. During routine circulation operations, the driving pressure must be sufficient to force the fluid down the injection wellbore, across the reservoir, and up the production wellbore.

Closed-cycle (binary) HDR power extraction—The recovery of heat from a confined HDR reservoir by the continuous, closed-loop circulation of pressurized fluid, ensuring emissions-free energy production. The thermal energy of the circulating fluid is transferred to a secondary working fluid via a heat exchanger on the surface, then used to drive the power-generation turbine.

Closed-loop circulation/flow—See *Closed-cycle (binary) HDR power extraction*.

Confined reservoir—A man-made HDR reservoir that is created in a previously sealed body of hot crystalline rock and whose boundaries remain sealed as the reservoir is grown and extended from its initial injection point. (In contrast, an unconfined HWR—hot wet rock—reservoir has open, unsealed boundaries.)

Cyclic (or load-following) operation—Operation of an HDR reservoir whereby the production flow rate is modulated, by adjusting the backpressure of the production well, to achieve a rapid and sustained increase in the production rate for a few hours each day. (See *Using an HDR Reservoir for Load-Following*, pp. 35–37.)

Diffusional water loss—The loss of water from the pressurized HDR reservoir by slow, outward flow at the periphery, through the network of microcracks in the otherwise sealed, surrounding rock mass.

Dispersion volume—A reservoir fluid volume measurement based on tracer data (see pp. 520–521).

First-arrival volume—A reservoir fluid volume measurement based on tracer data (see pp. 520–521).

Flow impedance—The total resistance to flow, from the surface at the injection wellbore to the surface at the production wellbore. It includes the resistance to movement through the wellbores themselves as well as the resistance to flow across the reservoir. (See also *Reservoir flow impedance*.)

Fluid-accessible reservoir volume—This volume comprises both the circulation-accessible reservoir volume *and* the zone near the periphery of the reservoir where fluid has permeated into the joint extensions. It is thus slightly larger than the circulation-accessible rock volume at any given reservoir pressure, and appears to offer a reasonable analog to the latter—but one that can be measured through static reservoir pressure testing.

GEOCRACK—The name given by Prof. Daniel Swenson to his discrete-element numerical model for the Fenton Hill jointed HDR reservoir.

Geothermal energy—Energy derived from the natural heat of the earth.

Geothermal gradient—The rate at which the temperature of a rock mass changes with depth. At depths beyond those affected by the climate at the surface, the geothermal gradient is a function of (1) the composition of the rock; (2) the presence of—or distance from—significant sources of geothermal heat (such as a magma body or a concentration of radioactive elements); and (3) the presence of fluids, which adds a convective component to the conductive gradient. In the HDR situation, since there are no open faults or joints for the convection of water, the geothermal gradient is controlled by the outward conduction of heat from the interior of the earth, augmented by heat generation from the decay of radioactive elements within the rock mass itself.

Heat flow—The flow of heat in a rock mass from regions of higher temperature to those of lower temperature. The rate of conductive heat flow in rock is a direct function of the thermal conductivity of the particular rock body and any fluids within it. The movement of fluids within a rock mass may also lead to convective heat flow, which can occur at a significantly greater rate than conductive heat flow, giving rise to a *hydrothermal* situation.

Heat mining—The term coined by Armstead and Tester (1987) to rename the closed-loop HDR heat-transport process (originally named by Don Brown in 1973), i.e., the generation of geothermal power by the circulation of pressurized water through a confined, man-made HDR reservoir. It is the process whereby heat is removed from the reservoir and transported to the surface by the circulation of pressurized water.

Heat-transfer volume—The volume of the pressure-stimulated rock mass in an HDR reservoir from which circulating fluid can effectively extract heat. This volume, which is dependent on the mean reservoir pressure, excludes the higher-pressure portions of the seismic volume (which are not accessible at the lower reservoir circulating pressure) and those regions that consist of "dead-end" fluid-filled joints. The heat-transfer volume is analogous to the circulation-accessible reservoir volume (see above).

High-backpressure flow testing—The term applied by Los Alamos field-testing personnel to flow testing of a confined HDR reservoir at production pressures much higher than those needed to prevent boiling of the production fluid (higher than several hundred psi).

Hot dry rock (HDR) geothermal energy—The totally new geothermal energy concept invented in 1971 (and later patented) by researchers at Los Alamos Scientific Laboratory.

Hot wet rock (HWR) geothermal energy—The term adopted by Japanese geothermal researchers in the early 1990s to describe open, jointed hydrothermal systems that are only marginally productive without pressure stimulation (see p. 27). In 1995, the U. S. DOE renamed such systems *EGS*—Enhanced Geothermal Systems. (As of 2012, there is still no example of an EGS system in the U. S.)

Huff-puff operational mode—An early concept of cyclic operation of an HDR reservoir, whereby water is periodically injected (huff) through a borehole into the confined reservoir, then produced (puff) from the same borehole.

Hydraulic stimulation (or pressurization)—The injection of a fluid, typically water, deep into an isolated section of a borehole at pressures high enough to open (dilate) one or more of the favorably oriented joint sets intersecting the borehole. In hard, crystalline basement rock, hydraulic stimulation will almost invariably open pre-existing—but resealed—joints rather than fracture (in tension) the solid rock surrounding the borehole. The opening up of this joint network creates the engineered HDR reservoir. (See also *Pressure stimulation.*)

ICFT (Initial Closed-Loop Flow Test)—The first extended circulation test of the deeper Phase II Reservoir at Fenton Hill, conducted in mid 1986.

IFT (Interim Flow Test)—The nearly 7-month period (August 1992–February 1993) between the first and second steady-state production segments of the LTFT, during which the reservoir was kept pressurized and circulation maintained while pump problems were resolved (see pp. 501–503).

Impedance—See *Flow impedance*, *Reservoir flow impedance*

Impedance distribution—The partitioning of the total impedance to flow in an HDR circulation system, among four components: the system piping (very minor), the reservoir region near the points of fluid entry from the injection wellbore (minor), the body of the reservoir (minor to major), and the reservoir region near the points of fluid entry into the production wellbore (major).

Injection impedance—The impedance associated with the level of pressure required to pry open the most favorably oriented set of joints intersecting the injection interval of a borehole (see p. 328). This impedance is associated with flow *into* a potential reservoir region, and is not to be confused with the impedance associated with flow *across* the reservoir (see *Reservoir flow impedance*).

Injection pressure—The pressure applied at the injection wellhead to force fluid into the HDR reservoir. In routine energy extraction operations, this pressure would need to be great enough to open the reservoir joints so that circulation is feasible, but not so great that renewed reservoir growth—as indicated by seismic activity—would take place.

Integral mean fluid volume—A reservoir volume measurement based on tracer data (see pp. 520–521).

Jacking Pressure—See *Joint-opening pressure*

Joints—The re-cemented (sealed) flaws or cracks in the crystalline basement rock, originally formed during deformation or subsidence. It is such sealed flaws that are reopened by hydraulic pressurization during the creation of an HDR reservoir.

Joint-closure stress—The component of the earth-stress tensor normal to the joint surface. This stress is equivalent to the fluid pressure required to just open a joint (*joint-opening pressure*).

Joint-extension pressure—A pressure just high enough to cause an opened joint to further extend. When an HDR reservoir is already inflated, injecting fluid at a pressure at least equal to the joint-extension pressure will induce microseismic activity, owing to slight shear displacement of the joints as they continue to pressure-dilate and extend.

Joint-filling material—The mineral material, deposited by natural chemical processes, that over time fills and seals the previously opened joints in the crystalline basement rock.

Joint-opening pressure—The fluid pressure required to just open a joint against the existing normal closure stress. This pressure is sometimes referred to as the *jacking pressure*.

Joint porosity—The porosity of the secondary joint-filling material, deposited at an earlier time by the continually decreasing flow of mineral-laden fluid through the slowly sealing joints. It is thus the residual porosity of the joint-filling material, after the joints became sealed, that is referred to as *joint porosity*. It is considerably higher than the porosity of the matrix (i.e., of the sparse array of interconnected microcracks in the crystalline basement rock). In some cases, the term "reservoir porosity" is used to refer to the aggregate porosity of the pressurized HDR reservoir, which is determined almost entirely by the degree of opening of the stimulated joints; this aggregate porosity is strongly dependent on the reservoir pressure.

Joint sets—The subparallel groups, or arrays, that characterize the disposition of the stimulated joints in a pressure-dilated HDR reservoir region.

LASL—Los Alamos Scientific Laboratory (the former name of Los Alamos National Laboratory, before its renaming in 1980).

Least principal earth stress (σ_3)—The minimum component of the *in situ* earth-stress tensor at a given depth.

Load-following—The capability of an HDR reservoir to be operated in a cyclic manner, with greatly increased thermal power production for several hours each day. Load-following is achieved by programmed changes in the production-well backpressure, resulting in corresponding changes in reservoir power production. Load-following permits an HDR system to generate power in concert with fluctuations in demand—the maximum amount of energy being produced at times when it is most needed (and commercially most valuable).

LTFT (Long-Term Flow Test)—The flow testing of the Phase II HDR reservoir at Fenton Hill (1992–1995), to assess the reliability of HDR power production and the longevity of the reservoir; and to demonstrate that geothermal energy could be extracted on a sustained basis. The LTFT was designed to simulate as closely as possible the conditions under which a commercial HDR power plant would operate.

Magnetic ranging—The technique utilized by the Laboratory to magnetically determine the *direction* from one borehole to another.

Makeup water—The amount of water that must be continuously added to the circulation fluid to make up for peripheral losses (to the far field) of fluid from the reservoir, enabling a constant pressure and flow rate to be maintained.

Manifolding joints—The continuous joint set(s) within an HDR reservoir that account for the cross-reservoir fluid connectivity (see p. 380).

MHF Test (Massive Hydraulic Fracturing Test)—The high-pressure, high-volume injection of almost 6 million gal. of water into the deepest part of the EE-2 borehole, which created the Phase II HDR reservoir. Carried out in December of 1983, it was designed to greatly enlarge the joint network pressure-stimulated during Expt. 2020 and to connect this enlarged reservoir to the EE-3 borehole above.

Microcracks—The small, thin, fluid-filled cracks occurring in crystalline basement rock. Typically formed at grain boundaries or within mineral crystals themselves, the arrays of interconnected microcracks are extremely "tight," explaining the very low "native" permeability of the matrix rock surrounding an HDR reservoir and its consequent very high impedance to fluid flow.

Microseismic activity—The very small earthquakes (microseisms) generated as water is injected into a sealed region of rock under pressures high enough to open previously sealed joints (this joint opening is mainly in tension, but often has a shear component as well). Detection of microseismic activity demonstrates that an HDR reservoir is being created or expanded, and identifying the locations of the individual seismic events is the most important means of locating the reservoir region, determining its approximate dimensions, and identifying some of the characteristics of its interior joint structure.

Microseismic cloud—Tens of thousands of microseismic events may be induced within a rock mass subjected to pressure stimulation—many more in some regions than in others. The cloud of microseismic events depicts the distribution and density of these events, representing the region of joint openings, which helps researchers evaluate the degree of joint connectivity in the pressure-stimulated rock mass.

Microseismic events—Movement at depth of jointed rock blocks in an HDR reservoir, as a result of hydraulic pressure applied along the interconnecting joints. These movements—caused by opening of joints and slippage along joints—are manifested as microearthquakes, the detection of which provides a means for locating zones of joint dilation and reservoir growth.

Modal volume—A reservoir fluid volume measurement based on tracer data (see pp. 520–521).

Near-wellbore inlet impedance—Resistance to the flow of fluid in the near-wellbore joints connecting the injection interval to the body of the reservoir. This impedance rapidly declines as the relatively cool injected fluid causes cooling—and contraction—of the rock blocks near the injection wellbore, opening the connecting joints.

Near-wellbore outlet impedance—Resistance to the flow of fluid in the near-wellbore joints connecting the body of the reservoir to the much-lower-pressure production interval. The impedance to flow is greatest in this region, because of the rapid decrease in fluid pressure as the flow converges to the production wellbore, resulting in a progressive pinch-off of the producing joints.

Open-cycle HDR power extraction—The circulation (atypical) of fluid through an HDR reservoir that is at some point open to the atmosphere. For power production, the produced fluid would be flashed to steam and the steam delivered to a turbine. Open-cycle operation has many drawbacks, among them water consumption and mineral scaling.

PBR (polished bore receptacle)—A length of pipe (typically 30–40 ft) having a honed (polished) bore, to form the outside surface of a high-temperature, sliding-sleeve seal mechanism. The PBR is used in conjunction with a seal assembly (sometimes called a PBR *mandrel*) to form a movable, high-pressure seal. PBR seal assemblies were used at Fenton Hill at differential pressures up to 7000 psi.

Penny-shaped fracture theory—The theory (based on the faulty assumption that the basement rock can be considered homogeneous and isotropic) that a "fracture" created in the rock by hydraulic pressurization will be vertical and shaped like a penny (see pp. 12–14).

Phase II assumption—The assumption, based on the joint orientations observed in the Phase I reservoir, that the continuous joints in the deeper Phase II reservoir region would be the same, i.e., essentially vertical rather than inclined. This assumption proved to be wrong (see pp. 239–240).

Phase II HDR reservoir—The deeper HDR reservoir at Fenton Hill, developed during the MHF Test in late 1983 and extensively flow-tested between 1985 and 1995.

Pore fluid—The fluid occupying the microcrack pore space within the matrix blocks and—more important—the fluid occupying the pore space within the joint-filling material itself. This latter pore space consists not of microcracks, but more equidimensional pores (see pp. 449–450).

Pressure dilation—The opening of joints in hard, crystalline rock as a result of pressure stimulation. Note that the joints do not have to fully jack open to pressure-dilate—only to expand slightly, so that not all the asperities are in contact. The dilation can continue until the joints are fully jacked open. The volumetric change resulting from this dilation is accommodated by the associated compression of the interior rock blocks and/or of the rock mass just beyond the periphery of the HDR reservoir.

Pressure propping—The holding open of joints by the applied pressure within the joints themselves (analogous to the sand-propping techniques used in the oil industry).

Pressure spallation—The pressure-induced spallation of joint surfaces. During reservoir development, high-pressure fluid from the joints slowly permeates into the network of microcracks in the rock matrix adjacent to the joint surfaces. If the pressure within the joints is then suddenly released (e.g., by a rapid venting of the reservoir), high-pressure fluid will become trapped in the microcracks. It is the very significant pressure differential thus created between the microcracks and the low-pressure joints that causes fragments of the rock matrix to break away, or "spall" from the joint surfaces. It appears that a significant time—several days—of pressure "soaking" of the matrix rock is required to establish the conditions necessary for pressure spallation.

Pressure stimulation—The injection of fluid into a borehole drilled into a rock mass, under pressures high enough to open pre-existing—but sealed—joints, or to extend already-opened joints in the region surrounding the zone of pressurization. (See also *Hydraulic stimulation (or pressurization)*.)

Production well backpressure—The pressure imposed on the production wellbore during operation of an HDR system. The backpressure may be increased (high-backpressure operation) to significantly reduce the near-wellbore outlet impedance, by pressure-dilating the joints entering the lower-pressure production wellbore from the high-pressure body of the reservoir.

Pumped storage—The ancillary use of an HDR reservoir for the additional storage of pressurized water during temporary operation at higher-than-normal pressures. This additional storage would be accommodated by the temporary hyper-compression of both the rock blocks within the reservoir and the rock mass just beyond the periphery of the reservoir. The additional stored water can be returned to the surface during hours of peak power demand, augmenting the HDR plant's power production.

Reservoir flow impedance—Resistance to flow through an HDR reservoir. This impedance is typically greatest in the region near the production wellbore(s), because of the rapid decrease in fluid pressure as the flow converges to the much-lower-pressure production wellbore(s), which causes the intersecting joints to be somewhat pinched off.

Reservoir rock volume—The volume of pressure-stimulated HDR reservoir rock. This volume can be measured or estimated on the basis of several types of information: seismic data, tracer data, hydraulic/hydromechanical measurements, or geometric analyses of the wellbore injection and production zones. The volume measurement most pertinent to reservoir operation is the *fluid-accessible reservoir volume* (see above), which is based static reservoir pressurization data.

Reservoir Verification Flow Test (RVFT)—The final circulation test of the Phase II HDR reservoir at Fenton Hill. The RVFT demonstrated that even after two years of inactivity, during which the pressure on the reservoir was at times allowed to decay to ambient levels, the system could rapidly be reactivated to operating conditions and productivity levels essentially the same as those of the preceding steady-state periods.

Seismic cloud—See *Microseismic cloud*

Seismic reservoir volume—The volume of a rock mass affected by pressure-stimulation operations, as determined by the distribution of detected seismic events. This volume is simply an estimate, because the seismic events tend to be somewhat unevenly distributed; it is usually expressed with a degree of confidence based on the mathematical rules of standard deviation (σ_1, σ_2, etc.), according to the fraction of the identified seismic signals included in the calculation.

Short-circuiting—Preferential fluid flow through one or a very few pathways directly from the injection to the production wellbores. Short-circuited flow could be expected to lead to rapid cooling of the preferred pathways and a resultant decline in energy production. However, experience has shown that as joints cool they tend to collapse and carry *less* fluid, diverting more flow to the more tortuous paths.

Stress cage—The annular region of hyper-compressed rock surrounding the pressure-dilated HDR reservoir, which acts to hold the peripheral joints more tightly closed than they were originally. This extra compression arises from the elastic response of the surrounding rock mass to the pressure-inflation of the reservoir region (see p. 346).

SUE (Stress-unlocking experiment)—An experiment conducted near the end of Phase I reservoir testing, to determine whether repressurization of the reservoir at significantly higher levels would reduce the flow impedance (see pp. 230–233).

Tag cementing—A method of cementing casing whereby only the bottom few hundred feet of pipe are actually cemented in the borehole.

Thermal dilation—The cooling-induced opening of the joints intersecting the injection borehole, through thermal contraction.

Thermal drawdown—The depletion of the stored heat in an HDR reservoir, as indicated by a drop in the temperature of the produced fluid.

Through-flow fluid volume—The fluid volume associated with the circulation-accessible rock volume, and determined on the basis of tracer data.

Travel-time algorithm—A seismic method for locating acoustic events in space. By inversion of arrival times for four or more P- and/or S-waves, recorded on at least two separate geophones, the position and time of the event can be determined.

Water loss—Diffusional loss of water from the boundaries of a pressurized HDR reservoir. This term is sometimes incorrectly used to refer to water flowing into an expanding HDR reservoir region as the joints at the periphery continue to open and pressure-dilate.

Wellbore impedance—Resistance to the flow of fluid down the injection wellbore and up the production wellbore. This impedance is a very minor component of the overall flow impedance in an HDR system.

Wellbore stress concentration—The circumferential compressive stress occurring at—and near—the borehole wall, created by the drilling of the hole.

Bibliography

Note Regarding the Bibliography

The principal source for the documents listed is a Department of Energy electronic database accessed through the Los Alamos National Laboratory Research Library. To the initial list we gradually added other documents as we put the chapters together. In several instances, after having used a document to add or clarify information, we checked the Bibliography to see whether that document was already present—and discovered that it was, but with the authors listed in exactly reverse order (except for the first author)! Unfortunately, it was only after numerous such discoveries had been made that it became apparent that there was a *pattern*—and by then it was too late to go back and find which of the entries had already been corrected. (The origin of the problem with this database is not known; it may be related to the process by which it was transferred from the Department of Energy to the Los Alamos system). Even scarier, in some cases the error was discovered via the *Georef* database, which we then began to trust and use for cross-checking, until a few cases—of Los Alamos Laboratory documents—were found in which the entry in Georef also had the authors' names in reverse order (verified through the Laboratory Publications database).

Obviously, the only way to be 100 percent sure of the correct order would be to check each reference against an actual hard copy of the document—an impossible task given the number of entries (not to mention the difficulty of acquiring a hard copy of each). We therefore caught all that we could, and we apologize for the unknown number that may still be listed with the second and following authors' names in reverse order. In addition, in a number of instances, references were listed (in various databases) without page numbers or with an ambiguous entry, such as "p. 128"—the latter having three possible interpretations: the item is an abstract on just one page; it is an article beginning on that page; or there are 128 pages in the entire document. We did our best to resolve as many of these as possible (if it was clear that the number represented total pages in the document, for instance, it is written "128 pp"). No doubt some entries remain that could not be fully clarified in this respect.

Aamodt, R. L., 1977. "Hydraulic fracture experiments in GT-1 and GT-2," Los Alamos Scientific Laboratory report LA-6712, Los Alamos, NM, 19 pp.

Aamodt, R. L., 1980. "Hot dry rock geothermal reservoir engineering," 3rd invitational well testing symposium, *Well testing in low permeability environments* (March 26–28, 1980: Berkeley, CA). Lawrence Berkeley Laboratory, Berkeley, CA, pp. 11–13.

Aamodt, R. L., and Smith, M. C., 1972. "Induction and growth of fractures in hot rock—artificial geothermal reservoirs," 10th annual American Nuclear Society conference (June 18, 1972: Las Vegas, NV). Los Alamos Scientific Laboratory report LA-DC-72-669, 31 pp.

Aamodt, R. L., and Zyvoloski, G., 1980. "Report on Phase I, Segment 5, Stage 1 (start up of experiment 217)," Los Alamos National Laboratory internal report G-5, Technical Memo No. 5, Los Alamos, NM, 31 pp.

Aamodt, R. L., and Kuriyagawa, M., 1981. "Measurement of instantaneous shut-in pressure in crystalline rock," workshop on hydraulic fracturing stress measurements (December 2–5, 1981: Monterey, CA). U. S. Geological Survey Open File report OF 82-1075, Reston, VA, pp. 394–402.

Abé, H., and Hayashi, K., 1992. "Fundamentals of design concept and design methodology for artificial geothermal reservoir systems," *Geotherm. Resour. Counc. Bull*. **21**(5):149–155.

Abé, H., Duchane, D.V., Parker, R. H., and Kuriyagawa, M., 1999. "Present status and remaining problems of HDR/HWR systems design," in *Hot Dry Rock/Hot Wet Rock Academic Review* (Abé, H., Niitsuma, H., and Baria, R., eds.), *Geothermics* special issue **28**(4/5):573–590.

Abé, H., Niitsuma, H., and Murphy, H., 1999. "Summary of discussions, structured academic review of HDR/HWR reservoirs," in *Hot Dry Rock/Hot Wet Rock Academic Review* (Abé, H., Niitsuma, H., and Baria, R., eds.), *Geothermics* special issue **28**(4/5):671–679.

Achenbach, J. D., Bazant, Z. P., Dundurs, J., Keer, L. M., Nemat-Nasser, S., Mura, T., and Weertman, J., 1980. "Hot dry rock reservoir characterization and modeling, October 1, 1978–September 30, 1979" (final report). Los Alamos Scientific Laboratory report LA-8343-MS, Los Alamos, NM, 154 pp.

Ahearne, J., 1979. "Fenton Hill: drilling for energy at 13,000 feet," *The Atom*, Los Alamos Scientific Laboratory, Los Alamos, NM, 5 pp.

Albright, J. N., 1975. "A new and more accurate method for the direct measurement of earth temperature gradients in deep boreholes," 2nd United Nations symposium on the development and use of geothermal resources (May 20–29, 1975: San Francisco, CA). CONF-750525-7, 17 pp.

Albright, J. N., 1975. "Temperature measurements in the Precambrian section of Geothermal Test Hole No. 2," Los Alamos Scientific Laboratory report LA-6022-MS, Los Alamos, NM, 11 pp.

Albright, J. N., and Hanold, R., 1976. "Seismic mapping of hydraulic fractures made in basement rocks," in *Proceedings* (Linville, B., ed.), second ERDA symposium on enhanced oil and gas recovery (September 9, 1976: Tulsa, OK), vol. 2—Gas. Petroleum Publishing Company, Tulsa, OK, pp. C8.1–C8.13.

Albright, J. N., and Pearson, C. F., 1980. "Location of hydraulic fractures using microseismic techniques," 55th Society of Petroleum Engineers of AIME annual technical conference and exhibition (September 21, 1980: Dallas, TX). SPE 9509, 19 pp.

Albright, J. N., and Newton, C. A., 1981. "The characterization of hot dry rock geothermal energy extraction systems," in *SQUID Applications to Geophysics* (Weinstock, H., and Overton, W. C., Jr., eds.), workshop on SQUID applications (June 2–4, 1980: Los Alamos, NM), pp. 166–171.

Albright, J. N., and Pearson, C. F., 1982. "Acoustic emissions as a tool for hydraulic fracture location: experience at the Fenton Hill hot dry rock site," *Soc. Petrol. Eng. J.* **22**(4):523–530.

Albright, J., Potter, R., Aamodt, L., and Linville, B., 1977. "Definition of fluid-filled fractures in basement rocks," 3rd ERDA symposium on enhanced oil and gas recovery and improved drilling methods (August 30, 1977: Tulsa, OK). CONF-770836-P2, pp. F.2.1–F.2.8.

Albright, J. N., Aamodt, R. L., Potter, R. M., and Spence, R. W., 1978. "Acoustic methods for detecting water-filled fractures using commercial logging tools," 4th ERDA symposium on enhanced oil and gas recovery and improved drilling methods (August 29, 1978: Tulsa, OK). CONF-780825-3, 19 pp.

Albright, J. N., Fehler, M. C., and Pearson, C. F., 1980. "Transmission of acoustic signals through hydraulic fractures," in *Transactions*, 21st annual symposium of the Society of Professional Well Log Analysts (July 8–11, 1980: Lafayette, LA). SPWLA, Houston, TX, pp. R1–R18.

Albright, J. N., Johnson, P. A., Phillips, W. S., Bradley, C. R., and Rutledge, J. T., 1988. "The Crosswell Acoustic Surveying Project," Los Alamos National Laboratory report LA-11157-MS, Los Alamos, NM, 121 pp.

Aldrich, M. J., and Laughlin, A. W., 1984. "A model for the tectonic development of the southeastern Colorado Plateau boundary," *J. Geophys. Res.* **89**:207–218.

Aldrich, M. J., Laughlin, A. W., and Gambill, D. T., 1981. "Geothermal resource base of the world: a revision of the Electrical Power Research Institute's estimate," Los Alamos Scientific Laboratory report LA-8801-MS, Los Alamos, NM, 59 pp.

Altseimer, J. H., Armstrong, P. E., Fisher, H. N., and Krupka, M. C., 1977. "Rapid excavation by rock melting—LASL Subterrene program" (Hanold, R. J., comp.), Los Alamos Scientific Laboratory report LA-5979-SR, Los Alamos, NM, 83 pp.

Anon., 1979. *Summary of talks, hot dry rock geothermal conference* (April 19–20, 1978: Los Alamos, NM). Los Alamos Scientific Laboratory report LASL-79-8, Los Alamos, NM, 31 pp.

Anon., 1981. *Summary of talks, third annual hot dry rock geothermal information conference* (October 28–29, 1980, Santa Fe, NM). Los Alamos National Laboratory report LAL-81-22, Los Alamos, NM, 41 pp.

Archuleta, J. R., and Todd, B. E., 1978. "Hot dry rock geothermal energy development project: cablehead assembly. Equipment development report," Los Alamos Scientific Laboratory informal report LA-7325-MS, Los Alamos, NM, 8 pp.

Armstead, H. C. H., 1983. Geothermal Energy, second edition, E. & F. N. Spon, London, 357 pp.

Armstead, H. C. H., and Tester, J. W., 1987. Heat Mining, E. & F. N. Spon, London and New York, 478 pp.

Armstrong, D. E., Coleman, J. S., McInteer, B. B., Potter, R. M., and Robinson, E. S., 1965. "Rock melting as a drilling technique," Los Alamos Scientific Laboratory report LA-3243, Los Alamos, NM, 39 pp.

Arney, B., Potter, R., and Brown, D., 1981. "When the hole is dry: the HDR alternative in the Cascades," Geothermal Resources Council symposium, *Geothermal potential of the Cascade mountain range: exploration and development* (May 19–22, 1981: Portland, OR). Geothermal Resources Council special report No. 10, Davis, CA, pp. 11–14.

Arney, B. H., Goff, F., and Harding Lawson Associates, 1982. "Evaluation of the hot dry rock geothermal potential of an area near Mountain Home, Idaho," Los Alamos National Laboratory report LA-9365-HDR, Los Alamos, NM, 65 pp.

Balagna, J., Vidale, R., Tester, J., Holley, C., Herrick, C., Feber, R., Charles, R., and Blatz, L., 1976. "Geochemical considerations for hot dry rock systems," Conference on scale management in geothermal energy development (August 2, 1976: San Diego, CA). COO-2607-4; CONF-760844, pp. 103–114.

Bechtel National, Inc., 1988. *Hot Dry Rock Venture Risks Investigation*, prepared for the U. S. Department of Energy, San Francisco operations office, San Francisco, CA, 217 pp.

Becker, N. M., Pettitt, R. A., and Hendron, R. H., 1981. "Power from the hot-dry-rock geothermal resource," ASME/IEEE joint power generation conference (October 4, 1981: St. Louis, MO). CONF-811008-3, 30 pp.

Berger, M. E., and Murphy, H. D., 1988. "Prospects for hot dry rock in the future," in *Proceedings*, Geothermal Energy Program Review VI (April 18–21, 1988: San Francisco, CA). U. S. Department of Energy document CONF-880477-5, 10 pp.

Birdsell, S. A. (ed.), 1988. "Experiment 2074 report," Group ESS-4 internal memorandum ESS-4-88-92, Los Alamos, NM, 29 pp.

Birdsell, S. A. (ed.), 1989. "Experiment 2076 report," Group ESS-4 internal memorandum ESS-4-89-82, Los Alamos, NM, 9 pp.

Birdsell, S. A., and Robinson, B. A., 1988a. "Prediction of thermal front breakthrough due to fluid reinjection in geothermal reservoirs," Geothermal Resources Council 11th annual symposium on geothermal energy (January 10–14, 1988: New Orleans, LA). American Society of Mechanical Engineers, New York, NY, CONF-880104, 7 pp.

Birdsell, S. A., and Robinson, B. A., 1988b. "A three-dimensional model of fluid, heat, and tracer transport in the Fenton Hill hot dry rock reservoir," in *Proceedings*, 13th annual workshop on geothermal reservoir engineering (January 19–21, 1988: Stanford, CA). SGP-TR-113, pp. 225–230.

Birdsell, S. A., and Robinson, B. A., 1989. "Kinetics of aryl halide hydrolysis using isothermal and temperature-programmed reaction analyses," *Ind. Eng. Chem. Res.* **28**(5):511–518.

Blackwell, D. D., 1983. "Heat flow—the technique for hot dry rock exploration and evaluation," in *Workshop on Exploration for Hot Dry Rock Geothermal Systems* (Heiken, G. H., Shankland, T. J., and Ander, M. E., comp.), June 21, 1982: Los Alamos, NM. Los Alamos National Laboratory report LA-9697-C, Los Alamos, NM, pp. 22–27.

Blair, A. G., Tester, J. W., and Mortensen, J. J., 1976. "LASL Hot Dry Rock Geothermal Project. Progress report, July 1, 1975–June 30, 1976," Los Alamos Scientific Laboratory report LA-6525-PR, Los Alamos, NM, 238 pp.

Block, L., Cheng, C. H., Fehler, M., and Phillips, W. S., 1991. "Inversion of microearthquake arrival time data at the Los Alamos hot dry rock reservoir," 60th annual international meeting of the Society of Exploration Geologists (September 23–27, 1991: San Francisco, CA). Expanded abstracts SI4.7, pp. 1226–1229.

Block, L. V., Phillips, W. S., Fehler, M. C., and Cheng, C. H., 1994. "Seismic imaging using microearthquakes induced by hydraulic fracturing," *Geophys.* **59**(1):102–112.

Bower, K. M., June 1996. "A numerical model of hydro-thermo-mechanical coupling in a fractured rock mass," Los Alamos National Laboratory report LA-13153-T, Los Alamos, NM, 179 pp.

Brittenham, T. L., 1978. "Drilling plan, Energy Extraction Well EE-2, Jemez Plateau, Sandoval County, New Mexico." Grace, Shursen, Moore & Associates, unpublished data.

Brittenham, T. L., Williams, R. E., Rowley, J. C., and Neudecker, J. W., 1980. "Directional drilling operations: hot dry rock Well EE-2," preprint, Geothermal Resources Council annual meeting (September 9−11, 1980: Salt Lake City, UT). Los Alamos Scientific Laboratory report LASL-80-36, Los Alamos, NM, pp. 5–8.

Brown, D. W., 1973. "Potential for hot-dry-rock geothermal energy in the western United States," Los Alamos Scientific Laboratory report LA-UR-73-1075, Los Alamos, NM, 22 pp.

Brown, D. W., 1982a. "Addendum to Experiment 2020 procedure," Group ESS-4 internal memorandum ESS-4-82-489, Los Alamos, NM, 4 pp.

Brown, D. W., 1982b. "Los Alamos hot-dry-rock project: recent results," in *Proceedings*, 8th annual workshop on geothermal reservoir engineering (December 14, 1982: Stanford, CA). SGP-TR-60, pp. 249–254.

Brown, D. W. (ed.), 1983. "Results of Experiment 186, the high back-pressure flow experiment" (unpublished), 86 pp.

Brown, D. W., 1988a. "Anomalous earth stress measurements during a six-year sequence of pumping tests at Fenton Hill, New Mexico," 2nd international workshop on hydraulic fracturing stress measurements (June 15–18, 1988: Minneapolis, MN). Los Alamos National Laboratory report LA-UR-88-3985, Los Alamos, NM, 25 pp.

Brown, D. W., 1988b. "Post Expt. 2074 temperature log in EE-3A," Group ESS-4 internal memorandum ESS-4-88-25, Los Alamos, NM, 4 pp.

Brown, D. W., 1989a. "Reservoir modeling for production management," in *Research and Development for the Geothermal Marketplace*, proceedings of Geothermal Energy Program Review VII (March 21–23, 1989: San Francisco, CA). U. S. Department of Energy document CONF-890352, pp. 153–156.

Brown, D. W., 1989b. "The potential for large errors in the inferred minimum earth stress when using incomplete hydraulic fracturing data," *Int. J. Rock Mech. Min. Sci. & Geomech. Abstr.* **26**:573–577.

Brown, D. W., 1990a. "Hot dry rock reservoir engineering," *Geotherm. Resour. Counc. Bull.* **19**(3):89–93.

Brown, D. W., 1990b. "Reservoir water loss modeling and measurements at Fenton Hill, New Mexico," in *Hot Dry Rock Geothermal Energy* (Baria, R., ed.), proceedings of the Camborne School of Mines international hot dry rock conference (June 27–30, 1989: Redruth, Cornwall, UK). Robertson Scientific Publications, London, pp. 498–508.

Brown, D. W., 1991. "Recent progress in HDR reservoir engineering," in *The Geothermal Partnership—Industry, Utilities, and Government Meeting the Challenges of the 90's*, proceedings of Geothermal Energy Program Review IX (March 19–21, 1991: San Francisco, CA). U. S. Department of Energy document CONF-9103105, pp. 153–157.

Brown, D. W., 1992. "Update on the Long-Term Flow Testing Program," *Geotherm. Resour. Counc. Bull.* **21**:157–161.

Brown, D. W., 1993a. "Cumulative experience of the U. S. Hot Dry Rock Program," in *Hot Dry Rock Geothermal Energy for U. S. Electric Utilities*, proceedings of an EPRI workshop (January 14, 1993: Philadelphia, PA). Project RP1994-06, 6 pp.

Brown, D. W., 1993b. "Recent flow testing of the HDR reservoir at Fenton Hill, New Mexico," *Geotherm. Resour. Counc. Bull.* **22**:208–214.

Brown, D. W., 1994a. "How to achieve a four-fold productivity increase at Fenton Hill," Geothermal Resources Council annual meeting, *Restructuring the geothermal industry* (October 2–5, 1994: Salt Lake City, UT). *Trans. Geotherm. Resour. Counc*. **18**:405–408.

Brown, D. W., 1994b. "Summary of recent flow testing of the Fenton Hill HDR reservoir," in *Proceedings*, 19th annual workshop on geothermal reservoir engineering (January 18–20, 1994: Stanford, CA). SGP-TR-147, pp. 113–116.

Brown, D., 1995a. "1995 verification flow testing of the HDR reservoir at Fenton Hill, New Mexico," Geothermal Resources Council annual meeting (October 8–11, 1995: Reno, NV). *Trans. Geotherm. Resour. Counc.* **19**:253–256.

Brown, D., 1995b. "The US hot dry rock program—20 years of experience in reservoir testing," in *Worldwide Utilization of Geothermal Energy: an Indigenous, Environmentally Benign Renewable Energy Resource*, proceedings of the World Geothermal Congress (May 18–31, 1995: Florence, Italy). International Geothermal Association, Inc., Auckland, New Zealand, vol. 4, pp. 2607–2611.

Brown, D. W., 1996a. "Experimental verification of the load-following potential of a hot dry rock geothermal reservoir," in *Proceedings*, 21st workshop on geothermal reservoir engineering (January 22–24, 1996: Stanford, CA). SGP-TR-151, pp. 281–285.

Brown, D. W., 1996b. "1995 reservoir flow testing at Fenton Hill, New Mexico," in *Proceedings*, 3rd international HDR forum (May 13–16, 1996: Santa Fe, NM), pp. 34–37.

Brown, D. W., 1996c. "The geothermal analog of pumped storage for electrical demand load following," in *Proceedings*, Intersociety Energy Conversion Engineering Conference (August 11–16, 1996: Washington, DC), pp. 1653–1656.

Brown, D. W., 1996d. "The hot dry rock geothermal potential of the Susanville (CA) area," *Trans. Geotherm. Resour. Counc*. **20**:441–445.

Brown, D. W., 1996e. "The load-following potential of an HDR reservoir," in *Proceedings*, 3rd international HDR forum (May 13–16, 1996: Santa Fe, NM), pp. 47–50.

Brown, D. W., 1997a. " Review of Fenton Hill HDR test results," in *Proceedings*, NEDO international geothermal symposium (March 11–12, 1997: Sendai, Japan), pp. 316–323.

Brown, D. W., 1997b. "Storage capacity in hot dry rock reservoirs," U. S. Patent No. 5,585,362, dated November 11, 1997.

Brown, D. W., 1999. "Evidence for the existence of a stable, highly fluid-pressurized region of deep, jointed crystalline rock from Fenton Hill hot dry rock test data," in *Proceedings*, 24th workshop on geothermal reservoir engineering (January 25–27, 1999: Stanford, CA). SGP-TR-162, pp. 352–358.

Brown, D. W., 2000. "A hot dry rock geothermal energy concept utilizing supercritical CO_2 instead of water," in *Proceedings*, 25th annual workshop on geothermal reservoir engineering (January 24–26, 2000: Stanford, CA). SGP-TR-165, pp. 233–238.

Brown, D. W., 2003. "Geothermal energy production with supercritical fluids," U. S. Patent No. 6,668,554 B1 (dated December 30, 2003).

Brown, D. W., 2009. "Hot dry rock geothermal energy: important lessons from Fenton Hill," in *Proceedings*, 34th workshop on geothermal reservoir engineering (February 9–11, 2009: Stanford, CA). SGP-TR-187, pp. 139–142.

Brown, D. W., and Potter, R. M., 1973. "LASL geothermal energy program: summary of *in-situ* experiments in the first exploratory hole," fall annual meeting of the American Geophysical Union (December 10–13, 1973: San Francisco, CA). *EOS, Trans. Am. Geophys. Union* **54**(11):1214.

Brown, D. W., and Fehler, M. C., 1989. "Pressure-dependent water loss from a hydraulically stimulated region of deep, naturally jointed crystalline rock," in *Proceedings*, 14th annual workshop on geothermal reservoir engineering (January 24–26, 1989: Stanford, CA). SGP-TR-122, pp. 19–28.

Brown, D. W., and Robinson, B. A., 1990. "The pressure dilation of a deep, jointed region of the earth," in *Rock Joints* (Barton, N., and Stephansson, O., eds.), proceedings of the international symposium on rock joints (June 4–6, 1990: Loen, Norway). Balkema, Rotterdam, pp. 519–525.

Brown, D. W., and Duchane, D., 1992. "Status and prospects for hot dry rock in the United States," Geothermal Resources Council annual meeting (October 4–7, 1992: San Diego, CA). *Trans. Geotherm. Resour. Counc.* vol. 16, 20th anniversary, Davis, CA, pp. 395–401.

Brown, D. W., and DuTeau, R., 1993. "Progress report on the long-term flow testing of the HDR reservoir at Fenton Hill, New Mexico" in *Proceedings*, 18th annual workshop on geothermal reservoir engineering (January 26–28, 1993: Stanford, CA). SGP-TR-145, pp. 207–211.

Brown, D. W., and DuTeau, R. J., 1995. "Using a hot dry rock geothermal reservoir for load following," in *Proceedings*, 20th annual workshop on geothermal reservoir engineering (January 24–26, 1995: Stanford, CA). SGP-TR-150, pp. 207–211.

Brown, D. W., and DuTeaux, R., 1997. "Three principal results from recent Fenton Hill flow testing," in *Proceedings*, 22nd workshop on geothermal reservoir engineering (January 27–29, 1997: Stanford, CA). SGP-TR-155, pp. 185–190.

Brown, D. W., and Duchane, D. V., 1999. "Scientific progress on the Fenton Hill HDR project since 1983," in *Hot Dry Rock/Hot Wet Rock Academic Review* (Abé, H., Niitsuma, H., and Baria, R., eds.), *Geothermics* special issue **28**(4/5):591–601.

Brown, D. W., Potter, R. M., and Smith, M. C., 1972. "New method for extracting energy from 'dry' geothermal reservoirs," 7th intersociety energy conversion engineering conference (September 25, 1972: San Diego, CA). Los Alamos Scientific Laboratory report LA-DC-72-1157, Los Alamos, NM, 23 pp.

Brown, D., Hendron, R. H., and Dennis, B., 1982. "Experiment 2020: third fracture connection attempt from just below the casing shoe in EE-2," Group ESS-4 internal memorandum ESS-4-82-410, Los Alamos, NM, 8 pp.

Brown, D. W., Dennis, B., and Hendron, R. H., 1984. "Experiment 2036: post-MHF evaluation of EE-2," Group ESS-4 internal memorandum ESS-4-84-4, Los Alamos, NM, 7 pp.

Brown, D. W., Potter, R. M., and Myers, C. W., 1990. "Hot dry rock geothermal energy—an emerging energy resource with a large world-wide potential," in *Energy and the Environment in the 21st Century* (Tester, J. W., Wood, D. O., and Ferrari, N. A., eds.), proceedings of the MIT conference (March 26–28, 1990: Cambridge, MA), pp. 931–942.

Brown, D. W., DuTeaux, R., Kruger, P., Swenson, D., and Yamaguchi, T., 1999. "Fluid circulation and heat extraction from engineered geothermal reservoirs," in *Hot Dry Rock/Hot Wet Rock Academic Review* (Abé, H., Niitsuma, H., and Baria, R., eds.), *Geothermics* special issue **28**(4/5):553–572.

Burns, K. L., 1987. "Geological structures from televiewer logs of GT-2, Fenton Hill, New Mexico. Part 1: feature extraction," Los Alamos National Laboratory report LA-10619-HDR, Pt. 1, Los Alamos, NM, 40 pp.

Burns, K. L., 1987. "Geological structures from televiewer logs of GT-2, Fenton Hill, New Mexico. Part 2: rectification," Los Alamos National Laboratory report LA-10619-HDR, Pt. 2, Los Alamos, NM, 40 pp.

Burns, K. L., 1987. "Geological structures from televiewer logs of GT-2, Fenton Hill, New Mexico. Part 3: quality control," Los Alamos National Laboratory report LA-10619-HDR, Pt. 3, 18 pp.

Burns, K. L., 1988. "Televiewer measurement of the orientation of *in-situ* stress at the Fenton Hill Hot Dry Rock site, New Mexico," Geothermal Resources Council annual meeting (October 9–12, 1988: San Diego, CA). *Trans. Geotherm. Resour. Counc.* **12**:229–235.

Burns, K. L., 1991. "Orientation of minimum principal stress in the hot dry rock geothermal reservoir at Fenton Hill, New Mexico," Geothermal Resources Council annual meeting (October 6−9, 1991: Sparks, NV). *Trans. Geotherm. Resour. Counc.* **15**:319−323.

Burns, K. L., and Potter, R. M., 1995. "Structural analysis of Precambrian rocks at the hot dry rock site at Fenton Hill, New Mexico," in *Worldwide Utilization of Geothermal Energy: an Indigenous, Environmentally Benign Renewable Energy Resource*, proceedings of the World Geothermal Congress (May 18–31, 1995: Florence, Italy). International Geothermal Association, Inc., Auckland, New Zealand, vol. 4, pp. 2619–2624.

Callahan, T. J., 1996. "Reservoir investigations of the hot dry rock geothermal system, Fenton Hill, New Mexico: tracer test results," in *Proceedings*, 21st annual workshop on geothermal reservoir engineering (January 22–24, 1996: Stanford, CA). SGP-TR-151, pp. 299–304.

Carden, R. S., Nicholson, R. W., Pettitt, R. A., and Rowley, J. C., 1985. "Unique aspects of drilling and completing hot-dry-rock geothermal wells," *J. Pet. Technol*. **37**:821–834.

Carter, J. J., 1990. "The effects of a clay coating on fluid flow through simulated rock fractures," M. S. thesis, University of California, Department of Materials Science and Mineral Engineering, Berkeley, CA, 75 pp.

Cash, D., Homuth, E. F., Keppler, H., Pearson, C., and Sasaki, S., 1983. "Fault plane solutions for microearthquakes induced at the Fenton Hill hot dry rock geothermal site: implications for the state of stress near a Quaternary volcanic center," *Geophys. Res. Lett.* **10**(12):1141–1144.

Chemburkar, R., Brown, L. F., Travis, B. J., and Robinson, B. A., 1988. "Numerical determination of temperature profiles in flowing systems from conversions of chemically reacting tracers," American Institute of Chemical Engineers annual convention (November 27, 1988: Washington, DC). CONF-881143-4, 16 pp.

Cummings, R. G., Erickson, E. L., Arundale, C. J., and Morris, G., 1979. *Economic Factors Relevant for Electric Power Produced from Hot Dry Rock Geothermal Resources: A Case Study for the Fenton Hill, New Mexico, Area*. U. S. Department of Energy report DOE/ET/27017-T1, 52 pp.

Cummings, R. G., Morris, G. E., Tester, J. W., and Bivins, R. L., 1979. "Mining earth's heat: hot dry rock geothermal energy," *Technol. Rev.* **81**(4):58–78.

Dash, Z. V., and Murphy, H. D., 1981. "Summary of hot dry rock geothermal reservoir testing 1978 to 1980," in *Proceedings*, 7th annual workshop on geothermal reservoir engineering (December 16, 1981: Stanford, CA), pp. 97–102.

Dash, Z. V., and Murphy, H. D. (eds.), 1983. "Hot dry rock geothermal reservoir testing: 1978 to 1980," in *Geothermal Energy from Hot Dry Rock* (Heiken, G., and Goff, F., eds.), *J. Volcanol. Geotherm. Res.* special issue **15**(1–3):59–99.

Dash, Z. V., and Murphy, H. D., 1985. "Estimating fracture apertures from hydraulic data and comparison with theory," Geothermal Resources Council annual meeting (August 26–30, 1985: Kailua Kona, HI). *Trans. Geotherm. Resour. Counc.* **9**(II):493–496.

Dash, Z. V., Murphy, H. D., and Cremer, G. M. (eds.), 1981. "Hot dry rock geothermal reservoir testing: 1978–1980," Los Alamos National Laboratory report LA-9080-SR, 62 pp.

Dash, Z., Dennis, B., Dreesen, D., Fehler, M., Walter, F., and Zyvoloski, G., 1984. "Experiment 2042," Group ESS-4 internal memorandum ESS-4-84-326, Los Alamos, NM, 39 pp.

Dash, Z., Burns, K., Kelkar, S., Dreesen, D., House, L., Miller, J., Zyvoloski, G., and Murphy, H., 1985a. "Experiment 2061—the unsuccessful attempt to connect EE-3A to EE-2 by injection in EE-3A below a packer set at 12555 feet," Group ESS-4 internal memorandum ESS-4-85-205, Los Alamos, NM, 40 pp.

Dash, Z. V., Dreesen, D. S., Walter, F., and House, L., 1985b. "The massive hydraulic fracture of Fenton Hill HDR Well EE-3," Geothermal Resources Council annual meeting (August 26–30, 1985: Kailua Kona, HI). *Trans. Geotherm. Resour. Counc.* **9**(II):83–88.

Dash, Z. V., Aguilar, R. G., Dennis, B. R., Dreesen, D. S., Fehler, M. C., Hendron, R. H., House, L. S., Ito, H., Kelkar, S. M., Malzahn, M. V., Miller, J. R., Murphy, H. D., Phillips, W. S., Restine, S. B., Roberts, P. M., Robinson, B. A., and Romero, W. R. Jr., 1989. "ICFT: an initial closed-loop flow test of the Fenton Hill Phase II HDR reservoir," Los Alamos National Laboratory report LA-11498-HDR, Los Alamos, NM, 128 pp.

Demuth, R. B., and Harlow, F. H., 1979. "Thermal fracture effects in geothermal energy extraction," Los Alamos Scientific Laboratory report LA-7963, Los Alamos, NM, 148 pp.

Demuth, R. B., and Harlow, F. H., 1980. "Geothermal energy enhancement by thermal fracture," Los Alamos Scientific Laboratory report LA-8428, 66 pp.

Dennis, B. R., 1978. "Hot dry rock, an abundant, clean energy resource," in *Combined Environments: Technology Interrelations*, proceedings of the 24th Institute of Environmental Sciences technical meeting (April 18–20, 1978: Fort Worth, TX). A79-16076 04-38, pp. 300–306.

Dennis, B. R., 1980. "Borehole survey instrumentation development for geothermal applications," in *Transactions*, 21st annual symposium of the Society of Professional Well Log Analysts (July 8–11, 1980: Lafayette, LA). SPWLA, Houston, TX, pp. D1–D16.

Dennis, B. R., 1984. "Logging technology for high-temperature geothermal boreholes," in *Observation of the Continental Crust through Drilling I* (Raleigh, C. B., ed.), international symposium (May 20–25, 1984: Tarrytown, NY), pp. 174–181.

Dennis, B. R., 1985. "Earth science instrumentation update review," in *Proceedings*, Geothermal Energy Program Review IV (September 11, 1985: Washington, DC). U. S. Department of Energy document CONF-8509142, pp. 115–118.

Dennis, B. R. (comp.), 1986. "Symposium on high-temperature well-logging instrumentation" (November 13–14, 1985: Los Alamos, NM). Los Alamos National Laboratory report LA-10745-C, Los Alamos, NM, 117 pp.

Dennis, B. R., 1987. "What is required to make good measurements in a geothermal wellbore? A team," in *Proceedings*, Geothermal Energy Program Review V (April 14–15, 1987: Washington, DC). U. S. Department of Energy document CONF-8704110, pp. 165–170.

Dennis, B., 1990. "High-temperature borehole instrumentation developed for the DOE Hot Dry Rock Geothermal Energy Program," *Geotherm. Resour. Counc. Bull.* **19**(3):71–81.

Dennis, B. R., and Horton, E. H., 1980. "Hot dry rock, an alternate geothermal energy resource—a challenge for instrumentation," *Trans. Instrum. Soc. Am.* **19**(1):49–58.

Dennis, B. R., Potter, R., and Kolar, J., 1981. "Radioactive tracers used to characterize geothermal reservoirs," preprint, Geothermal Resources Council annual meeting (October 25–29, 1981: Houston, TX). Los Alamos Scientific Laboratory report LALP-81-48, Los Alamos, NM, pp. 1–4.

Dennis, B. R., Koczan, S., and Cruz, J., 1982. "High-temperature borehole instrumentation," 10th annual Instrument Society of America symposium on instrumentation and control systems (May 4, 1982: Denver, CO). CONF-820564-1, 13 pp.

Dennis, B. R., Koczan, S. P., and Stephani, E. L., 1985. "High-temperature borehole instrumentation," Los Alamos National Laboratory report LA-10558-HDR, Los Alamos, NM, 46 pp.

Dey, T. N., and Brown, D. W., 1986. "Stress measurements in a deep granitic rock mass using hydraulic fracturing and differential strain curve analysis," in *Proceedings*, international symposium on rock stress and rock stress measurements (September 1–3, 1986: Stockholm, Sweden). Centek Publishers, Lulea, Sweden, pp. 351–357.

Dillinger, W. H., Harding, S. T., and Pope, A. J., 1972. "Determining maximum likelihood body wave focal plane solutions," *Geophys. J. Roy. Astron. Soc.* **30**:315–329.

Dreesen, D. S., and Nicholson, R. W., 1985. "Well completion and operations for MHF of Fenton Hill HDR Well EE-2," Geothermal Resources Council annual meeting (August 26−30, 1985: Kailua Kona, HI). *Trans. Geotherm. Resour. Counc*. **9**(II):89–94.

Dreesen, D. S., Malzahn, M. V., Fehler, M. C., and Dash, Z. V., 1987. "Identification of MHF fracture planes and flow paths: a correlation of well log data with patterns in locations of induced seismicity," Geothermal Resources Council annual meeting (October 11–14, 1987: Sparks, NV). *Trans. Geotherm. Resour. Counc*. **11**:339–348.

Dreesen, D. S., Cocks, G. G., Nicholson, R. W., and Thomson, J. C., 1989. "Repair, sidetrack, drilling, and completion of EE-2A for Phase II reservoir production service," Los Alamos National Laboratory report LA-11647-MS, Los Alamos, NM, 67 pp.

Duchane, D. V., 1990. "Hot dry rock: a realistic energy option," *Geotherm. Resour. Counc. Bull.* **19**(3):83–88.

Duchane, D. V., 1991. "Commercialization of hot dry rock geothermal energy technology," Geothermal Resources Council annual meeting (October 6–9, 1991: Sparks, NV). *Trans. Geotherm. Resour. Counc.* **15**:325–331.

Duchane, D. V., 1991. "Hot dry rock heat mining: an alternative energy progress report," in *Proceedings*, international symposium on energy and environment (August 25–28, 1991: Espoo, Finland). CONF-910809-1, 17 pp.

Duchane, D. V., 1991. "International programs in hot dry rock technology development," *Geotherm. Resour. Counc. Bull.* **20**(5):135–142.

Duchane, D., 1991. "Moving HDR technology toward commercialization," in *The Geothermal Partnership—Industry, Utilities, and Government Meeting the Challenges of the 90's*, proceedings of Geothermal Energy Program Review IX (March 19–21, 1991: San Francisco, CA). U. S. Department of Energy document CONF-9103105, pp. 143–148.

Duchane, D. V., 1992. "Hot dry rock: a new energy source for clean power," Ch. 45 in *Proceedings*, 15th World Energy Engineering Congress (October 27–31, 1992: Atlanta, GA). pp. 265–270.

Duchane, D. V., 1992. "Hot dry rock heat mining: an advanced geothermal energy technology," in *Emerging Energy Technology—1992*, PD-Vol. 41 (Gollahalli, S. R., ed.), proceedings of the American Society of Mechanical Engineers energy sources technology conference and exhibition (January 26–30, 1992: Houston, TX). American Society of Mechanical Engineers, New York, NY, pp. 71–78.

Duchane, D. V., 1992. "HDR opportunities and challenges beyond the long-term flow test," in *Geothermal Energy and the Utility Market—the Opportunities and Challenges for Expanding Geothermal Energy in a Competitive Supply Market*, proceedings of Geothermal Energy Program Review X (March 24–26, 1992: San Francisco, CA). U. S. Department of Energy document CONF-920378, pp. 147–154.

Duchane, D. V., 1992. "Industrial applications of hot dry rock geothermal energy," international conference on industrial uses of geothermal energy (September 2–4, 1992: Reykjavik, Iceland). CONF-9209147-1, 9 pp.

Duchane, D. V., 1993. "Expectations for a second U. S. hot dry rock site," in *Hot Dry Rock Geothermal Energy for U. S. Electric Utilities*, proceedings of an EPRI workshop (January 14, 1993: Philadelphia, PA). Project RP1994-06, 5 pp.

Duchane, D. V., 1993. "Hot dry rock flow testing: What has it told us? What questions remain?" Geothermal Resources Council annual meeting, *Utilities and geothermal: an emerging partnership* (October 10–13, 1993: Burlingame, CA). *Trans. Geotherm. Resour. Counc.* **17**:325–330.

Duchane, D. V., 1993. "Hot dry rock: What does it take to make it happen?" in *Geothermal Energy—the Environmentally Responsible Energy Technology for the Nineties*, proceedings of Geothermal Energy Program Review XI (April 27–29, 1993: Berkeley, CA). *Geotherm. Resour. Counc. Bull.* **22**(8):204–207.

Duchane, D. V., 1993. "Next stages in HDR technology development," in *Hot Dry Rock Geothermal Energy for U. S. Electric Utilities*, proceedings of an EPRI workshop (January 14, 1993: Philadelphia, PA). Project RP1994-06, 7 pp.

Duchane, D., 1994a. "Geothermal energy," in Kirk-Othmer Encyclopedia of Chemical Technology, 4th edition, vol. 12. John Wiley & Sons, New York, pp. 512–539.

Duchane, D. V., 1994b. "Geothermal energy production from hot dry rock: operational testing at the Fenton Hill, New Mexico HDR test facility," in *Emerging Energy Technology—1994* (Karim, G. A., ed.), proceedings of the American Society of Mechanical Engineers energy sources technology conference and exhibition (January 23–26, 1994: New Orleans, LA). American Society of Mechanical Engineers, New York, NY, vol. 57.

Duchane, D. V., 1994c. "Heat mining to tap hot dry rock energy," Los Alamos National Laboratory report LALP-94-73, Los Alamos, NM, 4 pp.

Duchane, D. V., 1994d. "Hot dry rock: a climate change action opportunity for industry," in *Geothermal's Role in Global Climate Change—Impacts on the Climate Change Action Plan*, proceedings of Geothermal Energy Program Review XII (April 25–28, 1994: San Francisco, CA), 11 pp.

Duchane, D., 1994e. "Hot dry rock geothermal energy: moving towards practical applications," New Mexico conference on the environment (April 24–26, 1994: Albuquerque, NM). CONF-9404107-3, 10 pp.

Duchane, D., 1994f. "Status of the United States hot dry rock geothermal technology development program," *Chinetsu Gijutsu* (Japan) **19**(1 & 2):12–32.

Duchane, D. V., 1995a. "Heat mining to extract hot dry rock (HDR) geothermal energy: technical and scientific progress," in *Federal Geothermal Research Program Update, Fiscal Year 1994*, U. S. Department of Energy, Washington, DC, pp. 4.183–4.195.

Duchane, D. V., 1995b. "Heat mining to extract hot dry rock (HDR) geothermal energy: technology transfer activities," in *Federal Geothermal Research Program Update, Fiscal Year 1994*, U. S. Department of Energy, Washington, DC, pp. 4.197–4.203.

Duchane, D. V., 1995c. "Hot dry rock: a versatile alternative energy technology," annual technical conference and exhibition of the Society of Petroleum Engineers (October 22–25, 1995: Dallas, TX). SPE 30738, 10 pp.

Duchane, D., 1995d. "Hot dry rock geothermal energy in the USA—moving toward practical use," in *Worldwide Utilization of Geothermal Energy*: *an Indigenous, Environmentally Benign Renewable Energy Resource*, proceedings of the World Geothermal Congress (May 18–31, 1995: Florence, Italy). International Geothermal Association, Inc., Auckland, New Zealand, vol. 4, pp. 2613–2617.

Duchane, D. V., 1995e. "Hot dry rock in the United States: putting a unique technology to practical use," Geothermal Resources Council annual meeting (October 8–11, 1995: Reno, NV). *Trans. Geotherm. Resour. Counc*. **19**:257–261.

Duchane, D. V., 1995f. "Putting HDR technology to practical use," in *The Role of Cost-Shared R&D in the Development of Geothermal Resources*, proceedings of Geothermal Energy Program Review XIII (March 13–16, 1995: San Francisco, CA). U. S. Department of Energy document DOE/EE-0075, pp. 8.19–8.26.

Duchane, D., 1996a. "Focus of the Hot Dry Rock Program after restructuring," in *Keeping Geothermal Energy Competitive in Foreign and Domestic Markets*, proceedings of Geothermal Energy Program Review XIV (April 8–10, 1996: Berkeley, CA). U. S. Department of Energy document DOE/EE-0106, pp. 89–95.

Duchane, D. V., 1996b, "Geothermal energy from hot dry rock: a renewable energy technology moving towards practical application," in *Renewable Energy* Vol. II (A. A. M. Sayigh, ed.), World Renewable Energy Congress on energy efficiency and the environment (June 15–21, 1996: Denver, CO), pp. 1246–1249.

Duchane, D. V., 1996c. "Heat mining to extract hot dry rock geothermal energy: technical and scientific progress," in *Federal Geothermal Research Program Update, Fiscal Year 1995*, U. S. Department of Energy, Washington, DC, pp. 4.215–4.230.

Duchane, D., 1996d. "Hydrothermal applications of hot dry rock technology," *Trans. Geotherm. Resour. Counc.* **20**:453–456.

Duchane, D. V., 1996e. "Progress in making hot dry rock geothermal energy a viable renewable energy resource for America in the 21st century," 31st Intersociety and Energy Conversion Engineering Conference (August 11–16, 1996: Washington, DC). Vol. 3, IEEE, Piscataway, NJ, pp. 1628–1632.

Duchane, D., 2002. "The history of HDR research and development," in *Geologisches Jahrbuch* special edition (Baria, R., Baumgärtner, J., Gérard, A., and Jung, R., eds.), international conference—4th HDR forum (September 28–30, 1998: Strasbourg, France). Hannover, Germany, pp. 7–17.

Duchane, D. V., Brown, D. W., House, L., Robinson, B. A., and Ponden, R., 1990a. "Progress in hot dry rock technology development," Geothermal Resources Council annual meeting and international symposium on geothermal energy (August 20–24, 1990: Kailua Kona, HI). *Trans. Geotherm. Resour. Counc.* **14**(II), Davis, CA, pp. 555–559.

Duchane, D. V., Brown, D. W., Robinson, B. A., and Ponden, R., 1990b. "Status of the hot dry rock geothermal energy development program at Los Alamos," in *The National Energy Strategy—the Role of Geothermal Technology Development*, proceedings of Geothermal Energy Program Review VIII (April 17–20, 1990: San Francisco, CA). U. S. Department of Energy document CONF-9004131, pp. 101–108.

Duffy, C. J., 1980. Unpublished data.

DuTeau, R., 1993. "A potential for enhanced energy production by periodic pressure stimulation of the production well in an HDR reservoir," Geothermal Resources Council annual meeting, *Utilities and Geothermal: an Emerging Partnership* (October 10–13, 1993: Burlingame, CA). *Trans. Geotherm. Resour. Counc*. **17**:331–334.

DuTeau, R., and Brown, D., 1993. "HDR reservoir flow impedance and potentials for impedance reduction," in *Proceedings*, 18th annual workshop on geothermal reservoir engineering (January 26–28, 1993: Stanford, CA). SGP-TR-145, pp. 193–197.

DuTeaux, R., Swenson, D., and Hardeman, B., 1996a. "Insight from modeling discrete fractures using GEOCRACK," in *Proceedings*, 21st workshop on geothermal reservoir engineering (January 22–24, 1996: Stanford, CA). SGP-TR-151, pp. 287–293.

DuTeaux, R., Swenson, D., and Hardeman, B., 1996b. "Modeling the use of tracers to predict changes in surface area and thermal breakthrough in HDR reservoirs," in *Proceedings*, 3rd international HDR forum (May 13–16, 1996: Santa Fe, NM), pp. 41–44.

Dyer, B. C., Schanz, U., Ladner, F., Häring, M. O., and Pillman, T. S., 2008. "Microseismic imaging of a geothermal reservoir stimulation," in *The Leading Edge* (Society of Exploration Geophysicists, Tulsa, OK), pp. 856–869.

East, J., 1981. "Hot dry rock geothermal potential of Roosevelt Hot Springs area: review of data and recommendations," Los Alamos National Laboratory report LA-8751-HDR, Los Alamos, NM, 46 pp.

Elsworth, D., 1990. "Lifetime calculations for multiple stimulated HDR reservoirs," in *Hot Dry Rock Geothermal Energy* (Baria, R., ed.), proceedings of the Camborne School of Mines international hot dry rock conference (June 27–30, 1989: Redruth, Cornwall, UK). Robertson Scientific Publications, London, pp. 487–497.

Evans, K., Cornet, F., Hayashi, K., Hashida, T., Ito, T., Matsuki, K., and Wallroth, T., 1999. "Stress and rock mechanics issues of relevance to HDR/HWR engineered geothermal systems: review of developments during the past 15 years," in *Hot Dry Rock/Hot Wet Rock Academic Review* (Abé, H., Niitsuma, H., and Baria, R., eds.), *Geothermics* special issue **28**(4/5):455–474.

Fehler, M. C., 1984. "Microseismic Analysis Review Panel summary report," ESS Division internal report ESS-84-002-DS, Los Alamos, NM, 25 pp.

Fehler, M., 1987. "A new method for determining dominant fluid flow paths during hydraulic fracturing," in *Proceedings*, Geothermal Energy Program Review V (April 14–15, 1987: Washington, DC). U. S. Department of Energy document CONF-8704110, pp. 153–156.

Fehler, M., 1989. "Stress control of seismicity patterns observed during hydraulic fracturing experiments at the Fenton Hill hot dry rock geothermal energy site, New Mexico," *Int. J. Rock Mech. Min. Sci. & Geomech. Abstr.* **26**(3–4):211–219.

Fehler, M., and Bame, D., 1985. "Characteristics of microearthquakes accompanying hydraulic fracturing as determined from studies of spectra of seismic waveforms," Geothermal Resources Council annual meeting (August 26–30, 1985: Kailua Kona, HI). *Trans. Geotherm. Resour. Counc*. **9**(II):11–16.

Fehler, M., and Phillips, W. S., 1991. "Simultaneous inversion for Q and source parameters of microearthquakes accompanying hydraulic fracturing in granitic rock," *Bull. Seism. Soc. Am.* **81**:553–575.

Fehler, M., and Rutledge, J., 1995. "Using seismic tomography to characterize fracture systems induced by hydraulic fracturing," SEGJ/SEG international symposium on geotomography (November 8–10, 1995: Tokyo, Japan). CONF-9511148-1, 8 pp.

Fehler, M., House, L., and Kaieda, H., 1987. "Determining planes along which earthquakes occur: method and application to earthquakes accompanying hydraulic fracturing," *J. Geophys. Res.* **92**(B9):9407–9414.

Ferrazini, V., Chouet, B., Fehler, M., and Aki, K., 1990. "Quantitative analysis of long-period events recorded during hydraulic fracturing experiments at Fenton Hill, New Mexico," *J. Geophys. Res.* **95**(B13):21871–21884.

Franke, P. R., 1979. "Hot dry rock geothermal energy development program," 2nd Miami international conference on alternative energy sources (December 10, 1979: Miami Beach, FL). CONF-791204-3, 16 pp.

Franke, P. R., 1988. "The U. S. hot dry rock geothermal energy development program," 11th annual symposium on geothermal energy (January 10–14, 1988: New Orleans, LA). American Society of Mechanical Engineers, New York, NY, CONF-880104, pp. 11–16.

Franke, P. R., and Nunz, G. J., 1985. "Recent developments in the hot dry rock geothermal energy program," Geothermal Resources Council annual meeting (August 26−30, 1985: Kailua Kona, HI). *Trans. Geotherm. Resour. Counc.* **9**(II):95–98.

Gérard, A., Genter, A., Kohl, T., Lutz, P., Rose, P., and Rummel, F., 2006. "The deep EGS (Enhanced Geothermal System) project at Soultz-sous-Forêts (Alsace, France)," *Geothermics* **35**(5):473–483.

Goff, F., and Decker, E. R., 1983. "Candidate sites for future hot dry rock development in the United States," in *Geothermal Energy from Hot Dry Rock* (Heiken, G., and Goff, F., eds.), *J. Volcanol. Geotherm. Res.* special issue **15**(1–3):187–221.

Gosnold, W. D. Jr., and German, K. E. Jr., 1983. "Geothermal investigations in Nebraska," in *Workshop on Exploration for Hot Dry Rock Geothermal Systems* (Heiken, G. H., Shankland, T. J., and Ander, M. E., comp.), June 21, 1982: Los Alamos, NM. Los Alamos National Laboratory report LA-9697-C, Los Alamos, NM, pp. 75–81.

Green, A. S. P., Pine, R. J., and Jupe, A., 1990. "*In situ* stress measurements in deep wells," in *Hot Dry Rock Geothermal Energy* (Baria, R., ed.), proceedings of the Camborne School of Mines international hot dry rock conference (June 27–30, 1989: Redruth, Cornwall, UK). Robertson Scientific Publications, London, pp. 85–97.

Grigsby, C. O., and Tester, J. W., 1989. "Rock-water interactions in the Fenton Hill, New Mexico, hot dry rock geothermal systems II: modeling geochemical behavior," *Geothermics* **18**(5/6):657–676.

Grigsby, C. O., Tester, J. W., Trujillo, P. E., Counce, D. A., Abbott, J., Holley, C. E., and Blatz, L. A., 1983. "Rock-water interactions in hot dry rock geothermal systems: field investigations of *in situ* geochemical behavior," in *Geothermal Energy from Hot Dry Rock* (Heiken, G., and Goff, F., eds.), *J. Volcanol. Geotherm. Res.* special issue **15**(1–3):101–136.

Grigsby, C. O., Tester, J. W., Trujillo, P. E., and Counce, D. A., 1989. "Rock-water interactions in the Fenton Hill, New Mexico, hot dry rock geothermal systems I: fluid mixing and chemical geothermometry," *Geothermics* **18**(5/6):629–656.

Harlow, F. H., and Pracht, W. E., 1972. "A theoretical study of geothermal energy extraction," *J. Geophys. Res.* **77**(35):7038–7048.

Harrison, R., Doherty, P., and Coulson, I., 1990. "HDR cost modelling," in *Hot Dry Rock Geothermal Energy* (Baria, R., ed.), proceedings of the Camborne School of Mines international hot dry rock conference (June 27–30, 1989: Redruth, Cornwall, UK). Robertson Scientific Publications, London, pp. 245–261.

Harvey, D. J., 1979. "LASL manages the national program," *The Atom*, Los Alamos Scientific Laboratory, Los Alamos, NM, 4 pp.

HDR (Hot Dry Rock Geothermal Energy Development Project), 1976. "Annual report, July 1975–June 1976," (Pettitt, R. A., ed.), Los Alamos Scientific Laboratory report LA-6504-SR, Los Alamos, NM, 92 pp.

HDR (Hot Dry Rock Geothermal Energy Development Project), 1978. "Annual report, fiscal year 1977," (LASL HDR Project staff, eds.), Los Alamos Scientific Laboratory report LA-7109-PR, Los Alamos, NM, 294 pp.

HDR (Hot Dry Rock Geothermal Energy Development Program), 1979. "Annual report, fiscal year 1978" (Brown, M. C., Smith, M. C., Siciliano, C. L. B., and Duffield, R. B., eds.), Los Alamos Scientific Laboratory report LA-7807-HDR, Los Alamos, NM, 132 pp.

HDR (Hot Dry Rock Geothermal Energy Development Program), 1980. "Annual report, fiscal year 1979 " (Cremer, G. M., Wilson, M. G., Smith, M. C., and Duffield, R. B., eds.), Los Alamos Scientific Laboratory report LA-8280-HDR, Los Alamos, NM, 255 pp.

HDR (Hot Dry Rock Geothermal Energy Development Program), 1981. "Annual report, fiscal year 1980" (Cremer, G. M., ed.), Los Alamos National Laboratory report LA-8855-HDR, Los Alamos, NM, 211 pp.

HDR (Hot Dry Rock Geothermal Energy Development Program), 1982. "Annual report, fiscal year 1981" (Smith, M. C., and Ponder, G. M., eds.), Los Alamos National Laboratory report LA-9287-HDR, Los Alamos, NM, 140 pp.

HDR (Hot Dry Rock Geothermal Energy Development Program), 1983a. "Annual operating plan, fiscal year 1984" (Nunz, G. J., Franke, P. R., and Brown, D. W., comp.), Los Alamos National Laboratory report HDR-84-AOP-01, Los Alamos, NM, 58 pp.

HDR (Hot Dry Rock Geothermal Energy Development Program), 1983b. "Annual report, fiscal year 1982" (Smith, M. C., Nunz, G. J., and Ponder, G. M., eds.), Los Alamos National Laboratory report LA-9780-HDR, Los Alamos, NM, 127 pp.

HDR (Hot Dry Rock Geothermal Energy Development Program), 1985. "Annual report, fiscal year 1983" (Smith, M. C., Nunz, G. J., and Wilson, M. G., eds.), Los Alamos National Laboratory report LA-10347-HDR, Los Alamos, NM, 91 pp.

HDR (Hot Dry Rock Geothermal Energy Development Program), 1986a. "Annual operating plan, fiscal year 1986" (Franke, P. R., Brown, D. W., and Hendron, R. H., comp.), Los Alamos National Laboratory report HDR-86-AOP-02, Los Alamos, NM, 41 pp.

HDR (Hot Dry Rock Geothermal Energy Development Program), 1986b. "Annual operating plan, fiscal year 1987" (Franke, P. R., and Hendron, R. H., comp.), Los Alamos National Laboratory report HDR-87-AOP-01, Los Alamos, NM, 41 pp.

HDR (Hot Dry Rock Geothermal Energy Development Program), 1986c. "Annual report, fiscal year 1984" (Franke, P. R., Brown, D. W., Smith, M. C., and Mathews, K. L., eds.), Los Alamos National Laboratory report LA-10661-HDR, Los Alamos, NM, 31 pp.

HDR (Hot Dry Rock Geothermal Energy Development Program), 1986d. Program Development Council, Minutes of meeting, July 15, 1986, Albuquerque, NM, 94 pp.

HDR (Hot Dry Rock Geothermal Energy Development Program), 1987. "Annual report, fiscal year 1985" (Brown, D. W., Franke, P. R., Smith, M. C., and Wilson, M. G., eds.), Los Alamos National Laboratory report LA-11101-HDR, Los Alamos, NM, 23 pp.

HDR (Hot Dry Rock Geothermal Energy Development Program), 1988a. "Annual operating plan, fiscal year 1988," (Franke, P. R., Hendron, R. H., and Murphy, H. D., comp.), Los Alamos National Laboratory report HDR-88-AOP-02, Los Alamos, NM, 40 pp.

HDR (Hot Dry Rock Geothermal Energy Development Program), 1988b. "Annual report, fiscal year 1988" (Dash, Z. V., Murphy, H. D., and Smith, M. C., eds.), Los Alamos National Laboratory report LA-UR-88-4193, Los Alamos, NM, 82 pp.

HDR (Hot Dry Rock Geothermal Energy Development Program), 1988c. "Annual operating plan, fiscal year 1989," (Franke, P. R., Hendron, R. H., and Murphy, H. D., comp.), Los Alamos National Laboratory report HDR-89-AOP-04, Los Alamos, NM, 40 pp.

HDR (Hot Dry Rock Geothermal Energy Development Program), 1989a. "Annual report, fiscal year 1986" (Dash, Z. V., Grant, T., Jones, G., Murphy, H. D., and Wilson, M. G., eds.), Los Alamos National Laboratory report LA-11379-HDR, Los Alamos, NM, 32 pp.

HDR (Hot Dry Rock Geothermal Energy Development Program), 1989b. "Annual report, fiscal year 1987" (Smith, M. C., Hendron, R. H., Murphy, H. D., and Wilson, M. G., eds.), Los Alamos National Laboratory report LA-11717-HDR, Los Alamos, NM, 55 pp.

HDR (Hot Dry Rock Geothermal Energy Development Program), 1990. "Annual report, fiscal year 1989" (Albright, J. N., Dash, Z. V., Hendron, R. H., and Smith, M. C., eds.), Los Alamos National Laboratory report LA-UR-90-230, Los Alamos, NM, 58 pp.

HDR (Hot Dry Rock Geothermal Energy Development Program), 1991. "Annual report, fiscal year 1990" (Duchane, D. V., ed.), Los Alamos National Laboratory report HDR-90-Annual Report, Los Alamos, NM, 66 pp.

HDR (Hot Dry Rock Geothermal Energy Development Program), 1992. "Annual report, fiscal year 1991" (Duchane, D., ed.). Los Alamos National Laboratory report LA-UR-92-870, Los Alamos, NM, 72 pp.

HDR (Hot Dry Rock Geothermal Energy Development Program), 1993. "Hot dry rock energy: Progress report, fiscal year 1992" (Winchester, W. W., ed.), Los Alamos National Laboratory report LA-UR-93-1678, Los Alamos, NM, 69 pp.

HDR (Hot Dry Rock Geothermal Energy Development Program), 1995. "Hot dry rock energy: Progress report, fiscal year 1993" (Salazar, J., and Brown, M., eds.) Los Alamos National Laboratory report LA-12903-PR, Los Alamos, NM, 40 pp.

Heiken, G., and Sayer, S., 1980. "Bibliography of the geological and geophysical aspects of hot dry rock geothermal resources," Los Alamos Scientific Laboratory report LA-8222-HDR, Los Alamos, NM, 51 pp.

Heiken, G., Murphy, H., Nunz, G., Potter, R., and Grigsby, C., 1981. "Hot dry rock geothermal energy," *American Scientist* **69**(4):400–407.

Heiken, G., Goff, F., and Cremer, G. (eds.), 1982. "Hot dry rock geothermal resource 1980," Los Alamos National Laboratory report LA-9295-HDR, Los Alamos, NM, 113 pp.

Helmick, C., Koczan, S., and Pettitt, R., 1982. "Planning and drilling geothermal Energy Extraction Hole EE-2: a precisely oriented and deviated hole in hot granitic rock," Los Alamos National Laboratory report LA-9302-HDR, Los Alamos, NM, 135 pp.

Hendron, R. H., 1978. "Hot dry rock energy project," international conference on alternative energy sources, *Geothermal energy and hydropower* (December 5, 1977: Miami Beach, FL). Vol. 6, Hemisphere Publishing Corp., Washington, DC, pp. 2655–2687.

Hendron, R. H., 1981. "Energy from hot dry rock," in *Proceedings*, international conference on long-term energy resources (November 26–December 7, 1979: Montreal, Canada). Pitman Publishing Co., Boston, MA, pp. 1617–1637.

Hendron, R. H., 1987. "Operations and flow testing at Fenton Hill," in *Proceedings*, Geothermal Energy Program Review V (April 14–15, 1987: Washington, DC). U. S. Department of Energy document CONF-8704110, pp. 143–151.

Hendron, R. H., 1988. "Hot dry rock at Fenton Hill, USA," international workshop on hot dry rock, *Creation and evaluation of geothermal reservoirs* (November 4, 1988: Tsukuba City, Japan). CONF-881196-1, 20 pp.

Herzog, H., Tester, J., and Frank, M., 1995. "Economic analysis of heat mining," in *Worldwide Utilization of Geothermal Energy: an Indigenous, Environmentally Benign Renewable Energy Resource*, proceedings of the World Geothermal Congress (May 18–31, 1995: Florence, Italy). International Geothermal Association, Inc., Auckland, New Zealand, vol. 4, pp. 2521–2527.

Hicks, T. W., Pine, R., Willis-Richards, J., Xu, S., Jupe, A., and Rodrigues, N., 1996. "A hydro-thermo-mechanical numerical model for HDR geothermal reservoir evaluation," *Int. J. Rock Mech. Min. Sci. & Geomech. Abstr.* **33**:499–511.

Hoffers, B., 1983. "Experiment 2018, first fracturing attempt below casing shoe in EE-2," Group ESS-4 internal memorandum ESS-4-83-81, Los Alamos, NM, 21 pp.

Holley, C. E. Jr., 1981. "Chemistry and the Los Alamos hot dry rock geothermal power project," *N.M. J. Sci.* **21**(1):1–9.

Holley, C. E. Jr., Blatz, L. A., Charles, R. W., Grigsby, C. O., and Tester, J. W., 1978. "Enhanced chemical dissolution of granite" (abstract), in *Proceedings* (Elsner, D. B., comp.), hot dry rock geothermal workshop (April 20, 1978: Los Alamos, NM). Los Alamos Scientific Laboratory report LA-7470-C, p. 49.

Holley, C., Charles, R., Blatz, L., Tester, J., Grigsby, C., and Campbell, A., 1980. "Interaction of water with crystalline basement rock in fractured hot dry rock geothermal reservoirs: tests and laboratory experiments," 3rd international symposium on water−rock interaction (July 14, 1980: Edmonton, Alberta, Canada). CONF-800718-1, pp. 161–162.

House, L., 1987. "Locating microearthquakes induced by hydraulic fracturing in crystalline rock," *Geophys. Res. Lett.* **14**(9):919–921.

House, L., and Fehler, M., 1988. "Microseismic mapping of an HDR reservoir: exploration and development of geothermal resources," International symposium on geothermal energy (November 10–14, 1988: Kumamoto, Japan). *J. Geotherm. Res. Soc. Japan*, pp. 359–362.

House, L., Keppler, H., and Kaieda, H., 1985. "Seismic studies of a massive hydraulic fracturing experiment," Geothermal Resources Council annual meeting (August 26−30, 1985: Kailua Kona, HI). *Trans. Geotherm. Resour. Counc*. **9**(II):105–110.

House, L. S., Fehler, M. C., and Phillips, W. S., 1992. "Studies of seismicity induced by hydraulic fracturing in a geothermal reservoir," in *Workshop on Induced Seismicity* (Ramseyer, C., ed.), proceedings of the 33rd U. S. symposium on rock mechanics (June 10, 1992: Santa Fe, NM), pp. 186–189.

Kaufman, E. L., and Siciliano, C. L. B., 1979. "Environmental analysis of the Fenton Hill hot dry rock geothermal test site," Los Alamos Scientific Laboratory report LA-7830-HDR, Los Alamos, NM, 63 pp.

Kelkar, S. M., 1985. "Expt. 2059 (the connection), EE-3A packer test #3 hydraulic data," Group ESS-4 internal memorandum ESS-4-85-150, Los Alamos, NM, 23 pp.

Kelkar, S., and Malzahn, M. V., 1987. "Recent U. S. hot dry rock reservoir testing and hydrothermal modeling," conference on forced flow through fractured rock masses (April 1987: Garcy, France). CONF-8704111-2, 15 pp.

Kelkar, S. M., Zyvoloski, G. A., and Dash, Z. V., 1986. "Pressure testing of a high temperature naturally fractured reservoir," in *Proceedings*, 11th annual workshop on geothermal reservoir engineering (January 21, 1986: Stanford, CA), pp. 59–63.

Kelkar, S., Dash, Z., Malzahn, M., and Hendron, R., 1987. "Hydraulic and thermal behavior of a hot dry rock reservoir during a 30-day circulation test," Geothermal Resources Council annual meeting (October 11–14, 1987: Sparks, NV). *Trans. Geotherm. Resour. Counc.* **11**:547–552.

Keppler, H., Pearson, C. F., Potter, R. M., and Albright, J. N., 1983. "Microearthquakes induced during hydraulic fracturing at the Fenton Hill HDR site: the 1982 experiments," *Trans. Geotherm. Resour. Counc.* **7**:429–433.

Khilar, K. L., and Folger, H. S., 1984. "The existence of a critical salt concentration for particle release," *J. Colloid. and Interface Sci.* **101**(1):214–224.

Kintzinger, P. R., West, F. G., and Aamodt, R. L., 1977. "Downhole electrical detection of hydraulic fractures in GT-2 and EE-1," Los Alamos Scientific Laboratory report LA-6890-MS, Los Alamos, NM, 13 pp.

Kowallis, B. J., and Wang, H. F., 1983. "Microcrack study of granitic cores from Illinois Deep Borehole UPH 3," *J. Geophys. Res*. **88**:7373–7380.

Kron, A., and Stix, J., 1982. "Geothermal gradient map of the United States," National Geophysical Data Center, National Oceanic and Atmospheric Administration, Boulder, CO (for the Los Alamos National Laboratory, Los Alamos, NM).

Kron, A., Wohletz, K., and Tubb, J., 1991. "Geothermal gradient contour map of the United States," Los Alamos National Laboratory, Los Alamos, NM.

Kruger, P., 1990. "Heat extraction from microseismic estimated geothermal reservoir volume," *Trans. Geotherm. Resour. Counc.* **14**:1225–1232.

Kruger, P., 1995. "Heat extraction from HDR geothermal reservoirs," in *Worldwide Utilization of Geothermal Energy: an Indigenous, Environmentally Benign Renewable Energy Resource*, proceedings of the World Geothermal Congress (May 18–31, 1995: Florence, Italy). International Geothermal Association, Inc., Auckland, New Zealand, vol. 4, pp. 2517–2520.

Landt, J. A., Koelle, A. R., Trump, M. A., and Nickell, J. D. Jr., 1978. "A magnetic induction technique for mapping vertical conductive fractures: electronic design," Los Alamos Scientific Laboratory informal report LA-7426-MS, Los Alamos, NM, 17 pp.

Laney, R., Laughlin, A. W., and Aldrich, M. J. Jr., 1981. "Geology and geochemistry of samples from Los Alamos National Laboratory HDR Well EE-2, Fenton Hill, New Mexico," Los Alamos National Laboratory report LA-8923-MS, Los Alamos, NM, 33 pp.

Laughlin, A. W., and Eddy, A. C., 1977. "Petrography and geochemistry of Precambrian rocks from GT-2 and EE-1," Los Alamos Scientific Laboratory report LA-6930-MS, Los Alamos, NM, 50 pp.

Laughlin, A. W., Eddy, A. C., Laney, R., and Aldrich, M. J. Jr., 1983. "Geology of the Fenton Hill, New Mexico, hot dry rock site," in *Geothermal Energy from Hot Dry Rock* (Heiken, G., and Goff, F., eds.), *J. Volcanol. Geotherm. Res.* special issue **15**(1–3):21–41.

Lehner, F. K., and Bataille, J., 1984. *Nonequilibrium Thermodynamics of Pressure Solutions*, Report No. 25, Division of Engineering, Brown University, Providence, RI, 52 pp.

Levy, S., 2010. "Subsurface geology of the Fenton Hill hot dry rock geothermal energy site," Los Alamos National Laboratory report LA-14434-HDR, Los Alamos, NM, 101 pp.

Liu, J., and Badalamente-Alexander, T. M., 1988. "Geothermal power generation options for Fenton Hill reservoir testing," Los Alamos National Laboratory report LA-11470-MS, Los Alamos, NM (available from NTIS, Springfield, VA), 134 pp.

Maceira, M., Rowe, C. A., Beroza, G., and Anderson, D., 2010. "Identification of low-frequency earthquakes in non-volcanic tremor using the subspace detector method," *Geophys. Res. Lett.* 37, L06303, doi:10.1029/2009GL041876, 2010.

Malzahn, M., Dreesen, D. S., and Fehler, M. C., 1988. "Locating hydraulically active fracture planes," in *Proceedings*, 13th annual workshop on geothermal reservoir engineering (January 19–21, 1988: Stanford, CA). SGP-TR-113, pp. 231–237.

Matsunaga, I., Kadowaki, M., and Murphy, H., 1983. "Current summary of hydraulic fracturing experiments in Phase II reservoir," Group ESS-4 internal memorandum ESS-4-83-80, Los Alamos, NM, 32 pp.

McFarland, R. D., 1975. "Geothermal reservoir models: crack plane model," Los Alamos Scientific Laboratory report LA-5947-MS, Los Alamos, NM, 18 pp.

McFarland, R. D., and Murphy, H. D., 1976. "Extracting energy from hydraulically fractured geothermal reservoirs," in *Proceedings*, 11th intersociety energy conversion engineering conference (September 12–17, 1976: State Line, NV). Vol. 1, American Institute of Chemical Engineers, New York, pp. 828–835.

McGarr, A., 1976. "Seismic moments and volume changes," *J. Geophys. Res.* **81**:1487–1494.

McNamara, J. J., and Kaufman, E. L., 1979. "Hot dry rock geothermal resource ownership and the law," Los Alamos Scientific Laboratory report LA-8027-HDR, Los Alamos, NM, 39 pp.

Miera, F. R. Jr., Montoya, C., McEllin, S., and Langhorst, G., 1984. "Environmental studies conducted at the Fenton Hill hot dry rock geothermal development site," Los Alamos National Laboratory report LA-9967-MS, Los Alamos, NM, 20 pp.

Milora, S. L., and Tester, J. W., 1976. Geothermal Energy as a Source of Electric Power, Massachusetts Institute of Technology Press, Cambridge, MA, 186 pp.

MIT (Massachusetts Institute of Technology), 2006. *The Future of Geothermal Energy*. Prepared for the U. S. Dept. of Energy under Idaho National Laboratory subcontract 63 00019; DOE Idaho Operations Office contract DE-AC07-05ID14517. Idaho Falls, ID. Available at http://www1.eere.energy.gov/geothermal/egs_technology.html

Mock, J. E., 1990. "The U. S. hot dry rock program (USA)," in *Hot Dry Rock Geothermal Energy* (Baria, R., ed.), proceedings of the Camborne School of Mines international hot dry rock conference (June 27–30, 1989: Redruth, Cornwall, UK). Robertson Scientific Publications, London, pp. 149–158.

Mortensen, J. J., (comp.), 1977. *Proceedings*, 2nd NATO-CCMS information meeting on dry hot rock geothermal energy (June 28, 1977: Los Alamos, NM). Los Alamos Scientific Laboratory report LA-7021-C, 77 pp.

Mortensen, J. J., 1978. "Hot dry rock: a new geothermal energy source," *Energy* (Oxford) **3**(5):639–644.

Mortimer, N. D., and Minett, S. T., 1990. "Hot dry rock geothermal energy cost modelling: drilling and stimulation results," in *Hot Dry Rock Geothermal Energy* (Baria, R., ed.), proceedings of the Camborne School of Mines international hot dry rock conference (June 27–30, 1989: Redruth, Cornwall, UK). Robertson Scientific Publications, London, pp. 224–244.

Muffler, L. J. P. (ed.), 1979. *Assessment of Geothermal Resources of the United States—1978*, U. S. Geological Survey circular C 790, Reston, VA, 163 pp.

Murphy, H. D., 1979. "Hot dry rock geothermal heat extraction experiments," Geothermal Resources Council annual meeting (September 24, 1979: Reno, NV). Los Alamos Scientific Laboratory report LASL-79-75, Los Alamos, NM, 5 pp.

Murphy, H. D., 1979. "Thermal stress cracking and the enhancement of heat extraction from fractured geothermal reservoirs," *Geothermal Energy* **7**(3):22–29.

Murphy, H., 1980. "Pressure losses in fracture-dominated reservoirs: the wellbore constriction effect," Geothermal Institute 1980 workshop (November, 1980: Auckland, New Zealand). CONF-801123-1, 7 pp.

Murphy, H., 1984. "Experiment 2032 report," Group ESS-4 internal memorandum ESS-4-84-70, Los Alamos, NM, 53 pp.

Murphy, H. D., 1985. "Hot dry rock Phase II reservoir engineering," in *Proceedings*, Geothermal Energy Program Review IV (September 11, 1985: Washington, DC). U. S. Department of Energy document CONF-8509142, pp. 91–96.

Murphy, H., 1987. "Highlights of the hot dry rock program," in *Proceedings*, Geothermal Energy Program Review V (April 14–15, 1987: Washington, DC). U. S. Department of Energy document CONF-8704110, pp. 139–142.

Murphy, H., 1987. "Hot dry rock reservoir engineering," NATO Advanced Study Institute on geothermal reservoir engineering (July 1–10, 1987: Antalya, Turkey). *NATO ASI Series E: Applied Sciences* No. 150, Noordhoff International Publishing, Leiden, Netherlands, pp. 177–193.

Murphy, H. D., and Tester, J. W., 1979. "Heat production from a geothermal reservoir formed by hydraulic fracturing—comparison of field and theoretical results," 54th annual conference and exhibition of the Society of Petroleum Engineers (September 23–26, 1979: Las Vegas, NV). SPE 8265, 10 pp.

Murphy, H., and Dash, Z., 1985. "The shocking behavior of fluid flow in deformable joints," Geothermal Resources Council annual meeting (August 26–30, 1985: Kailua Kona, HI). *Trans. Geotherm. Resour. Counc*. **9**(II):115–118.

Murphy, H. D., and Fehler, M. C., 1986. "Hydraulic fracturing of jointed formations," in *Proceedings*, Society of Petroleum Engineers international meeting on petroleum engineering (March 17, 1986: Beijing, China). Vol. 1, Society of Petroleum Engineers of AIME, Dallas, TX, pp. 489–496.

Murphy, H. D., Lawton, R. G., Tester, J. W., Potter, R. M., Brown, D. W., and Aamodt, R. L., 1977. "Preliminary assessment of a geothermal energy reservoir formed by hydraulic fracturing," *Soc. Pet. Eng. J.* **17**(4):317–326.

Murphy, H. D., Grigsby, C. O., Tester, J. W., and Albright, J. N., 1978. "Evaluation of the Fenton Hill hot dry rock geothermal reservoir: Part I. Heat extraction performance and modeling; Part II. Flow characteristics and geochemistry; Part III. Reservoir characterization using acoustic techniques," 4th annual workshop on geothermal reservoir engineering (December 13–15, 1978: Stanford, CA). SGP-TR-30, pp. 243–263.

Murphy, H. D., Aamodt, R. L., Albright, J. N., Becker, N., Brown, D. W., Butler, R., Counce, D., Fisher, H., Grigsby, C. O., Hendron, R. H., Pearson, C., Potter, R. M., Tester, J. W., Trujillo, P. E., and Zyvoloski, G., 1980a. "Preliminary evaluation of the second hot dry rock geothermal energy reservoir: results of Phase I, Run Segment 4," Los Alamos Scientific Laboratory report LA-8354-MS, Los Alamos, NM, 88 pp.

Murphy, H. D., Potter, R. M., Grigsby, C. O., and Tester, J. W., 1980b. "*In situ* heat transfer in man-made geothermal energy reservoirs," 19th national heat transfer conference (July 27, 1980: Orlando, FL). CONF-800723-17, 39 pp.

Murphy, H. D., Potter, R. M., and Tester, J. W., 1980c. "Comparison of two hot dry rock geothermal reservoirs," in *Proceedings*, 6th annual workshop on geothermal reservoir engineering (December 16–18, 1980: Stanford, CA), pp. 272–278.

Murphy, H. D., Aamodt, R., Fisher, H., Grant, T., Grigsby, C., Hendron, R., Keppler, H., Pearson, C., Potter, R., Suhr, G., and Zyvoloski, G., 1981a. "Relaxation of geothermal reservoir stresses induced by heat production" (Murphy, H. D., ed.), Los Alamos National Laboratory report LA-8954-MS, Los Alamos, NM, 33 pp.

Murphy, H., Fisher, H., Grigsby, C., and Aamodt, R. L., 1981b. "Growth of hot dry rock reservoirs" (abstract), in *Proceedings*, 5th annual EPRI geothermal conference and workshop (June 23–25, 1981: San Diego, CA). Electric Power Research Institute document EPRI-AP-2098, Palo Alto, CA, p. 3.29.

Murphy, H. D., Tester, J. W., Grigsby, C. O., and Potter, R. M., 1981c. "Energy extraction from fractured geothermal reservoirs in low-permeability crystalline rock," *J. Geophys. Res.* **86**(B8):7145–7158.

Murphy, H., Zyvoloski, G., Tester, J., and Drake, R., 1982. "Economics of a 75-MW(e) hot-dry-rock geothermal power station based upon the design of the Phase II reservoir at Fenton Hill," Los Alamos National Laboratory report LA-9241-MS, Los Alamos, NM, 39 pp.

Murphy, H., Keppler, H., and Dash, Z., 1983. "Does hydraulic fracturing theory work in jointed rock masses?" *Trans. Geotherm. Resour. Counc.* **7**:461–466.

Murphy, H., Zyvoloski, G., Tester, J., and Drake, R., 1985. "Economics of a conceptual 75 MW hot dry rock geothermal electric power-station," Seminar on utilization of geothermal energy for electric power production and space heating (May 14, 1984: Florence, Italy). *Geothermics* **14**(2/3):459–474.

Murphy, H., Hendron, R., Miller, J., and Dreesen, D., 1987. "Hot dry rock plans," in *Proceedings*, Geothermal Energy Program Review V (April 14–15, 1987: Washington, DC). U. S. Department of Energy document CONF-8704110, pp. 171–174.

Murphy, H., Fehler, M., Robinson, B., Tester, J., Potter, R., and Birdsell, S., 1988. "Hot dry rock fracture propagation and reservoir characterization," in *Proceedings*, Geothermal Energy Program Review VI (April 18–21, 1988: San Francisco, CA). U. S. Department of Energy document CONF-880477-5, 10 pp.

Murphy, H., Dreesen, D., Miller, J., Hendron, R., Hughes, E., Kruger, P., and Roberts, V., 1989. "The Hot Dry Rock Program: highlights and future," in *Basis for Expansion*, proceedings of the 11th EPRI geothermal conference and workshop (June 23–25. 1987: Oakland, CA). EPRI-GS-6380, pp. 209–218.

Murphy, H., Brown, D., Jung, R., Matsunaga, I., and Parker, R., 1999. "Hydraulics and well testing of engineered geothermal reservoirs," in *Hot Dry Rock/Hot Wet Rock Academic Review* (Abé, H., Niitsuma, H., and Baria, R., eds.), *Geothermics* special issue **28**(4/5):491–506.

Muskat, M., 1937. "Use of data on the build-up of bottom-hole pressures," *Trans. AIME* **123**:44–48.

Nakatsuka, K., 1999. "Field characterization for HDR/HWR: a review," in *Hot Dry Rock/Hot Wet Rock Academic Review* (Abé, H., Niitsuma, H., and Baria, R., eds.) *Geothermics* special issue **28**(4/5):519–531.

Narayan, S. P., Yang, Z., Rahmann, S. S., Jing, Z., and Hashida, T., 2002. "HDR reservoir development by fluid induced shear dilation: a numerical study of the Cooper Basin granite rock," in *Geologisches Jahrbuch* special edition (Baria, R., Baumgärtner, J., Gérard, A., and Jung, R., eds.), international conference—4th HDR forum (September 28–30, 1998: Strasbourg, France). Hannover, Germany, pp. 269–279.

Nemat-Nasser, S., Keer, L. M., and Oranratnachai, A., 1978. "Thermally induced secondary cracks" (abstract), in *Proceedings* (Elsner, D. B., comp.), hot dry rock geothermal workshop (April 20, 1978: Los Alamos, NM). Los Alamos Scientific Laboratory report LA-7470-C, pp. 39–40.

New Energy and Industrial Technology Development Organization, 1997b. *Proceedings*, NEDO international geothermal symposium (March 11–12, 1997: Sendai, Japan), 372 pp.

Nicholson, R. W., Pettitt, R., and Sims, J., 1982. "Production casing for hot dry rock wells EE-2 and EE-3," preprint, Geothermal Resources Council annual meeting (October 11–14, 1982: San Diego, CA). Los Alamos National Laboratory report LALP-82-21, Los Alamos, NM, pp. 9–16.

Nicholson, R. W., Dreesen, D. S., and Turner, W. C., 1984. "Improvement of tubulars used for fracturing in hot dry rock wells," *Trans. Geotherm. Resour. Counc.* **8**:275–280.

Niitsuma, H., Fehler, M., Jones, R., Wilson, S., Albright, J., Green, A., Baria, R., Hayashi, K., Kaieda, H., Tezuka, K., Jupe, A., Wallroth, T., Cornet, F. H., Asanuma, H., Moriya, H., Nagano, K., Phillips, W. S., Rutledge, J., House, L., Beauce, A., Alde, D., and Aster, R., 1999. "Current status of seismic and borehole measurements for HDR/HWR development," in *Hot Dry Rock/Hot Wet Rock Academic Review* (Abé, H., Niitsuma, H., and Baria, R., eds.) *Geothermics* special issue **28**(4/5):475–490.

Niitsuma, H., Baria, R., Fehler, M., Green, A., Hayashi, K., Kaieda, H., and Tezuka, K., 2002. "Results and the next step of MTC project: international joint research on new mapping technology for HDR/HWR development," in *Geologisches Jahrbuch* special edition (Baria, R., Baumgärtner, J., Gérard, A., and Jung, R., eds.), international conference—4th HDR forum (September 28–30, 1998: Strasbourg, France). Hannover, Germany, pp. 401–410.

Nunz, G. J., 1980. "DOE Hot Dry Rock Program," 2nd DOE-ENEL workshop for cooperative research in geothermal energy (October 20, 1980: Berkeley, CA). Lawrence Berkeley Laboratory report LBL-11555, pp. 173–188.

Nunz, G. J., 1980. "Status report—hot dry rock geothermal energy," *Mech. Eng.* **102**(12):26–31.

Nunz, G. J., 1993. "The xerolithic geothermal ('hot dry rock') energy resource of the United States: an update," Los Alamos National Laboratory report LA-12606-MS, Los Alamos, NM, 28 pp.

Nunz, G. J., and Franke, P. R., 1983. "HDR geothermal energy—a progress report," preprint, Geothermal Resources Council annual meeting (October 24–27, 1983: Portland, OR). Los Alamos National Laboratory report LALP-83-34, Los Alamos, NM, 4 pp.

Nunz, G. J., Franke, P. R., and Veziroglu, T. N., 1985. "Present status of hot dry rock technology," in *Alternative Energy Sources VII*, proceedings of the 7th international conference on alternative energy sources (December 9, 1985: Miami Beach, FL). Hemisphere Publishing, New York, NY, pp. 235–240.

Olsson, W. A., 1992. "The effect of slip on the flow of fluid through a fracture," *Geophys. Res. Lett.* **19**(6):541–543.

Pearson, C. F., 1981. "The relationship between microseismicity and high pore pressures during hydraulic stimulation experiments in low-permeability granitic rocks," *J. Geophys. Res.* **86**(B9):7855–7864.

Pearson, C. F., 1982. "Parameters and a magnitude moment relationship from small earthquakes observed during hydraulic fracturing experiments in crystalline rocks," *Geophys. Res. Lett.* **9**(4):404–407.

Pearson, C. F., and Albright, J. N., 1984. "Acoustic emissions during hydraulic fracturing in granite," in *Proceedings*, 3rd conference on acoustic emission/microseismic activity in geologic structures and materials (October 5–7, 1984: University Park, PA), pp. 559–575.

Pearson, C., Keppler, H., and Grigsby, C., 1982. "Location of microseismic events from Experiment 2025," Group ESS-4 internal memorandum (unnumbered), Los Alamos, NM, 6 pp.

Pearson, C. F., Fehler, M. C., and Albright, J. N., 1983. "Changes in compressional and shear wave velocities and dynamic moduli during operation of a hot dry rock geothermal system," *J. Geophys. Res.* **88**(B4):3468–3475.

Pettitt, R. A., 1975a. "Planning, drilling, and logging of Geothermal Test Hole GT-2, Phase I," Los Alamos Scientific Laboratory report LA-5819-PR, Los Alamos, NM, 42 pp.

Pettitt, R. A., 1975b. "Testing, drilling, and logging of Geothermal Test Hole GT-2, Phase II," Los Alamos Scientific Laboratory report LA-5897-PR, Los Alamos, NM, 21 pp.

Pettitt, R. A., 1975c. "Testing, drilling, and logging of Geothermal Test Hole GT-2, Phase III," Los Alamos Scientific Laboratory report LA-5965-PR, Los Alamos, NM, 8 pp.

Pettitt, R. A., 1977a. "Los Alamos hot dry rock geothermal energy project," Geothermal Resources Council meeting, *Geothermal: State of the Art* (May 9–11, 1977: San Diego, CA). Geothermal Resources Council, Davis, CA, CONF-770569, pp. 241–242.

Pettitt, R. A., 1977b. "Planning, drilling, logging, and testing of Energy Extraction Hole EE-1, phases I and II," Los Alamos Scientific Laboratory report LA-6906-MS, Los Alamos, NM, 66 pp.

Pettitt, R. A., 1978a. "Los Alamos hot dry rock geothermal energy experiment," Engineering Foundation conference on water for energy development (December 5, 1976: Pacific Grove, CA), pp. 151–162.

Pettitt, R. A., 1978b. "Testing, planning, and redrilling of Geothermal Test Hole GT-2, phases IV and V," Los Alamos Scientific Laboratory report LA-7586-PR, Los Alamos, NM, 64 pp.

Pettitt, R. A., 1981. "Development of man-made geothermal reservoirs," specialty conference on energy in the man-built environment: *The next decade* (August 3, 1981: Vail, CO). CONF-810808-4, 9 pp.

Pettitt, R. A., 1983. "Hot dry rock geothermal energy: the advanced technology," American Nuclear Society winter meeting (October 30, 1983: San Francisco, CA). *Trans. Am. Nucl. Soc.* **45**:16–17.

Pettitt, R. A., and Carden, R., 1981. "Sidetracking experiences in hot granitic wellbores," preprint, Geothermal Resources Council annual meeting (October 25–29, 1981: Houston, TX); Los Alamos National Laboratory report LALP-81-48, Los Alamos, NM, 4 pp.

Pettitt, R. A., and Becker, N. M., 1983. "Mining earth's heat: development of hot dry rock geothermal reservoirs," ASCE spring meeting (May 16, 1983: Philadelphia, PA). *Geothermal Energy* **11**(7):11–15.

Pettitt, R. A., and White, A. A. L., 1984. "Geothermal alternate energy: expanding the options," *J. Energy Eng.* **110**(2):143–156.

Phillips, W. S., Fehler, M. C., and House, L. S., 1992. "Seismic imaging of a hydraulically fractured reservoir," in *Workshop on Induced Seismicity* (Ramseyer, C., ed.), proceedings of the 33rd U. S. symposium on rock mechanics (June 10, 1992: Santa Fe, NM), pp. 190–194.

Phillips, W. S., House, L. S., and Fehler, M. C., 1992. "Vp/Vs and the structure of microearthquake clusters" (abstract), 87th annual meeting of the Seismological Society of America (April 13–15, 1992: Santa Fe, NM). *Seismolog. Res. Lett.* **63**(1):56.

Phillips, W. S., House, L. S., and Fehler, M. C., 1997. "Detailed joint structure in a geothermal reservoir from studies of induced microearthquake clusters," *J. Geophys. Res*. **102**(B6):11745–11763.

Plains Electric Generation and Transmission Cooperative, Inc., 1981. *Hot Dry Rock Feasibility Study*, prepared for the U. S. Department of Energy. Plains Electric Generation and Transmission Cooperative, Inc., Albuquerque, NM, 175 pp.

Ponden, R. F., 1991. "The design and construction of a hot dry rock pilot plant," in *The Geothermal Partnership—Industry, Utilities, and Government Meeting the Challenges of the 90's*, proceedings of Geothermal Energy Program Review IX (March 19–21, 1991: San Francisco, CA). U. S. Department of Energy document CONF-9103105, pp. 149–151.

Ponden, R. F., 1992. "Start-up operations at the Fenton Hill HDR pilot plant," in *Geothermal Energy and the Utility Market—the Opportunities and Challenges for Expanding Geothermal Energy in a Competitive Supply Market*, proceedings of Geothermal Energy Program Review X (March 24–26, 1992: San Francisco, CA). U. S. Department of Energy document CONF-920378, pp. 155–158.

Ponden, R. F., Dreesen, D. S., and Thomson, J. C., 1991. "Performance testing of the Phase II HDR reservoir," Geothermal Resources Council annual meeting (October 6–9, 1991: Sparks, NV). *Trans. Geotherm. Resour. Counc.* **15**:397–400.

Potter, R. M., Smith, M. C., and Robinson, E. S., 1974. "Method of extracting heat from dry geothermal reservoirs," U. S. patent No. 3,786,858.

Potter, R. M., Smith, M. C., Laughlin, A. W., and Eddy, A. C., 1978. "U. S. HDR resource base estimates" (abstract), in *Proceedings* (Elsner, D. B., comp.), hot dry rock geothermal workshop (April 20, 1978: Los Alamos, NM). Los Alamos Scientific Laboratory report LA-7470-C, p. 61.

Purtymun, W. D., Pettitt, R. A., and West, F. G., 1974. "Geology of Geothermal Test Hole GT-2, Fenton Hill site, July 1974," Los Alamos Scientific Laboratory report LA-5780-MS, Los Alamos, NM, 17 pp.

Ramey, H. J., and Gringarten, A. C., 1982. "Well tests in fractured reservoirs," 3rd circum-Pacific energy and mineral resources conference of the American Association of Petroleum Geologists (August 22–28, 1982: Honolulu, HI). Geothermal Resources Council special report No. 12, Davis, CA, pp. 11–16.

Rannels, J. E. (ed.), 1985. *Approved Minutes for the 11th IEA/HDR Steering Committee Meeting* (November 15–16, 1985: Los Alamos, NM). U. S. Department of Energy, Washington, DC, 138 pp.

Rannels, J. E. (ed.), 1986. *Approved Minutes for the 13th IEA/HDR Steering Committee Meeting* (November 19–20, 1986: Los Alamos, NM). U. S. Department of Energy, Washington, DC, 195 pp.

Rannels, J. E., 1987. "Final report for the IEA implementing agreement for a programme of research, development, and demonstration on hot dry rock technology," U. S. Department of Energy, Washington, DC, 14 pp.

Rannels, J. E., and Duchane, D. V., 1991. "Geothermal energy development in the USA: a vast potential resource," *Power Generation Technology (United Kingdom)*, 1990–1991 issue, pp. 177–180.

Rea, K. H., 1977. "Environmental investigations associated with the LASL hot dry rock geothermal energy development project," Los Alamos Scientific Laboratory report LA-6972, Los Alamos, NM, 25 pp.

Richards, H. G., Parker, R. H., Green, A. S. P., Jones, R. H., Nicholls, J. D. M., Nicol, D. A. C., Randall, M. M., Richards, S., Stewart, R. C., and Willis-Richards, J., 1994. "The performance and characteristics of the experimental hot dry rock geothermal reservoir at Rosemanowes, Cornwall (1985–1988)," *Geothermics* **23**(2):73–109.

Roberts, P. M., Aki, K., and Fehler, M. C., 1991. "A low-velocity zone in the basement beneath the Valles Caldera, New Mexico," *J. Geophys. Res.* **96**:21583-21596.

Robinson, B. A., 1982. "Quartz dissolution and silica deposition in hot dry rock geothermal systems," Los Alamos National Laboratory report LA-9404-T, Los Alamos, NM, 144 pp.

Robinson, B. A., 1986. "A field study of tracer and geochemistry behavior during hydraulic fracturing of a hot dry rock geothermal reservoir," 11th annual workshop on geothermal reservoir engineering (January 21–23, 1986: Stanford, CA). SGP-TR-93, pp. 189–196.

Robinson, B. A., 1988. "Fracture network modeling of a hot dry rock geothermal reservoir," 13th annual workshop on geothermal reservoir engineering (January 19–21, 1988: Stanford, CA). SGP-TR-113, pp. 211–218.

Robinson, B. A., 1990. "A discrete fracture model for a hot dry rock geothermal reservoir," in *Hot Dry Rock Geothermal Energy* (Baria, R., ed.), proceedings of the Camborne School of Mines international hot dry rock conference (June 27–30, 1989: Redruth, Cornwall, UK). Robertson Scientific Publications, London, pp. 315–327.

Robinson, B. A., 1990. "Pressure transient modeling of a fractured geothermal reservoir," in *Proceedings*, 15th annual workshop on geothermal reservoir engineering (January 23–25, 1990: Stanford, CA). SGP-TR-130, pp. 13–19.

Robinson, B. A., 1991. "Alternate operating strategies for hot dry rock geothermal reservoirs," Geothermal Resources Council annual meeting and exhibit (October 6–9, 1991: San Diego, CA). *Trans. Geotherm. Resour. Counc.* **15**:339–345.

Robinson, B. A., and Tester, J. W., 1984. "Dispersed fluid flow in fractured reservoirs: an analysis of tracer-determined residence time distributions," *J. Geophys. Res.* **89**(B12):10374–10384.

Robinson, B. A., and Tester, J. W., 1986. "Characterization of flow maldistribution using inlet-outlet tracer techniques: an application of internal residence-time distributions," *Chem. Eng. Sci.* **41**(3):469–484.

Robinson, B. A., and Birdsell, S. A., 1987. "Tracking thermal fronts with temperature-sensitive, chemically reactive tracers," in *Proceedings*, Geothermal Energy Program Review V (April 14–15, 1987: Washington, DC). U. S. Department of Energy document CONF-8704110, pp. 157–163.

Robinson, B. A., and James, G. F., 1987. "A tracer-based model for heat transfer in a hot dry rock reservoir," Geothermal Resources Council annual meeting (October 11–14, 1987: Sparks, NV). *Trans. Geotherm. Resour. Counc.* **11**:615–622.

Robinson, B. A., and Kruger, P., 1988. "A comparison of two heat transfer models for estimating thermal drawdown in hot dry rock reservoirs," in *Proceedings*, 13th annual workshop on geothermal reservoir engineering (January 19–21, 1988: Stanford, CA). SGP-TR-113, pp. 113–120.

Robinson, B. A., and Birdsell, S. A., 1989. "Hot dry rock geothermal reservoir model development at Los Alamos," in *Research and Development for the Geothermal Marketplace*, proceedings of Geothermal Energy Program Review VII (March 21–23, 1989: San Francisco, CA). U. S. Department of Energy document CONF-890352, pp. 157–163.

Robinson, B. A., and Pendergrass, J., 1989. "A combined heat transfer and quartz dissolution/deposition model for a hot dry rock geothermal reservoir," 14th annual workshop on geothermal reservoir engineering (January 24–26, 1989: Stanford, CA). SGP-TR-122, pp. 207–217.

Robinson, B. A., and Brown, D. W., 1990. "Modeling the hydraulic characteristics of the Fenton Hill, New Mexico hot dry rock reservoir," Geothermal Resources Council annual meeting and international symposium on geothermal energy (August 20–24, 1990: Kailua Kona, HI). *Trans. Geotherm. Resour. Counc.* **14**:1333–1337.

Robinson, B. A., and Fehler, M., 1991. "Estimates of rock volume suitable for heat transfer calculations," Group EES-4 internal memorandum EES-4-91-208, Los Alamos, NM, 5 pp.

Robinson, B. A., and Kruger, P., 1992. "Pre-test estimates of temperature decline for the LANL Fenton Hill Long-Term Flow Test," Geothermal Resources Council annual meeting, 20th anniversary (October 4–7, 1992: San Diego, CA). *Trans. Geotherm. Resour. Counc.* **16**:473–479.

Robinson, B. A., Brown, L. F., and Tester, J. W., 1984. "Using chemically reactive tracers to determine temperature characteristics of geothermal reservoirs," preprint, Geothermal Resources Council annual meeting (August 26–29, 1984: Reno, NV). Los Alamos National Laboratory report LALP-84-37, Los Alamos, NM, pp. 41–45.

Robinson, B., Dash, Z., Dreesen, D., Kelkar, S., Miller, J., Restine, B., Yamaguchi, T., and Zyvoloski, G., 1985. "Experiment 2062 results," Group ESS-4 internal memorandum ESS-4-85-209, Los Alamos, NM, 47 pp.

Robinson, B. A., Aguilar, R. G., Kanaori, Y., Trujillo, P. E. Jr., Counce, D. A., Birdsell, S. A., and Matsunaga, I., 1987. "Geochemistry and tracer behavior during a thirty-day flow test of the Fenton Hill HDR (hot dry rock) reservoir," 12th annual workshop on geothermal reservoir engineering (January 20–22, 1987: Stanford, CA). SGP-TR-109, pp. 163–171.

Robinson, B. A., Brown, L. F., and Tester, J. W., 1988. "Reservoir sizing using inert and chemically reacting tracers," *SPE (Society of Petroleum Engineers) Format. Eval.* **3**(1):227–234.

Robinson, E. S., Potter, R. M., McInteer, B. B., Rowley, J. C., Armstrong, D. E., and Mills, R. L., 1971. "A preliminary study of the nuclear Subterrene" (Smith, M. C., ed.), Los Alamos Scientific Laboratory report LA-4547, 62 pp.

Rodrigues, N. E. V., Robinson, B. A., and Counce, D. A., 1993. "Tracer experiment results during the Long-Term Flow Test of the Fenton Hill reservoir," 18th annual workshop on geothermal reservoir engineering (January 26–28, 1993: Stanford, CA). SGP-TR-145, pp. 199–206.

Roegiers, J. C., and Brown, D. W., 1974. "Geothermal energy: a new application of rock mechanics?" 3rd international congress on rock mechanics (September 1, 1974: Denver, CO). CONF-740909-P2A, vol. II, part A, National Academy of Sciences, Washington, DC, pp. 674–680.

Roegiers, J. C., and McLennan, J. D., 1978. "Rock mechanics problems associated with hot dry rock geothermal energy extraction" (abstract), in *Proceedings* (Elsner, D. B., comp.), hot dry rock geothermal workshop (April 20, 1978: Los Alamos, NM). Los Alamos Scientific Laboratory report LA-7470-C, p. 36.

Roff, A., Phillips, W. S., and Brown, D. W., 1996. "Joint structures determined by clustering microearthquakes using waveform amplitude ratios," *Int. J. Rock Mech. Min. Sci. & Geomech. Abstr.* **33**(6):637–639.

Rowley, J. C., and Carden, R. S., 1982. "Drilling of hot dry rock geothermal Energy Extraction Well EE-3," Los Alamos National Laboratory report LA-9512-HDR, Los Alamos, NM, 123 pp.

Rowley, J. C., Heiken, G., Murphy, H. D., and Kuriyagawa, M., 1982. "Experimental results and potential for hot dry rock geothermal resources," 3rd circum-Pacific energy and mineral resources conference of the American Association of Petroleum Geologists (August 22–28, 1982: Honolulu, HI). *Trans. Circum-Pacific Energy Minerals Res. Conf.* **3**:451–457.

Rowley, J. C., Pettitt, R. A., Hendron, R. H., Sinclair, A. R., and Nicholson, R. W., 1983. "Fracturing operations in a dry geothermal reservoir," annual technical conference of the Society of Petroleum Engineers of AIME (October 5, 1983: San Francisco, CA). *Soc. Pet. Eng. AIME Pap.* vol. SPE12100, p. 16.

Rowley, J. C., Pettitt, R. A., Matsunaga, I., Dreesen, D. S., Nicholson, R. W., and Sinclair, A. R., 1983. "Hot dry rock geothermal reservoir fracturing: initial field operations—1982," Geothermal Resources Council annual meeting (October 24–27, 1983: Portland, OR). *Trans. Geotherm. Resour. Counc.* **7**:467–472.

Sanyal, S. K., Wells, L. E., and Bickham, R. E., 1979. "Geothermal well log interpretation. Midterm report," Los Alamos Scientific Laboratory report LA-7693-MS, Los Alamos, NM, 178 pp.

Sarda, J. P., and Hsu, Y. C., 1975. "Angle of crack propagation for a vertical hydraulic fracture," Los Alamos Scientific Laboratory report LA-6175-MS, Los Alamos, NM, 6 pp.

Sass, J. H., and Robertson-Tait, A., 2002. "Potential for 'enhanced geothermal systems' in the western United States," in *Geologisches Jahrbuch* special edition (Baria, R., Baumgärtner, J., Gérard, A., and Jung, R., eds.), international conference—4th HDR forum (September 28–30, 1998: Strasbourg, France). Hannover, Germany, pp. 35–42.

Savage, W. U., 1977. *Review of the Los Alamos Seismic Monitoring Program in Relation to the Hot Dry Rock Geothermal Project*, prepared for the Los Alamos Scientific Laboratory of the University of California, Los Alamos, NM. Woodward-Clyde Consultants, San Francisco, CA, 30 pp.

Schillo, J. C., Nicholson, R. W., Hendron, R. H., and Thomson, J. C., 1987. "Redrilling of Well EE-3 at the Los Alamos National Laboratory HDR Project," Geothermal Resources Council annual meeting (October 11–14, 1987: Sparks, NV). *Trans. Geotherm. Resour. Counc.* **11**:67–73.

Shulman, G., 1992. "Administration's national energy strategy relating to the hot dry rock (HDR) geothermal energy program" (presented to U. S. House of Representatives Committee on Interior and Insular Affairs, Subcommittee on Energy and the Environment, January 23, 1992). *Geotherm. Resour. Counc. Bull.* **21**(5):175–176.

Sibbitt, W. L., Dodson, J. G., and Tester, J. W., 1979. "Thermal conductivity of crystalline rocks associated with energy extraction from hot dry rock geothermal systems," *J. Geophys. Res.* **84**(B3):1117–1124.

Simmons, G., and Eddy, A., 1976. "Microcracks in GT-2 core" (abstract), American Geophysical Union spring annual meeting (April 12, 1976: Washington, DC). *EOS, Trans. Am. Geophys. Union* **57**(4):353.

Simmons, G., and Richter, D., 1976. "Microcracks in rocks," in The Physics and Chemistry of Minerals and Rocks (Streus, R. G. J., ed.), John Wiley & Sons, London, pp. 105–137.

Simmons, G., and Cooper, H., 1977. "DSA of the microcracks in more GT-2 core: interpretation and implications," final technical report to the Los Alamos Scientific Laboratory under subcontract X67-69648-1, unpublished, 34 pp.

SKB (Svensk Kärnbränslehantering AB—Swedish Nuclear Fuel and Waste Management Co.), 1989. *Storage of Nuclear Waste in Very Deep Boreholes—Feasibility Study and Assessment of Economic Potential*, SKB Technical Report 89-39, Stockholm, Sweden, 100 pp.

Slemmons, D. B., 1975. "Fault activity and seismicity near the Los Alamos Scientific Laboratory geothermal test site, Jemez Mountains, New Mexico," Los Alamos Scientific Laboratory report LA-59-11-MS, 26 pp.

Smith, M. C., 1973. "Geothermal energy," Los Alamos Scientific Laboratory informal report LA-5289-MS, Los Alamos, NM, 31 pp.

Smith, M. C., 1973. "The potential for the production of power from geothermal resources," *Geotherm. Energy* **1**(2):46–51.

Smith, M. C., 1974. "Geothermal power," in *Proceedings*, AIP topical conference on energy (February 4, 1974: Chicago, IL). No. 19, pp. 401–411.

Smith, M. C., 1974. "Los Alamos dry geothermal source demonstration project," in *Proceedings*, geothermal power development conference (June 18, 1974: Berkeley, CA). Lawrence Berkeley Laboratory document LBL-3099, 6 pp.

Smith, M. C., 1974. "Los Alamos geothermal dry hot rock source demonstration project," *Geotherm. Energy Mag.* **2**(10):8–14.

Smith, M. C., 1974. "Progress of the LASL dry hot rock geothermal energy project," in *Proceedings*, conference on research for the development of geothermal energy resources (September 23, 1974: Pasadena, CA), pp. 207–212.

Smith, M. C., 1974. "Prospect for geothermal power," Power Engineering Society summer meeting and energy resources conference (July 16, 1974: Anaheim, CA). CONF-740709-2, 9 pp.

Smith, M. C., 1975. "Los Alamos Scientific Laboratory dry hot rock geothermal project," *Geothermics* **4**(1–4):27–39.

Smith, M. C., 1976. "LASL dry hot rock concept" (abstract), American Geophysical Union spring annual meeting (April 12, 1976: Washington, DC). *EOS, Trans. Am. Geophys. Union* **57**(4):349.

Smith, M. C., 1977. "Results of fluid-circulation experiments: LASL hot dry rock geothermal project," American Nuclear Society topical meeting on energy and mineral recovery research (April 12, 1977: Golden, CO). CONF-770440-3, 6 pp.

Smith, M. C., 1978. "Geothermal energy: the furnace in the basement," *Phys. Teach.* **16**(8):533–539.

Smith, M. C., 1978. "Initial results from the first Los Alamos hot dry rock energy system," symposium on geothermal energy (May 29, 1978: Gothenburg, Sweden). CONF-780513-1, 10 pp.

Smith, M. C., 1979. "The future of hot dry rock geothermal energy systems," 3rd national congress, pressure vessel and piping division of the American Society of Mechanical Engineers (June 24–29, 1979: San Francisco, CA). American Society of Mechanical Engineers publication 79-PVP-35, 12 pp.

Smith, M. C., 1980. "Hot dry rock pilot project," NATO/CCMS meeting on pilot studies (July 15, 1980: Paris, France). CONF-800704-2, 5 pp.

Smith, M. C., 1981. "The hot dry rock geothermal energy program," *Interstate Oil Compact Commission Committee Bull*. **23**(2):20–22.

Smith, M. C., 1982. "The hot dry rock geothermal energy program," Los Alamos National Laboratory report LALP-81-45, Los Alamos, NM, 4 pp.

Smith, M. C., 1982. "Progress of the U. S. hot dry rock program," in *Proceedings*, international conference on geothermal energy (Stephens, H. S., and Stapleton, C. A., eds.), May 11–14, 1982: Florence, Italy, pp. 303–319.

Smith, M. C., 1983a. "A history of hot dry rock geothermal energy systems," in *Geothermal Energy from Hot Dry Rock* (Heiken, G., and Goff, F., eds.), *J. Volcanol. Geotherm. Res.* special issue **15**(1–3):1–20.

Smith, M. C., 1983b. "Hot dry rock is where you find it," in *Workshop on Exploration for Hot Dry Rock Geothermal Systems* (Heiken, G. H., Shankland, T. J., and Ander, M. E., comp.), June 21, 1982: Los Alamos, NM. Los Alamos National Laboratory report LA-9697-C, pp. 18–21.

Smith, M. C., 1983c. "Major accomplishments of the hot dry rock program, 1970–1982," Los Alamos National Laboratory report LALP-82-37, Los Alamos, NM, 12 pp.

Smith, M. C., 1985. "The transfer of hot dry rock technology," Los Alamos National Laboratory report LA-10601-HDR, Los Alamos, NM, 38 pp.

Smith, M. C., 1987. "The hot dry rock geothermal energy program," Los Alamos National Laboratory report LALP-87-16, Los Alamos, NM, 5 pp.

Smith, M. C., 1995. "The furnace in the basement, Part 1: The early days of the hot dry rock geothermal energy program, 1970–1973," Los Alamos National Laboratory report LA-12809, Pt. 1, Los Alamos, NM, 215 pp.

Smith, M. C., *in preparation*. "The furnace in the basement, Part 2: The Phase I system, 1974–1978."

Smith, M. C., and Tester, J. W., 1977. "Energy extraction characteristics of hot dry rock geothermal systems," in *Proceedings*, 12th intersociety energy conversion engineering conference (August 28–September 2, 1977: Washington, DC). Society of Mechanical Engineers, New York, NY, pp. 816–823.

Smith, M., Potter, R., Brown, D., and Aamodt, R. L., 1973. "Induction and growth of fractures in hot rock," in *Geothermal Energy* (Kruger, P., and Otte, C., eds.), Stanford University Press, Stanford, CA, pp. 251–268.

Smith, M. C., Aamodt, R. L., Potter, R. M., and Brown, D. W., 1975. "Man-made geothermal reservoirs," 2nd United Nations symposium on the development and use of geothermal resources (May 20–29, 1975: San Francisco, CA). CONF-750525-6, 26 pp.

Smith, R. L., Bailey, R. A., and Ross, C. S., 1970. *Geologic Map of the Jemez Mountains, New Mexico*, U. S. Geological Survey Miscellaneous Investigations Series Map No. I-571, Reston, VA.

Sneddon, I. N., 1946. "The distribution of stress in the neighbourhood of a crack in an elastic solid," *Proc. Royal Soc. London* **A187**:229–260.

Somerville, M., van der Meulen, T., Estrella, D., Rahman, S. S., Chopra, P. N., and Wyborn, D., 1994. "Hot dry rock feasibility study," Energy Research and Development Corporation report ERDC-243, 133 pp.

Spence, R. W., Aamodt, R. L., Potter, R. M., and Albright, J. N., 1978. "Acoustic ranging and in-situ velocity measurements" (abstract), in *Proceedings* (Elsner, D. B., comp.), hot dry rock geothermal workshop (April 20, 1978: Los Alamos, NM). Los Alamos Scientific Laboratory report LA-7470-C, p. 20.

Steck, L. K., Lutter, W. J., Fehler, M. C., Thurber, C. H., Roberts, P. M., Baldridge, W. S., Stafford, D. G., and Sessions, R., 1998. "Crust and upper mantle structure beneath Valles Caldera, New Mexico: Results from the JTEX Teleseismic Experiment," *J. Geophys. Res.* **103**:24301–24320.

Sun, R. J., 1969. "Theoretical size of hydraulically induced horizontal fractures and corresponding surface uplift in an idealized medium," *J. Geophys. Res.* **74**(25):5995–6011.

Swanson, P. L., 1985. "Subcritical crack growth and other time- and environment-dependent behavior in crustal rocks," *J. Geophys. Res.* **89**:4137-4152.

Swenson, D., and Beikmann, M., 1992. "An implicitly coupled model of fluid flow in jointed rock," in *Proceedings*, 33rd U. S. symposium on rock mechanics (Tillerson, J. R., and Wawersik, W. R., eds.), June 3–5, 1992: Santa Fe, NM. A. A. Balkema, Brookfield, VT, pp. 649–658.

Swenson, D., Martineau, R., James, M., and Brown, D., 1991. "A coupled model of fluid flow in jointed rock," in *Proceedings*, 16th annual workshop on geothermal reservoir engineering (January 23–25, 1991: Stanford, CA). SGP-TR-134, pp. 21–27.

Swenson, D., DuTeau, R., and Sprecker, T., 1995. "Modeling flow in a jointed geothermal reservoir," in *Worldwide Utilization of Geothermal Energy: an Indigenous, Environmentally Benign Renewable Energy Resource*, proceedings of the World Geothermal Congress (May 18–31, 1995: Florence, Italy). International Geothermal Association, Inc., Auckland, New Zealand, vol. 4, pp. 2553–2558.

Takahashi, H., and Hashida, T., 1993. "New project for hot wet rock geothermal reservoir design concept," in *Proceedings*, 18th annual workshop on geothermal reservoir engineering (January 26–28, 1993: Stanford, CA). SGP-TR-145, pp. 291–296.

Tatro, C. A., 1986. "A study of pumps for the hot dry rock geothermal energy extraction experiment (LTFT [Long-Term Flow Test])," Los Alamos National Laboratory report LA-10862-T, 89 pp.

Tennyson, G. P. Jr., 1985. *Minutes*, 9th IEA Steering Committee meeting (October 3–4, 1984, Tokyo, Japan). U. S. Department of Energy, Washington, DC, 110 pp.

Tennyson, G. P. Jr., 1986. *Revised Draft Minutes*, 12th IEA/HDR Steering Committee meeting (June 17–18, 1986: Los Alamos, NM). U. S. Department of Energy, Washington, DC, 177 pp.

Tennyson, G. P. Jr., 1991. "Summary—hot dry rock," in *The Geothermal Partnership—Industry, Utilities, and Government Meeting the Challenges of the 90's*, proceedings of Geothermal Energy Program Review IX (March 19–21, 1991: San Francisco, CA). U. S. Department of Energy document CONF-9103105, pp. 139–141.

Tennyson, G. P. Jr., 1992. "Hot dry rock—summary," in *Geothermal Energy and the Utility Market—the Opportunities and Challenges for Expanding Geothermal Energy in a Competitive Supply Market*, proceedings of Geothermal Energy Program Review X (March 24–26, 1992: San Francisco, CA). U. S. Department of Energy document CONF-920378, p. 145.

Tester, J. W., 1974. *Proceedings*, NATO-CCMS information meeting on dry hot rock geothermal energy (September 17–19, 1974: Los Alamos, NM). Los Alamos Scientific Laboratory report LA-5818-C, 40 pp.

Tester, J. W., 1976. "Geothermal energy for power generation," in *Energy for the Future*, proceedings of the IEEE region six conference (April 7–9, 1976: Tucson, AZ). A76-39476 19-44, pp. 19–25.

Tester, J. W., 1979. "Issues facing the development of hot dry rock geothermal resources," 3rd annual EPRI geothermal conference (June 26, 1979: Monterey, CA). CONF-790679-2, 11 pp.

Tester, J. W., 1980. "Development of hot dry rock geothermal resources: technical and economic issues," in *Energy for Ourselves and Our Posterity* (Perrine, R. L., and Ernst, W. G., eds.), Rubey colloquium (January 28, 1980: Los Angeles, CA). Vol. 3, pp. 208–228.

Tester, J. W., 1982. "Energy conversion and economic issues for geothermal energy," in Handbook of Geothermal Energy (Edwards, L. M., Chilingar, G. V., Rieke, H. H. III, and Fertl, W., eds.), Gulf Publishing Company, Houston, TX, pp. 471–588.

Tester, J. W., 1992. "Testimony on hot dry rock geothermal energy" (presented to U. S. House of Representatives Committee on Interior and Insular Affairs, Subcommittee on Energy and the Environment, January 23, 1992). *Geotherm. Resour. Counc. Bull.* **21**(5):137–147.

Tester, J. W., and Milora, S. L., 1975. "Geothermal energy," energy sources of the future meeting (July 7, 1975: Oak Ridge, TN). Los Alamos Scientific Laboratory report LA-UR-75-1463; CONF-750733-1, pp. 74–88.

Tester, J. W., and Bivins, R. L., 1978. "An analysis of interwell tracer residence time distributions" (abstract), in *Proceedings* (Elsner, D. B., comp.), hot dry rock geothermal workshop (April 20, 1978: Los Alamos, NM). Los Alamos Scientific Laboratory report LA-7470-C, p. 31.

Tester, J. W., and Albright, J. N. (eds.), 1979. "Hot dry rock energy extraction field test: 75 days of operation of a prototype reservoir at Fenton Hill, Segment 2 of Phase I," Los Alamos Scientific Laboratory report LA-7771-MS, Los Alamos, NM, 104 pp.

Tester, J. W., and Potter, R. M., 1979. "Interwell tracer analyses of a hydraulically fractured granitic geothermal reservoir," 54th annual conference and exhibition of the Society of Petroleum Engineers (September 23–26, 1979: Las Vegas, NV). SPE 8270, 12 pp.

Tester, J. W., and Herzog, H. J., 1990. *Economic Predictions for Heat Mining: a Review and Analysis of Hot Dry Rock (HDR) Geothermal Energy Technology*, final report for the U. S. Department of Energy. Massachusetts Institute of Technology, Energy Laboratory, document MIT-EL 90 001, 180 pp.

Tester, J. W., and Herzog, H. J., 1991. "The economics of heat mining: an analysis of design options and performance requirements of hot dry rock (HDR) geothermal power systems," *Energy Sys. and Pol.* **15**:33–63.

Tester, J. W., Blatz, L. A., and Holley, C. E. Jr., 1977. "Solution chemistry and scaling in hot dry rock geothermal systems," 83rd national meeting of the American Institute of Chemical Engineers (March 20, 1977: Houston, TX). CONF-770310-2, 9 pp.

Tester, J. W., Grigsby, C., Holley, C., and Blatz, L., 1978. "Geochemical analysis of fluids circulated through a granitic hot dry rock geothermal system" (abstract), 2nd workshop on sampling and analysis of geothermal effluents (February 15–17, 1977: Las Vegas, NV). EPA/600/7-78-121, p. 174.

Tester, J. W., Morris, G. E., Cummings, R. G., and Bivins, R. L., 1979. "Electricity from hot dry rock geothermal energy: technical and economic issues," Los Alamos Scientific Laboratory report LA-7603-MS, Los Alamos, NM, 24 pp.

Tester, J. W., Brown, D. W., and Potter, R. M., 1989a. "Hot dry rock geothermal energy—a new energy agenda for the 21st century," Los Alamos National Laboratory report LA-11514-MS, Los Alamos, NM, 30 pp.

Tester, J. W., Murphy, H. D., Grigsby, C. O., Potter, R. M., and Robinson, B. A., 1989b. "Fractured geothermal reservoir growth induced by heat extraction," *SPE (Society of Petroleum Engineers) Reserv. Eng.* **4**(1):97–104.

Traeger, R., and Murphy, H., 1988. "Plumbing the Earth's depths," *Mech. Eng.* **110**(9):62–68.

Trice, R., and Warren, N., 1977. "Preliminary study on the correlation of acoustic velocity and permeability in two granodiorites from the LASL Fenton Hill deep borehole, GT-2, near the Valles Caldera, New Mexico," Los Alamos Scientific Laboratory report LA-6851-MS, Los Alamos, NM, 26 pp.

Trujillo, P. E., Shevenell, L., Goff, F., Grigsby, C. O., and Counce, D., 1987. "Chemical analysis and sampling techniques for geothermal fluids and gases at the Fenton Hill laboratory," Los Alamos National Laboratory report LA-11006-MS, Los Alamos, NM, 87 pp.

University of New Mexico, 1979. *Economic Modeling of Electricity Production from Hot Dry Rock Geothermal Reservoirs: Methodology and Analyses* (Cummings, R. G., and Morris, G. E., principal investigators), final report. Electric Power Research Institute document EPRI EA-630, 82 pp.

USDOE (U. S. Department of Energy), 1980. *Hot Dry Rock Research, Development, and Demonstration Program Plan*, U. S. Department of Energy, Division of Geothermal Energy, document HDR-PO1, 41 pp.

USDOE (U. S. Department of Energy), 1987. *Energy Security: a Report to the President of the United States*, U. S. Department of Energy, Washington, DC., 97 pp.

USDOE (U. S. Department of Energy), 1995. *Geothermal Progress Monitor*, report No. 17, DOE/EE-0091, U. S. Department of Energy, Washington, DC, 85 pp.

USGS (U. S. Geological Survey), 1979. *Assessment of Geothermal Resources of the United States—1978* (Muffler, L. J. P., ed.), U. S. Geological Survey circular C 790, Reston, VA, 163 pp.

USGS (U. S. Geological Survey), 2008. (Resources Assessment Team: Williams, C. F., Reed, M. J., Mariner, R. H., DeAngelo, J., and Galanis, S. P. Jr.), *Assessment of Moderate- and High-Temperature Geothermal Resources of the United States*. U.S. Geological Survey Fact Sheet 2008-3082, 4 pp.

Vidale, R., Gancarz, A., and Binder, I., 1981. "Application of fluid-chemistry studies to a hot dry rock geothermal system: I. Neutron-activation studies," Los Alamos Scientific Laboratory report LA-8766-MS, Los Alamos, NM, 25 pp.

Wald, M. L., 1991. "Mining deep underground for energy," *New York Times*, November 3, 1991.

Wang, H. F., and Simmons, G., 1978. "Microcracks in crystalline rock from the 5.3-km depth in the Michigan Basin," *J. Geophys. Res.* **83**:5849-5856.

Warren, N., 1983. "Quantitative petrostructure analysis," Los Alamos National Laboratory report LA-9711-MS, Los Alamos, NM, 39 pp.

West, F. G., 1976. "Geology of the LASL Fenton Hill site" (abstract), American Geophysical Union spring annual meeting (April 12, 1976: Washington, DC). *EOS, Trans. Am. Geophys. Union* **57**(4):350.

West, F. G., and Shankland, T. J., 1977. "Exploration methods for hot dry rock," Los Alamos Scientific Laboratory report LA-6659-MS, Los Alamos, NM, 58 pp.

West, F. G., Kintzinger, P. R., and Laughlin, A. W., 1975. "Geophysical logging in Los Alamos Scientific Laboratory Geothermal Test Hole No. 2," Los Alamos Scientific Laboratory report LA-6112-MS, Los Alamos, NM, 13 pp.

West, F. G., Kintzinger, P. R., and Purtymun, W. D., 1975. "Hydrologic testing of Geothermal Test Hole No. 2," Los Alamos Scientific Laboratory report LA-6017-MS, Los Alamos, NM, 8 pp.

Whetten, J., Potter, R., and Brown, D., 1983. "Hot dry rock update," in *Proceedings*, Geothermal Energy Program Review II (October 11, 1983: Washington, DC). U. S. Department of Energy document CONF-8310177, pp. 212–234.

Whetten, J., Dennis, B., Dreesen, D., House, L., Murphy, H., Robinson, B., and Smith, M., 1986. "The U. S. hot dry rock project," 1st EEC/U. S. workshop on geothermal hot dry rock technology (May 28–30, 1986: Brussels, Belgium). *Geothermics* **16**(4):331–339.

Whetten, J. T., Murphy, H. D., Hanold, R. J., Myers, C. W., and Dunn, J. C., 1988. "Advanced geothermal technologies," 15th annual energy technology conference and exposition, *Repowering America* (February 17–19, 1988: Washington, DC). CONF-880212-4, 16 pp.

Williams, R. E., 1978. "Geothermal drilling in hot granitic rock," Geothermal Resources Council meeting, *Geothermal Energy: a Novelty Becomes a Resource* (July 25–27, 1978: Hilo, HI). *Trans. Geotherm. Resour. Counc.* **2**(2):721–723.

Williams, R. E., Rowley, J. C., Neudecker, J. W., and Brittenham, T. L., 1979. "Equipment for drilling and fracturing hot granite wells," 54th annual conference and exhibition of the Society of Petroleum Engineers (September 23–26, 1979: Las Vegas, NV). SPE 8268, 8 pp.

Williams, R. E., Neudecker, J. W., Rowley, J. C., and Brittenham, T. L., 1981. "Directional drilling and equipment for hot granite wells," in *Proceedings*, international geothermal drilling and completions technology conference (January 21–23, 1981: Albuquerque, NM). CONF-810105-2, pp. 9.1–9.24.

Witherspoon, P. A., Wang, J. S. Y., Iwai, K., and Gale, J. E., 1980. "Validity of cubic law for fluid flow in a deformable rock fracture," *Water Resour. Res.* **16**:1016–1024.

Witherspoon, P. A., Bodvarsson, G. S., Pruess, K., and Tsang, C. F., 1982. "Energy recovery by water injection," 3rd circum-Pacific energy and mineral resources conference of the American Association of Petroleum Geologists (August 22–28, 1982: Honolulu, HI). Geothermal Resources Council special report No. 12, Davis, CA, pp. 35–44.

Won, I. J., and Son, K. H., 1982. "Determination of depth to the Curie isotherm from aeromagnetic data," in *Workshop on Exploration for Hot Dry Rock Geothermal Systems* (Heiken, G. H., Shankland, T. J., and Ander, M. E., comp.), June 21, 1982: Los Alamos, NM. Los Alamos National Laboratory report LA-9697-C, pp. 51–57.

Worley, W. G., and Tester, J. W., 1995. "Dissolution kinetics of quartz and granite in acidic and basic salt solutions," in *Worldwide Utilization of Geothermal Energy: an Indigenous, Environmentally Benign Renewable Energy Resource*, proceedings of the World Geothermal Congress (May 18–31, 1995: Florence, Italy). International Geothermal Association, Inc., Auckland, New Zealand, vol. 4, pp. 2545–2551.

Wunder, R., and Murphy, H., 1978. "Thermal drawdown and recovery of singly and multiply fractured hot dry rock reservoirs," Los Alamos Scientific Laboratory report LA-7219-MS, Los Alamos, NM, 18 pp.

Yamamoto, T., Kitano, K., Fujimitsu, Y., and Ohnishi, H., 1997. "Application of simulation code GEOTH3D on the Ogachi HDR site," in *Proceedings*, 22nd workshop on geothermal reservoir engineering (January 27–29, 1997: Stanford, CA). SGP-TR-155, pp. 203–212.

Zyvoloski, G., 1980. "Bottom-hole temperatures and pressures for Experiment 217," Los Alamos Scientific Laboratory G-5 internal report, technical memo 11, Los Alamos, NM.

Zyvoloski, G., 1982. "Non-Darcy flow in geothermal reservoirs," Geothermal Resources Council annual meeting (October 11, 1982: San Diego, CA). *Trans. Geotherm. Resour. Counc.* **6**:325–328.

Zyvoloski, G., 1984. "Reservoir modeling of the Phase II hot dry rock system," preprint, Geothermal Resources Council annual meeting (August 26–29, 1984: Reno, NV). Los Alamos National Laboratory report LALP-84-37, Los Alamos, NM, 4 pp.

Zyvoloski, G., 1985. "The sizing of a hot dry rock reservoir from a hydraulic fracturing experiment," in *Research and Engineering Applications in Rock Masses*, proceedings of the 26th U. S. symposium on rock mechanics (June 26–28, 1985: Rapid City, SD). A. A. Balkema Publishers, Accord, MA, pp. 355–362.

Zyvoloski, G. A., Aamodt, R. L., and Aguilar, R. G., 1981a. "Evaluation of the second hot dry rock geothermal energy reservoir: results of Phase I, Run Segment 5," Los Alamos National Laboratory report LA-8940-HDR, Los Alamos, NM, 94 pp.

Zyvoloski, G. A., Aamodt, R. L., Fisher, H. N., and Murphy, H. D., 1981b. "Some results of a long-term flow test of a hot dry rock reservoir," preprint, Geothermal Resources Council annual meeting (October 25–29, 1981: Houston, TX). Los Alamos National Laboratory report LALP-81-48, Los Alamos, NM, 4 pp.

Index